Modelling the magnetic properties of natural and environmental materials

Lees, Joan Anne

Award date:
1994

Awarding institution:
Coventry University

Modelling the Magnetic Properties of Natural and Environmental Materials

Joan Anne Lees

Thesis submitted in partial fulfilment of the University's requirements for the Degree of Doctor of Philosophy

August, 1994

Coventry University

Modelling the Magnetic Properties of Natural and Environmental Materials

Joan Anne Lees

Abstract

Magnetic properties have been used to characterize natural and environmental materials. An evaluation of magnetic properties, for the modelling of sources of materials and minerals, has been completed. A methodological framework has been developed for the application of magnetic techniques to studies involving the quantification of sources of materials and minerals in any environment. The framework includes the identification of sources using magnetic reconnaissance and multi-variate statistical classification techniques. Magnetic measurements used are susceptibility (both field and laboratory), remanence and magnetization measurements. The linear additivity of magnetic measurements, and classification and linear modelling techniques, have been tested using data for artificial laboratory mixtures and hypothetical mixing experiments. The limitations of using magnetic properties with these statistical and mathematical techniques are defined. The framework allows for the testing of suitability of magnetic modelling techniques in any sourcing study.

To test the methodological framework three environmental applications have been completed. The first, a coastal study, has allowed assessment of the methodology in sourcing beach sediments in a dynamic system. In the second application, a catchment study, evaluation of the spatial variability of sources is undertaken; including statistical definition of the source properties for modelling techniques. The final application covers modelling of magnetic minerals in several contrasting soil profiles. Hysteresis loop data are used for the purpose of modelling diamagnetic, paramagnetic, canted-antiferromagnetic and ferrimagnetic minerals in the soils.

The methodological framework is re-assessed according to the needs and results of each individual application. It has largely been the case that there are great limitations in the use of magnetism for sourcing environmental materials, and minerals quantitatively. At best only four potential sources of material in a 'mixture' can be successfully modelled. These are mainly defined by the four mineral magnetic properties listed above. Limitations and errors involved in each step of the methodology are tested, and quantified, and a final definition of the positive application of quantitative source modelling using magnetism is made.

From the experimental work it has been found that χlf is the most linearly additive measurement and field kappa can be widely used for mapping magnetic properties indicating soil, land-use, geology and topographical/drainage features. χlf versus $HIRM_{+100mT}$ bi-variate plots give vital preliminary information on the modelling suitability of the potential sources of mixtures. From the case study applications it has been found that environmental variability of sources can be incorporated into linear modelling routines. Often this gives source contributions which have a wide, often overlapping, range of values. In the coastal and mineral modelling work dominant ferrimagnetic minerals have been found to mask weaker magnetic signals which makes unmixing of the mineral contributions very difficult. However, also in the coastal study field tracing, using kappa has been utilised and gives information on short term beach and wave processes. In the catchment study sources of finer sediments have been quantified successfully and the reliability of answers tested. Ranges of source contributions overlap when the natural variability of sources is taken into account. In the future, wider incorporation of hysteresis parameters may improve characterization of minerals other than those which are ferrimagnetic.

Contents

SECTION B: Evaluation and Modelling

SECTION D: Discussion and Conclusions

CHAPTER 10: Discussion and Conclusions

List of Figures

Chapter 1

Chapter 2

Chapter 3

Chapter 8

Chapter 9

Appendices

List of Tables

Chapter 2

Chapter 3

Chapter 4

Chapter 5

Chapter 7

Chapter 8

Chapter 9

Chapter 10

Appendices

List of Plates

List of Appendices

Acknowledgements

This research was funded by a Coventry University Research Initiative Grant (formerly PCFC) held by Dr. J. Dearing and Dr. F. P. Lockett.

I thank Dr. John Dearing for supervision and advice on the writing of this thesis and for making corrections. I would like to thank Dr. Peter Lockett for his supervision and invaluable help with the mathematical aspects of this work and reading, correcting and making useful comments on this thesis. Special thanks also my father, Mr. S. J. Lees for reading and correcting a draft of the text and Dr. Angela Browne who so carefully proof read the final draft.

Continued encouragement and advice from many members of staff in the Geography Department at Coventry University have made it possible for me to complete this research, especially Prof. David Smith, Drs. Ian Foster, David Keen, Brian Ilberry, Alistair Dawson and Serwan Baban. I especially thank Drs. Hazel Barrett, Philip Nicholls and Angela Browne for giving much needed moral support throughout the research. I must also thank many of the postgrads for their 'life saving' support and 'interesting research ideas' (amongst other things) especially Sue Charlesworth, Rebecca Dann, Steven Wade, Lois Mansfield, Lewis Holloway, Sue Dawson, Keiran Hickey, Catherine Kelly, Dale Howes and Karen Hay. Mr. S. J. Lees and Rebecca Dann provided invaluable field assistance throughout the research.

Sincere thanks go to Prof. Roy Chantrell and Dr. Kevin O'Grady for help with fine particle physics and useful experimental ideas and δIRM data. Prof. John Pethick initiated the Holderness study and I thank him for showing us the Holderness area and its erosional problems. Dr. Barbara Maher provided useful discussions on synthetic magnetites and thanks go to her for allowing further measurement of her MT samples. I thank Dr. Nigel Parker for his interest and experimentation with 'magnetic bacteria'. Thanks to Dr. David Keen for identification of numerous geological samples. Useful discussion was also provided by Prof. Roy Carey, Drs. Lizhong Yu, Peter Loveland, Roy Thompson and Margaret Oliver on certain aspects of the work. I thank Mr. Chris White for allowing measurement of his dissertation soil samples.

Thanks also to Dr. Bob Jones for help with the photographing of the microscope slides and Mr. S. J. Lees for training in development and enlargement of the photographs. I would like to thank Mrs. Shirley Addleton, Miss Ruth Gaskell and Mr. Lorne Elliot for cartographic advice and computer assistance and Mrs. E Turner for laboratory guidance and technical discussion. I would also like to thank Mrs. Christene Dawson who provided the SEM and XRD analysis results.

I would like to thank my family for continued support and encouragement throughout.

SECTION A

Aims and Methods

CHAPTER 1

Introduction, Aims and Objectives

Science; not just an individual effort

"It is not in the nature of things for any one man to make a sudden, violent discovery; science goes step by step and every man depends on the work of his predecessors. When you hear of a sudden unexpected discovery - a bolt from the blue, as it were - you can always be sure that it has grown up by the influence of one man on another, and it is this mutual influence which makes the enormous possibility of scientific advance. Scientists are not dependent on the ideas of a single man, but on the combined wisdom of thousands of men, all thinking on the same problem and each doing his little bit to add to the great structure of knowledge which is gradually being erected", Rutherford.

1.1 Introduction

The environment is the most important factor affecting the quality of our lives. Wider publicity in the past few decades has brought attention to the degradation of the environment by the influence of society. Yet for many, the environment in which physical geographers or environmental scientists work is 'remote' and includes areas not readily habitable. Increasingly the effects of man are felt in such remote areas and, closer to home, it would be difficult to find any land surface not affected in one way or another by human influence. A major question posed in environmental science is where natural or polluting materials have originated and how much material from a particular source has been delivered to an area. Much scientific work has been done in the field of source identification and tracing, whether it be soils, airborne pollutants, river sediments or industrial wastes. Also the definition of rates of soil erosion and loss of materials through poor land management and application of the wrong management techniques to the wrong areas has received much attention. Many analytical and descriptive techniques have been employed to define environmental changes and degradation which have included using chemical properties (eg calcium and nitrogen), physical properties (eg particle size, density or magnetic properties) and anthropogenically derived properties (atmospheric particles and radioisotopes) of the materials of interest. In historical and continuing environmental change the above techniques and others such as pollen, diatom and fossil analysis, tree ring analysis and stratigraphical analyses are used.

Different techniques are often used in conjunction with one another, correlated, and theories based on all the evidence are then presented. Figure 1.1 outlines the analytical techniques which have been used to characterize the properties of materials and the 'fingerprinting' or matching techniques which can be used to identify the sources of materials.

Figure 1.1: Types of fingerprinting techniques used with physical, biological and chemical characterization analysis

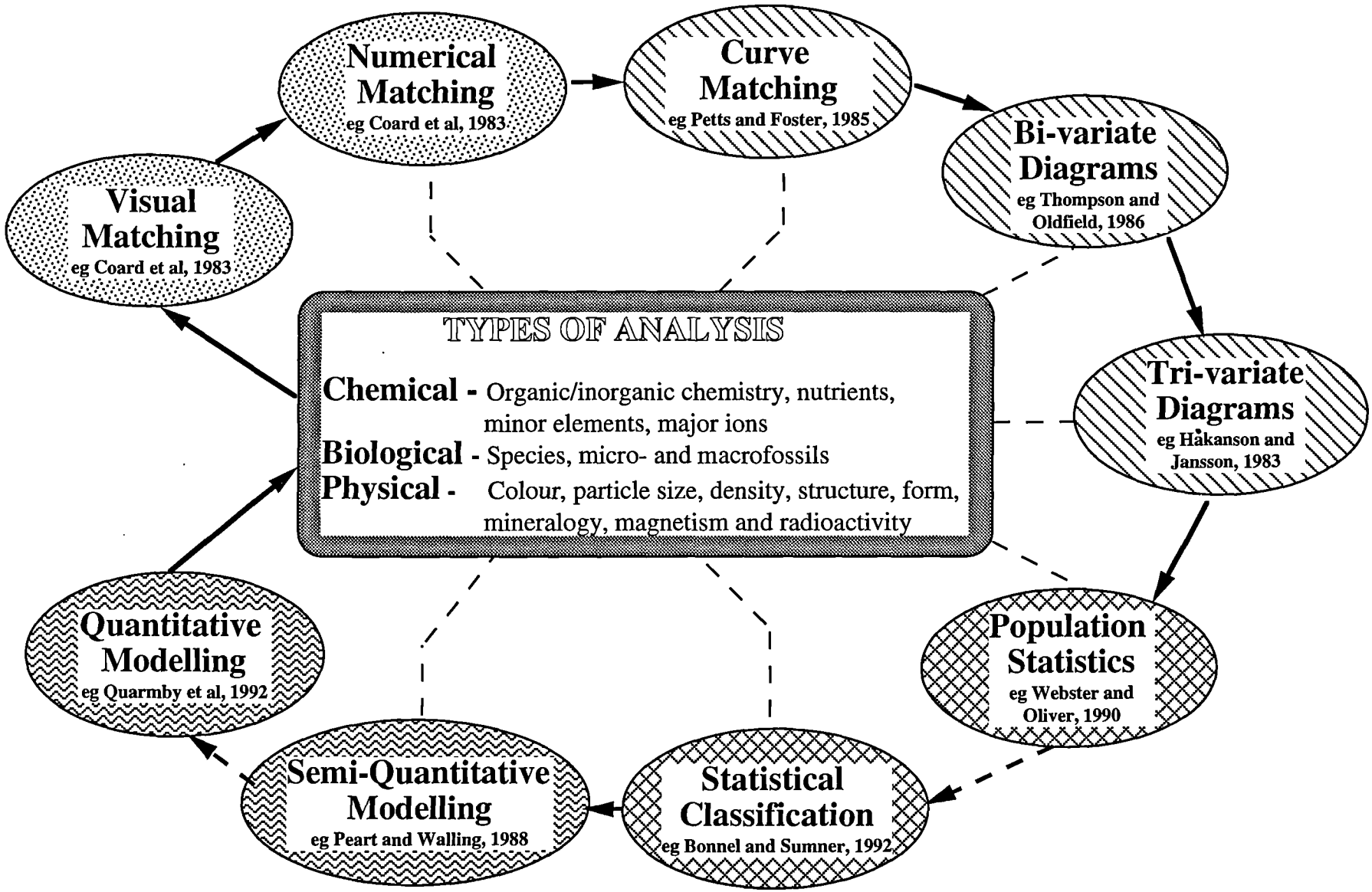

The most simple matching techniques are those of visual and single numerical matching where the colour or single parameter values for the materials are compared. For instance, Coard et al.(1983) used the colour of sediments and numerical values of properties of sediments to trace their source materials. Bi-variate and tri-variate diagrams employ two or three parameters to group like materials: for instance sand, silt and clay percentage contents of sediments can be represented on a tri-diagram (Håkanson and Jansson, 1983). Population statistics can be used to define ranges of source data and be used for discrimination (Webster and Oliver, 1990). More complex statistical classification techniques and modelling techniques can use many parameters to group and quantify the sources of materials in more mathematical terms. For instance, Bonnel and Sumner (1992) employed PCA analysis to group precipitation data from 121 sites in Wales and Quarmby (1992) used linear modelling to quantify crop coverage from remote sensing images. The present work is set between the progression from semi-quantitative modelling techniques to quantitative modelling techniques.

Some of the most important aspects of human interference on environments are the interactions of processes causing sediment selection, erosion, transportation and subsequent deposition. Such sediment can include river sediment, aeolian sediments both natural and anthropogenic, marine sediments, and glacial sediments. All sorts of anthropogenic materials such as chemical waste, mining mineral waste and general litter or tipped material must also be included in analysis in some way. Examples of such sediment and anthropogenic sources of material and mixtures are shown in Figure 1.2 and Plate 1.1. In Figure 1.2 a list of sources of materials include carbonaceous particles and dusts and geologies while mixtures listed include those of river bedloads and soil horizons. Plate 1.1 shows various sources and mixtures ranging from cliff sediments (a) to fly ash particles (f). Not only are the sources of materials of interest in environmental science but individual minerals and their origins are also of importance. Minerals can also be quantified as if they were a source of the total mineralogical property of a material. This approach also has been studied in this research and a few examples are given in Figure 1.3. For instance, the mineral magnetite can be found in geological samples and can be eroded and mixed into sediments; magnetites are also produced by soil burning and pedogenic activity and therefore they can be mixed in soils. The mixing processes of all these materials or minerals and the interactions between such mixed materials or minerals are of utmost importance. Two major questions arise from this. First, how are the 'pure' sources of material changed physically when they are mixed together and interact in the environment? Secondly, can the proportions of the contributing sources be extracted using certain measured properties of the sources and the mixture? Techniques are increasingly being expected to provide means whereby quantitative analysis of sediment source contributions in sediment mixtures can be made successfully while coping with vast environmental variability present in natural and anthropogenically derived material. In order to fulfil these aims using any technique, deductive evaluation and testing of the technique should be done to avoid invalid or erroneous results resulting from mis-application of non-suitable techniques. Many measured properties of materials have been used for this purpose. However, in this study the focus is the technique of Environmental Magnetism which is analysed and evaluated for the purposes of quantitative source modelling.

The questions raised above are answered using magnetic properties of materials as a mechanism for identifying and fingerprinting different materials and quantifying their contribution in environmental mixtures. This has been

Figure 1.2. Unmixing Sediment Sources: Examples

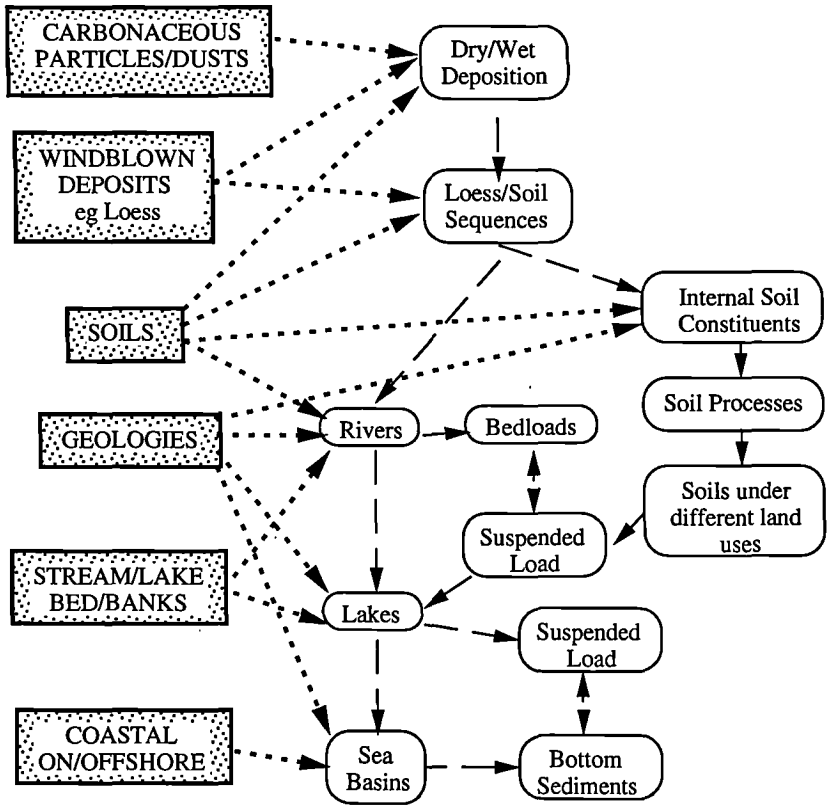

Figure 1.3. Unmixing Mineralogies of mixtures: Examples

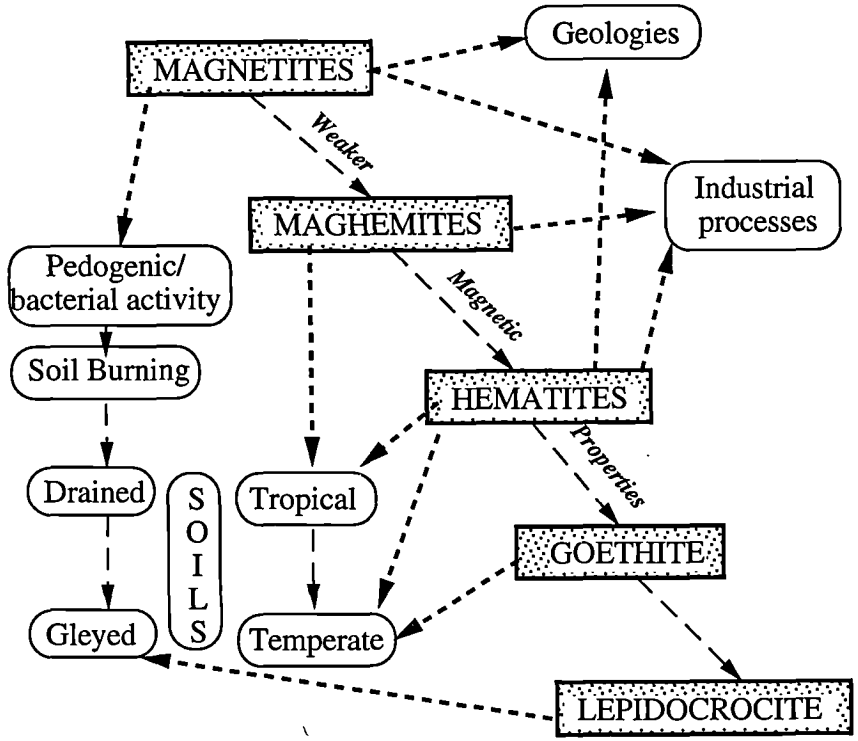

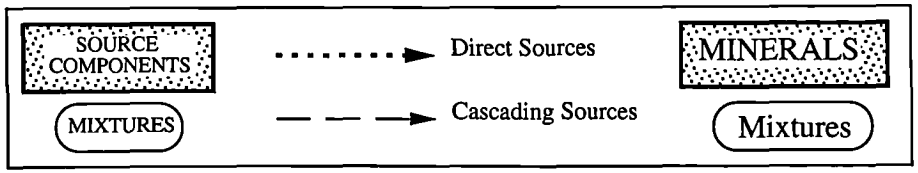

Plate 1.1a: Examples of natural sediment sources-coastal slumping

Plate 1.1b: Field erosion

Plate 1.1c: Stream bank construction

Plate 1.1d: Beach sediment sorting

Plate 1.1e: Anthropogenic sources-Finham sewage works

Plate 1.1f: Anthropogenic sources-fly ash in Seeswood Pool lake sediments

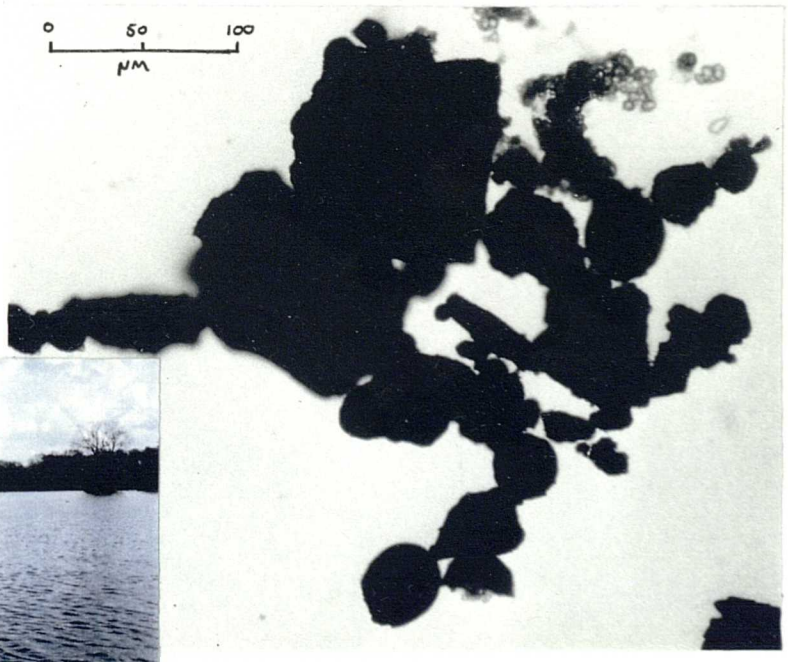

approached in two ways in this research using magnetic measurements. In the first instance laboratory and theoretical analysis has tested the technique and a preferred methodological procedure is defined. Laboratory and controlled data sets have been employed to test magnetic data for the purpose of evaluating the use of that data in the quantitative sourcing of sediments. For this purpose statistical and mathematical classification and modelling techniques are used. Secondly, application of the methodological procedure has been carried out in three environmental contexts. The environmental contexts chosen include a dynamic coastal unit, a small catchment system and single soil profile units. Overall a multidisciplinary approach has been employed to test systematically the use of magnetism in this relatively new field of research. Limits can then be realistically set on a technique and its mode of application defined accurately. Modelling the magnetic properties of natural and environmental materials should advance the use of the technique of environmental magnetism in the quantitative sediment sourcing of mixtures of sediments in environmental systems.

1.2 Background to Present Research

There are advantages in using magnetic techniques in environmental studies. The measurement of parameters is quick, easy, clean and involves no chemical or complicated preparation other than the (usual drying) and sieving. The measurements are also non-destructive and repeatable leaving the material free for other subsequent analyses. Field measurement (of magnetic susceptibility) holds a vital key to assessing the variability of natural materials spatially. Such field measurements can be used to infer short timescale changes in environmental systems and are not labour extensive or time consuming (Leeks et al, 1988). Laboratory measurements of soil cores or lake cores meanwhile give guides to erosional changes occurring over longer timescales (Walling et al, 1979, Oldfield et al. 1979, Flower et al, 1984, Foster et al, 1985) and often are associated with changes in land-uses in specific areas (Dearing, 1979, Dearing and Flower, 1982, Dearing, 1991, Higgitt et al. 1991). Overall, magnetism offers a mechanism for studying change in environmental systems (lake sediments for example) and thorough evaluation of the technique outlining its advantages, disadvantages and guides for its application are needed. Difficulties in interpretation of magnetic parameters in terms of minerals present and their concentrations may be resolved by modelling minerals using linear programming techniques.

Environmental Magnetism was an offshoot discipline of rock magnetism. This section aims to introduce some of the areas in environmental science (see also Annex) where magnetic techniques have been applied, including, soil, lake, atmospheric and geological studies. Le Borgne (1955) first studied the magnetic properties of topsoils and later Tite and Mullins (1971), Vadyunina and Babanin (1972) also looked at the magnetic susceptibility characteristics of soils in Britain and in the USSR respectively. It was found that magnetic properties were different between topsoil and subsoil horizons due to an enhancement mechanism in the upper soil layers and destruction of magnetic minerals in wet soils. Magnetic enhancement in topsoils is characterized by higher measurement values and many studies have attempted to show the causes of this. This enhancement can be due to burning (Rummery et al. 1979), pedogenic factors (Singer and Fine, 1989, Fine et al, 1989) and anthropogenic factors (Nezhdanova and Suetin, 1987). There is also geological input of minerals into soils (Tite, 1972 and Smith et al, 1990). Smith et al (1990) used susceptibility

and remanence measurements to characterize topsoils and subsoils of different land uses and glacial sand, till and colluvium. Subsoils were found to have lower magnetic values and overall the possibility of a mixing model for sources of the colluvium was proposed. Further to this initial characterisation of topsoils, Maher (1986) classified the magnetic properties of soil horizons using cluster analysis, and she also studied the formation of magnetites in soils with Taylor (1988). Taylor and Schwertmann (1974) and Taylor et al (1987) had already written on the origin of magnetic minerals in soils.

Magnetic techniques were then applied to lake sediments, for example Lough Neagh and Loch Lomond (Thompson et al, 1975, Thompson and Morton, 1978). Thompson et al (1975) found that magnetic susceptibility was positively correlated with the amount of inorganic material (detrital titanomagnetite) present in lake cores in Lough Neagh. Thompson and Morton (1978) analysed possible sources of lake sediments in Loch Lomond. These included bedrock, soil, till, stream and beach sediments. Changes in susceptibility in the lake cores were attributed to changes in particle size and iron oxides of either primary or secondary origin. Many studies then followed these, assessing the use of magnetic techniques for identifying the sources of lake sediments and for lake core correlation (Oldfield et al, 1978, Bloemendal et al, 1979, Dearing et al, 1981, Oldfield et al, 1983 and 1985, Dearing, 1983, Appleby et al, 1986 and Foster et al, 1988 and 1990). Also in lake sediment work identification of different magnetite grain sizes was attempted (King et al, 1982). During this time work extended into the study of suspended sediments filtered from stream sediments (Oldfield et al, 1979 and Walling et al, 1979) and were used to identify channel bank sources. Artificial magnetic enhancements of stream bedload have also been carried out and used as a tracer (Oldfield, 1981). In such studies sediments are heated causing enhancement of their magnetic properties so that identification and tracing of the sediments is easier in the field.

Magnetic techniques have been applied to sediments of other environmental systems including aeolian sediments (Blank et al, 1985, Liu et al, 1988 and Kukla et al, 1988, 1989, 1990) and atmospheric dusts (Oldfield et al, 1978, Kleinman, 1980, Zhou and Yi, 1989). In such studies the sediments have been characterized and discriminated from other deposits using magnetic parameters. Studies involving water pollution (Beckwith et al, 1986 and 1990) have used magnetic techniques along with heavy metal analysis to assess and identify the sources of pollution in water bodies. Bacterial magnetite studies (Bazilinski et al, 1988, Fassbinder et al, 1990) and geological mineral studies (Johnson and Hall, 1978) indicate contrasts between the types and sizes of mineral grains contributed to soil and sediment systems. Bacterial magnetic grains are much finer and more magnetic than primary magnetic grains. Glacial (Gravenor and Wong, 1987, Walden et al, 1987) and marine studies (Andrews and Jennings, 1986, Hilton, 1986) have incorporated magnetic analyses to discriminate till and marine sediments often in local geographical areas. Even layers of volcanic ash have been identified magnetically in Icelandic lakes (Thompson et al, 1986). Also many studies have concentrated on individual magnetic minerals, including magnetite (Dunlop, 1973, Maher, 1988), hematite (Chevallier and Mathieus, 1943, Dunlop, 1971) and iron oxides in general (Longworth and Tite, 1977, Dankers, 1978, Schwertman and Taylor, 1977).

Classification of samples into source groups and discrimination of those groups also plays a major part in the

modelling of sediment sources. Traditional discrimination/classification of materials has included use of bi-variate scattergrams which generally use two parameters indicating different magnetic minerals and/or grain sizes (domain states). Banerjee et al.(1981) used the magnetic measurements of susceptibility (χ, see Appendix 1 for list and explanation of all measurements appearing in the thesis) and anhysteretic remanent magnetization (ARM) to characterize fine grained magnetites ranging from sub-micron size to those of hundreds of microns. Regression lines were applied to show clearly discernible changes of average magnetic grain size with depth in sediment cores. The technique complemented pollen analysis in identifying past palaeoclimatic changes. It was concluded that magnetism could be used to model finer sediment flux of erosion sediments where sediments do not display major magnetic mineral character variation.

Susceptibility of ARM (χarm; calculated from ARM using a constant multiplier conversion) and susceptibility were also used by King et al.(1982) to differentiate grain sizes of magnetites. An idealized model was based on sized magnetite content of natural materials and it was hypothesized that the method be used as an initial means of identifying sub-groups of samples. A number of problems were highlighted by the study relating to lake sediments. First there was an effect of ultra-fine superparamagnetic grains contributing to the measurements in which other sizes of grains were being discriminated. Secondly, magnetic interactions between grains occurred with varying concentration affecting the grain measurements, and the shapes of grains also affected the true measurement. Finally it was found that transport mechanisms meant that grain size distributions of magnetites behave differently from the distribution of the whole sediment.

Oldfield and Clark (1990) used another classification technique, principal components analysis (PCA), to classify lake sediments using magnetism. Walden (1991) also used PCA to discriminate sediments including recent volcanic disturbances but ratio, or normalized, parameters were included in the analysis. Grew (1990) used magnetic parameters of S ratio and SIRM (IRM880) to classify soil sources and lake sediments of Seeswood Pool, North Warwickshire. A bi-variate scattergram presented percentage contributions of each of the two sources based on some laboratory mixtures of the same materials (see also Foster et al 1990). Dearing (1992) also used normalized parameters rather than linear parameters to infer sediment sources due to concentration problems. Walden et al (1992) presented a discussion of the potential and possible limitations of factor analysis using mineral magnetic data sets. However, evaluation of the magnetic data used in factor analysis was not covered and ratio or normalized parameters were included in the statistical analysis. Following this Yu and Oldfield (1993) working on source ascription in a reservoir catchment near Nijar, South East Spain also used PCA to classify sediments on the basis of parameters not then used in modelling the source contributions. Some methodological improvements in the modelling were made. For instance, a correction was made for organic dilution of the magnetic properties of the materials. Also sand, silt and clay fractions were used separately in modelling.

A move was then made towards linear modelling when Hilton et al.(1985) used magnetic measurements to model trace metals in sediment cores. The concentrations of trace metals were modelled by considering three components: first the background concentration (Cb); secondly that due to accelerated erosion (Ca) and thirdly that due to

anthropogenic pollution (Cp), so Ctotal = Cb + Ca + Cp. Regression analysis was used to identify the three components and to classify metals into three groups. Hilton (1986) then presented a simple model for the interpretation of magnetic records in lacustrine and ocean sediments. This extended the list made by Thompson et al. (1980) of magnetic mineral sources, which were soil/rock erosion and transport by water, authigenic formation, fly ash, atmospheric deposition of wind-blown soil, cosmic particles and volcanic ash and included local sources of pollution and mineral contributions from magnetic bacteria. A two-dimensional qualitative model of the total deposition rates and productivity rates for each source was presented.

Advances on these models and methodologies were made by Stott (1986) who developed a magnetic mixing model for sediment tracing in a reservoir system using susceptibility and a demagnetization ratio parameter (IRM-0.04/IRM0.3T). Topsoils and subsoil sources were identified and their relative proportions in lake sediments calculated. The lake system was simplified into a black box mechanism whereby four assumptions (limitations) were made of the mixing model: 1. that sediment sources can be classified with respect to magnetic characteristics into two components of geomorphic significance; 2. that the behaviour of magnetic properties during mixing are regular and consistent; 3. that no significant alteration, selective transport or enrichment occurs during erosion, transport and deposition; 4. that the deposition of sediments in a lake or reservoir preserves a chronological record of erosion and transport events in the catchment. A bi-variate scattergram was used to discriminate the sources and mass-mixing tests were incorporated. However as the demagnetization parameter was non-linear a hyperbolic function was fitted whereas a linear function was fitted to the susceptibility results.

In contrast to the sediment source problem, Thompson (1986) proposed a method for modelling mineral mixtures in materials using magnetization data. A linear modelling technique using a SIMPLEX algorithm was employed to model the proportions of magnetite and hematite crystals of varying sizes and concentrations in sediments. Bi-cubic spline functions were used to numerically characterize the magnetization curves of the minerals and interpolation was carried out between empirical data for mineral grain sizes to establish data for other grain sizes. The mineral data used was from Dankers (1978) who physically disintegrated and micro-sieved magnetites and hematites. This process, however, could have changed the internal structure of the minerals, so subsequently Maher (1988) precipitated magnetite crystals and sized them at different growth stages. These magnetite samples have been used in this research and are not problem free either. These samples contain a population of grain sizes but this may be smaller than that allowed by micro-sieving.

Linear modelling techniques were also employed by Yu (1989) and Yu and Oldfield (1989), where cluster analysis was first used to classify the samples into source component groups. Fractionated estuary sediments of the Rhode River catchment, Maryland, USA were separated or 'unmixed' using magnetic properties of source components visually identified in the field. Multiple regression was incorporated to obtain linearly additive data from ratio data, of the fine particle fraction, for use in the linear programming routine. By the very nature of linear programming, only linearly additive data can be involved (see Appendix 1, Part 4 for a definition of linear additivity). The results obtained included zero predictions for components which had been identified as being source components. Sampling

strategy used in the field for initial identification of sources was limited for the size of the catchment (63 samples from 35 Km^2). Sources could have been missed or included when they were not contributory. Classification of the sources and sediments using cluster analysis also proved to be problematical. Sources which are actually quite similar may be divided into separate clusters according to which scale of detail is picked from the linkage diagrammatical output (dendrogram) used by Yu (1989) and Yu and Oldfield (1989) for identification of source components.

Maher and Thompson (1992) have also applied the modelling techniques of Thompson (1986) to a Chinese loess/palaeosol environment. The contribution of each magnetic component to the loess magnetic record was estimated. The additivity of magnetic properties, where low concentrations of magnetic mineral existed, was attributed to Stacey (1963). Finally Caitcheon (1993) recently modelled bedload sediments (as sources) in tributary and trunk rivers in Australia. Gradients of the ratios of susceptibility and a number of remanence parameters were used to calculate proportions contributed from the tributary rivers. Bedload source and sediment mixture definition was limited to the collection of several samples from certain points along the tributaries and trunk rivers.

Overall however, magnetic minerals predominantly form only a small proportion of the total mineral material which make up earth materials. Much of the matrix carrying iron minerals is thought of as 'non-magnetic' but is generally diamagnetic (very weakly magnetic). Great complexity can be encountered in environmental studies such as those described when materials consist of primary (rocks) and secondary (anthropogenic, atmospheric, chemical or biogenic) minerals. The diverse nature of materials, soils or rocks or transported sediment mixtures for example, means that trying to model their mineral or sediment sources is a daunting task. The basic definition of 'pure' mineral sources presents many problems in itself, with inherent variation of natural minerals in the environment.

In environmental systems many processes during selection, erosion, transport and deposition of materials will act to change the original properties of materials/minerals. Such processes could include chemical transformations where weathering and soil formation processes, involving organic acids, water and oxygen for instance, may lead to changes in mineral magnetic status. Minerals being weathered in humid areas where goethite is produced as a by-product exhibit changes from canted-antiferromagnetic to paramagnetic properties. Cyclic wetting and drying also appears to cause reduction of goethites to magnetites and then in oxidizing conditions reforms to maghemite (Le Borgne, 1955, Mullins, 1977). Acidity and drainage conditions have been seen to affect the stability of magnetic minerals in soil environments (Maher, 1986). Where burning (Rummery et al, 1979) or intense heating occurs, paramagnetic or canted-antiferromagnetic minerals may be transformed into ferrimagnetic states. Physical processes of erosion and transport causes the comminution and abrasion of particles selected from source materials which can also lead to changes in magnetic properties especially where magnetic coatings may exist.

Preferential selection and transport of specific particle sizes leads to problems of matching sediment sources to mixtures. Dilution or extreme concentration of certain magnetic minerals can lead to major difficulties for sediment sourcing in the environment. The stability of certain minerals, in terms of weathering and destruction, may also

lead to concentrations of certain magnetic minerals, in particular soil horizons for example. Organic matter in surface soil horizons act as a dilution component of the magnetic properties and mineral concentrations detected for certain volumes of material. Material removed in solution, calcium carbonate for example, may also have profound effects on the differences between properties of original source materials and the final mixtures. Additions to primary and natural secondary minerals are made through atmospheric deposition of fly ash and other particles.

Also bacterial magnetite formation has been hypothesized to contribute much to the magnetic mineral assemblage in specific locations. Bacterially formed magnetites have been studied by Farina et al.(1990) and Fassbinder (1990). Bacteria utilize iron and produce extremely stable superparamagnetic and single domain magnetite particles extracellularly. Also intracellularly formed magnetite is used by some bacteria and animals for navigational purposes (Kirschvink and Gould, 1981). The presence of bacterially formed magnetites has important implications for environmental studies. Grains have been found to be of <0.05 μm size and would form a great component of the magnetic properties of soils and sediments. The quantification of these minerals and other mineral types and grain sizes in environmental materials would be of great advantage in mineral sourcing studies.

The methodology presented in this thesis considers the accurate definition of the spatial magnetic variability of sources caused by many of the factors described above. This is an aspect which has not been covered in many studies. In many cases mixtures such as lake sediments are extensively analysed but only a few samples are taken to characterize sources. In the use of modelling techniques, the environmental variability of materials which control the final 'mean' outcome must be addressed. The outcome of any model is set by the parameters which are entered; parameters which in the environment are dependent on the number of samples and the scale at which they are collected. Possibly the best that can be achieved is to solve a model for a range or distribution of values which take into account complex variability and experimental factors. Model calibration, accuracy, verification and definition of the limiting factors are as important as the model itself and are factors addressed in the deductive approach taken in this research.

1.3 Aims and Objectives

The present research follows a methodological base set especially by Yu, 1989. Much emphasis is given to evaluating not only the methodology used to study environmental systems using magnetic techniques, but also the magnetic techniques and measurements themselves. The aims and objectives reflect the need to test thoroughly the use of magnetism using as diverse a range of environmental materials as possible in the first instance and environmental systems in the second instance. There are two main aims of this research and a number of methodological objectives which are outlined as follows:

1. To model the movement of environmental materials through environmental systems and therefore be able to identify the sources of mixtures quantitatively.

2. To evaluate the prospects for modelling the magnetic mineralogies of natural and synthetic samples in terms of:

(a) Mineral magnetic properties
(b) Mineral type and concentration
(c) Mineral size

* To develop the means by which sources are identified and defined in the environment with respect to their spatial variability and likelihood of contribution of sediment.

* To identify the most useful magnetic measurements which can be used in classification and modelling and so define the limits of the technique.

* To develop and evaluate the use of magnetic properties in classification techniques for source and mineral identification, discrimination and sample matching from a base of traditional bi-variate discrimination.

* To develop and evaluate the use of magnetic properties in mathematical modelling techniques, for 'unmixing' environmental mixtures of sources and mineralogies and for tracing the movement of materials through environmental systems.

* To identify the most suitable materials which can be modelled according to their magnetic properties in order to define application limits of the technique.

* Subsequently to define an overall *Measurement - Modelling - Interpretation* methodological framework for application to any environmental system of interest.

Overall this thesis consists of four main sections:

A *Introduction to the area of research and the magnetic, statistical and modelling techniques used in this research.* Section A of the thesis contains this introduction and Chapter 2 reviews and describes the methodology and techniques used in this research.

B *Laboratory and hypothetical testing of classification and modelling techniques using linear magnetic measurements.* In this section tests of multi-variate classification (Chapter 3) and linear modelling (Chapter 4) are carried out using magnetic data from databases containing over 1200 samples. The databases contain materials which are as environmentally diverse as could be obtained, as well as many synthetic, commercially manufactured materials. Chapter 5 of this section presents work on the identification and statistical definition of sources of materials. The methodological procedure devised from the laboratory, theoretical and field tests is presented in Chapter 6.

C *Application of the methodology to several environmental systems for true appraisal and confirmation of the methodological procedure formulated in Section B.* In this section three case studies were conducted in different environments. These attempt to quantify sediment sources and mineral components of environmental 'mixtures' using the methodological procedure from Section B. Chapter 7 presents work completed in two coastal systems and in Chapter 8 a catchment system is studied. Finally in Chapter 9 work on the modelling of mineral mixtures in environmental materials is presented.

D *Discussion and Conclusion.* Summaries are provided at the end of each chapter but a final discussion and main findings are presented in Chapter 10.

An overall methodological structure of the research program is presented in Figure 1.4 for reference. The flow chart is split into main sections of research completed in order to answer the aims and objectives. These sections include equipment calibration (see Appendix 3), data collection (see Chapter 3), measurement, classification and modelling evaluation (Section B) and other experimental work not presented in full in this thesis.

Figure 1.4: Methodological Structure of Research Program

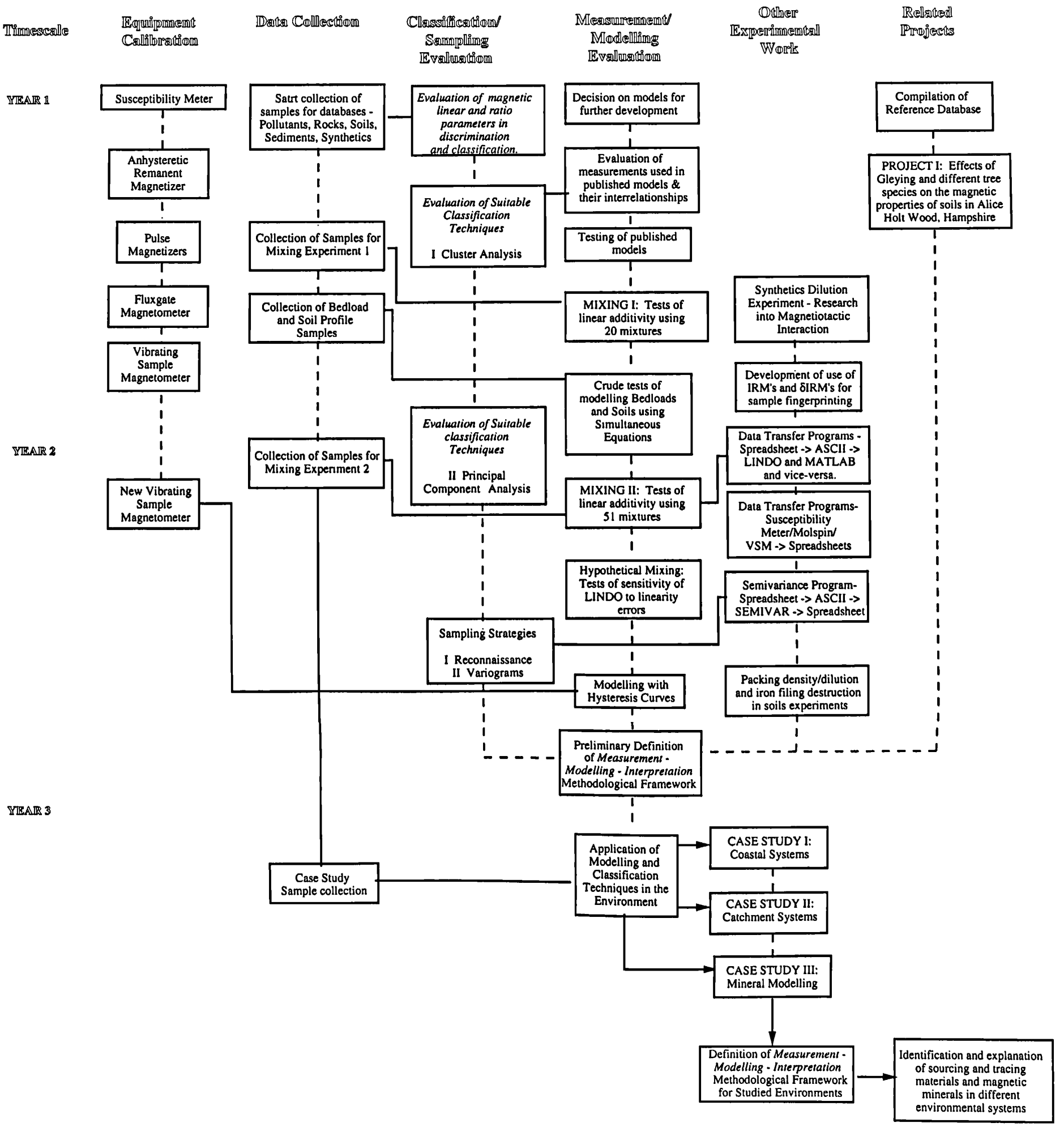

CHAPTER 2

Methodology and Techniques - A Review

Introduction

In this chapter the methodological techniques employed throughout the research are described. These include environmental magnetism, sampling strategies, statistical classification techniques and linear modelling. Most of the magnetic information has been summarized from various textbooks on magnetism including O'Reilly (1984), Jakubovics, 1987, Cullity (1972) and Jiles (1991) and Environmental Magnetism (Thompson and Oldfield, 1986). In the case of the sampling strategies, statistical classification and modelling techniques, a broad review of the techniques as used in geography and other disciplines is also included.

2.1 Environmental Magnetism

"few subjects in science are more difficult to understand than magnetism",

Encyclopedia Britannica, 1989, p685.

Magnetism is one of the most fundamental forces on earth; as is electricity which is very closely related to magnetism through electron movements. The magnetic property of natural materials lies in their atomic structure: all materials are magnetic but to varying degrees. Most environmental materials are relatively magnetically weak, such as organic material, whereas some materials such as iron and lodestone (magnetite) are magnetically very strong. At the atomic scale electrons orbit around the central nucleus generating an electric current which produces a magnetic force or field. The electrons (of which there are different numbers termed the atomic number) also spin on their own axes. This motion produces an electric current and a magnetic field. The product of these fields causes a dominant spin moment of the atoms depending on the interaction of the electrons, their numbers and configuration. External natural or artificial magnetic fields affect their overall magnetic behaviour which vary sympathetically. Where electrons are not paired in a material, a greater magnetic moment will result. Essentially the work in this thesis is based on the artificial application of various magnetic fields on samples, rather than their magnetic properties as found in their natural state produced by the Earth's magnetic field.

Basic Magnetic Properties

Five main types of magnetic behaviour can occur when magnetic fields are applied. These are, in order of strength, ferromagnetism, ferrimagnetism, antiferromagnetism, paramagnetism and diamagnetism. Often ferromagnetism is not discussed in environmental studies, however, as it only occurs in iron and similar substances. Ferromagnetism and ferrimagnetism are also very similar in nature and difficult to distinguish. The magnetic properties discussed here are summarized in Table 2.1 which gives a list of minerals and materials which can be classified according to their magnetic behaviour.

Table 2.1: *Classification of Materials according to their Magnetic Properties and Behaviour.* (Adapted from Jakubovics, 1987)

Class	Arrangement of Moments	Nature of Alignment	Net Magnetization.	Resulting Force	Examples
Diamagnetic	Electron and orbital spins balance out but induced magnetic moments align in the opposite direction to the applied field.		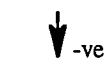 -ve	Very weak and negative, not capable of holding a remanence.	Noble gases; many metals, e.g. Cu, Hg, Bi; non-metallic elements, e.g. B, Si, P, S; many ions, e.g. Na^+, Cl^-, and their salts; most diatomic molecules, e.g. H_2, N_2; water; most organic compounds, e.g. wood, paper, leaves, chalk.
Paramagnetic	Electron and orbital spins have a small magnetic moment which tends to align with the applied field. Neighbouring moments do not interact.	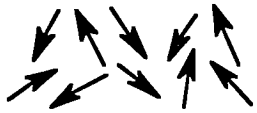		Very weak, not capable of holding a remanence.	Some metals, e.g. Cr, Mn; some diatomic gases, e.g. O_2, NO; rare earth metals; rare earth oxides; carbonates of iron; biotite, olivine, garnet.
Antiferromagnetic	Electron spins alternate, atom by atom, thus cancelling out each generated moment.	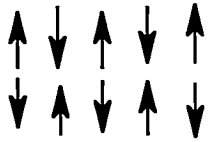		Weak, capable of remanence aquisition.	Many compounds of transition metals e.g. MnO, CoO, NiO, Cr_2O_3, MnS, MnSe, $CuCl_2$. Haematite.
Imperfect Antiferromagnetic	Caused by spin canting, impurities or lattice defects.	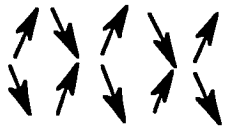		Capable of holding a remanence	Hematite, Goethite.
Ferrimagnetic	Two of every three atoms line up in one direction, third oppositely. Moments are unequal.	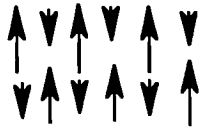		Strong, capable of remanence acquisition.	Fe_3O_4 (magnetite); l-Fe_2O_3 (maghemite); mixed oxides of iron and other elements.
Ferromagnetic	Atoms have permanent dipole moments.	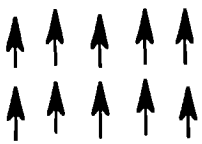		Strong, capable of holding a remanence	Transition metals, Fe, Co, Ni; rare earths with $64 < Z < 69$ alloys of ferromagnetic elements; some alloys of Mn.

Diamagnetism

Diamagnetism is the weakest of the magnetic behaviours which a material can exhibit. This is the result of interaction between the magnetic field and orbital motion of electrons. On application of a field a weak negative magnetization occurs. When the field is removed, all magnetization is lost. Only the orbital motion of the electrons around each atom's nucleus contributes to the moment. This is due to an electron configuration where all electrons are paired and electron spin motions cancel one another. Diamagnetic materials include wood, quartz, silica and water.

Paramagnetism

The next weakest magnetic behaviour is that of paramagnetism. Paramagnetic materials contain unbalanced free electrons which cause permanent magnetic moments. Application of an external field induces a weak positive magnetization in paramagnetic materials, which include olivine, salts, biotite, iron hydroxides, lepidocrocite and ferrihydrite. Spin moments tend to align themselves in the direction of the applied field. When the field is removed the moment within the material is lost due to thermal agitation. Unlike in diamagnetic materials, temperature is a factor in controlling paramagnetic behaviour, where the moment depends on field strength and absolute temperature. When certain magnetic minerals such as magnetite are heated to a controlled temperature (Curie temperature) they exhibit paramagnetic behaviour rather than ferrimagnetic behaviour.

Antiferromagnetism, Ferrimagnetism and Ferromagnetism

In ascending order the next strongest magnetic behaviours are antiferromagnetism, ferrimagnetism and ferromagnetism. In each case there is spontaneous magnetization in a material remote from applied magnetic fields. Such materials or minerals are capable of holding a magnetic remanence when an applied field is removed. In materials exhibiting these behaviours there is strong alignment of magnetic moments and interaction between neighbouring atoms (caused by the effects of quantum mechanics). This effect overcomes the thermal agitation of the atom. Ferromagnetism, the strongest magnetic behaviour, occurs when all electron moments are entirely parallel. Ferromagnetic materials are temperature dependent and, upon heating past the Curie temperature, a ferromagnetic property is transformed to a paramagnetic property. Below the Curie temperature ferromagnetic materials, including iron, carry strong remanence magnetizations.

Ferrimagnetic materials include magnetite, maghemite, manganese and zinc ferrites, which are magnetically weaker than ferromagnetic materials (but the two are difficult to distinguish). Magnetic moments are parallel in ferrimagnetic materials but are not totally aligned in one direction (Table 2.1). There is a net magnetization in one direction depending on the crystal structure. Ferrite (often an iron oxide) crystal structure is of a spinel type with two types of magnetic sites with anti-parallel magnetic moments.

Antiferromagnetic materials exhibit similar anti-parallelism to ferrimagnetic materials but the moments are equal and net magnetization is zero. However canted-antiferromagnetism is often seen in natural materials, where alignments of magnetic moments are imperfect or 'canted' (Table 2.1) and a weak net moment occurs in one

direction. Hematite and goethite display this magnetic behaviour where impurities and lattice defects cause spin canting, hence, such canted-antiferromagnetic minerals show remanence capability.

Magnetic Domains and Critical Grain Sizes

The magnetic behaviour of materials is dependent on the way in which their internal geometry defines their magnetic domains. Magnetic domain theory was first proposed by Weiss (1907) to explain how materials with spontaneous magnetization could exist in a demagnetized state (quoted in Thompson and Oldfield, 1986). Magnetic domains are regions within a materials' crystal structure which can be magnetized in a certain direction (Figure 2.1). Neighbouring domains can be magnetized in different directions with the domains being bounded by domain walls. Bloch Walls or domain boundaries are thought to be 100 atoms thick (10^{-8} to 10^{-7}µm thick), where a compromise between the energies of neighbouring domains is found (balance is found between exchange and anisotropy, Chantrell, pers. comm.). The most advantageous domain size is where a balance is achieved between competing energies and is about one micrometer thick (Thompson and Oldfield, 1986). Domain sizes have important effects on the measurement values of materials, depending on the shape, size and purity of crystals in the material.

There are three main types of domain behaviour found in ferrimagnetic and canted-antiferromagnetic materials: multidomain, single domain and superparamagnetic. These domain behaviours and their characteristics are shown in Table 2.2. It is clear that magnetic properties vary with grain size as described in the Table and this phenomenon is further discussed in Chapter 9. The grain size boundaries between these are important and are different for different minerals. This is controlled by grain shape and volume. Different minerals contributing to the magnetic property of a material, such as magnetite and hematite, have different critical grain sizes. This is most important for magnetite and related minerals and most of the work in critical grain sizes reflects the dominance of magnetite in the measurement of natural materials. Table 2.3 gives a range of important critical grain sizes (mainly for magnetite minerals) presented by different workers. It is clear that there are varying views and findings on the boundaries between ultra-fine superparamagnetic grains, and small stable single-domain grains, and single and multidomain grains.

Multidomain behaviour is controlled by the movement of domain walls. On the application of a strong field, the domain with a magnetization in the direction of the field will grow at the expense of other domains. Similarly due to magnetization, initial changes will be reversible, while in stronger fields changes in the positions of the domain walls will reach a new equilibrium for that field. On the removal of the applied field the domains may remain in their magnetized position thus causing a remanence to be held by the material. The material is 'saturated' when all the domains are aligned in the direction of the applied field. Neighbouring domains may have magnetizations in different directions as shown in Figure 2.1 until a field is applied. Multidomain grains are larger than 0.1-1µm in magnetite and 1000µm in hematite (Table 2.3).

Single domain behaviour cannot be explained by the movement of domain walls since there are no domain boundaries. The single domain grain has an axis of easy magnetization when a field is applied. The direction of

Figure 2.1: Magnetization of Domains in a Multidomain Grain

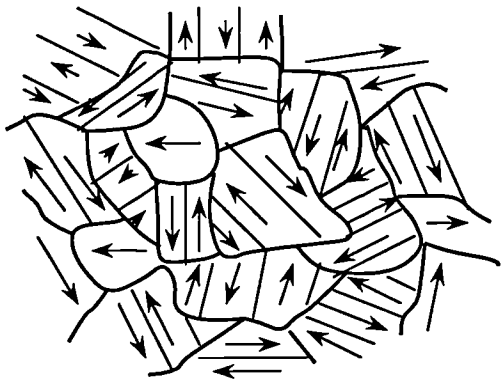

Figure 2.2: Hysteresis Loop, Initial Magnetization Curve and associated magnetic parameters

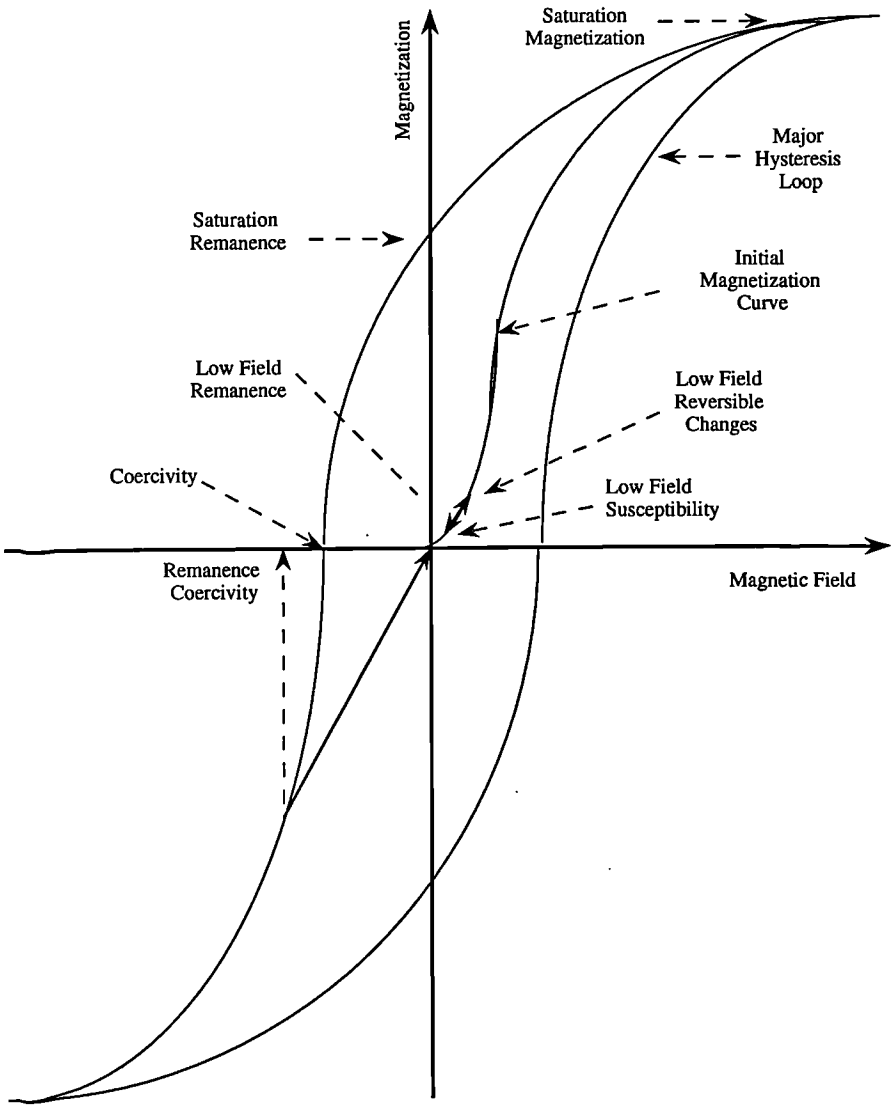

magnetization is forced into alignment with the field. The field required to do this may have to be very strong. The hysteresis properties of the grains will depend on the angle which the axis of easy magnetization makes with the field. Once the field is removed the magnetization returns to its original axis direction. An assemblage of single domain grains will then add or oppose each other in terms of magnetization (for reversible changes at low fields). Single domain grains in magnetite have been calculated at c. <0.1μm (Dunlop, 1973) but this may be larger in uniaxial grains where volume remains at a constant.

As grains become smaller (<0.05μm diameter) their magnetic properties become time dependent and changes in remanence occur in minutes and seconds; these grains are superparamagnetic or viscous. Such small grains have a thermal energy which can be as great as their magnetic energy; they are magnetically unstable and do not exhibit hysteresis or any remanence property. The thermal energy can also overcome an applied magnetic field which causes serious implications for measurement. However, this time dependency can be used to an advantage. Many of the affected grains are of the 'secondary' magnetite size (SP/SD) and can be detected when making high frequency susceptibility field measurements (χhf). χlf and χhf can be used to calculate χfd% which indicates the presence of superparamagnetic and/or stable single domain grains. Whilst in an applied field the grains exhibit alignment to the field, upon removal thermal agitations destroy this alignment. The property of the grains is similar to the overall property of paramagnetism, but is stronger. Superparamagnetic grains have a greater effect on the magnetic susceptibility of a material than both multidomain and single-domain grains.

Finally, a phenomenon which causes many problems in the interpretation of magnetic results is that of magnetostatic interaction. Grains which lie close to each other may interact leading to a demagnetization causing reduction of the overall magnetic moment. This occurs in superparamagnetic grains especially (Thompson and Oldfield, 1986, Petrovsky at al, 1993). Further discussion of these effects in natural and synthetic materials can be found in Paper 1, Appendix 7.

Natural Magnetic Minerals

Natural magnetic minerals are those minerals, mainly iron oxides, which are formed by primary (rock formation) or secondary (pedogenic) processes. Most of the natural minerals which display the stronger magnetic properties (ie canted-antiferromagnetic and ferrimagnetic) include iron oxides such as magnetite, hematite, maghemite and titanomagnetite. Iron oxides form one of the basic elements in rock formation and are well dispersed, but only make up a few percent of the total mineral content of rocks (Thompson and Oldfield, 1986). Iron sulphides, such as pyrite, display paramagnetic properties while other minerals in this less common group such as greigite and pyrrhotite, are ferrimagnetic. Such minerals make up the non-saturating component of the hysteresis loop, already discussed. In general there are certain common iron bearing minerals which occur widely in environmental materials. Table 2.4 shows the most common of these. In this section a brief description of each of the most important magnetic mineral groups is given (some have also been included in Table 2.1). Plates of the minerals described in the following section are included in Chapter 9 where samples of some of the minerals have been used in mineral modelling routines.

Table 2.2: Magnetic Domains and their Magnetic Properties (adapted from Yu, 1989)

Type of Crystal	Characteristics	Magnetic Properties
Multidomain (MD)	Large crystals. Magnetization explained in terms of movement of domain walls.	Show loss of magnetization between Ms and SIRM. Low SIRM/χ and ARM/χ, high SIRM/ARM ratio.
Pseudo Single Domain (PSD)	Between MD and SSD.	Intermediate characteristics.
Stable Single Domain (SSD)	Grains of 0.05μm. Each grain forms its own domain.	Higher remanences than MD. SIRM/χ, ARM/χ reach a maximum in SSD grains. SIRM/ARM is relatively low.
Viscous (V)	Between SSD and SP - 0.02μm in diameter.	Response to changes in magnetic fields is delayed. High χ - importance of a narrow band of grains.
Superparamagnetic (SP)	Extemely small grains - 0.001-0.01μm in diameter.	Too small to retain remanence at room temperature. Any magnetic moment induced in a strong field is immediately lost by thermal vibration. Zero SIRM and ARM. Disproportionately high susceptibility.

Table 2.3: Critical Grain Sizes of Magnetite Minerals

	Grain Sizes (μm)				
Crystal Type	**Yu (1989)**	**Dunlop (1973a)**	**Thompson & Oldfield (1986)**	**Maher (1986)**	**Dunlop (1981)**
Multi domain			60 - 100	10 - 100	>0.06
Pseudo Single domain			1 - 10	1 - 10	
Stable Single Domain	0.05	> 0.03 (spherical)	0.075 - 0.75	0.01 - 1	>0.03 <0.05
Fine Viscous	0.02				
Superparamagnetic	0.001-0.01	< 0.03 (spherical)	0.075 - 0.01	0 - 0.01	<0.025

Important Divisions: a) Ultra fine SP grains/ small SSD - 0.03μm in magnetite. All natural hematites are SD
b) MD/SSD - 1μm in magnetite certainly MD (Complicated by PSD (two domain). 1000μm in hematite

Iron Oxides

Iron oxides include the magnetic minerals of magnetite, maghemite and hematite. Magnetite is a very common black mineral found in many igneous and metamorphic rocks and subsequently in sedimentary rocks. Magnetite is ferrimagnetic but when heated to 580°C, its Curie temperature, it becomes paramagnetic. A structural transition occurs at this point from order to disorder in the directions of the magnetized areas of the mineral. On oxidation, transformation from magnetite to maghemite occurs. Maghemite is also ferrimagnetic, black in colour and is fairly common in earth materials. When maghemite is heated to 300°C it converts to the mineral hematite. Hematite is present in many rocks and is normally indicated by its red colour, in red sandstone for example. It is an oxidation product of rock minerals and is canted-antiferromagnetic. Hematite is a highly stable mineral due to its internal structure and has a higher Curie temperature of 675°C.

Iron Sulphides

Pyrrhotite and pyrite are the most common of a group of iron sulphides. Pyrrhotite, which is ferrimagnetic, is characterized by a high susceptibility and low remanence. Pyrite is paramagnetic and holds no or little remanence depending on the proportion of inclusions/impurities present.

Table 2.4: Iron Oxides in Soils (Adapted from Schwertmann and Taylor 1977, Maher 1986.)

Mineral	Formula	Magnetic Status	Reported Environmental Associations
Hematite	αFe_2O_3	Canted-antiferromagnetic	Relatively dry, highly oxidized soils - usually in areas of elevated temperatures
Goethite	$\alpha FeOOH$	Canted antiferromagnetic	Moister soils, abundant in well - drained temperate areas.
Maghemite	λFe_2O_3	Ferrimagnetic	Abundant in highly weathered tropical/ sub-tropical soils.
Lepidocrocite	$\lambda FeOOH$	Paramagnetic	Occurs in poorly drained soils.
Ferrihydrite	$5FeO_3.9H_2O$	Paramagnetic	Poorly drained and podzolized soils.
Magnetite	Fe_3O_4	Ferrimagnetic	Primary, soil firing, pedogenically and bacterially produced.

Iron Hydroxides

Goethite is another common magnetic mineral which forms as a weathering product and is found in soils of humid climates. Goethite varies in colour from yellowish brown to red and is canted-antiferromagnetic. Lepidocrocite is also a hydroxide and is brown in colour but is less common than goethite. Lepidocrocite is a paramagnetic mineral which when heated to 250-350°C breaks down to form maghemite. In contrast goethite dehydrates to hematite at temperatures of between 300-400°C.

Other magnetic minerals include elemental iron (ferromagnetic), ferromanganese minerals (ferrimagnetic or paramagnetic) and other paramagnetic minerals such as pyroxenes and biotites (magnesium, iron and aluminium silicates)

Magnetic Parameters and Instrumentation

Environmental materials contain a mixture of minerals of varying grain size and concentration. These exhibit an overall magnetic response. Magnetic parameters and their units used in this research are defined in Appendix 1. Most test parameters include the application of a magnetic field at various strengths between -1T and +1T. Most materials show a saturation at 1T where the material cannot increase magnetization with increasing field strength. In Appendix 1 measurements which are theoretically linear are marked (*) and it is these to which most precedence is set in this research. These measurements, when multiplied by the proportion of source components existing in a mixture, should, in theory, equal the measurement value of the mixture. It is this linear additivity that forms the basis of the present research and laboratory testing of this is discussed in Chapter 4. Ratio parameters (+) have also been described but are not used in the application of statistical techniques and linear modelling in this research. Much of the instrumentation has been analysed in terms of drift stability and linearity and results are presented in Appendix 3. All measurements made in this research which require the application of a magnetic field have been measured immediately (within 20 seconds) upon removal from the magnetometer.

Most of the magnetic parameters in use can be explained in terms of the magnetic hysteresis loop (Figure 2.2). Magnetic hysteresis is a measure of magnetization and the hysteresis loop represents the change in magnetization with changes in field strength. Continuous measurement of both in-field and remanent magnetization for magnetic fields (generally between -1 Tesla and +1 Tesla) can be produced. This presents many advantages over the standard procedure of measuring low field susceptibility and a few parameters of remanence magnetization on different pieces of equipment. The hysteresis loop gives clear graphical representation of the magnetic properties of materials which are often more easily interpretable at a glance than the sets of numbers obtained for standard measurements. For instance the width of the loop at the origin can indicate the presence of canted-antiferromagnetic minerals (eg Figure 2.2) and a thin, steep loop indicates the presence of ferrimagnetic minerals. Further description of hysteresis loop shape and related mineral type is given in Chapter 9 and examples are presented in Appendix 4. The loops are measured on a single piece of equipment which optimizes sample preparation, measurement and data handling time, and eliminates calibration comparisons between different measuring equipment. Thompson and Oldfield (1986) stated that the 'hysteresis diagram and parameters provide the most comprehensive magnetic characterization of natural materials without extravagant specialisation or excessive cost'. The field strengths of the Vibrating Sample Magnetometer (VSM) engaged in this research were between -1T and +1T. More information on the VSM and its accuracy are given in paper 3 in Appendix 7. Typically, after an initial magnetization curve beginning at zero field, the loop starts at +1T moves in reverse to -1T and then continues back to +1T.

When a material is first magnetized at small field strengths the effects are reversible. Initial magnetic susceptibility (χlow) is measured here indicating the concentration of ferrimagnetic minerals in a material. Beyond this reversible

Figure 2.3: Remanence curve, magnetization curve and associated magnetic parameters

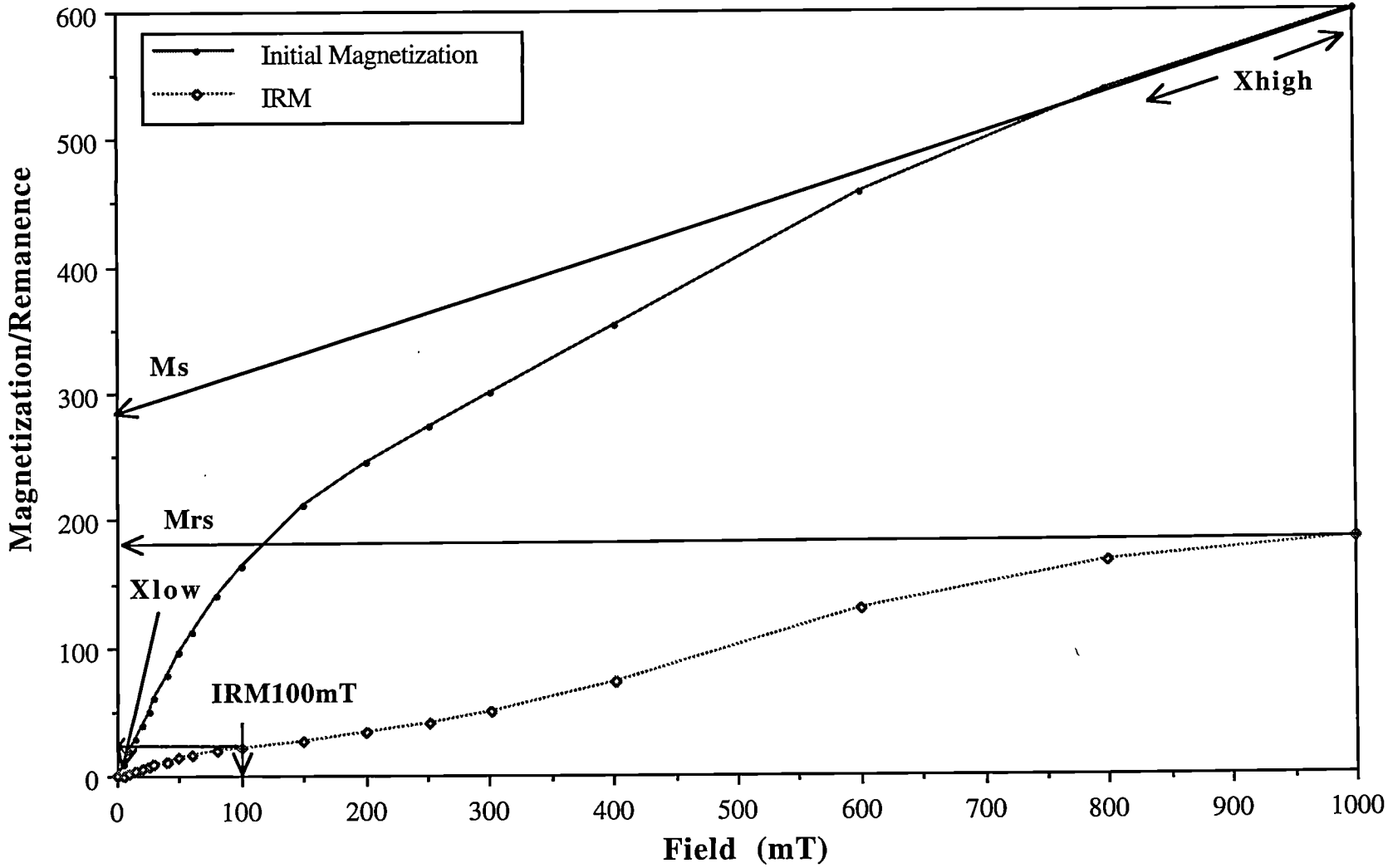

boundary the material may obtain a remanence and saturation of magnetization (Ms) and saturation remanence (Mrs) values can be obtained. Sometimes the loop does not saturate, but increases steadily indicating a paramagnetic component in a material. Ms and Mrs of the ferrimagnetic component which always saturates well within 1T is then calculated by correcting for the effect of this slope angle.

Remanence curves (IRM) measured at field strength stages between zero and 880mT have also been extensively used in this research. These indicate the concentration of remanence carrying minerals and by normalizing the curves to remanence at 880mT an indication of the mineral type is also obtained. Figure 2.3 shows parameters which are taken from the initial magnetization curve and the remanence curve. Examples of remanence curves for a variety of materials are included in Appendix 4 for reference. Remanence was observed using a Molspin pulse magnetometer, applying fields between zero and 880mT. The remanence measurements were made with a Molspin Fluxgate Magnetometer. In this research the common term SIRM for the highest field remanence is not used; IRM880 is preferred as certain minerals do not saturate within 880mT (IRM880 should not be referred to as SIRM; see also Appendix 1).

Two very important measurements are made using a susceptibility meter (Bartington Instruments) employing two different frequencies: low frequency 0.46khz and high frequency 4.6khz. Low frequency susceptibility (χlf) indicates the concentration of ferrimagnetic minerals in a material. The difference between χlf and χhf (χfd) gives an indication of the presence of fine-grained magnetic minerals in the viscous range between SP and SD. At low frequency all ferrimagnetic minerals contribute to the overall value; at high frequency however fine magnetite grains do not contribute to the overall value. The mechanism behind this is the relatively fast reversal of the field at high frequency to which the fine magnetites cannot respond. Larger grain sized minerals which do not reverse their magnetizations as quickly do contribute to the magnetization value. χfd can be calculated as a mass specific parameter by finding the difference between χlf and χhf or as a percentage of the χlf value (see Appendix 1). Initial non mass-specific susceptibility (kappa) can be measured in the field also, using a Bartington MS2 sensor and either a search loop ('D' loop) or probe sensor.

2.2 Source Identification and Sampling Strategies

Sourcing of sediments in environmental systems

As an example, one of the largest sediment source projects to date is that of Idbeken and Schleyer (1991) where within 19 basins, the provenance of river sediments contributing to larger basin fills and to the Ionian Sea (S. Italy) were studied. The sediments in the area were not widely affected by anthropogenic activity and sediment sources were studied from river head-waters to river mouth and onto beaches and continental shelf areas. 'Actuogeologic' properties used in this work included digitized data from maps, particle size distributions, petrography, mineralogy, light and heavy minerals and geochemistry. Multivariate techniques were used to cluster and discriminate the sources according to the hundreds of variables used. Fifty-five geo-units were reduced to eight main units which facilitated provenancing, to which the overall conclusion is "provenance is a complex topic" (p232).

Sampling design and spatial variability of properties of materials

One essential technique which has been generally overlooked is that of effective sampling design which incorporates environmental variability of sources (Webster and Oliver, 1992). In the classification and modelling of sources of mixtures, their properties need to be defined in a statistically viable way. There should be a population mean and standard deviation from a number of samples within the source groups which can be incorporated into the modelling techniques. Workers are aware of the natural variability in the properties of materials but it is often considered too difficult and uneconomical to include it in a sampling strategy; numbers of samples which can be handled realistically is often limited. In this section a number of studies are described where spatial variability and mechanisms employed to study them have been used effectively and economically.

Variability of soils is focussed upon in this section as most of the literature has been written within this field of physical geography. Beckett and Webster (1971) presented an early review of soil variability which clarified the need for thorough sampling and variability study by indicating that "users of soils maps have a requirement to establish how far they could assume that all the soil mapped as one class had equal potentialities" (p. 1). They report that lateral variability of soil properties including potassium, phosphorus, calcium and nitrogen were found to increase with size of area sampled. Up to half the variance within a field may occur in any one square metre in a field, but within-field variance often changed little with size of field. Between-field differences in soil nutrients however were clearly due to differing management strategies (but such patterns were not found in all properties, sand and clay contents for instance). On average 50% of randomly chosen sites within a mapped soil series matched the definition of the specified soil unit profile. Variability in the other 50% was due to factors other than land use-management strategies.

Finding and using mean values for soil properties are a common basis for many geographical field studies. McBratney and Webster (1981 and 1983) outline the need for taking account of the spatial dependence of properties of soils (or any material). Methods are presented for determining sample sizes needed to cover the spatial variability of soils. These methods move away from using the number of observations set out by classical sampling strategies. Variograms are presented which indicate the spatial variability of the area of interest over set distances. The variogram is based on measurements of a particular property in an area using grids or transects with regular sampling/measurement intervals. At least 100 and preferably 200 points are used in the grids or transects (Oliver and Webster, 1990, Webster and Oliver, 1992). Variograms (eg Figure 2.4a) use the calculation of semivariance, a measure of the variance between samples at different separation distances (termed 'lags') from large scale (many observations) to small scale (fewer observations, Figure 2.4b). For example, if the sampling interval was 1m, over a 200m transect, the largest separation for which semivariance could theoretically be calculated occurs at 200m; between observation numbers 1 and 200. Realistically however it is only statistically viable to use a distance of one-third (or even one-fifth) of the total transect or grid length. So that in this example the semivariance would be calculated up to 66m (Webster and Oliver, 1990). The variogram can then be used by reading the variance (or acceptable error) from the y-axis and reading the sampling distance, or lag, given by the curve at that point. For this research a BASIC program of Campbell (1985) which calculates semivariance has been adapted. Data output

Figure 2.4: The Variogram and its main components (a) and semivariance calculation for different lags (b). (after Webster and Oliver, 1990)

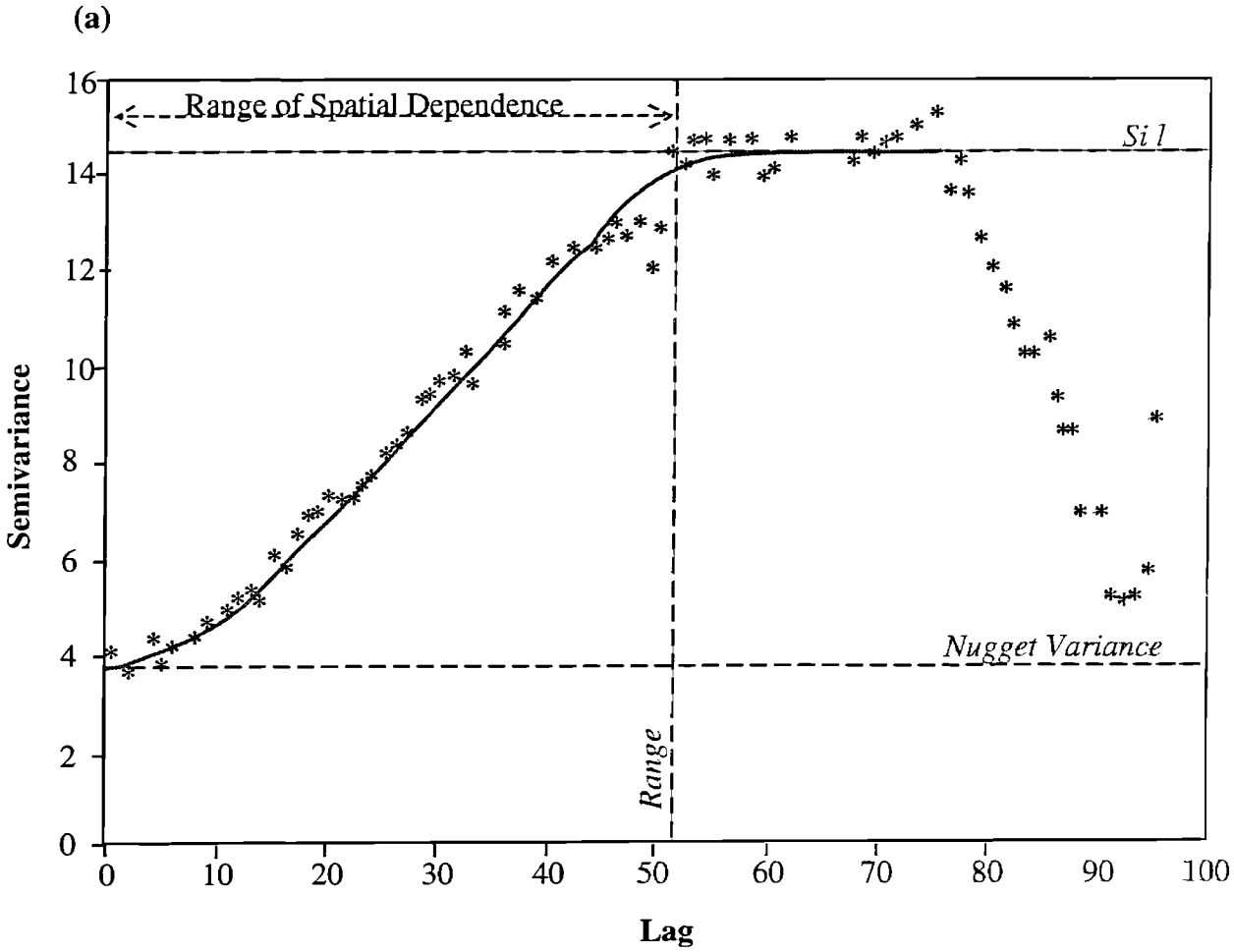

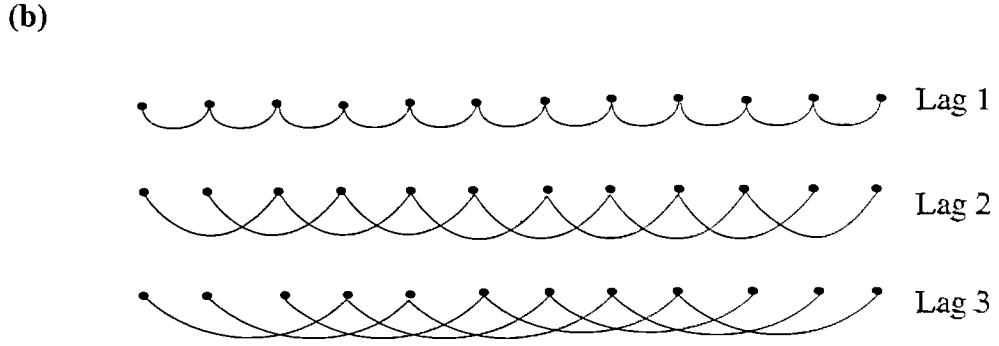

from the program is then manipulated in a spreadsheet and variograms such as that in Figure 2.4 constructed. The adapted version of the program is listed in Appendix 5.

The first example is drawn from McBratney and Webster (1981) who studied a 2km soil transect sampled every 20m (giving 101 points). Properties of the soils analysed were pH, nitrogen, colour, mottles and light and heavy minerals. Variograms showed that for colour variates, all the spatial variance was found within 360-400m, while for soil variates a nugget effect was found. The nugget effect is where the variation of a property is unaccounted for by the sampling interval and all variation is at a different (usually smaller) scale. The statistical basis of the semivariance measure has subsequently been applied to mapping soils at indicated scales (where economical) and for indicating numbers of samples required for sufficient statistical definition of soil units (Oliver and Webster, 1986). Oliver (1987) presents a useful review of geostatistics and its application to soil science and, similarly, Oliver with Webster (1991) discuss "how geostatistics can help you".

Other studies of soil variation include that caused by irrigation and cultivation (Buraymah and Webster, 1989) and nitrifers in a soil under pasture (Bramley and White, 1991). Work has been done on soil pH (Laslett et al, 1987) and Oliver and Webster (1987) studied many soil properties in the Wyre Forest including litter thickness, mottles, colour, percent sand and clay, structure, root and stone abundance and consistency. Variograms were then constructed for all properties based on nested sampling strategies. Webster and Boag (1992) have recently studied the spatial variability of cyst nematodes in agricultural soils. Nested sampling strategies have been used to cut down on the number of samples taken when using grid strategies and are best described by Webster and Oliver (1990). Also proposed is bulking of samples at the same scale to reduce the number of samples analysed but at the same time maintaining the spatial variability.

Finally the only variogram so far constructed using magnetic data is that of Williams and Cooper (1990). A 200m transect was used to study the variation in magnetic susceptibility of topsoils at 1m intervals (in America). The main aim was to locate soil boundaries using quickly made susceptibility measurements rather than other slower techniques. The magnetic susceptibility variogram showed a range of spatial variability at 60m and 120m which roughly coincided with the well- and poorly-drained soils along the transect. The conclusion suggested that magnetic susceptibility clearly defined soil boundaries and was related to texture, parent material and drainage characteristics. Smith et al, (1990) also indicate that susceptibility field surveys may represent a rapid surveying method (here relating to soil erosion and colluvial deposition).

Coefficient of variation (CV% = (usually 1 standard deviation/mean)*100) is a variance parameter which is used widely to compare variability between materials or soil units, for example (Webster and Oliver, 1990). CV% is affected by absolute and arbitrary zero values in a dataset where values contribute to the standard deviation measure, but not to the mean value of a population. This results in large CV% values. In this research the preferred methodology is that of the use of variograms for defining boundaries, spatial variability and required numbers of samples. CV% values are also used to assess and compare the variability of materials.

2.3 Multivariate classification techniques

Statistical multivariate classification techniques such as cluster analysis and principal component analysis (PCA) are essential tools in grouping materials according to their properties. In many areas they have been used in analysing patterns or groups using human and social, economic, biological, physical and chemical data. Continuous quantitative data and qualitative ranked or presence/absence data can be used in the techniques. Classification techniques have been used in many disciplines, often as a precursor to modelling techniques, and in many disciplines as a 'stand-alone technique'. Often it is difficult to interpret the outcome especially if transformed data has been used (Shaw and Wheeler, 1985). In environmental magnetism there has been little consistency between which parameters are used in classification techniques and those which can be used in modelling techniques (Yu and Yu and Oldfield, 1989 for example). The normality of the data is also often not considered and this has great effects on the success of a classification routine (Chapters 3 and 7).

Multivariate analyses present many advantages which Birks (1987a) reviews. The first is that the form of data simplification and the reduction of numbers of variables simplifies often complex and large data sets. This allows description and display of the data in fewer dimensions using two or three principal components linearly constructed from many original variables. In these terms exploration and hypothesis of large data sets becomes more easy. Communication of simplified data to non-specialists and repeatability of analysis are also important factors. Another useful review is given in Joreskog et al (1976) who concentrated on geological factor analysis and its correct application. Types of data used (linear data), data transformations and the differences and advantages of studying inter -sample relationships and inter-variable relationships are discussed. The latter is the more useful where samples are classified according to their properties.

Cluster analysis has in many cases been used as a stand-alone technique to group samples according to the variables or properties measured. There are several statistical methods which can be employed to group or 'agglomerate' samples into groups including single linkage (nearest neighbour), centroid and Ward's method. There is often confusion over which is the best agglomerative method to use. In this research (using SPSS-PC) different results were often obtained with each. Ward's method is the most widely used for continuous data (Bonnell and Sumner, 1992) and is the method adopted throughout this thesis. The output from a cluster analysis is generally presented in the form of a dendrogram, a type of tree diagram, an example of which is shown in Figure 2.5. The diagram shows the history of agglomeration from those samples grouped first to those 'outliers' grouped last or tagged onto the end of the diagram. It is clear in Figure 2.5 that similar samples are grouped according to their magnetic properties and groups are scaled in similar terms.

For cluster analysis environmental data, particularly magnetic data, often need to be normalized by performing a natural log transformation, as in many cases in physical science data are highly positively skewed and 'log-normal'. The effect of normalizing eliminates the differences in magnitude between the samples for the variables; the ratio of one number to another is not changed but the proportionality between the numbers is (Joreskog et al, 1976). Also

Figure 2.5: Example dendrogram of 49 samples in a database of possible 'source' samples including rocks, soils and pollutants and 3 sediment 'mixtures'

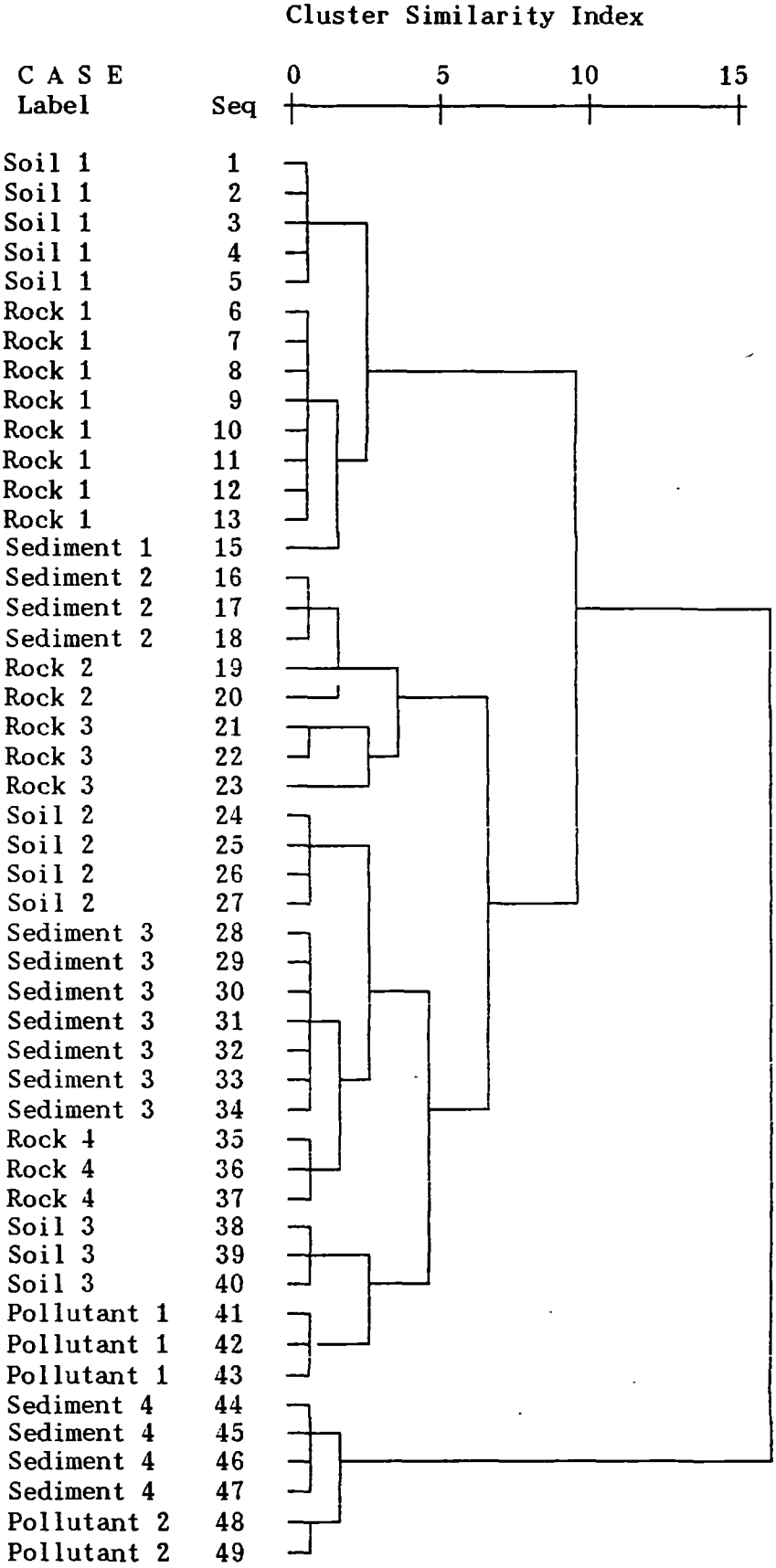

data are transformed into 'Z' scores which removes the effect of scale by standardizing the variable distribution and removing the mean (this is a linear transformation and does not change the shape of the original distribution however).

In soil science, cluster analysis has been used to group samples from different soil units as a basis for mapping (Webster and Burrough, 1972). Twenty-two field observations were made on samples from a 1400*600m grid and the resultant dendrogram was used at different scales of similarity from the finest scale where every sample is an individual group to the coarsest scale where there were two large groups. Maher (1986) grouped soil survey samples of different horizons using magnetic properties. At first many parameters were included in the analysis (including ratio, percentage and interrelated parameters). However, it was found that as good a classification could be obtained using only three parameters, χ, ARM and SIRM (IRM880). This result shows that there is intercorrelation between magnetic parameters which does not help the classification, a point further discussed in Chapter 3.

Classification of 65 soil profile descriptions from West Sussex was carried out by Wickramagamage and Fisher (1988). Two agglomeration methods were used and compared to the traditional soil classification. At high category levels, the composition of groups was different leading to a discussion on the difficulties of defining the best classification methods to use. Bonell and Sumner (1992) also review this. Cluster analysis can also be done using the scoring obtained from PCA for each sample to check the differences between original variables and principal components constructed from them.

Principal components are in fact new variables linearly constructed from the variables originally input (Joreskog et al, 1976). The original variables are reduced and drawn together to explain more simply the most important factors affecting the properties of the data set. Figure 2.6 shows an example ordination plot for a set of materials classified on the basis of a number of parameters. The relationship between the new components and the original variables is shown.

Bonnell and Sumner (1992) used PCA on precipitation data from 121 sites in Wales. Several principal component rotation methods were tried including non-rotation of PC's, varimax and oblimin rotations. Rotation of the components is used to maximize the relationships between the extracted PC's and the original variables contributing to them; varimax rotation is the most commonly used method which makes interpretation of the data easier. Bonnell and Sumner (1992) find that results gained by using different rotation techniques were broadly similar. PCA data for precipitation was then used in cluster analysis, as already mentioned, to identify clearly the groups of precipitation sites for mapping purposes.

In geology and geochemistry an introductory review of the use of multivariate statistics in stratigraphical analysis is given by Birks (1987a and 1987b). He states that many types of geological data can be used to classify stratigraphies including that of micro-fossils, pollen, sediment composition, chemical, mineral and stable isotope ratios. A useful section on the types of data suitable for use in multivariate techniques are also given by Birks (op

Figure 2.6: Principal Co-ordination plot for a set of different materials showing the relationships between principal components and original parameters used.

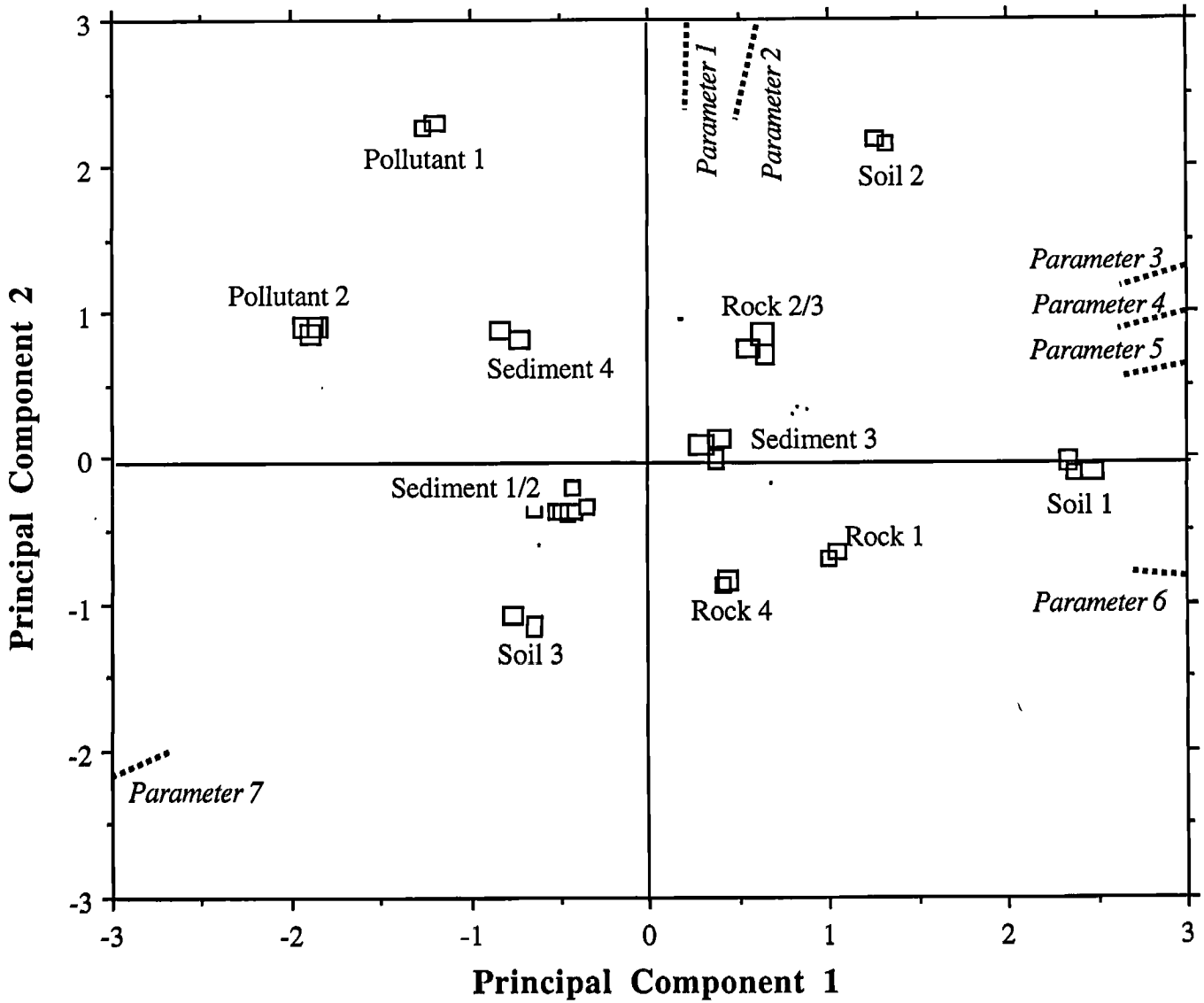

cit). Basically, data need to be linear and, if skewed, a transformation such as a log transformation needs to be carried out. However, Odeh et al (1991) found that log transformation does not affect the results significantly.

Mohan and Rao (1992) used PCA to analyse sediments of the Upper Siwalik conglomerates in India, where the PC's were related to erosion and transporting processes (size, sorting and shape), composition (quartz, sandstone) and depositional processes (orientation and packing). Mooers (1990) had used this approach already in order to discriminate texturally similar tills in central Minnesota. Magnetic parameters of χ and χarm and χarm/χ were included to discriminate between different sediment size fractions. This gave the first two PC's 95% of the original variance indicating the interrelationship between the parameters used. Walden et al (1987) had also used magnetic parameters in a similar way to discriminate tills. Magnetic parameters were again used by Yu and Oldfield (1989 and 1993) to classify sediments and sources of Chesapeake Bay and Nijar, Spain. Interrelated magnetic parameters were again included and in the second study the mixtures fell outside the range of the sources until another 'new' source was introduced, indicating source identification difficulties. Source contributions through linear modelling of the lake sediments could then be solved. Finally Saucy et al.(1991) applied classification techniques in order to identify the major characteristics of aerosol particles in Phoenix, Arizona. The composition and time-dependent concentrations of aerosol particles of 13,026 individual particles were used and 15 chemically distinct particle types were identified. Three major sources of the particles were attributed to crustal materials, copper smelters and marine air. This outlines the power of these techniques for reducing many variables and large data sets.

In this research cluster analysis is to be used for initial grouping of samples and to study the effects of magnetic data distribution on such classification. PCA will also be utilized to find the most useful discriminatory sets of linear magnetic parameters (identified as PC's) and to classify different materials/sources accordingly. Magnetic data from the sample databases will be used to test both techniques, and evaluation of the suitability of magnetic data for classifying materials will be made. The SPSS-PC statistical package is used throughout the research.

2.4 Linear Modelling - linear programming techniques

Between the mathematical and geographical disciplines the term 'model' has been interpreted in a variety of ways. Models can be conceptual/descriptive, black-box input/output only, statistical, empirical/process, simulation, physical/stochastic or mathematical, approaching the white box state. Kirkby et al.(1993) presents the definition "a model simulates the effect of an actual or hypothetical set of processes and forecasts one or more possible outcomes". Most models essentially represent a reduction of complex systems into analogues which have simplified inputs, outputs and internal processes. Stochastic modelling is the only type to include a random process element; for the most part models are deterministic (Kirkby et al.1993). In environmental magnetism, so far, most models have been deterministic. In this section a linear modelling technique is described which can incorporate error terms giving a range and limit to possible outcomes. The technique essentially poses an inverse modelling problem where the source proportions are to be found from the properties of the sources and mixtures. The technique is open to problems of source identification and variability with which, it is hoped, the sampling strategy and classification

techniques will provide useful precursor techniques to the modelling.

Linear programming (LP) algorithms are the mechanism by which linear modelling is carried out. More widely known as the basis of operational research, linear programming is mainly used in economics and industry to optimize certain assets, maximize profits and minimize raw goods, for example. By definition, linearly additive parameters are used to optimize conditions (finding solutions) whist being constrained by certain factors (constraints). The basic model is where several parameters are represented by linear equations and a solution is found where these meet and reach an 'optimum point' in multidimensional space. The point at which a solution may be found however is restricted by constraints or error limits set on the model. These may be the number of suppliers of goods or the number of individual processes of employees, for example. Coverage of such economic use is given in Winston (1991) where the standard routine used, as in this research, is a minimization program called LINDO (Linear interactive discrete optimizer) which uses a Simplex algorithm. Figure 2.7 shows, in two dimensions, the points made here. The advantage of linear programming is that many parameters can be included but difficulties occur with interrelated linear parameters and parameters of different scales. These factors are extensively discussed throughout this work with use of linearly additive magnetic parameters (see Appendix 1 for a list of linear parameters and definition of linearly additive). BASIC programs used in conjunction with LINDO are listed in Appendix 5 and an example input data matrix and LINDO data matrix are also provided.

In environmental sciences linear modelling has been used in a variety of ways. Water quality is one area in which linear models have proved useful especially with the increasing concerns for water quality and pollution (Rossman, 1976). Linear modelling of the mixing of chemical constituents of tributaries flowing into one major river has been successful and Kirkby et al.(1993) review a number of applications of linear modelling including a chemical mixing model. In another field of environmental pollution, Lehmann (1991a and 1991b) has analysed acid rain abatements by applying a linear modelling approach. Essentially as a management model, it attempted to determine (optimize) a pollution abatement strategy satisfying certain environmental targets (constraints). These targets form the uppermost constraints on the model while the costs of abatement of each pollution source are minimized. The effects of decreasing deposition targets in two countries effectively caused one country to allow an increase in its pollution levels. This indicates that great care has to be taken in interpretation of such optimization results.

Other geographical applications of LP include examples such as the work done by Dauer (1991) where the modelling of daily lake depths over a period of time (in terms of lake inflow and outflow, the effects of seepage, evaporations and minor tributaries) was carried out. The aim was to determine a set of parameters in the model which reflect the characteristics of the lake. In the model inflow + lake volume - outflow is maximized within certain lake water abundance constraints. Another application of LP is that of ground cover estimation from remote sensing data (Quarmby et al, 1992, Settle and Drake, 1993). Quarmby et al.(1992) estimate crop coverage using linear mixture modelling of multi-temporal advanced, very high resolution radiometer data (AVHRR) in Northern Greece. Identification of the problems, resolution of data and homogeneity of pure pixel source (end members) in this type of data are discussed. However, the estimation of the crop areas was successful to an average accuracy of 89%. In the

Figure 2.7: Linear Programming model showing constraints and optimum solution

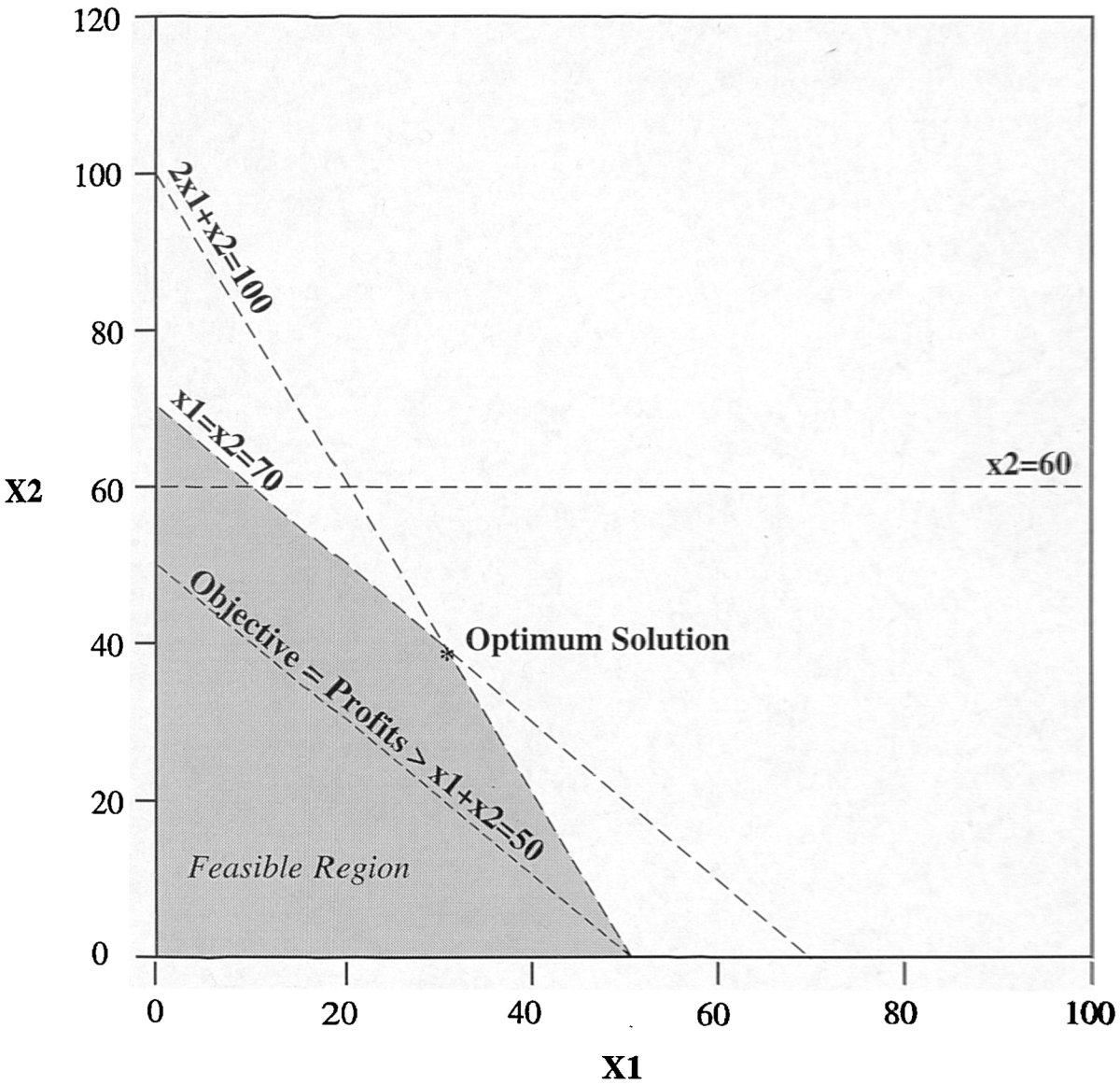

program each pixel of information is assigned several labels along with a proportion assigned to each label present. Linear programming is used to assign these label proportions using mixture modelling. The sources or labels are found when information on 'pure' pixels (end members containing only 1 label) are identified. The technique forms a rapid and potentially effective method for identifying crop coverage information. Also it is suggested that PCA can be used to define end members more successfully and accurately from the satellite data.

Often the type of linear modelling used in geographical studies involves only one or two parameters and is done using simultaneous equations. This often restricts the results to the specific factors affecting the parameters used rather than finding the average result from numerous parameters. Peart and Walling (1988) used geochemical sediment property ratios such as carbon/phosphorous and caesium-137 to determine the contributions from surface sources to suspended sediments in streams. The source properties were different to a significance level of 0.05 and calculations were done in respect to the values of the stream bank sediments. Much variation was seen however in the source contribution values for the different parameters.

It has been found that simultaneous equations can be used with magnetic measurements to quantify sediment delivered from tributaries into larger rivers. Considering the simplest case where one stream flows into a river simultaneous equations can be used to solve source proportions using all linear magnetic measurements. Basically the proportion of sediment from stream 'A' plus the proportion of sediment from upstream 'B' should equal the sediment at downstream 'C'. There have been varying degrees of success with this method. Nightingale (1991) used the means of χlf and IRM880 for the River Sherbourne and River Sowe near Coventry, which was reasonably successful. Also, since this work was completed, Caitcheon (1993) has used gradients of fitted lines for susceptibility and remanence parameters for source modelling of bedload. Values for source sediments were relatively unique using these parameters and the percentage contributions were calculated for a number of rivers in Australia. The difference parameter was used as it was explained to be "conceptually different" from those parameters which were used in its calculation (ie it indicated a difference in mineralogy). The success of this technique will depend on two factors: first, the particles in which the magnetic fraction exist, ie the geological, clay or organic materials which the magnetic minerals are related to; secondly, the degree to which particles mix together when they reach the downstream location.

The main advantage of LP is that full control of the error terms is allowed, ie the amount of 'room' in multidimensional space the program has in which to find a solution which fits the constraints. Also many parameters can be included from the outset and an average solution, satisfying all properties of the sediments for a particular mixture, can be established. However, simultaneous equations using one or two reliable parameters can give a good guide to the situation present in any environment. The methods presented here are tested in Chapters 4, 7, 8 and 9.

2.5 Summary

From this chapter it becomes clear that there are numerous areas in which variability studies, classification techniques and linear modelling can be applied successfully. In many cases, especially with classification techniques, different statistical methods are somewhat confusing and often data input into techniques is interrelated and non-linear. Care has to be taken with the joint use of the techniques so that modelling is carried out using the same parameters as those on which the classification has been carried out. In all cases of application of the various techniques, detailed description of the methods and statistics applied are needed in order to justify and explain results. This is summed up by Birks (1987), "it is better to be explicit but wrong than inexplicably right". The present work aims to improve the methodology and further the evaluation of the magnetic technique in the identification, classification and quantitative modelling of sediment and mineral sources of environmental mixtures.

SECTION B

Evaluation and Modelling

Introduction

This section presents the research which underlies formulation of the methodological framework (Chapter 6), with the overall aim being to simplify the methodology to ensure successful application of magnetism in sediment source modelling. The conceptual framework within which the research mainly lies is that of a critical rationalist approach. This approach eliminates any inductive reasoning whereby general conclusions or theories are induced from specific results and are then widely applied. 'Deductive' reasoning involves the deduction of specific conclusions from a set of general premises. Figure 3.1 outlines the deductive approach where first a problem is identified then critically tested and finally a preliminary hypothesis is adapted or refuted (Haines-Young and Petch, 1986). The deductive approach is affected by personal experience but always the experimental work and predicted results and theories are critically evaluated and verified. A very important factor in this process is the observation of critical conditions which affect the whole process which includes starting conditions and error bounds for models for instance. The chapters in this section incorporate experimental and hypothetical work not often used in geographical sciences. Experiments presented aim to present specific conclusions about the application of statistical and mathematical modelling techniques using magnetic properties to environmental systems and to resolve the following questions:

1. How can the sediment sources of mixtures be identified and defined taking into account geographical knowledge and statistical robustness?

2. How can sampling strategies take into account source variability and how can sources be statistically defined to give the range of contribution possibilities in modelling of sources? How many samples are needed to do this?

3. Which sources are most likely to be defined using magnetic techniques and how can sources be identified quickly and evaluated for their suitability for application of magnetic techniques for source modelling?

4. What types of materials can be successfully classified and modelled according to their magnetic properties? Can both sediment sources and minerals be modelled successfully?

5. Which are the best (linear) magnetic measurements to use in classification and modelling of sources? Are magnetic measurements truly linear and what restrictions does equipment accuracy and mixing of materials impose on the modelling?

This section is divided into 4 chapters which represent tests of the points raised above in that Chapter 3 tests existing methodologies and work, Chapters 4 and 5 test magnetic measurements for use in classification and modelling and Chapter 5 also tests magnetic parameters for use in reconnaissance work (source identification and assessment of source variability). Finally Chapter 6 presents the main findings of this section and defines the methodological framework devised from the evaluation and modelling work which is then applied to the environmental case studies presented in Section C.

Figure 3.1 : The Critical Rationalist View - Deductive Research Approach (adapted from Haines-Young and Petch,1986)

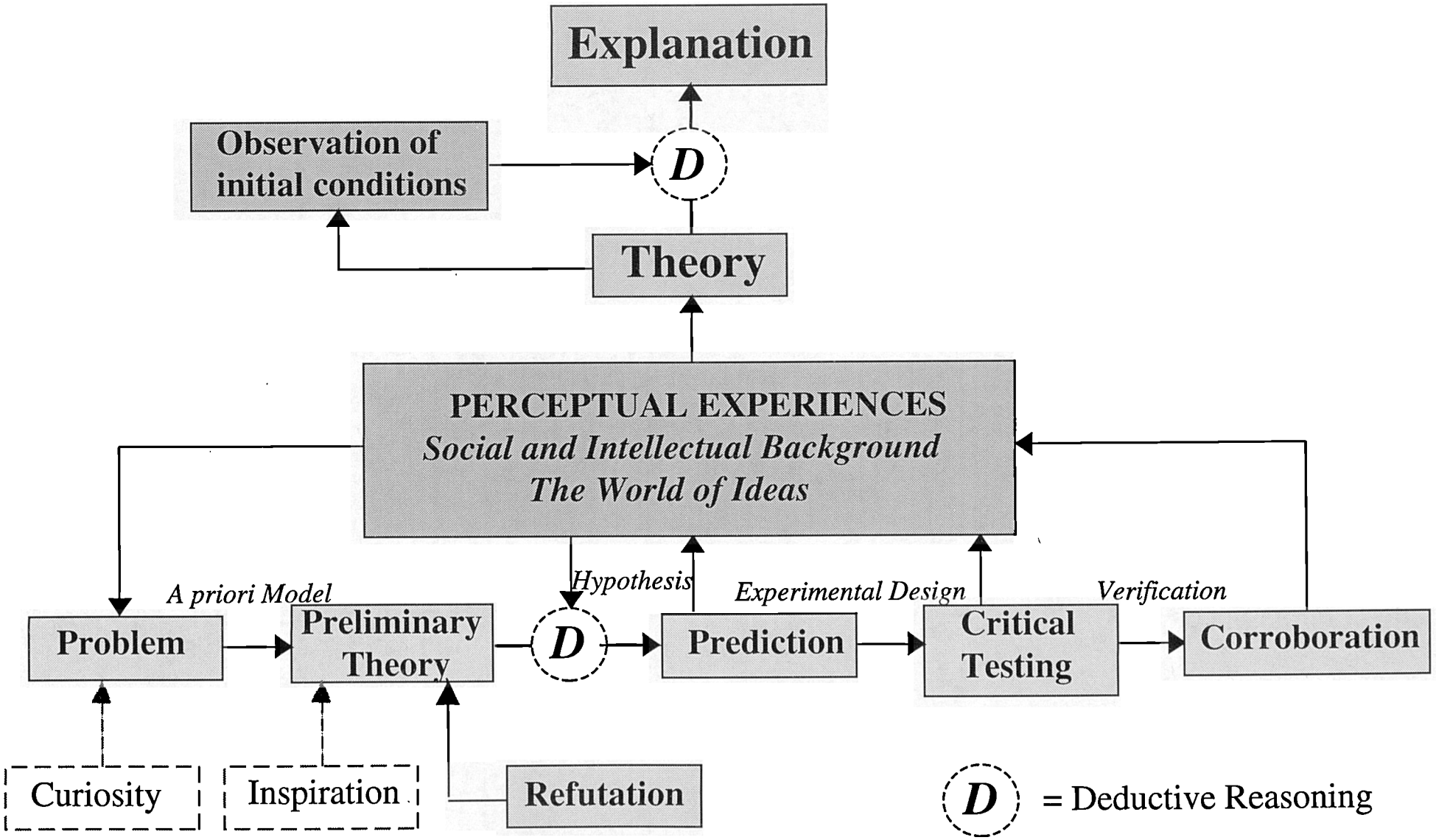

CHAPTER 3

Testing Existing Methodologies, Measurement Evaluation and Classification

Introduction

This chapter describes the initial testing of classification and modelling techniques using data collected by other workers, namely, Yu (1989) and Grew (1990) and testing of classification techniques using the databases constructed in this research. First, classification of sources using magnetic properties of Seeswood Pool sediments (Grew, 1990) was studied. The established identification of only two real sources, topsoil (field) and subsoil (from channel banks) was re-considered to highlight further research possibilities of the lake catchment. The work aimed to highlight the initial suitability of classifying sources using magnetic properties and to evaluate the classification techniques against existing bi-variate classifications for Grew's data. Secondly, the data of Yu (1989) was engaged in an assessment of the use of initial linear magnetic measurements rather than his linearly regressed ratio data in source modelling. The classification of sources which were subsequently used in the linear modelling of sediment mixtures is also re-appraised. The main aim was to examine the type of data which was used for classification and modelling of the sources. In the second part of this chapter bi-variate scattergraphs, cluster analysis and PCA are used to classify data from four databases. An evaluation and comparison of the techniques is given.

3.1 Testing Existing Methodologies

3.1.1 Seeswood Pool

Seeswood Pool has been a centre of attention in contemporary hydrology at Coventry University since the early 1980s and much work has been done by Drs I Foster, R Grew and J Dearing in the catchment involving monitoring of the two streams from the surrounding pasture and arable sub-catchments which feed the lake and lake sediment study. Preliminary modelling using magnetic properties in bi-variate scattergrams was done by R Grew (1990). Magnetic data for the lake sediments and suspended stream sediments were available; but little appraisal of soil variability had been carried out. S ratio (indicating remanence carrying ferrimagnetic and canted-antiferromagnetic minerals) and IRM880 (indicating all remanence carrying minerals) were used to discriminate between topsoil and subsoil sources of sediment in the catchment. The geology of the catchment is of a Keuper marl including both Keuper Clays and Triassic Red Sandstones. Soil types are of the Bromsgrove series and Salop series in the north of the catchment. Figure 3.2 shows the location and land-use of the reservoir catchment. Plates 3.1a-c show Seeswood Pool and associated in-flowing streams from the pasture catchment (Stream 1; Plate 3.1b) and the arable catchment (Stream 2; Plate 3.1c).

At Seeswood there are three different land-uses in the catchment. These needed either to be identified as individual sources or as being non-contributary; the stream channel itself needed to be counted as a source of material also.

Figure 3.2: Seeswood Pool catchment and land-uses. Core samples taken for this research are also marked

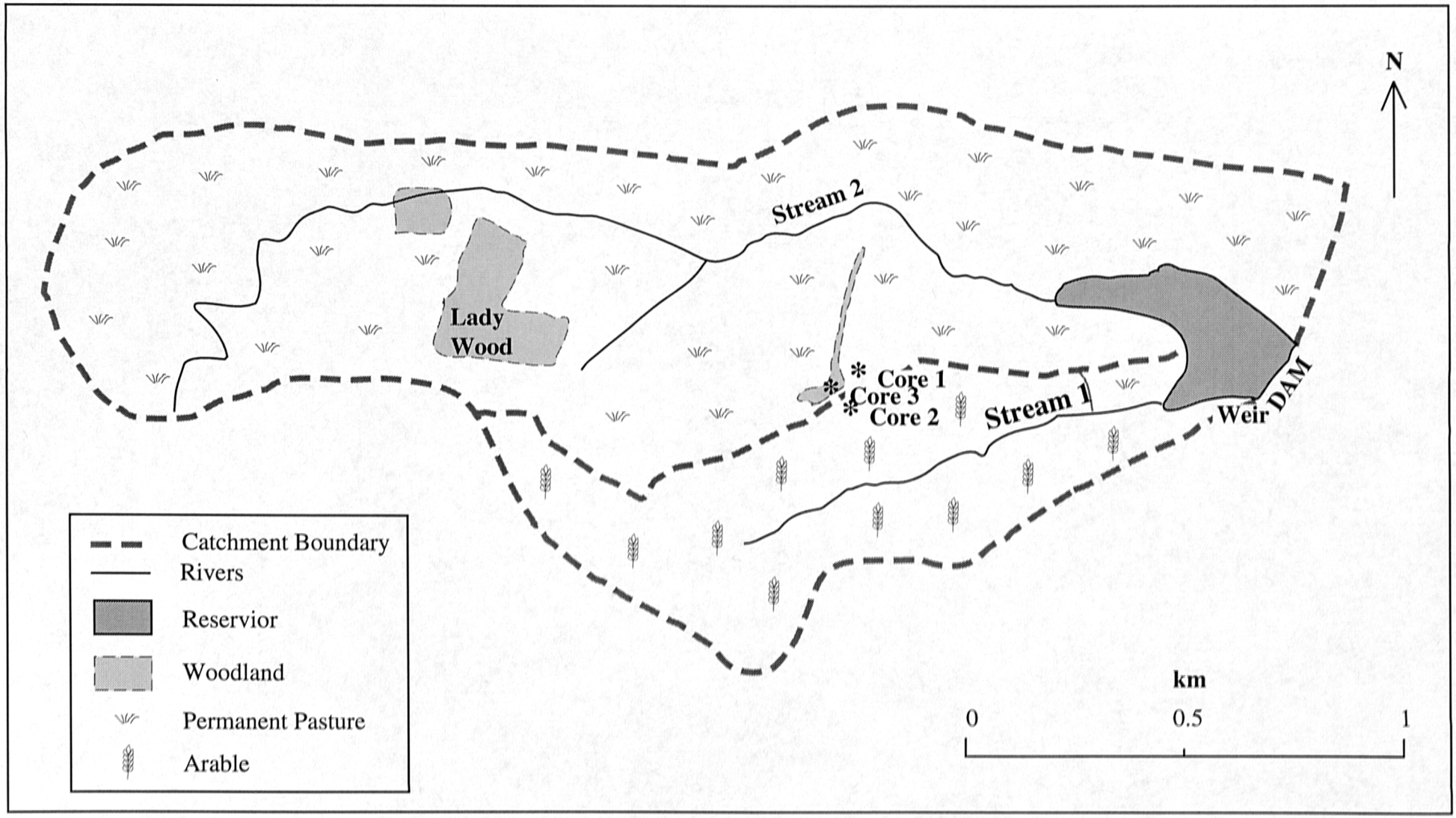

Plate 3a: Seeswood Pool from weir

Plate 3b: Stream 1-
Pasture catchment

Plate 3c: Stream 2-
Arable catchment

It seems that local woodland does not contribute sediment, but the possibility of this being a source needed further study, as it would in any unknown catchment. If the trees were felled this may open up the topsoil and subsoil to increased erosion where sediment would move via the ditch network. Grew (1990) identified the channel as being an important source of sediment for the lake and suggested that a sampling scheme similar to the land-use sampling schemes may be employed to study the properties of the two streams entering the lake. The existing data is re-classified here using PCA and the discrimination between topsoils and subsoils re-assessed. The suitability of sampling further the different land-use types is also evaluated using PCA.

Sediment Sources

The work carried out at Seeswood identified both ferrimagnetic topsoils and canted-antiferromagnetic clay subsoils as sediment sources. Well identified contrasts between topsoils and subsoils and the three main land-uses, pasture, arable and woodland were noted (Dearing, pers. comm.). Also the atmospheric component in this Midlands reservoir had been partially quantified as was suspended materials for the two streams (these comprised just 9 samples however). The data of Grew (1990) is given in Appendix 2, values of IRM-100 and HIRM-100 were recalculated from S ratio and IRM880. Soil sample data from a $100m^2$ grid over the catchment, lake core, air pollution and suspended sediment sample data were also included for further analysis.

Testing classification

The first test on Grew's data was designed to discriminate between topsoils and subsoils using the available magnetic data indicative of different mineralogies (Appendix 1). Figure 3.3a shows χfd plotted against HIRM-100 which makes it reasonably clear that by using χfd there is a division between topsoil (5-10 nm^3kg^{-1}) and subsoil (0-8 nm^3kg^{-1}) with a change in concentration of fine-grained ferrimagnetic minerals (through enhancement). HIRM-100 shows a smaller magnitude difference however, as the soils are generally clay derived. HIRM-100 is not indicative of the enhanced ferrimagnetic minerals in these topsoils but is of the canted-antiferromagnetic clay minerals. The magnitude difference of HIRM-100 between different land usages is just as low (Figure 3.3b) and there is no clear division between land-use samples. In both cases the lake core data spans that of the sources reasonably well, considering the selective transport and sorting processes which have occurred. Some lake core samples fall outside the range of the source data indicating either other sources or sorting of the magnetic fraction in the lake sediments.

PCA was carried out in order to test statistically the spatial discrimination (different land-use soils). Data distributions were found to be highly positively skewed and were log transformed accordingly. The PCA output (Figure 3.4) gave a similar output to that of the HIRM-100 /χfd scattergram. In this figure different land-use soils are not well discriminated as indicated by the mean values of the three land-uses (A, P and W). Topsoils and subsoils are well discriminated but some lake sediment values fall outside of the range of the soils as above. This reflects that either there is not enough magnetic discrimination to be able to model the land-use sources and/or that more samples are needed to define the land-use sources more exactly.

Figure 3.3: HIRM-100 versus Xfd for lake, topsoil and subsoil samples (a) and HIRM-100 versus Xfd for lake, topsoil and subsoil samples for different land-uses (b). (Data of Grew, 1990).

(a)

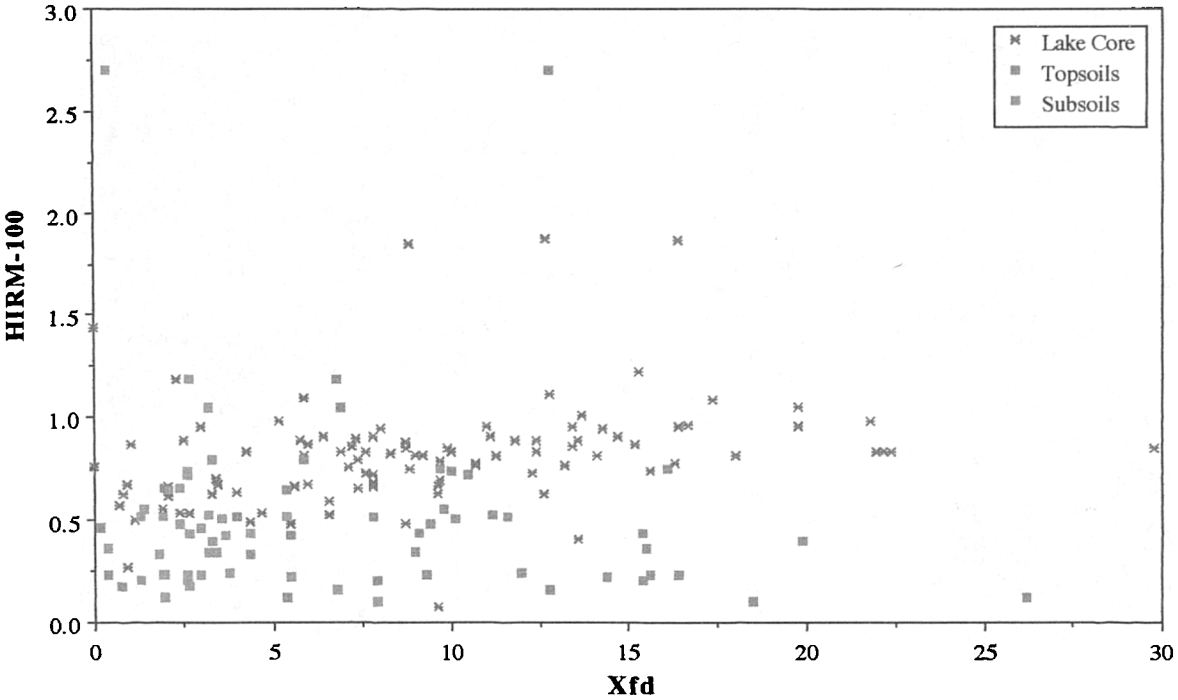

(b)

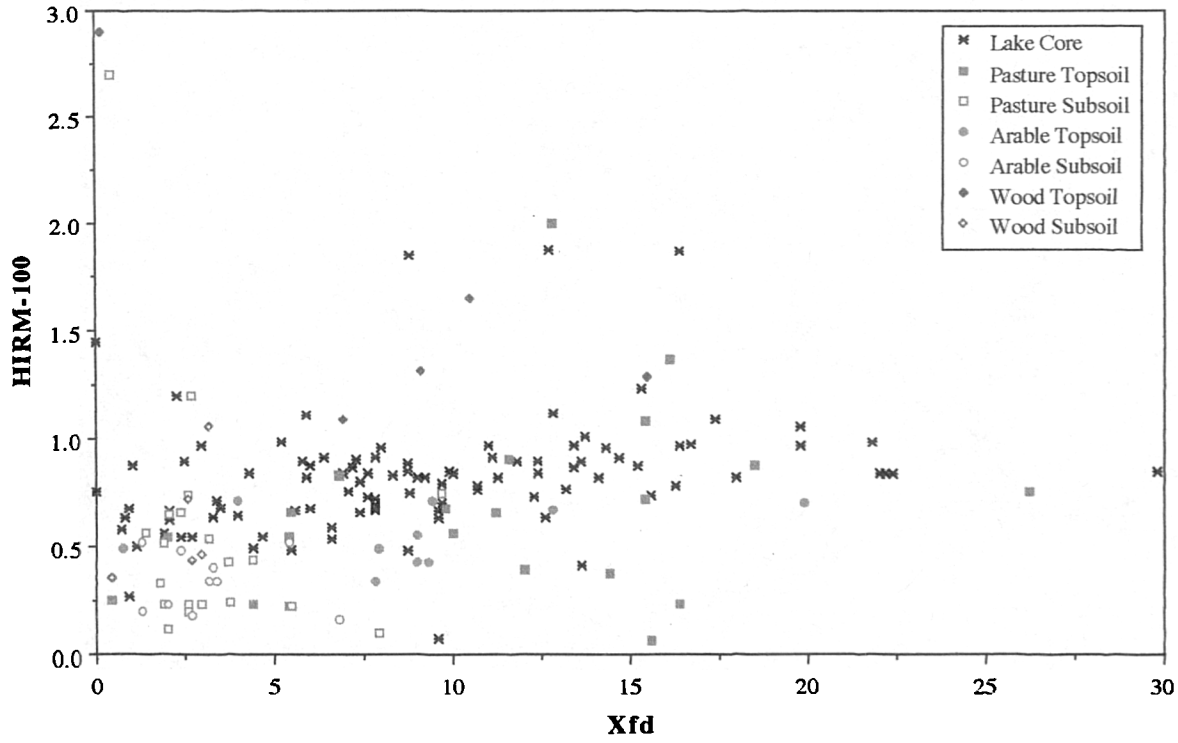

Figure 3.4: PCA plot of Seeswood Pool soil sources and sediments

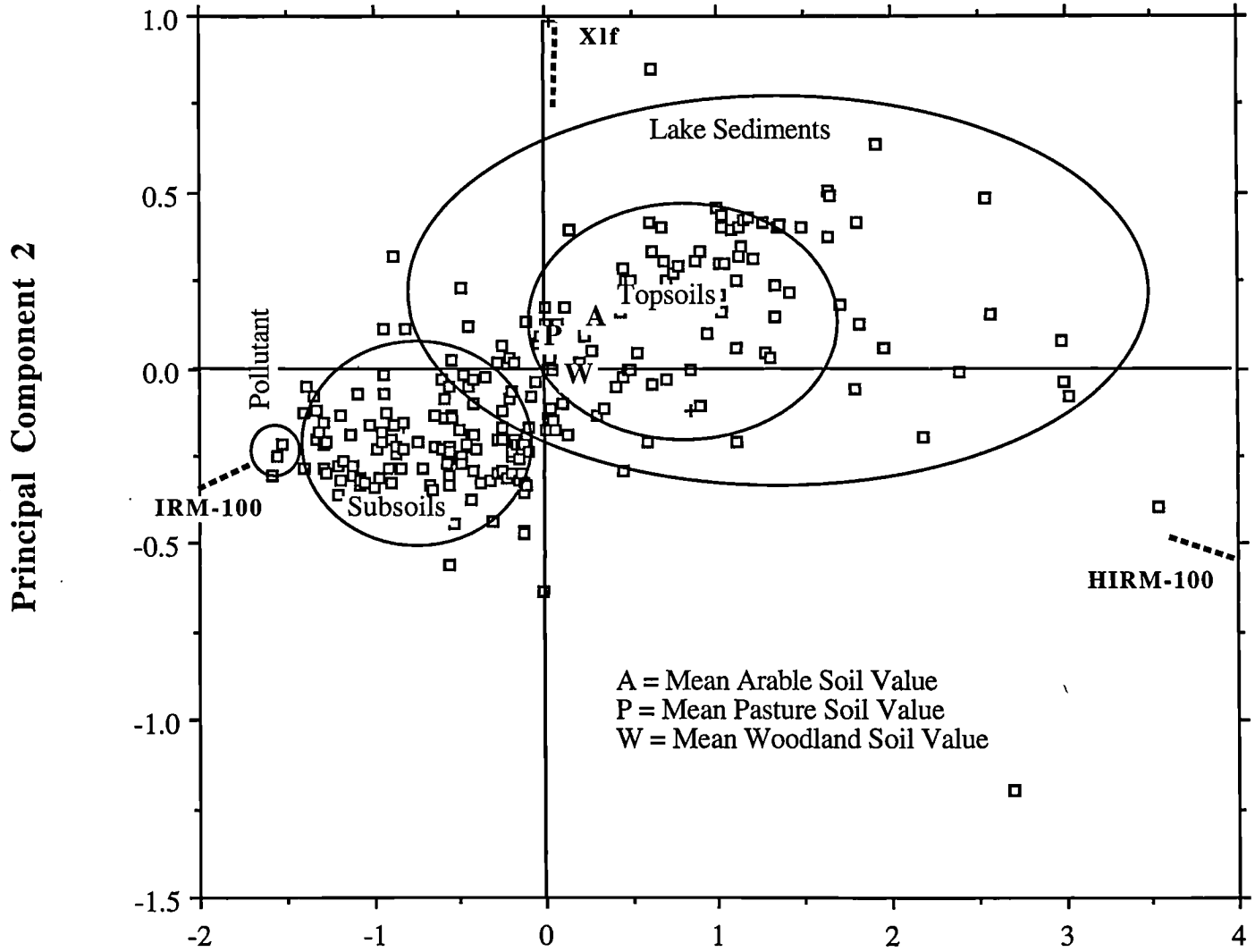

PC	*Eigenvalue*	*% of var.*	*Cum. Var.*
1	1.41	46.9	46.9
2	1.01	33.6	80.5

3.1.2 Rhode River

Data from Yu (1989) and Yu and Oldfield (1989) were used to test the classification and modelling techniques proposed for use in this research. Yu and Oldfield (1989) modelled the source contributions of the estuary of the Rhode River, Chesapeake Bay and its changing sources of sediment. In their study, sixty-three samples of the identified source components were collected in the field. The identified components were Talbot Parent Material, Talbot Subsoil, Nanjemoy Parent Material, Nanjemoy Subsoil and two surface soils. Samples were fractionated and the fine particle data regressed to obtain linearly additive data. The data was then input into the linear programming and used to unmix the estuary sediment mixture.

The source data were used by Yu in a linear programming routine and used to unmix an estuary mixture but their results contained zero proportions for two of the source components identified. In the present work regressed, fine particle and bulk linear data were used as input into linear programming. The results of Yu's regressed data was compared with the results obtained from using the original fine particle data in this research. Other investigations in this project included a re-evaluation of the classification of the sources using variables re-calculated from the original data. The work is split into stages of analysis, starting with cluster analysis, then assessing PCA and then evaluating the further linear programming results. The aims of the tests were as follows:

1. To assess the need for using regressed data in Linear Programming and the mathematical correctness of doing so.

2. To re-classify the identified source components and using parameters used in LP and to re-assess their suitability in terms of magnetic difference for use in modelling.

Rhode River Data

Data for 63 bulk samples from the Rhode River catchment were available from Yu (1989) and bulk, fine and regressed data were available for the source components and the mixture from Yu and Oldfield (1989). The 63 samples fell into one of eight groups: large mixed land use (101), pasture sub-catchment within 101 (111), forest (110), cultivated crop land (109), Nanjemoy Subsoil, Nanjemoy Parent material, Talbot subsoil and Talbot parent material. The source components used in the published paper were two surface materials, Nanjemoy subsoil, Nanjemoy parent material, Talbot subsoil and Talbot parent material. Table 3.1 shows the variables which were used and the data recalculated for the present work. A full listing of the data used is given in Appendix 2.

Classification

Data were entered into SPSS, found to be normally distributed, and data was then standardized. Many tests were carried out to find those variables which gave the best clustering (based on the dendrogram). Table 3.2 gives the list of tests carried out and the number of clusters identified, based on the eight groups of data in the file (listed previously). Ratio parameters were used in this analysis as they were used in the initial classification of the samples. In other studies presented in this research only those parameters which can be used in linear modelling are included in classification routines (Chapters 4, 7 and 8).

Table 3.1: Data used from Yu and Oldfield (1989), Yu (1989) and data recalculated for present re-assessment work

ORIGINAL DATA		RECALCULATED LINEAR DATA
Linear	**Ratio**	
χlf ($10^{-8}m^3$ kg^{-1})	χfd (%)	
χhf ($10^{-8}m^3$ kg^{-1})		χfd ($10^{-8}m^3$ kg^{-1})
ARM (mAm^2 kg^{-1})	ARM/χ (10^2Am^{-1})	
IRM880 (mAm^2 kg^{-1})	IRM880/χ (10^2Am^{-1})	
	IRM880/ARM	
	S-20mT (%)	IRM-20mT (mAm^2 kg^{-1})
	S-40mT (%)	IRM-40mT (mAm^2 kg^{-1})
	S-100mT (%)	IRM-100mT (mAm^2 kg^{-1})
	S-300mT (%)	IRM-300mT (mAm^2 kg^{-1})
	F+20mT (%)	IRM+20mT (mAm^2 kg^{-1})
	F+100mT (%)	IRM+100mT (mAm^2 kg^{-1})
		HIRM-100mT (mAm^2 kg^{-1})
		HIRM-300mT (mAm^2 kg^{-1})

Where:

$$\chi fd\ (\%) = \frac{\chi lf - \chi hf}{\chi lf} * 100 \qquad SxmT\ (\%) = \frac{IRMxmT * -1}{IRM880}$$

$$HIRMxmT = IRM880 + IRMxmT * 0.5$$

Table 3.2: Clustering Analysis Tests

Test	No. of Clusters Identified	Magnetic Parameters
a	7	χlf, χfd(%), ARM, IRM880, ARM/χlf, IRM880/χlf, IRM880/ARM, S-20, S-40, S-100, S-300, IRM-20, IRM-40, IRM-100, IRM-300
b	7	χlf, χfd(%), ARM, IRM880, ARM/χlf, IRM880/χlf, IRM880/ARM,S-20, S-40, S-100, S-300
c	7	χlf, χfd(%), ARM, IRM880, ARM/χlf, IRM880/χlf, IRM880/ARM
d	6	χlf, χhf, ARM, IRM880, IRM-20, IRM-40, IRM-100, IRM-300
e	6	χlf, χhf, ARM, IRM880, IRM-20, IRM-40, IRM-100
f	5	χlf, χhf, ARM, IRM880, IRM-20, IRM-40
g	5	χlf, χhf, ARM, IRM880, IRM-20
h	5	χlf, χhf, ARM, IRM880
i	3	χlf, χhf, ARM
j	3	χlf, χhf
k	3	χlf
l	2	ARM
m	2	IRM880
n	5	χlf, IRM880
o	7	χfd(%), ARM/χlf, IRM880/χlf, IRM880/ARM, S-20, S-40, S-100, S-300
p	7	χfd(%), ARM/χlf, IRM880/χlf, IRM880/ARM, S-20, S-40, S-100

Table 3.2 Continued

Test	No. of Clusters	Magnetic Parameters
q	6	χfd(%), ARM/χlf, IRM880/χlf, IRM880/ARM, S-20, S-40
r	6	χfd(%), ARM/χlf, IRM880/χlf, IRM880/ARM, S-20
s	5	χfd(%), ARM/χlf, IRM880/χlf, IRM880/ARM
t	6	χfd(%), ARM/χlf, IRM880/χlf
u	4	χfd(%), ARM/χlf
v	3	χfd(%)
w	7	χlf, χfd(%), ARM, IRM880, ARM/χlf, IRM880/χlf, IRM880/ARM, S-20, S-40, S-100, S-300, IRM-20, IRM-40, IRM-100, IRM-300 (Method Baverage)
x	7	χlf, χfd(%), ARM, IRM880, ARM/χlf, IRM880/χlf, IRM880/ARM, S-20, S-40, S-100, S-300, IRM-20, IRM-40, IRM-100, IRM-300 (Single Linkage)
y	4	IRM-20, IRM-40, IRM-100, IRM-300
z	6	χlf, χhf, χfd%, ARM, IRM880, IRM-20, IRM-40, IRM-100, IRM-300, HIRM-100, HIRM-300
aa	6	χlf, χhf, χfd, ARM, IRM880, IRM-20, IRM-40, IRM-100, IRM-300, HIRM-100, HIRM-300

The results of Table 3.2 were reproduced graphically and a Polynomial curve of order 3 fitted through the data (Figure 3.5). This aimed to identify the least number of parameters needed for a good classification result. The graph in Figure 3.5 shows that for the six components of Yu to be identified separately the least number of linear parameters needed was 7 (test e) and the least number of ratio parameters was 3 (test t). The cluster analysis does not identify how magnetically different the sources were nor their suitability for modelling however, so the data were then entered into PCA. Resulting principal co-ordination plots for the two sets of data (the 63 bulk samples and the fine particle component and mixture data) are shown in Figures 3.6 and 3.8a. Figures 3.7 and 3.8b show bi-variate scattergrams of χlf and HIRM-100 and are included for comparison with the PCA co-ordination plots. It can be seen that the χlf versus HIRM-100 plot would have indicated early on that certain sources were too magnetically alike and there was not enough variation in mineral type and concentration between the sources identified.

The two PCA co-ordination plots show that χlf, χfd and HIRM-100 and HIRM-300 are the most influential discriminatory variables. Both the plots show that the three sources, Nanjemoy subsoil, Nanjemoy parent material and Talbot parent material produced similar results, indicating that they are magnetically similar. For a successful modelling result it is shown in Chapter 4 that source samples have to fall in different areas of the plot. From this it can be seen that the three similar sources here should be amalgamated in the linear modelling routine. The bulk samples show this as clearly as the fine particle data, indicating that as the magnetic fraction lies in the fine particles it might be safe to classify bulk sediments first and then, if necessary, sieve and measure the finer sediments to match the sediment mixture. Further to the principal components, discriminant analysis was studied briefly to 'force' the 63 samples into groups identified in cluster analysis using principal component data for each source sample. Two tests were carried out, the first utilizing 6 source components and the second with four. The resulting territorial maps (Figure 3.9a and b) show that the four groupings look more reasonable than 6 groups indicating that this would be the most suitable classification on which to base modelling. In Figure 3.9b sources 1 and 2 are too similar to be discriminated (some labels used are identical but represent different land-uses).

Figure 3.5: Number of clusters versus number of different parameters with logarithmic curve fit

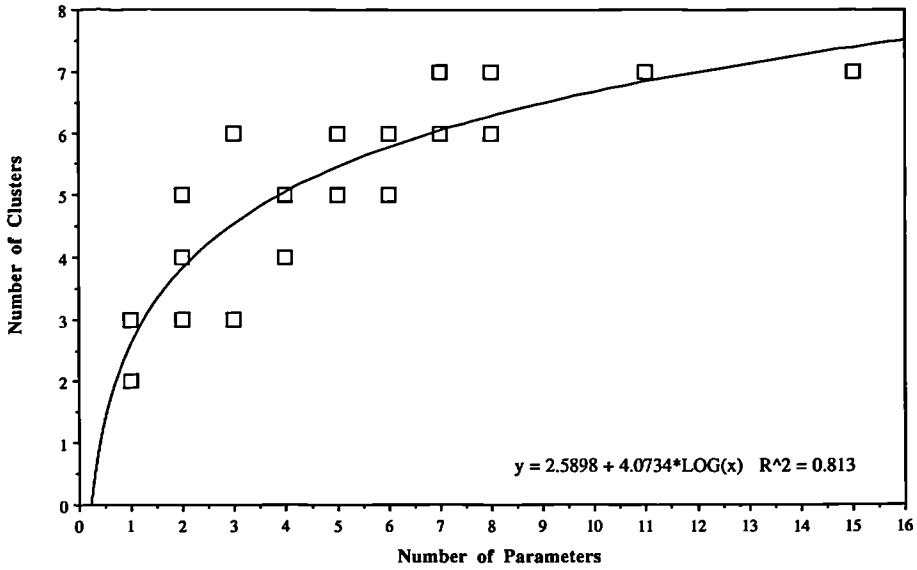

Figure 3.6: PCA Co-ordination for 63 bulk source samples. (Data of Yu, 1989; Yu and Oldfield, 1989).

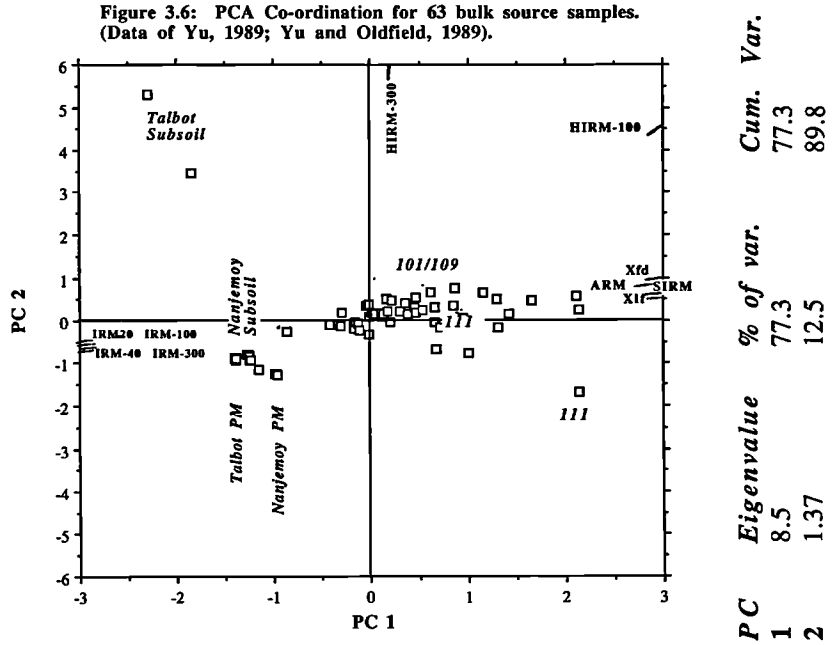

Figure 3.7: Xlf versus HIRM-100 for 63 bulk source samples. (Data of Yu, 1989; Yu and Oldfield, 1989)

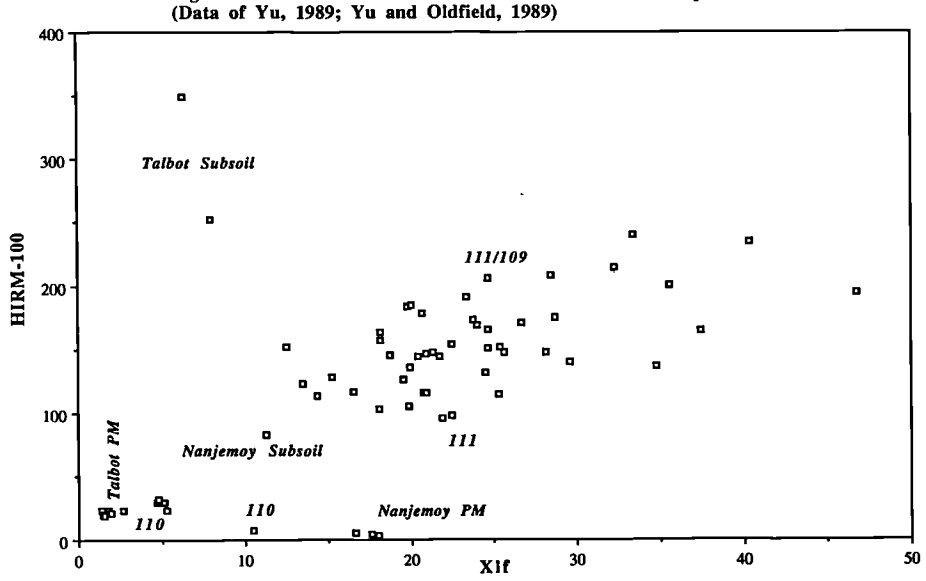

Figure 3.8: Principal Co-ordination plot (a) and HIRM-100 versus Xlf (b) for Fine particle source component and mixture

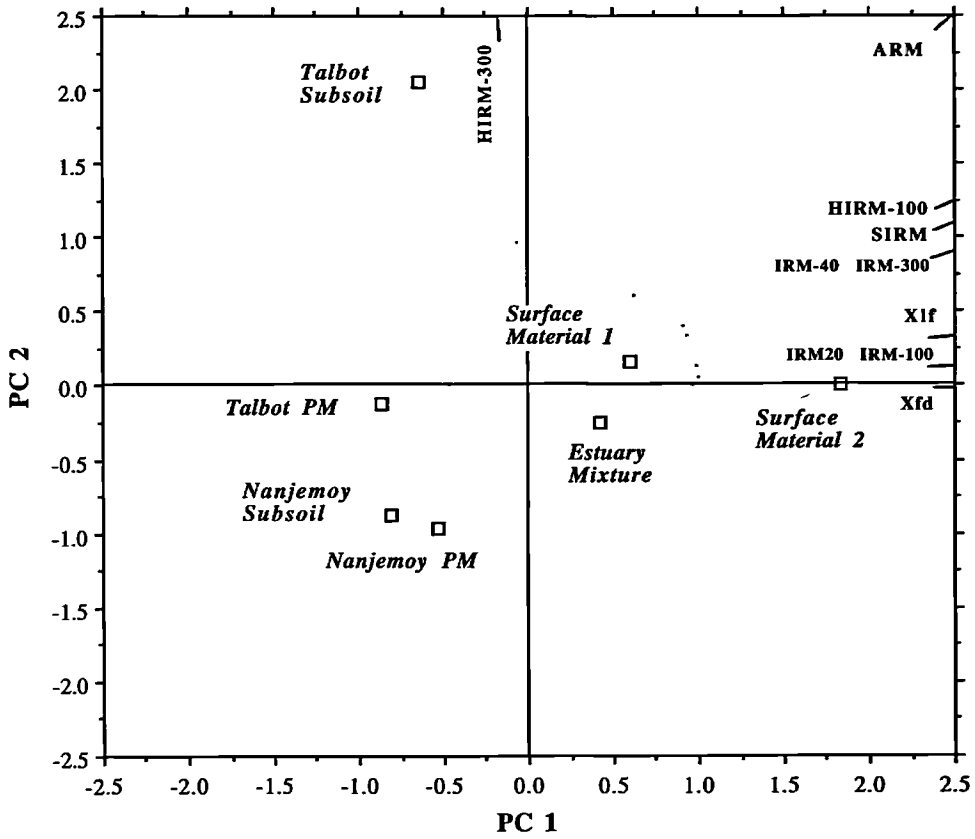

PC	*Eigenvalue*	*% of var.*	*Cum. Var.*
1	8.21	82.1	82.1
2	1.31	13.1	95.1

(b)

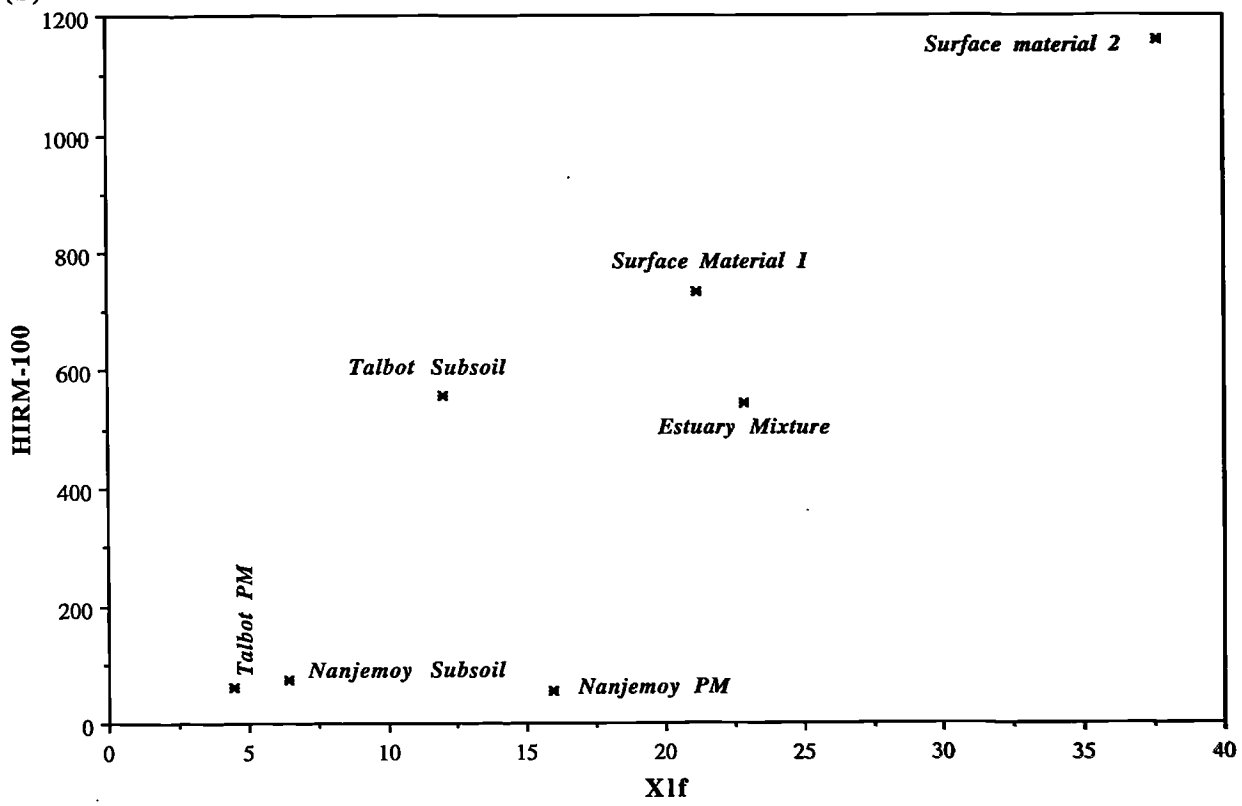

Figure 3.9: Territorial maps for 63 bulk samples using four (a) and six (b) source components. *=group centroid, across=function 1 and down=function 2.

(a) 1 = 101/109
2 = 101/109/111
3 = Talbot PM, Nanjemoy PM and subsoil, 110
4 = Talbot subsoil

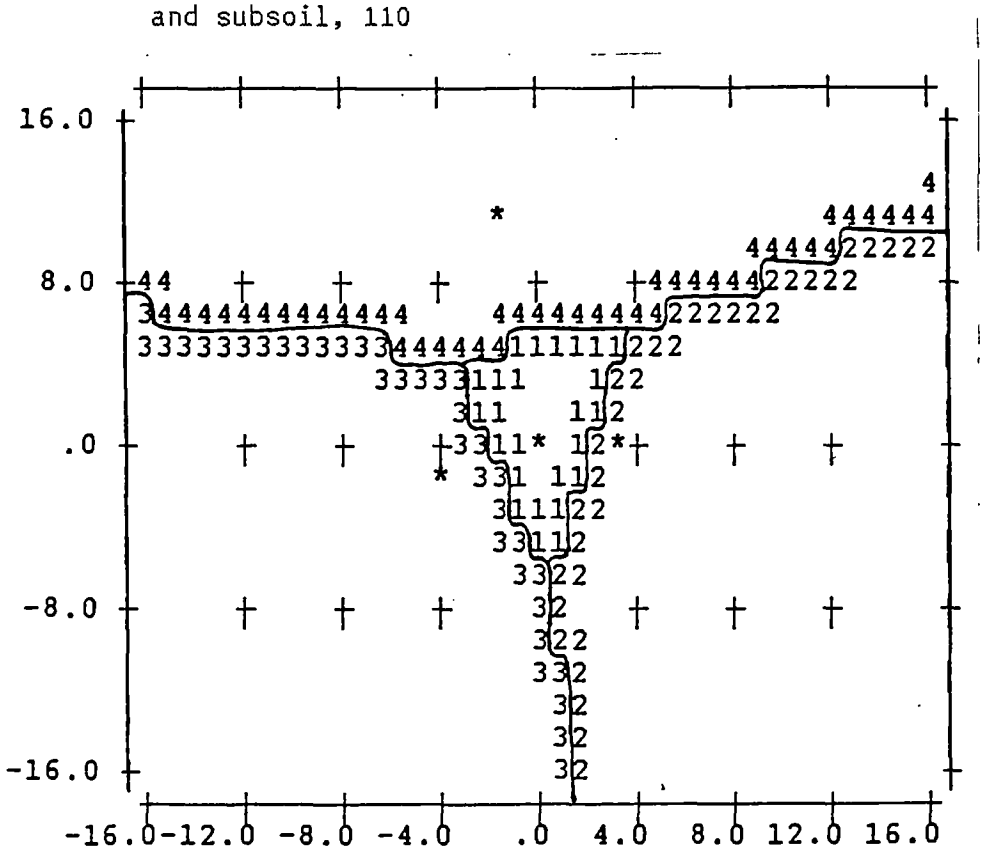

(b) 1 = 101/109
2 = 101/109
3 = 101/109
4 = 111
5 = Talbot PM, Nanjemoy PM and subsoil, 110
6 = Talbot subsoil

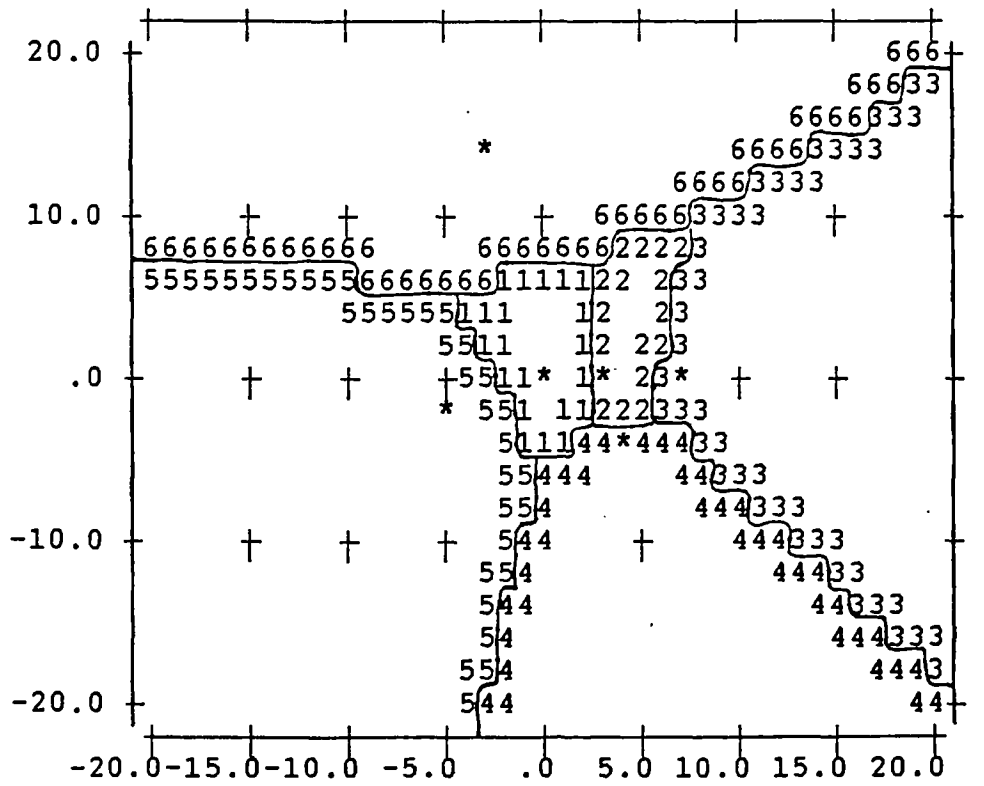

Linear Programming

Regressed, fine particle and bulk linear data were used in LINDO (Table 3.3a) and the results are given in Table 3.3b.

The Linear Model was constructed in the following way:

$$|| <= Ej <=> -Ej <= \sum_{i=1}^{m} aij\ xi - bj <= Ej$$

$$(i = 1, 2, 3, ... m)$$
$$(j = 1, 2, 3, ... n)$$

Where:-
- xi = Source proportions
- Ej = Error
- bj = Sample measurement
- aij = coefficient of regression model (source measurements)
- n = number of parameters
- m = number of sources

The errors for the new data were set at similar levels to the original data. It must be noted at this stage that the larger error terms given to IRM880 (Yu and Oldfield, 1989) only serve to bias the routine towards this variable. If possible all error terms should be kept in the same units (this is observed in the mixing experiments in Chapter 4 where consistent error terms (of 1 unit) are given to all measurements).

Reasonably similar results are gained for the fine particle data and are similar to the published results of Yu and Oldfield (1989). The only slight differences are seen in the proportion attributed to the Talbot subsoil (x4) where 1.67% is given for fine particle data and 4.7% for regressed data. In tests c and e, where only two parameters were used, results show similar results for the fine particle and regressed data. There is contradiction in proportions of surface material 1 (x5) however. Test j indicates that for regressed data using linear parameters the results are very similar to the published results. Tests k and l however, indicate further inconsistencies caused by similarity between Nanjemoy subsoil (x2) and Talbot parent material (x3).

Overall the results show that the fine particle data gives as good results as the regressed data, verifying that the regression analysis is not needed. The linear data are as good as the ratio data in predicting the result. Zero proportions were ascribed to three components in all, Nanjemoy subsoil, Nanjemoy parent material and Talbot parent material. Also the variability of the source sediments were not incorporated or could not be incorporated (some were the average of only 2 samples).

Essentially the linear programming routine used the component Nanjemoy parent material to correct for the mixture measurement with the surface materials and Talbot subsoil. This is shown diagrammatically in Figure 3.10, where vectors for the source samples are drawn for HIRM-100 and χlf. The two vectors for Talbot parent material and Nanjemoy subsoil are too similar for the program to discriminate and are near linear multiples of the Nanjemoy parent material. These factors were made clear from the classification results also, proving the importance of PCA as a precursor to linear modelling of sources using magnetic parameters.

Table 3.3: Linear Programming Tests (a) and Results (b).

(a)

Test	Data	Magnetic Parameters
a	Regressed	Original Data: χlf, χfd(%), IRM880, IRM880/χlf, S-20, S-40, S-100, S-300, F+20, F+300mT
b	Fine	Original Data: χlf, χfd(%), IRM880, IRM880/χlf, S-20, S-40, S-100, S-300, F+20, F+300mT
c	Bulk	Original Data: χlf, χfd(%), IRM880, IRM880/χlf, S-20, S-40, S-100, S-300, F+20, F+300mT
d	Regressed	Non Ratio Data: χlf, IRM880
e	Fine	Non Ratio Data: χlf, IRM880
f	Bulk	Non Ratio Data: χlf, IRM880
g	Regressed	Original Data plus recalculated parameters: χhf, IRM-20, IRM-40, IRM-100, IRM-300
h	Fine	Original Data plus recalculated parameters: χhf, IRM-20, IRM-40, IRM-100, IRM-300
i	Bulk	Original Data plus recalculated parameters: χhf, IRM-20, IRM-40, IRM-100, IRM-300
j	Regressed	All Non Ratio Data χlf, IRM880, χhf, IRM-20, IRM-40, IRM-100, IRM-300
k	Fine	All Non Ratio Data χlf, IRM880, χhf, IRM-20, IRM-40, IRM-100, IRM-300
l	Bulk	All Non Ratio Data χlf, IRM880, χhf, IRM-20, IRM-40, IRM-100, IRM-300

(b)

	Tests				
Sources	**Yu & Old's Values**	**a**	**b**	**c**	**d**	**e**
x1	46.195	46.52	37.75	11.24	52.22	43.29
x2	0	0	0	0	0	0
x3	0	0	0	0	0	0
x4	0.534	4.706	1.67	0	14.64	21.05
x5	33.443	29.25	43.53	84.22	0	0
x6	18.739	19.52	17.05	4.53	33.14	35.66

Sources	**f**	**g**	**h**	**i**	**j**	**k**	**l**
x1	22.91	46.61	32.79	13.397	46.68	21.27	14.67
x2	0	0	10.16	7.74	0	33.86	0
x3	0	0	0	0.16	0	0	5.82
x4	32.55	0.78	0	0	10.29	0.47	0
x5	0	24.25	33.44	59.05	20.21	3.02	60.5
x6	44.54	21.35	23.61	19.65	22.83	41.39	19.01

Where: x1 = Nanjemoy Parent Material; x2 = Nanjemoy Subsoil; x3 = Talbot Parent Material; x4 = Talbot Subsoil; x5 = Surface Material 1; x6 = Surface material 2

Figure 3.10: Actual mixing input for fine particle data showing similarity between source vectors

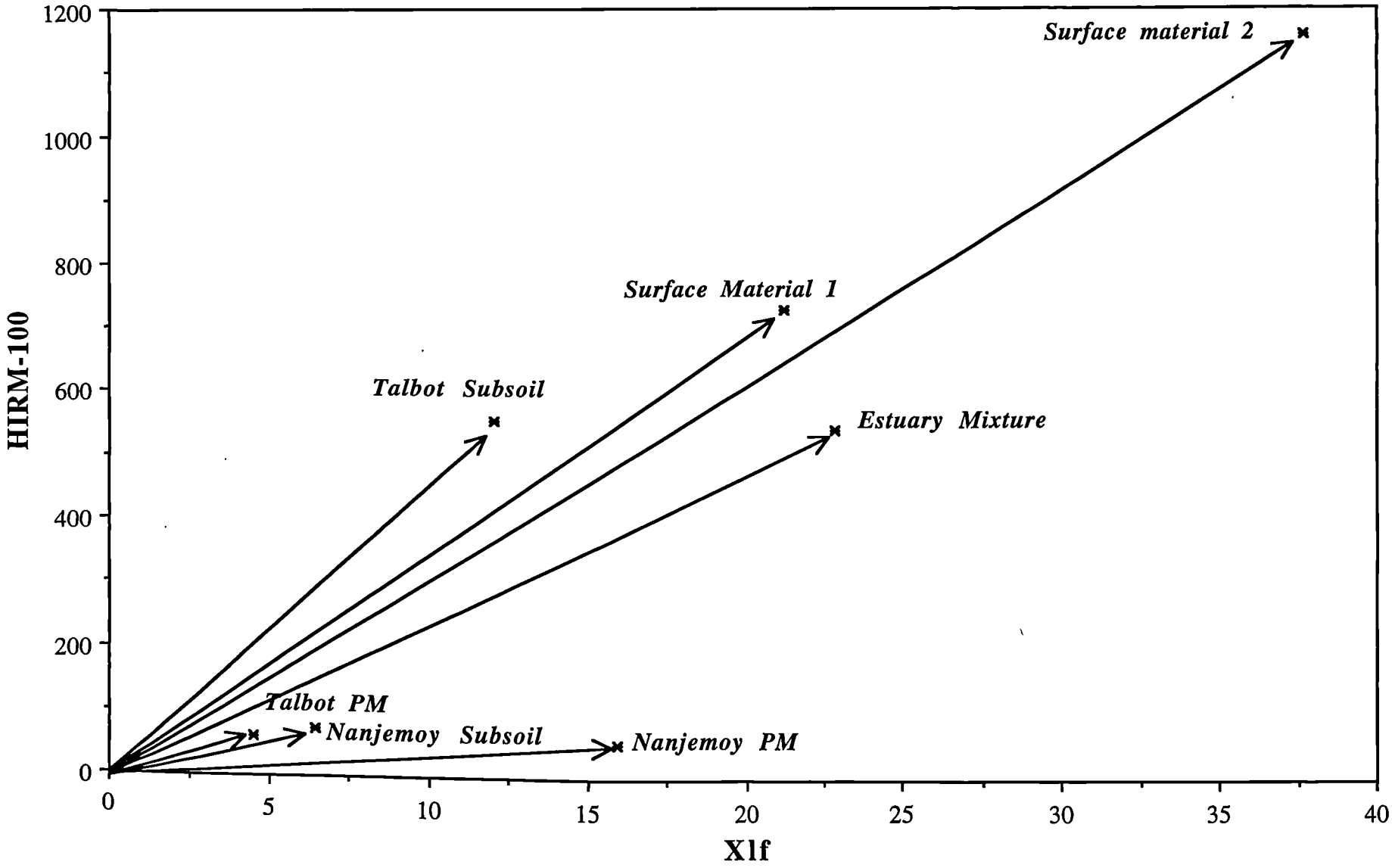

3.2 Evaluation of magnetic parameters

Introduction and Aims

This section explores the relationships between magnetic parameters in statistical and graphical terms using data from sample databases described below and listed in Appendix 2. The database measurement results were used to fulfil the following aims:

1. To set the ranges of magnetic values in different environments using databases with over 1000 samples
2. To study the interrelationships between magnetic parameters for the different databases
3. To evaluate the use of traditional bi-variate classification methods against multivariate statistical classification methods

Initial Data Collection

Four main databases were compiled during the first year of research, these were subsequently subdivided further as the research and sampling progressed (See Table 3.5). A full range of measurements (see Appendix 1) was made on the samples and a description of each sample in the databases can be found in Appendix 2. Samples collected as part of the work in Section C (Chapters 7 and 8) are listed in Appendix 2 but were not used in the preliminary work presented here. A brief outline is given here of the aims of using each set of samples in the preliminary work. All samples collected for the databases, despite their physical diversity, were air dried and sieved (where applicable) to less than 2mm. Leaf and filter samples were air dried and then cut into 2mm diameter disks using a brass tube cutter and stacked into 10ml pots horizontally. The main databases are as follows:

* *Rock Database* - Sixty one British samples from the Coventry University, Geography Department Rock Collection were measured (35 samples data supplied by Mr A P Lovejoy, 1991). Aim: Identification and classification of those rocks which may be discriminated for mineral and source modelling.

* *Soils/Sediments Database* - The database includes 13 soil profiles and 265 other samples from numerous areas including a range of parent materials, drainage and land use situations (150 gleyed soil samples were collected by Mr C. White). Forty bedload samples from the River Sowe and Finham Brook, Coventry were also included. Aim: Classification of topsoils, subsoils and bedloads in order to identify the types of materials suitable for source modelling.

* *Pollution Database* - Fifty-five samples were collected from the Coventry and Warwickshire area, including leaves, dusts, contaminated topsoils, organic materials and combusted material. A few fablon dust collectors were also obtained from the Environmental Health Department in Coventry. Aim: Classification of a wide range of materials in order to identify tracing and unmixing prospects for source and mineral modelling of atmospheric dusts.

* *Synthetics Database* - Thirty-eight samples were obtained from academic sources (including Dr B A Maher,

University of East Anglia) and commercial (Magnox) sources. The database also includes 82 samples of magnetites of different grain sizes, hematites, maghemites and goethites of varying dilutions and chemical reagents. Aim: To enable use of measurements of certain types of synthetic magnetic minerals and of different grain sizes in the modelling of mineralogies of environmental materials.

Measurement Evaluation

Evaluating magnetic measurements for classification and modelling is an important aspect of the research. The relationships between magnetic parameters have been analysed to determine those which were found to be the most important parameters for classification of materials in different sample databases. The fewer measurements needed to obtain a reliable classification the better, therefore correlation of large data sets and comparison between classification results using various numbers of measurements was carried out. The measurements used in modelling and classification have to be linearly additive and the list of measurements in Table 3.4 has been sub-divided on this basis. Linear measurements are considered here as these are the only parameters which can be used in modelling techniques but some of the ratios listed are used in bi-variate classifications in this section.

Table 3.4: Magnetic Measurements used in classifying database samples.

Initial Linear Measurements	**Linear Calculations**	**Ratios**
χlf (μm^3 kg^{-1})	χfd (nm^3 kg^{-1})	χfd (%)
χhf (μm^3 kg^{-1})		
ARM (mAm^2 kg^{-1})	χarm (μm^3 kg^{-1})	
IRM880 (mAm^2 kg^{-1})		χarm/IRM880 (mAm) IRM880/χlf (kA m^{-1}) IRM880/χfd (MA m^{-1})
IRM-100 (mAm^2 kg^{-1})	HIRM-100 (mAm^2 kg^{-1})	HIRM/χlf (kA m^{-1}) HIRM/χfd (MA m^{-1})
IRM+100 (mAm^2 kg^{-1})	HIRM+100 (mAm^2 kg^{-1})	
IRM Curves (20 point curves from fields of 0 --> 880 mT		IRM_X/IRM1T (Normalized IRM curve)
VSM IRM Curves (up to 200 points from fields of 0 --> 1T)		IRM_X/IRM1T (Normalized IRM curve)
Hysteresis Loops (+1 --> -1 Tesla) (All initial measurements also taken off curves)		Normalized Hysteresis Loop

Ranges in magnetic properties of databases

The ranges of selected linear magnetic parameters have been calculated in this section for all of the compiled databases. The main aim was to assess the possible overlaps in magnetic properties between similar groups of materials. Ranges of values for χlf and χfd% have been diagrammatically expressed for ease of reference in Figures 3.11a and b respectively. From the results in Table 3.5, mean values show that environmental groups of samples show great ranges of values and coefficients of variation are commonly above 50%. This is especially true of the geological and pollution databases where a diversity of mineral types and concentrations is found. A smaller range is seen in chemical and organic databases where consistently near-zero measurement values and no extreme values lower the overall range; CV% values however are large indicating the problems associated with using this measure in datasets containing arbitrary zeros (Chapter 2). In contrast, a large range is seen in the synthetics database with values of χlf for instance being between 0.8 and 1054.8 $\mu m^3 kg^{-1}$. CV% for χlf in this case is 70.8% however, compared to 151.6 in the chemical database. Lower variation was seen in the goethites in the synthetic database (although only 8 samples were available) indicating that in there was less contamination and fewer concentrational differences in this small set . However it was clear from the results for goethites and hematites that there were inclusions or contamination by ferrimagnetic minerals as shown by the high susceptibilities and IRM880 in some samples. This is more clearly shown in the IRM curves to be discussed shortly.

Table 3.5: Ranges of magnetic parameters for selected linear parameters for all databases giving statistical data and numbers of samples.

Environmental Databases

Variable	Mean	SD	CV%	Min	Max	N
Rock Database						
χlf	2.7	13.3	493.7	0	105.5	63
χfd	25.8	119.2	462.3	0	829.2	62
ARM	1.2	6.9	598.3	0	54.8	65
IRM880	29.4	92.7	315.1	0	502.1	65
HIRM-100	6.7	23.6	353.2	0	138.7	65
Soils Database						
χlf	0.5	0.6	135.6	0	8.3	392
χfd	27.3	44.0	161.4	0	293.7	381
ARM	0.1	0.1	142.9	0	1.1	393
IRM880	3.4	9.2	274.2	0	168.0	393
HIRM-100	0.4	1.4	342.5	0	17.7	393
Pollution Database						
χlf	3.3	5.7	171.6	0	38.6	98
χfd	27.5	52.4	190.5	0	407.0	94
ARM	2.2	17.3	795.4	0	177.8	110
IRM880	43.0	73.9	171.9	0	310.2	110
HIRM-100	4.0	10.4	256.7	0	85.4	110
Bedload Database						
χlf	0.3	0.2	78.6	0.1	1.0	60
χfd	4.5	4.5	100.0	0.8	28.2	60
ARM	0.0	0.0	133.3	0	0.2	59
IRM880	5.3	4.2	79.1	1.6	17.9	60
HIRM-100	0.9	0.9	98.9	0	3.9	60

Figure 3.11: Ranges of database Xlf measurements (a) and Xfd% values (b)

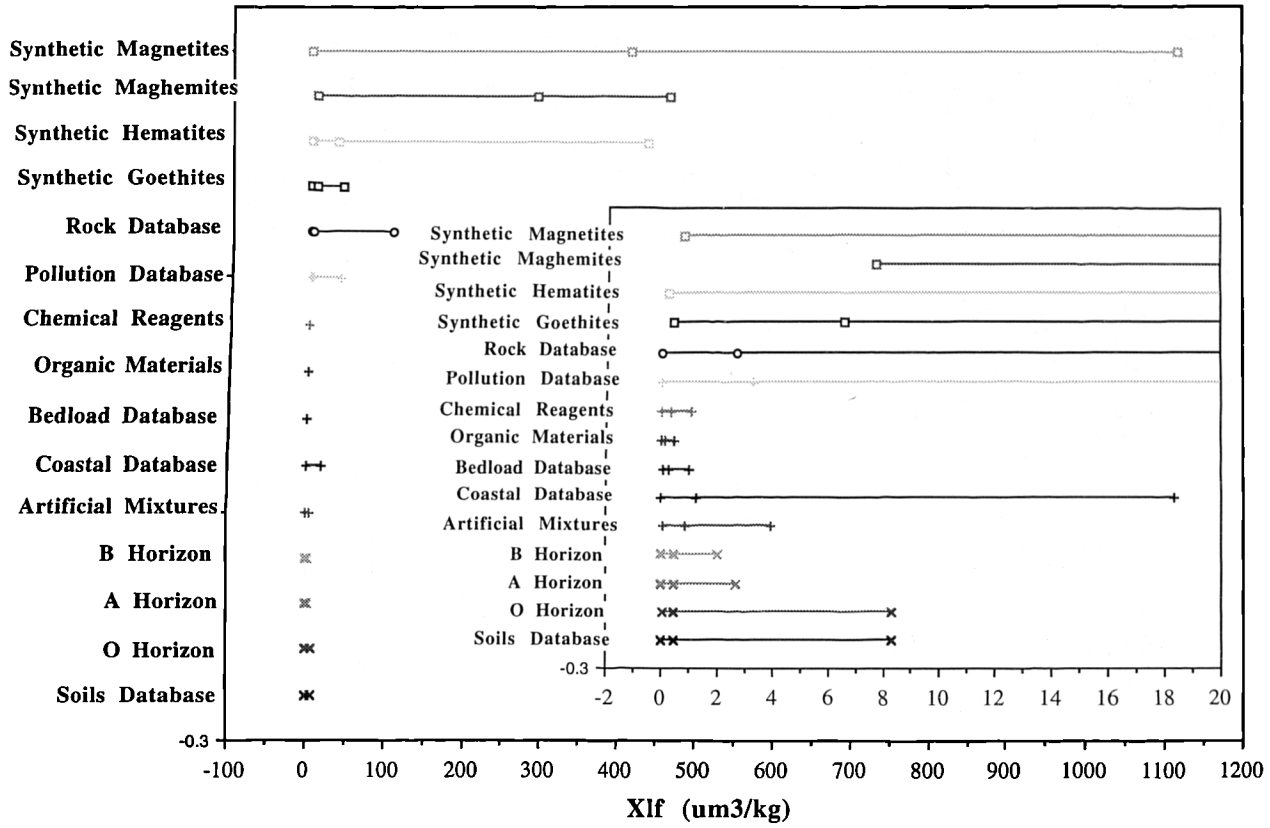

(b)

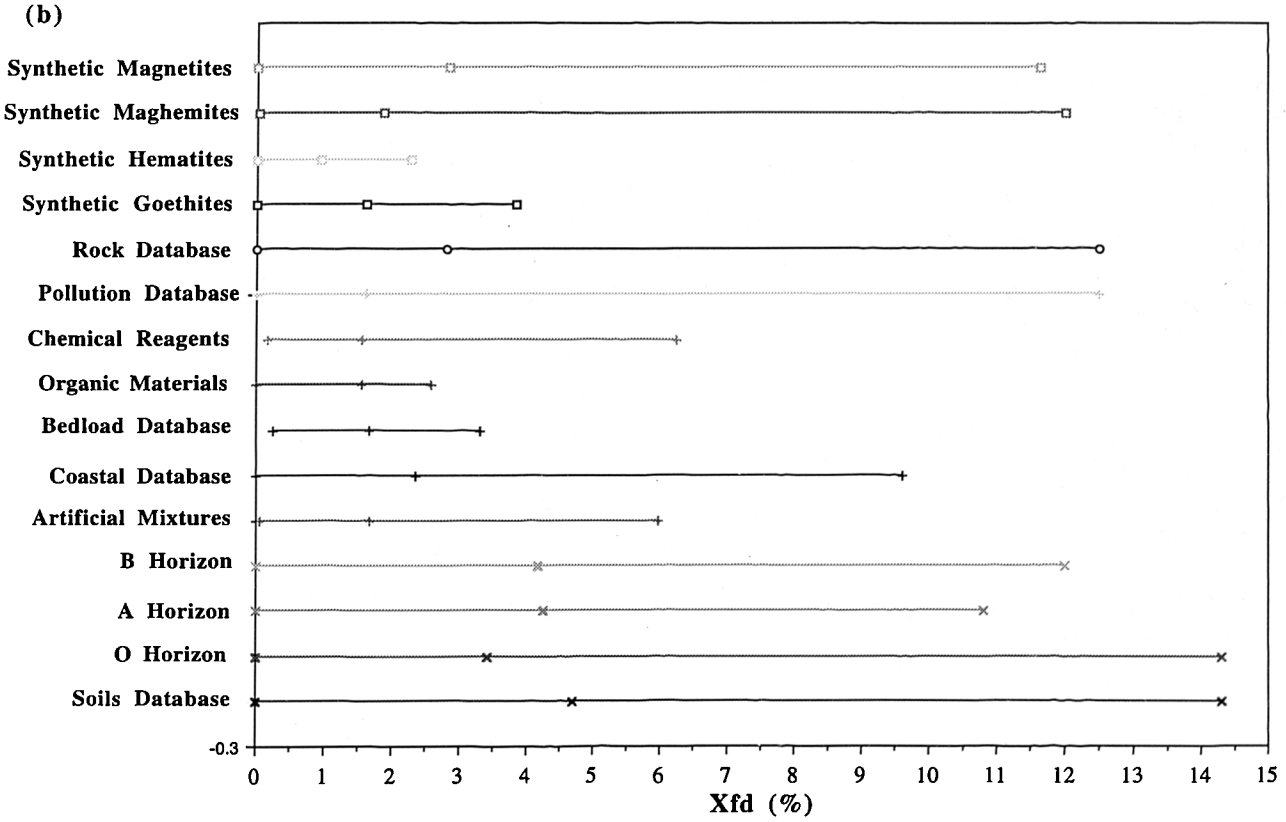

Table 3.5 continued

Variable	Mean	SD	CV%	Min	Max	N
Mixture Database						
χlf	0.9	1.0	112.5	0	4.0	71
χfd	8.6	7.1	82.5	0.4	36.2	71
ARM	0.1	0.1	100	0	0.3	71
IRM880	13.9	19.2	138.3	0.1	75.7	71
HIRM-100	1.7	1.5	91.1	0	6.8	71
Coastal Database						
χlf	1.3	3.1	244.9	0	18.3	77
χfd	11.5	22.1	191.9	0	138.4	76
ARM	0.5	3.5	694.0	0	30.6	78
IRM880	33.5	88.7	264.9	0	444.2	78
HIRM-100	4.9	15.1	308.8	0	101.9	78
Organic Database						
χlf	0.1	0.2	133.3	0	0.5	40
χfd	4.3	3.1	72.0	0	9.4	33
ARM	0	0	66.7	0	0.1	40
IRM880	1.6	2.3	140.6	0	6.9	40
HIRM-100	0.3	0.4	133.3	0	1.1	40
Chemical Database						
χlf	0.3	0.5	151.6	0	1.1	20
χfd	0.9	0.8	90.8	0.2	2.5	20
ARM	0	0	-	0	0.0	23
IRM880	0.2	0.1	80.0	0	0.3	23
HIRM-100	0	0	50.0	0	0	23

Synthetics Databases

Variable	Mean	SD	CV%	Min	Max	N
Magnetite Database						
χlf	414.2	293.3	70.8	0.8	1054.8	31
χfd	20533	33852	164.9	0.0	122174	21
ARM	121.4	125.9	103.7	0.1	372.7	30
IRM880	9711.3	9308.2	95.8	26.1	35129	24
HIRM+100	706.3	1091.7	154.6	9.9	4478.8	24
Maghemite Database						
χlf	291.8	179.9	61.6	7.7	464.1	24
χfd	1846.7	935.0	50.6	100.0	4800.0	24
ARM	92.4	23.7	25.7	26.0	122.6	23
IRM880	27684	9199	33.2	3681	33336	9
HIRM+100	5051.7	9452.3	187.1	130.8	30099	9
Hematite Database						
χlf	33.0	105.8	320.9	0.2	435.8	17
χfd	131.2	303.5	231.3	0.0	1128.7	16
ARM	5.8	19.8	343.8	0.0	79.8	16
IRM880	1670	6391	382.8	2.6	25635	16
HIRM+100	157.8	438.6	277.9	0.0	1791.1	16
Goethite Database						
χlf	6.6	14.4	218.4	0.4	41.5	8
χfd	97.5	231.8	237.8	0.0	666.7	8
ARM	0.9	1.9	202.2	0.0	5.5	8
IRM880	314.4	576.3	183.3	1.2	1335.8	8
HIRM+100	84.2	156.0	185.2	0.4	373.8	8

Maximum and minimum normalized IRM curves are shown for selected databases in Figure 3.12 and 3.13. Most of the database maximum curves are steep and remanence increases rapidly. The minimum curves have much gentler gradients and remanence increases more slowly with field. Many of the ranges of the curves appear to be very similar. It is clear that ferrimagnetic minerals indicated by maximum curves and canted-antiferromagnetic minerals indicated by minimum curves are represented in all the environmental sets. Chemical curves shown in figure 3.12d reveal the mainly ferrimagnetic contamination of the Analr chemical reagents. Soil curves given in Figure 3.13a have been subdivided into three soil horizons and synthetics curves in Figure 3.13b into four mineral types. From the soil curves it is clear that the O horizons are dominated by ferrimagnetic minerals and the B horizons are more dominated by canted-antiferromagnetic minerals. 'A' horizon soils fall between the two sets of curves. Synthetic curves shown in Figure 3.13b indicate the ferrimagnetic contamination or mineral inclusions in some of the goethite and hematite samples. Fine-grained magnetite curves (Figure 3.13b) rise more steeply than those of the other databases showing that curves of environmental samples generally indicate mixtures of different ferrimagnetic mineral grain sizes and other non-ferrimagnetic minerals.

Statistical inter-relationships of magnetic parameters

Five files were constructed for comparison between parameter correlations presented here and results of classification techniques presented in the following section. The first was a subset of the Alldata file containing 226 samples taken from the complete range of materials collected; secondly a geological file containing 45 samples; thirdly a soil file with 31 samples from a wide range of soil types; fourthly a pollution file (60 samples) and finally a synthetics file (79 samples). All samples and data used have been collected by the author apart from having access to Maher's synthetic magnetites (10 samples) for the synthetics database. Consistency of sample preparations and measurement made on all the database samples is therefore guaranteed. Correlations were performed on the five data-sets using the linearly additive magnetic parameters of χlf, χfd, χarm, IRM880, IRM100 and HIRM100. HIRM-100 and HIRM+100 have been used interchangeably in this section as in the early stages of research backfield (-100) measurements were used but +100 fields were then found to be more reliable in later tests. The implications of this are discussed in the next section of this chapter. Tables 3.6 to 3.10 give selected results and the probability values for the correlations (1-tailed correlation). χhf correlations always gave similar results to those of χlf as these two parameters generally only differ by up to 15% (χfd%).

Table 3.6: Correlations (r) and probability values (p) for selected samples of the Alldata database (n=226).

	χlf				
χfd	.7445				
	P= .000	**χfd**			
χarm	.1488	.1301			
	P= .013	P= .025	**χarm**		
IRM880	.6488	.3914	.2082		
	P= .000	P= .000	P= .001	**IRM880**	
IRM+100	.4499	.3045	.0447	.6812	
	P= .000	P= .000	P= .215	P= .000	**IRM+100**
HIRM+100	.1731	.0955	.4809	.6352	.3579
	P= .005	P= .076	P= .000	P= .000	P= .000

Figure 3.12: Maximum and minimum normalized IRM curves for selected databases

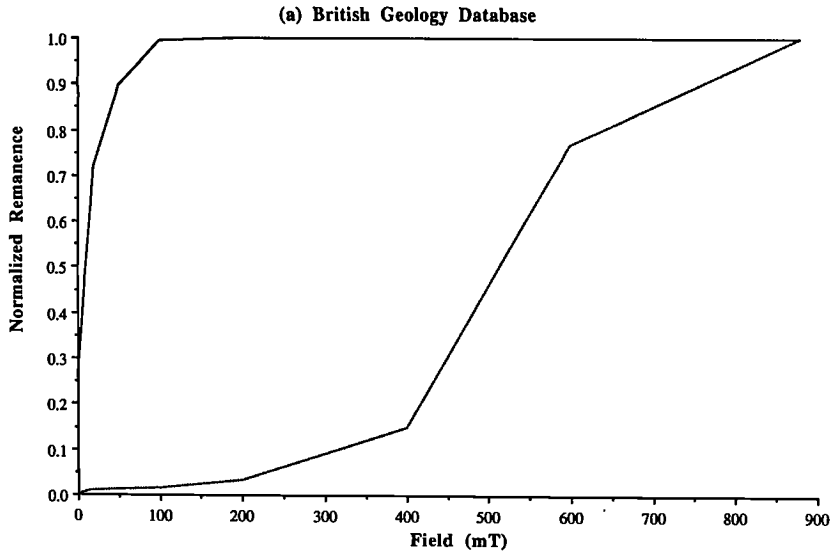

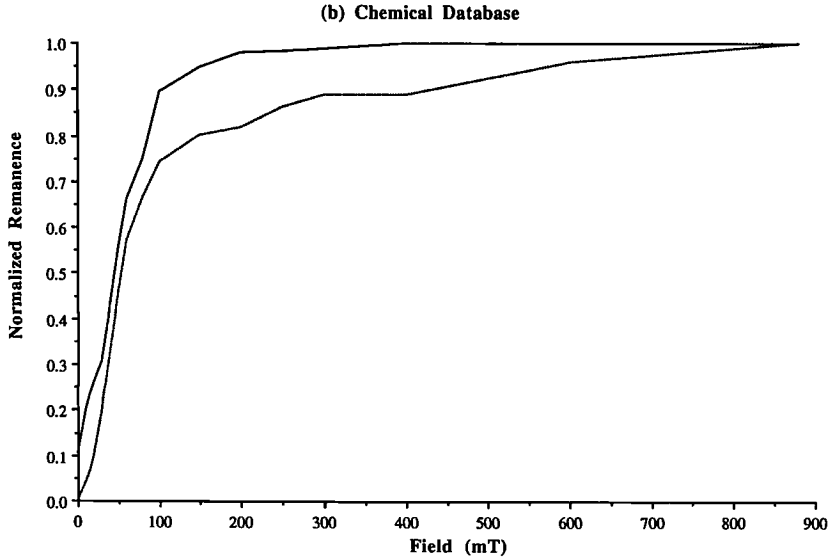

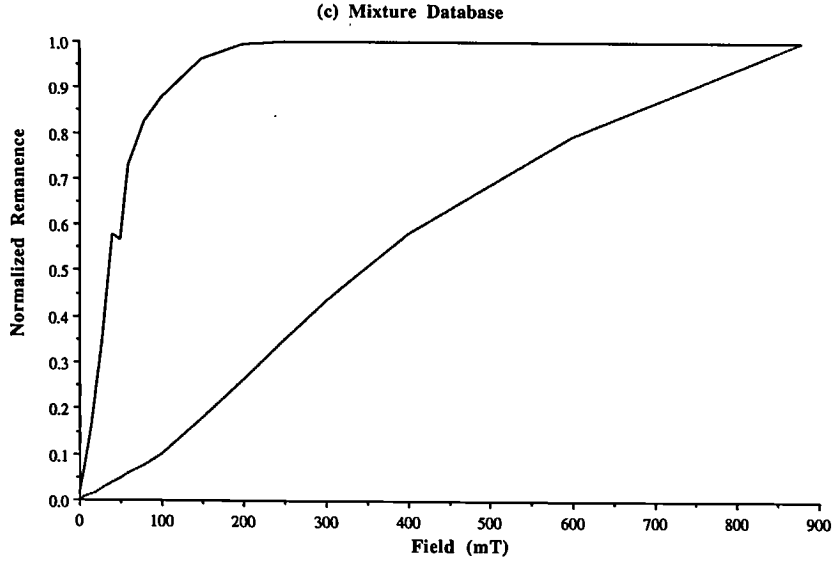

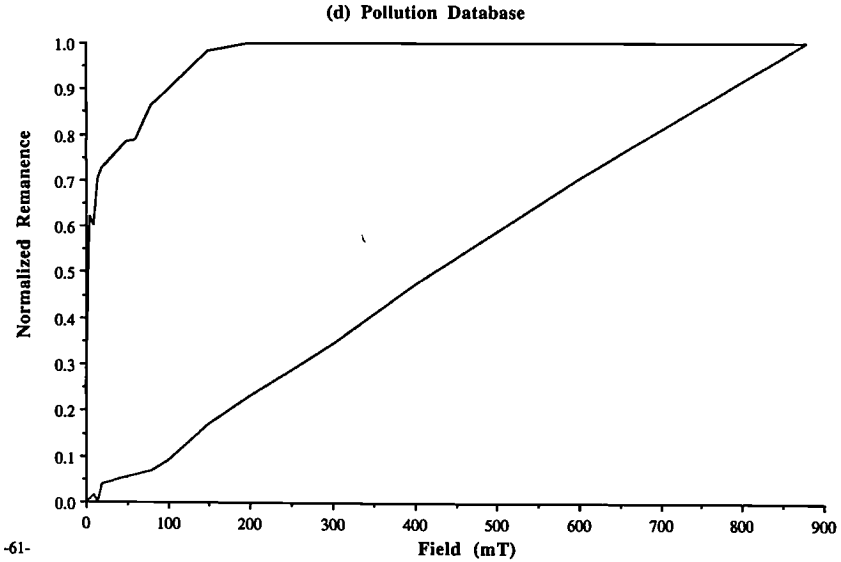

Figure 3.13: Maximum and minimum normalized IRM curves for soils database (a) and synthetic database (b)

(a)

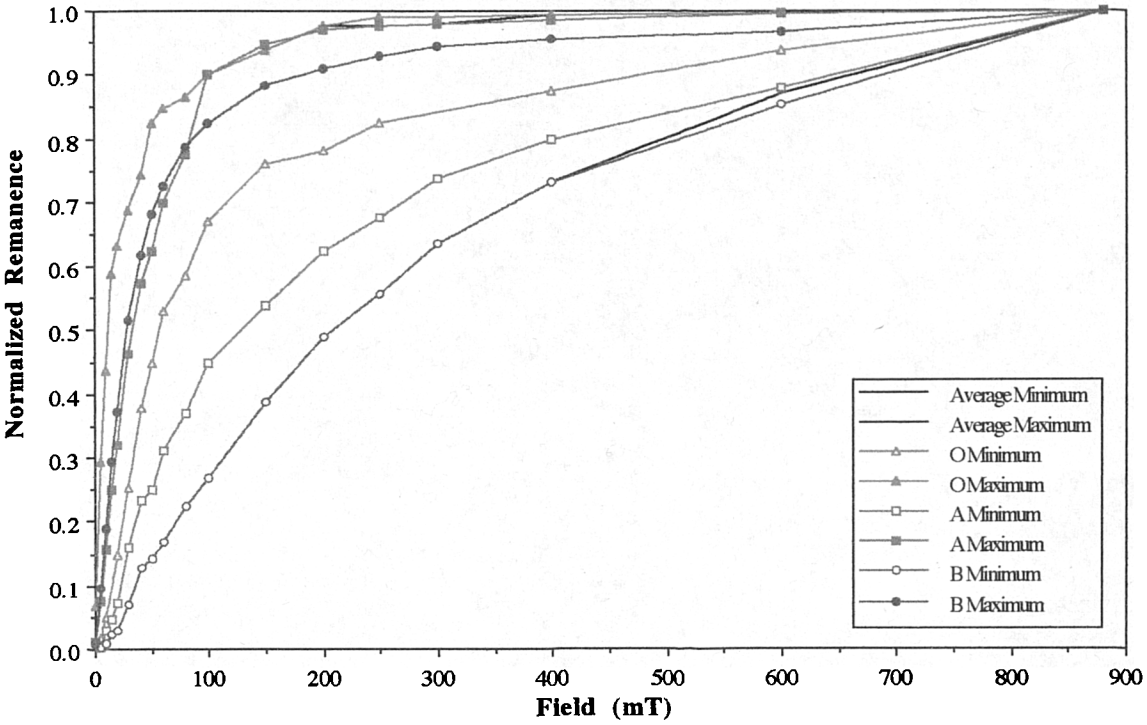

(b)

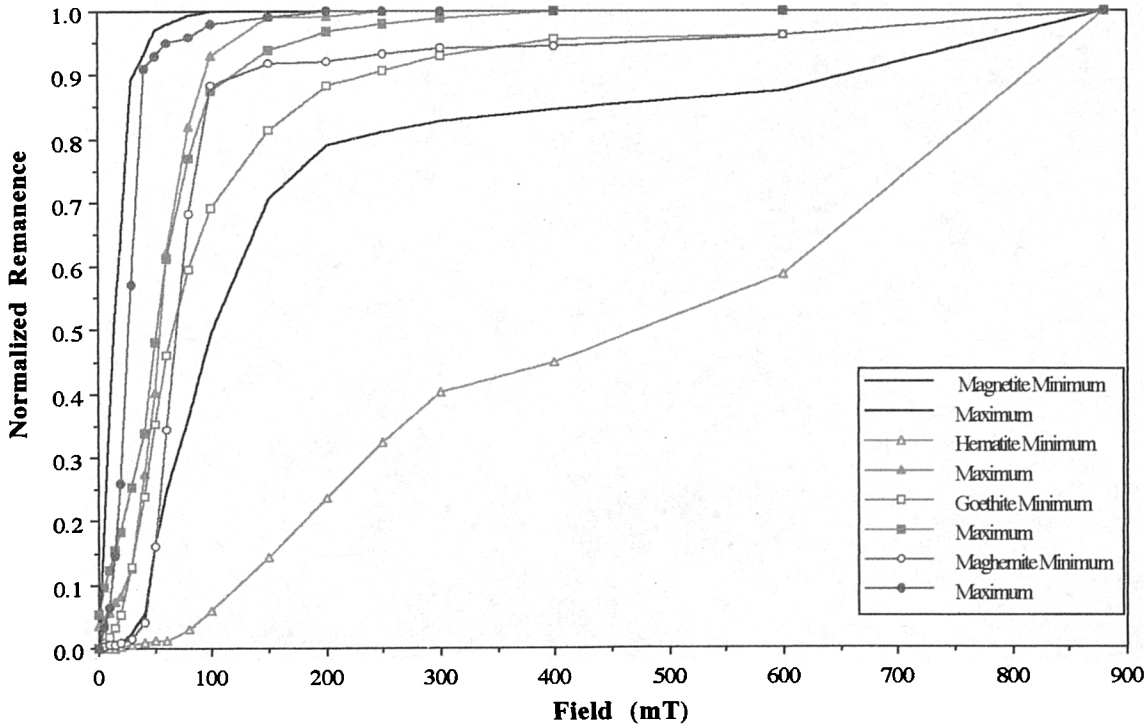

Most of the magnetic parameters in Table 3.6 are highly correlated with significance values of 0.0001, IRM-100 and HIRM-100 for instance (r=0.3579). χlf and χfd, IRM880, IRM-100 and HIRM-100 parameters are those which are interrelated through linear calculation and although they are widely used together, they are usually treated as independent parameters which indicate different properties of a material. Parameters which were surprisingly not related are χfd and χarm (r=0.1301) both of which are supposed to identify fine-grained magnetites. This may be because many samples contain mixtures of fine and coarse-grained magnetites. χarm is also not significantly correlated to IRM-100 (r=0.0447) indicating that perhaps the majority of samples in the database are dominated by coarser grained magnetites.

Table 3.7: Correlations (r) and probability values (p) for selected samples of the geology database (n=45)

	χlf				
χfd	.8951				
	P= .000	**χfd**			
χarm	.1217	.0619			
	P= .213	P= .343	**χarm**		
IRM880	.7048	.6651	.4392		
	P= .000	P= .000	P= .001	**IRM880**	
IRM-100	.8015	.7467	.2893	.9193	
	P= .000	P= .000	P= .027	P= .000	**IRM-100**
HIRM-100	.0624	.1378	.8021	.6780	.4588
	P= .342	P= .183	P= .000	P= .000	P= .001

For the geological samples (Table 3.7) again most magnetic parameters are closely correlated. χlf is not significantly related to χarm (r=0.1217) which may be explained in terms of coarse-grained minerals having low χarm, but also χlf has a paramagnetic influence not seen in the remanence measures. HIRM-100 and susceptibility measures are also not significantly related indicating that there is a wide range of minerals (ferrimagnetic and canted-antiferromagnetic) contributing to the overall magnetic properties of the data-set. In this sense HIRM-100 indicates canted-antiferromagnetic minerals and χlf and χfd indicates ferrimagnetic minerals.

Table 3.8: Correlations (r) and probability values (p) for selected samples of the soils database (n=31).

	χlf				
χfd	.9820				
	P= .000	**χfd**			
χarm	.9340	.9312			
	P= .000	P= .000	**χarm**		
IRM880	.6680	.5898	.7306		
	P= .000	P= .000	P= .000	**IRM880**	
IRM-100	-.8545	-.7855	.8707	-.9450	
	P= .000	P= .000	P= .000	P= .000	**IRM-100**
HIRM-100	-.0952	-.1568	.0458	.6413	-.3551
	P= .305	P= .200	P= .403	P= .000	P= .025

All parameters for the soils database (Table 3.8) are closely correlated in this soil data-set apart from χlf, χfd, χarm and IRM-100 with HIRM-100. χarm and HIRM-100 have the lowest correlation (r=0.0458) indicating both finer

grained ferrimagnetic mineral dominated soils (topsoils/brown earths/rendzinas) and canted-antiferromagnetic mineral dominated soils (subsoils/gleys) in the data-set. χarm and HIRM-100 or χlf and HIRM-100 would best classify the soils database.

Table 3.9: Correlations (r) and probability values (p) for the pollution database (n=60)

	χlf				
χfd	.7266				
	P= .000	**χfd**			
χarm	.2542	.2905			
	P= .025	P= .012	**χarm**		
IRM880	.8435	.4739	.2407		
	P= .000	P= .000	P= .032	**IRM880**	
IRM-100	-.8368	-.4745	.0550	-.9440	
	P= .000	P= .000	P= .338	P= .000	**IRM-100**
HIRM-100	.3392	.1794	.8539	.5261	-.2159
	P= .004	P= .085	P= .000	P= .000	P= .049

Pollution samples are dominated by coarse-grained ferrimagnetic particles such as fly ash. This is indicated in Table 3.9 by low r values for χlf, χfd with χarm (r=0.2542 and 0.2905 respectively). Canted-antiferromagnetic minerals such as hematite dominate some of the samples included in this database (tile works dust for example). These cause the low r values between HIRM-100 and the ferrimagnetic indicating parameters especially χfd (r=0.1794).

Table 3.10: Correlations (r) and probability values (p) for the synthetics database (n=79).

	χlf				
χfd	.6716				
	P= .000	**χfd**			
χarm	.7555	.6807			
	P= .000	P= .000	**χarm**		
IRM880	.5090	-.0325	.3580		
	P= .000	P= .413	P= .003	**IRM880**	
IRM+100	.5215	-.0044	.3772	.9422	
	P= .000	P= .488	P= .002	P= .000	**HIRM+100**
HIRM+100	0.1373	-.0784	.0693	.4846	.1635
	P= .154	P= .298	P= .304	P= .000	P= .112

The results in Table 3.10 indicate similar patterns to the previous correlation tables. χlf is significantly correlated with all parameters (no significant paramagnetic or canted-antiferromagnetic components) except HIRM-100 (r=0.1373, canted-antiferromagnetic minerals). χfd is also significantly correlated with all parameters except IRM880 (r=-0.0325), indicating samples with different ferrimagnetic grain size in this database. This is not seen in environmental materials due to the extensive mixing of widely dispersed ferrimagnetic minerals (both primary and secondary) of different grain sizes. In this data-set however, there are samples with discrete critical grain size ranges (Maher's fine-grained magnetites and Magnox coarse-grained magnetites and maghemites). Again HIRM-100 is not highly related to any of the parameters, except IRM880 (r=0.4846), with which it is linearly interrelated by calculation.

Most of the magnetic parameters used in the databases are highly correlated especially where domination by ferrimagnetic minerals exists. Only in cases where discreet grain-sized samples exist (for example the MT magnetite samples in the synthetics database) are the correlations between parameters indicating fine grains and total ferrimagnetic concentration not significantly related. In fact all remanence measurements were always found to be highly correlated in tests of sub-sets of the databases. In general low correlations between HIRM+100 with IRM+100 indicate that in most cases these two interrelated parameters may be used together with interpretational care. The implications of using interrelated parameters is further discussed in the classification section of this chapter. These results overall signify the most useful discriminatory parameters which are susceptibility parameters (χlf and χfd) and HIRM+100.

Evaluation of magnetic parameters using bi-variate scatter-graphs

In this section only bi-variate scattergrams of three database sub-sets are presented. First an Alldata file which contains all databases except the synthetic database has been collated; secondly the soils database is again subdivided into O, A and B horizons (not soil survey definitions, 0-5, 10-20 and 40-50cms generally) and the third a synthetics database is divided into four mineral types (magnetite, maghemite, goethite and hematite). Results from this research are compared with similar results for other workers' large databases where possible. In some cases all database results have been presented in log form due to the large positive skew in the databases (especially the synthetics database). An overview of the parameters discussed here is given in Appendix 1.

Susceptibility parameters can be used to discriminate between ferrimagnetic and canted-antiferromagnetic minerals and different grain sizes of ferrimagnetic minerals (especially SP/SD boundary, see previous section). Susceptibility parameters have been used here to discriminate between the database samples. χlf versus χfd% and χfd versus χfd% bi-variate scattergrams are presented for all databases in Figure 3.14, for the soils database in Figure 3.15 and for the synthetics database in 3.16. These two diagrams of each database can be compared directly to identify those samples which have minerals contributing to χlf but which are not ultrafine-grained ferrimagnetic minerals as indicated by medium to high χfd%. The scales on diagrams 3.14, 3.15 and 3.16 have been numerically matched according to the concentrational units of χlf (μm^3kg^{-1}) and χfd (nm^3kg^{-1}) assuming a sample volume of 10g. χfd% is effectively a normalized parameter (χfd/χlf*100) where effects of skew in the data are eliminated. Taking the pollution database as an example from Figure 3.14 a and b, high χlf values of 10 um^3kg^{-1} and lower χfd values of 10 nm3kg1 indicate that the materials are dominated by coarse-grained ferrimagnetic minerals and therefore the ratio gives a χfd% of only 1%. Soil samples on the other hand have larger concentrations of fine-grained ferrimagnetic minerals indicated by similar χlf and χfd values and a χfd% ratio with values of 6 and above. It is clear that all the databases contain widely varying concentrations of minerals and different grain sized ferrimagnetic minerals. The line drawn on Figure 3.14a indicates those samples which have kappa values of less than 10 and which are subject to unacceptably high measurement errors and consequently questionable χfd values.

Figure 3.14: Xfd % versus log Xlf (a) and Xfd% versus log Xfd (b) for all databases

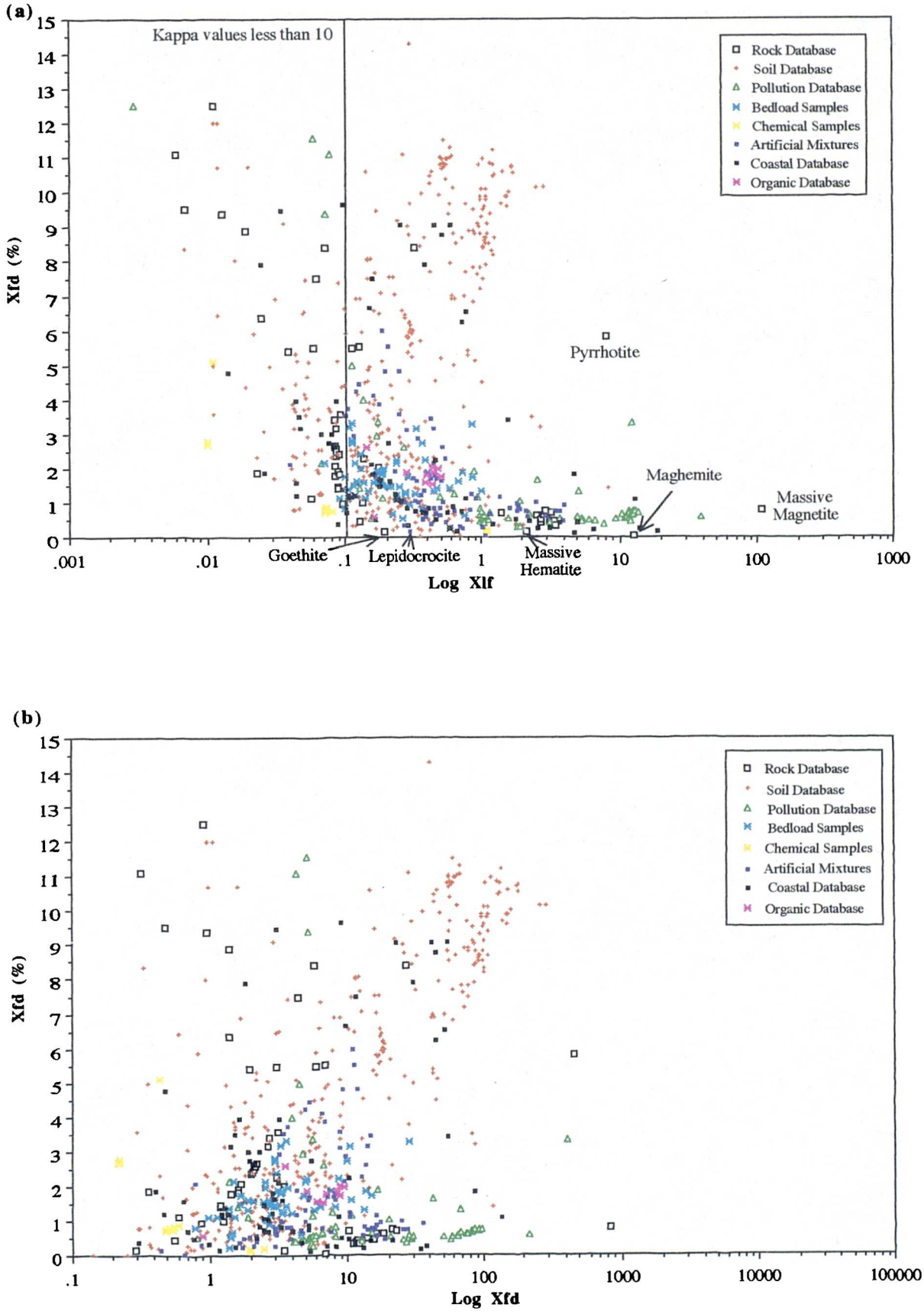

Figure 3.15: Xfd% versus Xlf (a) and Xfd% versus Xfd (b) for soil database

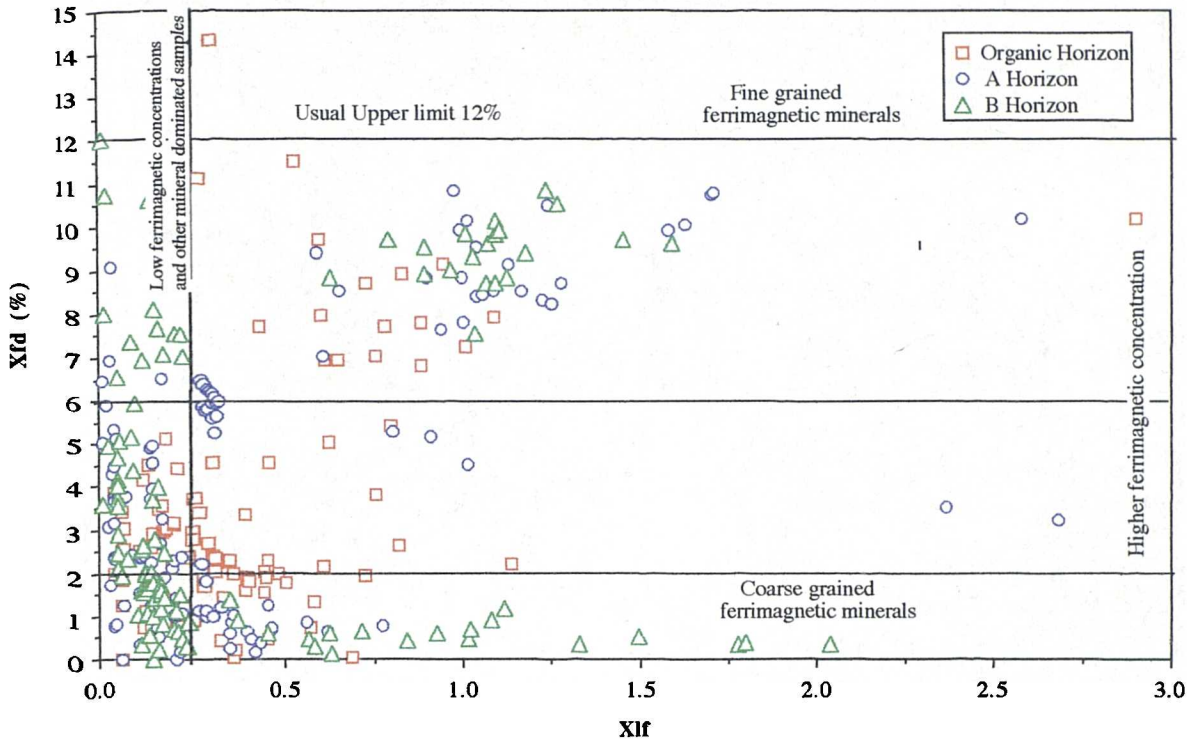

(b)

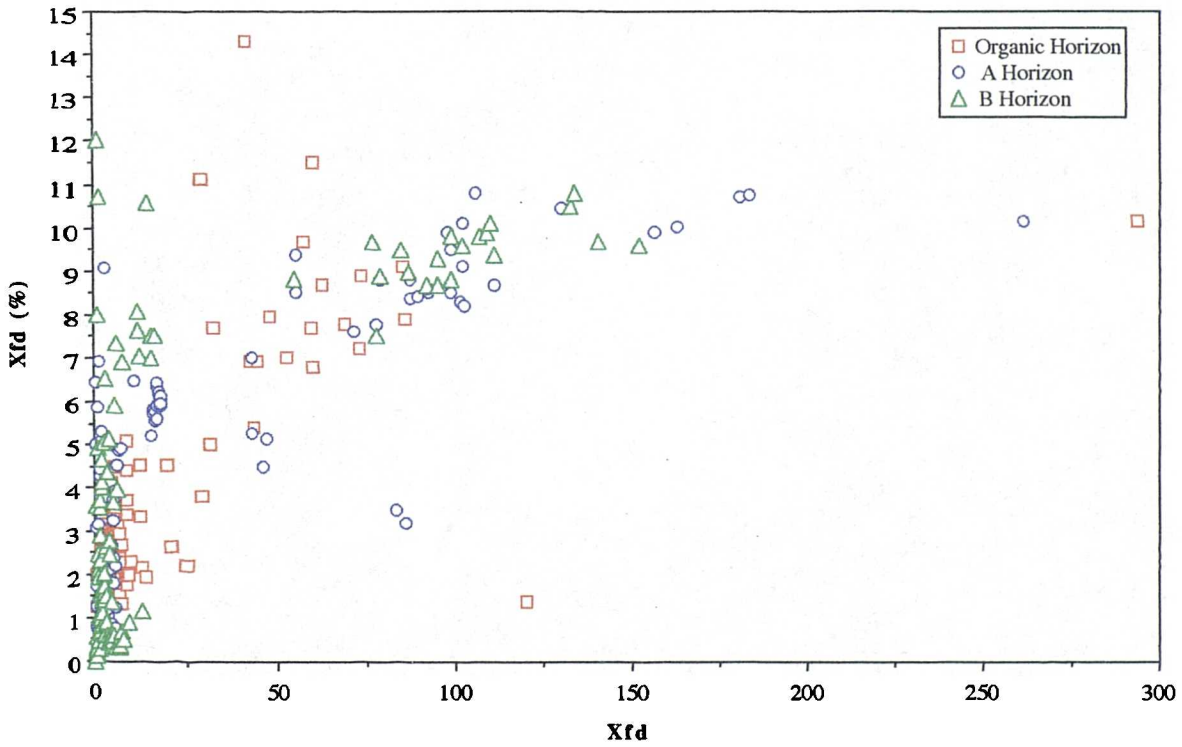

Figure 3.16: Xfd% versus Xlf (a) and Xfd% versus Xfd (b) for synthetic database

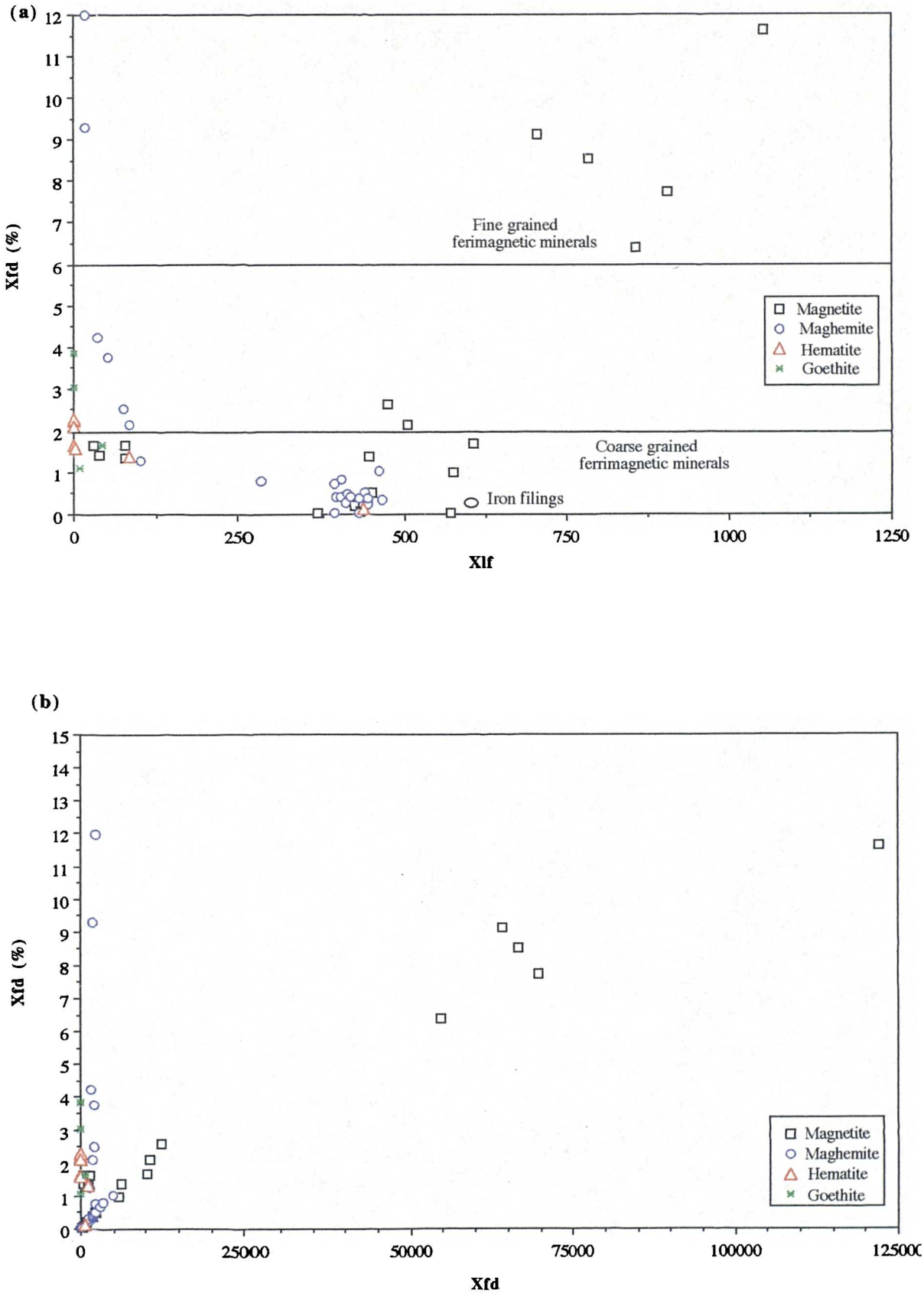

A simple classification can be made, especially with soil samples, as shown in Figures 3.15a and b. B horizon soils tend to span the extremes of the database including samples with coarse-grained ferrimagnetic minerals with χfd% values of less than 2% and fine-grained ferrimagnetic minerals with χfd% values of over 6%. These signify (subjectively) two broad soil drainage characteristics, (a) poorly drained gleyed soils and (b) well drained rendzinas and brown earths. 'A' horizon soils fall within these bounds and O horizon soils within the bounds of the A horizon, indicating mixing of O and B horizons. A few soil samples, which may be contaminated with iron for instance, are indicated in the far right of the diagram with χlf ($\mu m^3 kg^{-1}$) values over 2 and χfd ($nm^3 kg^{-1}$) values over 180. All coarse-grained dominated soil samples have moved towards the y axis (low x values) upon calculation of χfd. Some O horizon soils have higher mineral concentrations (χlf) and higher χfd%, (2-6%) indicating the presence of some fine-grained minerals and some atmospheric pollutant particles (see also Chapter 9). Values which appear above a χfd% of 10% and have low in mineral concentrations (low χlf) and represent samples of rendzina soils and limestones which had kappa values of less than 10. These samples have been left in the databases for completeness but probably have large measurement errors.

Figure 3.16a indicates a wide range of ferrimagnetic mineral concentrations and grain sizes. Maher's fine-grained magnetite samples have high χlf (500-1000 $\mu m^3 kg^{-1}$) values and a range of χfd% values between 2 and 12%. Most of the Magnox magnetites, maghemites, hematites and goethites and a sample of dispersed iron filings display low χfd% values (<2%). A few maghemite samples with lower concentration values but higher χfd% values of up to 12 are also present. These samples were not those with kappa values in the high error range (K<10). In Figure 3.16b the linear relationship seen between χfd and χfd% for many of the samples indicates the dominance of a ferrimagnetic mineral content with different critical grain sizes (as described in Chapter 2). Samples which span the x=0 axis with χfd% between 1 and 12 indicate the presence of other minerals as well as a proportion of fine-grained ferrimagnetic minerals (contaminated hematite and goethite samples).

ARM versus χlf parameters have been used to indicate superparamagnetic grains (SD size) and mineral type and concentration. Banerjee et al.(1982) used these parameters to discriminate between different lake core data with reasonable success. Figure 3.17a, 3.18a and 3.19a show ARM versus χlf for the three data-sets. A relatively linear relationship between the two parameters is shown in Figure 3.17a (note the log axis however). Some samples of the organic database have higher ARM values but lower mineral concentrations (χlf), indicating that these samples have a fine-grained component. Bedload samples however display lower ARM values but higher χlf values indicating some canted-antiferromagnetic minerals and coarse-grained ferrimagnetic minerals in these samples. There are groups of database samples which display set ratios of ARM/χlf. For instance, some soil samples have ratios above and below the main groups, whilst some pollutants have a ratio value between those of the soils but have larger concentrations of ferrimagnetic minerals.

Figure 3.18a indicates two main ARM/χlf ratio values, one which indicates fine-grained ferrimagnetic minerals and one which indicates coarse-grained ferrimagnetic minerals. Samples which fall centrally between these two ratios are those which contain mixtures of fine and coarse-grained minerals. These ratios have also been marked on Figure

Figure 3.17: Log ARM versus log Xlf (a) and log Xarm versus log IRM880 (b) for all databases

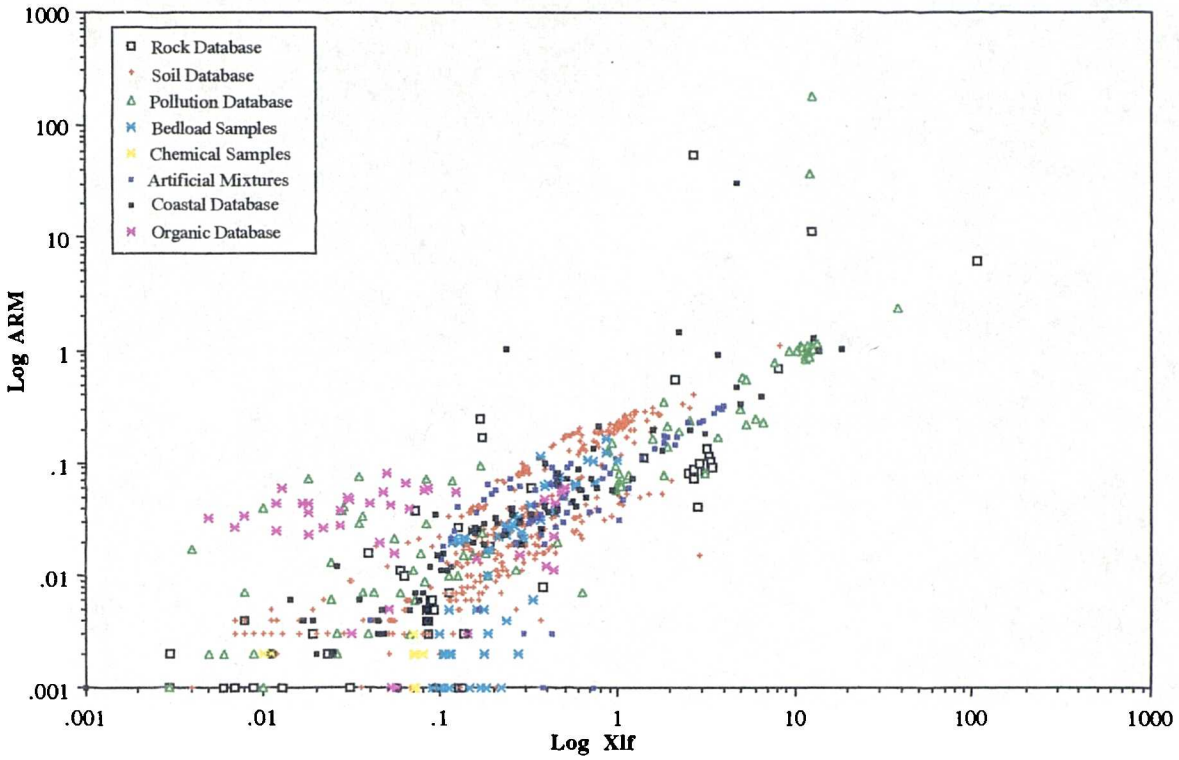

(b)

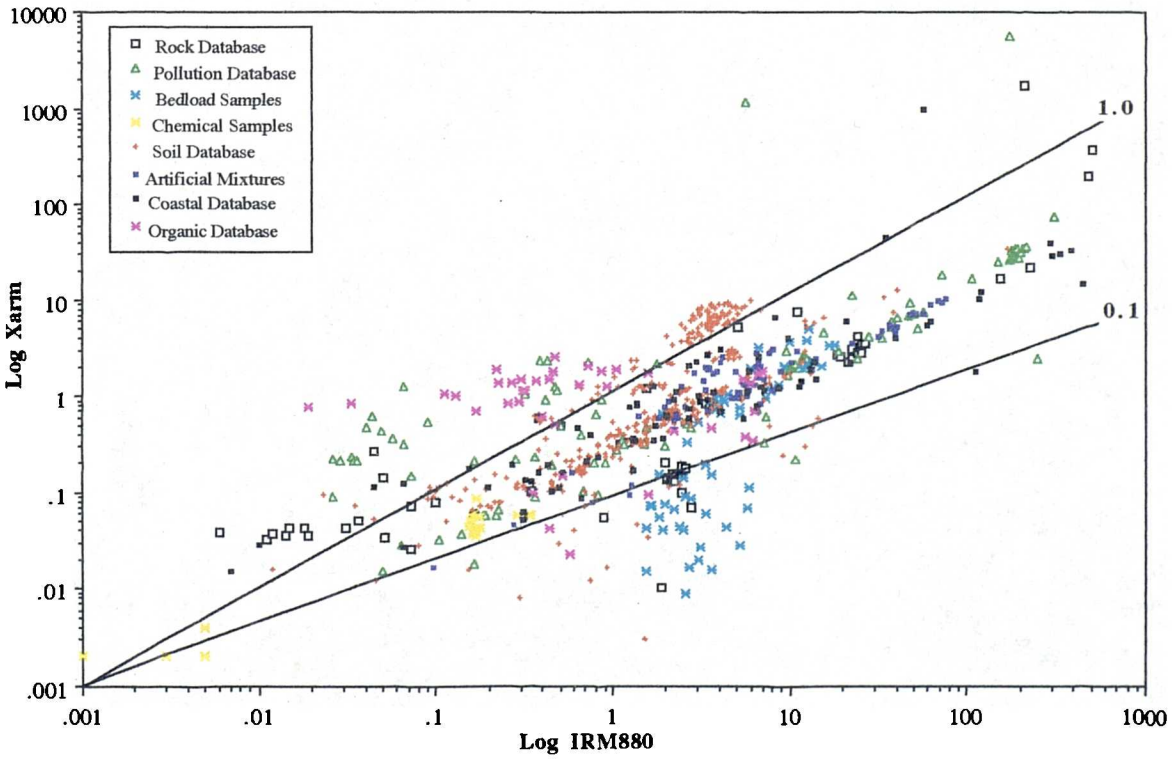

Figure 3.18: ARM versus Xlf (a) and Xarm versus IRM880 (b) for soils database

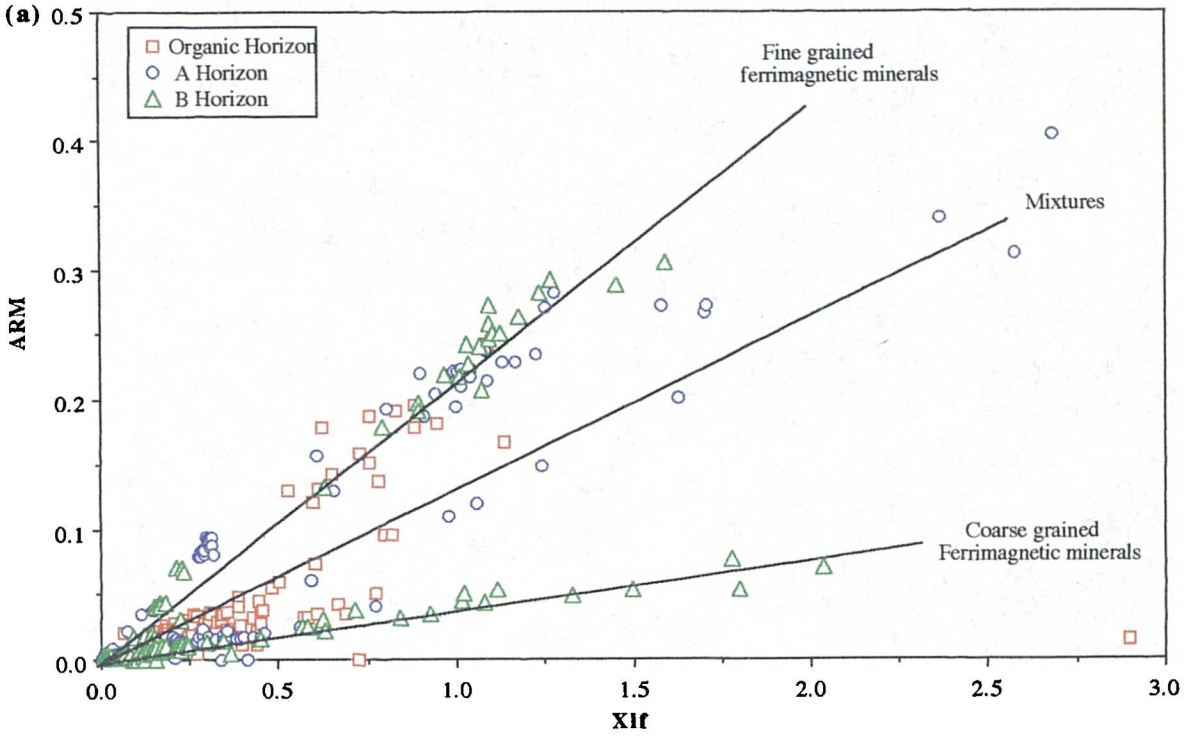

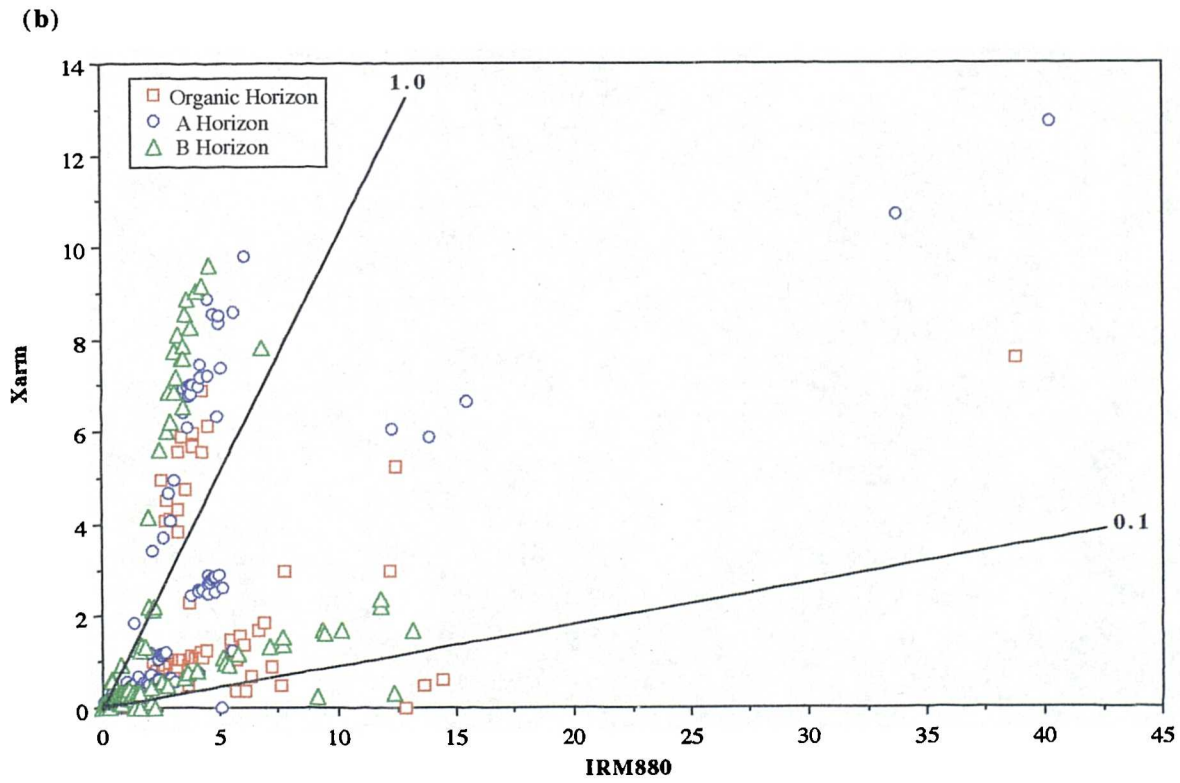

Figure 3.19: ARM versus Xlf (a) and Xarm versus IRM880 (b) for Synthetic database

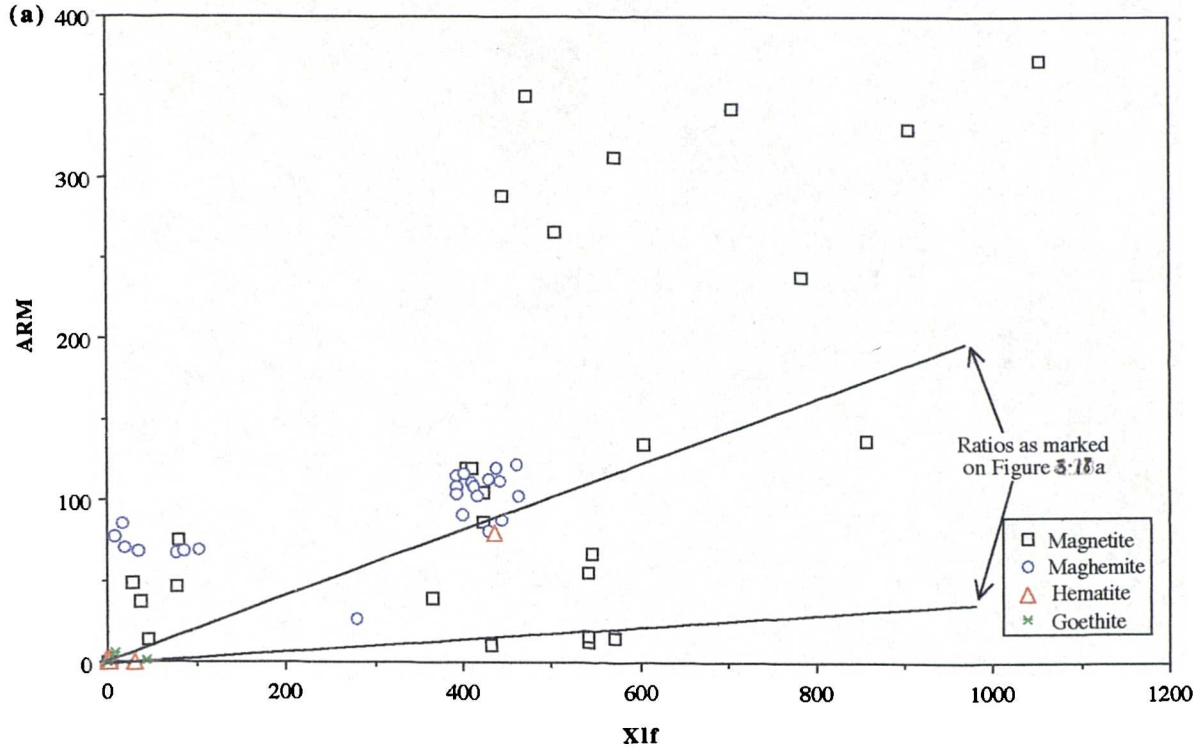

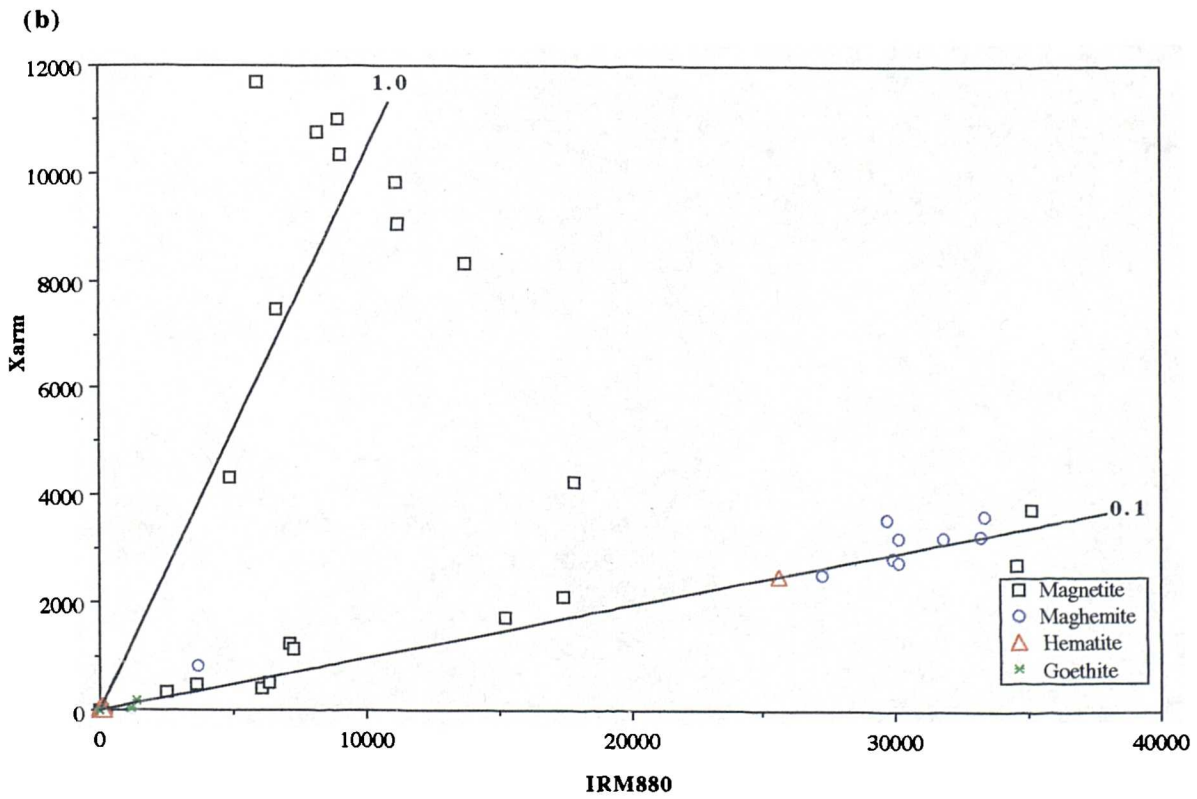

3.19a for comparison. Coarse-grained magnetites fall along the lower line (higher ratio) while most of the other samples and especially fine-grained magnetites appear above the higher line (lower ratio). Approximate percentage concentrations of certain grain sizes of ferrimagnetic minerals in the environmental materials can be calculated from these data. For example, taking a χlf value of 550 um^3kg^{-1} for a coarse-grained magnetite and a B horizon soil with a χlf of 2 μm^3kg^{-1}, a percentage concentration value of 0.36% is found. A similar answer is gained using ARM data.

Diagrams of the relationship between χarm and IRM880 are shown in conjunction with the ARM and χlf diagrams. χarm/IRM880 ratios are sensitive to grain size dimensions in magnetite and maghemite where a ratio of 0.1 indicates coarse-grained primary minerals and 1.0, indicates fine-grained secondary minerals (Maher, 1988). These ratios are marked on Figures 3.17b, 3.18b and 3.19b. Most database samples fall between the marked ratios indicating mineral and grain-size mixtures, but some bedload samples appear below the ratio of 0.1 (hematites) and organic samples appear above the ratio of 1 (paramagnetic minerals). Some soils and rock samples appear above the ratio of 1.0 also indicating the presence of canted-antiferromagnetic and/or paramagnetic minerals in these mainly gley soils and sedimentary rocks. Figure 3.18b shows the two distinct sub-sets of soil types within the soils database; soils with ratios of 0.1 are mainly gleys and soils with ratios of 1.0 are mainly rendzinas and brown earths. A set of polluted organic matter samples from beneath a pine wood falls between the two ratios, indicating coarse and finer-grained ferrimagnetic minerals. Many of the Magnox synthetic samples of magnetite, maghemite, contaminated hematite and some goethites appear along the 0.1 ratio while the fine-grained magnetite samples fall just above and below the ratio value of 1.0.

Figures 3.20a, 3.21a and 3.22a show the relationship between χlf and IRM880 indicating the concentration of mainly ferrimagnetic minerals and the volume concentration of remanence carrying minerals. There is a strong correlation between these two parameters for all the databases reflecting the dominance of ferrimagnetic minerals in most environmental samples. Pure minerals are labelled in Figure 3.20a showing the different areas of the scattergram in which certain mineral types and concentrations appear. Increasing concentrations of ferrimagnetic minerals are found towards the top right of the diagram. Lower ratios of IRM880 and χlf indicate paramagnetic minerals with lower remanence and high susceptibilities. Canted antiferromagnetic minerals appear above the main group at higher ratio values. These minerals have higher remanences and lower susceptibilities. Slightly different ratio values from the ARM/χlf diagrams can be seen in Figure 3.21a for the soils database. The discrimination between soil types is not as good however. Figure 3.22a also shows a strong linear relationship (on a linear scale also) between IRM880 and χlf. Hematites have a slightly higher ratio again compared to the magnetites.

Finally, a HIRM-100 parameter is used with χfd% to discriminate canted-antiferromagnetic minerals from ferrimagnetic minerals and critical grain sizes of ferrimagnetic minerals respectively. Hematite and magnetite appear at either end of the HIRM-100 scale. Most databases have a wide span of HIRM-100 values, especially the pollution database. Soils do not show such a wide range of HIRM-100 values as for χfd% (Figure 3.21b). Predominantly B horizon soils have lower ratios than A and O horizons even though many of the subsoils are

Figure 3.20: Log IRM880 versus log Xlf (a) and log HIRM-100 versus Xfd% (b) for all databases

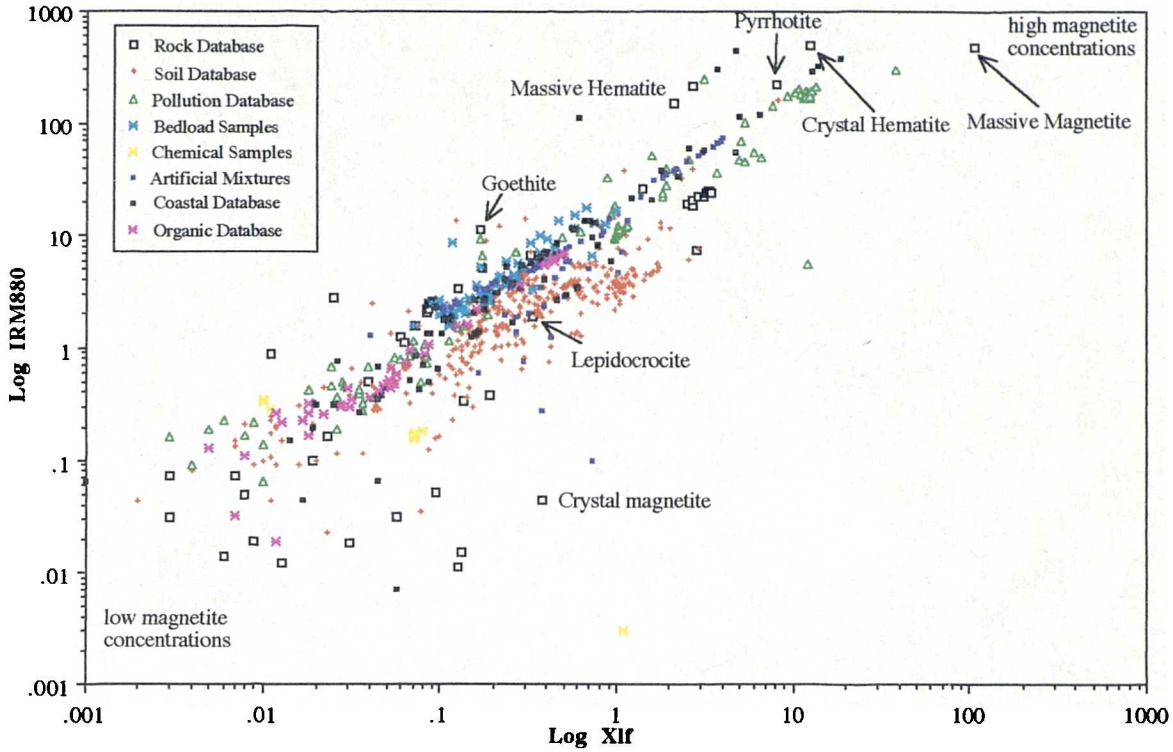

(b)

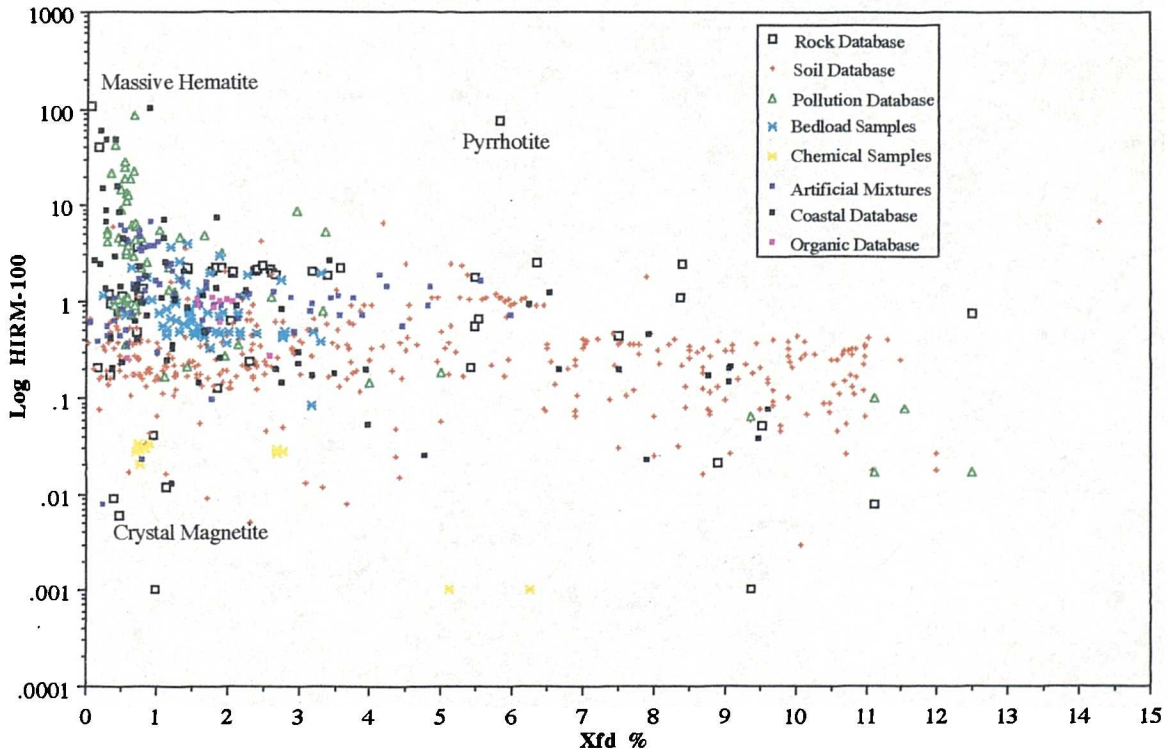

Figure 3.21: IRM880 versus Xlf (a) and HIRM-100 versus Xfd% (b) for soils database

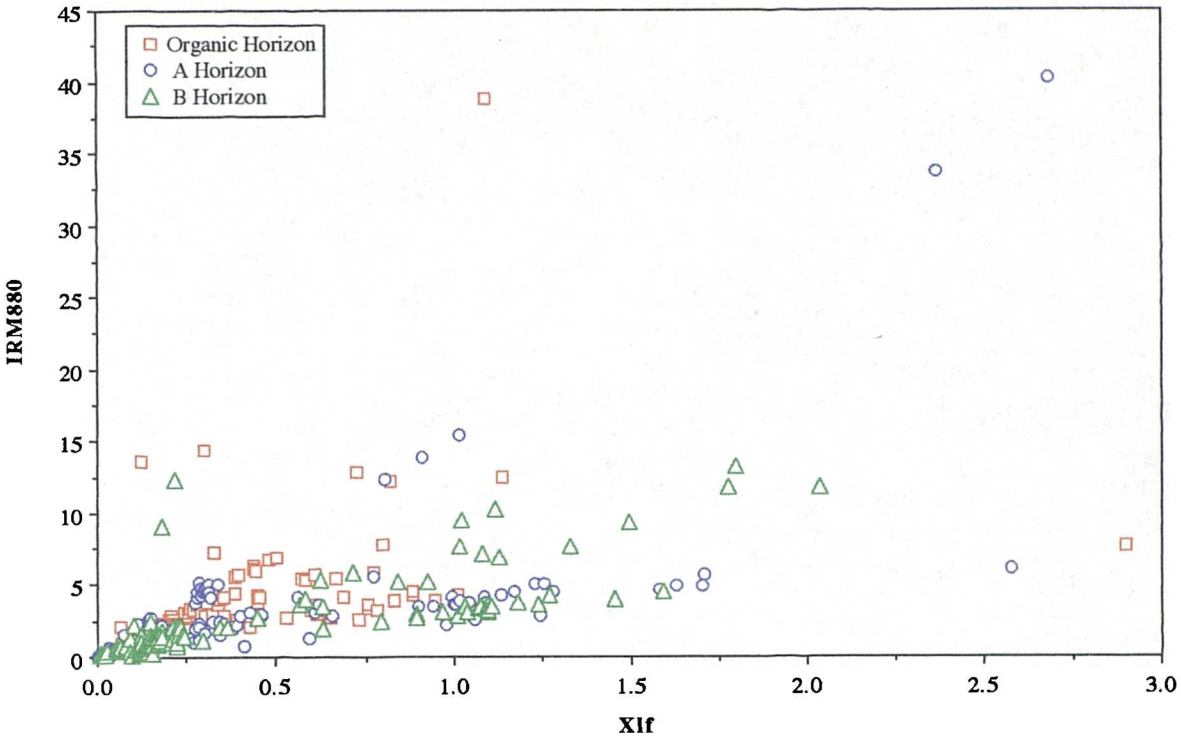

(b)

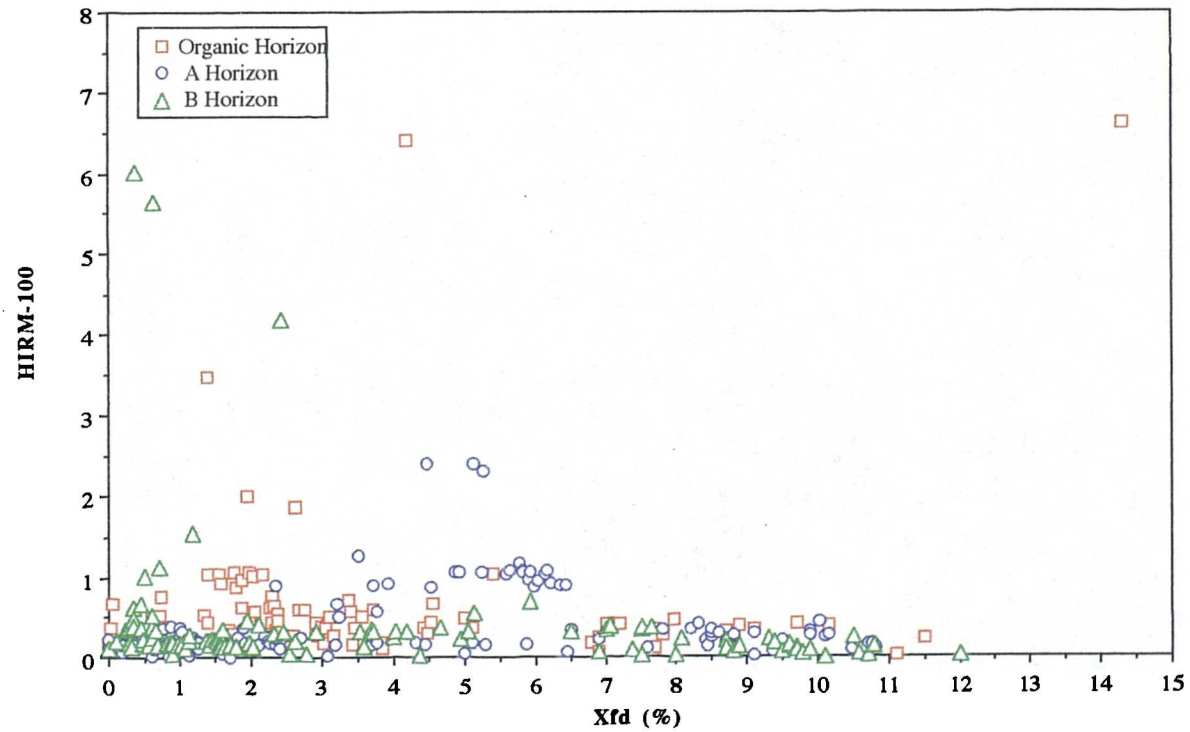

Figure 3.22: Log IRM880 versus log Xlf (a) and log HIRM+100 versus Xfd% (b) for synthetic database

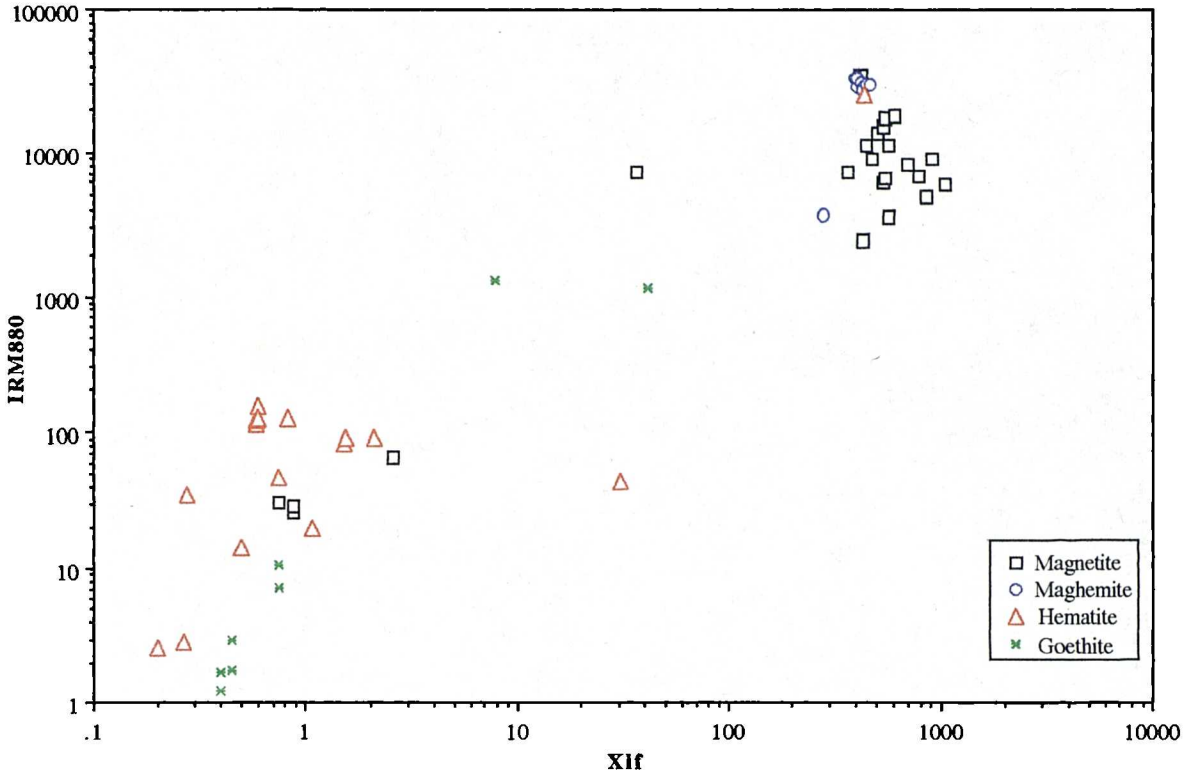

(b)

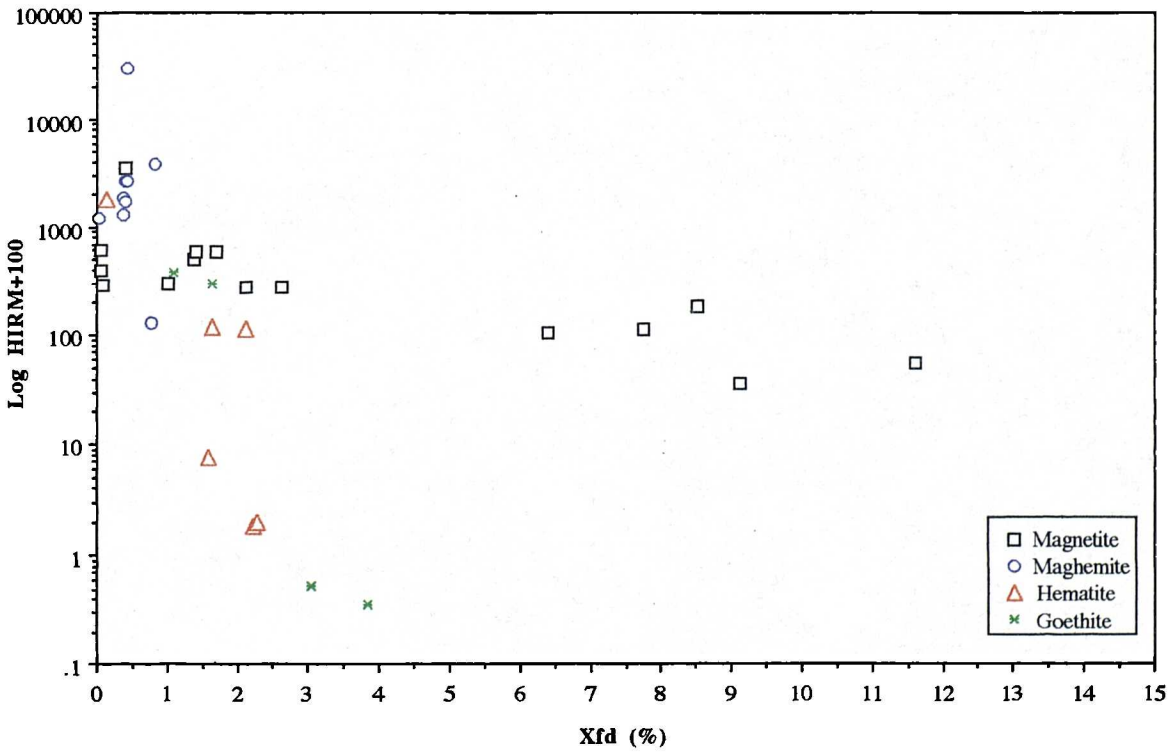

clayey. A differen pattern in the ranges of values for HIRM-100 appears in Figure 3.22b, where synthetic magnetite and maghemite values are higher than those for hematites and goethites. HIRM-100 is however influenced by canted-antiferromagnetic inclusions in strongly ferrimagnetic samples.

The use of HIRM+100 in the synthetics database must be noted here. The range over which the synthetic minerals could be saturated and exposed to a backfield was limited. At this point it was decided that forward HIRM values should be used instead. Upon testing the relationships between HIRM-100 and forward HIRMs of 20, 100 and 300mT it was found that a 1:1 highly significant relationship between HIRM-100 and HIRM20 existed. This essentially meant that some of the backfield magnetization was used in reversing the magnetization of the saturated sample and effectively reducing remanence values. Also some value was lost through division by 2 in the calculation of HIRM-100. This is due to the crossing of the y-axis (field mT) which produces addition of values (through a double negative), larger than the saturation remanent magnetization. HIRM-100 was linearly related to HIRM+100 and +300 but not at a 1:1 ratio; ratios were 1:7 and 1:21 respectively.

The database samples collected in this research have been compared with those of Thompson and Oldfield (1986). Thompson and Oldfield present a diagram of kappa (m^3kg^{-1}) versus SIRM (Am^2kg^{-1}), to which the same χlf (μm^3kg^{-1}) and IRM880 (mAm^2kg^{-1})values in this research have been compared and the scales recalculated accordingly (Figures 3.23a and b). The χlf scale rises above that of Thompson and Oldfield by a factor of 100, which could be a reflection of units still being different, or the strongly magnetic samples in the Coventry database. IRM880 and SIRM were found to be equal. A classification of the types and concentrations of magnetic minerals is given in Figure 3.23a and is an inverted version of Figure 3.20a. The ranges of values in concentration terms are similar in the two databases.

Figure 3.23: Xlf versus IRM880 for all databases (a) similar data of Thompson and Oldfield, 1986 (b) whose classification is applied to (a)

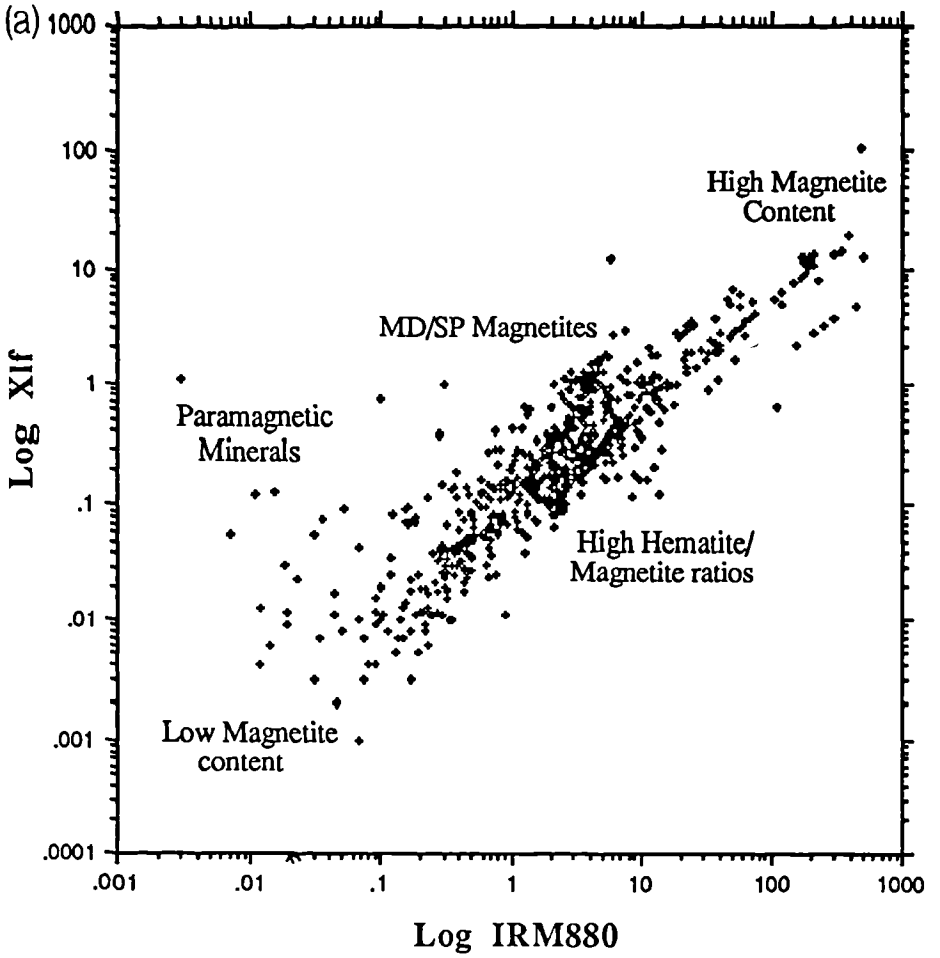

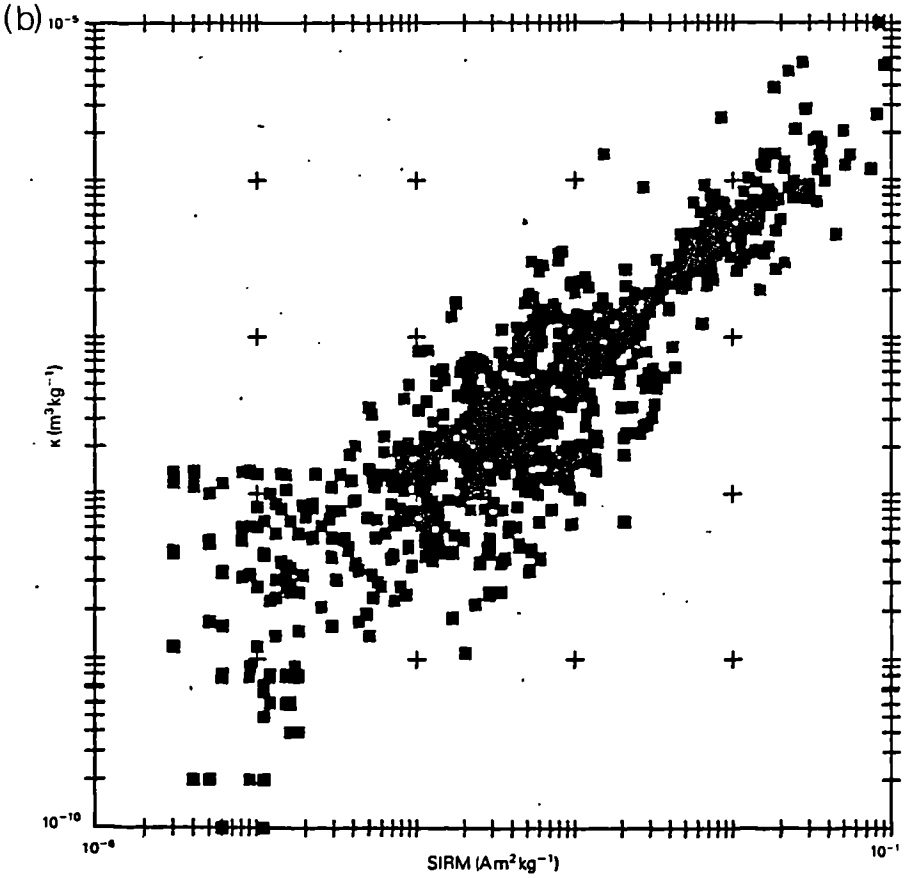

3.3 Classification of databases using linear magnetic parameters

Sample Matching/Source Classification

Results for two multi-variate techniques are described in this section: Cluster Analysis and Principal Component Analysis. The application of these techniques have been tested extensively using the sample databases described earlier in this chapter. Selected results are presented here for sub-sets of the alldata database, the soils database and the synthetics database and all the samples in the geology and pollution databases. The same datafiles have been used for both cluster analysis and PCA in this section for direct comparison.

Cluster Analysis

The SPSS Cluster analysis routine using Ward's agglomeration method has been used throughout for sample matching and discrimination in the databases. Two sets of results are presented here, one using the original raw data and one using normalized (log transformed) data. The mathematical basis of the classification techniques includes linear amalgamation of the parameters. As the raw data have to be used in linear programming, classification results for these non-transformed data are presented also. Ratio parameters have been widely used in classification routines (Yu, 1989 Yu and Oldfield, 1989 and 1993 and Walden et al 1991 and 1992) but such parameters appear not to have perfectly linear relationships in this research and are certainly not linearly additive. Therefore all classifications presented here are based only on those linearly additive parameters which can be used in linear modelling techniques. Continuity between those parameters used in the classification and those which can be used in modelling is essential otherwise potentially unsuccessful modelling attempts will occur when sources have been discriminated using ratio parameters alone.

Interpretation of the two-dimensional output (dendrogram) from cluster analysis is difficult as the results are very variable depending on which measurements are input and which clustering method is utilized. Input of data for Cluster Analysis has to be in the form of Z Score, where the data is standardized. Three different clustering methods were tried, (a) single linkage, (b) centroid and (c) Ward's methods. Single linkage effectively finds the nearest neighbouring sample. Centroid finds the closest groups by calculating the distance between the group means. In Ward's method the means for all variables are calculated and the distance between each case and each cluster is calculated. Dendrograms created using Ward's method also provided the best results in tests of various agglomerative techniques.

All data dendrograms for raw data and log transformed data are shown in Figures 3.24 and 3.25. The effects of the positive skew in the data are clear from Figure 3.24 where pure minerals (pyhrrotite, magnetite and maghemite) and strongly magnetic rocks (basalt, igneous rock) pull out the classification into two main groups (a) strongly magnetic materials at the base and (b) all other materials. Log transformed data (with 38 cases rejected through missing values), however, produced a much more useful dendrogram. Figure 3.25 shows clustering of similar groups of samples from soil types, rock types and leaves and glacial tills.

Figure 3.24: Dendrogram using raw data for X1f, Xfd, Xarm, IRM880 and HIRM100 and Ward's agglomeration method for Alldata database subset (147 cases)

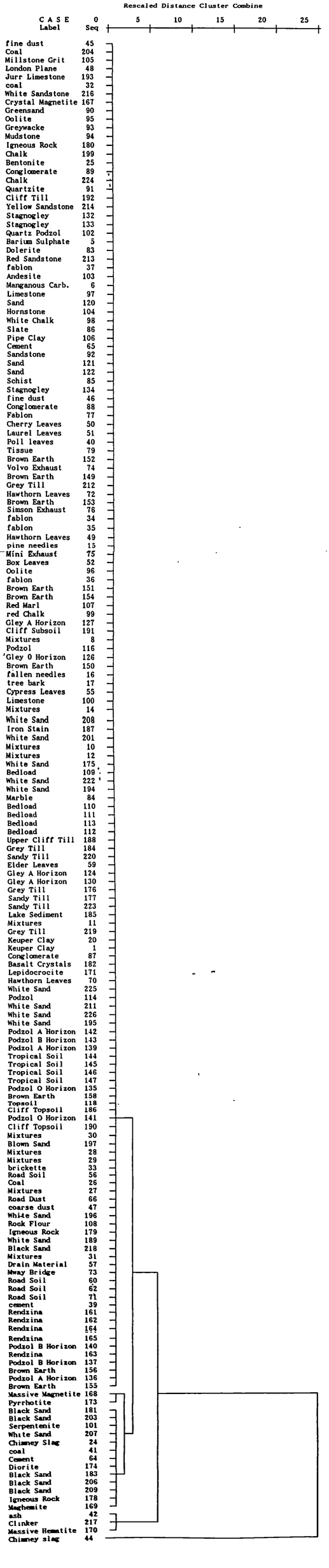

Figure 3.25: Dendrogram using log data for X1f, Xfd, Xarm, IRM880 and HIRM100 and Ward's agglomeration method for Alldata database subset (188 cases)

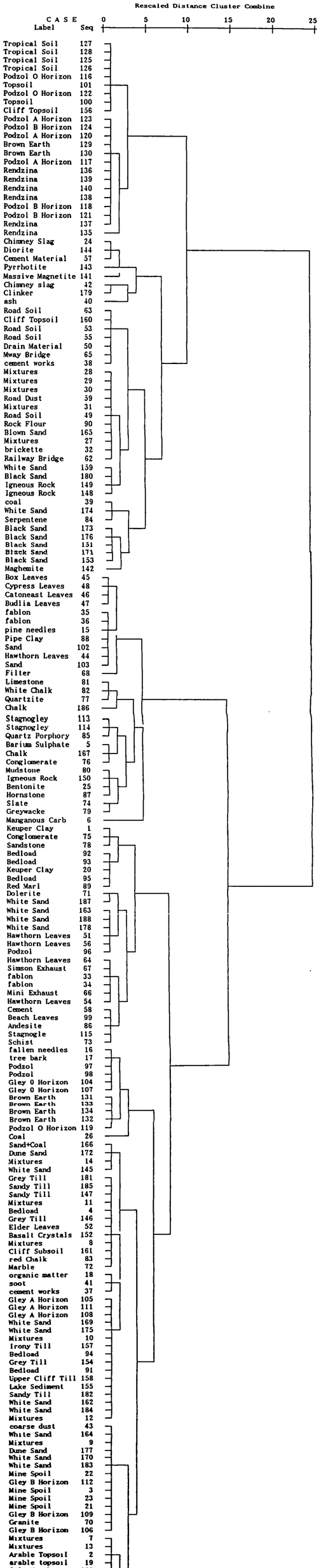

The soils database subset shows a lesser difference between raw and log transformed results (Figures 3.26 and 3.27) due to the fact that the range of samples chosen for this exercise happened to be not as skewed as in other databases. However the log transformed dendrogram seems to give slightly clearer groupings and here no cases were lost through missing values.

Figures 3.28 and 3.29 show the results of the cluster analysis for the geology database. It can be seen that very strong samples, such as the basalt, mask the rest of the geology samples which form only one cluster. Depending on the scale (along the top of the dendrogram), different numbers of groups can be identified. The log transformed dendrogram however (even with 10 cases rejected through missing values) shows a much improved classification and clear groupings into canted-antiferromagnetic clays, ferrimagnetic coal and granite, for instance. Diamagnetic chalks and limestones and quartzite also feature in a group in association with conglomerates containing quartzite minerals.

The pollution database dendrograms are shown in Figures 3.30 and 3.31. Again, through positive skew in the data, a few magnetically strong samples, such as chimney slag and ash, draw out the classification. All other weaker materials were not usefully classified. This indicates that modelling in atmospheric systems would be problematical due to pollutants containing ferrimagnetic minerals in large concentrations. The log transformed dendrogram (with 10 cases rejected through missing values) also shows classification of magnetically strong and weak materials. At the coarsest scale there are still two main groups, samples with large concentrations of ferrimagnetic and samples with low concentrations of ferrimagnetic minerals. But at a finer scale the canted-antiferromagnetic component of some materials has been identified, mine spoil and clays for instance.

Finally, the synthetics database dendrograms are shown in Figures 3.32 and 3.33. Figure 3.32 shows two broad groupings of samples, those that are ferrimagnetic (magnetites and maghemites) and those that are canted-antiferromagnetic (hematites and goethites). Distinction is made between fine-grained magnetites (MT series) and the other magnetite samples however. The log transformed dendrogram has only 36 cases as 12 were omitted due to missing values. However, the classification is excellent with clear discrimination between fine and coarse-grained MT samples and other magnetites and maghemites. Hematites and goethites are also classified usefully and a hematite sample which exhibited a ferrimagnetic component in Figures 3.22a and b, classifies with the group of maghemites in the dendrogram.

Figure 3.26: Dendrogram using raw data for Xlf, Xfd, Xarm, IRM880 and HIRM100 and Ward's agglomeration method for soils database subset (31 cases)

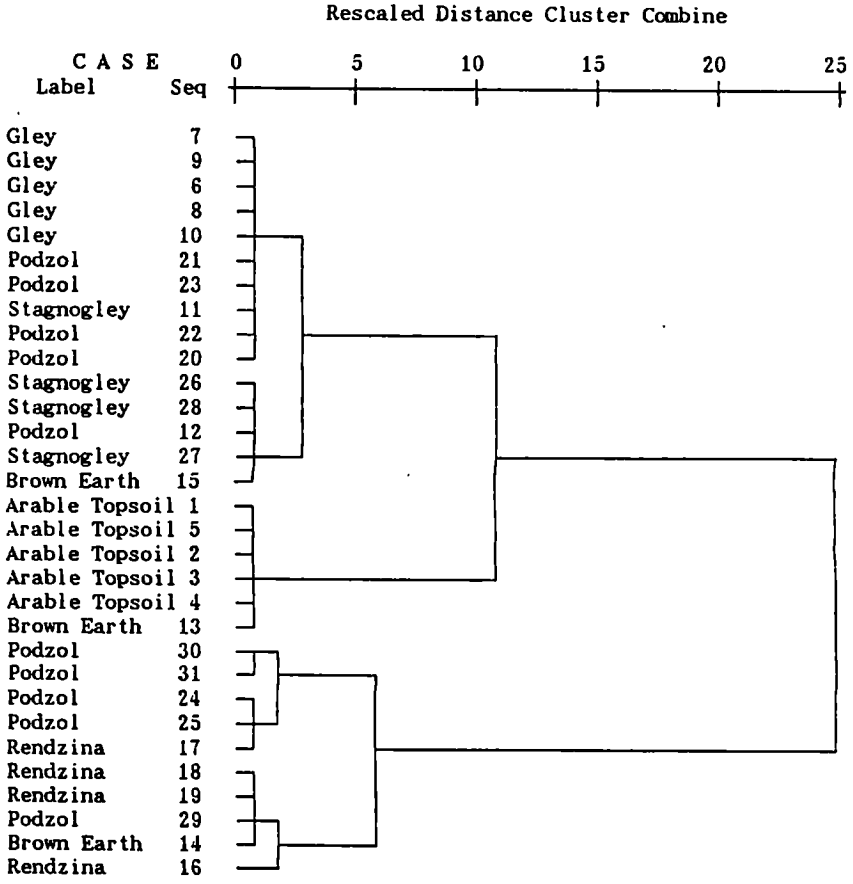

Figure 3.27: Dendrogram using log data for Xlf, Xfd, Xarm, IRM880 and HIRM100 and Ward's agglomeration method for soils database subset (31 cases)

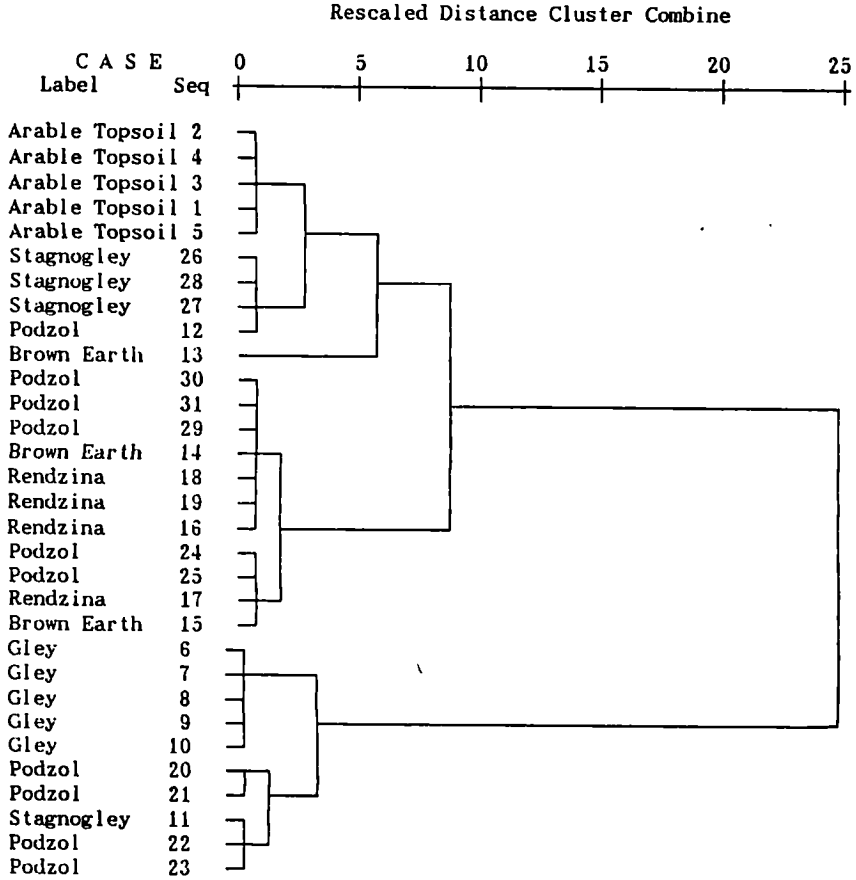

Figure 3.28: Dendrogram using raw data for Xlf, Xfd, Xarm, IRM880 and HIRM100 and Ward's agglomeration method for geology database (42 cases)

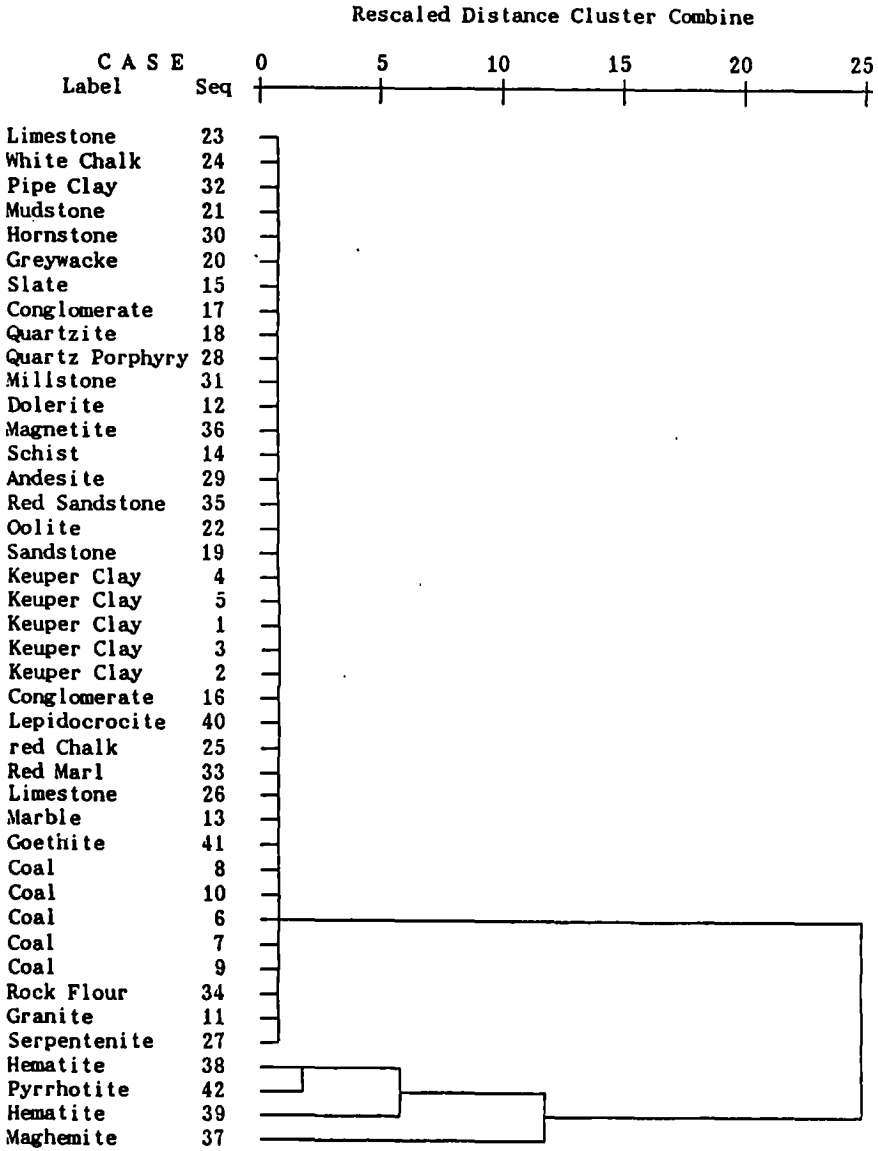

Figure 3.29: Dendrogram using log data for Xlf, Xfd, Xarm, IRM880 and HIRM100 and Ward's agglomeration method for geology database (35 cases)

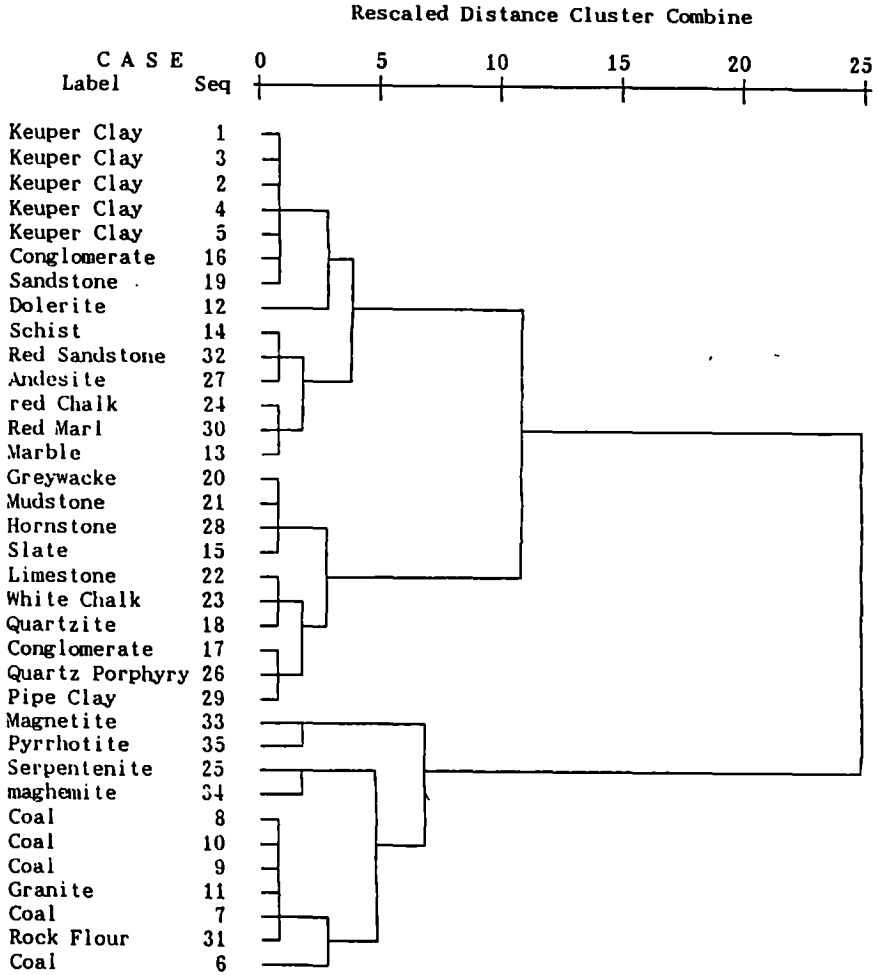

Figure 3.30: Dendrogram using raw data for X1f, Xfd, Xarm, IRM880 and HIRM100 and Ward's agglomeration method for pollution database (53 cases)

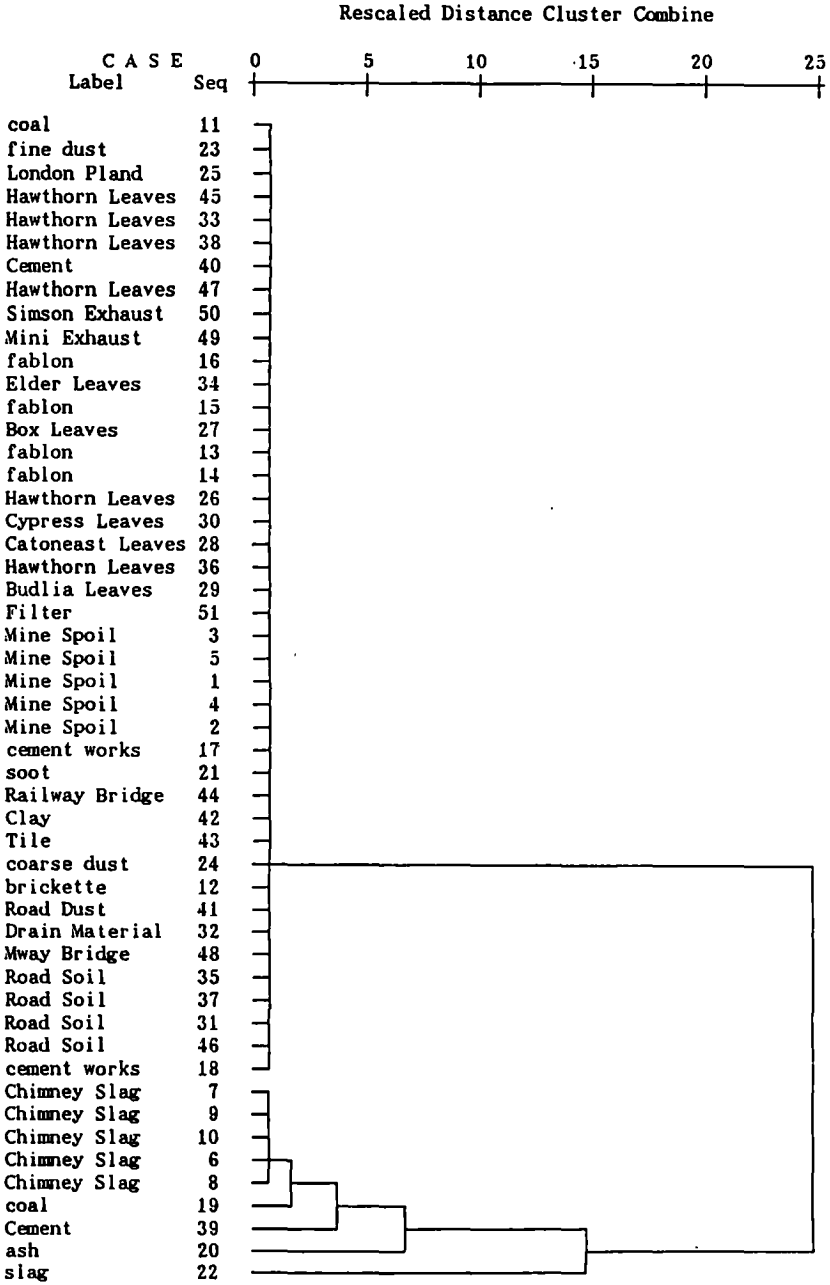

Figure 3.31: Dendrogram using log data for X1f, Xfd, Xarm, IRM880 and HIRM100 and Ward's agglomeration method for pollution database (48 cases)

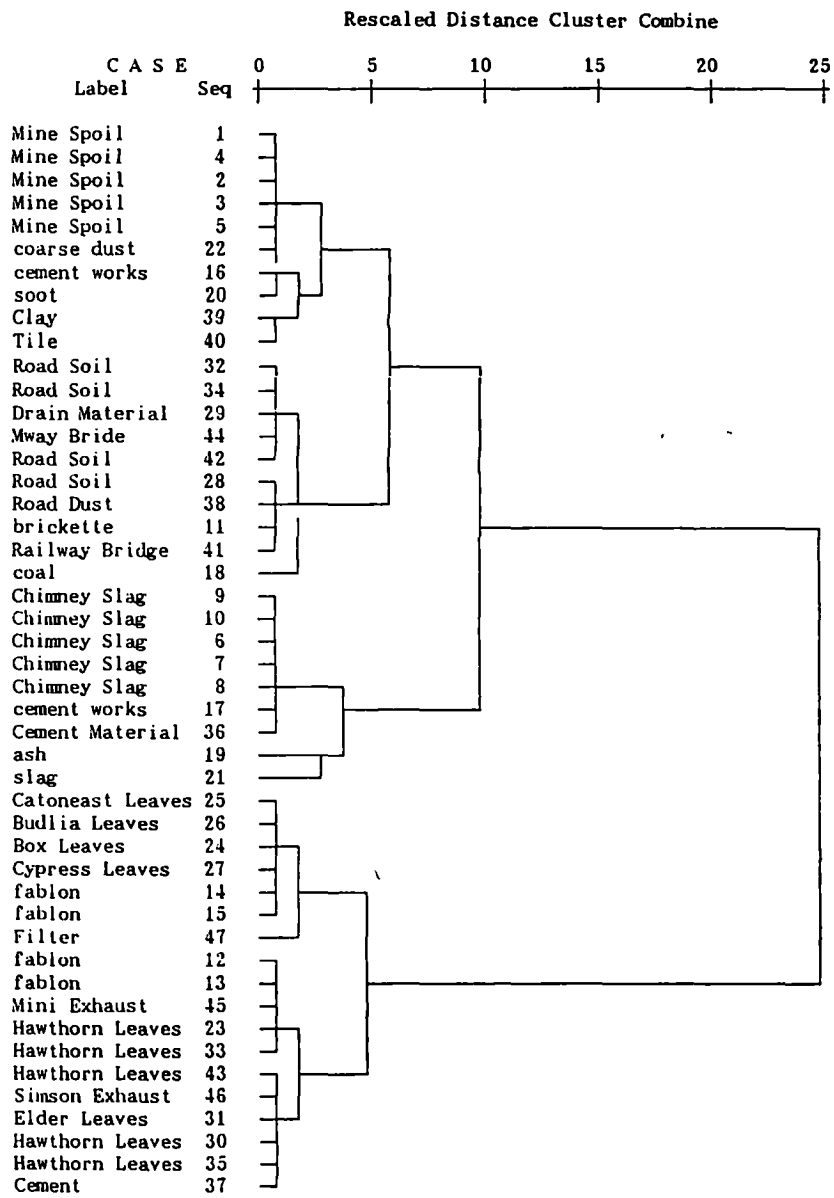

Figure 3.32: Dendrogram using raw data for Xlf, Xfd, Xarm, IRM880 and HIRM100 and Ward's agglomeration method for synthetic database (48 cases)

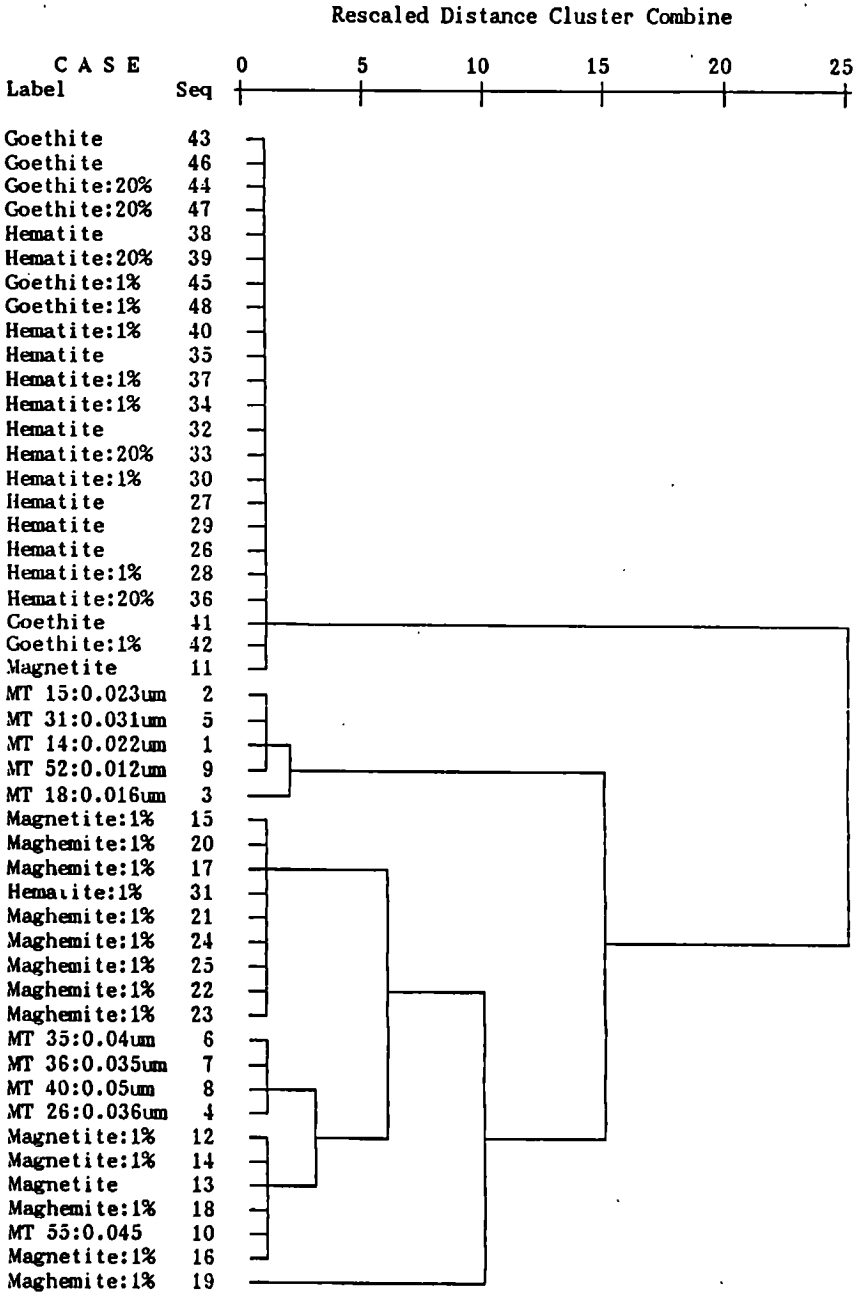

Figure 3.33: Dendrogram using log data for Xlf, Xfd, Xarm, IRM880 and HIRM100 and Ward's agglomeration method for synthetic database (36 cases)

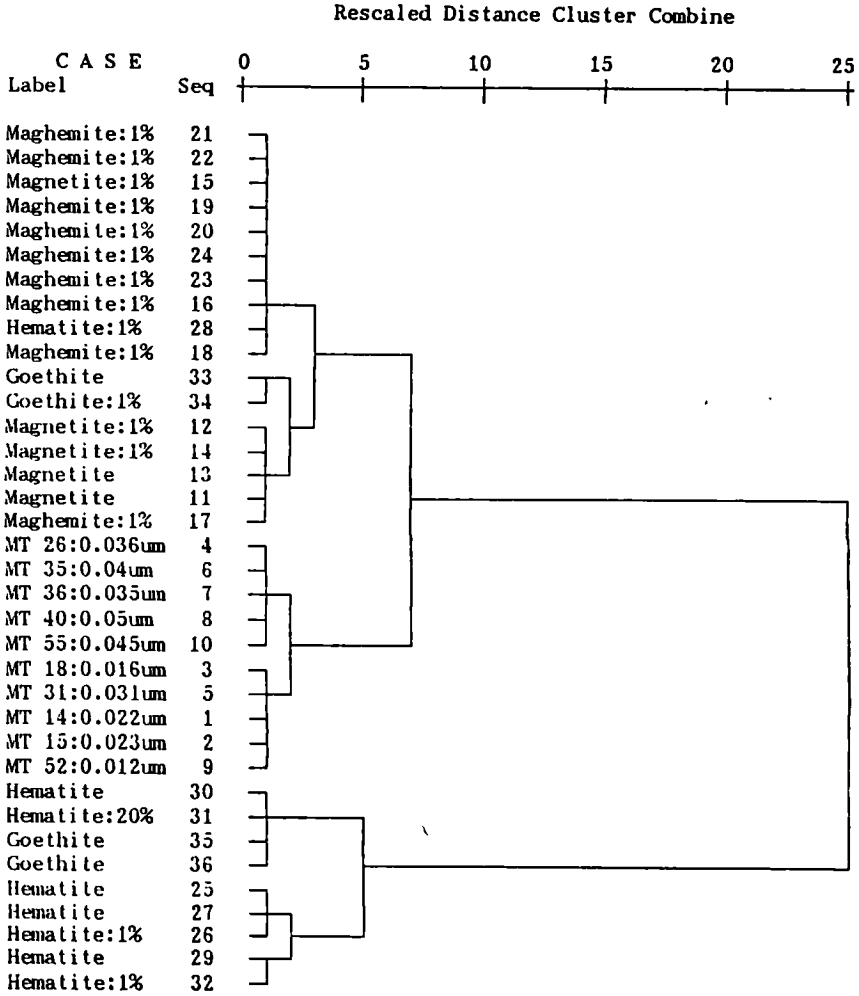

Principal Component Analysis

Principal Component. Analysis reduces the number of variables and constructs several components which are orthogonal (uncorrelated) as introduced in Chapter 2. These represent the major properties of the data set. The output which can be generated, from the SPSS routine, is that of a principal co-ordination plot as seen in Chapter 2 (Figure 2.6). Co-ordination plots presented here are created using original raw data only as too many cases were lost through log transformation.

Principal component analysis transforms the input data into standardized variables within the routine and again only linear variables can be used. A correlation matrix is first calculated for all the variables. Often a warning that the matrix is ill-conditioned appears, caused by many of the variables indicating similar magnetic properties and being interrelated (as in the previous correlation section). Principal components are extracted from the correlation table to represent the variables. Eigenvalues are calculated for the principal components which is, effectively, the total variance for each component accounted for in the data set. Significant components are those which have eigenvalues greater than 1; no other components are included. The relationship between each sample in the data set and the new component is calculated (by correlation) and can be used to plot the data in the principal co-ordination plot.

The principal components are then subject to a varimax rotation which effectively re-evaluates the relationship between the variables and the principal components. This emphasises those variables which most influence the components for interpretational purposes. Generally these were found to be χlf, χfd and HIRM+100 in this research, corresponding to the total ferrimagnetic, fine-grained ferrimagnetic and canted-antiferromagnetic properties of samples in the data set. The results of principal components analysis, ie the components themselves, can be used in classification techniques such as cluster analysis instead of the original variables. However, very similar results were gained in this research by performing cluster analysis both ways.

Figures 3.34 to 3.38 show PCA co-ordination plots and bi-variate scattergrams for all the databases and subset databases used in the cluster analysis. In all cases the linear parameters used to construct the co-ordination plots are given and the two most important parameters have been used to construct the bi-variate scattergrams. Figure 3.34a and b give results for the alldata database. The two figures are very similar and the two most important components in the database are ferrimagnetic concentration (χlf and χfd) and canted-antiferromagnetic concentration (HIRM+100). The co-ordination plot (Figure 3.34a) shows slight grain size discrimination along the χfd vector (PC 1). This is not seen in the bi-variate scattergram. However the two diagrams are not substantially different indicating that the bi-variate scattergrams would present almost as much information about the database as PCA does.

A similar phenomenon is seen in Figure 3.35 where the soils topsoil database is best classified using χlf against HIRM+100. The bi-variate scattergrams displays much the same patterns as the co-ordination plot. Again, in Figures 3.36a and b of the rock database and Figures Figure 3.37a and b of the pollution database, classification is best observed using the parameters χlf and HIRM+100.

Figure 3.34: PCA Co-ordination plot for alldata database (a) and Xlf versus HIRM100 bi-variate plot (b)

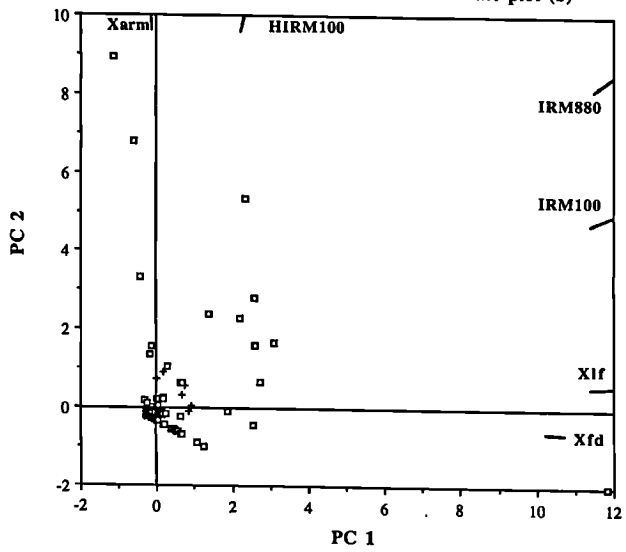

PC	Eigenvalue	% of var.	Cum. Var.
1	2.94	49.0	49.0
2	1.33	22.1	71.1

(b)

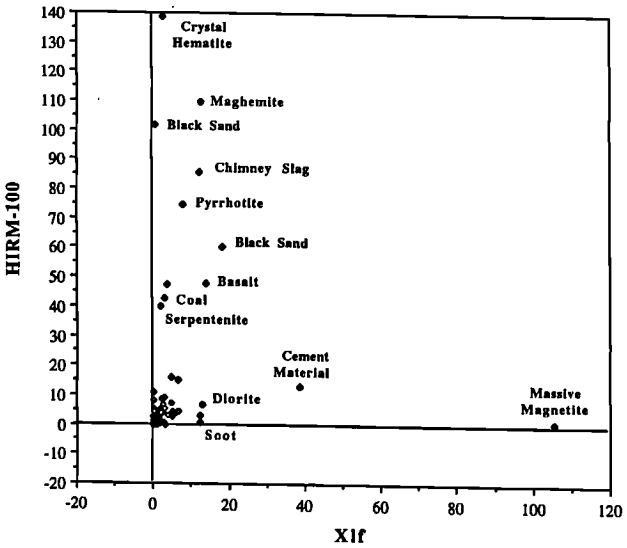

Figure 3.35: PCA Co-ordination plot for topsoils database (a) and Xlf versus HIRM-100 bi-variate plot (b)

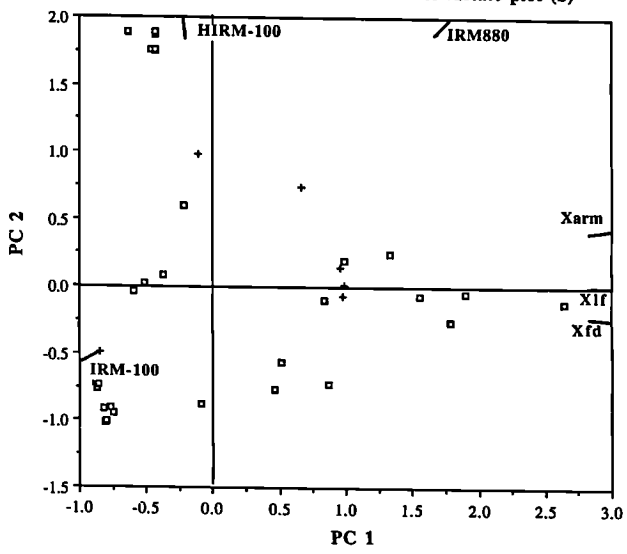

PC	Eigenvalue	% of var.	Cum. Var.
1	4.36	72.7	72.7
2	1.48	24.6	97.3

(b)

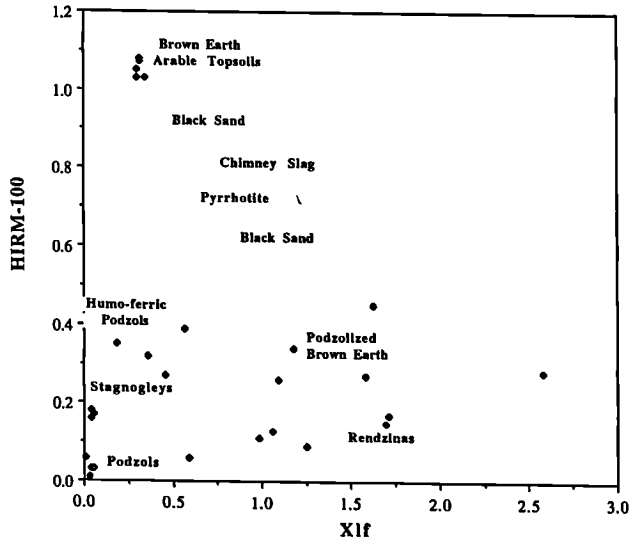

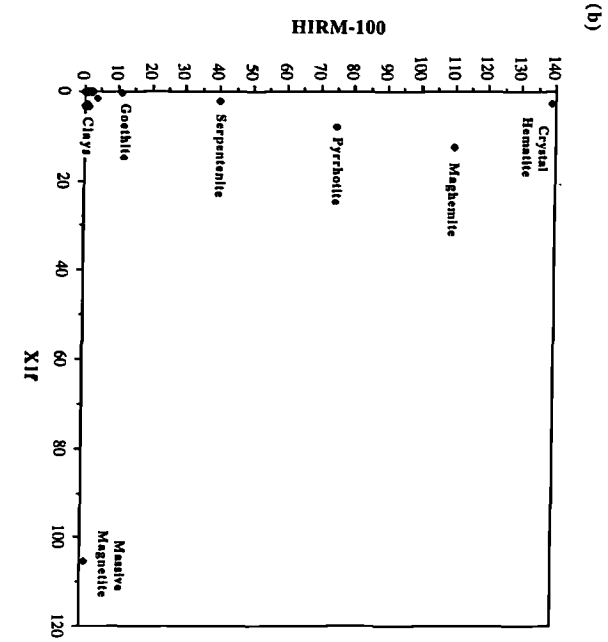

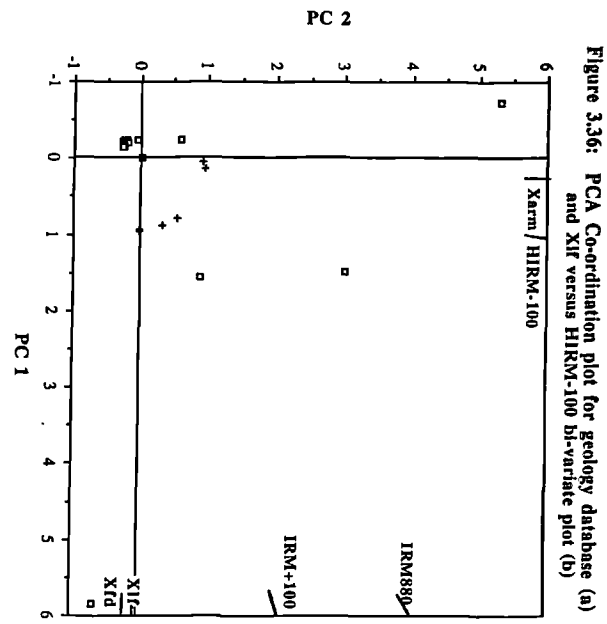

Figure 3.36: PCA Co-ordination plot for geology database (a) and Xlf versus HIRM-100 bi-variate plot (b)

PC	*Eigenvalue*	*% of var.*	*Cum. Var.*
1	3.71	61.9	61.9
2	1.68	28.1	90.0

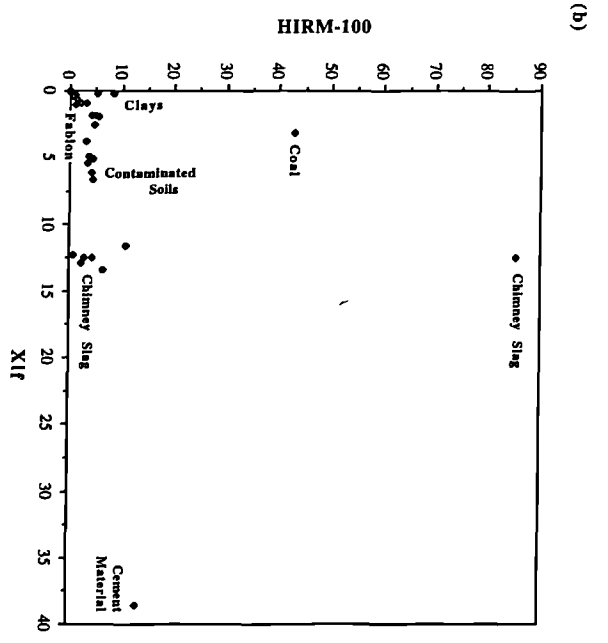

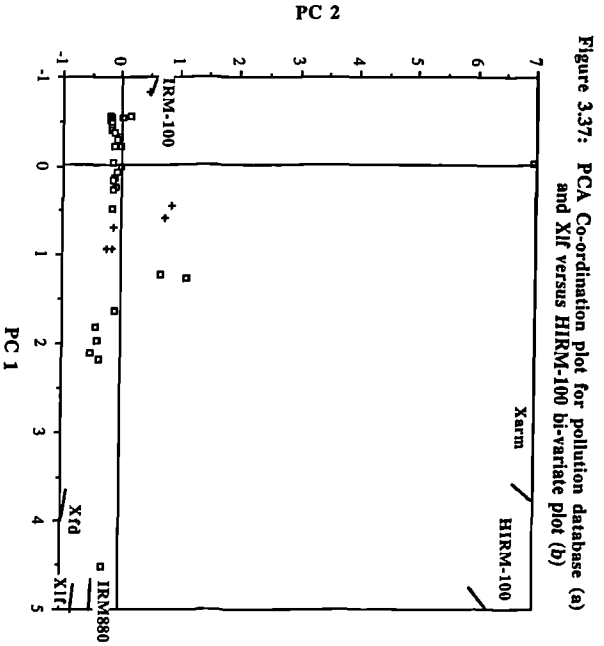

Figure 3.37: PCA Co-ordination plot for pollution database (a) and Xlf versus HIRM-100 bi-variate plot (b)

PC	*Eigenvalue*	*% of var.*	*Cum. Var.*
1	3.45	57.6	57.6
2	1.63	27.2	84.8

Figure 3.38: PCA Co-ordination plot for synthetic database (a) and Xfd versus IRM880 bi-variate plot (b)

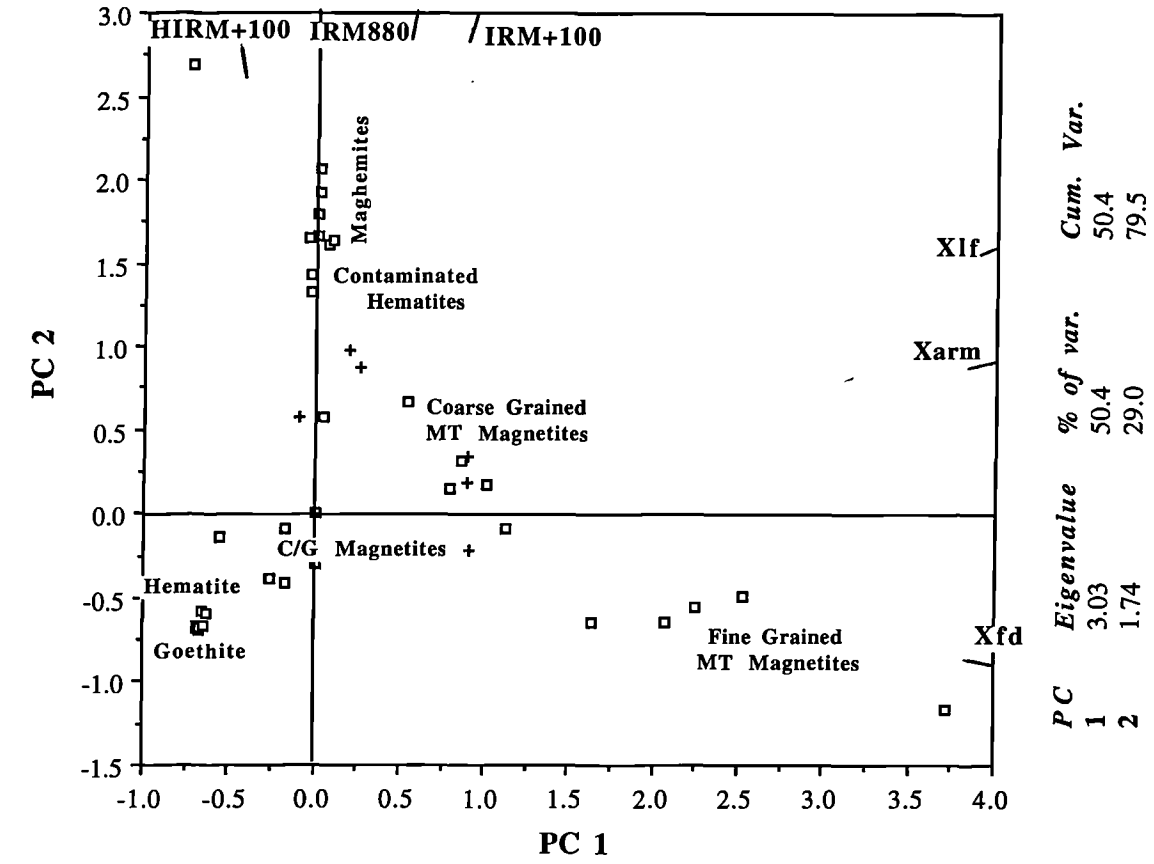

(b)

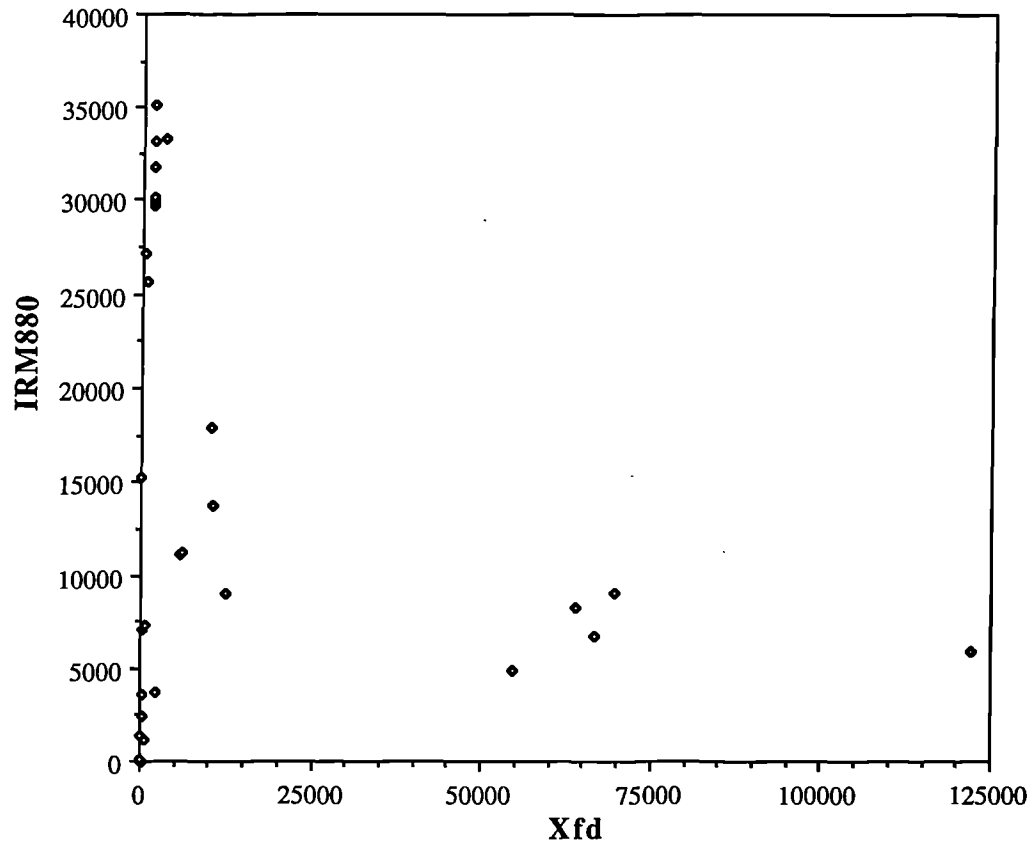

Figures 3.38a and b shows a different pattern however. Classification of the synthetic database is much clearer in the co-ordination plot than in the bi-variate scattergram. This is due to the strong ferrimagnetic grain-size differences and concentrations (and the canted-antiferromagnetic component as in the other databases). The bi-variate scattergram of χfd and IRM880 does not give as clear a classification of the grain size variation. In the synthetics database PCA routine, three principal components were extracted, a ferrimagnetic component and fine-grained ferrimagnetic component and a canted-antiferromagnetic component. Co-ordination plots of the second and third factors (not shown) were not as useful as plots of the first two factors, although the numerical scale problem of the ferrimagnetic minerals was lessened somewhat.

Comparison of PCA with Traditional Sample Discrimination

It is clear that in many cases the PCA and bi-variate scattergram results are similar and PCA does not add any further significant information. Ratio parameters have been used to discriminate samples in many studies. Oldfield et al (1985) used IRM880/ARM versus χfd (%) to discriminate pollutants and Hunt et al (1984) used IRM-20/IRM880 versus IRM-200/IRM880 for the same purpose. IRM880 versus χlf has been used to discriminate samples of different mineralogy and grain size as has ARM/χlf and IRM880/ARM. Maher (1988) used χarm/IRM880 versus χfd (%) to indicate ultrafine-grained magnetites in soils. It is felt that these grain size indicators are very useful for interpretational purposes (for example in the bi-variate plots presented earlier) but unfortunately they are not suitable for linear unmixing which is a main aim of this work. HIRM+100 versus χlf, indicating different mineralogy (magnetite and hematite) and different properties (ferrimagnetic, antiferromagnetic and paramagnetic), present the most useful linear discriminating parameters. HIRM+100 versus χfd is potentially more useful as it discriminates between ferrimagnetic mineral grain sizes, but it is prone to measurement error in weak samples. In most cluster analysis and PCA tests HIRM+100 and χlf seem to be the most influential parameters, therefore a comparison between the simple bi-variate plot and the PCA output has been appropriate (see Chapter 2). The interpretational quality of the PCA plot is possibly better as more variables can be taken into account, but the HIRM+100 versus χlf scattergram gives a good indication of sample groupings and concentrations for assessment of modelling suitability.

3.4 Summary

From the initial tests presented in this section conclusions can be drawn which form part of the methodological framework of the present research (presented in Chapter 6), especially with respect to the environmental applications described in Section C (Chapters 7, 8 and 9).

1. There is great need for thorough identification of sources not only through field experience but also through field survey and statistical discrimination. Parameters used in the classification must be those on which the modelling is to be based.
2. The main methodological flaw in many studies can be attributed to unrealistic sampling strategies which fail to

incorporate the variability of source materials. Proper identification of such variability may save unviable application of modelling techniques where variability causes overlap in the properties of two or more sediment sources. Field surveys and bulking of many samples to incorporate spatial variability might be a valid technique to use in pilot studies of systems of interest.

3. Care must be taken with the distributions of magnetic data (normality) and the interrelationships between parameters which are calculated from initial measurement. The type of data used should be as unchanged as possible; initial linear parameters should give as good a result as ratio parameters. This saves both time and the complication of regression line fitting to non-linear parameters.

4. It is clear that PCA is a good indicator of materials which can be modelled successfully and those which are too magnetically alike, or a multiple of one another, which are likely to fail.

5. If sources are too magnetically alike there is great scope for incorporating other parameters from geochemical or other analysis in linear modelling. This may make the difference between having to amalgamate two sources into one, or being able to quantify them individually.

Significant interrelationships have been found to exist between many magnetic parameters which are used widely in magnetic discrimination work. χlf and HIRM+100 seem to provide the best means for classification of most environmental materials where χlf indicates ferrimagnetic minerals and HIRM+100 indicates canted-antiferromagnetic minerals. The inter-correlations between parameters causes ill-conditioning of classification techniques where there are no significant orthogonal parameters on the basis of which to classify the materials. Overall conclusions of the classification work completed (and that not presented here) is given in Figure 3.39 for four of the main databases, soils, geologies, pollutants and synthetic samples. In the figure, evaluation of measurements used to discriminate the samples is presented first. In general, ratio parameters have been found to indicate grain size differences of ferrimagnetic minerals in samples more successfully than linear parameters which are affected by concentrations of minerals. From classification tests it is clear that without log transformation much information is lost due to the scale of mineral concentration present within most of the databases. However log transformation causes the loss of information in datasets with many weak or negative values and the PCA techniques partly fail as a result. A constant value could be added to all parameter values in the dataset to overcome data loss through negative or near zero values; this has not been carried out as yet but should be approached with caution especially when interpreting the data.

Principal components which are extracted always correspond to ferrimagnetic minerals first and canted-antiferromagnetic minerals second, except in the case of the synthetics database where there are stronger grain size differences between samples. In Figure 3.39 initial proposals for modelling and tracing minerals have been made based on the classification results alone. From the pollution database it is clear that further work in tracing and modelling pollutants using standard magnetic properties would not be successful. Limitations are also present in the geology database where basic igneous rocks with strong ferrimagnetic signals would mask weaker geologies. From this chapter, definition of the materials which could not be used in modelling studies can be made and the parameters which successfully discriminate materials can be identified.

Figure 3.39: Summary of Database Contents and Classification work done on each

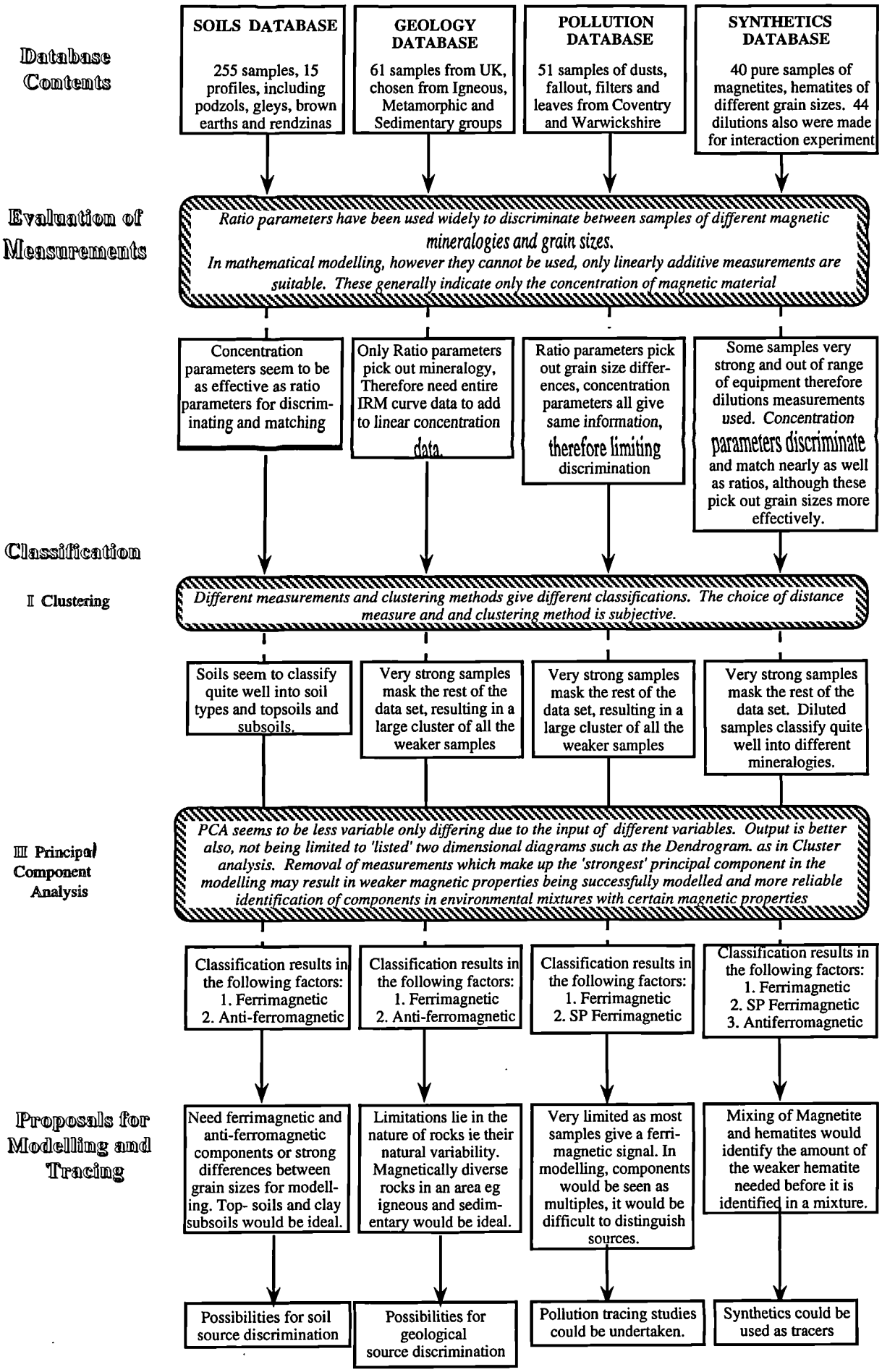

CHAPTER 4

Modelling the Magnetic Properties of Materials

Testing linear systems

"Lulled into a false sense of security by his familiarity with the unique response of a linear system, the busy analyst or experimentalist shouts 'Eureka, this is the solution', once a simulation settles onto an equilibrium or steady cycle, without bothering to explore patiently the outcome from different starting conditions. To avoid dangerous errors and disasters, industrial designers must be prepared to devote a greater percentage of their effort into exploring the full range of dynamic responses of their systems". H.B. Stewart and J.M. Thompson on the Border between Calm and Catastrophe, Non-linear Dynamics and Chaos, pxiii.

Introduction

Linear additivity is the most widely assumed property in sediment source and mineral modelling studies which use magnetic properties (see Appendix 1, Part 4 for a definition). Yu (1989) tested the additivity of magnetic measurements using artificial sediment mixtures and obtained reasonable results. More recently Maher and Thompson (1992) quote Stacey (1963) as stating that 'in small or modest concentrations of a few percent magnetic properties are linearly additive'. It has also been stated that mixtures are necessary in order to calibrate the quantification of sources in environmental systems (Walden et al, 1991). It is suggested here that in order to test linearity of both measurements and equipment only one artificial mixing exercise should be needed to define limitations. Effects of interaction between magnetic grains may affect the linearity of magnetic properties where the interaction may serve to reduce the mixture measurement (considered in more detail in Paper 1, Appendix 7). Two main issues are tested in this chapter, that of the linear additivity of proportions of source sediments to a mixture (ie linear additivity of magnetic properties) and that of linearity of measuring equipment. These two issues are closely interlinked, however, and limitations placed on the linearity of magnetic properties by equipment is tested.

In this chapter, results are presented for linear additivity tests carried out firstly in two artificial mixing experiments and secondly in two case studies. In the first set of experiments, 71 artificial mixtures have been made using environmental and synthetic materials. The artificial mixing experiments test the linear additivity of magnetic properties in relation to linearity of the measuring equipment. The linear additivity of the source component magnetic properties and that of the mixture is tested. A hypothetical mixing experiment is also carried out to test the sensitivity of LINDO to errors in measurement. In the second instance the two case studies consist of the use of bedload samples from Finham Brook and the River Sowe in Coventry, Central England, and samples of a gley soil (Bromsgrove soil series) from Corley, North Warwickshire, England. In each case bulk samples have been fractionated and the linear additivity of the fraction magnetic properties against that of the original bulk sample is tested. In both sets of experiments linear additivity errors are expressed and in the artificial mixing experiment limitations on the application of magnetic properties in modelling of sources and minerals are defined.

4.1 Linear additivity of magnetic parameters and unmixing: Laboratory and hypothetical mixing experiments

Introduction

Mixing experiments were used to test the additivity of linear magnetic measurements through matrix inversion and linear modelling in LINDO (already described in Chapter 3 and an example is given in Appendix 5). Linear additivity of magnetic measurements is tested here with the use of 71 artificial mixtures of environmental and synthetic materials and a hypothetical mixing experiment. In the main, standard parameters are used in the artificial mixing experiments and the hypothetical experiment, but mixing experiments using hysteresis loop data are also briefly presented. Another approach could be that of fitting regression lines through data plotted for two parameters for use in linear modelling (Yu, 1989 and Yu and Oldfield, 1989). In the first instance this does not add further information than that attained from the original parameters (Chapter 3) and variation away from the line fitted will result in further variation within the dataset and hence non-linearity. From this section a definition of the limits as to the use of magnetic properties in linear modelling of sediment sources and minerals can be given (see Chapter 6 for final summary).

4.1.1 Mixing Experiments

Two laboratory mixing experiments using environmental and chemical materials were devised to evaluate the following:

* The linearity of magnetic measurements
* The effectiveness of linear programming (LINDO) in unmixing laboratory mixtures with different numbers of component materials, including materials which were magnetically weak, strong, or similar
* The minimum number of parameters and the most useful parameters needed for the modelling to give reliable source proportions

Methodology

The methodology of the experiments is shown in Figure 4.1 and source materials used in the two experiments are listed in Table 4.1. Initially materials or sources were collected for experiment 1 on the basis of their discrimination using χlf and HIRM-100 (Chapter 3). Six materials were chosen, as listed in Table 4.1, for their breadth of magnetic properties and magnetic mineral content. Figure 4.2a shows the χlf versus HIRM-100 plot for 10 sub -samples (<2mm) of each source. The variation within these sub-samples is clear from the figure (CV% results are presented in Chapter 5). Most of the variation between the source samples is seen in χlf where each source has a discrete value of its own. For instance, mine spoils have values of approximately 1 $\mu m^3 kg^{-1}$ while coal samples have values spread around 3 $\mu m^3 kg^{-1}$. Less variation is seen in the HIRM-100 values where chimney slag has values of around 16 $mAm^2 kg^{-1}$ (with much variation) and other sources have values below 2 $mAm^2 kg^{-1}$.

Figure 4.1: Mixing Methodology and Analysis

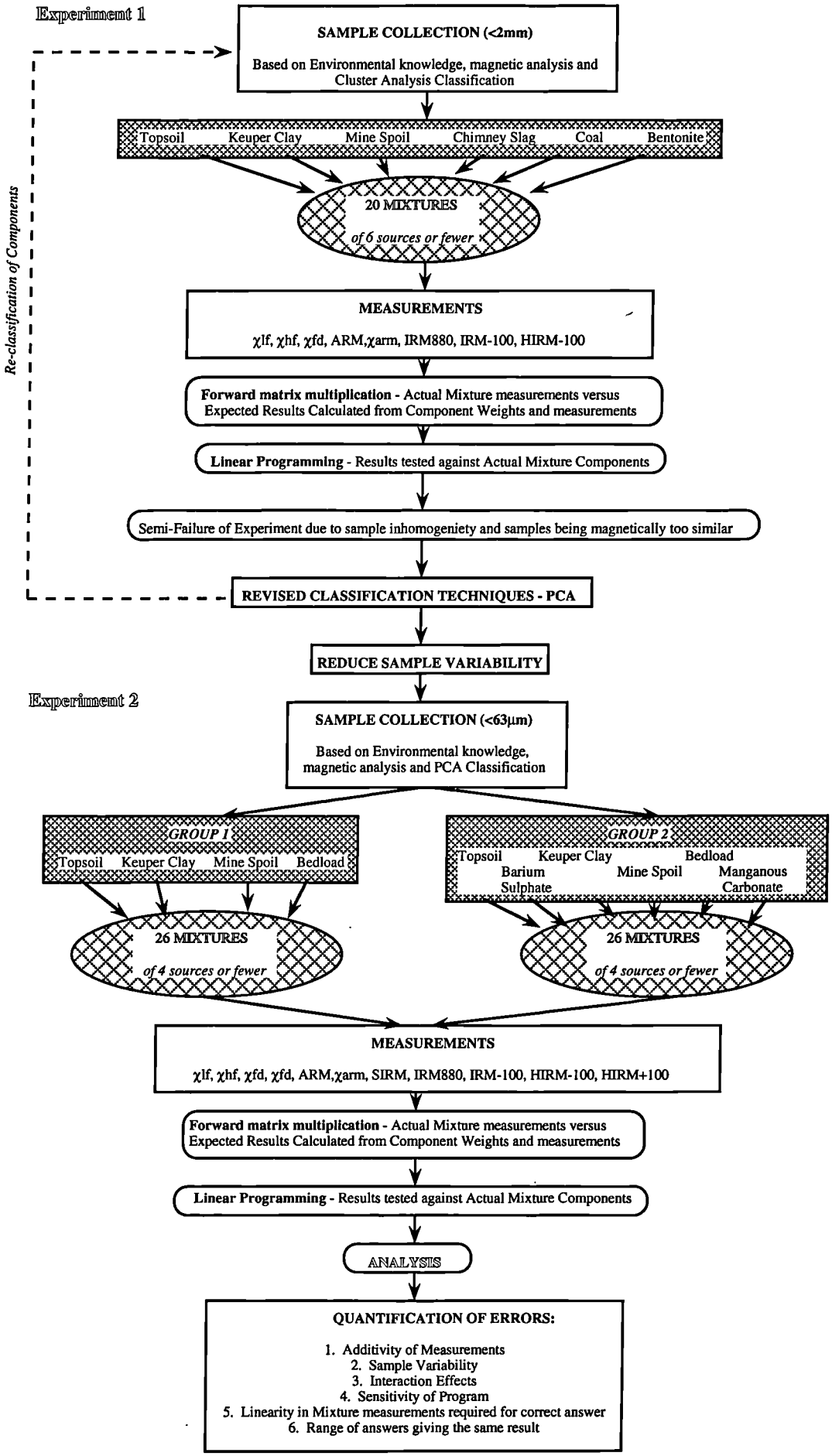

A similar process was adopted for mixing experiment 2, but PCA classification was employed to test source discrimination and some of the source materials used in the first experiment were also used in the second experiment. Figure 4.2b shows a co-ordination plot of the source components used in experiment 2; each quadrant of the plot can be classified according to the magnetic properties of the source materials. For instance, the quadrant in which Keuper clay and Finham Brook bedload fall, defines samples containing canted-antiferromagnetic materials. Each point in the figure represents 5 sub-samples. This is shown more clearly in the barium sulphate group where measurement of this diamagnetic material was affected by the noise of the equipment. Only 5 sub-samples were taken from each source material in mixing experiment 2 as the material was more finely sieved and ground (<63 μm) than that used in the first experiment. This was to overcome the in-homogeneity seen in the subsamples of materials used in experiment 1 (especially the chimney slag and coal). The influence of packing density and dilution on the materials used in these experiments has also been studied and the results are presented in Appendix 6.

A list of measurements made on each set of source samples is given in Figure 4.1. Mean values for each parameter in both experiments were found from the respective numbers of source sub-samples (these mean values were used in linear modelling). Twenty mixture specimens were mixed by hand from the first set of six source components (or fewer) and fifty one from the second set. The second set of mixtures are further divided as shown in Figure 4.1 into an environmental set (with four source components or fewer) and an environmental and chemical set (with six source components or fewer). Each source component was weighed and added to the mixture until approximately 15 grams of material was achieved. The mixtures were then packed into 10ml pots and measured along with the source components. The actual proportions of each source component in each mixture are presented in Table 4.3. A wide range of mixture properties was achieved and a co-ordination plot of the mixtures and source components of mixing experiment 2 is shown in Figure 4.2c. Predicted mixture measurements were calculated by multiplying the percentage source proportions by their magnetic parameter values and summing them.

Table 4.1: Materials used in the Mixing Experiments

Mixing Experiment 1

Component	Assumed Magnetic Property
a1 Arable Topsoil, Corley (Bromsgrove Series)	Fine-grained ferrimagnetic
a2 Keuper Clay, Seeswood Pool	Canted-antiferromagnetic
a3 Mine Spoil (Soil and Coal Spoil)	Course-grained ferrimagnetic
a4 Chimney Slag (Gulson Hosp Boiler)	Ferrimagnetic
a5 Coal, Daw Mill Colliery	Canted-antiferromagnetic
a6 Commercial Bentonite (Analr)	Paramagnetic

Mixing Experiment 2

Component	Assumed Magnetic Property
a1 Keuper Clay, Seeswood Pool	Canted-antiferromagnetic
a2 Arable Topsoil, Corley (Bromsgrove Series)	Fine-grained ferrimagnetic
a3 Mine Spoil (Newdigate Colliery)	Course-grained ferrimagnetic
a4 Bedload (Finham Brook, Coventry)	Ferrimagnetic
a5 Barium Sulphate (Analr)	Diamagnetic
a6 Manganous Carbonate (Analr)	Paramagnetic

Figure 4.2: (a) HIRM-100 versus Xlf for Mixing Experiment 1 source components

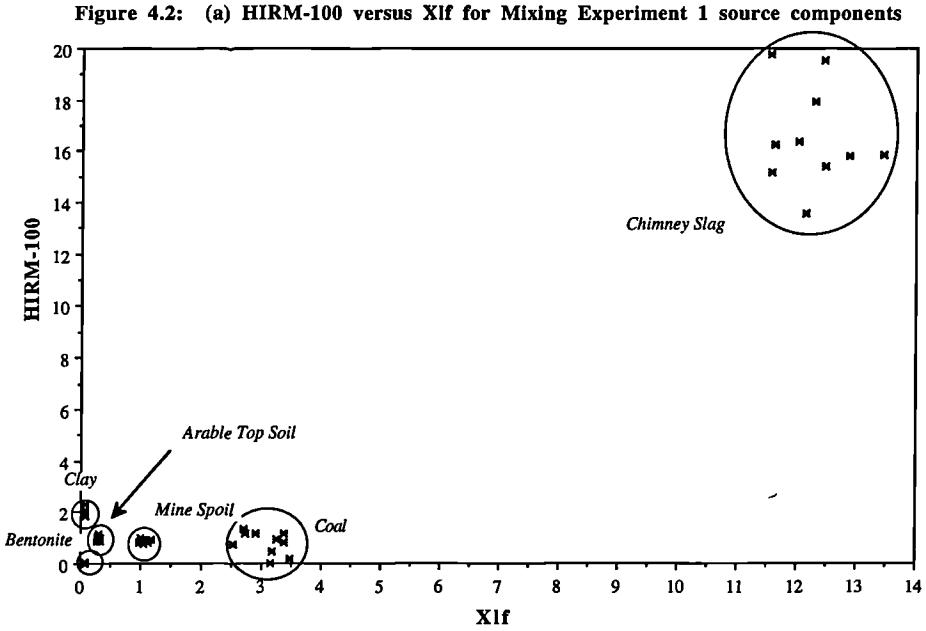

(b) Principal Co-ordination plot for mixing experiment 2 source components

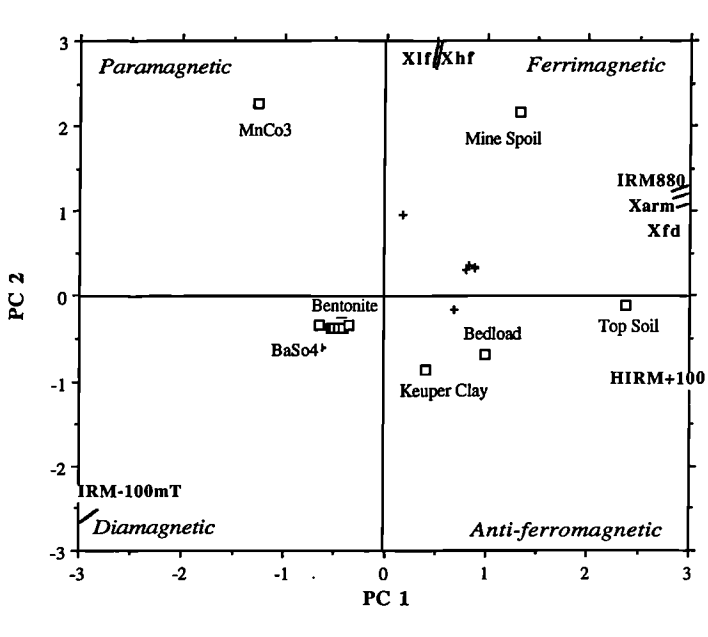

(c) Principal Co-ordination plot for mixing experiment source components and mixtures

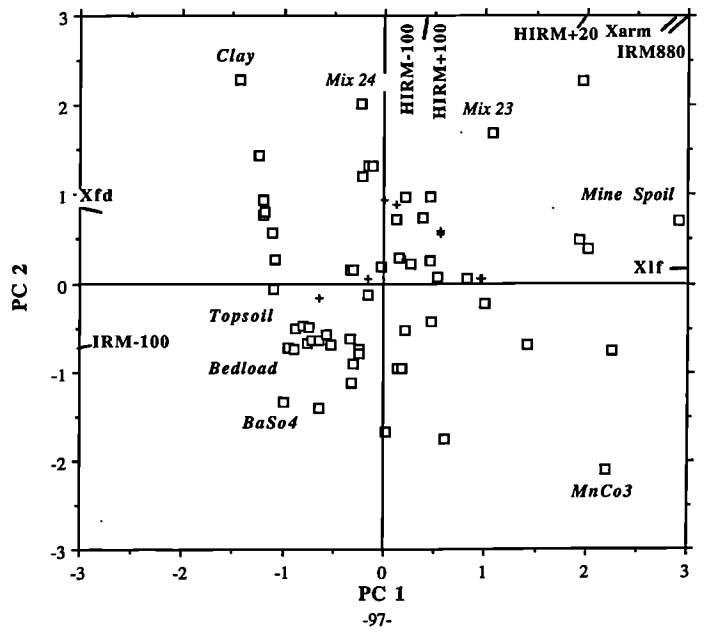

Linear Additivity

The actual mixture measurements were plotted against the predicted mixture parameter to test the linearity of each parameter. Figures 4.3 and 4.4 present results for selected representative parameters (χlf, χarm, IRM880 and HIRM-100) for mixing experiments 1 and 2 respectively. Overall there is a linear relationship between the actual and predicted values for the parameters shown but the relationships are not 1:1 (except for the χlf measurements of both mixing experiments). On the whole, the linearity worsens towards greater measurement values in experiment 1. This is especially shown in Figure 4.3c where greater deviation from the y=x line occurs with greater IRM880 values. Generally there is a 'systematic offset' in the predicted values which are lower than the actual values. Since no material could have been lost in these mixtures it indicates a magnetic phenomenon occurring in the original source samples. Much spread is seen in the HIRM-100 results which is compounded by the fact that HIRM-100 is a difference parameter and errors in the two original parameters, IRM880 and IRM-100, are effectively added. In Figure 4.4 the environmental mixtures appear to have lower deviations from the y=x line than the environmental and chemical mixtures. This is due to the errors involved in measuring the diamagnetic chemical reagents used in these mixtures.

Numerical comparison between the errors of the actual versus predicted measurements can be made from Table 4.2. In the table, error statistics are presented for each mixture (based on all parameters) and each parameter (based on all mixtures in each experiment). Percentage linearity errors were calculated by finding the difference between the predicted and actual values as a percentage of the predicted parameter values. The percentage errors are very variable in the first set of mixtures, for instance minimum errors range between 0 and 10% and maximum errors range between 20 and 200%, whereas in the second experiment minimum errors range between 0 and 15% and maximum errors range between 4 and 555%. Linearity errors for the magnetic parameters also show great variation. χlf measurements have the lowest errors of 7 and 5% in experiments 1 and 2 respectively. Remanence measurements have much higher average errors of between 9 and 30. The largest errors are found in those parameters which were difference calculations of two other measurements; for example χfd (not shown) and HIRM-100 (especially in experiment 1). Overall average parameter errors are lower in experiment 2 due to improved homogeneity of source samples. Some extreme error values were calculated for certain mixtures (mixtures 5, 51 and 63 for example); these are mixtures which completely failed, the reasons for which are presented later.

Table 4.3 shows the actual component proportions in each of the mixtures (in both experiments) and those predicted by LINDO using all linear measurements. Where a source component was not included in a mixture a zero is entered but the source was still included in the linear programming routine. For instance, mixture 1 contained all six source components but mixture 2 contained only 5 components. If the mixture and source properties were perfectly linear the actual and LINDO results would be equal. However this is not the case for the majority of the mixtures. For instance in mixture 9 the first and fifth components (Keuper clay and coal) are not attributed proportions by LINDO; the second component (topsoil) however is attributed 79% when only 18% was included in the mixture. In the first mixture set such inconsistencies can be related mainly to the strong and variable chimney

Figure 4.3: Predicted versus actual mixture measurements for mixing experiment 1

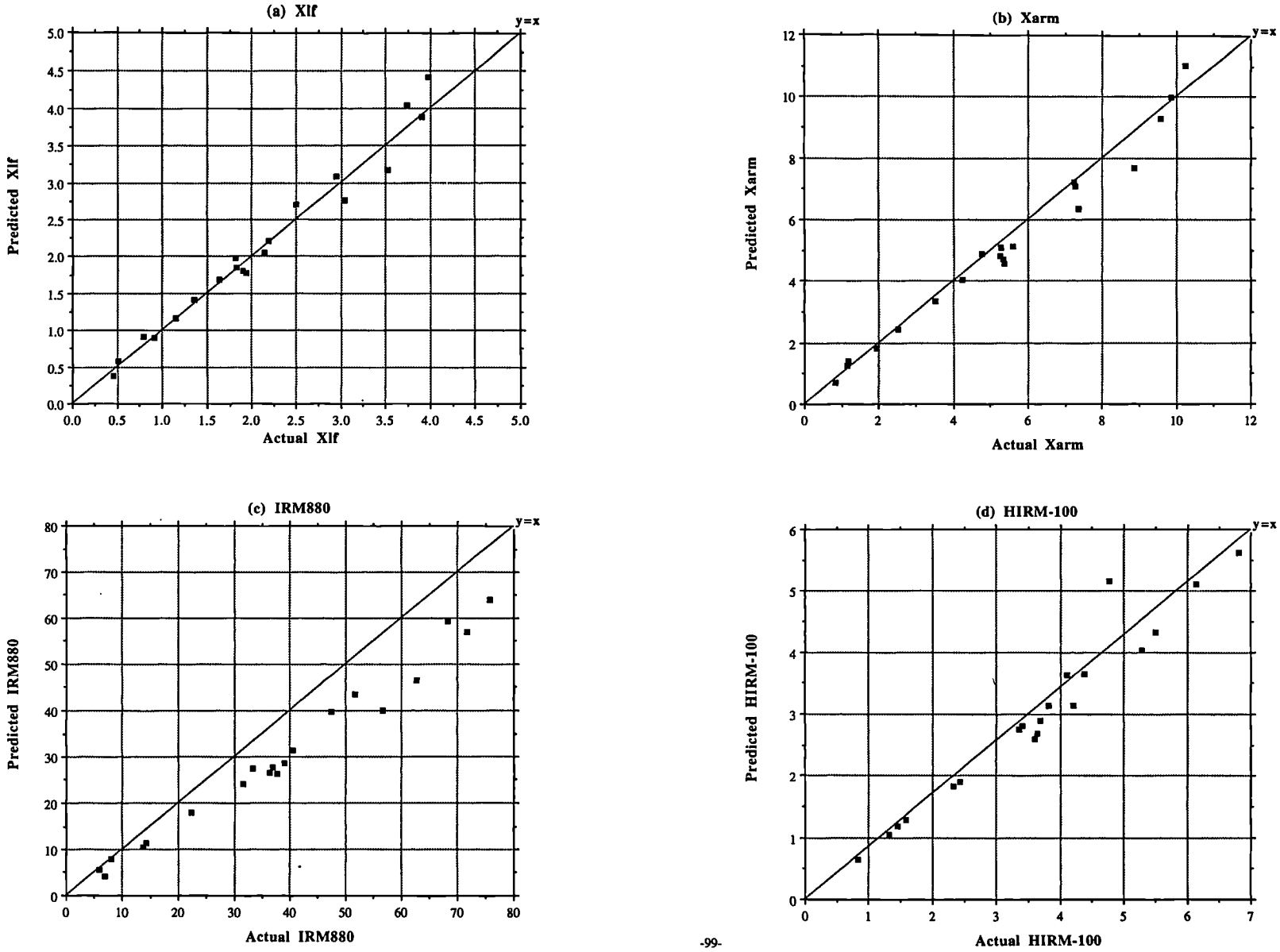

Figure 4.4: Predicted versus actual mixture measurements for mixing experiment 2

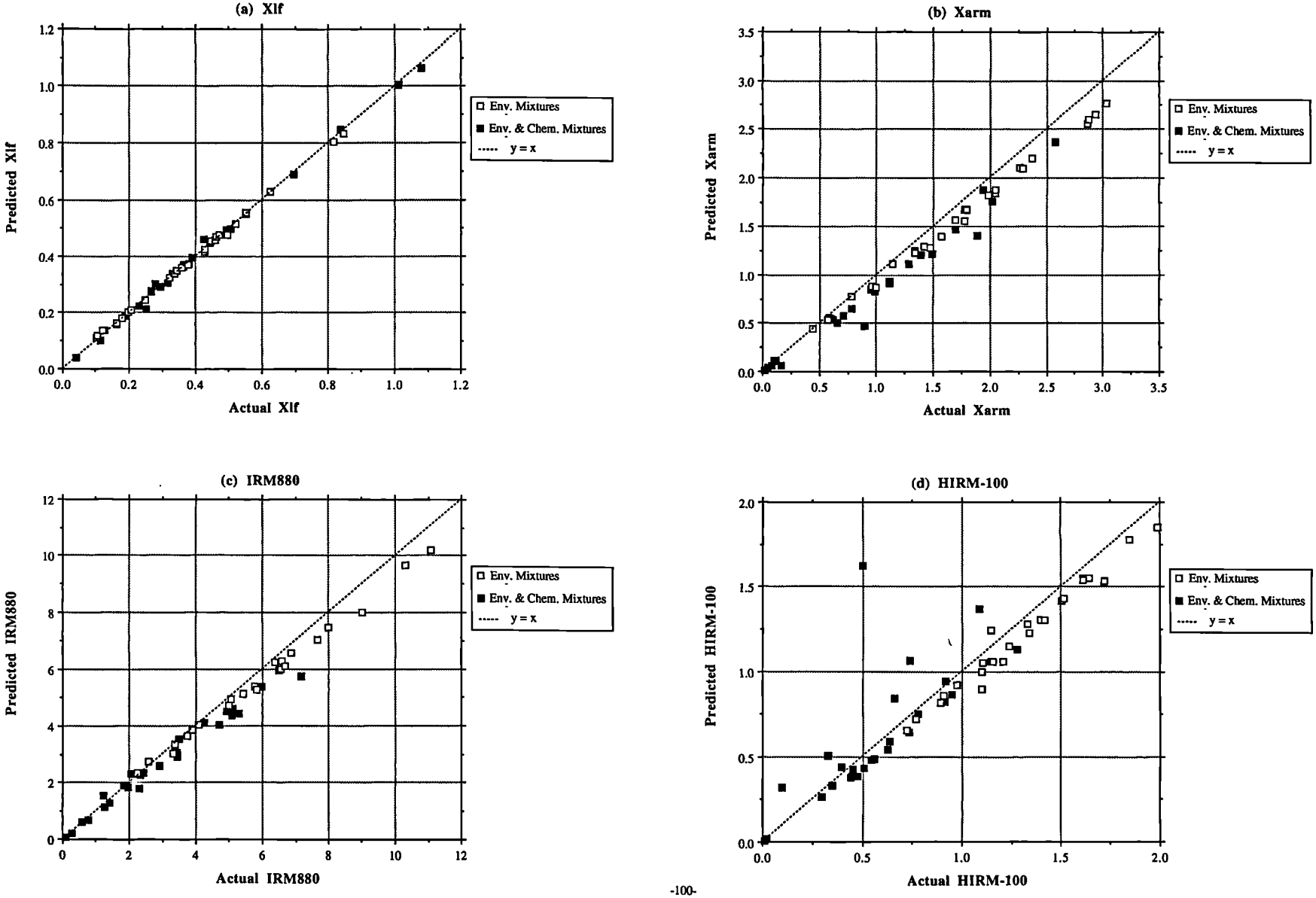

slag material and similar samples within the source set. When a PCA analysis was performed on the components and mixtures of mixing experiment 1, only one factor, a ferrimagnetic property, was identified. This indicates that the chimney slag dominated the magnetic mineralogy of most of the mixtures and masked other similar but weaker sources (such as coal) which were not then mathematically identified (eg mixture 14). In contrast, in the second set of mixtures, a mixture of magnetically similar materials works only in the case that they are the only two source components. But when one of the components is diamagnetic (barium sulphate) or paramagnetic(manganous carbonate) the mixture fails (eg mixtures 20 and 63). It was found during experimentation with different numbers of parameters that better results were gained using the parameters χlf, χfd, χarm, IRM100, IRM880 and HIRM100. Further interrelated parameters such as other IRM parameters worsened the results.

Table 4.2: (a) Linearity Errors for each mixture and measurement ((predicted-actual)/predicted)*100) and (b) Errors for each mixture and measurement between LINDO predicted mixture measurement and actual measurement (%)

Mixing Experiment 1

(a) Expected versus Actual Errors					**(b) LINDO Predicted versus Actual Errors**			
Mixture	**Mean**	**SD**	**Min**	**Max**	**Mean**	**SD**	**Min**	**Max**
1	10	7	0	30	5	7	0	30
2	6	7	0	30	5	7	0	30
3	16	45	0	200	27	19	10	100
4	9	9	0	30	4	7	0	20
5	7	5	0	20	55	4	50	70
6	22	10	10	50	7	8	0	30
7	17	8	0	40	5	8	0	30
8	10	8	0	30	5	7	0	20
9	12	8	0	30	8	9	0	30
10	9	8	0	30	9	7	0	30
11	5	7	0	30	11	6	10	30
12	6	8	0	30	7	8	0	30
13	13	8	0	40	5	7	0	30
14	15	8	0	40	5	7	0	30
15	24	10	10	50	7	9	0	30
16	12	21	0	90	13	21	0	90
17	12	19	0	90	10	20	0	90
18	42	21	0	60	10	13	0	40
19	16	7	10	40	6	7	0	30
20	10	9	0	30	5	8	0	30
n = 19								
Parameter	**Mean**	**SD**	**Min**	**Max**	**Mean**	**SD**	**Min**	**Max**
χlf	7	5	1	20	10	11	0	50
χhf	7	5	1	20	11	11	0	50
χarm	18	43	0	198	13	23	0	95
IRM5	22	12	2	48	20	13	7	60
IRM10	19	12	2	45	19	13	8	59
IRM20	30	7	13	40	29	11	14	66
IRM40	18	11	0	45	14	13	0	54
IRM60	12	13	0	55	6	12	0	54
IRM80	12	13	0	59	7	14	0	61
IRM100	11	13	0	59	6	13	0	55

Table 4.2 continued

Parameter	Mean	SD	Min	Max	Mean	SD	Min	Max
IRM150	18	27	0	89	14	28	0	90
IRM200	12	13	0	60	7	12	0	54
IRM250	11	13	0	62	6	12	0	53
IRM300	10	13	1	59	6	12	0	53
IRM400	10	11	0	46	6	12	0	53
IRM500	12	12	1	53	7	13	0	56
IRM600	10	11	1	53	5	12	0	53
IRM700	10	11	0	53	6	12	0	52
IRM880	11	11	0	49	7	12	0	54
HIRM-100	107	54	14	181	88	55	0	193

n= 20

Mixing Experiment 2

(a) Expected versus Actual Errors **(b) LINDO Predicted versus Actual Errors**

Mixture	Mean	SD	Min	Max	Mean	SD	Min	Max
21	2	2	0.06	6.18	2	2	0	10
22	2	1	0.56	4.9	2	2	0	10
23	13	4	0.39	20.42	3	5	0	20
24	14	6	0.16	23.36	4	4	0	10
25	10	5	0.02	18.59	4	5	0	20
26	9	5	2.42	22.81	4	5	0	20
27	6	4	0.51	15.54	3	4	0	10
28	8	2	1.4	10.62	2	3	0	10
29	4	2	0.83	7.45	2	2	0	0
30	12	7	0.46	37.51	4	9	0	40
31	11	3	4.11	15.46	2	2	0	10
32	11	17	1.25	89.19	5	18	0	90
33	5	2	1.11	9.09	2	3	0	10
34	9	3	1.01	14.81	3	4	0	10
35	3	1	0.3	6.48	1	2	0	0
36	5	2	0.1	8.49	1	2	0	10
37	9	3	2.01	13.24	2	2	0	10
38	13	12	5.12	52.04	7	15	0	60
39	5	8	0.64	40.28	3	5	0	30
40	12	6	0.27	17.97	3	5	0	30
41	8	3	0.42	11.97	2	2	0	10
42	5	3	1.55	12.72	2	3	0	10
43	8	2	1.86	14.01	1	2	0	10
44	2	2	0.09	7.7	2	1	0	10
45	6	2	0.53	11.62	2	3	0	10
46	17	5	0.94	25.42	2	4	0	20
47	9	4	0.08	14.99	2	2	0	10
48	44	109	1.43	555.41	19	86	0	420
49	3	3	0.02	10.3	2	2	0	10
50	13	13	1.69	73.11	11	15	0	70
51	35	10	13.43	54.55	10559	816	8720	10290
52	21	6	15.48	39.43	2	3	0	10
53	6	4	0.92	11.78	6	4	0	10
54	19	6	0.82	28.67	7	16	0	60
55	20	5	7.82	33.68	4	8	0	30
56	10	4	1.03	17.15	2	4	0	10
57	5	4	0.58	14.97	4	6	0	30

Table 4.2 continued

Mixture	Mean	SD	Min	Max	Mean	SD	Min	Max
58	16	5	1.19	22.51	1	1	0	0
59	11	4	1.51	18.32	2	2	0	10
60	16	5	0.86	20.67	1	2	0	10
61	84	59	2.02	159.03	9	16	0	60
62	13	4	0.28	19.05	7	17	0	60
63	87	75	.21	226.55	134	203	0	770
64	9	3	0.57	13.27	1	1	0	0
65	15	5	1.32	22.22	2	3	0	10
66	2	2	0.25	7.57	2	2	0	10
67	8	4	0.57	16.03	2	4	0	20
68	30	10	12.11	41.64	1	2	0	10
69	12	4	0.01	18.43	1	1	0	10
70	9	11	2.14	58.78	4	13	0	60
71	7	5	1.57	19.95	3	4	0	10

n = 48

Parameter	Mean	SD	Min	Max	Mean	SD	Min	Max
χLF	5	10	0	51	10	15	0	60
χHF	5	10	0	52	10	15	0	61
ARM	13	12	0	86	6	6	0	26
IRM5	12	17	1	112	4	4	0	20
IRM10	13	19	0	131	3	3	0	14
IRM15	12	20	0	142	4	3	1	12
IRM20	13	20	1	142	3	3	0	12
IRM30	15	22	1	154	4	6	0	45
IRM40	14	23	1	159	2	2	0	16
IRM50	15	25	1	158	3	13	0	90
IRM60	13	22	0	152	1	2	0	14
IRM80	13	21	0	148	1	2	0	13
IRM100	12	20	0	136	1	2	0	12
IRM150	13	18	0	105	2	11	0	74
IRM200	11	12	0	77	1	1	0	7
IRM250	10	9	0	57	1	1	0	6
IRM300	10	8	0	43	0	1	0	3
IRM400	9	6	0	23	0	1	0	3
IRM600	9	6	0	20	0	1	0	3
IRM880	9	5	1	21	1	1	0	5
IRM880-IRM20	11	6	0	25	3	2	0	12
IRM880-IRM100	12	10	1	65	3	3	0	14
HIRM+100	14	13	2	69	16	61	0	424

n = 24

Table 4.3: Component proportions of the mixtures and those predicted by LINDO (L)

Mixing Experiment 1

Mixture No.	Keuper Clay	Topsoil	Mine Spoil	Chimney Slag	Coal	Bentonite
1	25.24	19.02	27.55	5.76	10.51	11.92
L	36.1974	20.0442	38.0106	5.7478	0	0
2	16.22	17.	21.95	11.97	0	32.86

Table 4.3 continued

Mixture No.	Keuper Clay	Topsoil	Mine Spoil	Chimney Slag	Coal	Bentonite
L	50.0742	10.9459	27.6022	11.3777	0	0
3	14.33	19.49	18.13	12.35	8.79	26.9
L	83.0498	0	0	16.9502	0	0
4	8.46	26.9	11.75	14.06	9.63	29.2
L	9.999	10.5934	67.6057	11.802	0	0
5	0	37.85	25.25	18.13	7.61	11.17
L	0	0	39.1719	41.5194	19.3087	0
6	7.33	7.19	33.02	0	16.82	35.64
L	0	15.3642	42.2314	0	8.8951	33.51
7	21.61	0	34.7	27.78	6.84	9.08
L	48.2495	0	28.02	23.73	0	0
8	41.57	41.42	0	3.05	12.19	1.7
L	53.0777	28.996	0	2.0182	15.908	0
9	21.06	18.38	46.24	10.62	3.69	0
L	0	78.6228	9.8286	11.5486	0	0
10	9.85	13.64	18.12	27.21	10.13	21.05
L	0	71.2725	0	28.7275	0	0
11	14.47	18.37	20.21	21.61	7.99	17.34
L	0	74.5594	0	25.4406	0	0
12	39.94	30.33	4.45	12.52	3.91	9.18
L	15.1722	67.36	4.3066	13.1587	0	0
13	0	0	54.9	18.82	6.28	20
L	0	0	84.0358	15.9642	0	0
14	49.76	0	0	18.45	9.27	22.32
L	83.7578	0	0	16.2422	0	0
15	28.57	44.34	0	0	14.6	12.49
L	29.9072	60.7464	0	0	9.3464	0
16	15.21	28.82	30.65	0	25.32	0
L	33.329	23.1285	0	0	33.5425	0
17	22.59	27.97	38.72	10.72	0	0
L	52.2371	21.1812	14.7005	11.8812	0	0
18	0	38.72	31.14	0	0	30.14
L	0	43.3705	49.9915	0	0	6.638
19	50.68	0	0	29.95	19.37	0
L	73.1716	0	0	26.8284	0	0
20	10.58	27.67	23.93	10.26	3.71	23.85
L	21.3895	26.338	43.2392	9.0334	0	0

Mixing Experiment 2

Environmental Mixtures

Mixture No.	Keuper Clay	Topsoil	Mine Spoil	Finham Bedload
21	44.4437	55.5563	0	0
L	44.1873	55.8127	0	0
22	65.126	34.874	0	0
L	64.5901	35.4099	0	0
23	42.3882	0	57.6118	0
L	33.6061	0	66.3939	0
24	71.0079	0	28.9921	0
L	66.2026	0	33.7974	0
25	44.5055	0	0	55.4945
L	36.319	0	0	43.681
26	23.6442	0	0	76.3558
L	35.6031	0	0	64.3987

Table 4.3 continued

Mixture No.	Keuper Clay	Topsoil	Mine Spoil	Finham Bedload
27	0	65.3444	34.6556	0
L	0	59.1659	40.8341	0
28	0	26.4087	73.5913	0
L	0	14.3091	85.6909	0
29	0	65.2111	0	34.7889
L	0	68.4005	0	31.5995
30	0	28.278	0	71.722
L	0	39.8188	0	60.1812
31	0	0	38.9445	61.0555
L	0	0	45.1498	54.8502
32	0	0	75.3981	24.6019
L	0	0	82.0539	17.9461
33	33.3609	32.589	34.0501	0
L	34.5358	27.2646	38.1996	0
34	8.1633	60.1926	31.6441	0
L	7.4963	52.7217	39.782	0
35	33.5536	0	39.7027	26.7438
L	35.3842	0	41.1184	23.4975
36	46.8774	0	23.8985	29.224
L	51.2984	0	26.6144	22.0872
37	0	72.0314	18.0477	9.9209
L	0	78.2358	21.7642	0
38	0	24.7943	32.0455	43.1602
L	0	34.0002	35.6505	30.3492
39	32.0648	48.0476	0	19.8876
L	38.4994	53.4553	0	8.0453
40	43.3761	14.7863	0	41.8376
L	50.7553	9.0722	0	40.1725
41	22.8777	34.8943	27.427	14.801
L	27.5927	39.7909	31.3337	1.2828
42	8.2698	47.6858	27.3127	16.7317
L	15.0869	45.149	31.2837	8.4804
43	48.5407	16.9325	26.0278	8.499
L	49.8738	21.8055	28.3207	0
44	15.7733	34.6825	17.1843	32.3599
L	20.7815	35.6042	18.2468	23.3675
45	49.0317	15.9556	23.7253	11.2874
L	49.8146	25.0619	24.3051	0.8184

Environmental and Chemical Mixtures

Mixture No.	Keuper Clay	Topsoil	Mine Spoil	Finham Bedload	Barium Sulphate	Manganous Carbonate
46	0	0	34.951	0	65.049	0
L	0	0	42.0258	0	57.9742	0
47	0	60.092	0	0	39.908	0
L	0	65.693	0	0	34.307	0
48	0	0	47.466	0	0	52.534
L	0	0	59.35	0	0	40.65
49	0	82.39	0	0	0	17.61
L	0	84.1563	0	0	0	15.844
50	38.062	0	0	0	61.938	0
L	43.9604	0	0	0	56.0396	0
51	0	0	0	75.814	24.186	0
L	0	0	0	100	0	0

Table 4.3 continued

Mixture No.	Keuper Clay	Topsoil	Mine Spoil	Finham Bedload	Barium Sulphate	Manganous Carbonate
52	63.139	0	0	0	0	36.861
L	50.2367	0	0	0	0	49.763
53	0	0	0	85.047	0	14.953
L	0	0	0	82.3897	0	17.610
54	0	0	0	0	66.423	33.551
L	0	0	0	0	78.8091	21.191
55	0	0	0	0	23.202	76.798
L	0	0	0	0	27.6978	72.302
56	28.171	0	30.179	0	41.69	0
L	24.2938	0	34.7182	0	40.988	0
57	0	31.548	0	27.681	40.772	0
L	0	22.5334	0	55.4369	22.0297	0
58	0	0	34.99	0	35.435	29.575
L	0	0	41.1788	0	34.1964	24.625
59	0	50.91	0	0	18.229	30.861
L	0	57.5544	0	0	12.6937	29.752
60	6.856	0	31.862	0	0	61.128
L	5.7188	0	37.7077	0	0	56.574
61	68.876	12.245	0	0	0	18.879
L	5.726	39.1286	0	0	0	55.145
62	19.652	0	0	0	55.769	24.589
L	22.1521	0	0	0	63.5208	14.327
63	13.807	0	0	0	73.398	12.794
L	11.4235	0	0	0	88.5765	0
64	37.131	0	30.143	0	18.931	13.795
L	41.8101	0	33.3163	0	14.7568	10.117
65	9.221	0	20.72	0	56.811	13.247
L	10.4871	0	24.6891	0	55.8318	8.9919
66	0	59.081	0	25.294	7.435	8.19
L	0	54.9348	0	34.4783	4.2278	6.359
67	0	11.907	0	25.183	44.404	18.506
L	0	9.2554	0	37.0891	36.4636	17.192
68	25.937	46.783	0	0	23.075	4.204
L	0.7674	67.6655	0	0	27.6796	3.8876
69	0	0	36.864	38.642	13.341	11.153
L	0	0	41.2382	43.9331	8.215	6.6136
70	27.618	20.271	0	0	39.836	12.275
L	30.6917	21.5352	0	0	35.6026	12.17
71	0	0	9.881	43.365	25.127	21.627
L	0	0	9.7048	50.0502	19.7471	20.498

The causes of the failure for each mixture have been subjectively classified in Table 4.4. These causes range from inexplicable failure to those mixtures which fail due to strong or weak components. Mixtures which were given certain error limits have also been classified and these form the basis of Figure 4.5. In Figure 4.5 the 71 mixtures have been classified into three groups: those which fail (error>10%), those which have a linearity error between 5 and 10% and those which were most successful (error <5%). The proportion of mixtures with two or three components which had a linearity error of <5% is 55%. The proportion of mixtures which fail increases from 5% with two source components to 100% for 6 source components. Mixtures which contained one source from each of the four main magnetic properties failed in a proportion of 35% and only 30% were successful (error <5%).

Figure 4.5: Success rate for mixing experiments (71 mixtures)

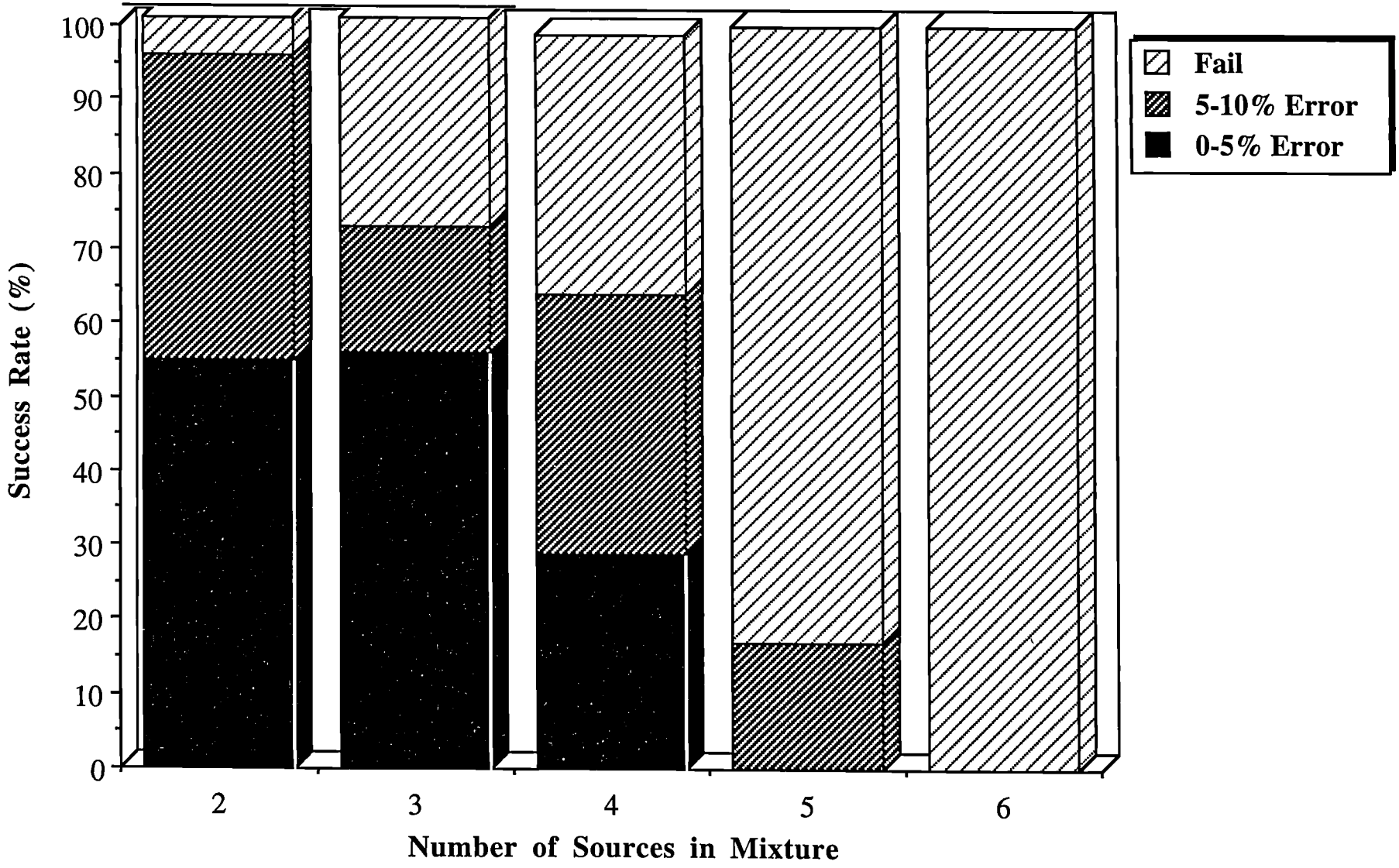

Table 4.4: Success and failure explanations for the mixtures in experiments 1 and 2. Results are graphically summarized in Figure 4.5.

A. Mixtures which failed Inexplicably

Mix Number	*No. of Components*
3	6

B. Mixtures which failed due to weak components

Mix Number	*No. of Components*	*Reason*
2	5	Bentonite
51	2	Barium Sulphate
63	3	Manganous Carbonate

C. Mixtures which failed due to strong components

Mix Number	*No. of Components*	*Reason*
5	5	Chimney Slag

D. Mixtures which failed due to very similar components

Mix Number	*No. of Components*	*Reason*
1	6	Mine Spoil+Coal; Clay+Bentonite
4	6	Mine Spoil+Coal+Bentonite
6	5	Clay+Soil
7	5	Mine spoil+Coal; Clay+Bentonite
9	5	Mine Spoil+Clay
10	6	Top Soil+Mine Spoil+Clay
11	6	Top Soil+Mine Spoil+Clay
12	6	Top Soil+Clay
13	4	Mine Spoil+Coal+Bentonite
14	4	Clay+Coal+Bentonite
15	4	Top Soil+Bentonite
16	6	Top Soil+Mine Spoil+Clay
17	4	Top Soil+Mine Spoil+Clay
18	3	Mine Spoil+Bentonite
19	3	Clay+Coal
20	6	Mine Spoil+Coal; Clay+Bentonite
37	3	Top Soil+Bedload
41	4	Bedload+all others
43	4	Top Soil+Bedload
45	4	Top Soil+Bedload
61	3	Manganous Carbonate+Clay
63	3	Manganous Carb.+Barium Sulph.
68	4	Top Soils+Clay

E. Mixtures which worked reasonably well (± 5-10%)

Mix Number	*No. of Components*	*Mix Number*	*No. of Components*
8	5	44	4
23	2	45	4
25	2	46	2
26	2	48	2
28	2	52	2
30	2	54	2
38	3	57	3
39	3	67	4
41	4	71	4
42	4		

Table 4.4 continued

F. Mixtures which worked perfectly (± 1-5%)

Mix Number	*No. of Components*	*Mix Number*	*No. of Components*
21	2	50	2
22	2	53	2
24	2	55	2
27	2	56	3
29	2	58	3
31	2	59	3
32	2	60	3
33	3	62	3
34	3	64	4
35	3	65	4
36	3	66	4
40	3	69	4
47	2	70	4
49	2		

Modelling with VSM Hysteresis Loops

Eight VSM 'source' mixtures were made and tested in a similar way to those of mixing experiments 1 and 2. However, the mixtures contained only two source components and the same source materials as the previous mixing experiments were used. Results of two of the mixtures are presented here. Mixture number 73 consisted of 65.603% Keuper clay and 34.397% mine spoil, and mixture 75 contained 40.145% arable topsoil and 59.855% manganous carbonate. The source components were mixed in these proportions into a total of 0.4g for a VSM sample holder.

The two source components for each mixture were forward multiplied to find the predicted curve. Again difference errors were calculated and are presented in Table 4.5. Errors are much larger at lower fields than at higher fields, for instance the error for mixture 73 at 1000mT is 1.3% but at 5mT it is 6.55. In small negative fields, however, errors rise to 61%. Figures 4.6 a and b show the hysteresis curves for each mixture, its source components and the predicted curve. Mixture number 73 is linearly accurate to within 10% except for very weak negative field measurements which are prone to inaccuracy. Mixture 75 however shows clearly that the mixture falls outside the range of the two source components in the paramagnetic section of the curve. From the eight VSM mixtures results were more similar to that of mixture 75. Mixture 73 was by far the most successful. No further VSM artificial mixing was proposed due to this experiment until causes of the errors could be identified and quantified.

Table 4.5: Hysteresis loop magnetization results (half curve) for source components and VSM mixtures 73 and 75. Expected results and error differences are also presented. (Error = Expected-Actual/Expected*100).

Field	Keuper	Top	Mine	Mang.	Mix 73			Mix 75		
(mT)	Clay	soil	Spoil	Carb.	Act.	Exp.	%Err.	Act.	Exp.	%Err.
1000	69.44	68.76	206.70	97.78	115.14	116.65	1.30	59.29	86.13	31.16
799	56.57	64.88	195.13	77.71	102.51	104.23	1.65	47.47	72.56	34.58
599	43.71	60.89	183.28	58.14	89.66	91.72	2.25	35.79	59.24	39.59
398	30.95	55.74	169.19	38.74	76.24	78.50	2.88	24.19	45.57	46.91
298	24.43	52.68	159.28	29.08	68.55	70.82	3.20	18.37	38.56	52.35
249	21.16	50.61	152.29	24.23	64.03	66.27	3.37	15.48	34.82	55.54

Figure 4.6: Hysteresis loops for VSM mixing experiment (a) Mixture No. 73

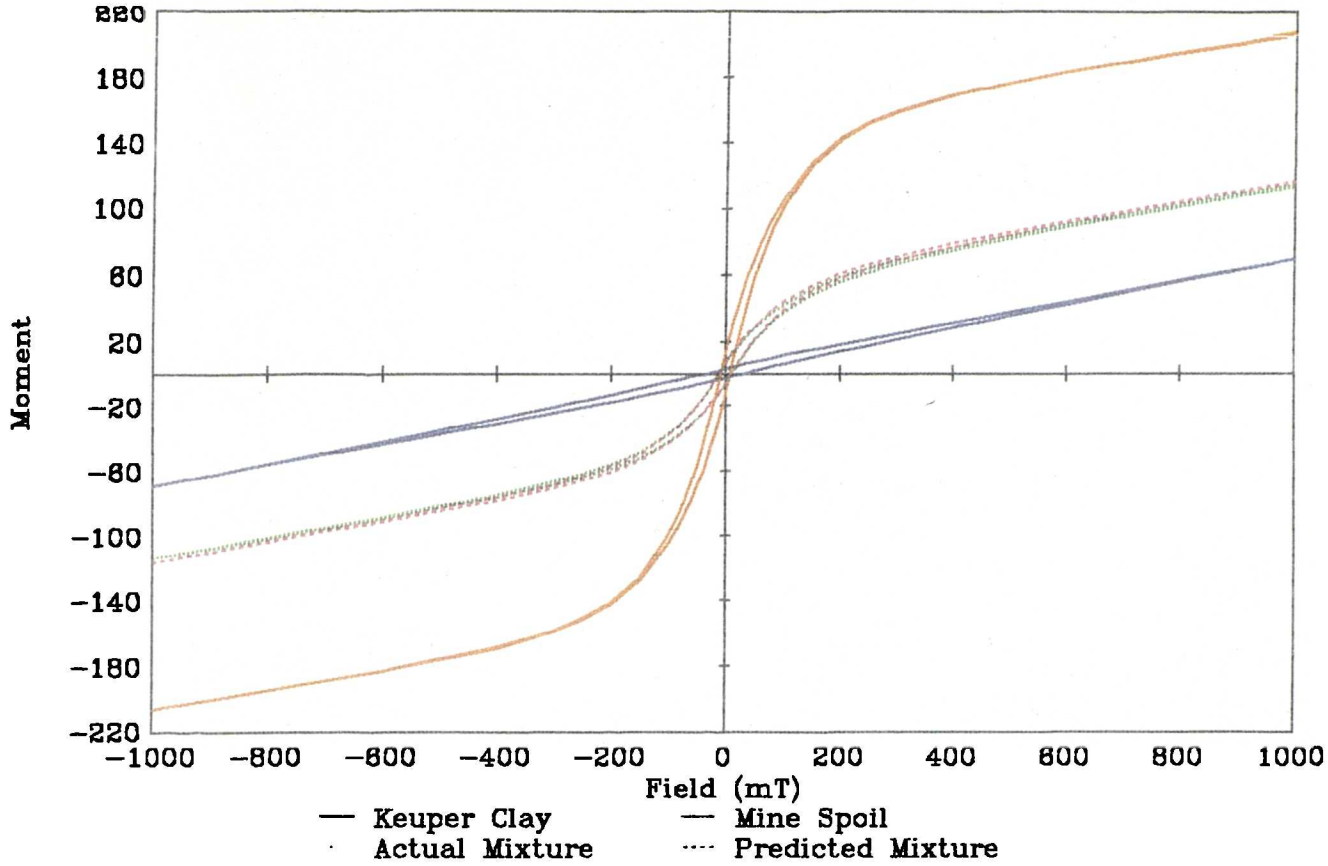

(b) Mixture No. 75

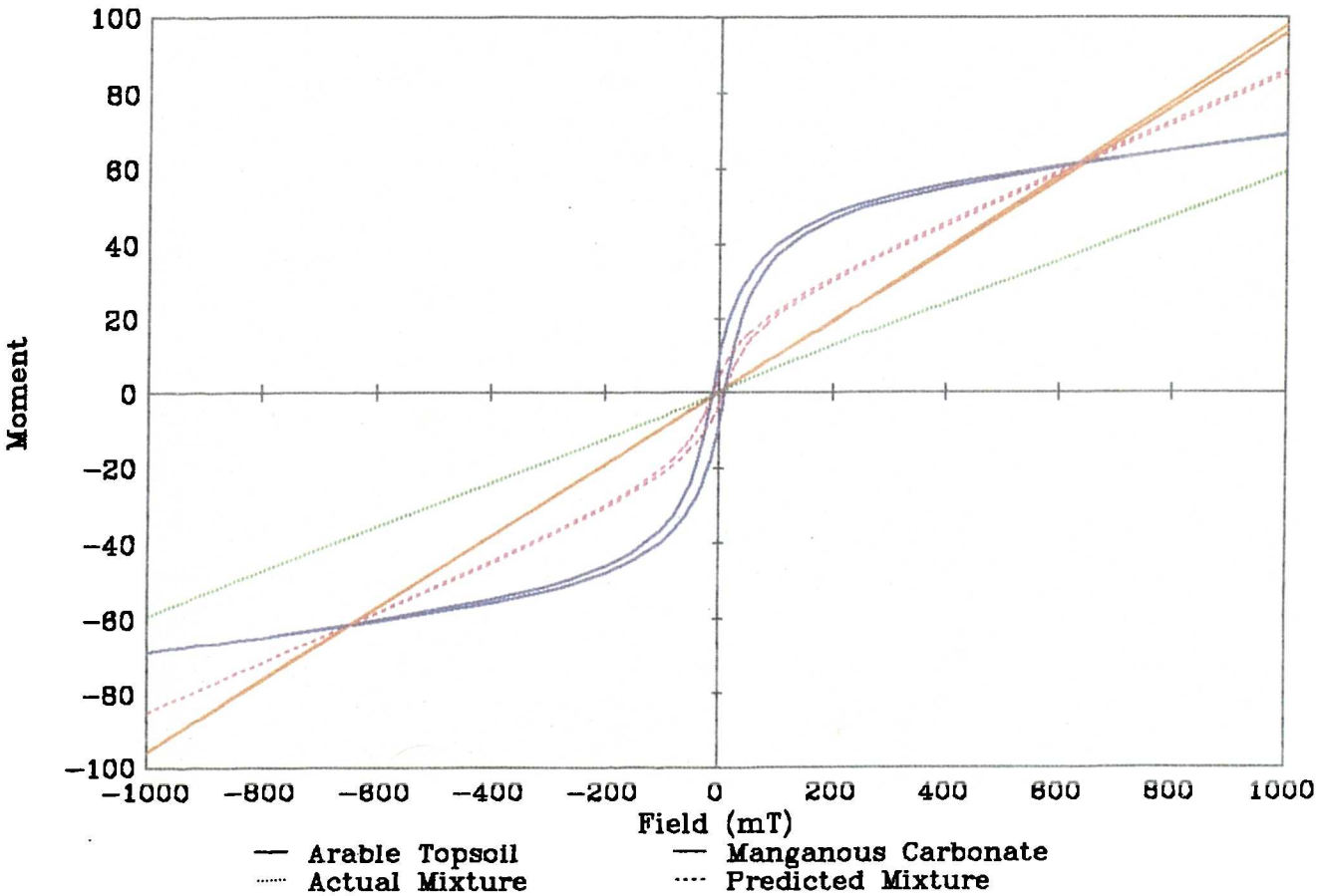

Table 4.5 continued

Field	Keuper	Top	Mine	Mang.		Mix 73			Mix 75	
(mT)	Clay	soil	Spoil	Carb.	Act.	Exp.	%Err.	Act.	Exp.	%Err.
198	17.83	48.03	142.52	19.38	58.63	60.72	3.44	12.54	30.88	59.38
148	14.49	44.76	128.09	14.53	51.61	53.57	3.66	9.56	26.67	64.14
99	11.05	39.65	105.14	9.63	41.72	43.41	3.89	6.55	21.68	69.81
78	9.54	36.71	92.82	7.71	36.75	38.19	3.77	5.32	19.35	72.53
59	7.99	33.02	77.80	5.77	30.84	32.00	3.64	4.09	16.71	75.55
49	7.26	30.64	69.16	4.80	27.56	28.55	3.47	3.45	15.17	77.28
39	6.61	27.88	59.96	3.83	23.98	24.96	3.94	2.81	13.48	79.15
29	5.83	24.61	49.87	2.85	20.14	20.98	4.00	2.17	11.59	81.24
24	5.33	22.63	44.39	2.37	17.90	18.76	4.59	1.84	10.50	82.48
19	4.92	20.47	38.34	1.88	15.69	16.41	4.39	1.52	9.34	83.76
14	4.55	18.13	32.50	1.41	13.40	14.16	5.37	1.20	8.12	85.18
9	4.13	15.32	25.94	0.90	11.02	11.63	5.23	0.87	6.69	86.97
4	3.69	12.57	19.91	0.46	8.67	9.27	6.55	0.57	5.32	89.37
0	3.29	9.13	13.02	0.03	6.11	6.64	7.98	0.22	3.68	94.14
0	3.24	8.95	12.81	0.00	6.08	6.53	6.97	0.19	3.59	94.75
0	3.13	8.87	12.72	0.02	6.11	6.43	4.99	0.17	3.57	95.22
-5	2.61	4.62	4.67	-0.52	2.99	3.32	10.02	-0.23	1.54	115.12
-10	2.22	0.46	-3.18	-0.99	0.14	0.36	61.01	-0.61	-0.41	-48.78
-15	1.70	-3.68	-11.07	-1.48	-2.67	-2.69	1.03	-0.97	-2.36	58.98
-20	1.30	-7.75	-18.38	-1.98	-5.59	-5.47	-2.15	-1.35	-4.30	68.66
-25	0.91	-11.16	-25.57	-2.46	-8.33	-8.20	-1.63	-1.67	-5.95	71.92
-30	0.35	-14.35	-32.33	-2.97	-10.89	-10.89	-0.03	-2.02	-7.54	73.19
-40	-0.42	-19.95	-45.47	-3.91	-15.92	-15.92	0.00	-2.69	-10.35	73.96
-50	-1.28	-24.37	-57.38	-4.89	-20.29	-20.58	1.42	-3.37	-12.71	73.51
-60	-2.13	-27.81	-68.07	-5.87	-24.42	-24.81	1.59	-4.00	-14.68	72.78
-80	-3.79	-32.96	-86.37	-7.80	-31.56	-32.20	1.98	-5.28	-17.90	70.51
-100	-5.45	-36.59	-100.98	-9.69	-37.44	-38.31	2.26	-6.50	-20.49	68.28
-150	-9.34	-42.57	-126.70	-14.53	-48.58	-49.71	2.27	-9.55	-25.79	62.98
-200	-13.18	-46.39	-141.85	-19.31	-56.06	-57.44	2.40	-12.51	-30.18	58.55
-251	-17.06	-49.11	-151.67	-24.10	-61.85	-63.36	2.38	-15.48	-34.14	54.66
-301	-20.85	-51.40	-158.74	-28.90	-66.67	-68.28	2.36	-18.40	-37.93	51.49
-401	-28.15	-54.85	-169.01	-38.44	-74.83	-76.60	2.31	-24.22	-45.03	46.21
-601	-42.19	-60.41	-183.37	-57.51	-88.87	-90.75	2.08	-35.83	-58.68	38.94
-800	-55.71	-64.86	-195.29	-76.67	-101.74	-103.72	1.91	-47.48	-71.93	33.99
-1000	-69.11	-68.73	-206.55	-96.18	-114.35	-116.39	1.75	-59.33	-85.16	30.33

Summary

Identification of the magnetic 'distance' needed between materials which can be unmixed successfully can be inferred from PCA co-ordination plots (eg Figure 4.2b). If the source components occur in different quadrants of the plot then mixtures of those components will be more successful than those of components which occur in the same quadrant. The co-ordination plot also gives us the means to see which mixtures contain which source components. All the mixtures fall within the bounds of the relevant source components (plus associated errors). If they had not then PCA would have identified first those source components which do not contribute to the mixture (ie the mixtures would fall out of the range of certain source components), and secondly, erroneous mixtures.

Referring again to Figure 4.1, the evaluation of the linearity of magnetic properties and specific measuring equipment can be quantified using the linearity errors. The linearity of measurements for each mixture set varies but follows a similar pattern. Susceptibility measurements have the lowest errors (5-7%,) indicating that the Bartington

Meter is linear. Remanence measurements made on the Molspin Fluxgate magnetometer are not so linear, with errors generally well over 10%. Linearity of the VSM magnetization data for successful mixtures was good, with errors of only 6.5% at low positive fields (5mT). Great difficulties were encountered in the mixing of such small samples and this could be the cause of the high failure rate of the VSM mixtures. The VSM samples especially are affected by intra-sample variability caused by sub-sampling procedures. The parameters which obtained the best linear programming results were χlf (χhf), χfd, χarm, IRM100, IRM880 and HIRM100.

The predicted mixture values were consistently lower than the actual mixture values in both experiments. The variability and scale of the chimney slag component used in experiment 1 caused other components in the mixtures to be masked. The scale and positive skew associated with most magnetic databases as shown in Chapter 3 cannot be overcome by mathematical transformation for linear modelling. The variability in the chimney slag is responsible for the increasing deviation from the y=x line in IRM880 measurements. One prospect of improving linearity and excluding such large scale differences might be to exclude parameters such as IRM880 which accentuate the scale of the unit numbers in the modelling. Another possibility of the cause of the predicted values being systematically less than those of the actual measurements is more interaction (or other unidentified process) in the source samples than in the mixtures; this factor is further explored in Paper 1, Appendix 7. However from synthetic mineral dilution experiments (not presented in the thesis), where 5 dilutions were made of 15 synthetic minerals, interaction only affected the linearity of χlf measurements in dilutions containing more than 20% of the mineral. Such clear results were not gained when testing remanence measurements, however, due to the scale of remanence values overloading the attenuation on the Molspin equipment. Realistically, no more than four sources could be modelled successfully and these would have to be of the four main magnetic properties shown in Figure 4.2b. Sources which contribute less than 10% of material would probably not be recognized in the linear programming and for weaker materials this figure could be as high as 25%. Overall it is the linear program, LINDO, which fails to incorporate the linearity errors seen in the mixing experiments. Section 4.2.2 aims to test the sensitivity of LINDO to various linearity errors using a hypothetical mixing experiment to further define this failure.

4.1.2 Modelling with Hypothetical Mixtures

Further to the mixing experiments which identified homogenous, linearity and mixing errors, five sets of data were chosen and hypothetical mixtures calculated to test the sensitivity of LINDO, with the aims being to:

1. Test the sensitivity of LINDO to changes in the mixture measurement (RHS of the problem)
2. Test the sensitivity of LINDO to repeat samples (with the same magnetic properties, LHS of the problem)
3. To find the largest error which can exist in the mixture measurement while obtaining a reasonable prediction of source component proportions.

Methodology

Magnetically diverse source samples were chosen from the databases using their normalized IRM curves (such that they were as magnetically different as possible in terms of mineralogy and grain size). The flow diagram in Figure

4.7 shows the methodology of the hypothetical experiment. For the most part remanence measurements were tested in this experiment, as a systematic reduction in the predicted mixture remanence measurements were found in the mixing experiments. Therefore a systematic error rather than a randomly generated error was applied to change the mixture measurements made in this hypothetical experiment. Figure 4.8 shows the IRM curves for the source components. 18 remanence data points were used in the experiment as linear data and in some cases χlf data were also incorporated to see if an improvement in the results was gained. A 'dilution factor' had to be calculated into the files for three of the synthetic samples used as the measurement values were of a different order to those of the natural samples. This would never be done in any situation other than a hypothetical experiment. The only scaling process which can be used in a real data set is that of scaling all the source components and mixtures for the large value measurements (scaling all the measurements of one or two strong source components or mixtures is mathematically incorrect). Five files (IRM groups 1-5) were constructed from different configurations of source component samples and these are listed in Table 4.6. Also, some source component samples were calculated as 'multiples' of some of the original source components by multiplying all the original data by a constant value (constant values are shown in Table 4.6).

Table 4.6: Samples chosen for each Hypothetical Mixing file

IRM Group 1

	Component	**Magnetic Property**
x1	MT 18 (0.016μm dispersed magnetite gr)ains	Fine-grained Ferrimagnetic
x2	CCm1B15 0.5-2mm Corley topsoil	Ferrimagnetic
x3	JL1X1 Volvo Exhaust particles	Course-grained ferrimagnetic
x4	JD-S2 Synthetic Hematite	Canted-antiferromagnetic
x5	BE2A1 Clay Dust	Canted-antiferromagnetic

IRM Groups 2 and 3

	Component	**Magnetic Property**
x1	MT 18	(as above)
x2	JD-S22 Maghemite (MT 31)	Ferrimagnetic
x3	EW1B1 Coniferous Organic matter	Fine-grained Ferrimagnetic
x4	DM1N1 Daw Mill Colliery Leaf samples	Course-grained Ferrimagnetic
x5	JD-S70 Red Iron oxide	Canted-antiferromagnetic
x6	BE2A1	(as above)

IRM Group 4

x1	MT 18
x2	JD-S2
x3	JL1X1
x4	CCm1B15
x5	Multiple of x4 (* 3)

IRM Group 5

x1	MT 18
x2	JD-S2
x3	Multiple of x2 (* 0.75)
x4	JL1X1
x5	CCm1B15
x6	Multiple of x4 (* 3)

Figure 4.7: Experimental Testing of LINDO using a Hypothetical Data Set

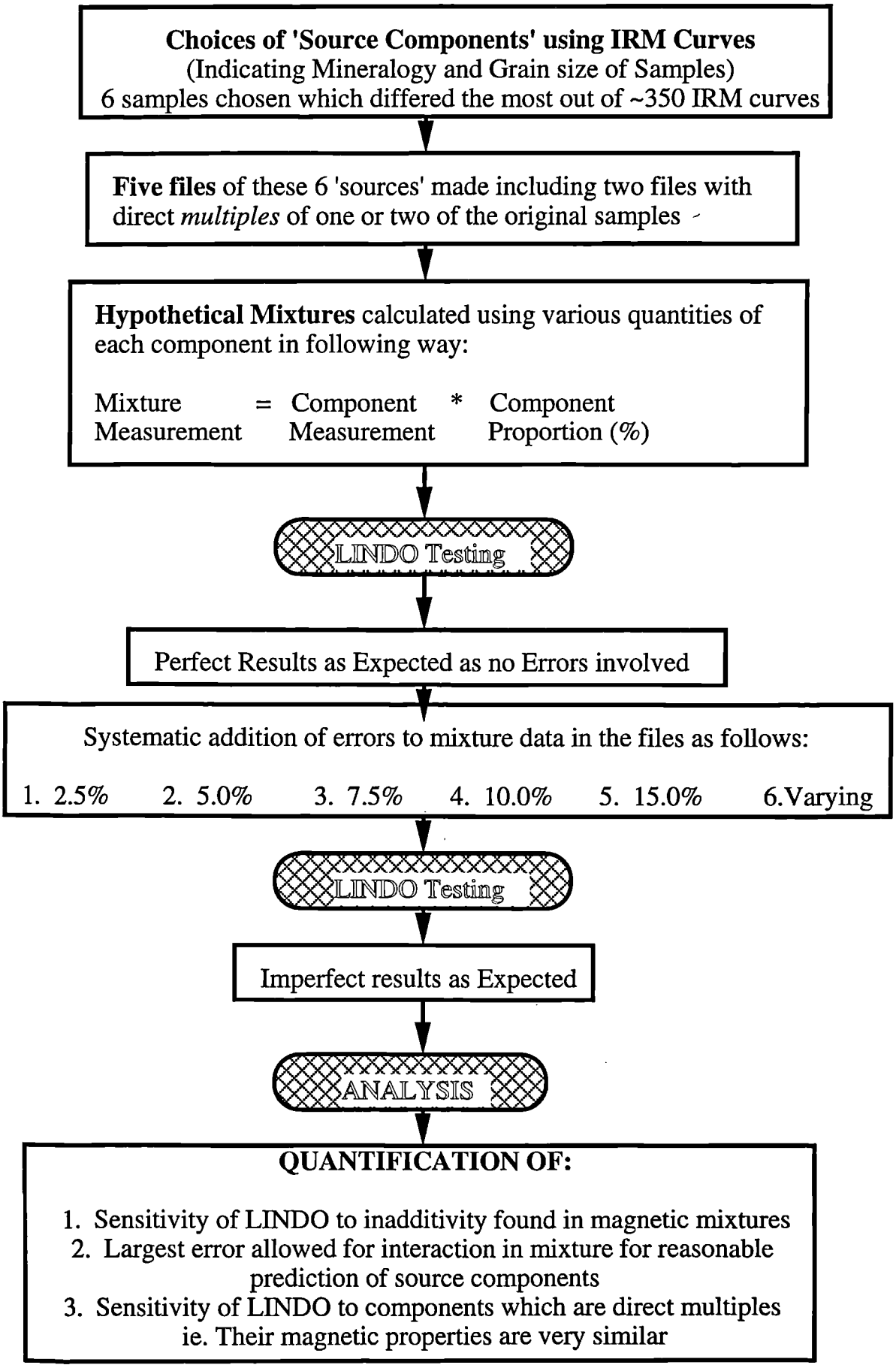

Figure 4.8: Normalized IRM Curves for source components used in the hypothetical mixing experiment

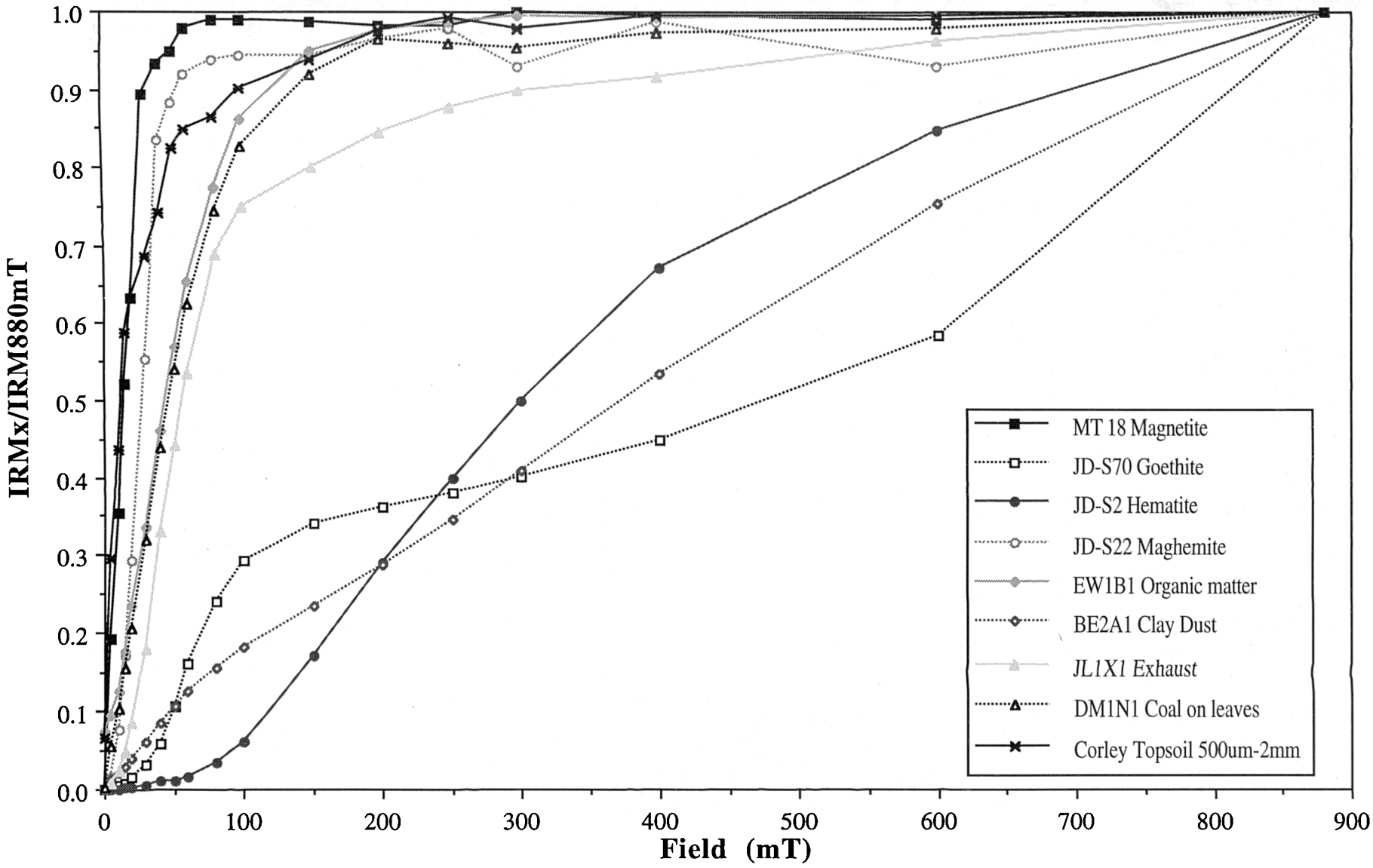

Hypothetical mixture values used in this experiment were forward calculated from the measurements of the components and their proportions, which were chosen subjectively. For example, the mixture component proportions for IRM Group 1 were set at 20% each therefore each mixtures' parameter value was calculated as follows:

$$a1*0.2 + a2*0.2 + a3*0.2 + a4*0.2 + a5*0.2 = b$$

Where: x1+x2+x3+x4+x5 = 1
ai = source components
b = mixture measurement

Errors were added to the mixture parameter values by calculating a set percentage of the mixture value and adding them to the values of the original mixture. For example in each file B = Actual + 5% of Actual.

Results

The results of the linear programming are shown in Table 4.7 and the sum of squares of differences error between the actual and predicted results are also summarized in Figure 4.9. This figure gives an indication of the variations in proportions predicted as caused by each error included in the hypothetical mixtures. The figure shows a progressive increase in error with increasing linearity errors imposed in the mixtures. In IRM groups 1 and 2 we can see that the component proportions cannot be predicted accurately with an error of over 10%. A sum of squares of the differences between the actual and predicted over a value of 7% means the result is poor. In IRM group 3 with very small components, of 3% and 8%, we can see that even with a large error (10%) the result is good and the components are identified by the program. Groups 4 and 5 incorporate small component values and multiple samples and due to this the situation is worsened. With an error of -7.5% in group 4 the multiple source sample (x5) could not be identified and in group 4 at an error of 2.5% the multiples were not identified.

Table 4.7: Results of Hypothetical Mixing Experiment with modelled source component proportions and the sum of sqaures error between the tests and the actual proportions.

IRM Group 1

Test	Error	x1	x2	x3	x4	x5	SSqDiff
	Actual	20.00	20.00	20.00	20.00	20.00	$\sqrt{((xi-x)^2/n)}$
A	0.00	20.00	20.00	20.00	20.00	20.00	0.00
B	2.50	21.15	20.95	19.65	20.83	17.42	1.39
C	-2.50	18.90	19.09	20.29	19.25	21.84	1.10
D	5.00	22.31	21.91	19.29	21.65	14.83	2.79
E	-5.00	19.89	19.91	20.03	19.93	20.19	0.11
F	7.50	23.47	22.87	18.94	22.48	12.25	4.19
G	-7.50	17.70	17.88	20.85	17.75	25.53	3.21
H	10.00	27.17	25.93	17.80	25.12	3.97	8.66
I	-10.00	21.83	21.51	19.44	21.31	15.91	2.21
J	15.00	26.93	25.74	17.87	24.96	4.49	8.37
K	-15.00	13.40	16.35	21.70	17.50	31.05	5.97
L	χlf 5 IRM 10	24.26	26.25	13.41	23.61	12.47	5.84
M	χlf-5 IRM-10	16.06	17.01	26.23	16.75	23.94	5.65

Figure 4.9: Graphical representation of the linearity errors calculated between predicted and expected measurements for the hypothetical mixing experiment

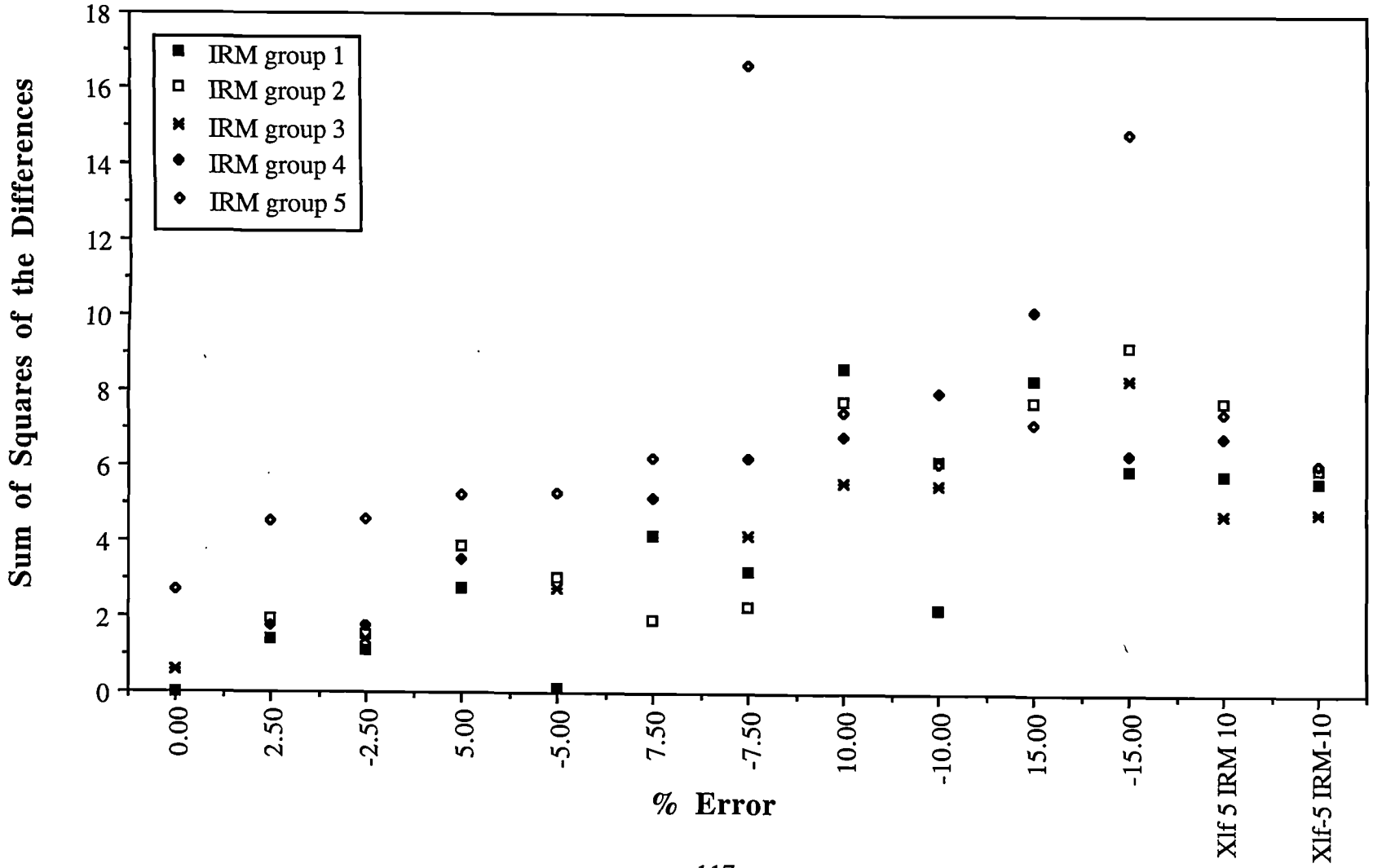

Table 4.7 continued

IRM Group 2

Test	Error	x1	x2	x3	x4	x5	x6	SSqDiff
	Actual	17.00	17.00	17.00	17.00	17.00	15.00	$\sqrt{((xi-x)^2/n)}$
A	0.00	16.99	17.00	16.99	17.04	16.96	15.00	0.00
B	2.50	17.05	17.83	17.44	18.77	12.78	16.14	1.94
C	-2.50	16.57	16.60	15.43	20.39	16.39	14.62	1.55
D	5.00	17.09	18.66	17.87	20.52	8.57	17.28	3.90
E	-5.00	16.14	16.22	13.86	23.66	15.89	14.23	3.07
F	7.50	17.05	17.83	17.44	18.77	12.78	16.14	1.94
G	-7.50	16.99	17.79	17.42	19.54	12.10	16.16	2.31
H	10.00	17.19	20.33	18.75	23.92	0.25	19.56	7.76
I	-10.00	15.29	15.43	10.73	30.30	14.79	13.45	6.16
J	15.00	17.94	21.27	21.52	18.68	0.00	20.60	7.76
K	-15.00	14.43	14.66	7.60	36.89	13.74	12.67	9.22
L	χlf 5 IRM 10	17.19	20.33	18.75	23.92	0.25	19.56	7.76
M	χlf-5 IRM-10	15.32	15.37	10.86	29.92	15.18	13.35	5.98

IRM Group 3

Test	Error	x1	x2	x3	x4	x5	x6	SSqDiff
	Actual	3.00	18.00	27.00	33.00	11.00	8.00	$\sqrt{((xi-x)^2/n)}$
A	0.00	2.99	18.99	28.03	32.99	11.01	7.99	0.58
B	2.50	3.10	18.45	28.76	30.14	11.35	8.23	1.39
C	-2.50	2.92	17.55	25.24	35.85	10.67	7.76	1.39
D	5.00	3.15	18.90	30.51	27.28	11.69	8.47	2.79
E	-5.00	2.85	17.10	23.49	38.70	10.33	7.53	2.78
F	7.50	3.23	19.35	32.27	24.42	12.03	8.70	4.18
G	-7.50	2.77	16.65	21.74	41.55	9.99	7.29	4.17
H	10.00	3.30	19.80	34.04	21.57	12.37	8.94	5.57
I	-10.00	2.70	16.20	19.99	44.40	9.66	7.05	5.55
J	15.00	3.45	20.70	37.53	15.86	13.04	9.41	8.35
K	-15.00	2.54	15.30	16.48	50.09	9.01	6.57	8.33
L	χlf 5 IRM 10	3.12	20.10	33.47	23.56	10.50	9.26	4.78
M	χlf-5 IRM-10	2.09	15.90	20.51	42.55	11.41	6.76	4.84

IRM Group 4

Test	Error	x1	x2	x3	x4	x5	SSqDiff
	Actual	47.00	13.00	25.00	12.00	3.00	$\sqrt{((xi-x)^2/n)}$
A	0.00	47.00	13.00	25.00	12.00	3.00	0.00
B	2.50	48.18	13.33	25.63	8.55	4.32	1.76
C	-2.50	45.83	12.67	24.38	15.45	1.67	1.76
D	5.00	49.35	13.65	26.25	5.10	5.65	3.53
E	-5.00	44.65	12.35	23.75	18.90	0.35	5.29
F	7.50	50.53	13.98	26.88	1.65	6.98	5.17
G	-7.50	42.96	12.04	22.86	22.15	0.00	6.23
H	10.00	52.71	13.39	27.69	0.00	6.21	6.83
I	-10.00	41.08	11.74	21.87	25.32	0.00	7.98
J	15.00	58.92	10.56	29.67	0.00	0.84	10.19
K	-15.00	37.31	11.25	19.89	31.68	0.00	6.36
L	χlf 5 IRM 10	50.42	12.37	28.24	0.00	8.97	6.83
M	χlf-5 IRM-10	41.08	11.74	21.87	25.32	0.00	20.52

Table 4.7 continued

IRM Group 5

Test	Error	x1	x2	x3	x4	x5	x6	SSqDiff
	Actual	23.00	19.00	8.00	33.00	11.00	6.00	$\sqrt{((xi-x)^2/n)}$
A	0.00	22.99	22.82	2.90	32.99	12.91	5.36	2.73
B	2.50	23.57	25.62	0.00	33.83	10.60	6.38	4.53
C	-2.50	22.42	24.37	0.00	32.18	17.40	3.63	4.56
D	5.00	24.15	26.25	0.00	34.65	7.20	7.75	5.24
E	-5.00	21.85	23.75	0.00	31.35	20.80	2.25	5.29
F	7.50	24.72	26.87	0.00	35.48	3.80	9.13	6.26
G	-7.50	21.27	0.00	30.83	30.53	12.64	4.73	16.66
H	10.00	25.30	27.50	0.00	36.30	0.40	10.50	7.45
I	-10.00	20.70	19.51	3.99	29.70	26.11	0.00	6.13
J	15.00	26.38	24.06	0.00	38.45	0.00	11.11	7.18
K	-15.00	19.55	1.74	26.01	28.05	24.65	0.00	14.91
L	χlf 5 IRM 10	25.30	27.50	0.00	36.30	0.40	10.50	7.45
M	χlf-5 IRM-10	20.70	19.52	3.97	29.70	26.11	0.00	6.13

Summary

LINDO is sensitive to errors as low at 2.5% which cause differences between the actual and predicted result. With one or two multiple samples at very low error noise (2.5%) the multiple cannot be identified in the routine. It can be seen that when small components of 3% are included the routine identifies the component, even when a large error is included. However it must be concluded that a component of less than 10% probably would not be identified properly in environmental mixtures unless it was a magnetically strong sample. However these values do not take into account the noise of the environment even if all the source components in the mixtures are known.

4.2 Environmental Linearity Tests

The artificial mixing experiments have tested the linearity of magnetic measurements and equipment. Large variability in laboratory source samples has been found to affect the modelling results. In this section two environmental experiments are presented which test the linear additivity of environmental mixtures. In both experiments small bulk samples, first of bedload and secondly of soil, have been collected and conservatively fractionated (ie no material was lost). The addition of the magnetic properties of the fractions multiplied by their relative proportions in the bulk samples is tested against the bulk magnetic properties. The experiments aim to confirm the importance of intra-sample variability and to test the linearity of fractionating samples and mathematical mixing.

4.2.1 Modelling Bedload using Simultaneous Equations

Introduction and Aims

An experiment was conducted on the River Sowe and Finham Brook, Stoneleigh, Coventry. Bulk bedload samples were collected and the additivity of fraction magnetic properties compared to the bulk properties was tested. Simultaneous equations (allowing no errors) were applied in order to test this. The linear programming model was also applied to the samples to test linearity of the magnetic measurements.

Plate 4.1a: River Sowe just below confluence of upper Sowe and Finham Brook

Plate 4.1b: Corley Moor soil pit

Three main aims were identified for this experiment:

1. To test the suitability of simultaneous equations for determining sediment contributions from the two input rivers (Finham Brook and Upper Sowe) to the main river (Lower Sowe)
2. To test the linear additivity of the magnetic measurements
3. To find the nature of the magnetic properties of different bedload fractions, in order to ascertain the grain sizes which affect the bulk (<2mm) sample

Methodology: Sample Collection

Eight samples were taken from the rivers as shown in the Table 4.8. Six of the samples were taken from several points across the river bed where the water was shallow enough to wade (sample type 1). Two samples were collected using a scoop from the bank, where the rivers were inaccessible (sample type 2) and these sediments were of a finer nature than the type 1 pebbly bedload samples. Plate 4.1a shows the confluence of the River Sowe and Finham brook.

Sample Preparation

Bulk samples were thoroughly mixed, dried at room temperature, and 10 sub-samples were potted into 10ml pots. All standard measurements were made including 18 point IRM curves. Wet sieving was used to fractionate 200g of each bulk sample. Sieves used were, 63, 125, 250, 500, 710μm, 2, 4, 8, 16mm. The fractions were also air dried and potted and measurements made as on the bulk samples (and at the same time).

Table 4.8: Collected Bedload Samples (Pairs of samples 1 and 2, 4 and 5 and 7 and 8 were bulked together).

Sample	River	NGR	Sample Type	Location
1	Finham Brook	SP 330 739	1	
2	Finham Brook	SP 330 739	1	
3	Finham Brook	SP 336 738	2	nr. confluence, concrete bed
4	Upper Sowe	SP 337 738	1	
5	Upper Sowe	SP 337 738	1	
6	Lower Sowe	SP 335 738	2	adjacent to sewage outlet
7	Lower Sowe	SP 334 738	1	below sewage outlet
8	Lower Sowe	SP 333 735	1	

Results and Discussion: Particle Size Distributions

Frequency histograms of the particle size distributions of each bedload sample are shown in Figure 4.10a to e. Particle size distributions for Finham Brook 1 (FB1), Upper Sowe 1 (US1) and Lower Sowe 2 (LS2) have similar distributions with 25-30% being between 2-4mm. The data for these samples were used in the simultaneous equations. Similarly, the two samples collected from the bank-side, Finham Brook 2 (FB2) and Lower Sowe 1 (LS1) have similar distributions with 80% of materials being between 250-710μm.

Figure 4.10: Particle size distributions for Bedload samples

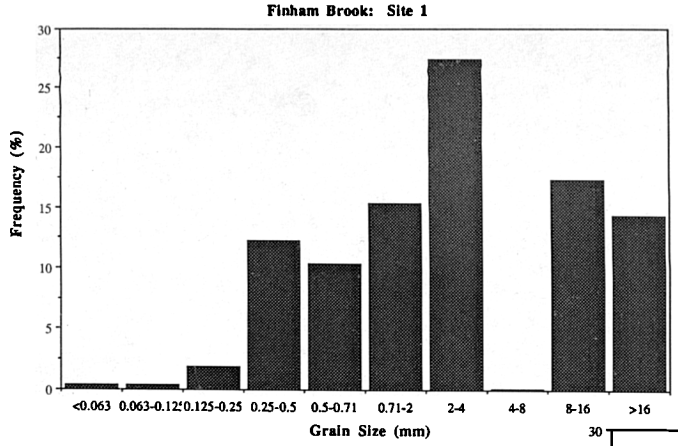

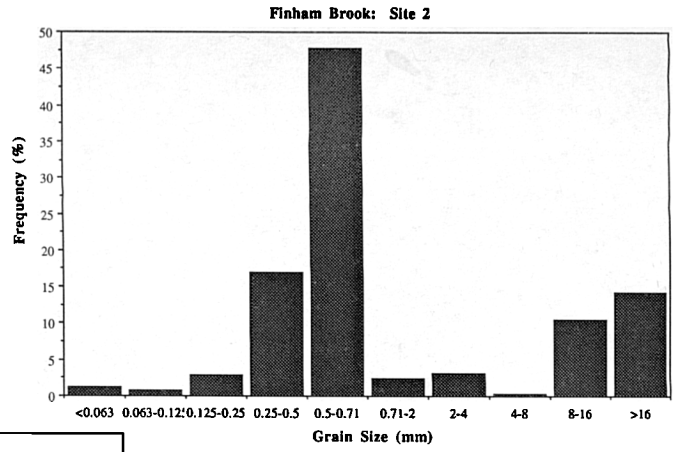

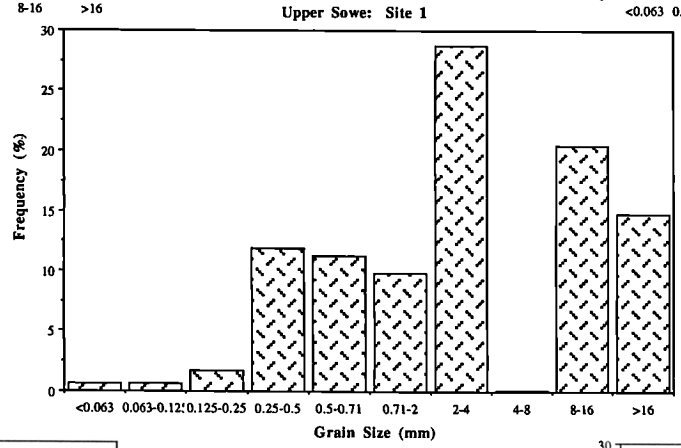

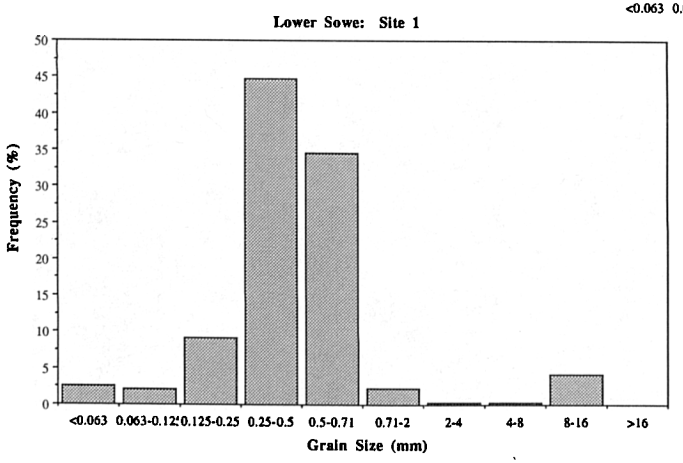

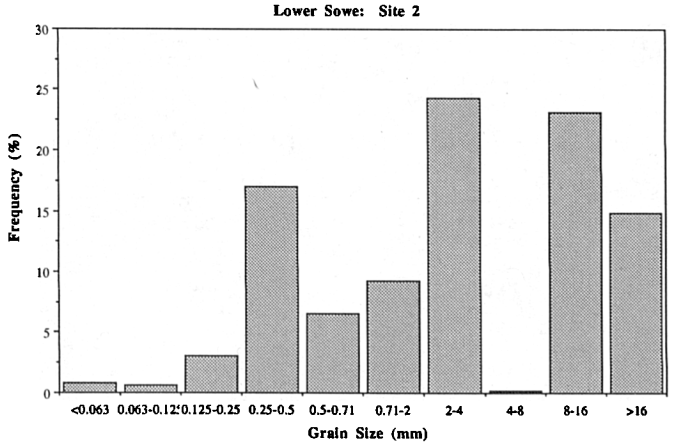

Magnetic Properties of Bedload Samples

It was found that the variability in the ten bulk sub-samples of each bedload sample was small (CV<15%) and had an acceptable standard deviation similar to the second laboratory mixing experiment sources (also see Chapter 5). Figures 4.11a to d show selected results of the measurements for the particle sizes <63μm, 63-125μm, 125-250μm, 250-500μm, 500-710μm, 710μ-2mm. No clear pattern of measurements emerged in any of the particle size ranges between the five samples. χlf and HIRM-100 appear to have the most consistent values between the five samples while χfd% and IRM880 show a greater range between the samples. Also there is no consistency between the samples with the largest or smallest values in all size ranges, and overall there is much variation. For instance, Finham Brook 1 shows the highest IRM880 measurement (18 mAm^2kg^{-1}) in the <63μm ranges while in the 63 -125μm range Lower Sowe 1 has the highest value (17 mAm^2kg^{-1}). It seems that ferrimagnetic minerals are controlling the properties of the smallest and largest ranges (<63, 63-125, 710μ-2mm), as values for χlf for these size ranges are four times those of the middle size ranges. Canted-antiferromagnetic minerals on the other hand are controlling the intermediate grain size ranges (125-250, 250-500, 500-710μm) which are indicated by the lower values. χfd% results show that all sample fractions have values less than 3.5%, indicating that only coarse-grained ferrimagnetic minerals are present in the ferrimagnetic component.

Normalized IRM curves in Figures 4.12a to g show gently-sloping curves indicating that hematites and goethites are present in the middle size ranges (125-250, 250-500, 500-710μm) and steeper curves which saturate at fields of 200mT in the finer and coarser grain-sizes (<63, 63-125, 710μm-2mm). The properties for bulk samples in all cases fall between these two extremes. Least variation in mineralogy is seen in IRM curves for the Upper Sowe sample (ferrimagnetically dominated) which flows southwards from Coventry. The widest variation in mineralogy between fractions is seen in the Finham Brook samples indicating possible sources of the local Keuper Clay and arable topsoils. The 125-250μm curve for both Finham Brook samples indicates the strongest canted-antiferromagnetic component (this is also true for the Lower Sowe samples). This could indicate the presence of SD hematite minerals which are thought to have a grain size of about 100μm (Thompson and Oldfield, 1986). Strongest ferrimagnetic curves are displayed by either the <63μm fractions and 710-2mm fractions in all cases.

Linear Additivity of Bedload Samples

The mean values of the ten bulk sub-samples and the fraction sample values were used to test the linearity of the mathematical mixing of the bedload samples. The linearity of the measurements χlf, χhf, χfd, ARM, χarm, IRM880, IRM-100 and HIRM-100 between the fraction and bulk samples was tested using matrix algebra in the following way:

$$\text{Predicted bulk measurements} = \Sigma \text{ Measurement of each fraction} * \%_{00} \text{ Weight of each fraction}$$

A percentage error for each measurement was calculated as follows:

$$\% \text{ Error} = \frac{(\text{Predicted bulk measurement} - \text{Actual bulk measurement})}{\text{Actual bulk measurement}} * 100$$

Figure 4.11: Measurment results for bedload particle size fractions (River Sowe (US - Upper Sowe; LS - Lower Sowe) and Finham Brook (FB) Bedload Fractions

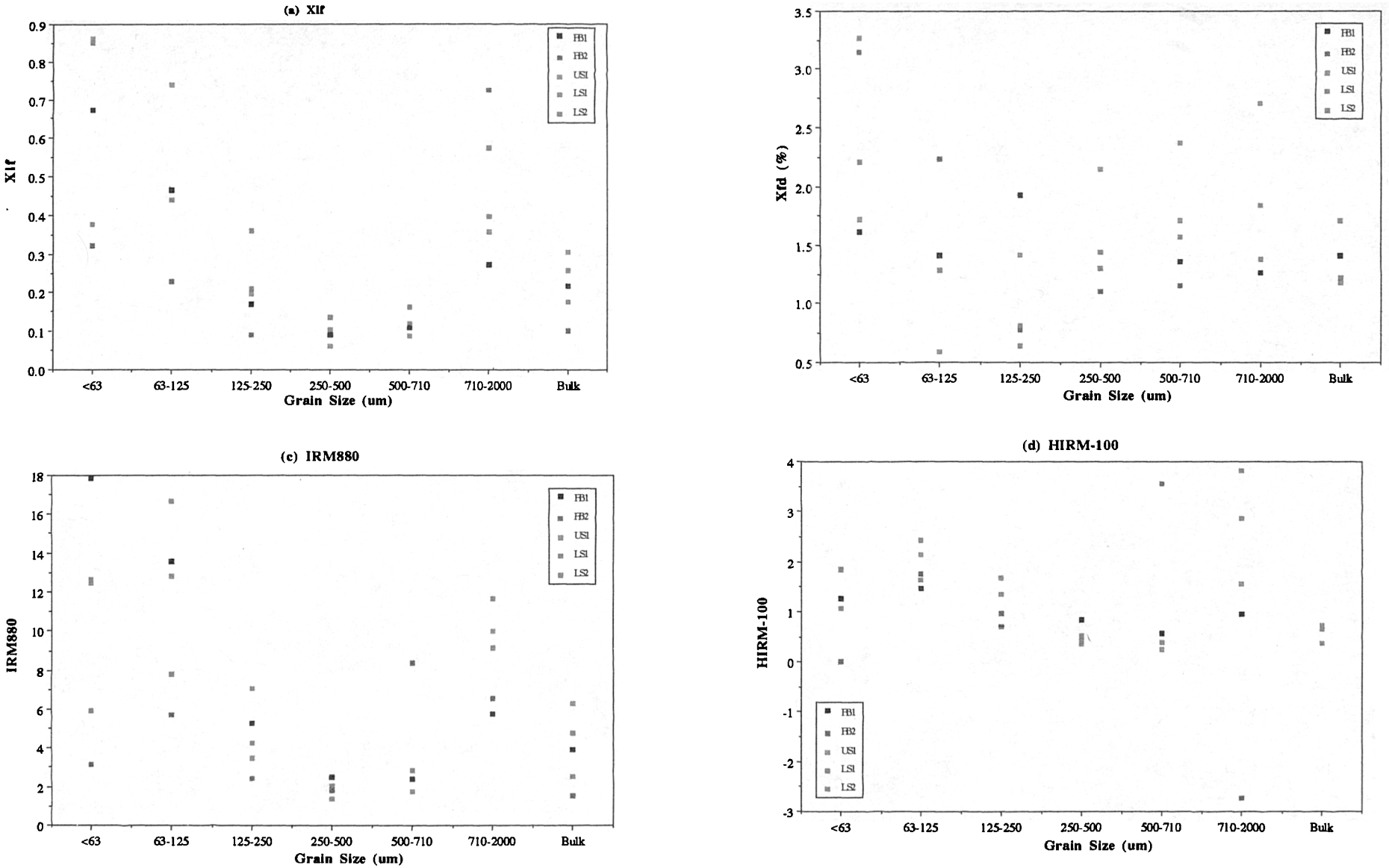

Figure 4.12: Selected Normalized IRM curves for bedload particle size fractions

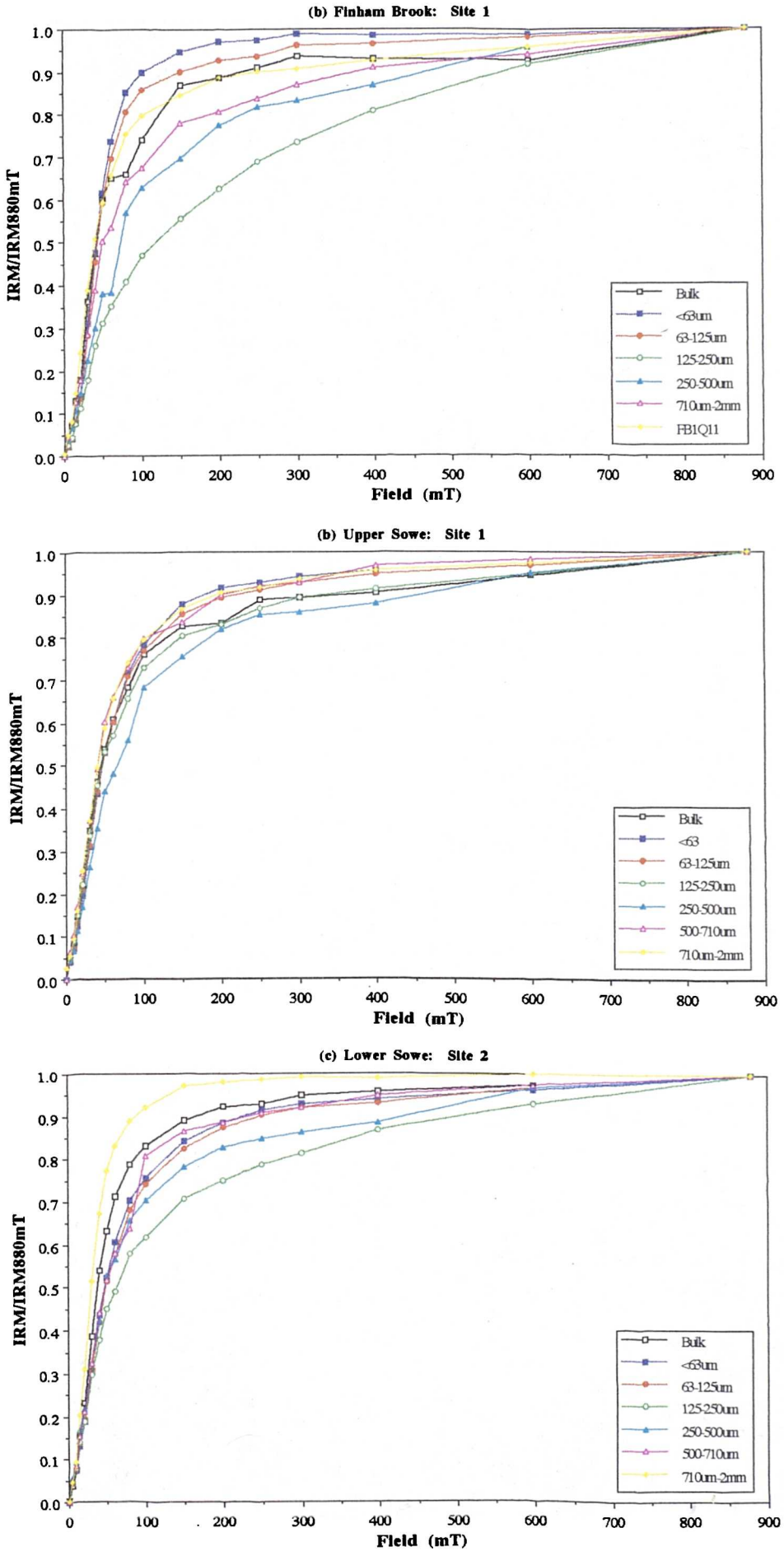

Component proportions (weight of each fraction) of the particle size fractions can be inferred from Figure 4.10. The results of the linear additivity tests are presented in Table 4.9. The results for the predicted measurement of the bulk bedload are less than those of the actual measurement. For instance, in Finham Brook 1 the predicted χlf is 0.175 μm^3kg^{-1} whereas the actual χlf is 0.217 μm^3kg^{-1} giving an error of 19.36%. It can be seen that if an error of 5% were acceptable for source modelling, for instance, then the above results are not valid. The lowest error (0.758%) is seen for the HIRM-100 measurement on the Upper Sowe 1 sample where predicted and actual values were 0.798 mAm^2kg^{-1} and 0.792 mAm^2kg^{-1} respectively. ARM (χarm) measurements are low and have large errors associated with them, for instance in Finham Brook 1 errors are 72.7 and 71.3% respectively while for the same sample the next largest error is 20.8% for χfd.

Table 4.9: Results of linear additivity tests giving predicted and actual measurement results and percent errors.

	Finham Brook 1			Upper Sowe 1			Lower Sowe 2		
Parameter	**Pred.**	**Act.**	**% Err.**	**Pred.**	**Act.**	**% Err.**	**Pred.**	**Act.**	**% Err.**
χlf	0.17	0.217	19.355	0.192	0.316	39.241	0.211	0.302	30.132
χhf	0.173	0.214	19.159	0.188	0.313	39.940	0.207	0.299	30.769
χfd	2.253	2.845	20.808	4.211	3.171	32.797	3.587	4.676	23.289
ARM	0.003	0.001	72.727	0.035	0.032	9.375	0.019	0.039	51.282
χarm	0.102	0.356	71.348	1.107	1.018	8.743	0.617	1.22	49.426
IRM880	4.065	3.922	3.646	4.504	6.445	30.116	4.425	7.104	37.711
IRM-100	-2.425	-2.416	0.373	-2.908	-4.862	-40.189	-1.915	-1.68	13.988
HIRM-100	0.819	0.753	8.765	0.798	0.792	0.758	1.255	0.895	40.223

Simultaneous Equations

Simultaneous equations were applied to three of the bedload samples, FB1, US1 and LS2. The proportions of the two proposed sources of bedload sediment (FB1 and US1) were found using the magnetic properties of the proposed sediment mixture, LS2. Bulk samples and samples for the six particle sizes were modelled for the two sources and mixture. Three source component values were tested for the bulk samples, mean, mean-1 standard deviation and mean+1 standard deviation to allow for the range of the 10 bulk sub-samples (even though the range was small). Actual measurements were used for the different particle sizes as only one sample of each was available. Results are shown in Table 4.10. Simultaneous Equations were formulated in the following way:

$$Ax + By = C$$
$$x + y = 1$$

Where: $A >= C <= B$
x and $y >= 0$
A = FB1, B = US1 and C = LS2

For the most part, from Table 4.10 it can be seen that some solutions were found using all the linear magnetic parameters (χlf, χhf, χfd, ARM, χarm, IRM880, IRM-100, HIRM-100). IRM880 and IRM-100 were the only parameters to give solutions for the three source values used. The first source component, Finham Brook 1 (x), ranged between 59 and 83% for IRM880 and between 55 and 88% for IRM-100. For some parameters ARM(χarm)

solutions were only found using the mean+1sd. The average proportions show that FB1 proportions range between 53 and 69% and US1 between 31 and 47%. The results show that with small ranges (CV%<15%) in sub-sample data quite different results are gained.

Table 4.10: Results of simultaneous equations. x = FB1, y = US1

Fraction	Parameter	mean		mean - 1sd		mean + 1sd	
		x	y	x	y	x	y
Bulk	χlf	0.495	0.505	No Solution		0.872	0.128
	χhf	0.495	0.505	No Solution		0.872	0.128
	χfd	No Solution		0.044	0.956	No Solution	
	ARM	No Solution		No Solution		0.429	0.571
	χarm	No Solution		No Solution		0.450	0.550
	IRM880	0.588	0.420	0.648	0.352	0.833	0.167
	IRM-100	0.552	0.448	0.683	0.362	0.880	0.120
	HIRM-100	No Solution		0.597	0.403	No Solution	
Average Proportion (%)		53	47	54	46	69	31

Fraction	Parameter	mean	
		x	y
63-125μm	χfd	0.671	0.329
	HIRM-100	0.687	0.313
125-250μm	ARM	1.0	0.0
	IRM880	0.472	0.528
250-500μm	IRM880	0.714	0.286
	HIRM-100	0.40	0.60
500-710μm	HIRM-100	0.587	0.413
710μm-2mm	χfd	0.368	0.632
	ARM	0.434	0.566
	χarm	0.433	0.567
	IRM880	0.185	0.815

The simultaneous equations for the particle size fractions were not as consistent, indicating either selective transport of certain size fractions or very variable deposition on the channel floor (although samples were collected from across the rivers and bulked). The <63μm fraction is not included in Table 4.10 as this range gave no viable solutions. The 63-125μm range gave similar solutions for χfd and HIRM-100 (68:32%) ARM and IRM880 worked in the 125-250μm range, although the ARM answer was not useful (100% for one component). For the 250-500μm range IRM880 and HIRM-100 gave contradictory solutions of 71:29% and 40:60% respectively. Similarly HIRM-100 gave a solution in both the 500-710μm range and in the 710μm-2mm range. χfd and ARM gave similar results of 40:60% while IRM880 gave results of 18:81%.

Summary

Overall the linearity of the fraction properties in the bulk sediment is poor and the results for the simultaneous equations were limited. Errors may result from the use of intra-variability of the sub-samples taken from the bedload samples. Even in a well-mixed sample one grain of a contaminant (iron for instance) may cause complete

failure of this type of experiment. Also errors may be compounded through the use of means of the bulk samples. But modelling of individual bulk sub-samples represents a more difficult problem, and individual sub-samples may be affected by random contaminants or dilution. Parameters such as HIRM-100 have smaller errors as they indicate mineralogically purer components of the mixtures and there is less variability between sub-samples. Parameters which indicate ferrimagnetic minerals (eg ARM) are subject to greater variability errors due to the grain size variability in such minerals (see also Chapter 9). In the mixing of tributary sediments there is no guarantee that the sources contribute wholly to the bedload mixture collected from the trunk river.

4.2.2 Corley Soil Experiment

Introduction and Aims

Three 200g soil samples were collected from Corley Common, North Warwickshire (NGR SP 280 853). A sample of each of organic matter (O), A horizon and B horizon were collected from the stagnogleyic argillic brown earth (Whimple 2 Series) which is derived from a clayey substrate. The aims of this experiment are similar to those of the bedload experiment and are re-iterated as follows:

1. To test the linear additivity of measurements using the soil bulk and fraction data
2. To find the nature of the magnetic properties of different soil fractions, in order to ascertain the grain sizes which affect the bulk (<2mm) sample

Methodology and Results

The samples were collected from a 50*50*100cm deep soil pit (Plate 4.1b) at depths of 0-5cm (O), 20-30cm (A) and 40-50cm (B). 200g of each sample was thoroughly mixed and wet sieved using 63, 125, 250, 500μm and 2mm sieves. Coarse organic matter in the samples was floated off during 2mm mesh sieving. Bulk and conservatively fractionated samples were dried at room temperature and one sample of each was then packed into 10ml pots (this process used nearly all the material available). Standard measurements were made on all samples.

The particle size distribution of each sample is shown in Figure 4.13a to c. The distributions are very similar in all three horizons with the largest component (28-32%) being the <63μm fraction. The smallest contribution (2-5%) is provided from the >500μm fraction. Figures 4.14a to d give selected results of the measurements made on the samples. χlf and IRM880 show greater values in the O horizon; in fact for the most part the O horizon has the strongest magnetic properties. Since the O horizon values are not corrected for loss on ignition (this was not required for the purposes of this experiment) the values indicate a large source of magnetic minerals which could be either atmospheric fallout or burning. HIRM-100 data shows that the B horizon has a greater hematite/magnetite ratio than the O horizon but the A horizon has a lower canted-antiferromagnetic contribution than the O horizon. χfd% results show that more finer-grained ferrimagnetic minerals are present in the B and A horizons (up to 6.5%) than the O horizon, where values are less than 4%. This means that there is a slightly greater concentration of course-grained ferrimagnetic minerals in the O horizon.

Figure 4.13: Particle size distributions for Corley soil horizons

(a) O Horizon

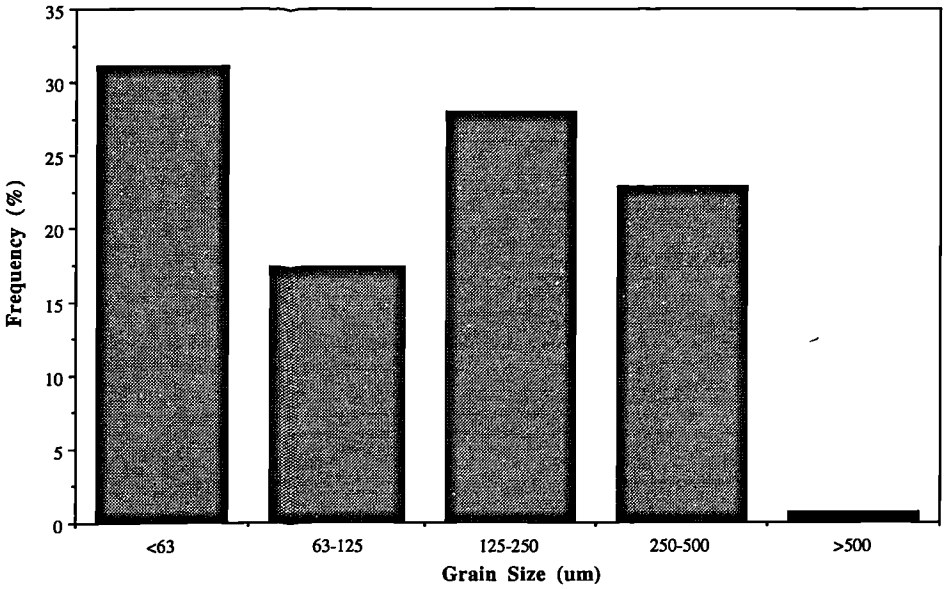

(b) A Horizon

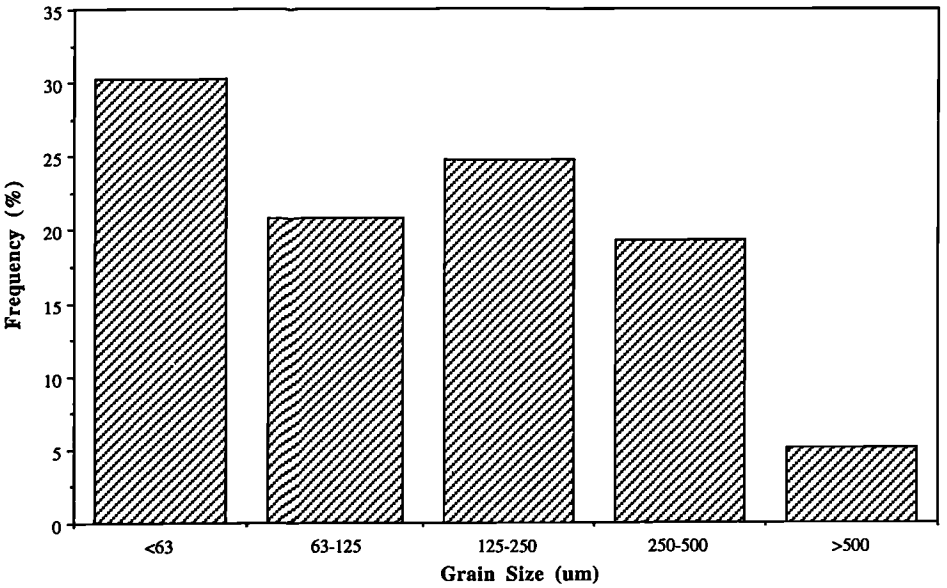

(c) B Horizon

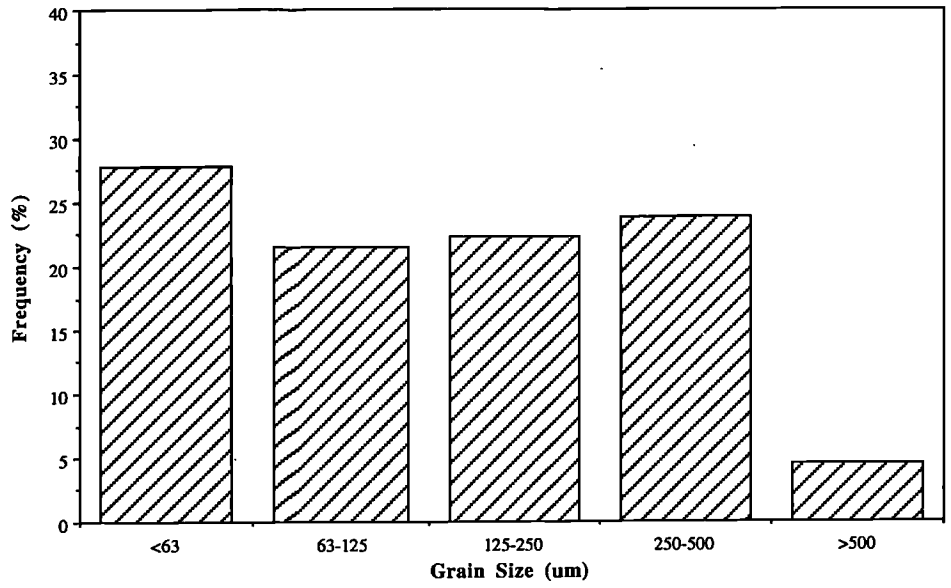

Figure 4.14: Selected measurement results for soil particle size fractions

(a) Xlf

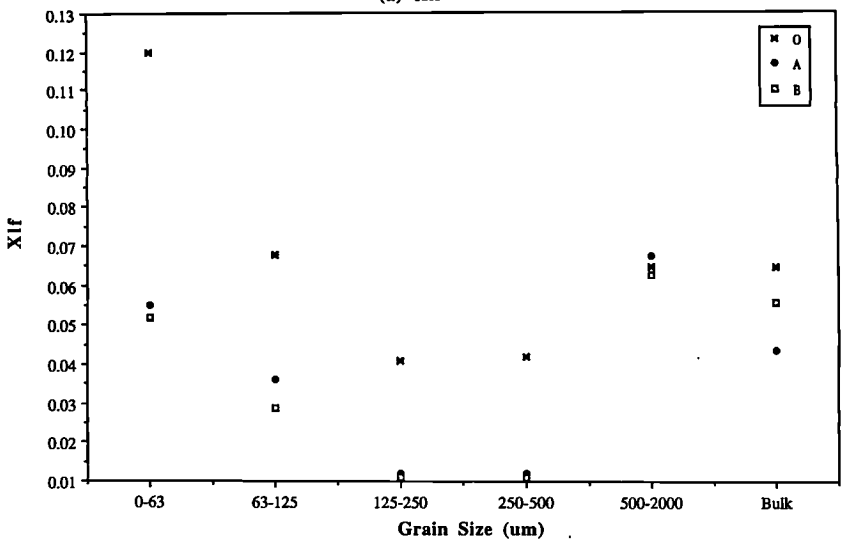

(b) Xfd%

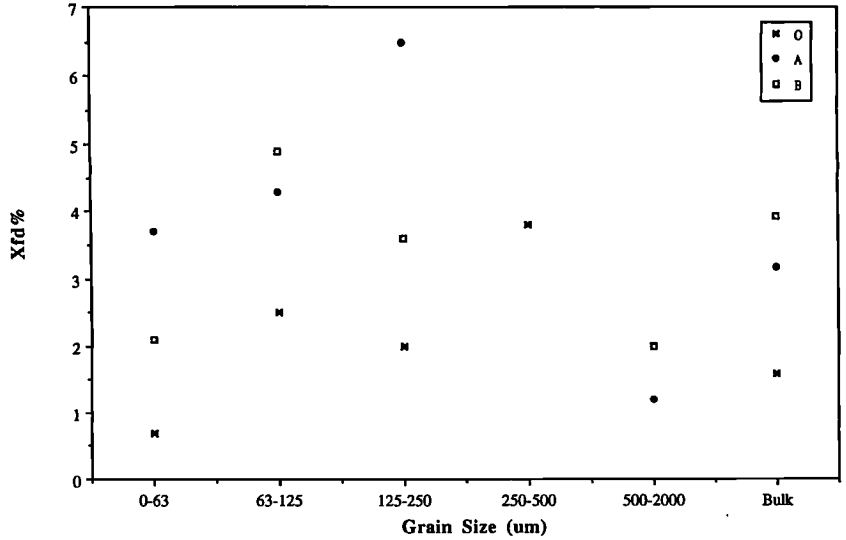

(c) IRM880

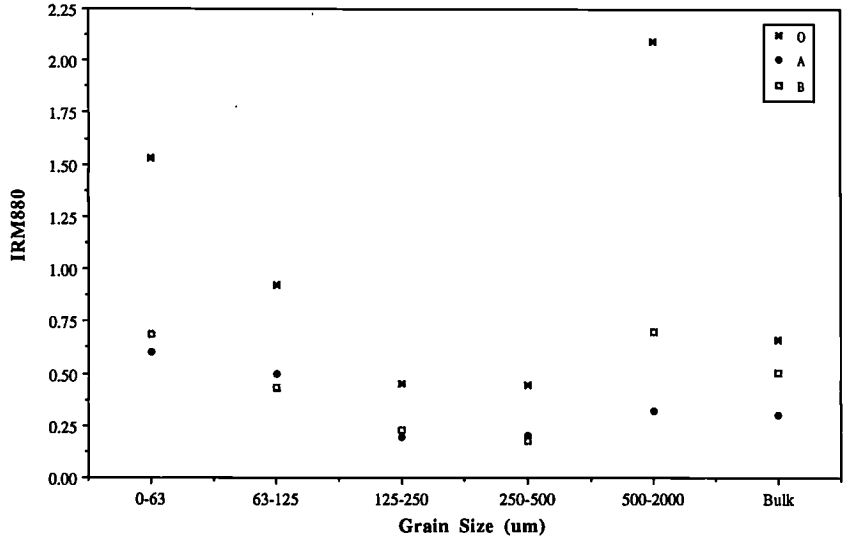

(d) HIRM-100

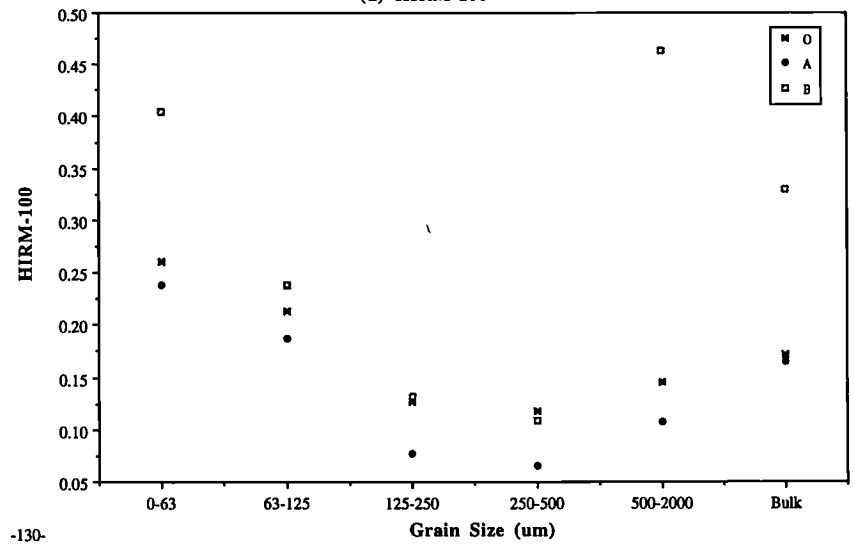

Figure 4.15: Normalized IRM Curves for soil horizons and particle size fractions

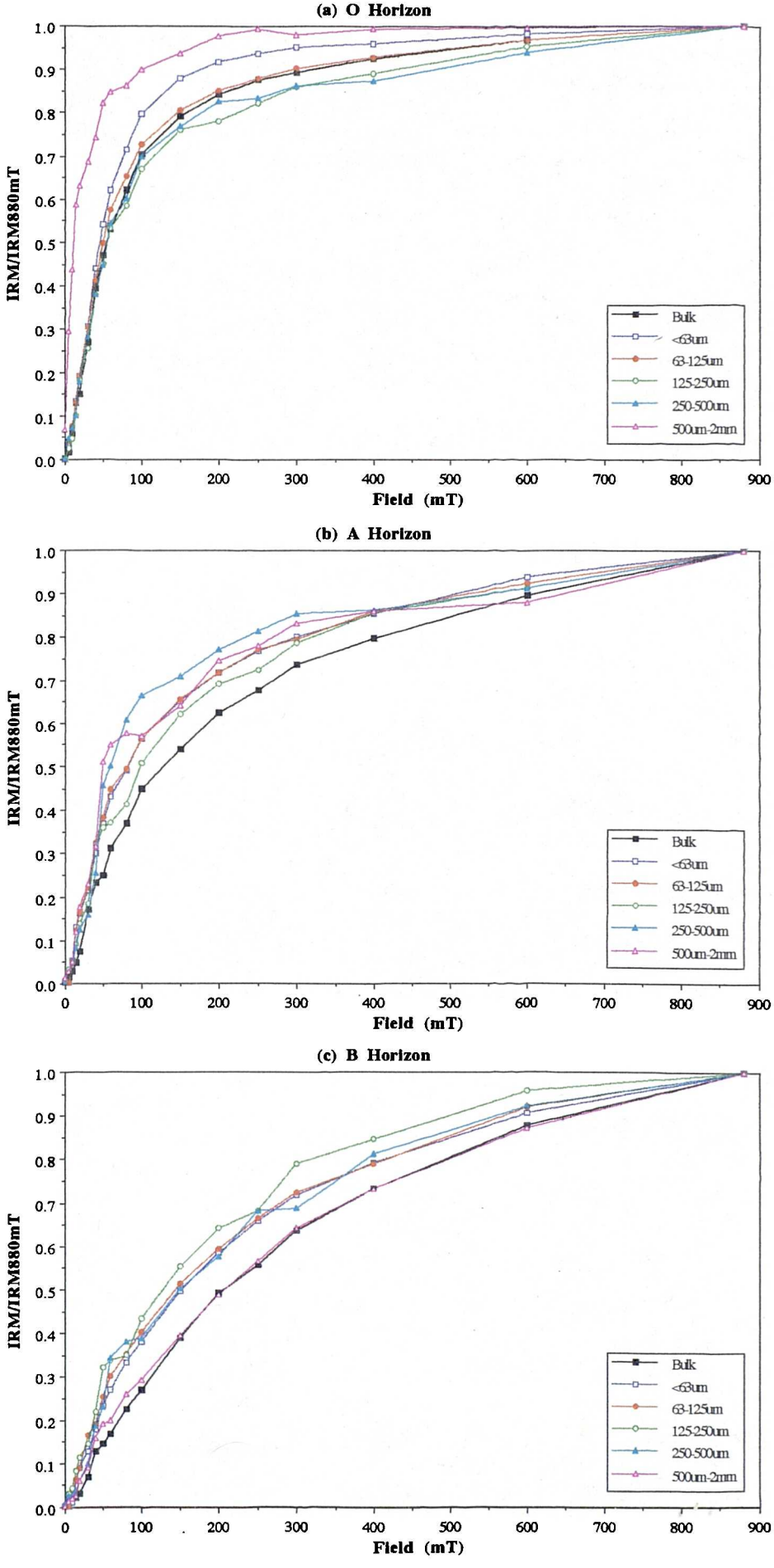

IRM curves essentially display similar results to Figure 4.14c where in the organic layer there were greater concentrations of course-grained magnetites. Normalized IRM curves (Figures 4.15a to c) show a distinct change from a soft ferrimagnetic remanence in the <63μm fraction to a harder canted-antiferromagnetic remanence through the intermediate grain sizes returning to a soft remanence in the 500μm-2mm grain size again. This pattern is also displayed between the three horizons where curves for the B horizon show harder remanence and A horizon curves lie in between the O and B horizons, indicating mixing of ferrimagnetic and canted-antiferromagnetic minerals within the soil profile. There is greater variation between the IRM curves of the three horizons than between the particle size fractions of each horizon.

Linear Additivity

The results of the data were used to test the linear additivity of the magnetic parameters for the soil horizon samples. The test was carried out in a similar manner to that described in the river bedload experiment (Section 4.2.1). Theoretically, as no material was discarded in the sieving, effects attributable to organic matter dilution should not occur in this experiment. Table 4.11 shows the results of the predicted and actual bulk sample measurements calculated by forward multiplication using matrix algebra of the fraction weights and their properties. The percentage error between the predicted and actual results of the bulk samples is also presented in Table 4.11.

Table 4.11: Linear Additivity results giving predicted and actual measurements and percent errors.

	O Horizon			A Horizon			B Horizon		
	Pred.	**Act.**	**% Err.**	**Pred.**	**Act.**	**% Err.**	**Pred.**	**Act.**	**% Err.**
χlf	0.071	0.065	8.769	0.033	0.044	25.455	0.029	0.056	48.930
χhf	0.070	0.064	8.750	0.031	0.042	25.238	0.028	0.054	48.333
χfd	1.139	0.974	16.952	1.458	1.304	11.833	0.960	2.045	53.046
ARM	0.002	0.005	54.0	0.002	0.004	62.50	0.003	0.003	16.667
χarm	0.074	0.170	56.412	0.056	0.119	53.277	0.082	0.109	24.404
IRM880	0.879	0.663	32.564	0.391	0.298	31.040	0.411	0.506	18.874
IRM-100	-0.516	-0.320	61.188	-0.093	0.032	391.25	0.069	0.153	54.641
HIRM-100	0.182	0.172	5.523	0.148	0.165	10.121	0.240	0.330	27.182

Predicted values are higher than actual values in the O horizon by between 5 and 61% (except for ARM). The opposite is true of the A and B horizons, however, where actual values are greater than predicted values by between 10 and 54%. If an acceptable error is again taken to be 5%, none of these calculations give precise enough answers. Errors for HIRM-100 and susceptibilities in the O horizon are generally the lowest (5-9%). It seems that errors for the B horizon are greater than those for the A horizon and similarly the A horizon shows greater linear additivity errors than the O horizon. Errors for ARM (χarm) measurements are again the highest; for instance in the A horizon they reach 62.5%.

Summary

The linearity of the addition of the properties of the soil fractions has been tested and found to incorporate large errors. It seems that for the most part the actual values in the O horizon are less than expected while in the other horizons the predicted value is greater than expected. This could indicate interactions (or other phenomenon) in the

bulk organic sample and the fractioned samples of the A and B horizons led to a reduction in the measurements. However as the measurements of the soils were not particularly high in respect to synthetic minerals, for instance, (Chapter 3) this probably is not the case. The suitability of the magnetic fraction in modelling different particle sizes in bulk soil samples is therefore under question. Addition of magnetic properties of fractions does not seem to be representative of the whole soil (as a bulk sample). Materials in the soil may be contributing to the dilution of the magnetic properties, organic matter and quartz for instance, such that it cannot be expected that reliable answers for the properties of the soil fractions and bulk can be modelled. Larger errors in the A and B horizons than the O horizon indicate that organic matter dilution is not the cause of the failure in this instance. However, variability in sub-sampling again may be a cause of poor linearity. It may not be the case that materials can be fractioned, even conservatively, and their properties in relative proportions be expected to add up to the properties of a bulk sample. This has quite serious implications for source modelling as a whole where sources are not positively known.

4.3 Linear additivity of magnetic properties - Summary

A final methodological summary of the results presented in this chapter and their effect on the formulation of a methodological framework for applying magnetic techniques to environmental sourcing is presented in Chapter 6. There is scope for modelling sources of sediments using magnetism but there are severe limitations. At best only four sources will be able to be modelled and great care in interpretation of the results is needed. Best results will be obtained using only 6 susceptibility and remanence parameters. Results are significantly worsened when further IRM points are included. Errors can be attributed to non-linearity of equipment, mixing small quantity mixtures (for VSM) and possibly grain interaction. Also it has been found that LINDO is sensitive to linearity greater than 2.5%. This indicates that, as most of the mixtures have errors greater than this, great care is needed for application of this technique and the interpretation of results. In the experiments in this chapter mixtures have been made artificially and environmental materials artificially fractioned. These procedures in themselves may produce artificial intra-sample variability and interaction effects not seen in naturally produced mixtures in environmental systems. In environmental mixtures no test of the source inputs can be made and results rely more on the initial identification of source and environmental variability. It has been found here that susceptibility represents the most linearly additive and reliable measurement. In the next chapter work is presented on the evaluation of magnetic susceptibility (at present the only field parameter easily measurable) for the identification of sources of sediments and for the definition of their spatial variability. The possible effects of spatial variability on modelling prospects of sources of environmental mixtures is assessed with respect to the limitations found in this chapter.

CHAPTER 5

Magnetic Variability, Reconnaissance and Sampling Strategies

5.1 Source Identification and Variability

This chapter discusses the different types of variability in the environment which can affect source modelling. Three levels of variability are discussed: intra-sample variability, within-unit variability and larger scale spatial variability. The three scales of variation are compared using CV% values and the modelling limits found from intra-sample variability in Chapter 4 are re-assessed here in the light of larger-scale variability. The intra-sample variability defines the lower level of magnetic variation in materials. Intra-sample variability may be predominantly related to sub-sampling and single grain contamination, of iron for example. Discussion on the grain and particle size controls on magnetic measurement are also included. From chapter 4 it has been shown that linear modelling is sensitive to such variation in sub-samples. The within-unit section assesses variation within single environmental units, geology and soil type for example. Within-unit variation, in soils for instance, may be caused by small-scale factors such as translocation, soil fauna, vegetation and micro-structural changes such as mottling, aggregation and deflocculation. The spatial variability section aims to improve the statistical definition of sources in defined study areas (catchments for example). Spatially, a much wider set of factors affect variability, including topography, drainage, land-use, parent materials and soil processes.

The main aim of this chapter is to formulate suitable reconnaissance survey and sampling strategies to identify sources and define spatial variability using magnetic field susceptibility (Kappa, Bartington MS2 meter and loop sensor-Plate 5.1d). Kappa measured in the field has been used to formulate a simple magnetic mineral concentration classification and an indication of the suitability of application of magnetic techniques for source and mineral modelling. Classification and modelling work has justified the use of susceptibility/kappa as one of the most useful discriminatory magnetic parameters and the most linearly additive (Chapter 4). Kappa transects and variograms have been used to identify source boundaries to identify scales of magnetic variability in the environment.

5.2 Magnetic Variability of Environmental Materials - Setting the Limits

Study of intra-sample variability of 'homogeneous' materials was completed using the environmental materials and chemical reagents (for comparison) from the mixing experiments presented in Chapter 4. Ten sub-samples of nine (200g) samples were measured and the variability of homogeneity of the materials quantified. Materials used included Keuper Clay, topsoil, mine spoil, coal, chimney slag, bedload and Analr bentonite and Barium Sulphate and Manganous Carbonate. The first set of sub-samples were taken from air-dried material of <2mm in size. The second set were sub-sampled from a finely ground (using a pestle and mortar) proportion of the materials such that the material passed through a 63μm sieve.

Table 5.1 gives the CV% results for this experiment. It must be re-iterated that CV% is greatly affected by data sets with arbitrary zeros and the results for difference parameters, such as χfd, are affected by inaccuracies on a higher magnitude of scale. In Table 5.1 it can be seen that the CV% is much reduced in the ground materials, especially for mine spoil, than in the <2mm samples. This is not true for chimney slag however, which for χlf, χfd, IRM880, IRM-100 and HIRM-100 exhibits a near twofold increase in the ground sample. This could indicate that in this material, of originally large-size particles, grinding has induced some form of structural change increasing the range of effective magnetic grain sizes (to microns rather than mm). The chemical reagents bentonite, barium sulphate and manganous carbonate exhibit zero variability, but difference parameters again exhibit the problems of calculating such parameters for weak magnetic materials (also see section 3.2). Even in finely ground materials, therefore, for linear parameters a CV of 10% can be expected in 10 sub-samples of a 200g total sample. This presents a basis for studying wider scale variability of environmental materials of similar particle size ranges (<2mm and <63μm). However it is noted that these particle size ranges include all the critical grain sizes discussed in Chapter 2.

Table 5.1: Coefficients of Variation (%) for <2mm (a) and ground (<63μm (b)) environmental materials

(a) <2mm materials

Variable	**(a)**	**(b)**	**(c)**	**(d)**	**(e)**	**(f)**
χlf ($\mu m^3\ kg^{-1}$)	0	3.45	5.77	4.98	5.37	0
χhf ($\mu m^3\ kg^{-1}$)	0	3.57	5.83	4.93	5.41	0
χfd ($nm^3\ kg^{-1}$)	20.29	4.89	21.02	15.68	13.93	133.3
ARM ($mAm^2\ kg^{-1}$)	0	0	14.29	10.31	10.0	0
χarm ($\mu m^3\ kg^{-1}$)	7.14	4.96	9.66	9.77	9.7	20
IRM880mT ($mAm^2\ kg^{-1}$)	6.45	8.76	8.61	2.29	8.83	5.88
IRM-100mT ($mAm^2\ kg^{-1}$)	7.1	9.3	10.33	2.89	10.34	9.1
HIRM-100mT ($mAm^2\ kg^{-1}$)	6.5	10.1	9.41	11.78	27.28	0

Where: (a) Keuper Clay (b) Arable Topsoil (c) Mine Spoil
(d) Chimney Slag (e) Coal (f) Bedload

(b) <63μm materials

Variable	**(a)**	**(b)**	**(c)**	**(d)**	**(e)**	**(f)**	**(g)**
χlf ($\mu m^3\ kg^{-1}$)	0	0	0.98	7.83	7.7	0	0
χhf ($\mu m^3\ kg^{-1}$)	0	3.45	0.98	7.81	7.7	0	0
χfd ($nm^3\ kg^{-1}$)	26.39	5.16	14.12	12.8	19.8	37.04	13.3
ARM ($mAm^2\ kg^{-1}$)	0	0	0	5.37	0	0	0
χarm ($\mu m^3\ kg^{-1}$)	0	1.05	0.78	5.36	3.1	0	0
IRM880mT ($mAm^2\ kg^{-1}$)	0.82	2.7	1.16	5.19	7.2	6.1	0
IRM-100mT ($mAm^2\ kg^{-1}$)	1.1	3.6	1.2	4.39	12.96	0	0
HIRM-100mT ($mAm^2\ kg^{-1}$)	0.92	1.9	1.89	25.17	6	50	0

Where: (a) Ground Keuper Clay (b) Ground Arable Topsoil (c) Ground Mine Spoil
(d) Ground Chimney Slag (e) Ground Bedload (f) Barium Sulphate
(g) Manganous Carbonate

Plate 5.1a: Site of Corley kappa transect. In-field survey (b), tractor wheelings affect soil density and kappa values (c) and field loop sensor, susceptibility meter and Psion data logger (d)

b

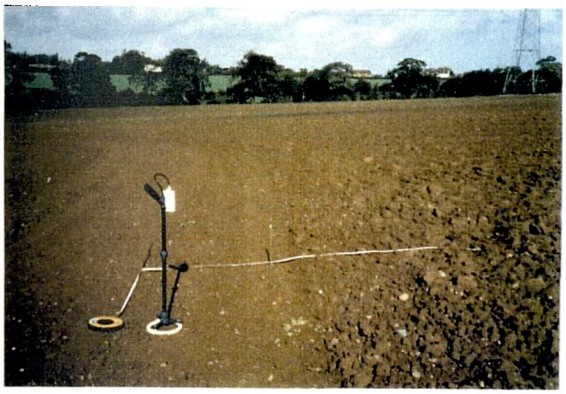

c

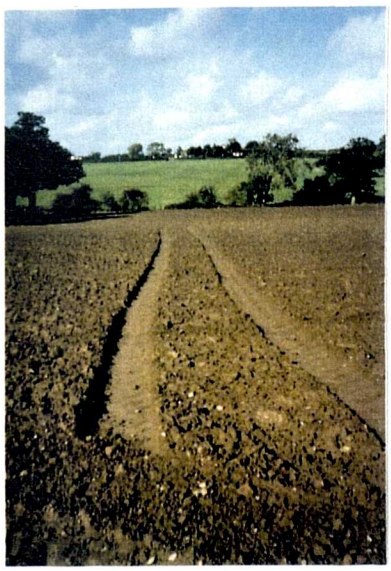

d

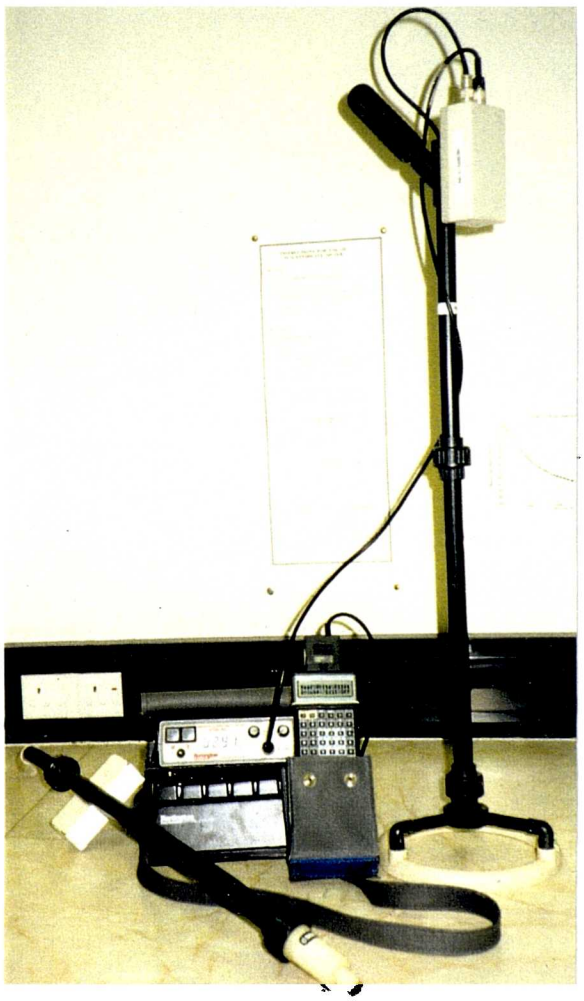

Grain-size controlled magnetic variation

The most important mineral displaying variation with grain size is magnetite. Such critical grain sizes have already been described in Chapter 2. Often the grains do not exist as individual particles, but occur as mineral inclusions and/or mineral coatings. Magnetite is also the most studied mineral due to its ferrimagnetic behaviour which dominates the magnetic properties of many environmental materials. In determining the mineralogy of natural materials, natural and synthetic magnetites have been used as an analogy, to indicate possible concentrations of certain grain sizes (Parry, 1965, Dunlop, 1973, Mullins, 1977, Dankers, 1978, Maher, 1988). In production of magnetite grain sizes Dankers (1978) physically disintegrated natural magnetite into a range of sieved grain sizes. This approach is thought to change the internal structure, and thus magnetization capability, of the resultant mineral grains, however. Maher (1988) precipitated ultra-fine grained magnetites synthetically and set certain grain sizes by stopping crystal growth at certain times (TEM analysis was used to measure c.100 grain diameters in each sample).

Ten of Maher's samples have been re-measured in this research but the measurements were less than those obtained by Maher (1988) . Results for Maher's samples measured for the present project are not presented as they were found to be reduced due to their slow oxidation to maghemite (B. Maher, pers. comm.) (but since magnetization data did not originally exist, the magnetization data collected for this research was used in Chapter 9 for mineral modelling). Figure 5.1 shows variation in χlf with grain size (Maher, 1988). The diagram shows clearly that there is variation with grain size. Small grains of less than 0.02μm have susceptibilities of up to 1100 $\mu m^3 kg^{-1}$ while coarser grains of 1μm have susceptibilities of only 300 $\mu m^3 kg^{-1}$. Also certain grain sizes have the same χlf (eg 0.05μm and 10μm grains). This overlap presents problems for concentrational calculations of certain grain sizes. Finer grain sizes can only be further discriminated by using ratios of two measurements, χfd% and IRM880/χarm, for instance (see Appendix 1 and Chapter 3). These grains however may be included in larger particles of sediment and this causes great difficulties in determining original sources of material. Groups of grain sizes in any particular size range of a sediment may average out the original fine and coarse-grained magnetic properties, making discrimination between particle sizes more difficult (see Chapter 3).

Particle-size controlled magnetic variation

Variation in the magnetic properties of particle size ranges in sediments and soils have been studied by many workers, for instance Mullins (1977), Bjorck et al (1982), King et al (1982), Oldfield (1985), Maher (1986), Yu (1989) and Yu and Oldfield (1993). Magnetic measurements can show as much variability between particle sizes of a bulk sample (Chapter 4) as they can between, say, samples of different soil types (Figure 5.2). This variation imposes many problems on the identification and unmixing of sediment sources, especially as sorting mechanisms during selection and transport of sediments may alter the particle size and make-up in the final mixture. In most environmental studies incorporating magnetic techniques particle size distribution properties are a foremost consideration. Mullins (1977) grouped susceptibility data for sized magnetite samples and used the resulting data to calculate percentages of grain sizes in soils developed on basalt. Finer grains (20-50μm) were present in topsoils in greater percentages while in lower horizons more coarser grains (200-500μm) were present. King et al (1982) used χarm to indicate finer magnetite grain sizes in fractioned lake sediments. Magnetites were also extracted from

Figure 5.1: Variation in susceptibility with critical magnetite grain sizes in samples (after Maher, 1988)

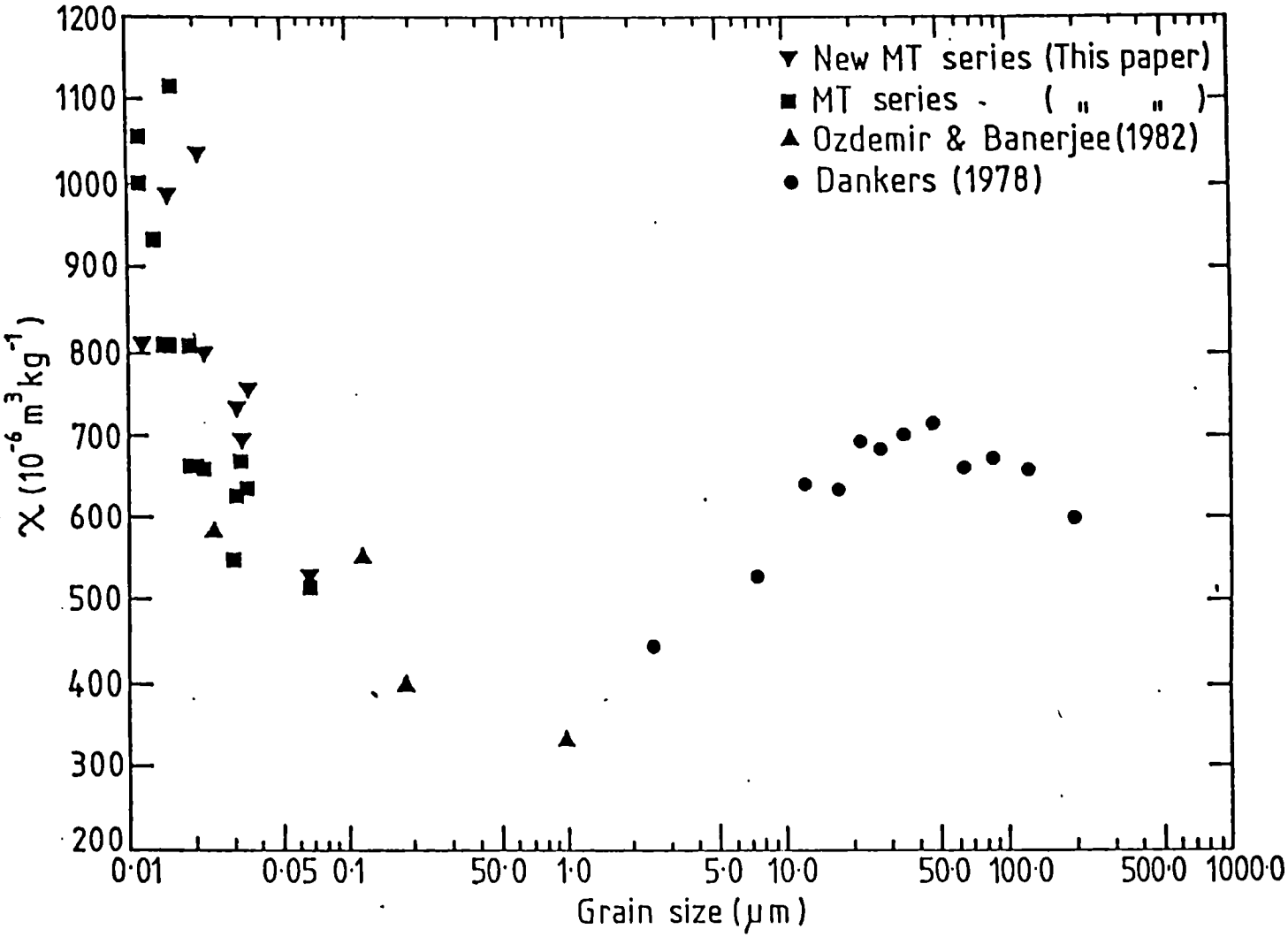

the sediments and the numbers of grains in each sediment particle range were estimated. The grain size distribution of the magnetite grains were comparable to the distribution in the whole sediment in this case.

Maher (1986) studied fractions of soil profiles and found distinct variation in magnetic properties (using χlf, χarm, IRM880 and χfd%) for clay, fine silt, silt and sand fractions. These were a direct result of prevalent soil-forming factors. Yu (1989) found that in sediments of Chesapeake Bay finer clays displayed greater magnetic values related to concentrations of fine-grained magnetites of single and superparamagnetic size. Particle size variations in bedload samples (already presented in Chapter 4) show that there is wide variation in properties of different particle size ranges from <63μm to >2mm. In samples collected in a close vicinity variation of size ranges between samples is large.

5.3 Variability of Environmental Materials - Sampling Strategies

Much of the work on spatial variability has been done in the area of soil science, as discussed in Chapter 2. The approach of Webster and Oliver (1990) has been applied in this work whereby variograms of kappa are used to assess sampling scales and sample numbers required. Variograms have been constructed using the adapted program of Campbell (1985, listed in Appendix 5). In sediment unmixing the measured parameter values input for sources are of utmost importance. Typically, too few samples are collected for statistical ranges of sources to be determined. Here variograms of topsoils are employed to assess spatial variability and define sample numbers required to define sources statistically. From the results obtained, grid sampling schemes on several scales can be selected to cover in-field and between-field variability affected by land-use management (even for the same soil types) and across catchment variability to identify boundaries of soil/geology types.

Within-unit variability

Many susceptibility surveys with normally c.50 measurements of K were carried out to assess the within-unit variability of, for instance, a soil type or rock outcrop. Figure 5.2 shows the distribution results for many of these surveys for different environmental materials. A magnetic mineral classification is included on the kappa axis. The data relating to the diagram is given in Table 5.2 presenting the numbers of measurements and values used in calculations of variance and coefficient of variation. All of the sets of measurements were normally distributed except for the granite groynes which were log-normally distributed. Sedimentary geologies (eg limestones) indicated low values and domination by paramagnetic and canted-antiferromagnetic minerals. The 'granites' used in groynes at Mappleton (including some metamorphic rocks) show a wide range of values, some of the rocks have very high ferrimagnetic mineral concentrations (K=2300). CV% results show again that for materials which are magnetically weak (with contain arbitrary zeroes) CV% is very large. Quartzite, for example, has a CV% of 78.7%. A value for chalk has not been calculated due to actual zero values in the data set.

Figure 5.2: Kappa Field Surveys of Environmental Material

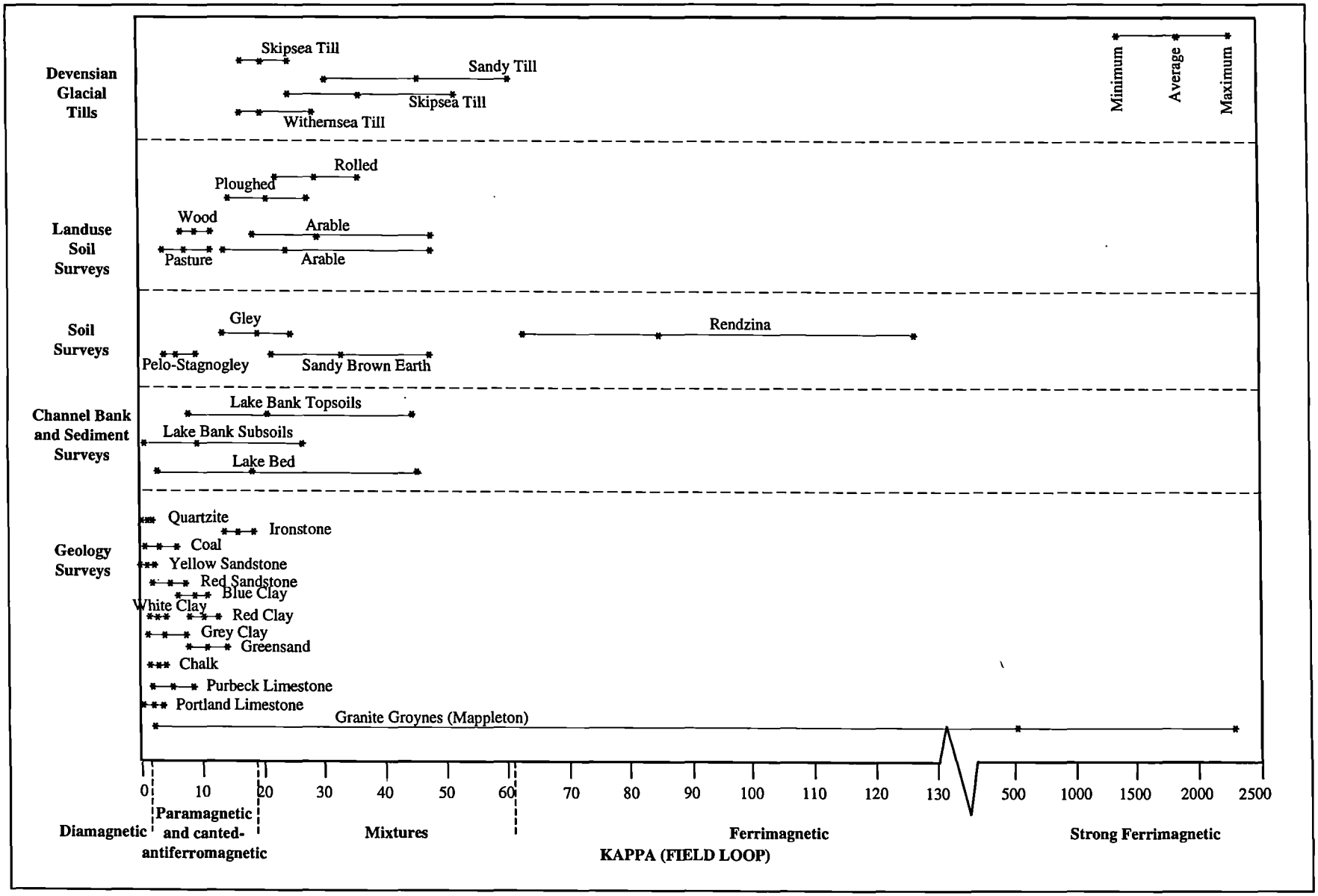

Table 5.2: Variability results for within-unit measurements relating to Figure 5.2

Group	Material/Location	Mean	SD	Min	Max	CV%	N
Glacial Tills	Red Till (Holderness)	20.6	2.8	17	29	13.4	50
	Sandy Till (Holderness)	46.0	7.8	31	61	17.0	50
	Black Till (Holderness)	36.9	4.9	25	52	13.3	50
	Red/Black Till (Holderness)	20.5	1.9	17	25	9.3	50
Soil/ Landuse Surveys	Rolled (Corley)	28.8	2.8	23	36	9.6	121
	Ploughed (Corley)	20.7	2.8	15	28	13.3	121
	Wood (Corley)	9.4	2.1	7	12	22.0	5
	Arable (Corley)	24.0	8.9	14	48	37.0	57
	Pasture (Corley)	7.7	2.0	4	12	26.0	56
	Arable (Corley)	29.7	7.2	19	48	24.1	39
	Pasture (Seeswood)	14.3	4.4	7	28	30.6	50
	Arable (Seeswood)	29.0	5.8	14	42	20.0	50
Soils and Sediments	Keuper Clay (Seeswood)	19.4	3.1	14	25	15.9	47
	Sandy Brown Earth (Corley)	33.0	6.8	22	48	20.6	49
	Pelo-Stagnogley (Great Rollright)	6.0	1.2	4	9	20.6	400
	Rendzina (Great Rollright)	93.0	12.6	63	124	13.6	400
	Lake Bank Topsoil (Seeswood)	19.4	8.6	7	44	44.2	33
	Lake Bank Subsoil (Seeswood)	8.1	5.6	2	26	69.0	33
	Lake Bed surface (Seeswood)	16.6	9.9	3	46	59.9	33
Geology Surveys	Quartzite (Lulworth)	0.9	0.7	0	2	78.7	50
	Ironstone (Lulworth)	16.6	1.4	14	19	8.6	50
	Coal (Lignite) (Lulworth)	2.3	0.7	1	4	30.9	50
	Yellow Sandstone (Lulworth)	1.1	0.7	0	2	66.7	50
	Red Sandstone (Lulworth)	3.81.1	2	6	28.3	50	
	Blue Clay (Lulworth)	8.1	1.0	6	11	12.6	50
	White Clay (Lulworth)	2.9	0.8	2	4	27.3	50
	Red Clay (Lulworth)	10.6	1.6	8	13	15.0	50
	Grey Clay (Lulworth)	6.4	1.3	1	8	19.9	50
	Greensand (Lulworth)	11.1	1.7	8	15	14.8	50
	Lower Chalk (Lulworth)	1.4	0.5	1	2	35.0	50
	Lower Purbeck (Lulworth)	5.4	2.3	2	9	42.4	50
	Portland Limestone (Lulworth)	2.0	0.9	0	4	46.5	50
	Granite Groynes (Holderness)	536.8	532.8	2	2269	99.3	50

Soils are fairly well discriminated in Figure 5.2 showing the low magnetic mineral concentration in gleys and magnetic enhancement in well-drained rendzinas. Also, differences in land-use values are observed, exhibiting lower values for pasture and woodland where measurements are made through grass or leaf litter. This is caused by the distance between the loop sensor and the mineral soil which is controlled by the thickness of organic matter or leaf litter. A value measured through organic matter represents approximately one sixth of the true measurement (Bartington Instruments). However, correction for this would increase values to above that for arable topsoils. For instance, Corley arable soil has a mean K of 24 while the adjacent pasture has a mean value of 7.7. Correction for the pasture would give a K of 46.2, which is nearly twice the value for the arable soil.

Density of the soil also has an effect on kappa as seen between the ploughed and compressed/rolled (more compacted) fallow soils which were situated directly adjacent to one another (Plates 5.1). Plate 5.1c shows more

clearly the difference in surface texture between the ploughed soil and the rolled soil (although in this case the compression is caused by a tractor wheel). The ploughed and rolled soils were measured using a $10m^2$ grid with 1m intervals (121 measurements). Using a student t-test the means were tested and found to be significantly different (t= -23.4, p=<0.0001). This result indicates that kappa variability is very large even within an area of $10m^2$ with differences in soil management. CV% for the two soils is also different by a factor of 4%, with ploughed soil varying by 13.32% and rolled soil varying by 9.6%. Most of the other soils, and soils under different land-uses, have CV's lying typically between 20% and 30%.

A test of the reliability of field susceptibility measurements was carried out to validate its use in spatial variability surveys. Figure 5.3 shows, for a set of geological samples, the mean of 50 field measurements plotted against their respective laboratory kappa values (for one sub-sample). A 1:1 relationship does not exist but there is a good linear relationship with a critical r value of 0.845 (p=>0.001). The effective differences between the two sets of measurements are that more accurate diamagnetic values are recorded in the laboratory whereas positive or zero values are recorded in the field. The spread of data indicates the difficulties in sampling any soil or geological unit at just one point. In this case 50 field measurements proved a good guide to assessing within-unit variability.

Overall this section shows that care needs to be taken when comparing results from different soils (because of density and organic changes) and weak magnetic geologies (because of near-zero measurements). The measurements however are made quickly, are not labour intensive and give a good initial guide to the magnetic mineralogies, their concentrations and variability within environmental materials.

Spatial Variability

In the identification and definition of sediment sources, spatial surveys need to be employed. This section introduces methods of assessing spatial variability of mainly topsoils and statistical definition of sources without having to collect excessive numbers of samples. The use of variograms was introduced in Chapter 2. Here, worked examples are presented of single transects of different sampling intervals. Normally a number of transects would be carried out in an area situated perpendicular to one another to assess spatial variability in different directions (Chapter 8).

Examples of variograms presented here represent variation in kappa measurements made on topsoils in North Warwickshire. The soil is of the Bromsgrove series and overlays Triassic Sandstones and Keuper Marls. First a kappa transect, 800m long and measured at 5m intervals, was completed along a part pasture/part arable/part woodland transect (Plate 5.1). Kappa results and land-use data are shown in Figure 5.4. Several boundaries were observed in the data which match soil, geological and land-use boundaries. First there is a difference between kappa measurement of the pasture and arable land-uses, partly due to the pasture measurements being made through a layer of grass. Kappa values for the arable soils are on average 20 for clay soils, 35 for sandy soils and only 9 for pasture soils and woodland soils. Woodland measurements are reduced due to the measurement through leaf litter layer. Another boundary exists at 350m where there is a soil type and geology boundary from a brown earth on sandstone to a gley on clay. Values also increase at 630m where there is another section of brown earths. There are

Figure 5.3: Correlation between lab and field kappa measurements for geological samples

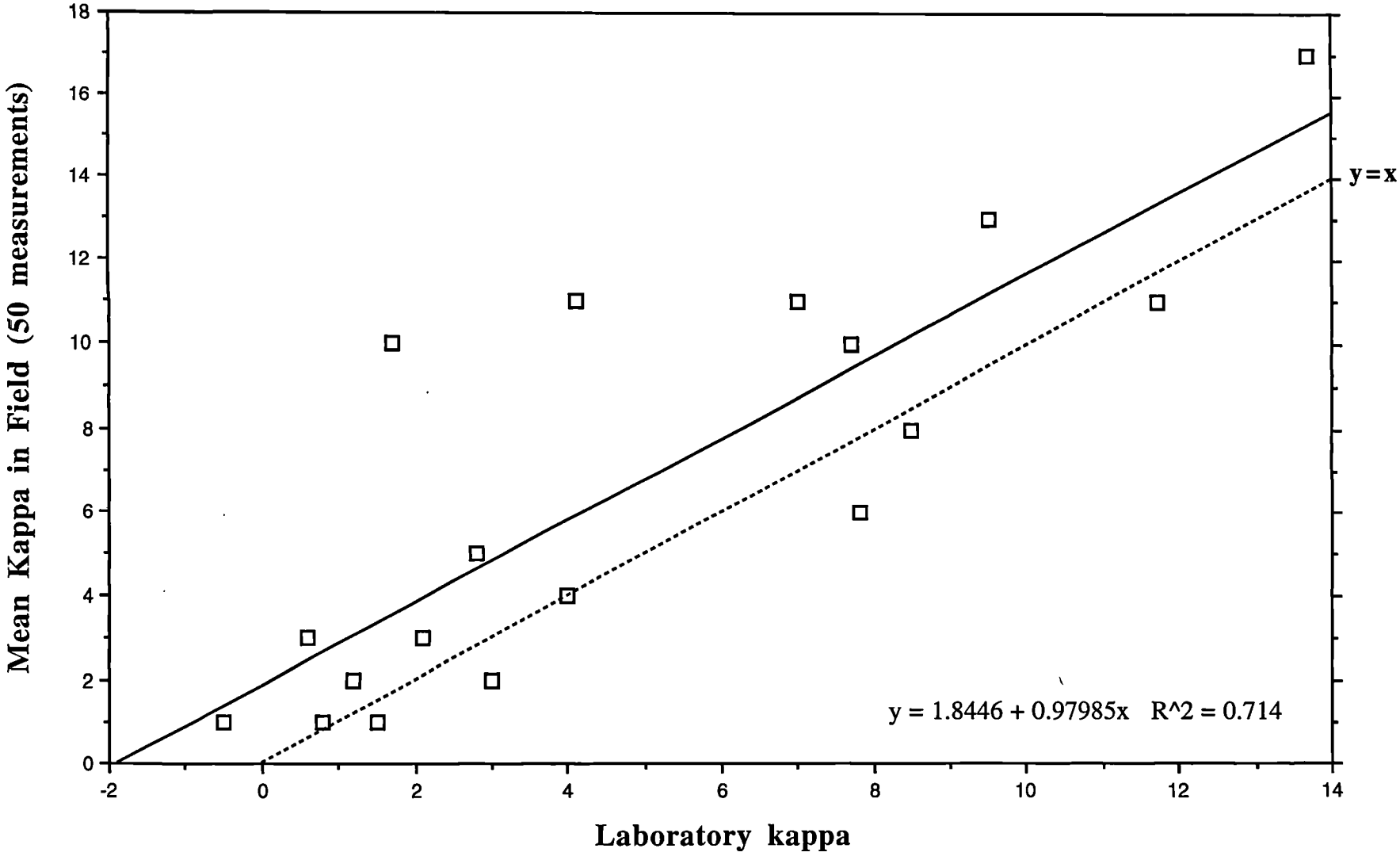

Figure 5.4: Kappa transect and associated environmental information

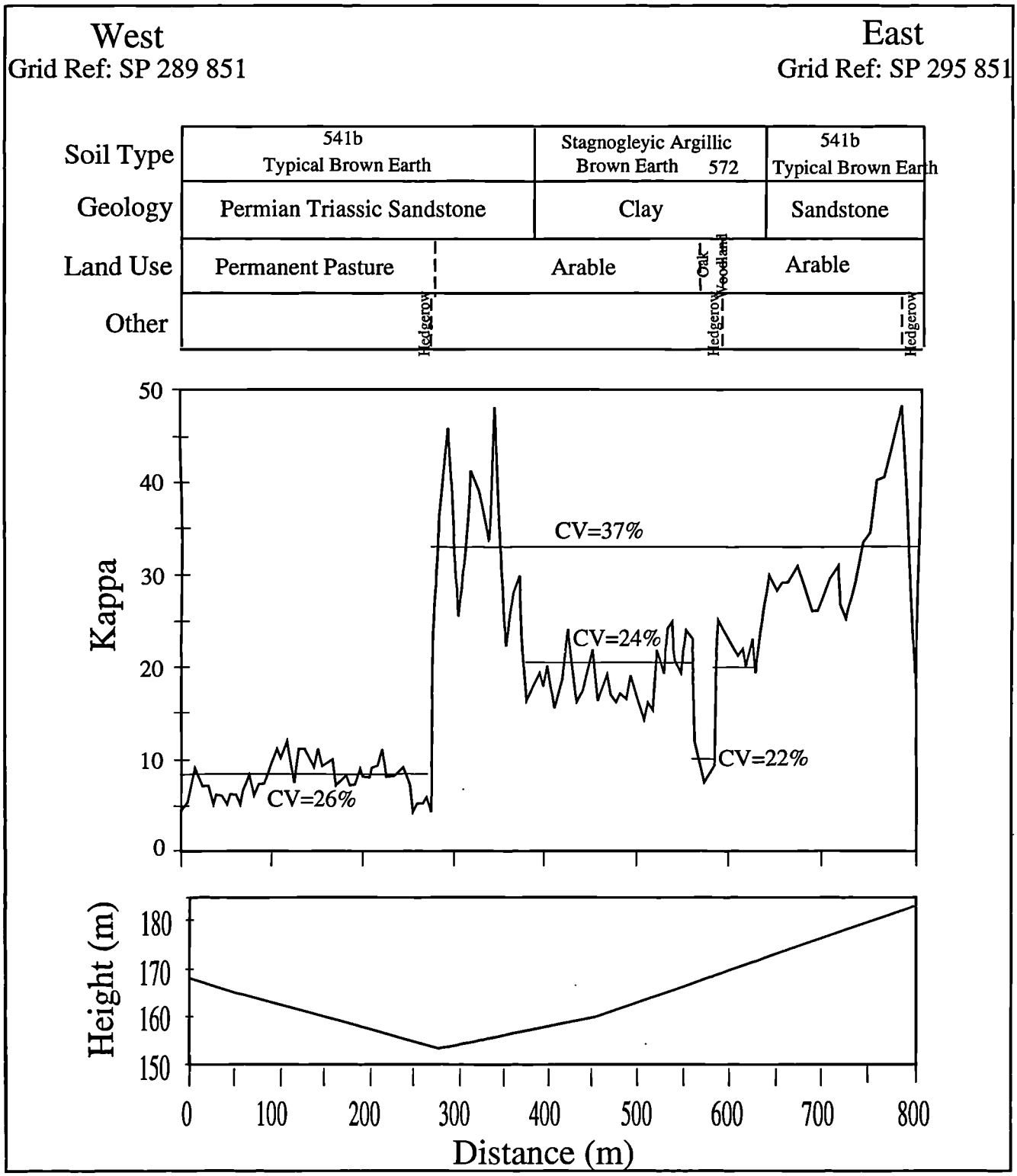

apparently insufficient topographical changes (angles are less than 3°) or drainage changes to affect the kappa values other than that related to soil and geology. Mean values for each section are marked on the transect. The kappa values exhibit a marked variation reflected by the CV% results (also marked on Figure 5.4). The CV values are reasonably constant for pasture and clays (~25%) but more variable in sandstones (~37%).

A variogram of the kappa transect data was constructed (Figure 5.5) and, whereas normally the variogram would be truncated at one third of the total distance, the entire curve is shown here for reference. There are two sills at 270 and 550m which confirm breaks in the kappa transect at the pasture/arable boundary and the second clay/sandstone boundary. This indicates that a sampling grid framework of 270m would cover the range of spatial variability of different soil/geology and land-use units of importance (ie samples taken at every $270m^2$ grid node). Above 600m on the variogram the curve tends towards infinity where the variance calculation is unstable and breaks down randomly (at the last point the calculation is between only two points). This feature may indicate a long-range trend or a nested feature showing two distinct scales of variation (M Oliver, pers. comm.). In this data there are two distinct scales of variation, one in the pasture section and one in the brown earth arable section.

The transect and corroborating variogram indicate how potential source sections in the landscape can be identified using magnetic susceptibility and aids the identification of sources which are magnetically differentiable. In order to assess the variability of individual source types, in-field or in-unit surveys can be employed or the original data can be sectioned. Figure 5.6a and b show variograms for the pasture and arable sections of the Corley transect. A sill at approximately 80m sets the range of spatial dependence for the pasture soil and a sampling grid on this scale would suffice for spatial definition of this source. There are a number of small sills in the arable variogram at 25m intervals. This variogram shows a cyclic feature in the field which could be related to patterns of ploughing, for instance, undertaken by the farmer or more likely old ridge-and-furrow patterns. A sampling grid of $20\text{-}25m^2$ would take into account the range of spatial variability on arable land. Webster and Oliver (1990) discuss bulking of samples over small scales as a valid means of cutting sample numbers while still accounting for spatial variability. This could be employed in the arable sections of this area and it has been found from experiment that the mean value for many samples is similar to the value of a sub-sample from bulked samples (also R Dann, pers. comm.).

A small survey was also completed in the arable field at Corley. A $20m^2$ grid was overlain onto a ploughed section and a rolled section of the field and measurements were taken at 1m intervals (121 measurements). Figure 5.7a and b give the resulting variograms for the ploughed and rolled data. The ploughed data shows a typical nugget pattern where the variation is below the scale measured meaning that at this scale the factors controlling variation are probably micro-soil processes at the aggregate level. The rolled grid shows a similar pattern but exhibits a small trend towards the variance (7.54) indicating that at 5m there is a scale of variation probably related to the width of the roller used to compress the soil. This again indicates the effects of density of the soil and land management upon the kappa measurement. (The rolled soils are 20m wide around the circumference of the field and have been planted with fine grasses and wild flowers. This area represents a buffer zone or land taken out of production).

Figure 5.5: Variogram for example kappa transect

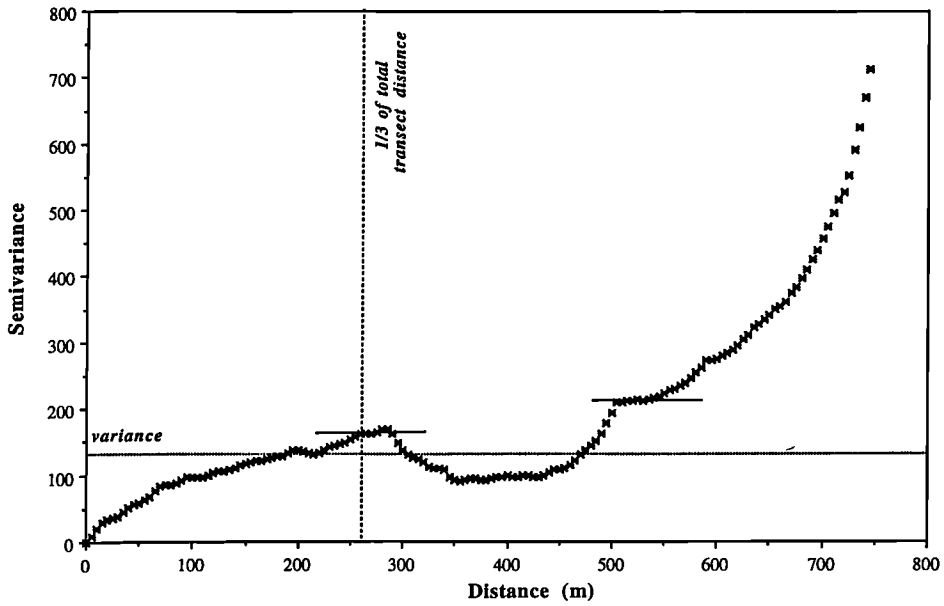

Figure 5.6: Variograms for pasture (a) and arable (b) sections of the transect

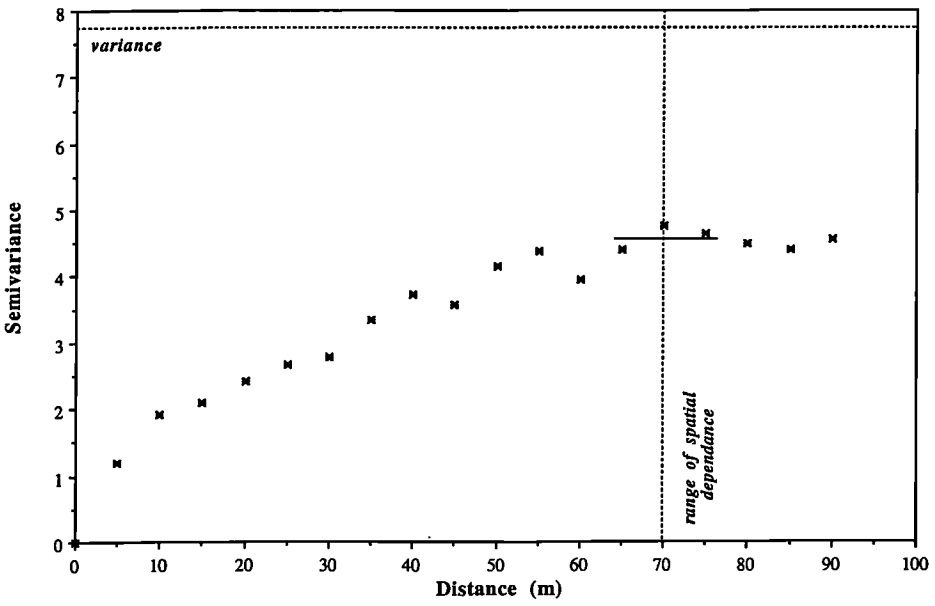

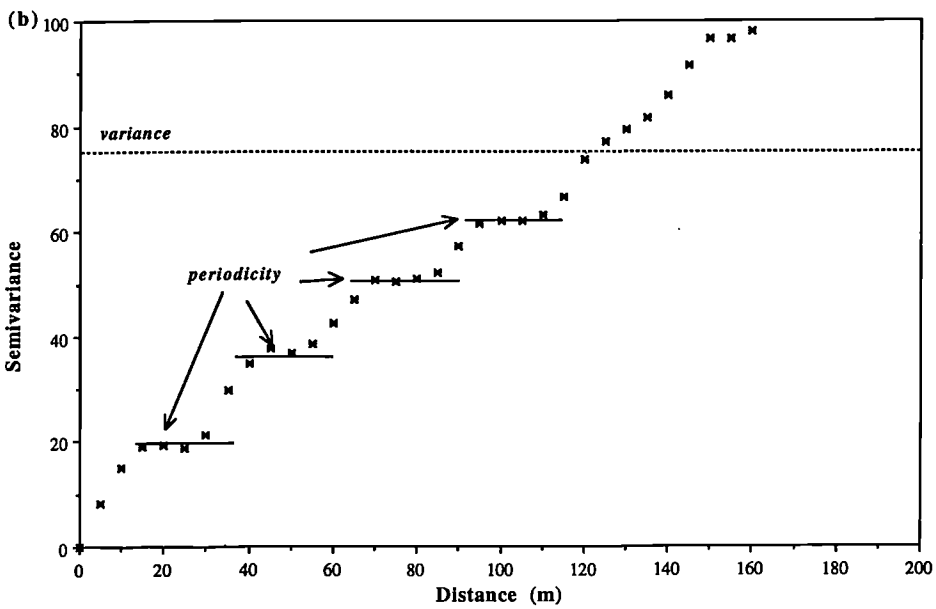

Figure 5.7: Variograms for ploughed soil (a) and rolled soil (b)

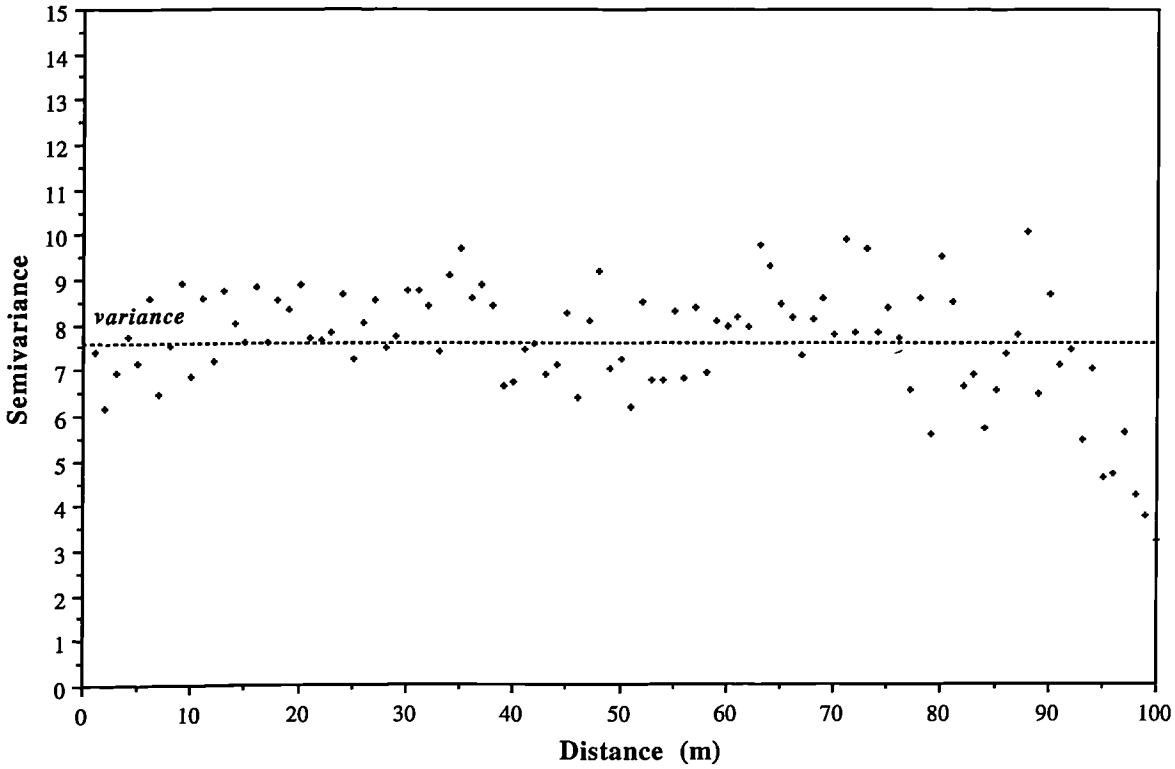

(b)

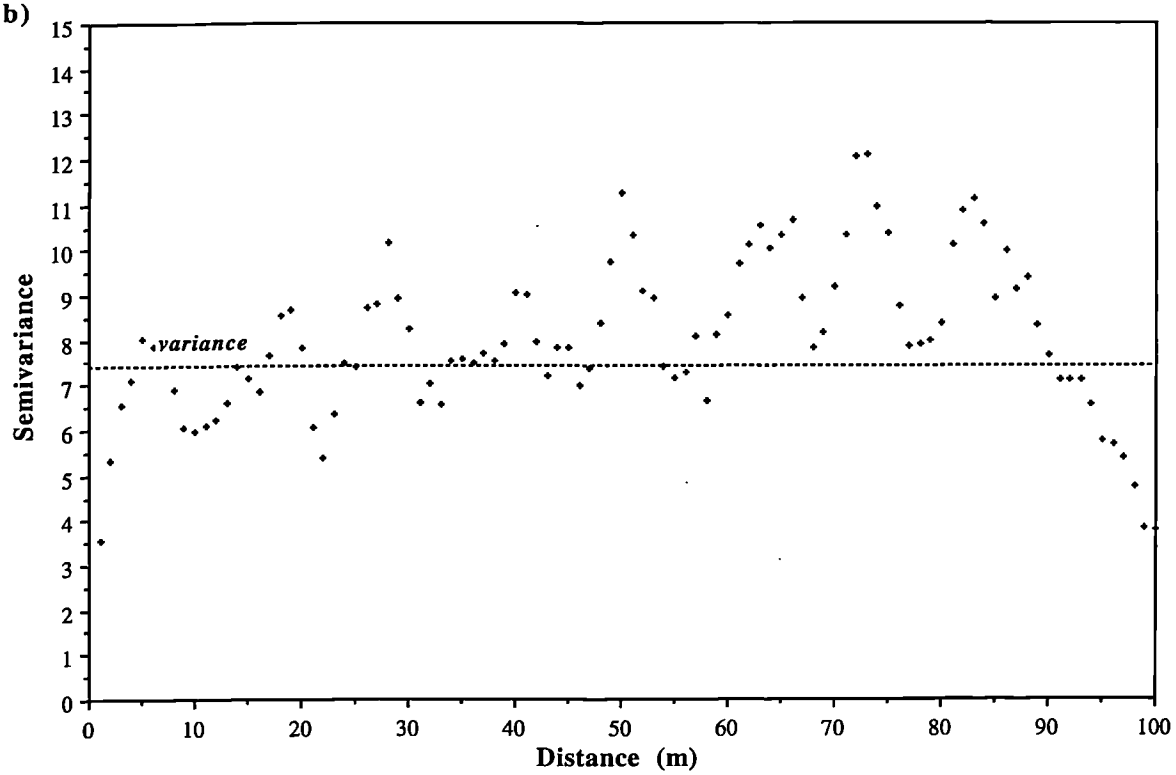

These small-scale variograms represent definition of the lower limits of environmental spatial variability. Overall from this section it can be seen that variograms using kappa measurements present a valuable survey tool in the assessment of spatial variability of potential sources and within- and between-field variation in small-scale single -unit studies.

5.4 Summary

This chapter has presented information on various aspects of variability from that found in sub-samples of materials to that found in larger spatial areas. Intra-sample variability sets the lower limit on the amount of variability which can be expected at all times. This has been found to be up to 10% in this research. Further to this, in the environment small changes in ferrimagnetic mineral grain size and particle size can have great effects on magnetic properties. Within-unit variability has shown that great variations exist in measurements taken at small distances from one another. CV% for such units has usually been found to be above 20%. Kappa measurements are most affected by density and presence of organic matter. At larger scales potential sources may be identified using kappa surveys and their boundaries statistically defined using variograms. Kappa measurements have been found to provide information on the concentration and type of minerals present in environmental materials. Kappa can also be used to discriminate between soil and geology types for instance and can indicate areas which might contain magnetically differentiable sources for application of modelling using magnetism. The following chapter summarizes the findings of the previous three chapters and presents the methodological framework devised from the evaluation and modelling work presented in this section.

CHAPTER 6

Methodological Findings: Formulating the Methodological Framework

Introduction

Chapter 4 presented much of the work on the basis of which a measurement-modelling-interpretation methodology or routine framework was defined. Much information collected and critically tested as shown in Chapters 3, 4 and 5 has led to evaluation of each stage of the proposed methodology. The main aim for the methodological framework is its adaptability to any environmental application as shown in Chapters 7, 8 and 9. This chapter provides an overview of the methodological framework constructed from the work described in Section B (before it was tested in an environmental situation).

6.1 Main Findings from evaluation and modelling in Section B

An overview is given here as to the main advantages and limitations of the use of magnetism which can be drawn from Chapters 3, 4 and 5. These define the realistic framework within which the methodological framework can be applied. The points are divided into individual steps of the methodology in the order in which it should be carried out (ie source identification , measurement, classification and modelling).

Source Identification

* Magnetic susceptibility surveys provide a sound mechanism for identifying the possibility of discriminating sediment sources in an area. Soil, geological and land-use boundaries can be identified using kappa.

* The variability of sub-samples as defined by CV% has been found to be <8% for χlf but higher for difference parameters .. For example χfd has CV%s up to 26% for environmental materials.

* Variability of source samples can be defined using kappa and CV% and have been found to be high (>20%).

* Upon application of the methodology to environments other errors such as environmental variability may outweigh experimentally-defined errors.

Initial bi-variate classification and statistics

* The normality of magnetic data should be tested as log transformation will almost certainly be required.

* Correlation of parameters quickly identifies those linearly additive measurements which would form the best discriminatory classification.

* Bi-variate scattergrams often give as much information with use of the appropriate parameters as do statistical classifications. Use of ratio parameters also gives a good indication of patterns other than concentrational factors occurring in the data.

Multivariate Classification

Cluster Analysis

* In using raw data, magnetically strong samples mask the results and cause weaker samples to be grouped together regardless of their apparent difference on a weaker magnetic scale. This indicates the scale to which the linear programming will be suitable for application to certain datasets.

* With normalized data the classification is more accurate but often much information is lost from samples with negative susceptibilities. Arbitrary zeros also present a problem in interpretation of transformed data.

* Different results are gained by using different clustering methods and inputting different variables. Interpretation of the way in which certain magnetic parameters affect this is extremely difficult.

* Using cluster analysis on its own would be insufficient to identify those sample groups which are different enough to model. The dendrogram output from cluster analysis is quite difficult to interpret in terms of just how alike samples are. For example, two samples which were exactly alike would plot out next to each other in the dendrogram rather than on the same spot as in PCA.

* Samples cluster just as well with a few well-chosen, relatively uncorrelated parameters (χlf, χfd, χarm and HIRM+100, for example) as they do with all the measurements available.

PCA

* Very strong samples mask the results; these samples have to be removed to expose any grouping in the weaker, but more environmentally 'normal', samples. Normalizing the data set often results in the loss of many of the cases through zero susceptibility values and arbitrary zeros.

* Interpretation of the way in which certain magnetic parameters affect PCA results is easier than that for cluster analysis.

* Inputting principal component data for each sample in cluster analysis rather than the raw data seems to produce similar results. With PCA data the orthogonality of the PCs brings out the groups suitable for modelling. With raw data emphasis is placed on the larger magnetic influences in the sample set but the fine detail (small eigenvalues) is lost.

* Principal Components are identified equally well with a few well-chosen relatively uncorrelated variables (χlf, χfd, χarm and HIRM+100 for example) as when all linear measurements available are included.

* If PCA cannot be carried out (ie only one factor) then the situation is suitable for tracing only.

Traditional Magnetic Interpretation versus PCA Classification

* Most PCA plots are strongly influenced by χlf and HIRM+100 identifying the two strongest magnetic properties, and great similarities were found between these and bi-variate scattergrams.

* The χlf versus HIRM+100 plot would be a very good initial indicator of the spread of samples and an early indicator of modelling suitability of sources and mixtures.

* One advantage of a PCA co-ordination plot is that it can take many variables into account at once. In mixing experiments these plots generally fit the samples into quadrants which reflect the four main magnetic properties. However if all main properties were not present this would not be the case.

Linear Programming

Modelling with Sources

* Magnetic measurements of environmental materials are linearly additive in low concentrations. With the addition of stronger materials the linearity decreases.

* Susceptibility produces the most linear results with only a 5% error occurring (mixing experiment 2) between the predicted results and the actual measurements. Remanence measurements showed, on average, a 10 % reduction from the predicted results.

* Possible causes of poor linearity: Interaction effects (see Paper 1, Appendix 7) cannot be ruled out as only the remanence measurements were affected, however it could be caused by equipment calibration (Appendix 3) or other aspects of the methodology such as packing density of the mixtures or mixing methodology (see Appendix 6).

* The number of sources which can be identified using magnetism is limited by the strength and number of magnetic properties and grain sizes existing in any environment. Difficulty has been encountered in mixtures of more than 4 components in this research. Even in mixtures with the linearity error as low as 2% for susceptibility and 10% for the remanences the linear programming failed in most cases with over 4/5 components.

* Great improvement was seen between the result of the first and second mixing experiments, mainly due to the removal of the chimney slag material and also due to the increased homogeneity of the samples in experiment 2.

* It is important to note that even when subjected to light grinding, the materials magnetic properties may change slightly, especially if the material contains large multidomain grains (Appendix 6).

* Six out of eight two-source component VSM mixtures suffered from large linearity errors and did not unmix successfully.

* The hypothetical mixing experiment showed that with errors as large as 10% we can still get fairly reasonable answers but can expect an error range of about 5 to 10% on each predicted component proportion.

* Great difficulties were encountered in the classification and modelling of sources which were either magnetically weak and/or were constant multiples of other sources.

Modelling with Magnetic Mineralogies

* There are possibilities for modelling magnetic minerals and determining the possible make up of the magnetic mineralogy of environmental materials.

* The scale of ferrimagnetic mineral measurements (magnetites) poses the largest disadvantage for modelling. Their properties often mask the properties of much weaker magnetic minerals unless the data are normalized. Such normalized data cannot then be used in linear modelling, however.

* There are many advantages in being able to model in this way, as other methods of identification of the mineralogy of a material involve lengthy electron microscopy or X-ray diffraction.

6.2 The measurement-modelling-interpretation routine

The proposed methodological framework is shown in Figure 5.1. It is essentially a set order of tasks with various options relating to application of magnetic techniques. The diagram has been formulated through work presented in Chapters 3, 4 and 5 and each section is described in detail here.

Statement of the Problem and sampling

First a statement of the problem is formulated whereby precise definition of the aims and objectives of working in any particular environment and the advantages of classification and modelling of sediment sources are defined. At this stage perceptual experience (relating back to Figure 3.1) plays a part in determining the initial suitability of using magnetic techniques in an area. Having determined the validity of this approach, careful delineation of the 'area of interest' (river catchment for example) can be carried out with the use of maps and field survey. This 'area of interest' may not be the effective sediment contributory area, however. In a river catchment the effective contributory area may be a subset of the whole catchment due to sediment barriers (roads, hedges or tracks). The effective area (subjectively defined) can be defined once the sediment sources are identified. The definition of 'area of

Figure 6.1: *MEASUREMENT - MODELLING - INTERPRETATION* Methodological Framework

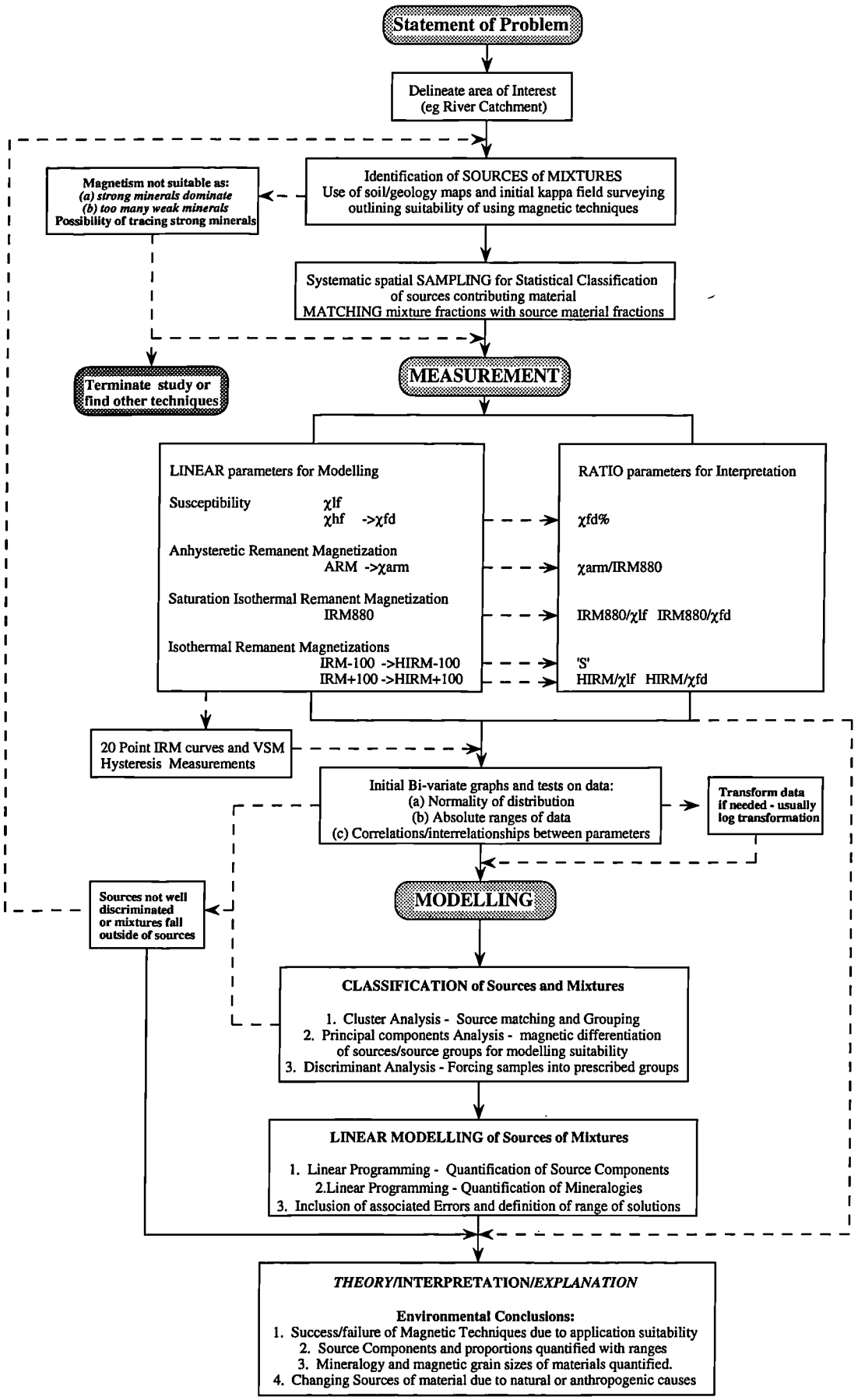

interest' will always prove more difficult to determine in more open systems such as the atmosphere and coastal environments than in catchment or soil systems.

For identification of sources, the methodology proposes the use of maps and magnetic susceptibility field survey as a basis for identifying the source units. The variability in magnetic properties, within and between sources, would also be examined. Experience backed by susceptibility results will outline the suitability of an area within which there may be a number of sources suitable for the application of magnetic techniques. For instance, the colour of soils and subsoils may indicate presence of ferrimagnetic minerals (brown/black) and canted-antiferromagnetic minerals (red/orangey-brown). At this stage in the methodology there is a route which by-passes systematic survey in cases where either, (a) strong minerals dominate the magnetic signal, or (b) there are tóo many magnetically weak sources which cannot be measured accurately enough. At this stage systematic survey can be by-passed. The possibility of tracing strong minerals (eg mining materials) in the particular environment then becomes viable; or the use of other analytical techniques which may discriminate the sources may be the best option.

If sources are thought to be magnetically different and not dominated by too magnetically strong or weak minerals then further systematic survey can be undertaken. Variograms from field survey can be incorporated to define sampling grids at several spatial scales within and across source units and to identify the number of samples needed. If the number of samples needed is large, bulking of samples within a source unit is a viable option (Webster and Oliver, 1990). The final modelling results will be as good as the initial identification of sources using their magnetic properties and the definition of the ranges in those properties within and between source units. Matching of relevant source particle size fractions to those of the proposed 'mixture' must also be addressed at this stage. Much environmental work is done using <63μm fractions but fractionating sediment sources is not always necessary if all magnetic properties are controlled by this fraction anyway. Consideration must also be given to the fact that the magnetic properties of the fractions may not discriminate them as well as the bulk material. A related problem is that sediments may not be selected, transported or deposited conservatively; this assumption remains in the methodology however.

Measurement

The methodological framework then moves on to linear measurement for use in classification and modelling and associated ratio parameters to aid initial bi-variate discrimination (and for final interpretation). χfd% is perhaps the most useful of the ratio parameters for this purpose, but only its mass specific counterparts, χlf, χhf and χfd, can be used in linearly additive modelling. Addition of other linear data from IRM curves and hysteresis loops can also be incorporated but often do not add any further information to the main linear parameters listed. Modelling using IRM curve and hysteresis loop data only is a possibility, but suffers from higher linear additivity errors and increased collinearity between parameters. The most linearly additive and useful parameters in terms of discrimination are susceptibility parameters (χlf or χhf), ARM (or χarm), high field IRMs and HIRM at +100mT.

Initial classification

Bi-variate scattergrams and simple statistical tests on the data can indicate the level of discrimination within a data set and identify those parameters which are significantly correlated. Often bi-variate scattergrams of the two least correlated parameters will match the results of statistical classification techniques. But statistical classification can classify on the basis of more than two parameters. Also the ranges of concentrations within and between identified sources can be shown. Sometimes the variation within source materials may be larger than that between different sources and may overlap the parameter value range of those sources. In this case the mean properties of the source materials become more important. Variance measures (standard deviation) used in modelling will indicate the range of source values and aid discrimination (ie mean-1sd or mean+1sd).

Normality of the distribution of the data is of utmost importance if useful results are to be gained using the classification techniques. This is unfortunately a factor that cannot be incorporated into the linear modelling. Classification of the original raw data will identify the realistic options for linear modelling of the sources of materials. As seen in Chapter 4, the majority of magnetic data-sets are highly positively skewed (log normal). Essentially a natural log transformation will 'normalize' the distribution. But the presence of arbitrary zeros in the data has to be carefully analysed otherwise large negative log values result and diamagnetic materials with negative susceptibility values are lost. A constant can be added to all the data to rectify the situation but overall it is the classification on the raw data which gives the most useful indication of the possible success or failure of linear modelling in any particular situation.

At this stage in the methodology it may be the case that the properties of the proposed mixtures fall outside the range of the sources, or that the sources are not as well discriminated as first hoped (they are direct linear multiples of one another). Further analysis can be by-passed at this stage; two options are available, (a) re-identification of the sources and further fieldwork or (b) termination of the study with interpretation and explanation of the results gained so far.

Statistical Classification

Statistical classification of sources and mixtures has the advantage of incorporating any number of variables in the analysis. First, cluster analysis defines in a two-dimensional dendrogram the groupings of samples within a data-set. Secondly, principal components analysis can identify the most important magnetic variables in a data-set and set out in a two dimensional co-ordination plot the sample groupings and the parameters related to each principal component. PCA can be carried out on the original raw data and on data constructed in cluster analysis for each individual sample. This has the advantage of checking any disparity between the two techniques and verifying the cluster analysis classification.

Discriminant analysis (Chapter 3) can be used and has the effect of forcing samples into defined groupings and can mislead the modeller into thinking the sources are better discriminated and have less variation than really exists. At this stage mixtures may again be found to be outside the range of the sources, or sources may be found to be direct

linear multiples of one another. Again, further analysis can be by-passed at this stage with two options available as above, (a) re-identification of the sources and further fieldwork or (b) termination of the study with interpretation and explanation of the results gained so far.

Usually patterns seen in magnetic data are caused by two main components: a ferrimagnetic component, indicated by χlf, χfd or IRM parameters; and a canted-antiferromagnetic parameter indicated by HIRM parameters. The main limitations in magnetic data intended for use in classification techniques are due to these two common magnetic characteristics of environmental materials.

Linear Modelling

A good indication of the likelihood of success of linear programming can be given by using the same linear (untransformed) parameters to classify the sources and mixtures. The linear programming routine may be used with any linearly additive data which are not subject to large measurement error. Linear modelling may be used to find the source proportions of spatial sediment sources or individual magnetic minerals. Usually the mean value is used for a sediment source or mineral input, however the mean$\pm$1sd should identify the range of source proportion values which are likely to be encountered in environmental studies. In the light of less than perfect results in artificial mixing experiments however it must be noted that source proportions calculated using magnetic properties of materials are at best only estimates.

Theory/Interpretation/Explanation

This section of the methodology is one of the most important in terms of (a) answering the statement of the problem and identifying and quantifying sediment and/or mineral sources and (b) evaluating magnetic techniques as applied. Also in using core data (lake cores for instance) changes in sources of material can be identified and quantified (and dated!). Environmental variability of materials will always present limitations over and above those of the linear additivity of magnetic properties in the quantification of sources. Intra-sample variability affects modelling results but is lower, in general, than spatial variability because of more control over the size of sample. Such variability in environmental materials may result in the calculation of a large range of source proportions in a modelling study.

6.3 Summary

The limitations imposed on the application of magnetism by the inter-correlation of the magnetic parameters themselves presents the largest single problem in this work. Classification and linear modelling techniques require parameters to be more independent than the magnetic parameters have been found to be. However with care the methodological framework presented in Figure 6.1 can be used and has been applied to various case studies as described in the following chapters of Section C. Further to this, the framework has been re-assessed in the light of each of the case studies. It is presented in revised form at the end of each of Chapters 7, 8 and 9 according to the suitability of application of the magnetic, statistical and modelling needs and findings in each individual case.

SECTION C

Environmental Applications

Introduction

In the following three chapters the methodological framework presented in Chapter 6 is applied to three contrasting environmental situations. The first applications are made to two coastal systems, one in Holderness, North Yorkshire, and one at Lulworth Cove, Dorset. The Holderness study is a large-scale study of a section of the eastern coastline of Britain between Scarborough (North Yorkshire) and Mablethorpe (Lincolnshire). Along the Holderness coastline there are many geologies, both solid and drift, and longshore drift of sediments occurs down coast towards the south. The Lulworth study is a smaller scale application in an area of sedimentary geologies and little longshore drift. The second application is that of a small catchment system near Chipping Norton, Oxfordshire. Soil and geological sources of sediments of two small streams are classified and modelled. The study incorporates definition of the spatial variability of sources using kappa surveys as described in Chapter 5. The third study is that of mineral sources in soil profiles. Five contrasting soil profiles are studied and an attempt is made to quantify the magnetic mineral content of the soils at certain depths. In each chapter the methodological framework has been re-evaluated and adjusted according to the individual needs and results of each of the case studies.

CHAPTER 7

Quantitative sediment sourcing and tracing in coastal systems

Introduction

No previous work has been done using magnetic techniques to trace coastal sediment sources. Mineralogical tracing studies using radiometric measurements have been carried out in Denmark by Greenfield et al. (1989) and Schuilling et al. (1985). Also Chauris (1989) used percentage mineral concentrations to trace minerals along the coast of Brittany, France. In these studies heavy minerals such as magnetite, hematite, pyrite and biotite and their properties were utilized to find their sources. Little, if any, quantification of sediment sources in coastal areas has been accomplished. With the increased interest and importance of the stability of our coastlines it is vital to be able to apply fingerprinting techniques to find historical and contemporary sediment sources. Foster et al.(1991) attempted to trace and describe the sediments found in three cores from coastal lagoons on the Isles of Scilly. Tsunami deposits, deposited in a series of large waves generated by the 1755 Lisbon earthquake, were thought to have filled the lagoons. Several source samples and the cores were analysed and the magnetic measurements of S ratio and SIRM (IRM880) discriminated between the ferrimagnetic contents of topsoils and beach sands.

A study of fjord and shelf deposits in Baffin Bay by Andrews and Jennings (1986) used magnetic susceptibility to identify sources of sediments. Major changes in magnetic susceptibility in some cores were attributed to sediment source and textural changes. High susceptibilities were found to be associated with nearby gneiss and granite outcrops, while low values were associated with Proterozoic geologies. The results show that magnetic susceptibility may provide valuable data in identifying sources of sediments in Baffin Bay. A more specific study by Scoullos et al.(1979) characterizes point sources of iron oxide particulate contamination in the Elefsis Gulf, Greece. Ferrimagnetic minerals emitted into the atmosphere by an iron and steel works were monitored using measurements of filter samples and Gulf sediments. SIRM (IRM880) was found to have a 'reasonable' calibration with iron content in the filter samples indicating a more rapid method of monitoring the particulate pollution in the area. These studies show in the main that magnetic measurements may be used for sourcing coastal sediments and especially in the tracing of highly magnetic minerals.

There are many problems associated with beach tracing and sand provenance in coastal studies over both short and long timescales. The first study presented in this Chapter attempts to trace the sources of sediments of the beaches along the Holderness coastline between Scarborough and Mablethorpe using magnetic techniques. The application of statistical classification and linear modelling in an essentially coarse-grained high-energy environment represents a major test of magnetic techniques. Reference to and comparison between the limitations of magnetic techniques researched in the laboratory and theoretically determined are made. The results presented give a good guide for the application of magnetic techniques in situations where discrimination of sediment sources is less than satisfactory.

The second study carried out at Lulworth Cove aims primarily to test the use of field measured kappa to identify sources of beach sediments in an area not affected by longshore drift and glaciation. The survey incorporates 50 measurements of each geology and a beach transect around the cove. The suitability of applying magnetic classification and modelling techniques is assessed from the initial field survey. Direct comparison between magnetic properties of the two coastal areas, 1, a glacial till covered area and 2, non-glacially affected area, produces useful conclusions. Some of the work carried out in Holderness is also presented in Paper 2, Appendix 7.

Part 1: Studying the Holderness Coastline

7.1 Area of study

This area of study was chosen on two grounds. First the Coastal Studies Unit, University of Hull, wished a particular black sand sediment on the beaches to be sourced. Secondly, in a preliminary study of the area the local geologies seemed to fulfil the criteria (given previous knowledge on magnetic minerals from the geology database) for magnetic sourcing. The actual complexity of the geologies of the area (with glacial tills) could not have been realized from geology maps however, and initial susceptibility field surveys were employed. The beaches and cliffs of the Holderness coastline are eroding rapidly at an average rate of 2 metres per year. This figure is a conservative estimate in some areas where erosion may have increased due to the building of local sea defences. This problem is compounded by the naturally unstable till cliffs of the area. Along most of the Holderness coastline the low water mark is moving inland at a rate of 1m per year due to both rising sea levels (Pearce, 1993) and isostatic readjustment of the land taking place since the last glaciation. Along the coastline of Holderness it is estimated that 480 square kilometres of land have fallen into the sea along with 36 villages since Roman times (Pearce, op cit). This stretch of coastline is the North Sea's largest single source of sediment; some of the coarser sediment moves south to Spurn Head (a natural spit) while finer sediments move off-shore and may eventually reach the Essex saltmarshes or the coastlines of Denmark, the Netherlands and Germany (Dossor, 1955; Pearce op cit).

The chosen area, the coastline between Scarborough and Mablethorpe (Figure 7.1), includes coastal features such as Spurn Head (shingle spit) a chalk headland (Flamborough Head) and salt marshes in and south of the Humber Estuary (Spurn Head and Saltfleet). The solid geology of the area is also given on Figure 7.1. The only site at which the chalk is clearly visible on the coast is at Flamborough head where the chalk is uplifted and resistant. Between Flamborough, Filey and Spurn Head the beaches are backed by glacial tills with complex stratigraphies. Further south at Cleethorpes and Mablethorpe the till cliffs are not evident, the beaches are wide and possibly receive mainly Humber estuary sediments. Plates 7.1a-g show many of the sites, tills and erosional features described in this chapter.

The glacial tills of the area are of the Wolstonian and late Devensian ages. A Wolstonian basement till is thought to exist below the Devensian tills (Jones and Keen, 1993) but this was not observed at sampling locations. The

Figure 7.1: Area of Study showing solid geology and sampling sites

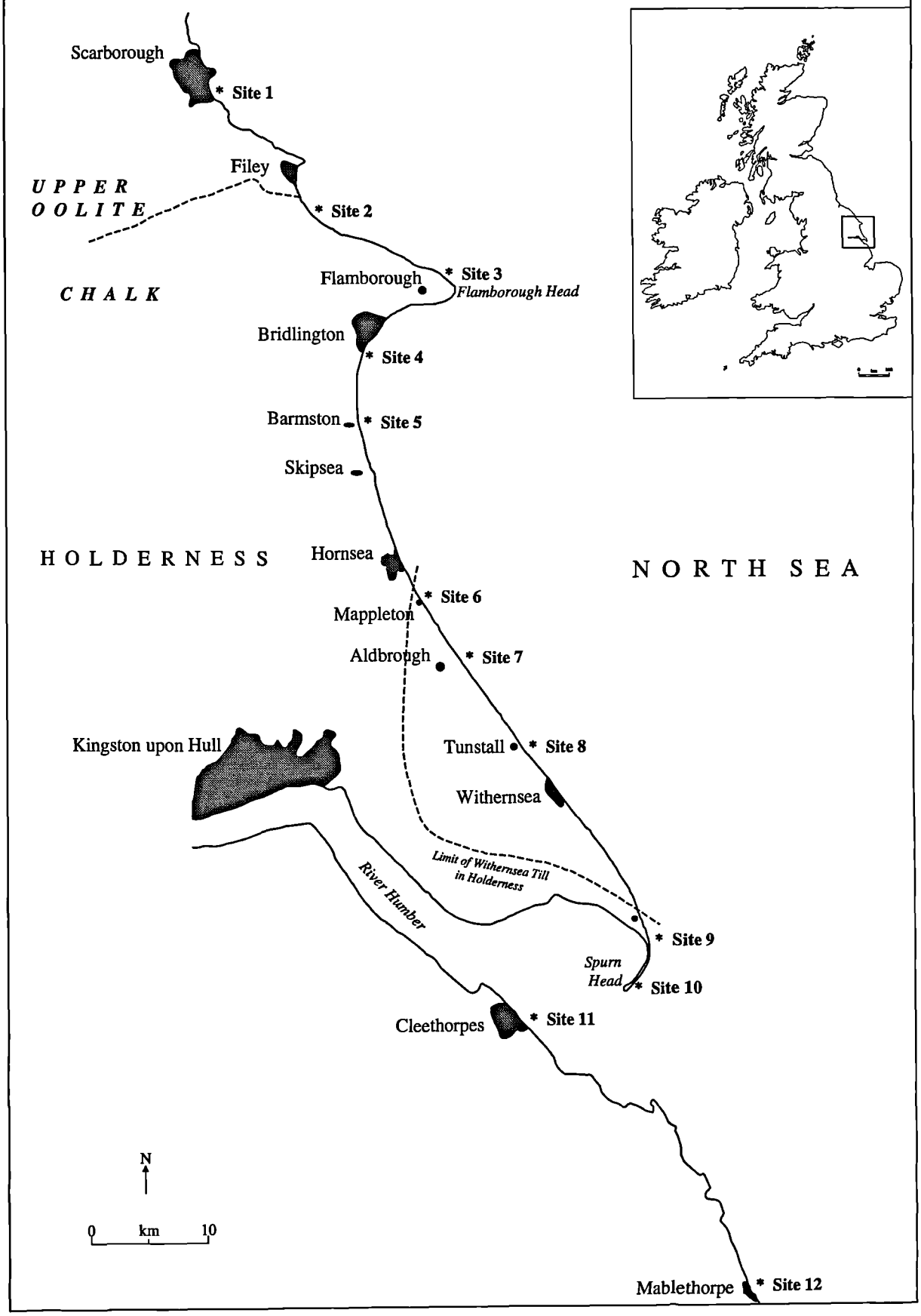

Plate 7.1a. Coastal erosion at Aldbrough

Plate 7.1b. Cliff collapse at Aldbrough

Plate 7.1c. Cliff collapse and black sand at Barmston

Plate 7.1d. Barmston cliff stratigraphy

Plate 7.1e. Cliff slumps and flows at Mappleton

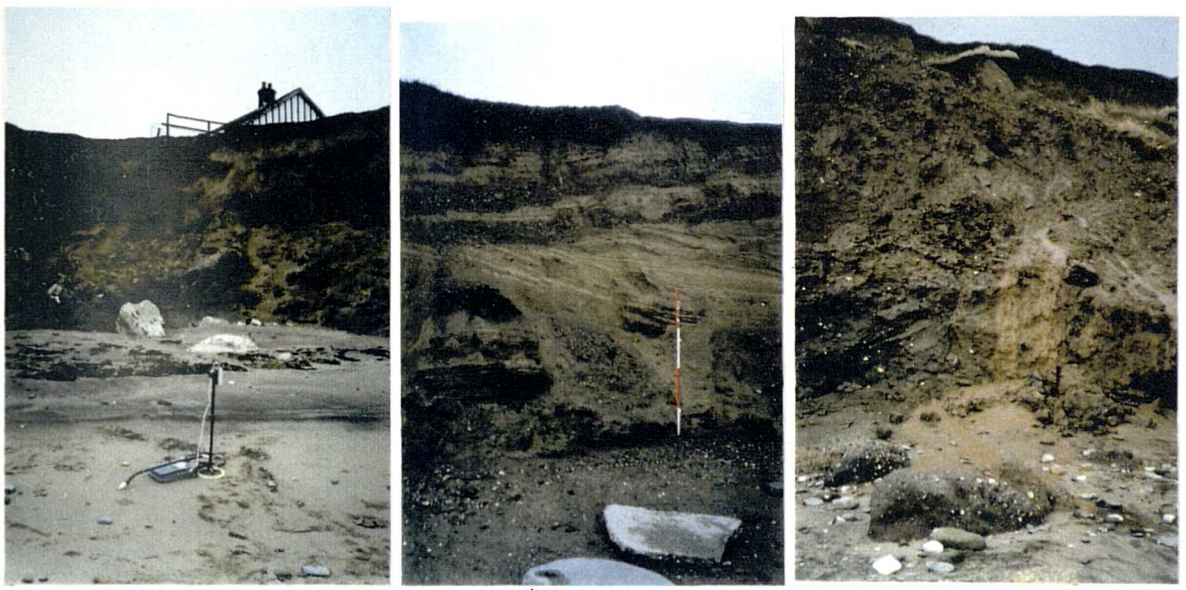

Plate 7.1f. Skipsea and Withernsea tills at Barmston

Plate 7.1g. Sorted black sand on ripples at Tunstall

tills which were sampled in the field are, first, a dark brown drab till termed Skipsea till which lies at the base of the cliffs. This was only exposed from Mappleton northwards. Secondly, between Hornsea and Spurn a red/purple till outcrops (Withernsea Till), the limit of which is marked on Figure 7.1. The Withernsea till overlays the Skipsea till and in between them in places there are lacustrine varved sediments with clear laminations and sand and gravel layers (Plate 7.1d). At Barmston (outside the Withernsea till limit) there is a complex stratigraphy where a sand layer/till, approximately 7m in depth overlies the Skipsea Till and is clearly bedded which suggests a fluvio-glacial origin. Above this was a clearly defined soil profile with dark topsoil (50cm) and weathered subsoil (1m). A till similar to the Withernsea till has been identified in Filey Bay (Edwards, 1981), but it was difficult to distinguish between the Filey tills and Withernsea tills in the field. The till cliffs range in height from 1m to 30m along the coastline and at the sites studied the cliffs were about 15m in height reducing to 1m at the landward end of Spurn. The tills carry many erratics and these were considered as potential sources for the beach (see Table 7.1). Many erratics were local chalks and limestones with negligible magnetic mineral concentration but some were igneous and sedimentary rocks.

The beaches were found to consist of mainly quartz sands with black sands which were concentrated in lines parallel to and near to the cliffline. In summer, clear banding of the black sand could be seen in the vertical beach profiles. In winter, black sand was concentrated at the surface of the beach and no depth banding was apparent as shingle and till underlay about 5 cm of sand. Shingle contained erratics from the tills and many flint and limestone pebbles.

Table 7.1. Erratics reported in the tills (Catt and Madgett, 1981) and those measured (*).

Skipsea Till	**Withernsea Till**
chalk*, pink chalk, liassic shales*	chalk*, greywackes*
Carboniferous limestone*	Carboniferous limestone*
limestone*, Magnesian limestone*	Magnesian limestone*
Bunter Sandstone*, yellow sandstone*	Triassic shales, Liassic shales*
Scottish granites*, granites*	Cheviot porphyrites, igneous pebbles*
Norwegian larvikite*, Diorite*	
grey flints*, black flints*	
green greywackes*, rhomb porphyry	
Cheviot porphyrites, quartz porphyry*	

7.2 Aims and objectives

The main objective of this study was to source the beach sediments along a section of the eastern coastline of Britain and to identify the number of lithological units which contribute sediment. The aims of the study, listed below, concentrate on the application of magnetism in the coastal sediment system rather than studying the coastal geomorphology and sedimentation of the area in any great detail. It was generally accepted, given local erosion rates, that there was contribution from a wide range of material - local geologies, drift geologies and related erratics to the beaches. The potential source materials covered are diamagnetic, paramagnetic, canted-antiferromagnetic and ferrimagnetic behaviours.

The aims of this study are:

1. To use magnetic properties to identify and quantify the sources of the beach sediment
2. To find the source of and quantify a specific sediment (black sand) on the beach and to trace that sediment by determining its magnetic properties
3. To evaluate the use of magnetism in the classification and modelling of coastal sediments

Also several questions were raised from the aims and are answered where possible during the course of this systematic study:

1. Is the stretch of coastline between Bridlington and Spurn sediment 'tight' or is sediment gained and lost from longshore/offshore sources?
2. How far north and south does the black sand on the beaches extend?
3. Where does all the till material go in the light of the thin beaches?

7.3 Source identification, field mapping and sample collection

Preliminary study

Potential sources of the beaches were defined primarily from solid and drift geology maps and secondly from observations in the field. Sources of all contemporary materials on the beaches of Holderness were included (this does not account for the original sources of the glacial till and erratics or the direction of circulation and deposition of North Seas sediments). Only landward sources of sediment were included and the glacial tills were considered the main source of material to the beach. It was not possible to collect any offshore sources of material. Many other beach materials such as wreckage from sea defences, housing collapse and industrial waste seemed to be very localised and were not included. Another material which was distributed on some beaches (especially Spurn) other than the sand and shingle was washed coal and jet which could have come from mine waste tips further north and from the tills (Skipsea Till). Figure 7.2 shows a conceptual diagram of all possible beach sediment sources.

Field survey

Initial fieldwork included a kappa survey of the tills and beach sediments. The variability of the tills and the beach sands was found using at least 50 measurements at each location (Table 7.2). Beach kappa transects were carried out at Barmston, Mappleton and Tunstall in order to trace the black sands over the beach profiles. Transects were surveyed every 5m using an Abney level and kappa was measured every 1m along the transect; resultant profiles are shown in Figure 7.3. The high values indicate accumulations of black sand along swash lines or in the lee of groynes, stones and slopes. Patterns in kappa resulting from sedimentation patterns on the beach are also marked. For instance kappa values vary sympathetically with small ridges at Barmston and groynes at Mappleton.

Figure 7.2: Defining all possible sources of beaches along the Holderness Coastline

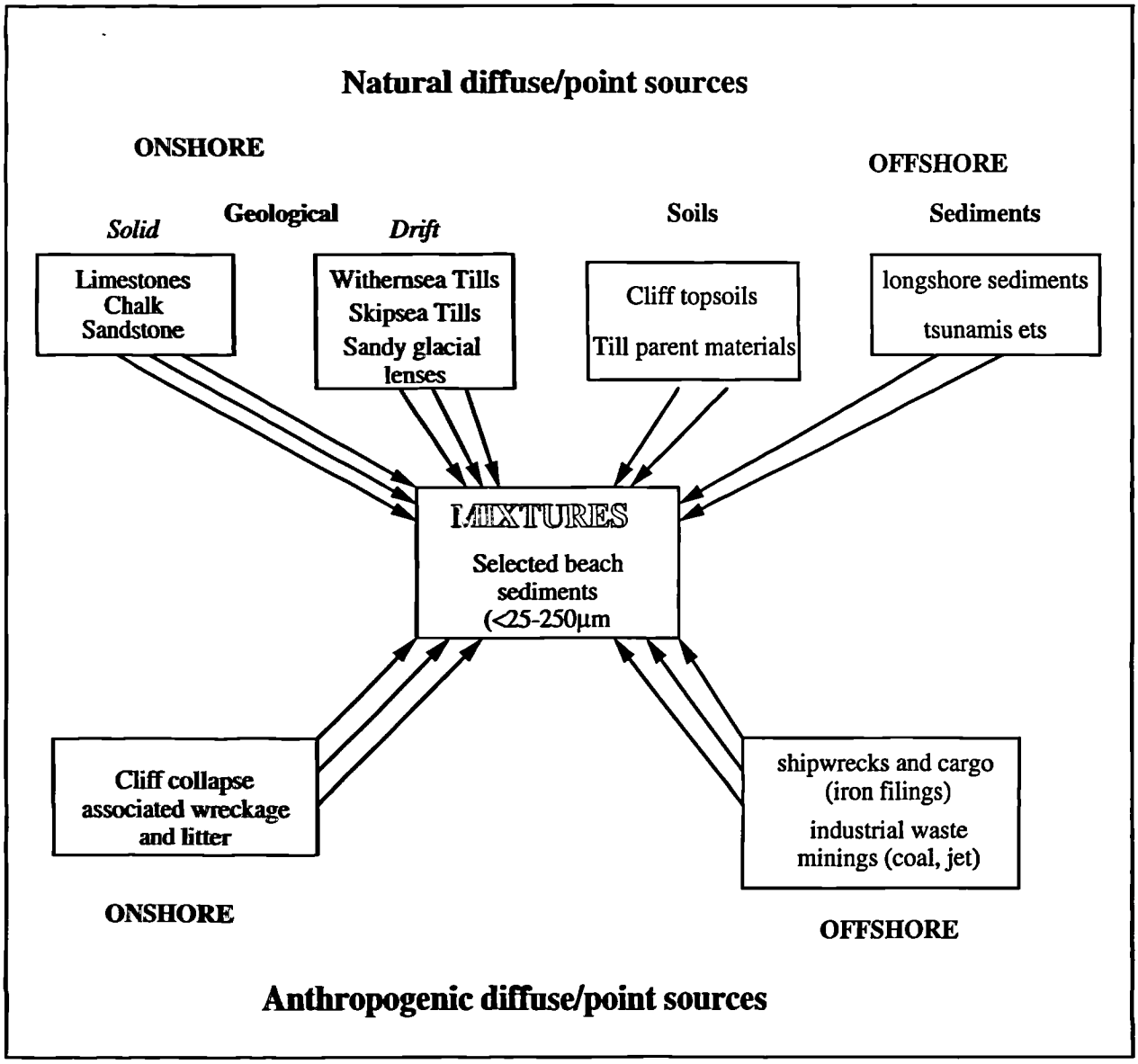

Figure 7.3: Beach and Kappa transects for selected

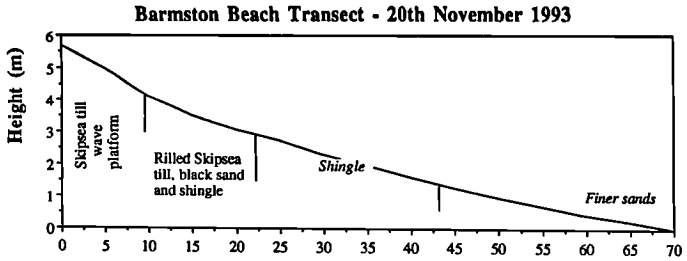

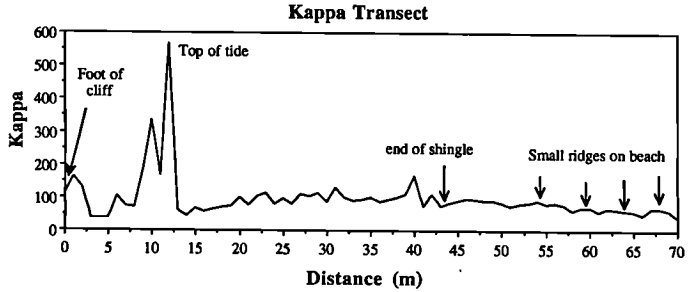

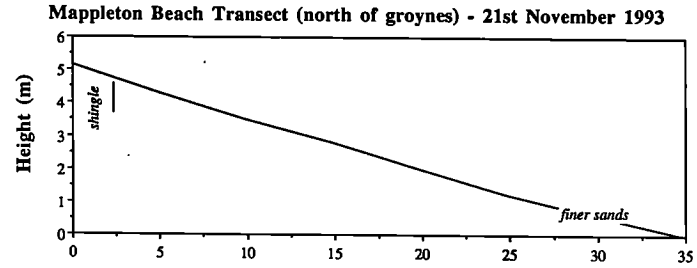

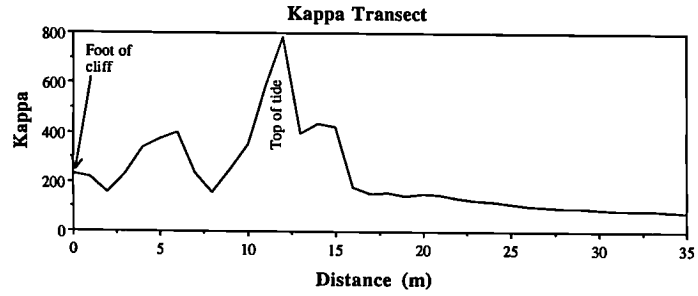

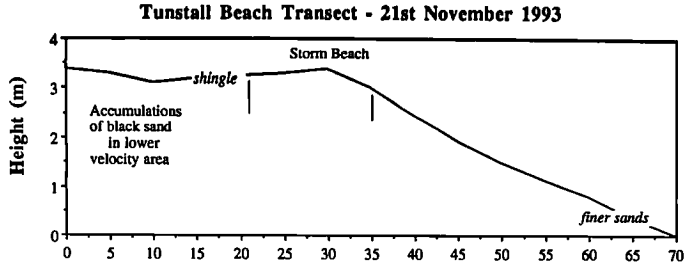

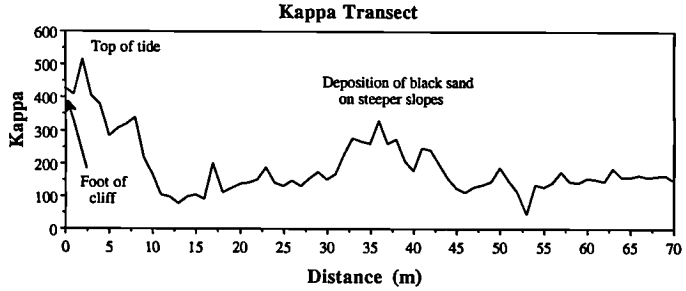

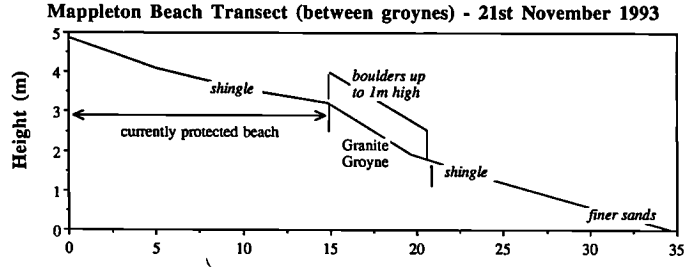

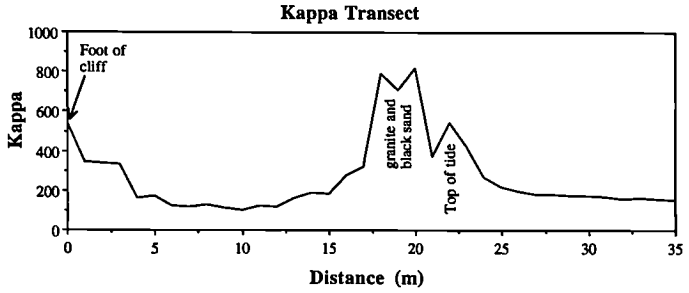

Table 7.2. Variability results for kappa surveys of the tills (matrix) and beach sediments and for granite boulders used to build the groynes at Mappleton

Site/sample	mean	standard deviation	coefficient variation (%)	sample no.
Barmston				
beach transect	87.95	64.58	73.44	70
Skipsea till	36.88	4.86	13.19	50
sandy till	46.0	7.75	16.86	50
Mappleton				
beach transect 1	267.25	188.81	70.65	35
beach transect 2	217.42	157.79	72.58	35
cross beach survey	452.9	119.57	26.4	50
Withernsea Till	20.52	1.88	9.16	50
granite groynes	536.78	527.41	98.25	50
Tunstall				
beach transect	187.54	90.18	48.09	70
Withernsea till	20.58	2.72	13.22	50

High variability (CV%=48-73%) is seen in beach transects because kappa is controlled by the concentration of black sand. The CV% of the till matrix varied by up to 17% and granite groynes showed CV% values of 98%.

Sampling and sample preparation

Spot samples of tills, black sands near the cliffs and white sands towards the sea were taken. Other samples included erratics from the tills and other geological specimens collected from the beach. Some data were available from a magnetic database of UK geologies (Appendix 2). In total, fifty-three samples were collected from points indicated on Figure 7.1. These are listed in Table 7.3. The samples were air dried, sieved to 2mm and packed into 10ml pots ready for magnetic measurement. Remaining sample material was sieved into 6 particle-size ranges and where enough material existed, fractions were packed again for magnetic measurement. Magnetic black sand particles were extracted using a 200mT hand magnet and dispersed in magnetically weak calcium carbonate so that the true magnetic properties of the black sand could be obtained. An X-ray diffraction was done on the black sand particles (not affected by interaction) and they were found to contain 60.6% iron, 17.9% titanium, 10.6% silica, 5.8% calcium, 3.2% aluminium, 0.8% potassium, 0.7% manganese and 0.4% magnesium. The black sand was also examined under a light microscope (Plate 7.2a) and identified as comprising basalt crystals probably of Scandinavian origin (D. Keen, pers. comm.).

Table 7.3. Holderness Sample descriptions

Code	Sample Type	Location	Other Information
Aldbrough			
AB1A1	Diorite	Aldbrough, Holderness	Beach Sample
AB2C1	White Sand	Aldbrough, Holderness	Beach Sample
AB3G1	Grey Till	Aldbrough, Holderness	Cliff Sample
AB4G1	Sandy Till	Aldbrough, Holderness	Cliff Sample
AB5A1	Igneous Rock	Aldbrough, Holderness	Beach Sample
AB6A1	Igneous Rock	Aldbrough, Holderness	Beach Sample
AB7A1	Igneous Rock	Aldbrough, Holderness	Beach Sample

Table 7.3 continued

Code	Sample Type	Location	Other Information
Barmston			
BS1C1	Black Sand	Barmston, Holderness	Beach Sample
BS1C9	Magnetic Particles	Barmston, Holderness	Beach Sample
BS2C1	Black Sand	Barmston, Holderness	Beach Sample
BS3G1	Grey Till	Barmston, Holderness	Cliff Sample
BS4L1	Lake Sediment	Barmston, Holderness	Cliff Sample
BS5B1	Cliff Topsoil	Barmston, Holderness	Cliff Sample
BS6G1	Iron Stain	Barmston, Holderness	Cliff Sample
BS7G1	Upper Cliff Sand	Barmston, Holderness	Cliff Sample
BS8C1	White Sand	Barmston, Holderness	Beach Sample
BS9B1	Cliff Topsoil	Barmston, Holderness	Cliff Sample
BS10B1	Cliff Subsoil	Barmston, Holderness	Cliff Sample
BS11G1	Cliff PM Till	Barmston, Holderness	Cliff Sample
BS12A1	Jurassic Limestone	Barmston, Holderness	Beach Sample
Bridlington			
BD1C1	White Sand	Bridlington, Holderness	Beach Sample
BD2C1	White Sand	Bridlington, Holderness	Beach Sample
BD3C1	White Sand	Bridlington, Holderness	Beach Sample
BD4E1	Blown Sand	Bridlington, Holderness	Dune Sample
BD5C1	Sand and Coal	Bridlington, Holderness	Beach Sample
BD6A1	Chalk	Bridlington, Holderness	Cliff Sample
Spurn Head			
SH1F1	Salt Marsh	Spurn Head, Holderness	Beach Sample
SH2C1	White (E) Sand	Spurn Head, Holderness	Beach Sample
SH3C1	White (E) Sand	Spurn Head, Holderness	Beach Sample
SH4C1	Black (E) Sand	Spurn Head, Holderness	Beach Sample
SH5A1	Coal	Spurn Head, Holderness	Beach Sample
SH6E1	Dune (E) Sand	Spurn Head, Holderness	Beach Sample
SH7C1	Black (E) Sand	Spurn Head, Holderness	Beach Sample
SH8C1	White (S) Sand	Spurn Head, Holderness	Beach Sample
SH9C1	White (S) Sand	Spurn Head, Holderness	Beach Sample
SH10C1	Black (S) Sand	Spurn Head, Holderness	Beach Sample
SH11E1	Dune (S) Sand	Spurn Head, Holderness	Beach Sample
Scarborough			
SB1C1	White Sand	Scarborough, Holderness	Beach Sample
SB2G1	Grey Till	Scarborough, Holderness	Cliff Sample
SB3A1	Red Sandstone	Scarborough, Holderness	Cliff Sample
SB3A2	Yellow Sandstone	Scarborough, Holderness	Cliff Sample
SB3A3	Brick	Scarborough, Holderness	Beach Sample
SB3A4	White Sandstone	Scarborough, Holderness	Cliff Sample
SB3A5	Clinker	Scarborough, Holderness	Beach Sample
Filey Bay			
FB1C1	Black Sand	Filey Bay, Holderness	Beach Sample
FB2G1	Grey Till	Filey Bay, Holderness	Cliff Sample
FB3G1	Sandy Till	Filey Bay, Holderness	Cliff Sample
FH1C1	White Sand	Flambobough Head, Holderness	Beach Sample
FH2C1	White Cave Sand	Flambobough Head, Holderness	Beach Sample
FH3G1	Sandy Till	Flambobough Head, Holderness	Cliff Sample
FH4A1	Chalk	Flambobough Head, Holderness	Beach Sample
Cleethorpes			
CT1C1	White Sand	Cleethorpes, Lincolnshire	Beach Sample
Mablethorpe			
MT1C1	White Sand	Mablethorpe, Lincolnshire	Beach Sample

Plate 7.2a. Black sand in 63-125mm grain size range from Spurn Head

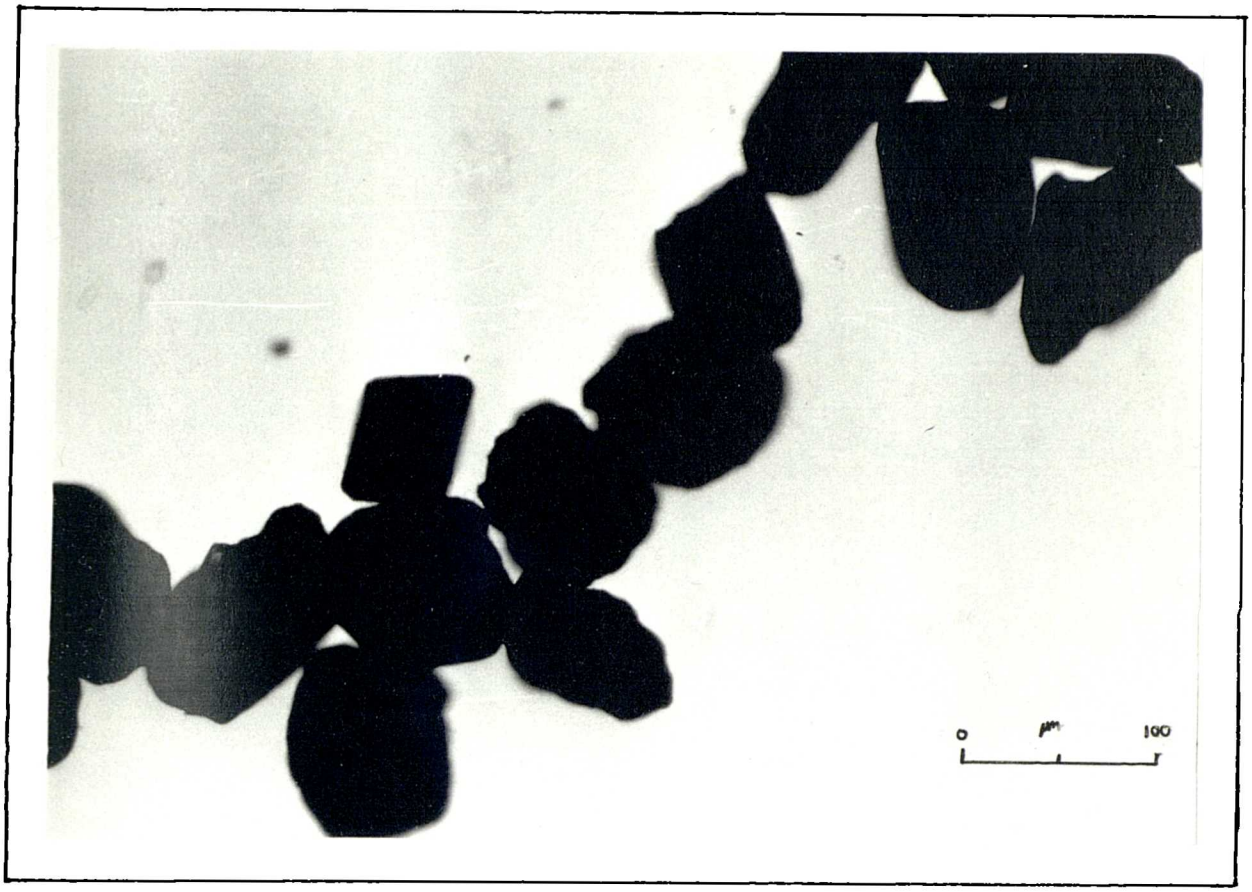

Plate 7.2b. Black sand in 63-125mm grain size range from Barmston upper cliff sand lenses

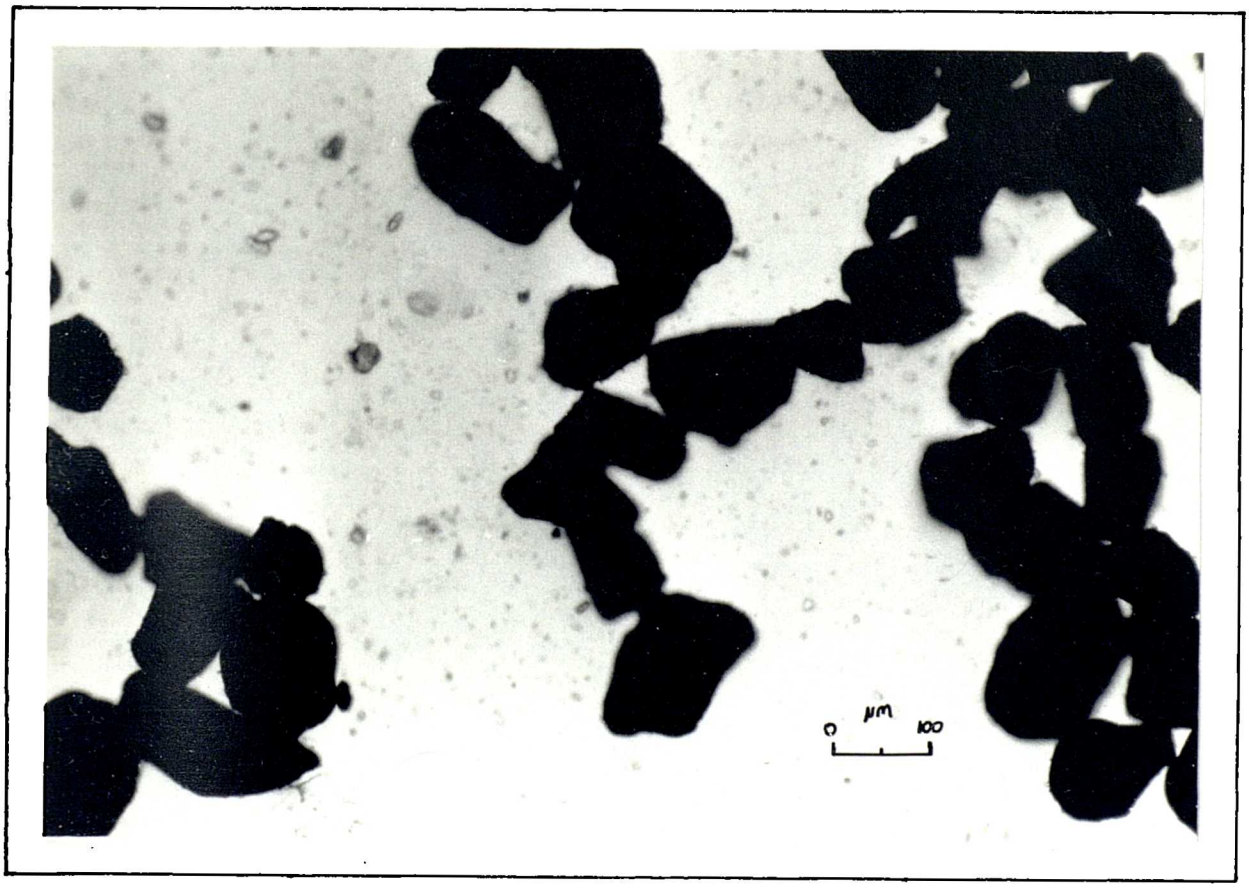

Magnetic Measurement

A range of magnetic measurements was made on bulk and fractioned samples including low and high frequency susceptibility (χlf and χhf), anhysteretic remanent magnetization (ARM) and isothermal remanent magnetizations measured at various field strengths between zero and 880mT so that IRM curves could be plotted (as described in Chapter 2). Ten hysteresis curves were also measured for clear graphical representation of magnetic properties of sources and mixtures. Saturation magnetization (Ms) at 1000mT was eventually used from the hysteresis loops to model the black sand. This measurement, of the total magnetic component of a sample, is not affected by interaction; however the small VSM samples are prone to in-homogeneity through sub-sampling especially in coarser materials (as seen in Chapter 4).

7.4 Initial data analysis and results

Normality and correlations

The data distributions were first analysed and correlations between parameters were calculated in SPSS so that an assessment could be made of the possible application of classification and modelling techniques. Frequency distributions for linear parameters χlf, χhf, χfd, ARM, IRM880, IRM+100 and HIRM+100 showed clearly a positive skew, where skew values were $3.2\ \mu m^3\ kg^{-1}$ (χlf) and $3.9\ mAm^2\ kg^{-1}$ (HIRM+100). To normalize the distributions, log transformations were made which reduced the skew in the data to -0.7 (χlf) and -0.8 (HIRM+100). The effects of skew in data on classification statistics are shown in section 7.7 (also discussed in Chapter 3).

Correlations of linear parameters showed that a dominant magnetic signal in the data, controlled by parameters indicating ferrimagnetic minerals was present, similar to that seen in the rock and pollution databases (Chapter 4). Some correlation results are presented in Table 7.4. Those parameters not significantly correlated offer the best means of discrimination for the samples collected.

Table 7.4. Selected correlation results for magnetic parameters

Variables	R value	Prob.	N
Significant Correlations			
χlf v IRM+100	0.82	0.001	53
χlf v IRM880	0.84	0.001	53
χlf v HIRM+100	0.51	0.001	53
IRM+100 v IRM880	0.99	0.001	53
IRM880 v HIRM+100	0.57	0.001	53
Non-significant Correlations			
χlf v χarm	0.18	-	53
χfd v HIRM+100	0.17	-	53
χarm v IRM880	0.07	-	53
χarm v IRM+100	0.07	-	53
χarm v HIRM+100	0.04	-	53

Figure 7.4: Particle size distributions for selected samples,
(a) Barmston black sand sample

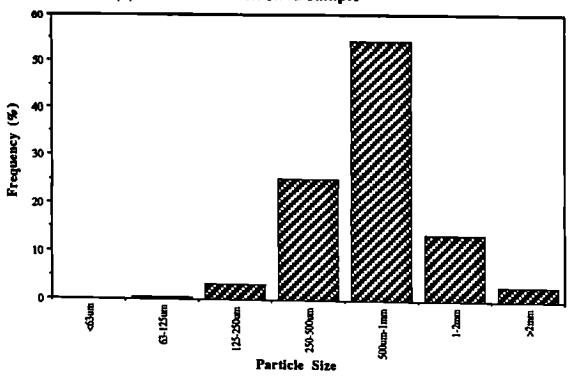

(b) Filey Bay black sand

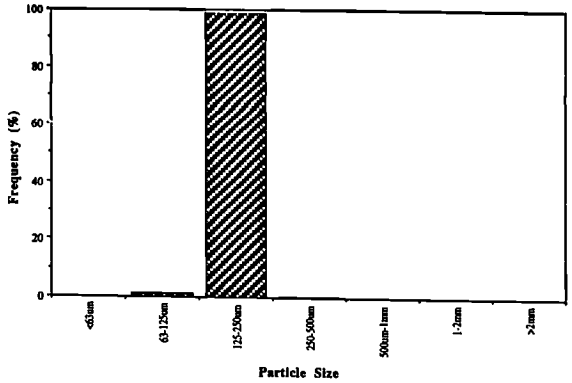

(c) Barmston white sand sample

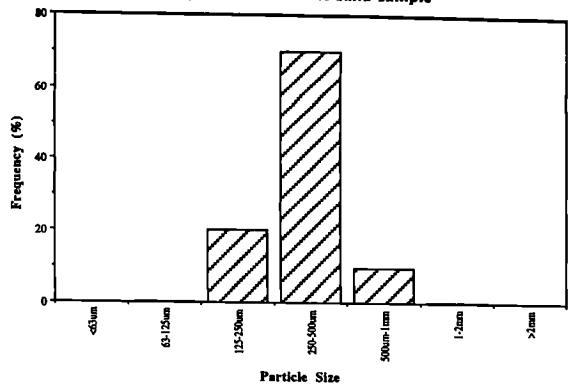

(d) Barmston Upper cliff sand sample

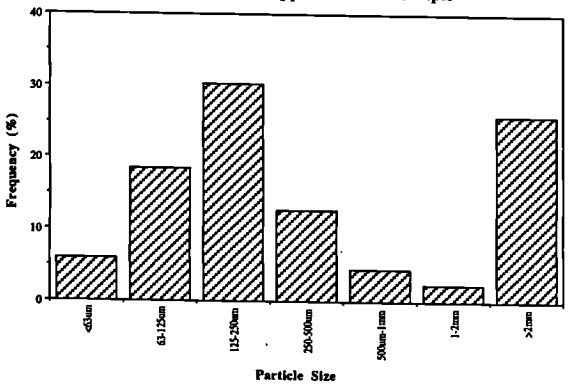

(e) Barmston grey till sample

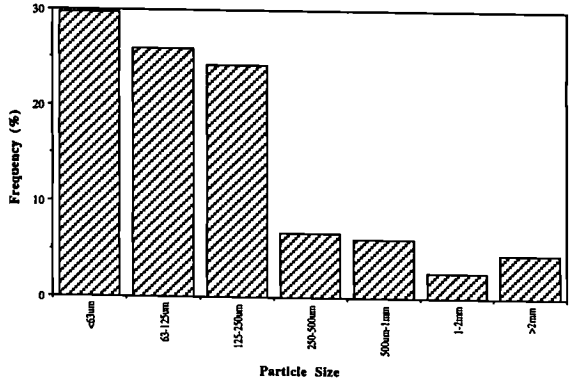

(f) Barmston cliff topsoil sample

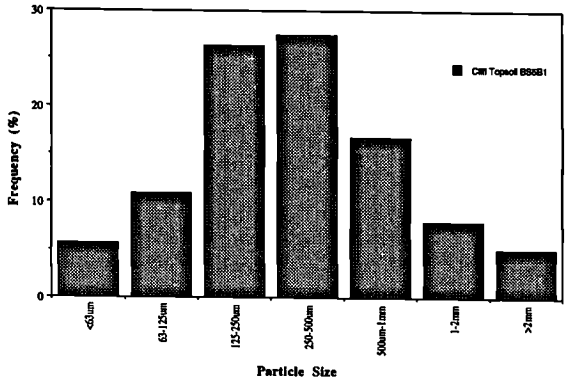

(g) Spurn Head salt marsh sample

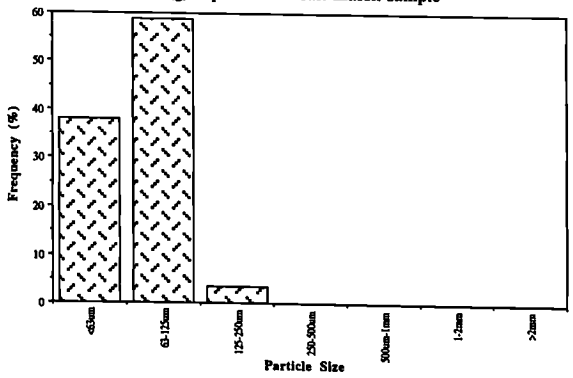

Particle-size results

Results of particle-size analysis shown in Figure 7.4 indicate that in general white sands (taken 50m from the cliffs) were between 125μm and 1mm with 50 to 80% lying between 250 and 500μm. Black sand mixtures collected from the foot of the cliffs ranged from 63μm to 2mm. The dominant black sand fractions are between 125 to 250μm and are associated with coarser quartz sands with 55% lying between 500μm and 1mm. This reflects grain size and density relationships similar to those found by Schuiling (1983), where heavy minerals are deposited with coarser grains of lighter minerals. The particle-size distributions of the tills ranged between <63μm and >2mm, with 80% lying between 63μm and 250μm. Cliff topsoils have a more normally distributed particle-size distribution whereas the bulked salt marsh sample has a distribution of less than 250μm with 97% less than 125μm.

The black sand did not appear, visually, to fall into a single particle-size range. The source of the black sand was inferred from the susceptibility results and upon magnetic extraction of cliff sand, black sand was found and compared magnetically using χfd% values which were <2%. The main source of the black sand was found to be upper cliff sands and the Skipsea Till between Barmston and Bridlington. Beach and till black sand was also compared microscopically. Plate 7.2a shows black sand extracted from Spurn head beach sand and Plate 7.2b shows black sand extracted from an upper cliff sand from Barmston.

Discrimination of Sediment Sources

The 53 bulk and the 125-250μm samples were initially classified separately using bi-variate scattergrams of χlf versus χfd% and χfd% versus HIRM+100. These parameters best indicated the two main trends in the data; one of ferrimagnetic grain size and one of ferrimagnetic mineral concentration (HIRM+100 being controlled by the black sand as it contains canted-antiferromagnetic mineral inclusions). χfd% is used here as a normalized parameter not affected by the positive skew in the data set (cf Chapter 3). Figures 7.5a and b show bulk and fractioned samples plotted and tentatively classified using χlf and χfd%; the horizontal axis on Figure 7.5a has been truncated to allow the lower concentration samples to be shown more clearly. The beach mixtures do not have χfd% values over 1%, indicating coarser multi-domain primary minerals present, whilst in topsoil and saltmarsh samples much finer secondary ferrimagnetic (superparamagnetic/viscous) grains are present and χfd% values are greater than 2. Till samples have fewer fine-grained (SP/SD) ferrimagnetic minerals which partly suggests the properties of their original sources of material during the Devensian glaciation (MD basalt bedrock for instance). There is no real difference in the trends in the data between the bulk and fractioned samples other than the concentration factor (the dominant black sand grain size being 125-250μm).

Figure 7.6a shows discrimination using χfd% and HIRM+100 for the bulk samples. The situation is similar to that seen in Figure 7.5a (with reversed axes). The black sands contain hard remanence carrying minerals, in greater concentration than the tills, or any other sources of material in the area. These results are highly related to the actual particle-size results and reflect the energy of the environments in which each material was created and deposited. The finer magnetic minerals contributing to the χfd% of the topsoils and tills are not found in the beach sediments because they are removed in suspension by the sea.

Figure 7.5: Xlf versus Xfd% for bulk samples (a) and 125-250um fractions (b) and classifications

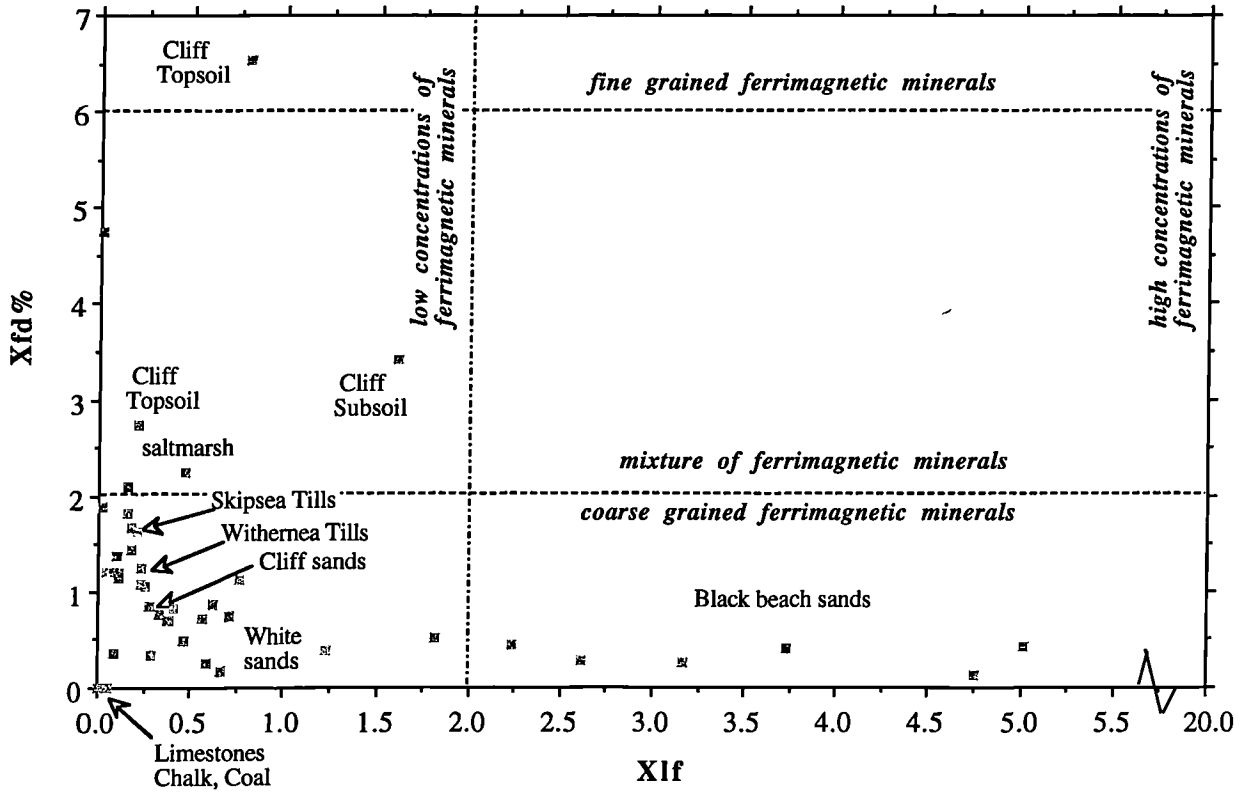

(b)

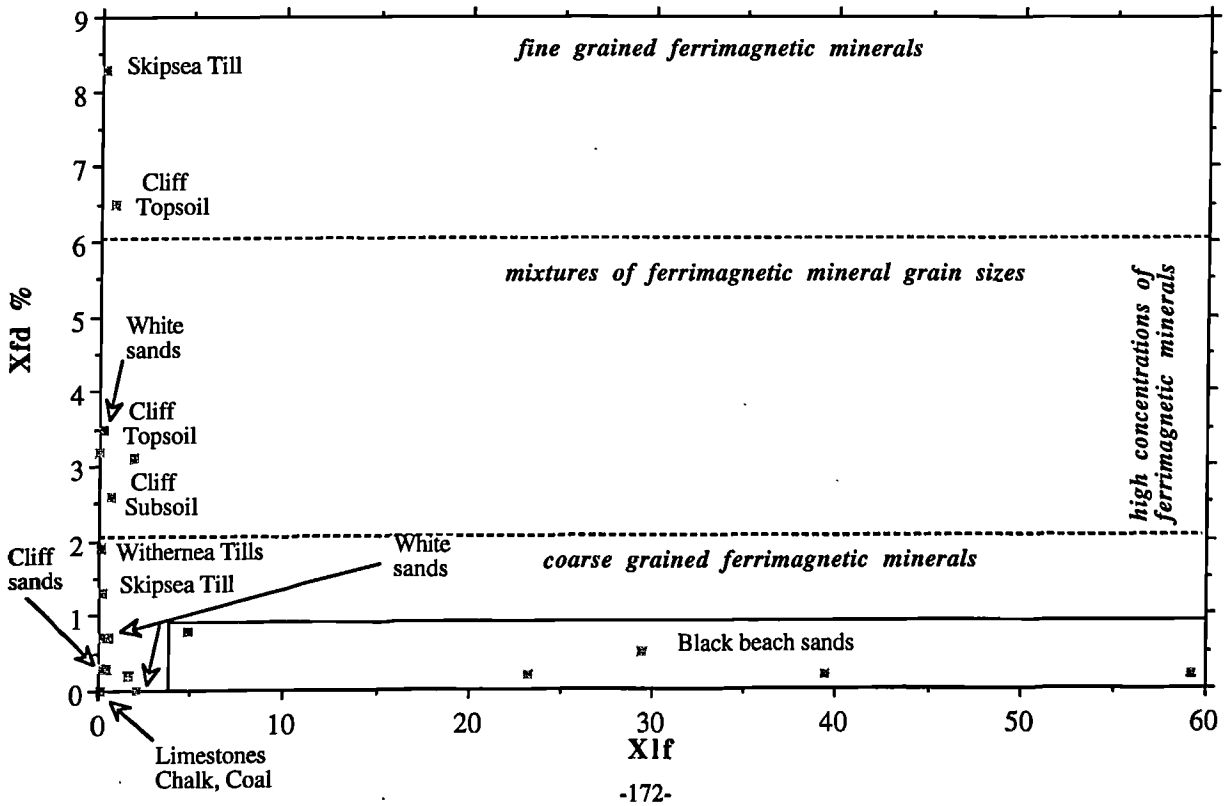

Figure 7.6a: HIRM100 versus Xfd% for bulk samples and classification

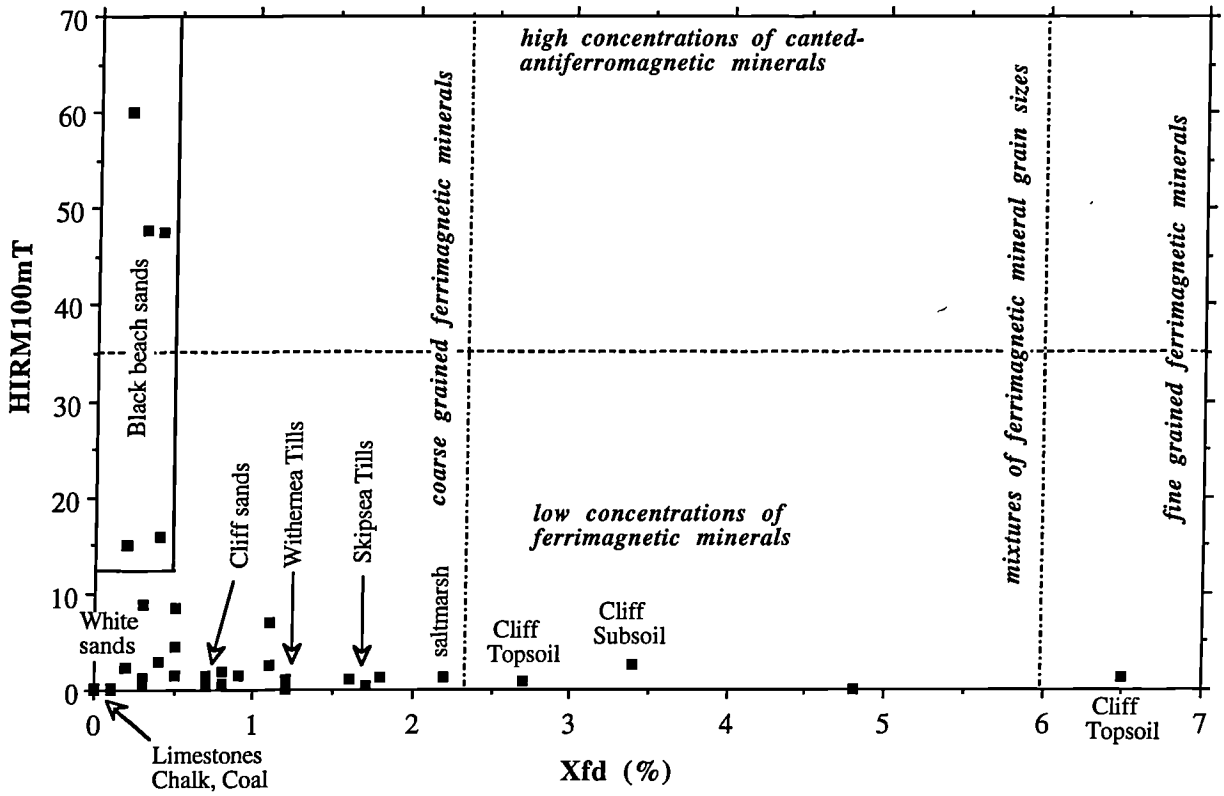

Figure 7.6b: Normalized IRM curves for selected samples

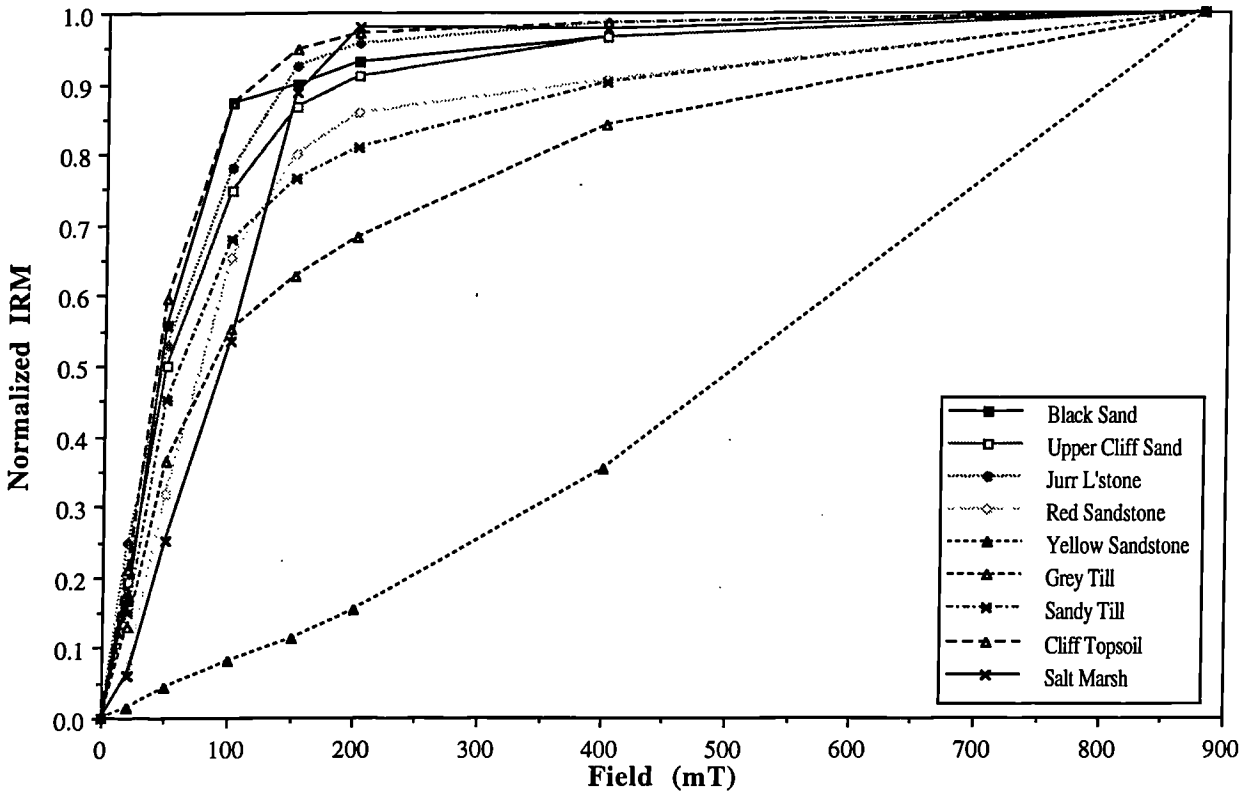

Better sample discrimination is seen using ratio data as shown in the normalized IRM curves for selected samples in Figure 7.6b. In terms of concentration parameters this spread of mineralogical content is masked and as a result limits the application of further statistics and linear modelling. The steepness of the curves and their field of saturation show the presence of canted-antiferromagnetic minerals (shallow and no saturation within 1000mT) in the sandstones and tills and the ferrimagnetic nature (steep curves saturating at 200mT) of the black sand and cliff topsoils. There is also a ferrimagnetic mineral content in the Jurassic limestone. Paramagnetic minerals in the sediments are not indicated by remanence curves and standard parameters but they are indicated in hysteresis loops.

Hysteresis loops (normalised to Ms) for the 125-250μm sand fractions of the Withernsea till, Skipsea till, cliff sand and a black sand beach mixture from Barmston are shown in Figure 7.7. The loops indicate that the two tills and sandy lenses contribute both ferrimagnetic (steep part of the curve) and paramagnetic minerals (eg paramagnetic limestone) to the beach, but only coarser ferrimagnetic minerals remain in the beach sediment. The loops also discriminate the tills more effectively than the susceptibility parameters used in Figure 7.5. The Skipsea till and upper cliff sand have a higher ferrimagnetic mineral content than the Withernsea till which has a higher paramagnetic and canted-antiferromagnetic mineral content. It can be inferred that the ferrimagnetic minerals from mainly the upper cliff sand and Skipsea tills contribute to the beach but are more concentrated in the beach than in the original source. However all the sediment mixtures fall outside of the numeric ranges of the proposed sediment sources. This led to the dispersed black sand sample being used in further analysis and modelling as an 'end member' (theoretical source) for the range beach mixture values. This is further explained in section 7.6

7.5 Statistical classification: an analysis

From the initial results and parameter correlations it was clear that any classification technique would not really improve the discrimination given by the bi-variate scattergrams. This inter-correlation was caused by the dominance in the mixtures of the strong ferrimagnetic black sand. There was no other material with a sufficiently different magnetic property to counteract this effect. In this section therefore an analysis and example is given of using classification techniques in this situation. It will be sufficient to classify materials with magnetic parameters using only bi-variate scattergram as in section 7.4 (and as in Chapter 3).

Two cluster analysis and principal component analysis routines were run, the first using raw data and the second using log transformed data. Six linear parameters, χlf, χfd, χarm, IRM880, IRM+100 and HIRM+100 were used in the cluster analysis and more IRM parameters were used in the PCA. Also samples which are diamagnetic and have a negative susceptibility are omitted - with missing log transformed values. Figures 7.8 and 7.9 show the dendrograms from the cluster analysis. Figure 7.8 is drawn out by the concentrational positive skew in the data distributions and three main groups of samples are shown: white sands, topsoils and lower concentration black sands, black sands and erratics and finally the dispersed sample of basalt crystals. Figure 7.9 is more balanced with the input of normalized data and samples are clustered into groups of magnetically weak white sands, tills, further white sands and dune sands, lower concentration black sands, topsoils, higher concentration black sands and

Figure 7.7: Hysteresis loops of beach sediments and sources (125-250um fraction)

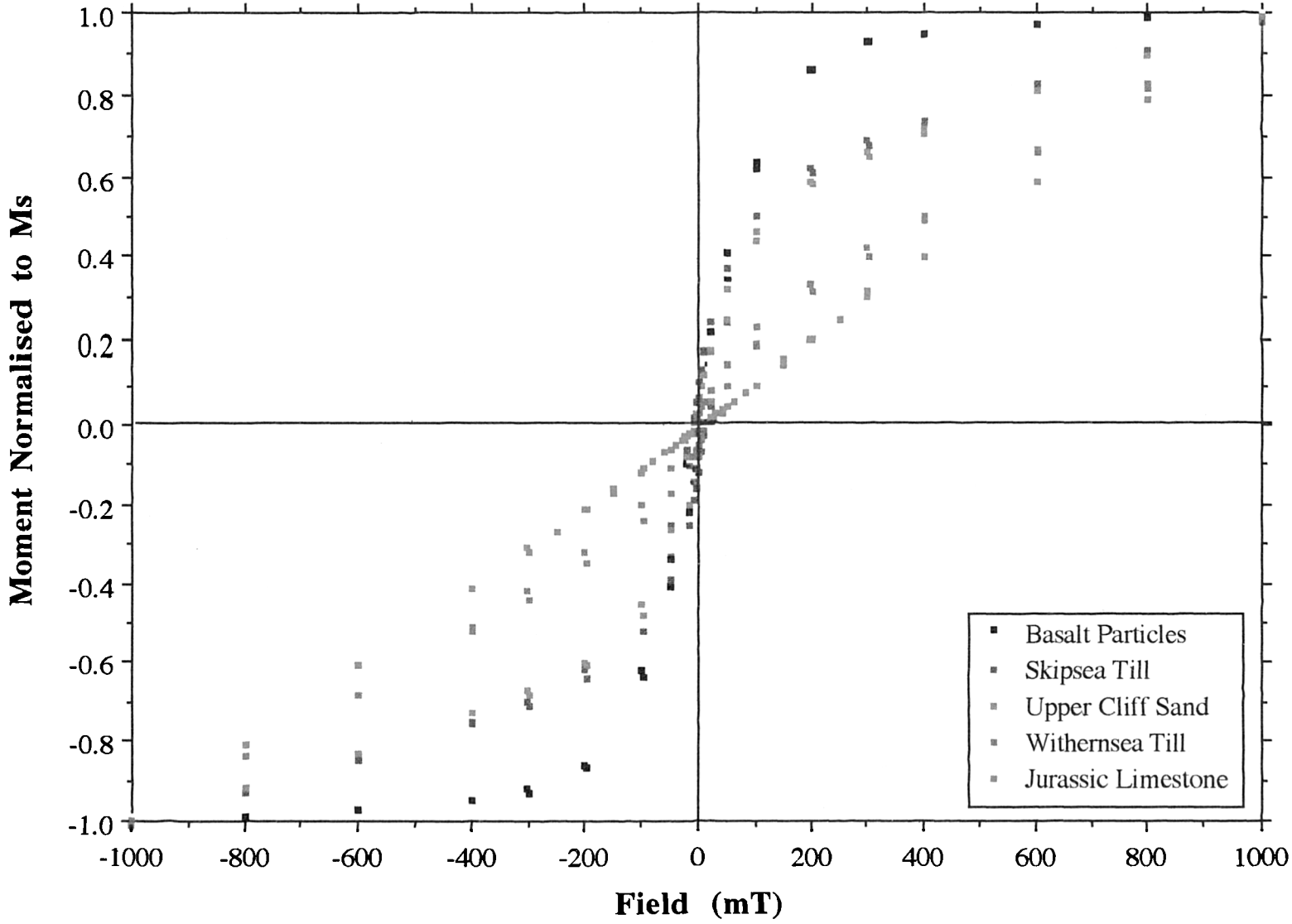

Figure 7.8: Dendrogram using raw positively skewed data and Ward's agglomeration method

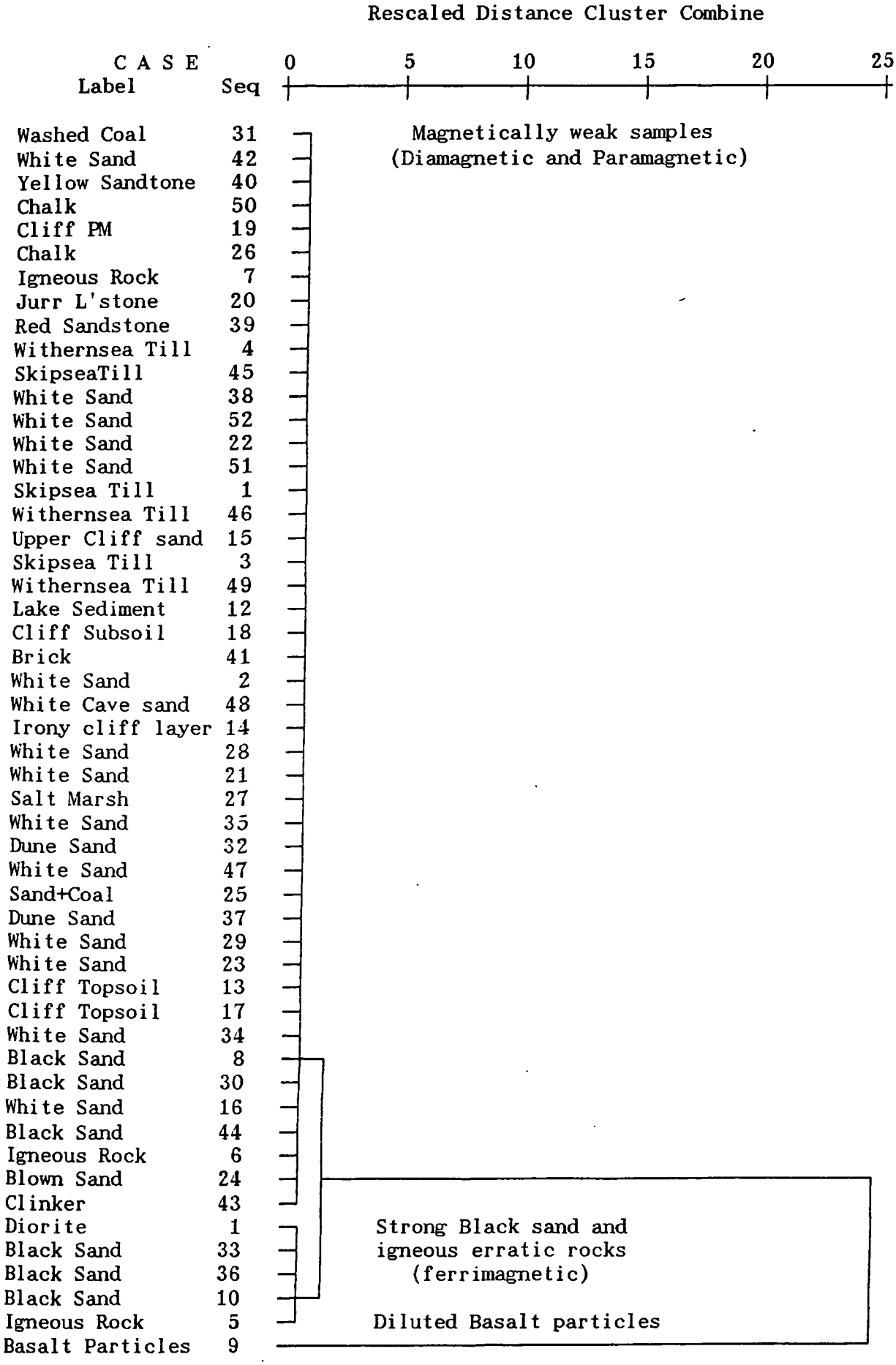

Figure 7.9: Dendrogram using log transformed data and Ward's agglomeration method

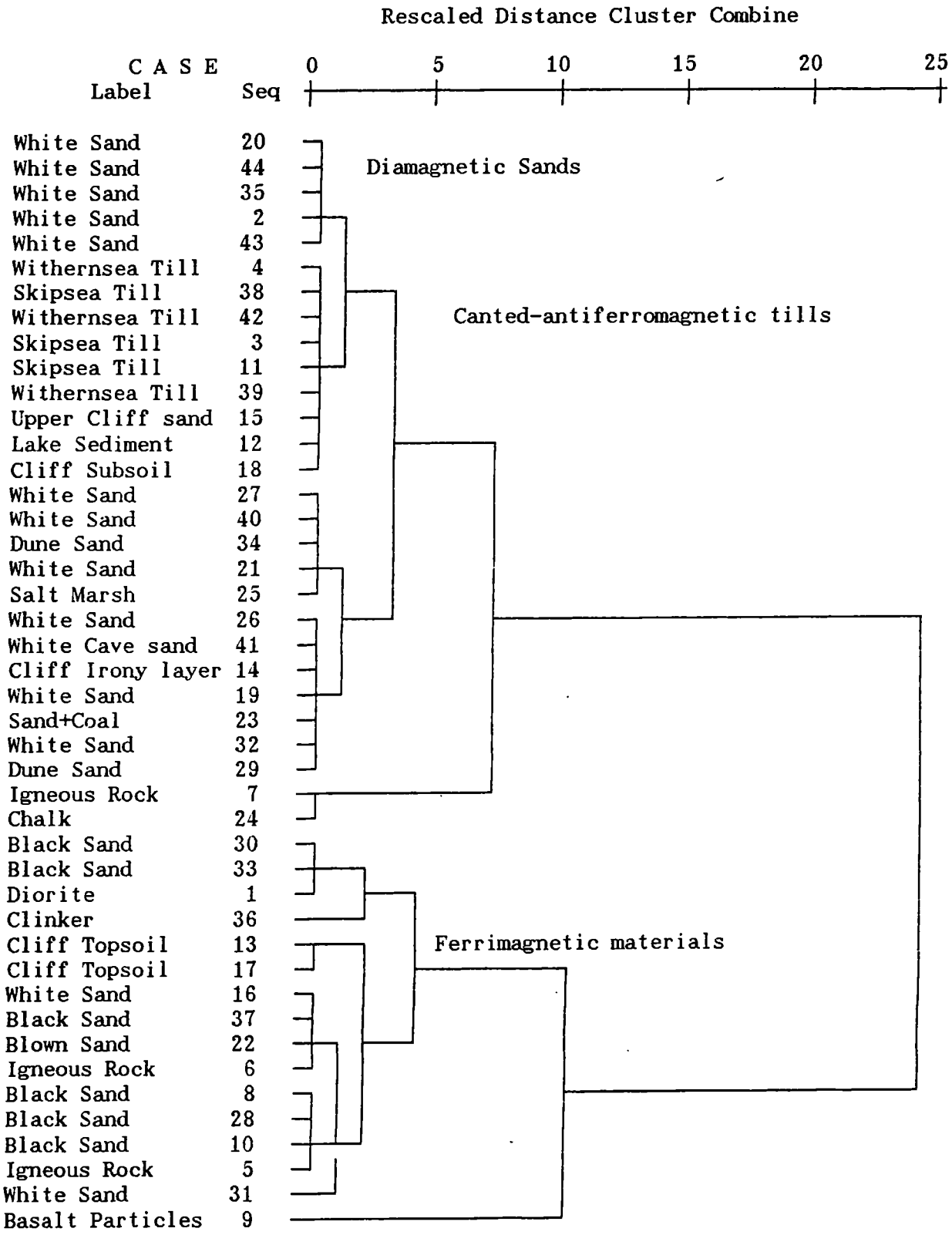

finally the dispersed sample of basalt particles. Comparing the two dendrograms (apart from missing cases in the second), the order in which the samples have been chosen is very similar. Generally in cluster analysis, magnetically weakest samples are grouped first and the magnetically strongest samples last.

The PCA suffers from the same problems as it is based on similar mathematics; ie the linear combination of the parameters into principal components. Generally in performing a PCA with log transformed data many cases are lost through the nature of magnetic data (with negative values and arbitrary zeros as seen in Chapter 3). In this case using log transformed data only one component was identified, as black sand samples with high values were still included in the data set. A co-ordination plot is shown in figure 7.10 which was constructed using the original data but with the strongest black sand samples omitted. It is clear that the two factors are controlled by a concentration of ferrimagnetic minerals and their fineness in grain size as displayed by χfd and χarm. The classification offers no new information to that of the bi-variate scattergram but has the advantage of using all parameters and indicating their relations to the principal components visually and spatially as if in a multidimensional map. These results from an environmental situation highlight and confirm those problems encountered in Chapter 4 when classifying samples from the sample databases.

7.7 Linear modelling and quantification of sediment sources

From the classification results, difficulties are exposed in completing further analysis especially quantification of the sources of the beach sands. Care must be taken in this section with interpretation of the results presented, as at best they offer only a guide to the environmental sedimentation in the area. Classification of the sources of the sediments and beach sand mixtures have shown that the tills are magnetically similar using standard magnetic parameters (there are slight paramagnetic differences shown by the hysteresis loops). Only slight differences are seen between Skipsea, Withernsea and cliff sands with respect to the scale of the black sand samples. The parent geologies of chalk, limestone and sandstones classify according to their diamagnetic, paramagnetic and slightly canted-antiferromagnetic nature respectively, but are too magnetically weak to discriminate. Finally the black sands in varying concentrations span the range of sand results but the end member sample of the dispersed black sand offers the only mechanism for modelling the proportions of the sources in the beach sands.

Linear modelling attempts

Any linear programming routine which has one component source of sediment with parameter values 1500 times that of the next strongest source is very poorly scaled. The application presented in this chapter highlights the problems associated with using strongly magnetic materials in mixtures discussed in Chapter 4. Despite this, the parameter values can be scaled down such that they are in similar units, but the actual difference between the source parameter values remains the same. Large parameter values for one source leads to the inclusion of errors of similar units in which the program has to find a solution. This means that the errors themselves become larger than the parameter values for the other important sources of material, limestone and tills for example.

Figure 7.10: PCA co-ordination plot for Holderness bulk samples and parameters used in constructing principal components

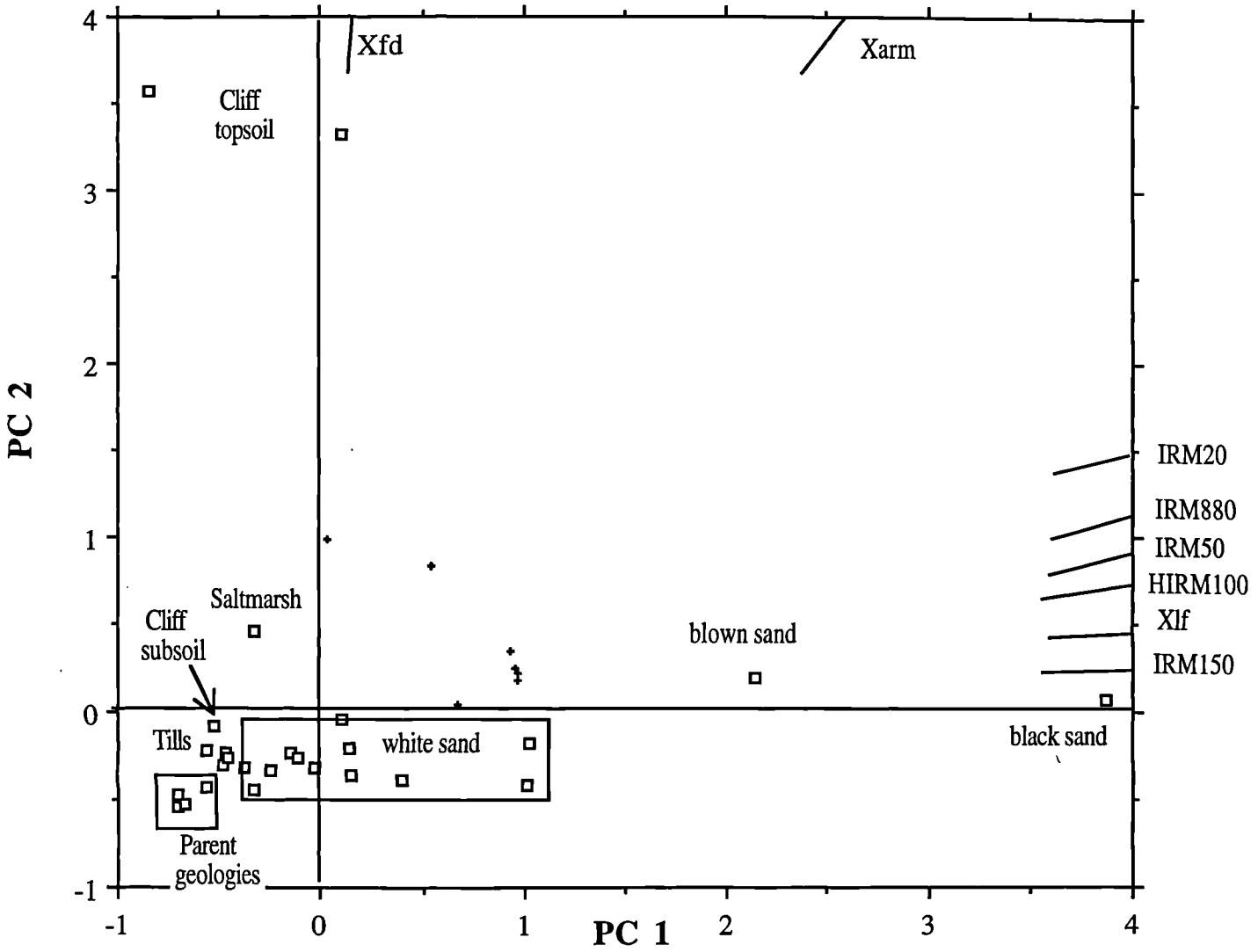

PC	*Eigenvalue*	*% of var.*	*Cum. Var.*
1	6.01	75.2	75.2
2	1.3	16.3	91.5

In the routines presented here, eight bulk (<2mm) beach sands including 'white' and 'black' sands collected from the foot of the cliffs have been used as mixtures. The sources chosen (described above) are listed in Table 7.5 along with some of their magnetic parameter values included to indicate the scale differences. The description of 'white' to beach sands is from appearance only as the sands contain smaller proportions of the black basalt minerals. Typical values for the bulk sources have been used rather than the means of groups of samples as the variability within each source group was not covered spatially by the sampling over this stretch of coastline (this is a factor considered in Chapter 8). Also bulk values have been used here as the sources contain chalks and limestones and the dispersed sample of basalt crystals which could not be fractioned. In the dispersed basalt sample the magnetically extracted crystals could not be separated during sieving once they had been magnetized with the 200mT hand magnet. Finally it is noted that the tills used contain minute quantities of the black sands themselves but it would require much work to extract this fraction and re-measure with any accuracy. This overlap is indicated in Figure 7.11 and the implications of this are discussed later.

Table 7.5. Cliff sources and beach mixtures used in linear programming tests

	Sources		χlf	χarm	IRM880	HIRM+100
			μm^3	kg^{-1}	mAm^2	kg^{-1}
x1	Basalt Particles		413.3	4760.5	9903.0	8776.2
x2	Upper Cliff Sand		0.23	0.72	4.12	1.04
x3	Skipsea Tills		0.28	0.94	3.45	0.72
x4	Chalk/Limestone/Quartzite		0.01	0.18	0.15	0.03
	Mixtures		χlf	χarm	IRM880	HIRM+100
	Site	**Situation**	μm^3	kg^{-1}	mAm^2	kg^{-1}
Mix 1	Aldbrough	White Sand/cliff sands	0.29	0.61	5.46	0.41
Mix 2	Barmston	Black Sand/Skipsea tills	3.73	29.09	302	47.4
Mix 3	Bridlington	White Sand/dunes	1.2	2.25	22.0	2.91
Mix 4	Spurn Head	Black Sand/dunes	5.02	10.51	117.4	16.0
Mix 5	Scarborough	White Sand/sandstones/ Skipsea tills	0.11	1.23	0.49	0.36
Mix 6	Filey Bay	Black Sand/Withernsea tills	2.61	6.99	6.17	6.68
Mix 7	Flamborough	White Sand/chalks/ cliff sands	0.71	5.23	2.25	2.34
Mix 8	Mablethorpe	White Sand-built up	0.11	1.23	0.35	0.25

Table 7.6 gives the results of the linear programming routines for the eight beach sand mixtures. The samples chosen for this linear programming exercise are shown graphically in Figure 7.11 and the results can be explained more clearly in terms of this diagram. With reference to the environmental situation and the knowledge of the accumulations of black sand at each site the percentage proportions calculated seem to be sensible. The greatest difficulty is in matching the grain sizes of the sources and mixtures effectively. Bulk samples have been used here but from the particle-size results it is clear that the fines from the tills do not remain in the beach sediments and as such the proportions given for the tills is of the sand fraction only. Mixture 2 represents the only possibly incorrect answer where Skipsea till is accounted for by the model but the coastline was concreted at this point. Till material could, however, have been supplied from offshore bars of the tills or from further upshore. At the two sites where no black sand was present, Scarborough and Mablethorpe, zero proportions are calculated. At Barmston and

Figure 7.11: Log Xlf versus Log HIRM100 for sources and beach mixtures used in linear programming routines

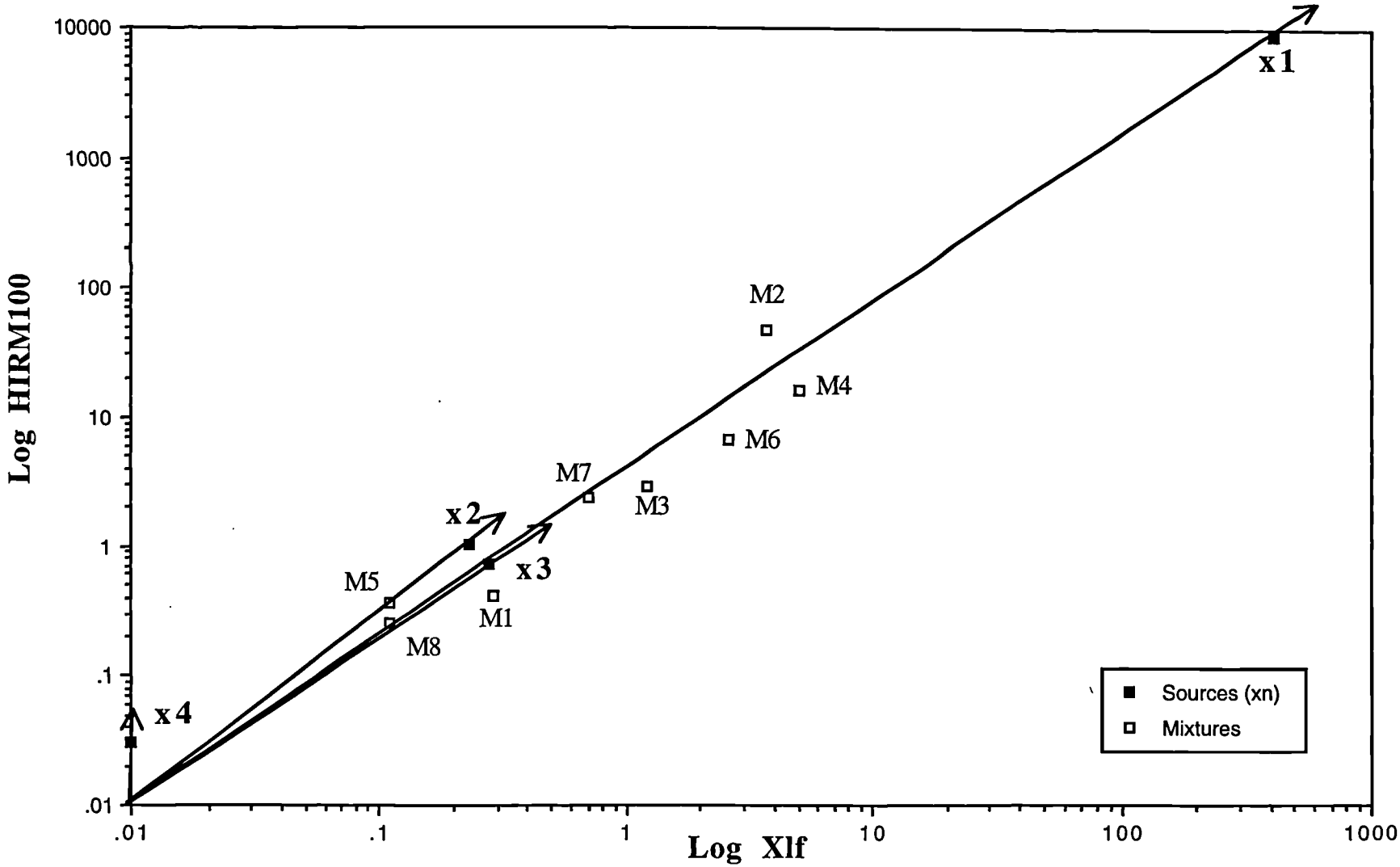

Spurn Head, where most black sand accumulation was seen, the proportion of x1 is the highest at 0.53% and 0.18% respectively. At Flamborough Head and Bridlington, where association with the chalk outcrop was highest and the tills were the thinest, proportions of black sands are the lowest at 0.03%.

Figure 7.11 shows source component vectors for the two parameters χlf and HIRM+100. The vectors for x1 and x3 are very similar highlighting the control of the black minerals in this till (even in tiny concentrations). The vectors for the two tills are also very similar which causes the ill-conditioning of the whole technique. The vector for x4 the diamagnetic sources is in a direction which allows the program to distinguish this source from the rest.

Table 7.6. Linear programming results (% proportions, refer to Table 7.5 for descriptions)

	x1	x2	x3	x4
Mix 1	0.03	99.97	0	0
Mix 2	0.53	0	99.47	0
Mix 3	0.03	99.97	0	0
Mix 4	0.18	99.82	0	0
Mix 5	0	12.68	34.91	52.41
Mix 6	0.08	85.75	14.18	0
Mix 7	0.03	99.97	0	0
Mix 8	0	9.79	28.3	61.91

Quantification of black sand concentrations in beach mixtures

The contribution of the black sand in the tills to the beaches was quantified at particular points over a specified time. χlf and Ms values for the black sand dispersions were used to calculate the amount of black sand in the Barmston cliff sands. χlf has been found to be the most reliably linear magnetic measurement in laboratory tests (Chapter 4) and from preliminary experiment Ms is more reliably linear than remanence measurements (Paper 3, Appendix 7). Ms is not affected by interaction between strongly magnetic particles but it is prone to sub-sampling variability (cf Chapter 5) as shown by the calculation for the Skipsea till. First, assuming the total magnetic signal is caused by the black minerals in the till matrix, the following proportion values can be calculated:

Upper cliff sand, bulk sample:

χlf ($\mu m^3\ kg^{-1}$): 0.0556% black sand in till matrix

Ms ($mAm^2\ kg^{-1}$): 0.05999% black sand in till matrix

Skipsea Till bulk sample:

χlf ($\mu m^3\ kg^{-1}$): 0.0665% black sand in till matrix

Ms ($mAm^2\ kg^{-1}$): 0.0388% black sand in till matrix

From the above calculations estimates of the contributions of black sand from the sandy cliffs to the beach can be made; taking a 1m section of cliff and beach where the sandy material comprises 7m of the cliff and the beach is 50m wide and erosion rates are 2m yr (depth of beach not accounted for):

Upper cliff sand, bulk sample:

χlf ($\mu m^3\ kg^{-1}$): covering of black sand on 50 * 1m surface of beach = 0.156cm

Ms ($mAm^2\ kg^{-1}$): covering of black sand on 50 * 1m surface of beach = 0.168cm

Skipsea Till bulk sample:

χlf ($\mu m^3 kg^{-1}$): covering of black sand on 50 * 1m surface of beach = 0.186cm

Ms ($mAm^2 kg^{-1}$): covering of black sand on 50 * 1m surface of beach = 0.109 cm

However the black sands are generally concentrated in the first 10m of the beach, near the cliffs or in swash lines, so re-calculating the above for a 10m wide beach gives 0.778cm, 0.84cm, 0.93cm and 0.54cm respectively. The lighter fractions could also be indicated as inputs from the cliff to the beach from the sandy cliffs at specific points along the cliffs possibly by the other 99.94% of the sand. Sand fractions from other tills would have to be included, however.

Quantification of numbers of black sand grains in beach mixtures

An attempt was also made to calculate the approximate numbers of black sand particles in any particular beach sample from magnetic measurements. The great advantage of the magnetic property of the black sand is that it can be traced and mapped in the field very quickly as shown in Figure 7.2. The laboratory susceptibility measurements were calibrated with the field susceptibility measurements by counting and measuring black sand grains of different grain sizes held apart in 2 * 6cm sellotape strips. The results of this experiment are given in Table 7.7. There was a good linear relationship between the kappa (laboratory) of the sellotape strips and the number of grains, and the following values were calculated:

kappa of 1 grain of black sand = 0.0222
kappa 1g of black sand = 4033.33
where 1g = 181,682 grains

The field sensor measures approximately 75% of the total susceptibility as measured by the laboratory susceptibility meter (Bartington Instruments Ltd.) in 6cm depth of material. For the most part when the kappa transects were undertaken much of the beach was only 5-10cms thick and underlain by till or shingle. If a kappa measurement on the beach was 75, the total laboratory susceptibility measurement would be approximately 100. The number and weight of grains being measured can be estimated using the above calculations. This assumes that all the magnetic minerals on the beach are black sand grains:

kappa of 100 ~ 4505 grains of black sand
~ 0.025 g of black sand

This gives an indication of the quantity of black sand in a homogeneous area of beach being measured by the loop ($270cm^2$ by 6cm depth). Field susceptibility transects, shown in Figure 7.2, indicate concentrations of the black sand found in swash lines, at the turn of the tide and in low velocity steeper areas of the beach. The kappa values could also be directly related to the number of grains of black sand in the beach using the above results. At Mappleton black sand was deposited in the lee of granite groynes built parallel to the cliffline. The Mappleton transects also indicate that changes have occurred in the beach profiles between and beyond the groynes since construction in 1989. The major difference is caused by the waves being reflected by the granite groynes and not proceeding up the beach to the cliff foot (a difference in height of 9m). The transects indicate how magnetic surveys can be used to map the distribution of the black sand and thus some aspects of coastal processes on the beach.

Table 7.7. Calibration between numbers of black sand grains of different sizes and kappa measurements.

Grain Size (μm)	No of grains	Calculated actual wt (g)	Kappa	Kappa per grain
75-90	3876	0.0213	71	0.0183
90-125	2156	0.0119	39	0.0181
125-180	2312	0.0127	42	0.0182
180-250	2015	0.0111	51	0.0253
250-300	1837	0.0101	47	0.0256
300-500	539	0.0030	15	0.0278
Mean	2123	0.0117	44	0.0222

Sample	No of grains	Calculated actual wt (g)	Kappa	Kappa per grain
Mixture	817	0.0045	18.15	0.0222

7.7 Further Discussion

The methodology outlined in Chapter 6 has been applied successfully and the methodological framework has been readjusted according to the needs and results of this study. This is shown in Figure 7.12. Magnetism was identified as being not fully suitable to model the sources of the beach mixtures in this study; but a further possibility of tracing the black sands was realised. Particular source fractions were matched according to the dominant particle-size of the black sand. An analysis and explanation of the failure of classification techniques using skewed data has been presented and provides useful information as to when such techniques should and should not be applied. Often less complicated bi-variate scattergrams and parameter correlations suffice. The initial bi-variate classification indicated that modelling of the sources of the beach materials would be impossible without diluting the effects of the sorting of the black sands. Linear programming techniques had limited application in this particular study due to the scale of the ferrimagnetic signal of the black sand. But some reasonable results were gained.

A means of tracing materials on the beaches is provided by the black sand and further analysis of its associated quartz grain sizes (in terms of density) may prove useful. The beach sediments can be sourced but only in very limited terms but results of the amounts of black sand in the beach sediments can be used to infer the movement of sands down the coastline. The northern and southern limits of the black sand are Scarborough and Spurn. Given that there is a southerly longshore drift, either tills further down the coast do not contain black sand, or the movement of sediments is sent out to sea at the Humber estuary. At Flamborough Head and Bridlington little contribution is made from thin tills and no extra black sand seems to have been transported here. Again sediment may flow offshore around Flamborough Head. Large accumulations of black sands were seen at the foot of Skipsea till cliffs in the summer and the sand was not being re-distributed along beaches at this stage. Sands were 1m thick and layers of the black sands indicating spring and summer storms were clear in vertical profiles. In the winter however the beaches were much coarser, thinner (5-10cm) and shingly. Sand fractions which were present were very black and were re-distributed at every tide into swash lines and areas of lower backwash energy on the beaches.

Day-to-day, or season-to-season, susceptibility surveys of the beaches may provide useful information on the

Figure 7.12 : Methodological framework and routes taken in Holderness study

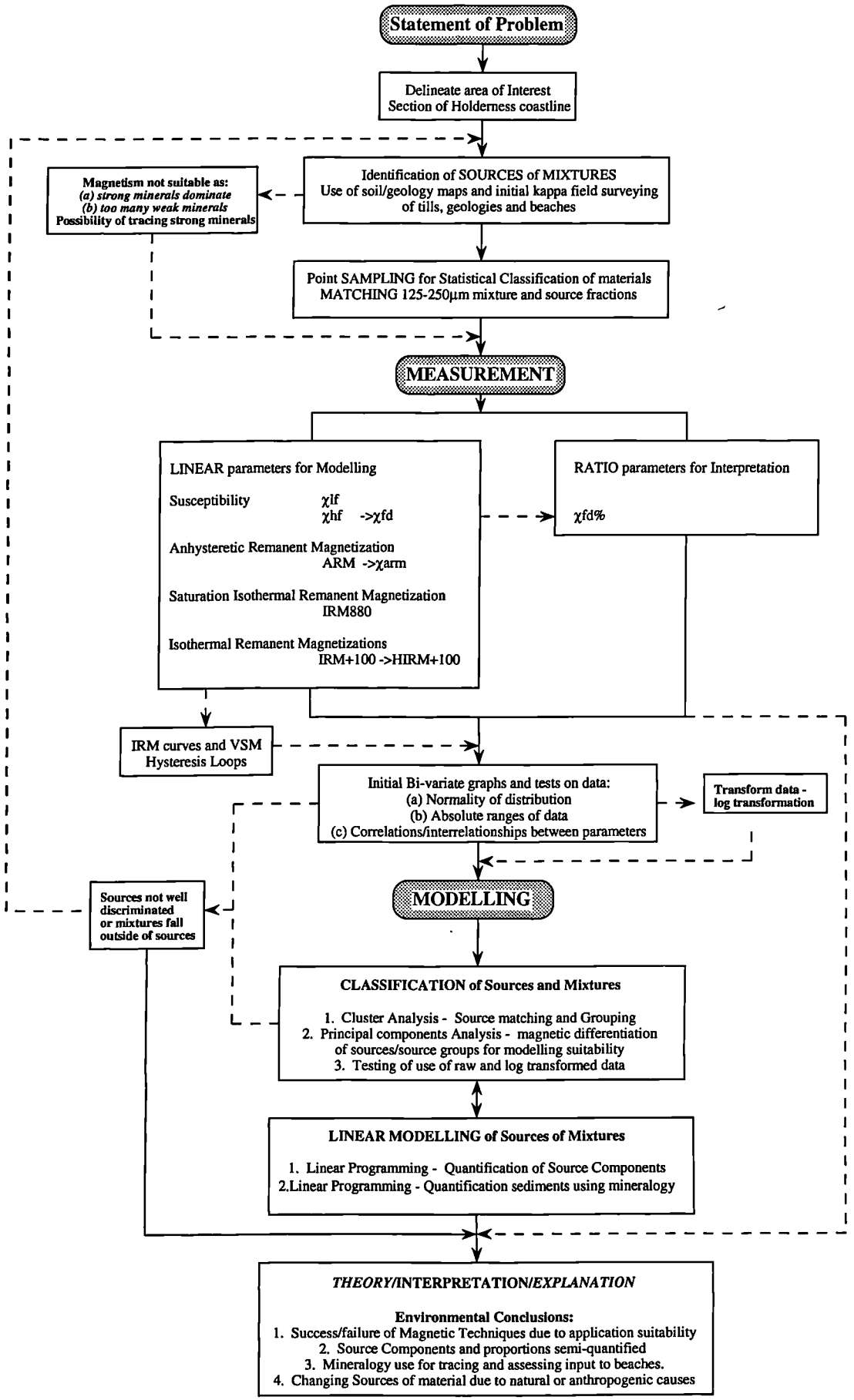

dynamics of the beaches especially if the energy needed to move the black sands was established. Intensive magnetic surveys could possibly reveal the spatial extent and movement of the black sand more easily than that done using radiometric surveys elsewhere (Greenfield, 1989 and Schuilling, 1993). Calculations of the energy required to move the black sand might indicate possible modelling avenues of the movement of sands in this area using the black sand as a tracer. Past energy requirements, preserved in raised coastal stratigraphies, could also be indicated by the presence of heavy minerals like the black sand detected through using magnetic analysis (D. Smith, pers. comm.).

Part 2: Lulworth Cove Source Identification Survey

7.8 Area of Study

Lulworth Cove is a semi-circular bay created as the sea breached Portland Limestone and excavated the soft Wealden beds of sand and clays and cretaceous chalks behind. The cove is not affected by longshore drift processes and is protected from large waves from the south-east by the Isle of Purbeck. The cliffs contribute sediments to the beaches, especially the highly erodible Wealden clays and sands which outcrop in between the limestone cliffs at the front of the cove and the chalk backwall of the cove. These are shown in Plate 7.3 by the lower cliffs on either side of the chalk backwall. This study was essentially an exercise in the initial identification of sources of the beach materials using kappa and the assessment of its use in classifying those source materials which could be modelled using linear programming further to that done in Chapter 5.

Aims, Field and laboratory methods

The main aims of this second coastal study were as follows:

1. To assess the application of magnetic sourcing techniques in brief to another coastal site
2. To confirm the use of magnetic susceptibility surveys in the assessment of sites of possible magnetic work

After initial study of the local geology maps susceptibility loop surveys completed on 21 separate geologies and a beach transect from the west to the eastern side of the cove was carried out. Fifty separate measurements were made of the geologies, some of which are shown in Plate 7.3. For the beach transect measurements were made at 5m intervals over 615m of curved beach at a constant distance away from the cliffs. The coefficients of variation give an idea of the variability in the set of 50 measurements but must be interpreted with care especially as some of the sets of measurements contain arbitrary zeros which contribute to the standard deviation but not the mean.

Twenty-four samples of the geologies and three bulked beach sands from the west, north and east beaches of the cove were collected. Table 7.8 gives details of the samples collected and their geological associations. The 24 samples were air dried and sieved to less than 2mm and potted into 19ml pots and sub-samples into VSM holders. The measurements of χlf, χhf and VSM IRM and hysteresis loops were carried out.

Plate 7.3a. Lulworth Cove

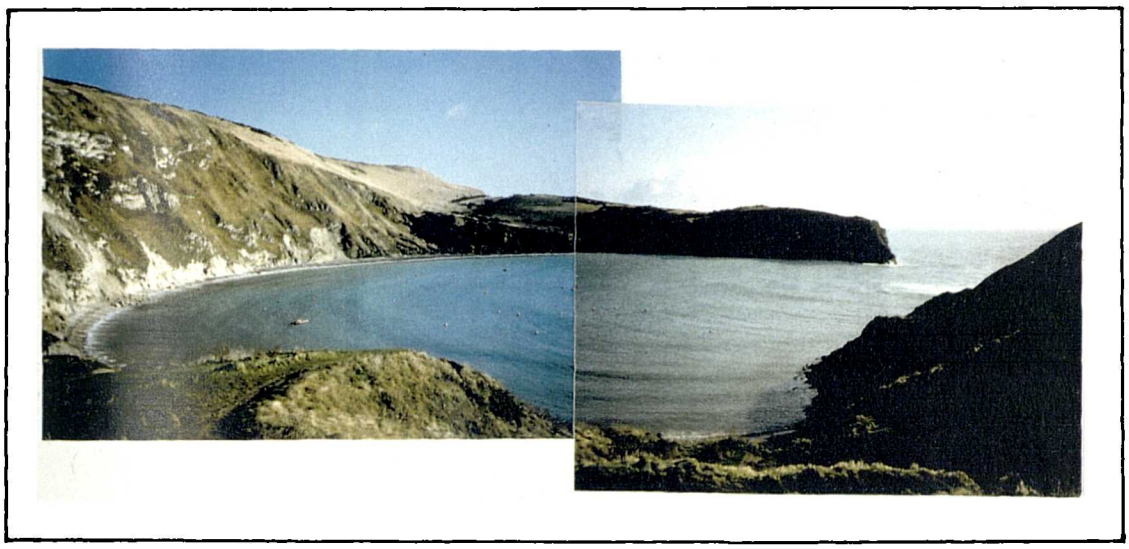

Plate 7.3b. Chalk bedrock and shingle ridges on beach

Plate 7.3c. Greensand and eroded chalk

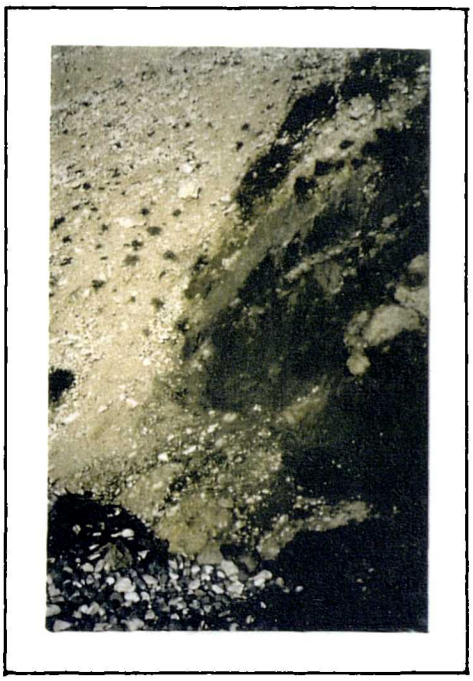

Plate 7.3d. Wealden beds on western side

Plate 7.3e. Wealden beds on eastern side

Table 7.8. Samples collected from Lulworth Cove

Sample	Description	Magnetic Property
Portland	LC1A1	Paramagnetic
Purbeck	LC1A2	Paramagnetic
Purbeck S'stone	LC1A3	Paramagnetic
Brown Soil/Clay	LC1A4	Paramagnetic
White S'stone	LC1A5	Diamagnetic/Paramagnetic
Grey Clay	LC1A6	Paramagnetic
Blue Clay	LC1A7	Paramagnetic
Yellow S'stone	LC1A8	Paramagnetic/ferrimagnetic
Iron S'stone	LC1A9	Paramagnetic
Lignite	LC1A10	Paramagnetic
Ironstone	LC1A11	Paramagnetic
Red Clay	LC1A12	Canted-antiferromagnetic
Black S'stone	LC1A13	Paramagnetic/ferrimagnetic
White Clay	LC1A14	Paramagnetic/ferrimagnetic
S'stone+Iron	LC1A15	Paramagnetic/ferrimagnetic
Quartz Conglom	LC1A16	Paramagnetic/ferrimagnetic
Or+Red+Pink Clay	LC1A17	Canted-antiferromagnetic
Greystone	LC1A18	Paramagnetic
Greensand	LC1A19	Paramagnetic
Chalk	LC1C20	Diamagnetic
Hard Chalk	LC1A21	Paramagnetic/diamagnetic
Low X Sand	LC1C22	Ferrimagnetic/paramagnetic
High X Sand	LC1C23	Ferrimagnetic/paramagnetic
Chalky Sand	LC1C24	Ferrimagnetic/paramagnetic

7.9 Results and Discussion

Figure 7.13 shows results for field kappa, lab kappa and χlf for the geologies listed in Table 7.9 on a base map of the location of the geological sections. The beach transect is also shown. The values for the beach transect fall outside those of the geologies contributing sediments. The maximum geological value is 12 whereas the beach values reach 155 in areas of fine sands. Most of the low values of the beach transect can be associated with in situ geologies in the beach profile, for instance chalk (kappa=1.4). In these areas the beach materials were the bedrock and shingle rather than sands. However in areas of the Wealden clays where streams ran from the cliffs some sorting of a 'black sand' could be seen; these beach areas were predominantly sandy. A magnetic extraction of the sands collected revealed (in samples 2 and 3) black particles which when studied under a light microscope appeared to be grains of silvery-grey iron and were certainly not primary minerals (D. Keen, pers. comm). A subsequent X-ray diffraction showed an iron content of 96.7%. Such a mineral in this pure a form would not be present in any of the geologies of the area. The black sand may have been present in other areas of the beach underlying the shingle but only surface beach sediments were measured in this reconnaissance survey.

Laboratory and field kappa measurements were compared to indicate the reliability of field measurements for identifying magnetic mineralogies. Figure 7.14 gives the results of a correlation between field kappa and lab kappa; the result is an r value of 0.845 significant to 0.001 (n=18). This indicates that the results for the field measurements can give a reliable guide to the suitability of an area for magnetic study even where the variability of

Figure 7.13: Laboratory and field kappa measurements for Lulworth Cove geological samples and beach kappa transect

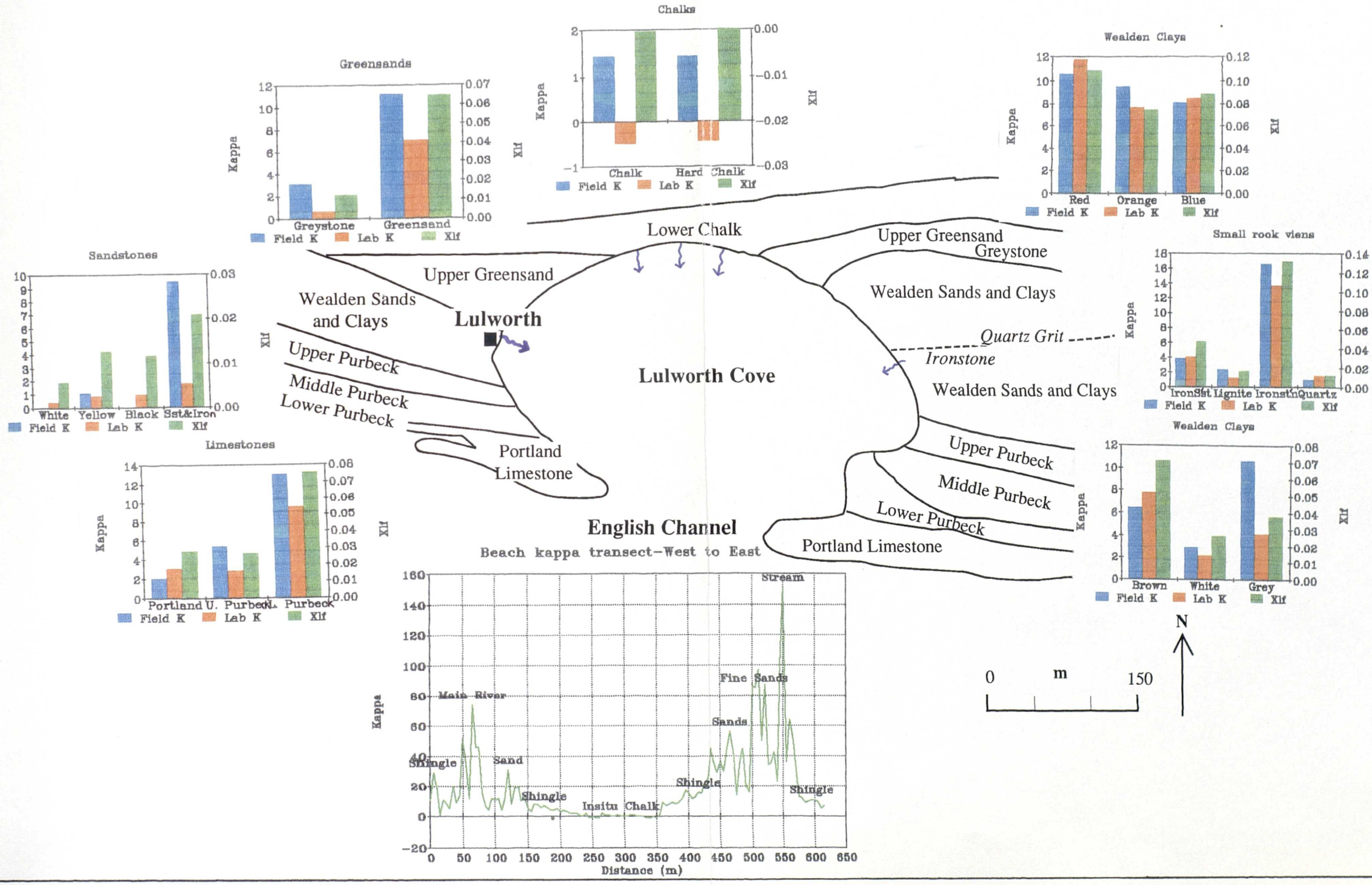

the material is quite high (CV are up to 77% for weak materials). However the field measurements are consistently higher than the laboratory measurements indicating that the level of noise in the field does not allow for sensitive diamagnetic measurements.

Table 7.9. Kappa results for loop survey of Lulworth Cove geologies

Sample	Mean	SD	Min	Max	CV%	N
Portland Stone	2	0.9	0	4	45.8	50
Lower Purbeck	5.4	2.3	2	9	42.1	50
Upper Purbeck	5.7	1	3	7	16.8	50
Portland Sand	13	1	11	15	7.4	50
Brown Clay	6.4	1.3	1	8	19.7	50
Grey Clay	10.6	1.6	8	13	14.9	50
Blue Clay	8.1	1	6	11	12.5	50
Red Sandstone	3.8	1.1	2	6	28.1	50
Yellow Sandstone	1.1	0.7	0	2	66.4	50
Lignite	2.3	0.7	1	4	30.4	50
Iron Stone	16.6	1.4	14	19	8.6	50
White Clay	2.9	0.8	2	4	27.1	50
S'stone&Iron conglom	9.5	1.4	8	12	14.5	50
Quartz Grit	0.9	0.7	0	2	77.9	50
Red Clay	11.1	1.6	8	15	14.7	50
Upper Greensand	9.5	2.6	6	16	27.7	50
Greystone	3.1	0.7	2	4	23.7	50
Lower Chalk	1.4	0.5	1	2	35	50

Hysteresis curves revealed the paramagnetic and diamagnetic nature of many of the minerals present in the geologies. Figure 7.15 gives a selection of hysteresis curves and those of the sand samples and measured dispersed magnetic extract of the black iron particles. It is clear from these normalized curves that the iron mineral is foreign to the natural environment. The sands collected from the three beach sites are all more ferrimagnetic than any of the natural geologies, even sand sample 1 collected from the base of the chalk backwall. Most of the geologies are paramagnetic, including all clay samples, black and yellow sandstone, greystone, limestones and greensand. Pink clay has a slightly open loop indicating the presence of canted-antiferromagnetic minerals also. Diamagnetic properties are displayed by chalks and white sandstone (which also has a small ferrimagnetic component).

Figure 7.14: Field and laboratory kappa measurements for Lulworth Cove samples

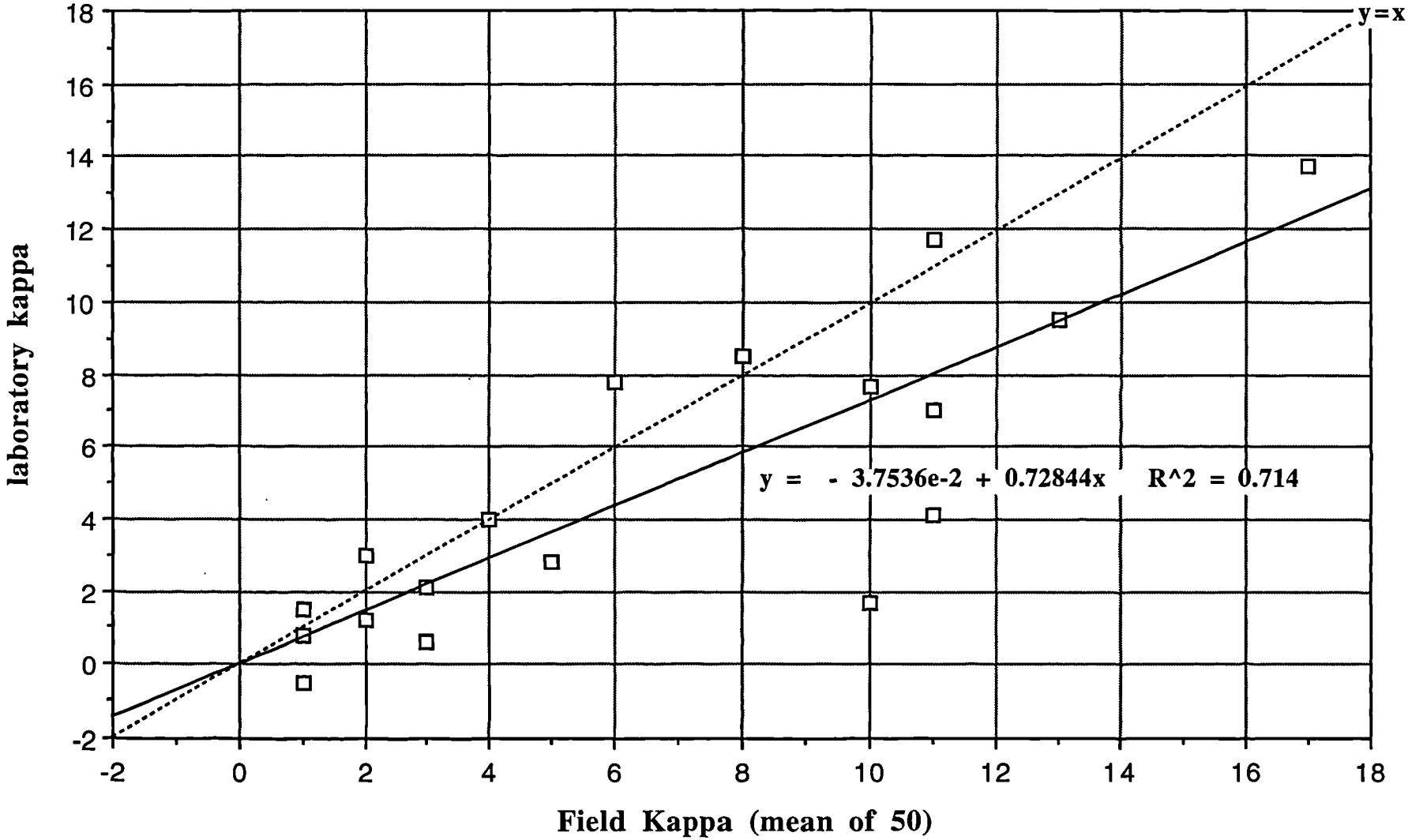

Figure 7.15: Hysteresis curves for Lulworth Cove geological samples, sands and magnetic mineral extracted from beach sand

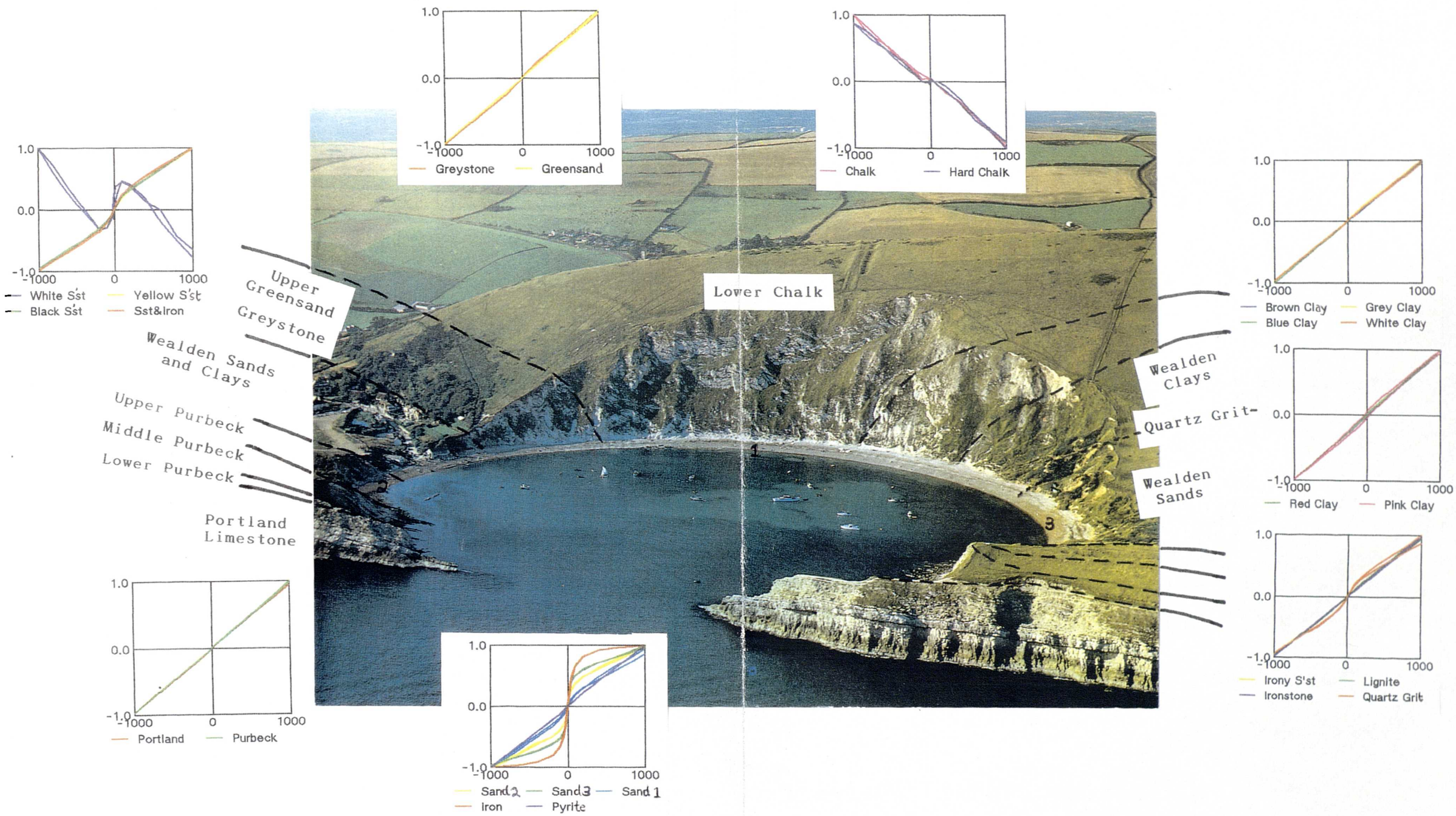

7.10 Summary

The application of magnetic techniques to the Holderness area has given information on the nature of the sources of the beach mixtures and identified the source of the black sand to the Skipsea Tills and upper cliff sands. The specific questions raised earlier can be fully answered here. The beaches can be sourced magnetically but only in terms of the ferrimagnetic black sand fractions in the till, which limits the application of magnetism here. The tills are magnetically weaker and less variable than the beach sands and the different tills can be discriminated. Erratics and till sands are the major contributing sources of the beaches between Scarborough and Spurn. Estuarine sands may contribute to beaches south of the Humber Estuary. The black sand could be used to trace the movement of its associated larger quartz grains (lighter fractions of the beach) probably down to Spurn head. The black sand is delimited to the north by the outcrop of Oolite near Scarborough, where the tills end. Sediments of beach zones are variable because of particle sorting and zones of different minerals, particle sizes and particle densities are created. It is clear from both particle-size distributions and magnetic measurement that the fines from the tills are removed and enter North Sea circulation and are deposited elsewhere. The southward movement of the black sand is interrupted by the Humber River as it was not found in Mablethorpe and Cleethorpes sands; here the sand flow must move out into the sea.

The Lulworth Cove site was assessed in one day and again a 'black sand' was present which dominated the magnetic properties of the beach sands. The application of kappa field survey proves to be a useful precursor tool in determining the suitability of an area for application of further sediment sourcing using magnetic techniques in coastal areas. Hysteresis loops have also proved useful for discriminating between geologies and beach sediments. Further application of the methodology to coastal environments would take the form of these studies where unexpected problem sediments, such as the black sands, can be identified using field kappa in the early stages.

CHAPTER 8

Quantitative Sediment Sourcing in a Small Catchment

8.1 Introduction

Lake catchment studies aside, there have only been a small number of studies undertaken dealing with the quantification of stream and river sources. These generally use suspended sediments as already outlined, but some studies have used bedload sediments (Nightingale, 1991, Caitcheon, 1993). In itself studies of bedload may give valuable information in determining point sources and storage of sediments, especially pollutants. Oldfield et al. (1979) and Walling et al. (1979) introduce the use of magnetic measurements for sourcing suspended sediments in Jackmoor Brook, Devon. Differences in susceptibility and coercivity IRM profiles for hematite rich Triassic sandstones and ferrimagnetically enhanced topsoils provide a basis for good source determination. Work by Oldfield (1985), Yu (1989), Yu and Oldfield (1989) shows the progression from the earlier qualitative/semi-quantitative studies to those using statistical regression techniques for sediment sourcing. These studies were all based on the Rhode River catchment, Maryland, USA and were discussed in Chapter 3.

In this chapter application of the methodological framework is made to a small catchment system near Great Rollright, Oxfordshire. The application fulfils all of the parts of the methodology from initial source sampling through classification stages to final modelling, thus allowing a wider interpretation of modelling results than the coastal studies. Initial work focuses on finding a catchment with soils and geologies which can be magnetically discriminated. This is carried out using a transect survey of soils and geologies in Midland and Southern England. The Great Rollright catchment was chosen on the basis of soils and geologies which were magnetically discriminated in the transect survey.

The identification of sources and an assessment of the variability of soils and geologies in the catchment using magnetic measurements consisted of several stages. Large and small scale field loop susceptibility surveys were carried out within and between different soil and geological units. The aim of the initial surveys was to assess the scales of the properties of the soils and geologies in the catchment and assess the variability within and between the soil units in terms of magnetic susceptibility. Advantages and disadvantages of using magnetic susceptibility surveys have already been discussed in Chapter 5. The catchment covered a relatively small area which could be studied more thoroughly, and its steep arable slopes presented likely contributory sediment source areas. The statistical and geomorphological base of these source contributory factors are discussed and source variability of the soils is accounted for in the definition of the sources to be incorporated in modelling of the sediment 'mixtures'. Mixtures which are modelled in this study are of fine stream bed and point bar sediments. The outcome of the modelling is reviewed with reference to experimental error discussed in Chapter 4 and in the light of the environmental variability within the sources of the sediments. Finally an assessment is made of the reliability of the tests and possible application to catchments with magnetically less well discriminated sediment sources.

8.2 Aims and Objectives

Essentially the main objective of the catchment study is to test thoroughly the methodological procedures to provide a widely applicable system of study. The main aims are as follows:

1. To define statistically the spatial variability of all the sediment sources chosen on the basis of soil/geology maps and magnetic susceptibility survey; and to determine the number of samples needed to cover the variability
2. To use classification techniques such that the samples could be reduced into four well-discriminated sources with discrete mean±1 standard deviation ranges
3. To test the linear programs using four source components
4. To set the limits of the classification and modelling techniques using magnetic properties in a catchment with well-defined sediment sources

In order to identify a catchment which might enable these aims to be met an initial study of soils of southern England was undertaken to find those soils which discriminate well using magnetic properties. This is discussed in the next section.

8.3 Transect of Soils of Southern England

The transect along which predominantly brown earth soils were collected ran from Coventry (SP40 80-SP50 80) to Basingstoke (SU40 20-SU50 20). This transect survey served two purposes; first, the range of magnetic properties of brown earth soils on different sedimentary geologies would be identified, and secondly, to give an indication of the types of soils and geologies needed in a catchment for sediment modelling to succeed.

Arable brown earth topsoils (surface samples) were collected from fifteen points along the transect, details of which are given in Table 8.1. The samples were air dried, lightly ground and sieved to remove >2mm fraction. The samples were potted into 10ml and 0.4g VSM holders and the measurement of χlf, χhf and VSM IRM curves and hysteresis loops were made on all samples.

Bi-variate scattergrams were used to assess the spread of soils according to their low frequency susceptibility (χlf), percentage frequency dependant susceptibility (χfd%) and high field remanence (HIRM300). Figures 8.1 a and b give the χlf and χfd% results for the soils and geologies. The variation in values indicate variation in factors such as aspect, land usage and drainage which alter soil magnetism. In general, rendzinas on chalk and limestones have a high χlf of 2 $\mu m^3 kg^{-1}$ and high χfd% of 9% indicating enhancement of the topsoils and production of secondary fine-grained ferrimagnetic minerals. Heavier soils on clays have much lower χlf (<0.4) and χfd% (<4%) due to poorer drainage, sub-optimal enhancement and possibly even destruction of ferrimagnetic minerals through slight gleying. Soils on Oldhaven and Bagshot beds and Middle and Upper Lias have χfd% of approximately 6 but varying χlf's (0.3-2.1 $\mu m^3 kg^{-1}$) indicating the varying mixtures of clay and limestone parent material components which cause slightly different drainage classes.

Figure 8.1: Xlf (a) and Xfd% (b) results for southern England transect survey

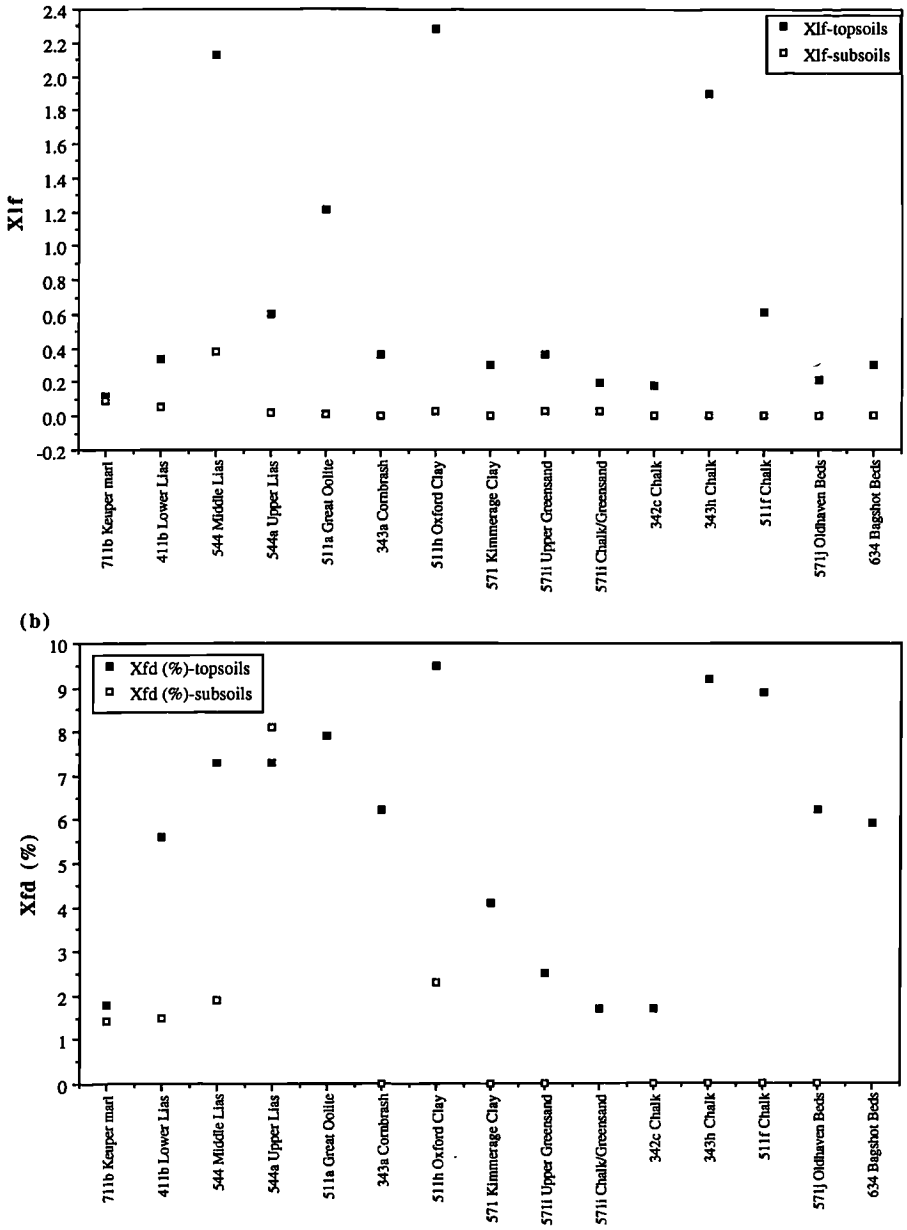

Figure 8.2: Xlf versus HIRM for southern England transect survey soils

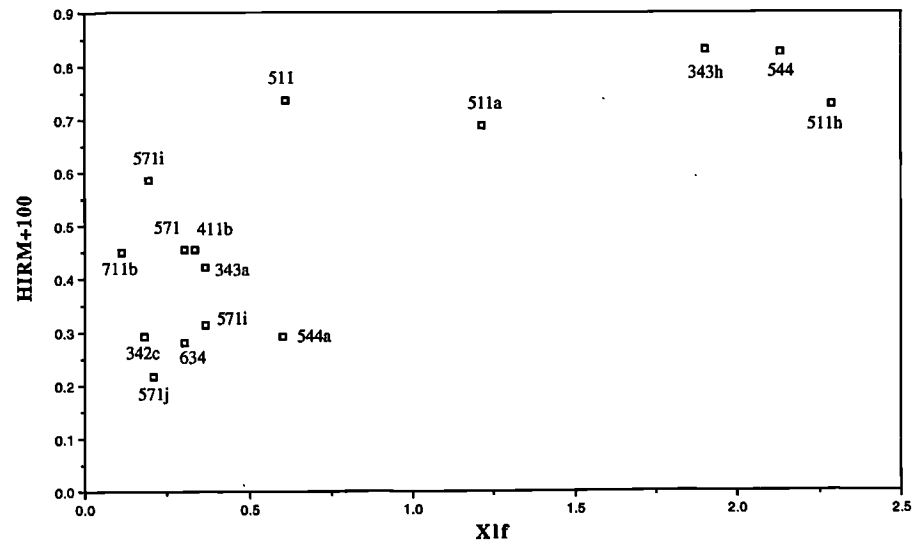

Table 8.1. Transect Survey Soil Sample Descriptions

Grid Ref	Site	Soil Type	Geology	Map Symbol
423 624	Southam, A423	Calcareous Pelosols	Lower Lias	411b
446 476	Mollington, A423	Brown Earth	Middle Lias	544
448 216	Wooton, A423	Typical Brown Calcareous Earths	Great Oolite	511a
455 187	Wooton, A423	Brown Rendzina	Cornbrash	343a
398 055	Stanton Harcourt, A415	Typical Brown Calcareous Earths	Oxford Clay	511h
482 956	Drayton, A4017	Typical Argillic Brown Earth	Kimmerage Clay	571
444 890	West Hendred, A417	Typical Argillic Brown Earths	Chalk/ Greensand	571i
432 894	West Hendred, A417	Typical Argillic Brown Earths	Upper Greensand	571i
447 876	West Hendred, A417	Grey Rendzinas	Chalk	342c
480 840	West Ilsley, A34	Brown Rendzinas	Chalk	343h
485 846	Chilton, A34	Typical Brown Calcareous Soils	Chalk	571f
482 737	Cheively, A34	Typical Argillic Brown Earths	Oldhaven Beds	571j
485 630	Burghclere, A34	Pelo-argillic Podzols	Bagshot Beds	634
466 258	Steeple Aston, A423	Ferritic Brown Earths	Upper Lias	544a
404 789	Coombe Abbey, A427	Typical Stagnogley Soils	Keuper Clay	711b

Based on the results of Chapter 4, where assessment was made of the best discriminatory magnetic parameters, χlf and HIRM300 were used to classify the fifteen soils. Figure 8.2 shows the resulting scattergram. The best discrimination is seen between the brown rendzina (343a) with χlf values of 2.0 $\mu m^3 kg^{-1}$ and brown earths soils on clays and coarse beds (571, 411b, 571j, 634 and gley 711b) with χlf values of less than 0.5 $\mu m^3 kg^{-1}$. HIRM300 values are 0.8 $mAm^2 kg^{-1}$ for rendzinas and <0.45 $mAm^2 kg^{-1}$ for clays. The criteria set for choosing a catchment on which to test the methodology were that it should contain a brown rendzina (fine-grained ferrimagnetic) on a limestone parent material (diamagnetic/paramagnetic) and a clayey soil on a clay parent material (both canted-antiferromagnetic/paramagnetic).

8.4 The Catchment Study

The catchment lies 2 miles north-east of Chipping Norton, Oxfordshire and contains the village of Great Rollright. The catchment, shown in Figure 8.3, is approximately $5km^2$. The countryside within the catchment boundary is typical Cotswold rolling hills where some slopes are moderately steep (above 5°). Two streams drain the catchment and both contribute to the River Swail which flows south-west from this area into the River Evenlode which flows south-east towards the Oxford Canal. The smaller stream flows partly through Danes Bottom which is a very steep-

Figure 8.3: Great Rollright Catchment

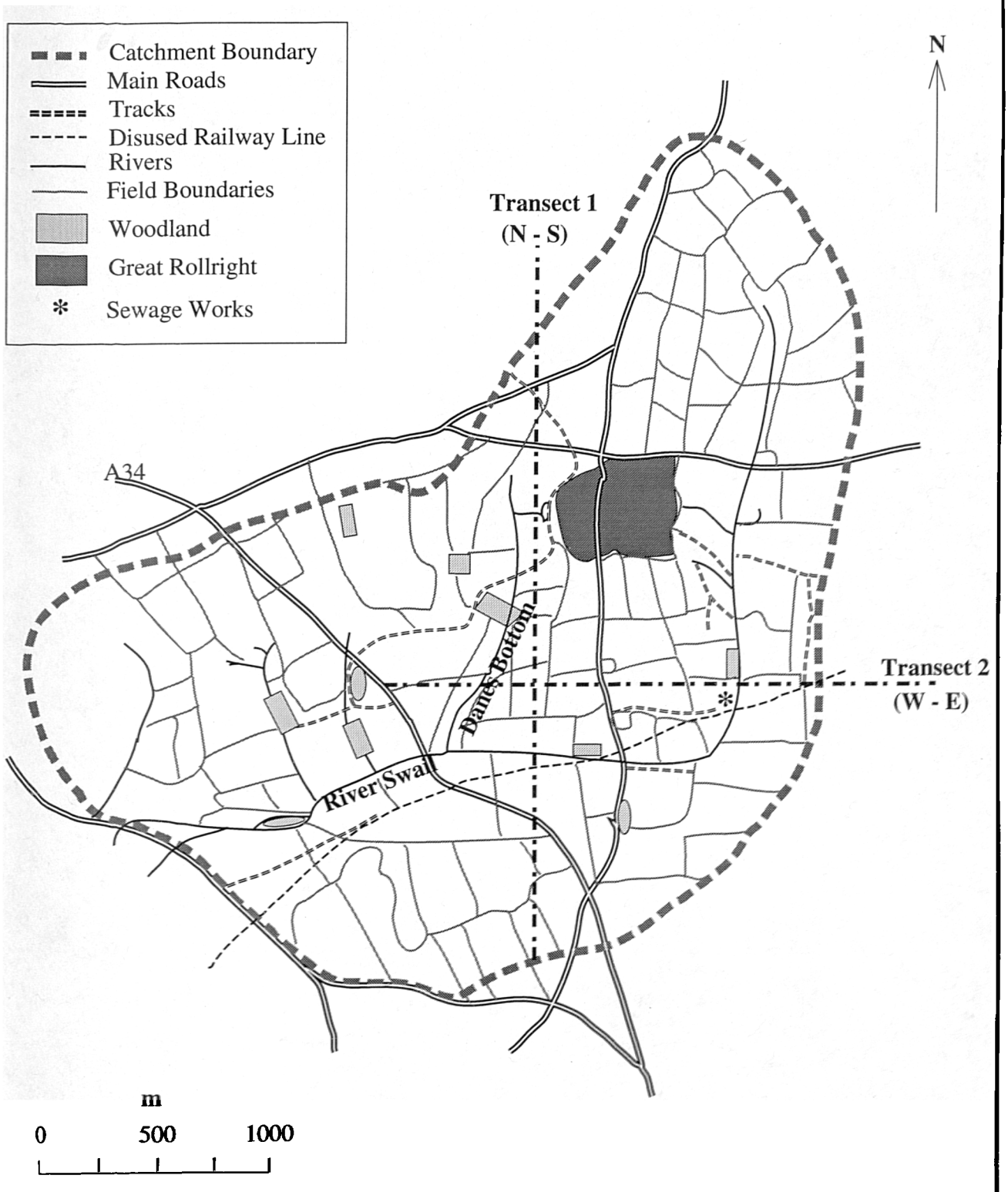

sided deep valley, possibly a fluvio-glacial outlet channel. The streams are visually clear and reasonably fast flowing except in localized areas where they were dammed by roads and farm tracks.

No highly magnetic pollutants appeared to be entering the streams other than agricultural drains and possible atmospheric fallout. No metal, litter or other contaminant was found in or near the streams apart from metal fencing along some stretches of the streams. Tile drains were evident throughout the catchment. There is a small sewage works in the catchment also. It was assumed then that the major sources of sediment were soils and geologies from the effective catchment area and channel banks and bed. Some parts of the catchment and some of the sampling points described later are shown in Plates 8.1 and 8.2.

The catchment contains two main soil types and a small area of a third soil type. The soils in the area are mapped on the 1:250 000 scale (Soil Survey Sheet 3, Midlands and Western England). Figure 8.4a shows the three soils: a brown rendzina (Elmton 1 series), a pelo-stagnogley (Denchworth series) and a stagnogleyic argillic brown earth (Oxpasture series). The rendzinas are described by the soil survey as shallow, well-drained brashy calcareous fine loamy soils over Jurassic limestones. The most typical associated land-use found in the catchment was arable crops which included cereals, mainly barley. The pelo-stagnogley is a slowly permeable, seasonally waterlogged clayey soil over Jurassic Clays (in this case) and is used to grow winter cereals and for grazing dairy herds. The Oxpasture soil is a fine loam over clayey, slowly permeable subsoil and is seasonally waterlogged. The main land use is as for the Denchworth soils.

Figure 8.4b gives the geology of the area mapped at the 1:63 000 scale (Sheet 218, Chipping Norton). Jurassic limestones and clays underlie the rendzinas and clays respectively, however as will be seen later the soil and geology boundaries do not match up exactly and some deeper rendzina soils overlie the clayey/calcareous subsoils near geological boundaries. The clays are of the Upper Lias series and the limestones, cornbrash and forest marble are of the Great Oolite series. Little geological difference was observed between the limestones in the catchment. The Great Oolite limestones made up the steepest slopes (10°) and the arable fields were largely armoured with platy stones of limestone.

Pastures were associated with the presence of clays and grazing for cattle and horses was observed. In Danes bottom the land was rough common and appeared unused. Some land use in the 'effective catchment' is marked on Figure 8.5a (effective catchment will be discussed in the following sections). Along most of the streams riparian buffer zones of at least 1-2 meters existed. In arable fields the streams were usually fenced and wooded, in pasture reaches and in two arable situations the streams were open. For most of the stream's length the channel bed was armoured with limestone except for points 2, 4, 11, and 12 (Figure 8.5b) which were very clayey and fine-grained.

Plate 8.1a: Part of the Great Rollright Catchment from the South.

Plate 8.1b: Confluence of Streams 1 and 2, stream 2 flowing through Danes Bottom is on the left.

Figure 8.4: Catchment soils (a) and geology (b)

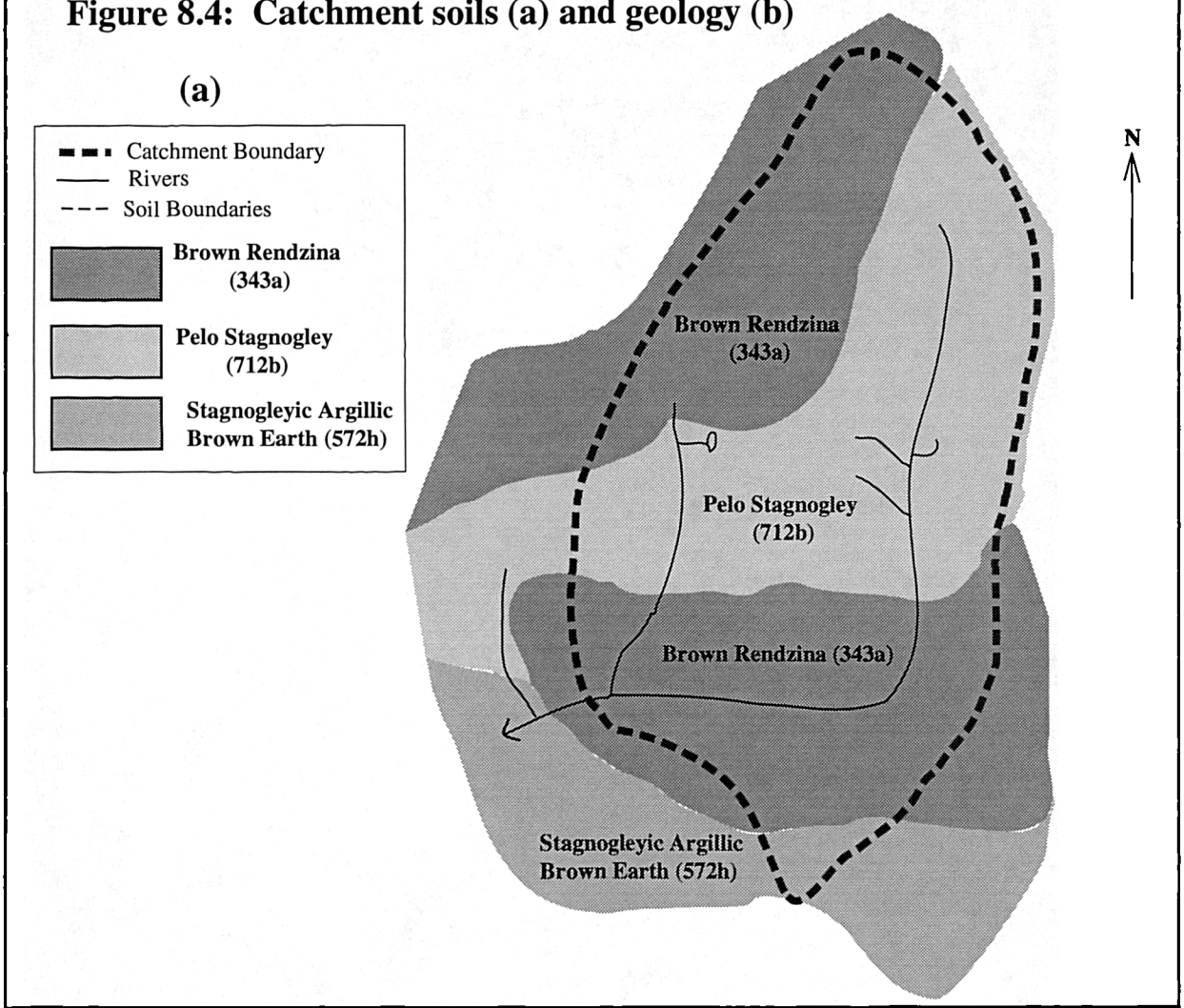

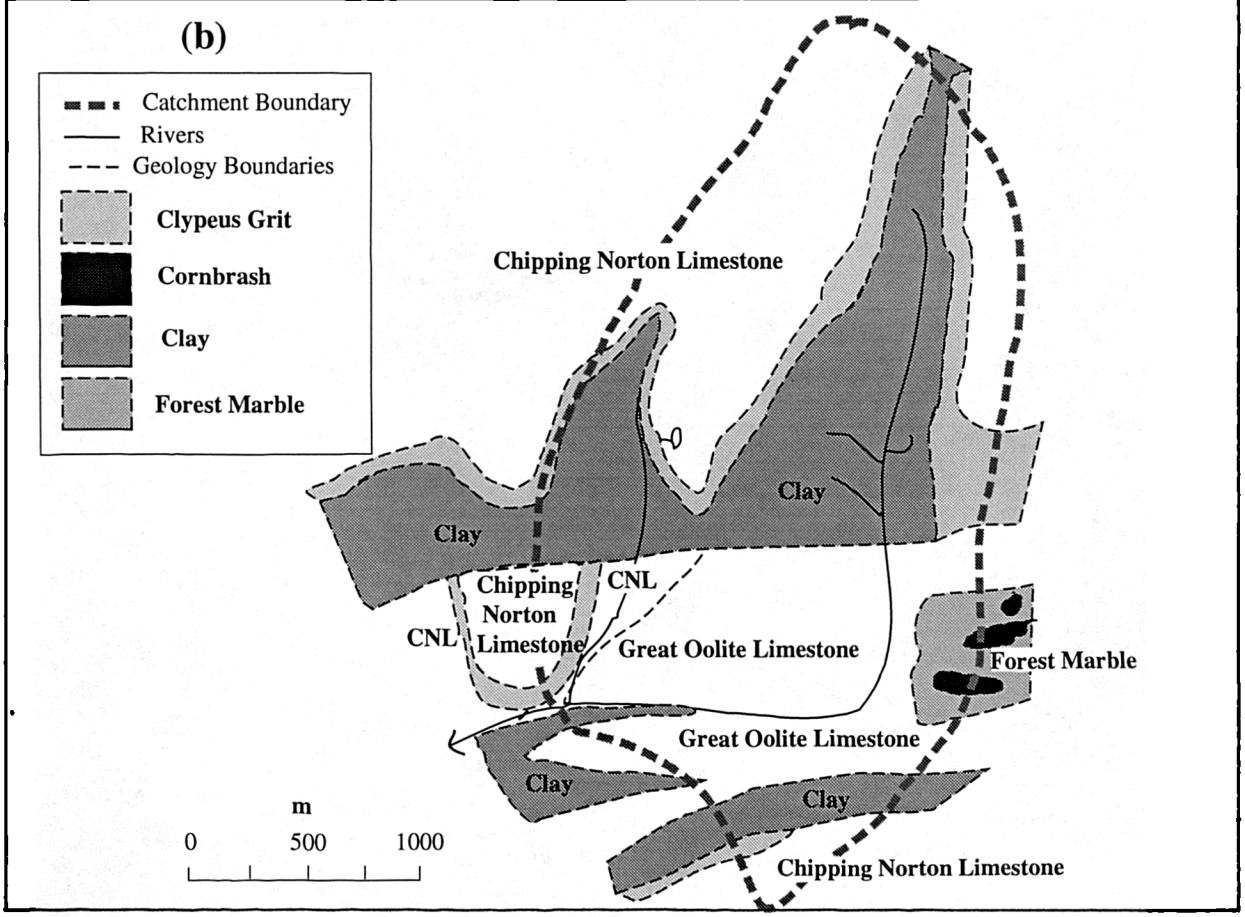

Figure 8.5: Land use (a) and sampling grid (b)

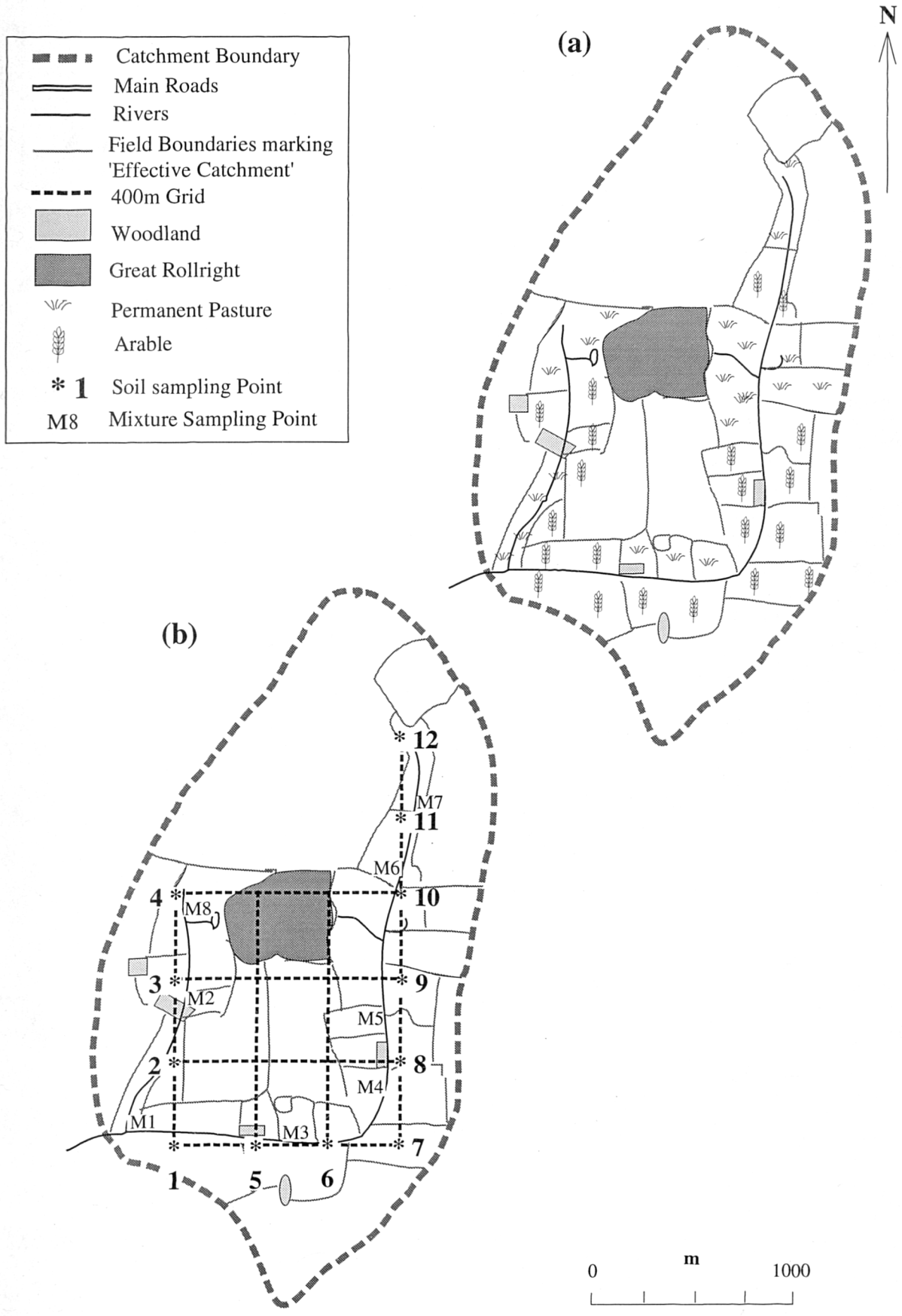

8.5 Identifying sediment sources and assessing spatial variability

Field Surveys

Kappa measurements were carried out every 10m along two 2km transects running perpendicular to one another. The transect positions (marked on Figure 8.3) were chosen to run across all the geologies from north to south and along the centre of the catchment from west to east. Figures 8.6 and 8.7 give the results of the transect surveys which are presented with the soil, geology and land use boundaries for comparison. These figures were used to identify source units and the data were used to construct variograms to verify the boundaries in the data and indicate the levels of spatial variability within the data. A view of the north-to-south transect is shown in Plate 8.1, where the transect ran from top to bottom of the photograph.

From Figure 8.6 (transect 1) a relationship between kappa and soil type and geology can be seen. The distinction between rendzina and pelo-stagnogley at 300m is evident from the reduction in kappa from 50 to 10. Other boundaries however are less clear being affected by boundary integration of geologies. For instance distinction between the clay and Chipping Norton Limestone at 800m is more limited. At 1500m, a small clay band running along stream 1 and the wetter soil characteristics reduces readings to 20 even within the brown rendzina unit (where values are as high as 70). The relationship between kappa and topsoil is not clear cut and many factors, especially those such as magnetic enhancement caused by burning stubble in the fields, may affect the overall pattern. The variability within each unit is large: for example the pelo-stagnogley unit covers the range from minimum values to 75% of the maximum value at the clay/limestone boundary. The clay soil boundaries and the clay geology boundaries do not match for this transect, perhaps reflecting wide intermediate areas of clay and limestone parent materials which are inter-mixed.

Figure 8.7 (transect 2) shows different relationships again, mainly being between topography and land use and the kappa values. Values for rough land and arable land with crops left in are lower than those for the arable fields (30 as opposed to 60). The fields with the fodder crop have values half that of the fallow even though bare soil was being measured (30:60). Two main minima in the values associated with large hedgerows are present but it is unclear why the values start to fall 50m either side of the hedges. Statistical means have not been calculated for the units subjectively identified in Figure 8.6 and 8.7; instead variograms, presented in the next section, have been used to identify the major boundaries in the data (as in Chapter 5).

A second smaller-scale survey was carried out within both a clay field and a rendzina field chosen from the results of the above survey. In each field a 20m grid and a 150m transect were measured at 1m intervals. An assessment of the within-field scale variability was then be made. Table 8.2 gives statistics for these shorter surveys. The 150m transect results are affected by topography more than the grids as in both cases they ran from the top to the bottom of each field. The difference between the means of the clays and rendzinas is clear and its significance was tested statistically. For the grid surveys a t-test value was -135.71 ($p=<0.0005$) and for the transect $t=-63.95$ ($p=<0.0005$). These t-test results indicate that for magnetic susceptibility the two soils are statistically distinguishable.

Figure 8.6: Kappa transect 1 (north to south)

North
Grid Ref:320 316

South
Grid Ref:320 299

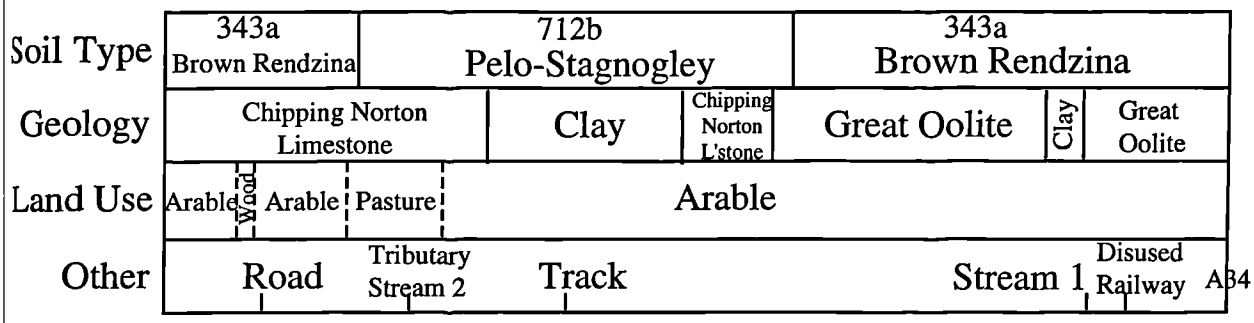

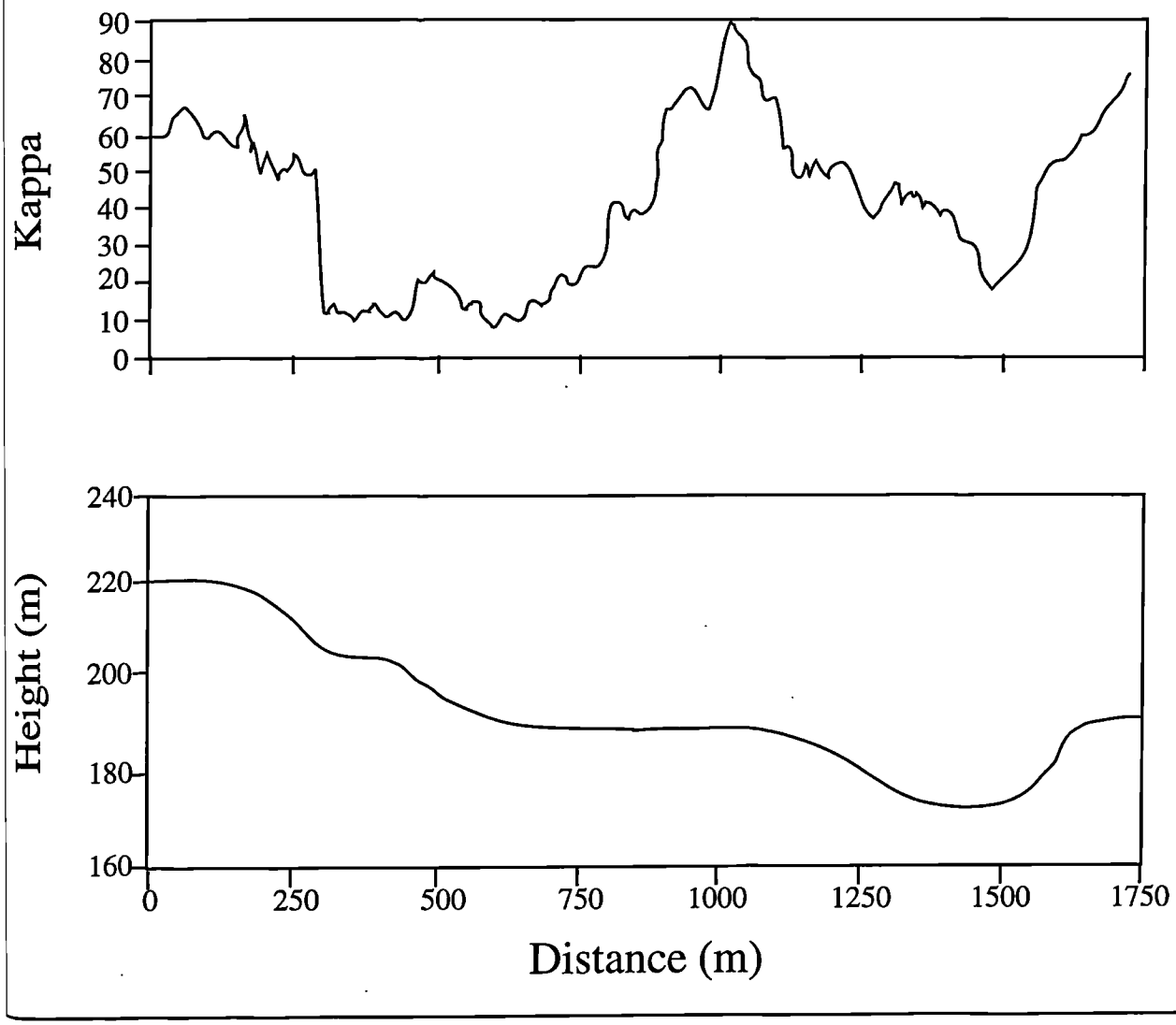

Figure 8.7: Kappa transect 2 (west to east)

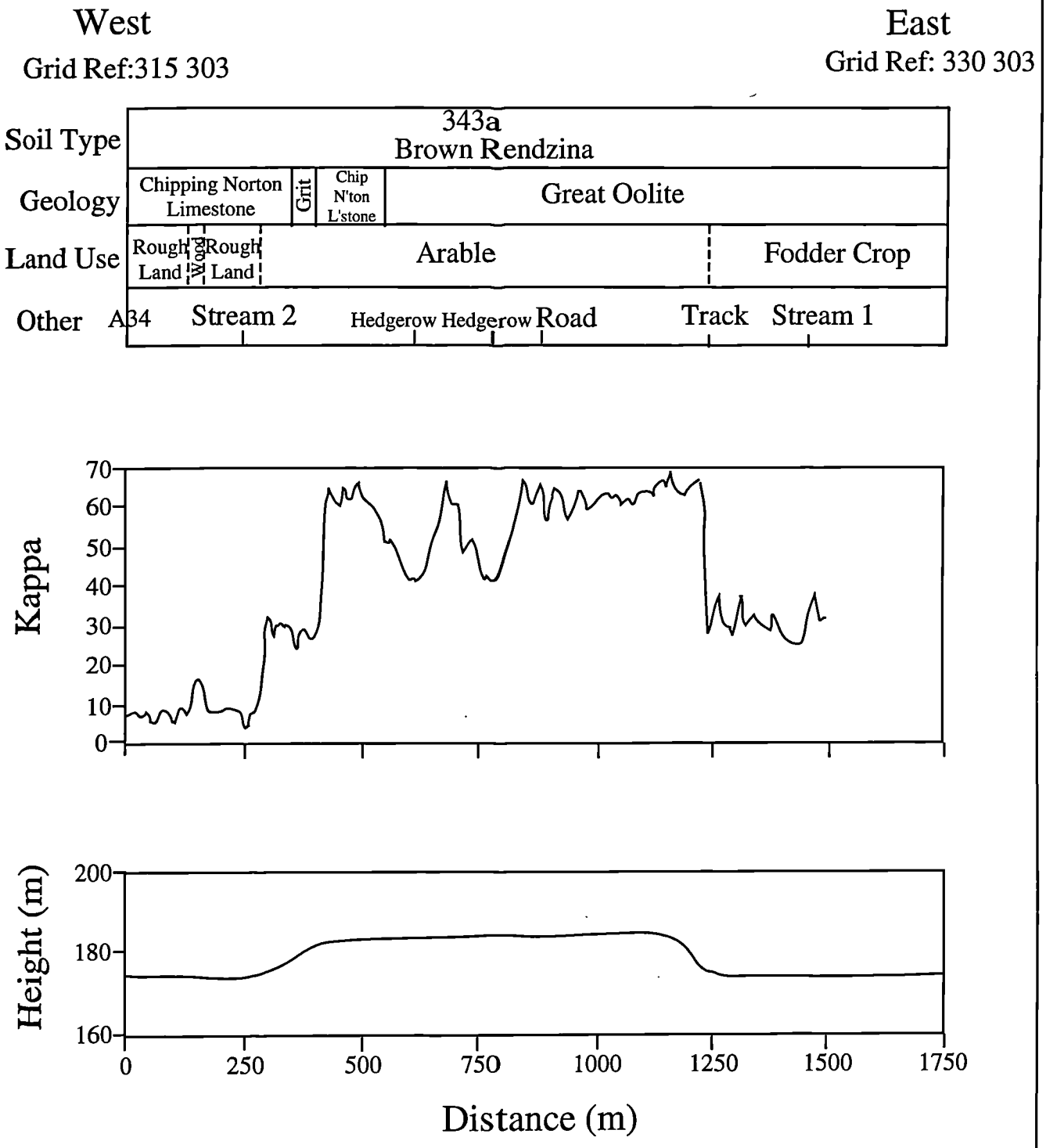

Table 8.2. Statistics for small scale grid and transect Kappa surveys

	Mean	SD	Var	Min	Max	CV%	N
Clay Grid	6.0	1.2	1.5	4	9	20.5	400
Transect	9.0	2.6	6.7	5	18	28.7	150
Rendzina Grid	93	12·6	158·7	63	124	13·6	400
Transect	96.6	15.6	243.5	63	126	16.2	150

Spatial Variability

Data from the 2km transects were analysed first. Individual variograms and a variogram of joint data (for both transects) are shown in Figures 8.8a, b and c. Sills are shown at 500m (8.8a) and 400m (8.8b) and the average 400m (8.8c) indicating that the boundaries between clays and rendzina soils are real for kappa values and that the range of spatial dependence is approximately 400m. Variograms of the arable soils in the catchment (a subset of the larger transects) also show a boundary at 400m (Figure 8.8d). It must be noted that variograms generally tend to the variance of a dataset, but in Figure 8.8 the sills are defined at higher levels than the variance. This may be caused by the large variation within each soil unit. Data from the shorter 150m transects were then used to construct variograms to look at the smaller within-field variation in soil susceptibility. Figures 8.9a and b show that in both cases there are small sills at approximately 15m intervals (marked by horizontal lines) and the variance is reached at 45m. There is no clear reason why these sills are present but they may be associated with topographic factors or in-field land-use factors such as ploughing patterns or old ridge-and-furrow.

Sampling Strategy

From the survey and variogram results a sampling strategy for sediment sources was formulated. First an effective sediment source area or 'effective catchment' was identified on the basis that all fields adjacent to the stream bank could deliver soil sediment to the stream (Figure 8.5b). Fields which were one field boundary away realistically would not supply materials because of sediment storage behind the boundaries. Stream bank topsoils and subsoils were also sampled. A sampling grid of $400m^2$ was overlain onto the effective catchment and twelve sampling sites were identified (Figure 8.5b). At each of the twelve sites a further grid of $45m^2$ was overlain and split into 9 squares of $15m^2$ giving 16 grid nodes. At each of the 12 sites, 16 topsoil samples were collected and bulked into one bag. Adjacent to each of the twelve sites stream bank topsoil and subsoil samples were also collected. Subsoils in the fields were not considered as potential sources; only the channel bank subsoils were included. Samples of limestone were also taken from the soils at each point and adjacent stream channel beds. Samples of leaves from oak and cypress trees and fablon pollution collectors left out for six weeks were also analysed to assess the atmospheric pollution input to the soils and sediments of the catchment. The sampling strategy is shown in Figure 8.10.

Stream sediment sampling points were chosen at stages above roads and tracks in the catchment (Figure 8.5b) and in all, eight sediment mixtures were collected by bulking fine sediments across the channel at each point. Mixture 1 was a confluence mixture taken from just downstream of the confluence of the two streams. Details of all sampling points are listed in Table 8.3. The strategy covered all major soil types, geologies, land uses and topographic units in the effective catchment. At this stage it was possible to define all the potential sources of sediment which are

Figure 8.8: Variograms for Great Rollright Transects 1 (a), 2 (b), a joint v and arable soils (d)

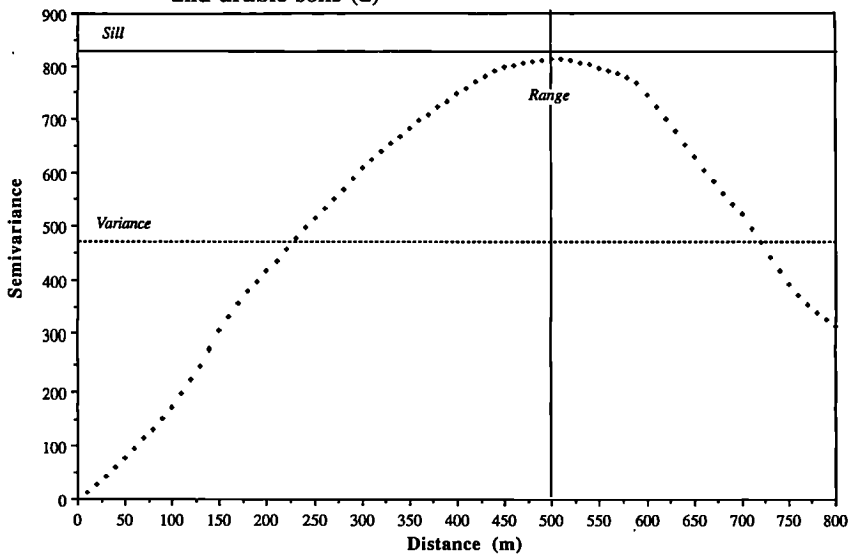

(b)

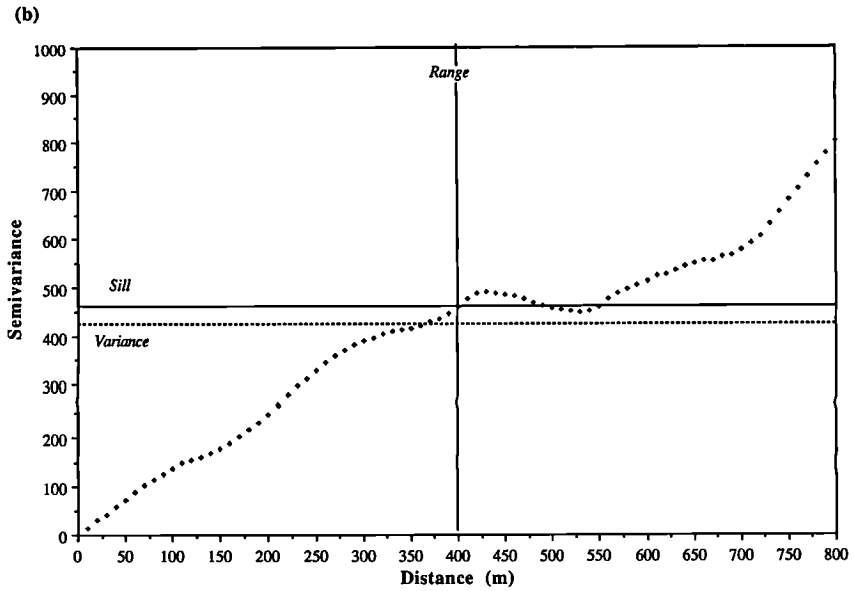

(c)

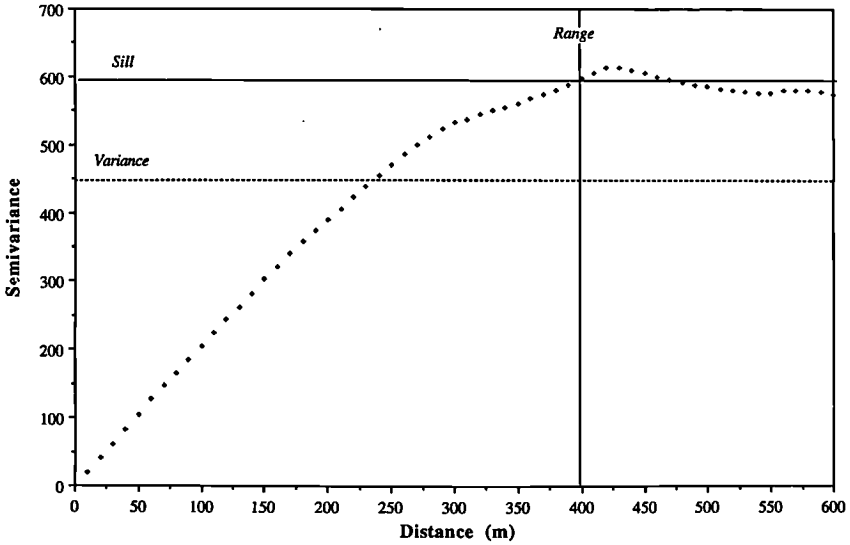

(d)

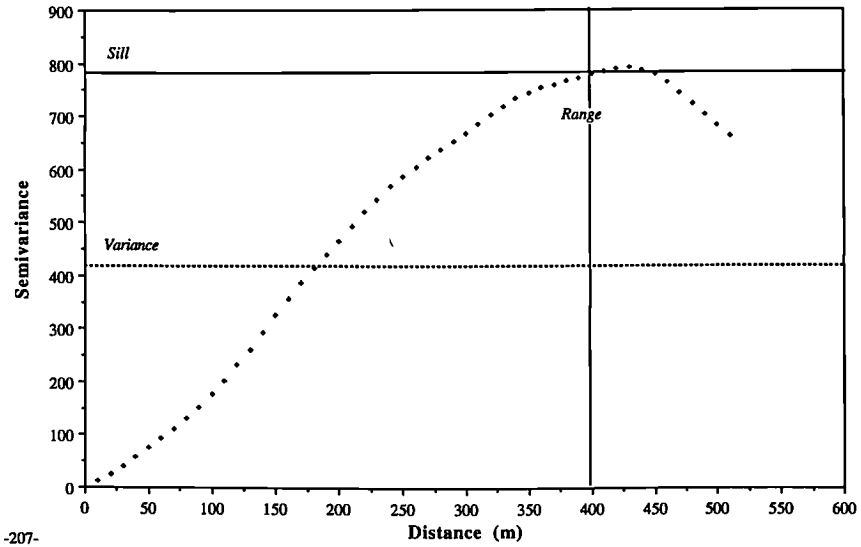

Figure 8.9: Variograms for in-field clay transect (a), rendzina transect (b)

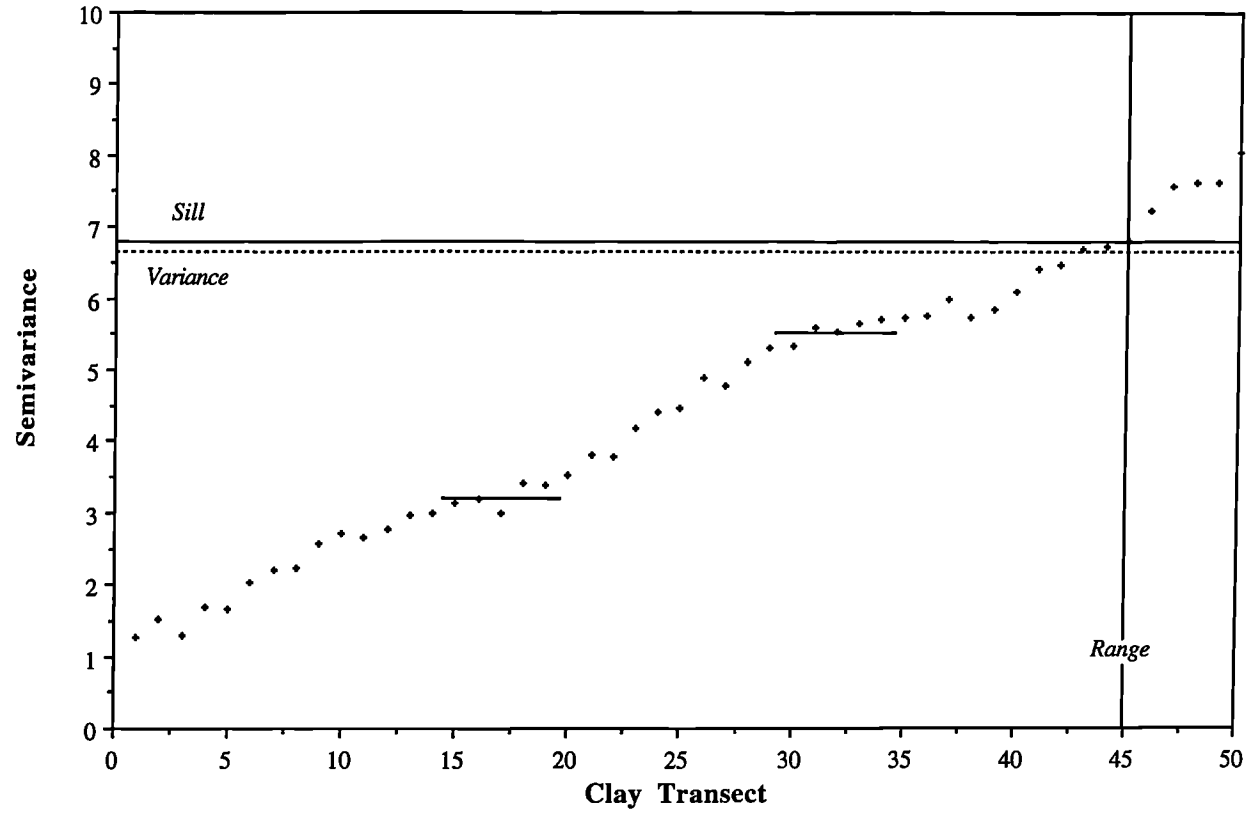

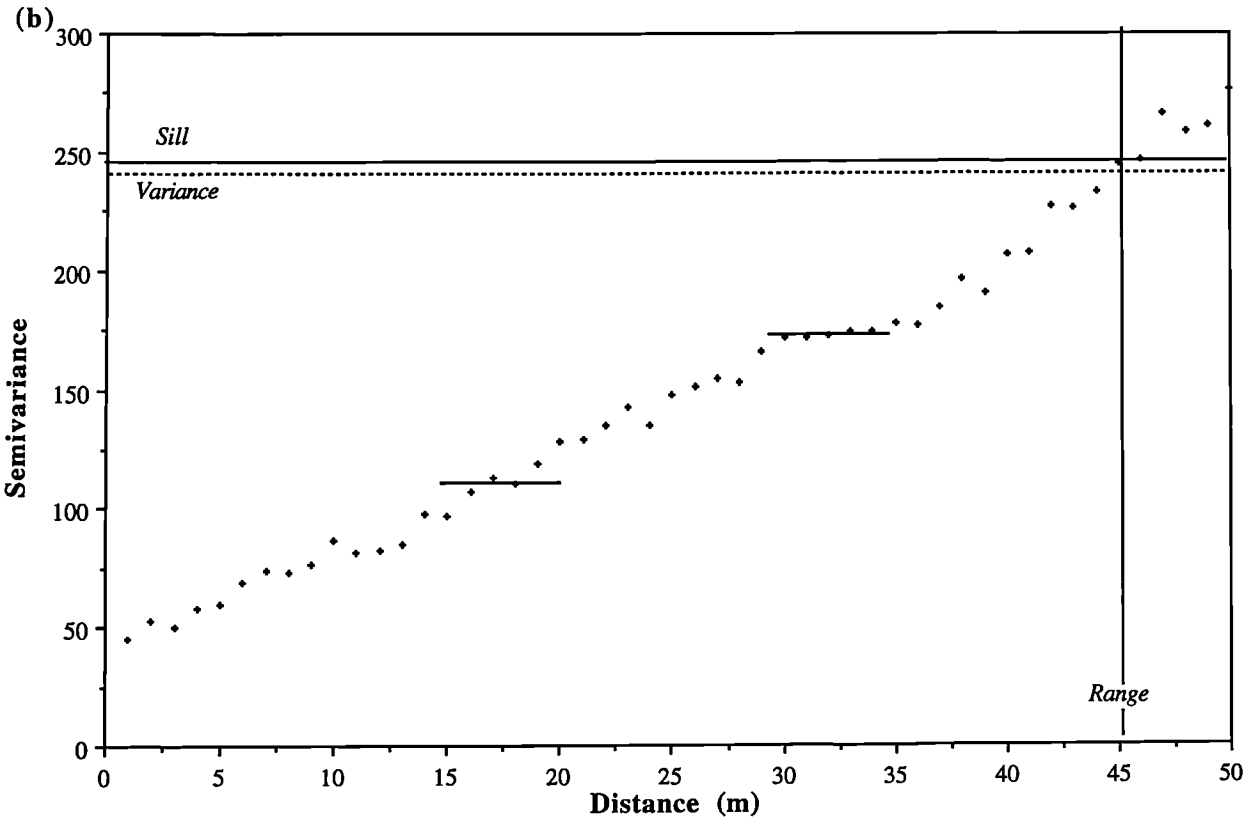

Figure 8.10: Sampling strategy

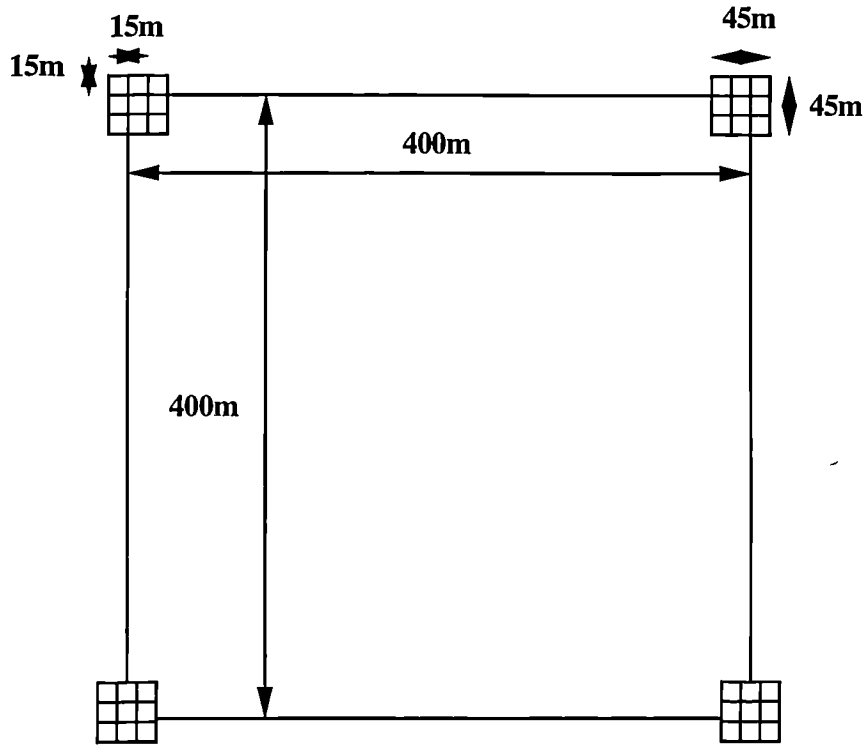

Figure 8.11: Defining potential sources within the Great Rollright Catchment

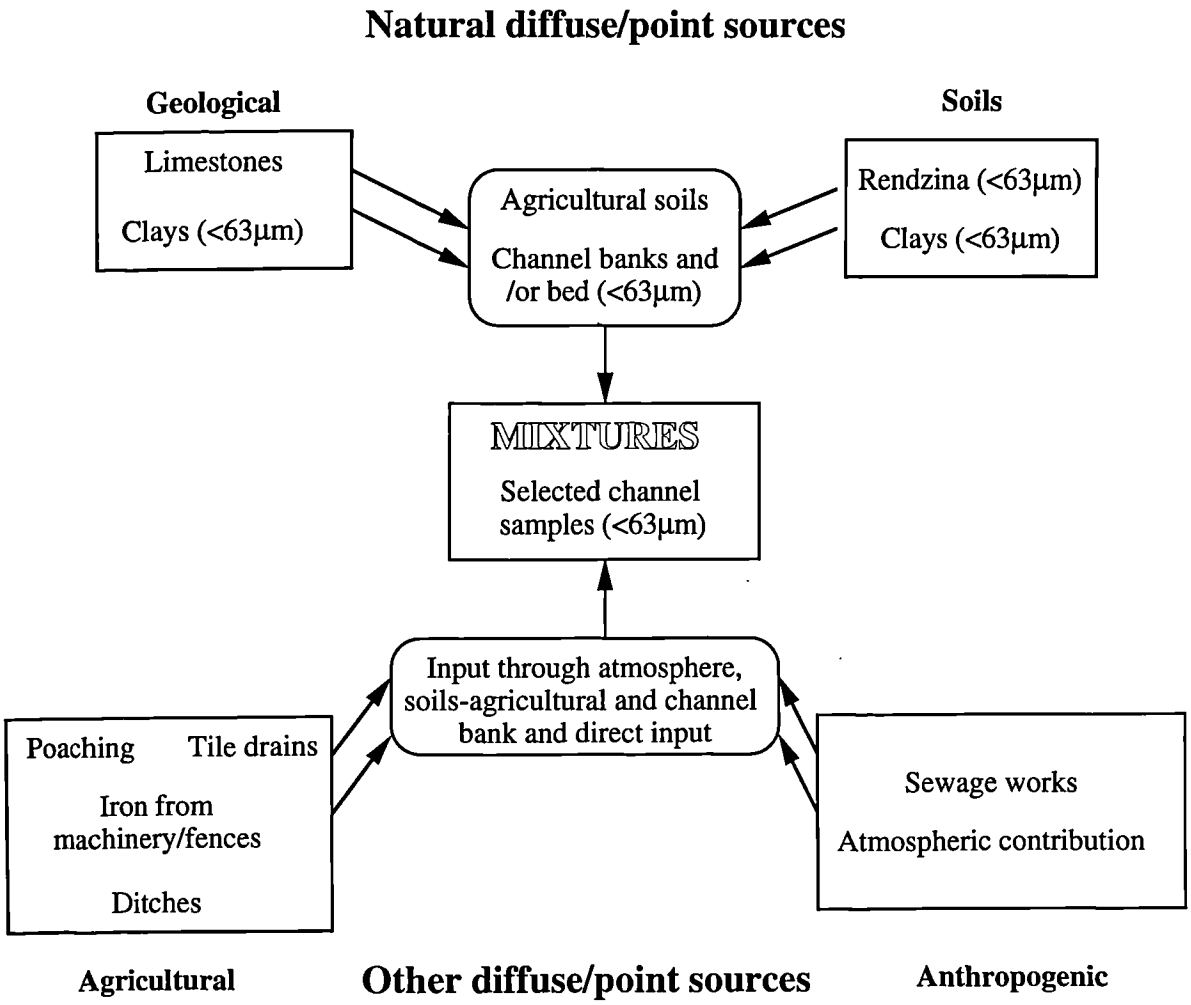

shown diagrammatically in Figure 8.11. The potential sources which have been included in this study are the natural sources. Views of many of the sampling points are shown in Plate 8.2a-i.

Table 8.3. Sample Descriptions of bulked soils and of stream sampling points (topsoils, a and subsoils, b) at each site. CNL=Chipping Norton Limestone, GO=Great Oolite, CG=Clypeus Grit, pelo-stag=pelo-stagnogley and rend=rendzina.

No	Grid ref	Soil	Geology	Land-use	Colour
1	318 302	Rendzina	CNL	Arable	10YR 4/3
1a	adjacent			Wooded/fenced	10YR 3/1
1b	"				10YR 5/2
2	318 306	Rendzina	CNL	Rough Grass	10YR 4/3
2a	adjacent			Open/marches	10YR 3/2
2b	"				10YR 4/3
3	308 310	Pelo-stag	Clay	Arable	10YR 6/4
3a	adjacent			Wooded/fenced	10YR 3/1
3b	"				10YR 5/2
4	308 314	Pelo-stag	Clay	Pasture	10YR 4/2
4a	adjacent			Open/fenced/	10YR 3/2
4b	"			bushes	10YR 4/2
5	322 302	Rendzina	GO	Arable	10YR 4/2
5a	adjacent			Open/fenced/	10YR 3/2
5b	"			bushes	10YR 5/3
6	326 302	Rendzina	GO	Arable	10YR 4/3
6a	adjacent			Open/fenced/	10YR 4/3
6b	"			bushes	7.5YR 4/3
7	330 302	Rendzina	GO	Arable	10YR 3/2
7a	adjacent			Open/fenced/	10YR 5/3
7b	"			bushes	10YR 4/2
8	330 306	Rendzina	GO	Arable	10YR 4/3
8a	adjacent			Wooded/fenced	10YR 5/3
8b	"				10YR 5/6
9	330 310	Clay/Rend	Clay/CG	Arable/Pasture	10YR 4/4
9a	adjacent			Open/marches	10YR 4/2
9b	"				2.5YR 4/3
10	330 314	Pelo-stag	Clay	Pasture	10YR 4/2
10a	adjacent			Open	10YR 3/2
10b	"				10YR 6/3
11	330 318	Pelo-stag	Clay	Arable	10YR 6/4
11a	adjacent			Open/bushes	10YR 5/2
11b	"				10YR 5/3
12	330 322	Pelo-stag	Clay	Arable	10YR 4/2
12a	adjacent			Open/bushes	10YR 4/3
12b	"				10YR 5/4

Sample Preparation and Measurement

Samples were air dried, thoroughly mixed (especially bulked soils) and sieved. The <63μm fraction of each of the bulked soils, stream topsoils and subsoils and the eight mixtures were sieved and potted into 10ml plastic pots. Twelve limestone samples and the twelve bulked soil samples were also placed in bulk into 10ml pots. Measurements made on the 78 samples were χlf, χhf, ARM and IRM's at 20, 100, 300 and 880mT.

Plate 8.2a: Rendzina field on the north bank of stream 1 near site 1.

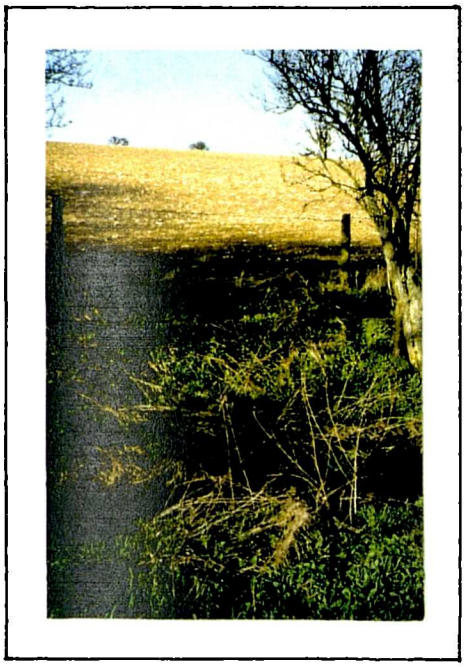

Plate 8.2b: Marshy area at the base of Danes Bottom, site 2.

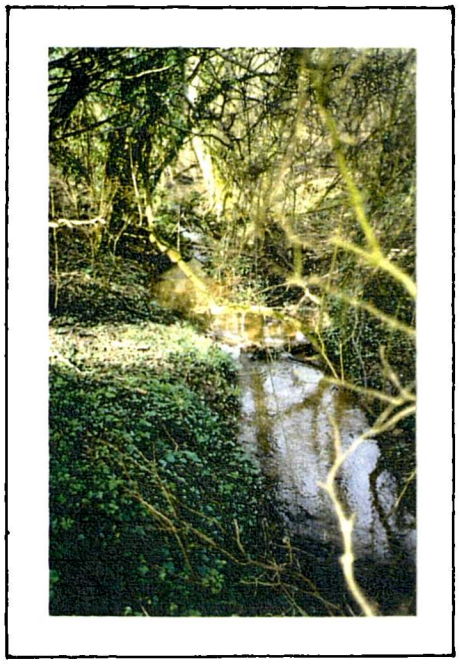

Plate 8.2c: Wooded stretch of stream 2 near site 3.

Plate 8.2e: Right angle bend in stream 1 near site 7.

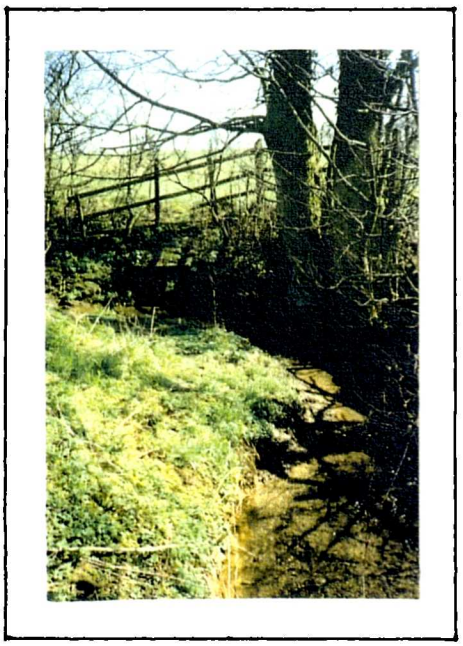

Plate 8.2d: Rendzina field either side of stream 1 at site 5. Platy limestone stones cover the fields in between streams 1 and 2.

Plate 8.2f: Sewage works on stream 1 between sites 7 and 8.

Plate 8.2g: Open banks of stream 1 and makeshift crossing near site 9.

Plate 8.2h: Tile drains and poaching delivering sediment to stream 1 between sites 11 and 12.

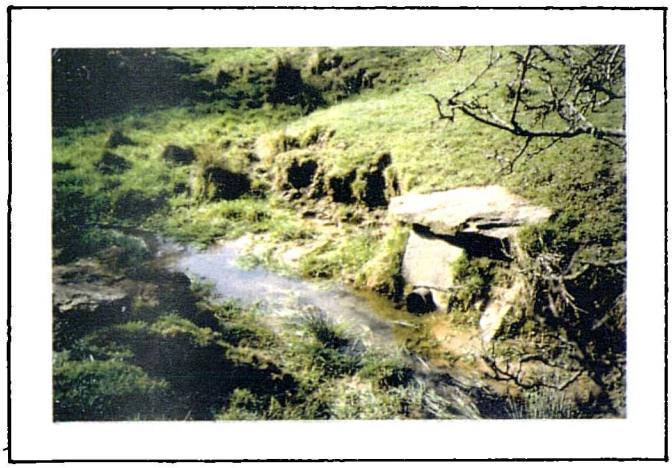

Plate 8.2i: Marshy stream 1 bed and evidence of poaching/bank collapse at site 12.

8.6 Initial Data Analysis and Results

Data for 66 (<63μm) soils and limestone samples were used in the remainder of the study. Data for the 12 bulked soil samples (not shown) were not included in further analysis other than for comparing with their respective <63μm sample results. The relationship was significant to 0.001 indicating similar discrimination in both sets of samples and justifying the use of the <63μm fraction for sourcing. Initial frequency tests on the data showed that they were slightly positively skewed with skew values of 1.2 generally. Log transformation of the data reversed the skew such that is was generally -1.8. Transformation was therefore not conducted on the data. Data were also correlated to check for collinearity between the magnetic variables such that an indication of discriminating parameters could be ascertained. Most parameters were correlated to a significance of 0.001 indicating that the use of magnetic techniques is limited. The five highest correlations between non-related variables and all the variables which were not significantly correlated are shown in Table 8.4.

Table 8.4. Selected correlation results for magnetic parameters

Variables	**R value**	**Prob.**	**N**
Significantly Correlated			
χlf v χarm	0.947	0.001	44
χarm v IRM100	0.948	0.001	44
χarm v IRM880	0.954	0.001	44
χarm v HIRM20	0.955	0.001	44
IRM20 v IRM300	0.98	0.001	44
Non-significantly Correlated			
HIRM300 v χarm	0.342	-	44
HIRM300 v IRM20	0.28	-	44
HIRM300 v IRM100	0.295	-	44
HIRM300 v IRM300	0.314	-	44
HIRM300 v IRM880	0.333	-	44
HIRM300 v HIRM20	0.348	-	44

HIRM300 offered the only independent variable from most other parameters. Although HIRM300 and IRM's 300 and 880mT are not independent parameters the values were not significantly correlated. Two bi-variate scattergrams were studied to assess the spread of the data. Figures 8.12a and b show χlf versus χfd% and χlf versus HIRM300 respectively. The first indicates the ranges in concentration of magnetic minerals versus fine-grained ferrimagnetic minerals and the second shows the concentration of magnetic minerals versus canted-antiferromagnetic minerals. The clay samples show a wide span in χfd% of between 1 and 6%, perhaps indicating that changes in waterlogging with topography cause variations in the production of fine-grained ferrimagnetic minerals (Foster et al, 1987). The concentration of the minerals within the clays is constant. The rendzinas display the opposite with constant χfd% and varying concentrations perhaps attributable to burning of the soils (Le Borgne, 1955). The stream topsoil sample from site 5 has been omitted from these plots as it showed values for χlf and HIRM300 more than twice that of the next strongest sample, indicating possible contamination from a nearby metal fence (Plate 8.2d).

Figure 8.12: Great Rollright source samples - Xlf versus Xfd% (a) and Xlf versus HIRM300 (b)

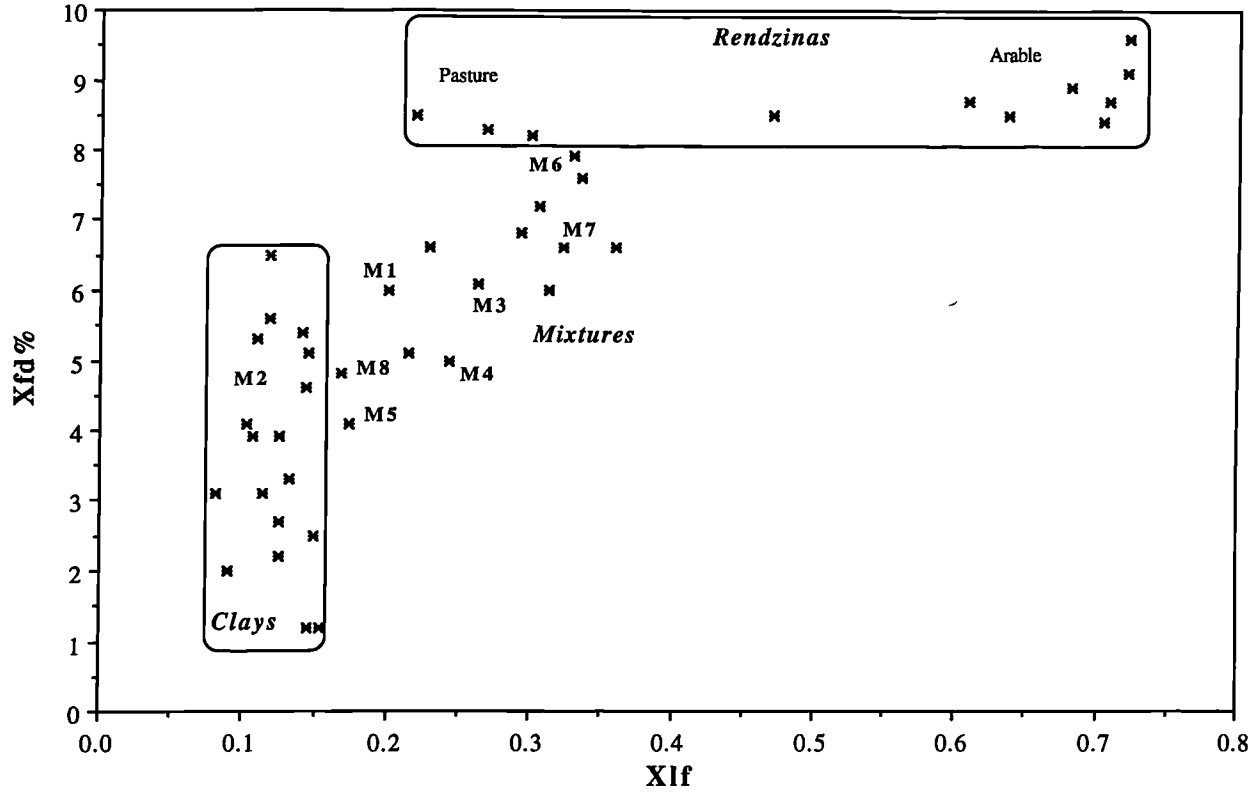

(b)

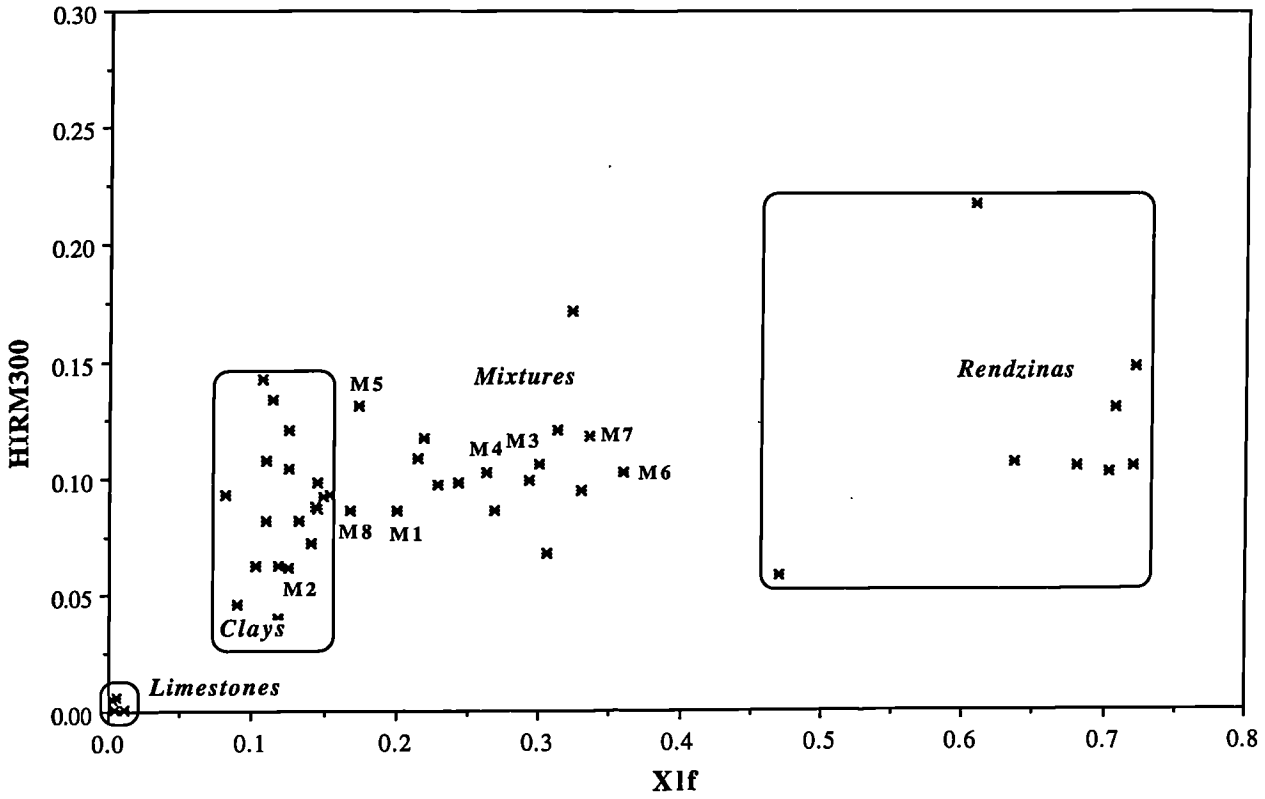

The scattergrams show that all the sediments fall within the ranges of the identified source samples. The mixtures also cross the span between clay soils and rendzina soils and mixture 1 falls centrally between those mixtures sampled from nearer the stream head-waters. Much variation is present within the two soil types and subsoil types indicating the spatial variability span covered in the sampling of different geologies, topographies and land-uses. In order to be able to model successfully a reduction in the data is required to four (or less) meaningful sediment sources (Chapter 4). The results from the pollution samples (not shown) showed that on average their magnetic contribution for one year's leaf growth was equal to that of the limestone magnetic properties and 1.15% of the rendzina topsoil using χlf and IRM880 results (urban and semi-rural leaf samples in the pollution database (Chapter 3) have been found to be highly magnetic). Pollution samples were not therefore included in subsequent analysis.

8.7 Statistical Classification Techniques

The 44 topsoil, subsoil and limestone samples were classified, first using cluster analysis and second using principal component analysis. The samples were classified using all the variables except those which are highly interrelated and prone to error (χhf, χfd and ARM). However it was found that classifying on the basis of χlf, χarm, IRM20 and HIRMs 100 and 300mT achieved the same results as using all the parameters (cf. Chapter 3).

The dendrogram produced using the variables listed above is shown in Figure 8.13. Ward's agglomeration technique was employed (cf Chapter 4). The samples classify at the coarsest scale (25) into two groups and at the finer scale (5) into five groupings of limestones, heavy field clays, stream bank clays, an intermediate group of sediments and some soils, channel bank rendzinas and field rendzinas. There is no clear distinction between topsoils and subsoils for either the clays or rendzinas in the catchment. All five categories contain both topsoils and subsoils. A principal component analysis was performed on the data and the ordination plot is presented in Figure 8.14. The routine was ill-conditioned reflecting the high correlations between the variables. This is shown in the first factor where a linear representation of all the variables except HIRMs 100 and 300 accounts for 84.4% of the variability of the data. Only two factors are significant (ie their eigenvalues are 1 and above); the second factor however has an eigenvalue of 1.00861 as opposed to the first factor eigenvalue of 10.13. Comparing the two classification techniques shows that samples B1, B5, B6, B7 and B8 are clustered into one group in the cluster analysis but are spread out on the ordination plot.

Grouping Samples into Sources

In grouping the samples into sources both classification techniques were used. Five sources were chosen, limestone, clay topsoil, clay subsoils, rendzina topsoils and rendzina subsoils. This includes four sources which are realistically discriminated and two clays which were similar but were included to test the linear modelling technique. Table 8.5 lists the samples used to construct each 'source' and Table 8.6 gives the population statistics of these sources. CV% values reflect the variability of the magnetic properties of the source groups. For example CV% is generally 30% for clays but between 25-60% for rendzinas and up to 65% for the limestones (reflecting the error in measuring such weak materials, as in Chapter 3).

Figure 8.13: Dendrogram for Great Rollright source samples using Ward's Method.

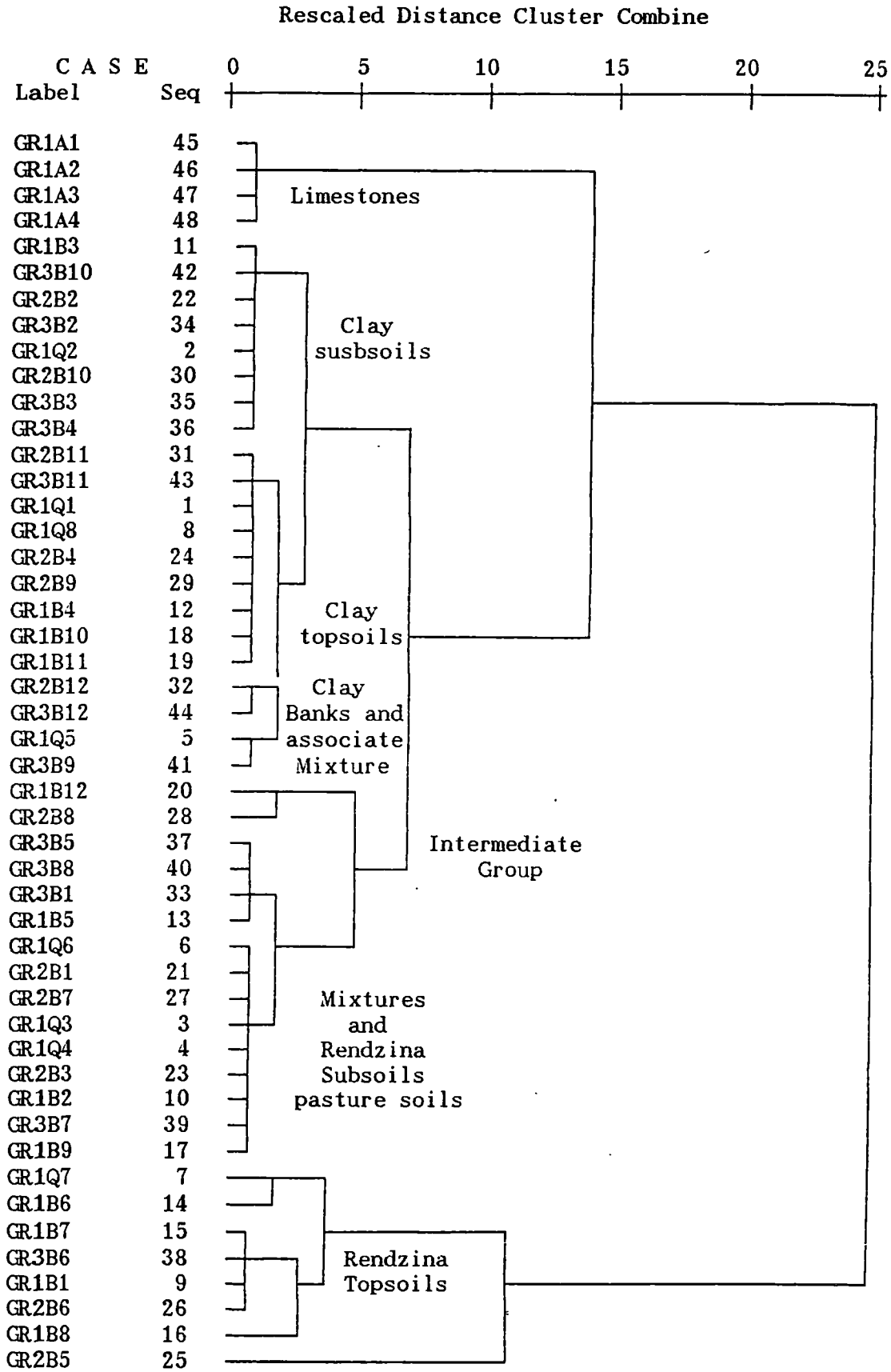

Figure 8.14: PCA ordination plot showing linear variables in relation to principal components

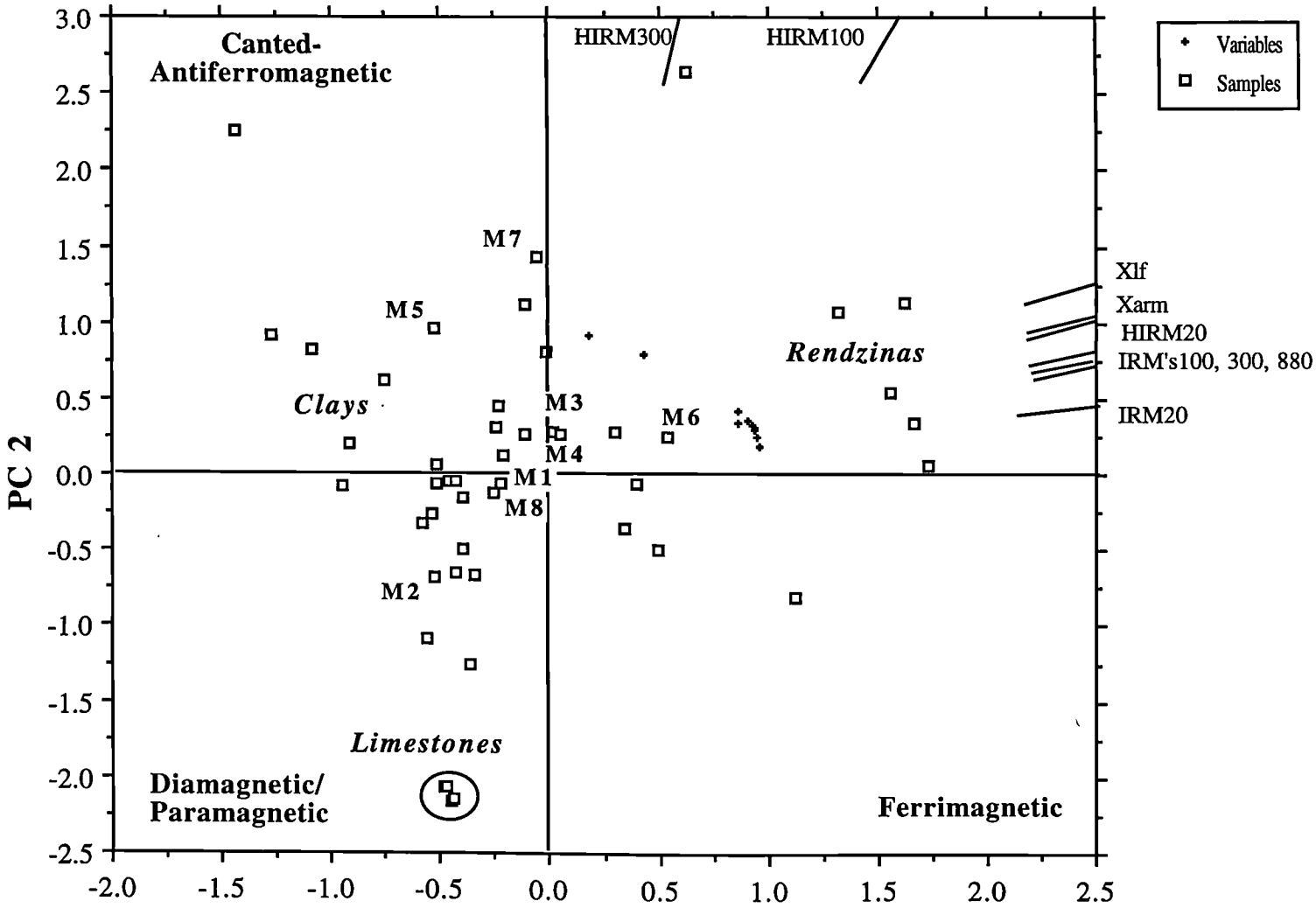

PC	*Eigenvalue*	*% of var.*	*Cum. Var.*
1	10.13	84.4	84.4
2	1.1	9.2	93.6

Table 8.5. Construction of sediment sources for modelling purposes. L=Limestone, S=stream band subsoil, T=stream bank topsoil and B=bulked field topsoils.

Geological Sources	Subsoil Sources		Topsoil Sources	
Limestones	*Rendzina*	*Clay*	*Rendzina*	*Clay*
PM S 1	*SUB S 1*	*SUB S 2*	*TOP S 1*	*TOP S 2*
L1	S1	S2	B1	B2
L2	S5	S3	B5	B3
L3	S6	S4	B6	B4
L4	S7	S9	B7	B9
L5	S8	S10	B8	B10
L6		S11	T1	B11
L7		S12	T5	B12
L8			T6	T2
L9			T7	T3
L10			T8	T4
L11				T9
L12				T10
				T11
				T12

Table 8.6. Population statistics for the grouped samples

	Var	χlf	χfd	χarm	IRM 880	IRM 300	HIRM 300
Sediment Mixtures	AVE	0.23	12.8	1.78	2.04	1.93	0.11
	STD	0.08	6.83	0.8	0.57	0.55	0.03
	MIN	0.1	4	0.65	0.8	0.73	0.06
	MAX	0.33	25.06	3.09	2.65	2.48	0.17
	CV %	33.26	53.37	45.15	28.05	28.41	28.96
	SUM	1.81	102.36	14.25	16.33	15.47	0.86
	COUNT	8	8	8	8	8	8
Limestone PM S 1	AVE	0.01		0.01	0.02	0.01	0
	STD	0		0	0	0	0
	MIN	0		0.01	0.01	0.01	0
	MAX	0.01		0.02	0.02	0.02	0.01
	CV %	55.72		22.93	30.35	21.94	65.75
	SUM	0.02		0.06	0.06	0.05	0.01
	COUNT	8		8	8	8	8
Rendzina SUB S 1	AVE	0.37	30.63	3.1	2.43	2.33	0.1
	STD	0.18	19.57	1.19	0.63	0.61	0.03
	MIN	0.23	14.81	1.74	1.66	1.56	0.07
	MAX	0.72	69.13	5.31	3.57	3.42	0.15
	CV %	48.26	63.89	38.25	26.06	26.34	26.78
	SUM	1.85	153.14	15.52	12.14	11.65	0.49
	COUNT	5	5	5	5	5	5
Clay SUB S 2	AVE	0.12	5.44	0.67	0.91	0.82	0.09
	STD	0.01	1.66	0.29	0.4	0.4	0.03
	MIN	0.11	2.62	0.32	0.46	0.32	0.04
	MAX	0.14	7.28	1.13	1.61	1.5	0.14
	CV %	9.41	30.58	43.36	43.66	49.06	38.52
	SUM	0.85	32.63	4.02	5.47	4.94	0.53
	COUNT	7	6	6	6	6	6

Table 8.6 continued

	Var	χlf	χfd	χarm	IRM 880	IRM 300	HIRM 300
Rendzina TOP S 1	AVE	0.65	51.51	4.59	4.07	3.96	0.11
	STD	0.38	28.72	1.86	1.85	1.84	0.04
	MIN	0.29	18.32	2.28	2.42	2.32	0.06
	MAX	1.68	121.06	8.98	9.14	9.04	0.22
	CV %	58.45	55.76	40.55	45.31	46.57	33.29
	SUM	6.47	515.14	45.9	40.74	39.59	1.15
	COUNT	10	10	10	10	10	10
Clay TOP S 2	AVE	0.15	6.67	1.05	1.21	1.11	0.09
	STD	0.06	6.46	0.56	0.44	0.44	0.02
	MIN	0.08	1.57	0.27	0.46	0.37	0.05
	MAX	0.3	24.09	2.44	2.01	1.9	0.13
	CV %	37.01	96.97	53.62	36.71	39.2	23.29
	SUM	2.11	93.33	14.73	16.89	15.57	1.33
	COUNT	14	14	14	14	14	14

Some results of Table 8.5 are presented in Figure 8.15 for the discriminatory parameters χlf and HIRM300. This highlights the relationships between the groups of samples and their minima, maxima and standard deviations (sd). Only one standard deviation measure was used as values of the mean-1sd were very similar to the minimum values of the source groups. This is shown in the figure and the range between the mean±1sd is used in the linear modelling. It is clear that the two clay sources and even the rendzina sources are relatively close and the significance of this is shown in the linear modelling results in the next section. Overall the rendzina and clay topsoils and limestones are the best discriminated sample groups.

8.8 Linear Modelling

Linear modelling was carried out on 108 separate files of the 8 mixtures and an average mixture (mixave). For each of the mixtures and mixave the source proportions were found using the source variable means, the mean-1sd and the mean+1sd. This would give a range of possible proportions which each source may contribute to the mixtures in terms of the natural variability of the source properties in the catchment. Variables used in the modelling are those linear measurements and calculated variables used in the classification routines, χlf, χarm, IRMs 20, 100, 300 and 880 and HIRMs 20, 100 and 300. Four test source configurations were carried out in the linear modelling of the stream sediments. These were chosen because the clay topsoils and subsoils, and the rendzina topsoils and subsoils, were magnetically similar. Table 7 gives details of the modelling routines carried out. Two routines included four sources, the third included three sources and the fourth included only two sources.

Table 8.7. Sources used in the four linear modelling routines. Source codes are as for Table 8.4.

Routine	x1	x2	x3	x4
1	PM S 1	SUB S 1	SUB+TOP S 2	TOP S 1
2	PM S 1	SUB S 2	TOP S 1	TOP S 2
3	PM S 1	SUB+TOP S 2	TOP S 1	-
4	-	SUB+TOP S 2	TOP S 1	-

Figure 8.15: Identifying ranges of grouped sample 'sources', asterixes indicate mean, minimum, maximum, mean-1sd and mean+1sd

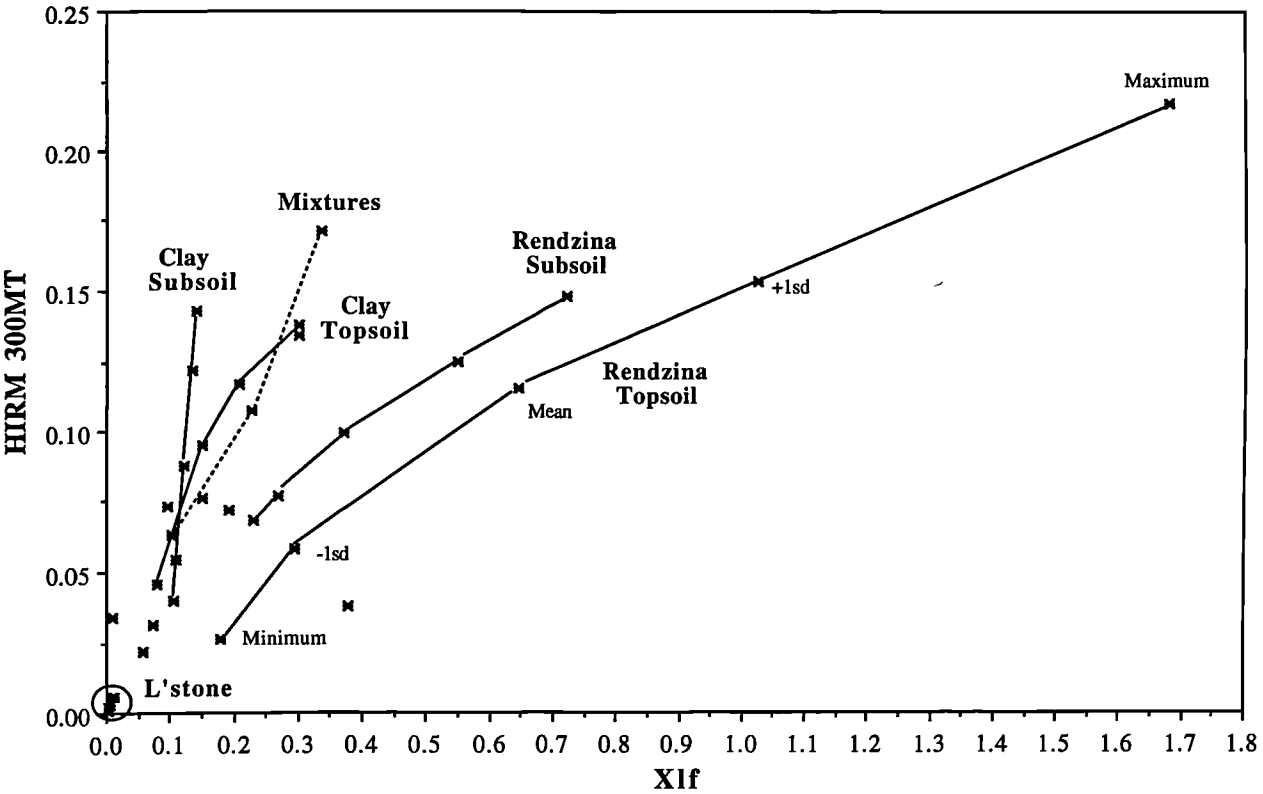

Figure 8.16: Explaining failure in linear programming applied to sediment sources of Great Rollright

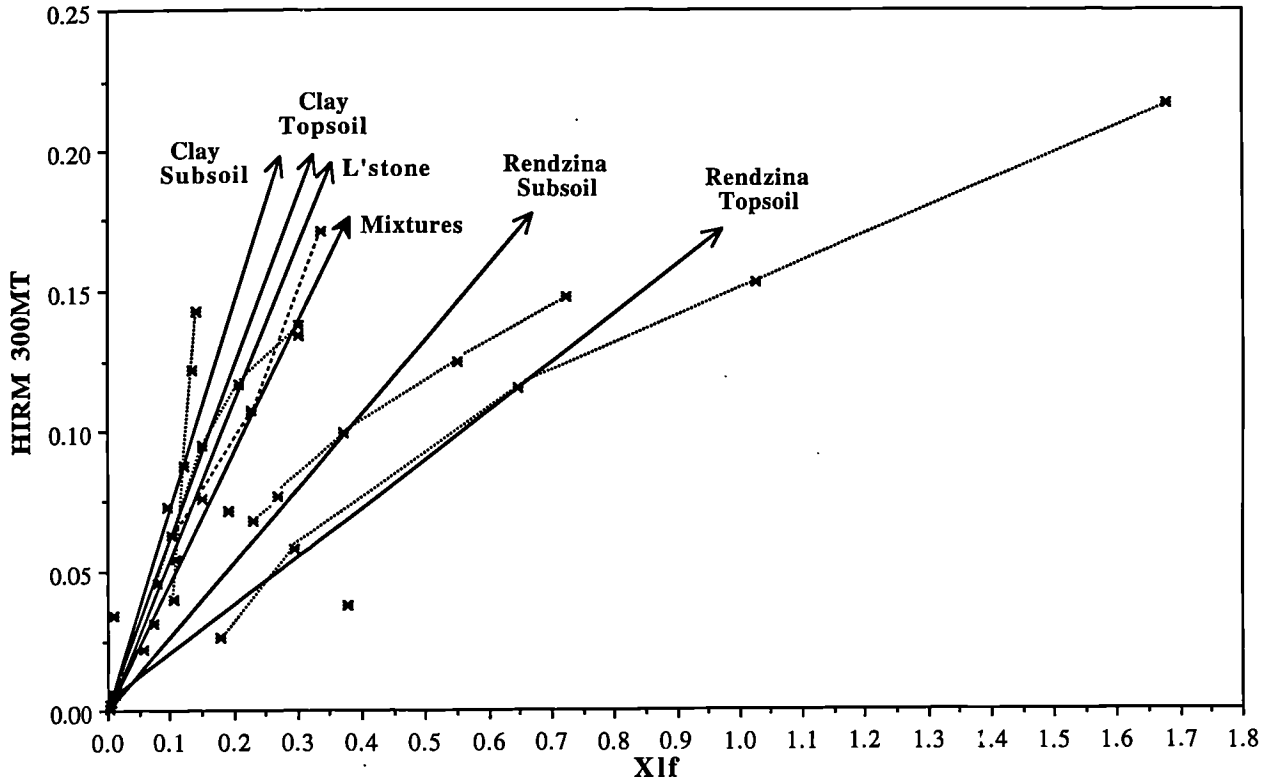

Results of the linear programming are given in Table 8.8. Errors given in the linear programs were between 0.1 and 0.5. This allows, for example, a 12.3% variation on the IRM880 of the rendzina topsoil (magnetically the strongest source) in which 'multidimentional space' LINDO can find a solution. This reflects both errors associated with the routine and linearity discussed in Chapter 4 and with the natural variability within the source sample sets.

Table 8.8. Results of the linear programming routines (a) routine 1, (b) routine 2, (c) routine 3 and (d) routine 4.

(a) routine 1

Mixture Number	Source Values	x1 Limestone	x2 Rend Sub	x3 Clay Ave	x4 Rend Top
1	Mean	59.1	0	0.53	40.38
	Mean-1sd	10.92	68.01	0.45	20.62
	Mean+1sd	72.49	0	0.47	27.08
2	Mean	81.22	0	0.47	18.32
	Mean-1sd	61.0	23.44	0.54	15.02
	Mean+1sd	87.3	0	0.33	12.36
3	Mean	46.52	0	0.48	53.0
	Mean-1sd	0	34.43	0.41	65.16
	Mean+1sd	61.86	0	0.38	37.77
4	Mean	48.67	0	0.51	50.82
	Mean-1sd	0	0	0.35	99.65
	Mean+1sd	57.44	0	0.31	42.25
5	Mean	45.9	28.31	0.92	24.87
	Mean-1sd	7.77	91.1	1.14	0
	Mean+1sd	72.26	0	0.84	26.9
6	Mean	17.31	56.38	0.43	25.88
	Mean-1sd	0	0	0	100
	Mean+1sd	43.14	32.94	0.38	23.54
7	Mean	15.29	50.66	1.04	33.02
	Mean-1sd	0	0	0	100
	Mean+1sd	36.38	44.82	8.23	17.98
8	Mean	63.02	0	0.59	36.39
	Mean-1sd	12.07	87.43	0.5	0
	Mean+1sd	75.52	0	0	24.48
Mixave	Mean	42.86	21.97	0.6	34.56
	Mean-1sd	0	53.48	0.62	45.9
	Mean+1sd	67.85	0	0.57	31.58

(b) routine 2

Mixture Number	Source Values	x1 Limestone	x2 Clay Sub	x3 Rend Top	x4 Clay Top
1	Mean	0	0	14.69	85.31
	Mean-1sd	0	0	61.61	38.34
	Mean+1sd	0	24.10	3.56	72.34
2	Mean	33.33	3.03	0	63.63
	Mean-1sd	14.94	0	10.34	74.71
	Mean+1sd	32.79	56.63	0	10.59
3	Mean	0	0	36.44	63.56
	Mean-1sd	0	0	100	0
	Mean+1sd	0	11.77	17.38	70.85
4	Mean	0	0	38.0	62.0
	Mean-1sd	0	0	100	0
	Mean+1sd	0	0	19.7	80.3

Table 8.8 continued

Mixture	Source	x1	x2	x3	x4
5	Mean	0	0	27.54	72.46
	Mean-1sd	0	0	78.57	21.43
	Mean+1sd	0	0	8.23	91.77
6	Mean	40.39	0	59.61	0
	Mean-1sd	0	0	100	0
	Mean+1sd	0	71.52	28.48	0
7	Mean	0	28.16	54.68	17.16
	Mean-1sd	0	0	100	0
	Mean+1sd	0	48.68	30.37	20.95
8	Mean	0	0	17.8	82.2
	Mean-1sd	0	0	68.03	31.97
	Mean+1sd	0	34.27	5.57	60.16
Mixave	Mean	0	0	26.27	73.73
	Mean-1sd	0	0	79.91	20.09
	Mean+1sd	0	18.23	10.8	70.97

(c) routine 3

Mixture Number	Source Values	x1 Limestone	x2 Clay Ave	x3 Rend Top
1	Mean	0	79.87	20.13
	Mean-1sd	0	37.39	62.61
	Mean+1sd	0	90.59	4.41
2	Mean	27.1	72.9	0
	Mean-1sd	0	89.9	10.06
	Mean+1sd	50.0	50.0	0
3	Mean	0	59.2	40.8
	Mean-1sd	0	0	100
	Mean+1sd	0	83.21	16.79
4	Mean	0	50.7	49.3
	Mean-1sd	0	10.68	90.32
	Mean+1sd	0	78.35	21.65
5	Mean	0	66.89	33.11
	Mean-1sd	0	7.55	92.45
	Mean+1sd	0	89.27	10.73
6	Mean	40.46	0	59.54
	Mean-1sd	0	0	100
	Mean+1sd	18.49	54.77	26.34
7	Mean	0	47.65	19.83
	Mean-1sd	0	0	70.44
	Mean+1sd	0	74.66	25.34
8	Mean	0	80.17	19.83
	Mean-1sd	0	29.56	70.44
	Mean+1sd	12.29	78.92	8.79
Mixave	Mean	0	68.58	31.42
	Mean-1sd	0	19.57	80.43
	Mean+1sd	2.23	86.4	11.37

(d) routine 4

x1 Clay Ave	x2 Rend Top
79.87	20.13
37.39	62.61
97.18	2.92
100	0
89.94	10.06
100	0
59.23	40.77
0	100
82.13	17.87
50.68	49.32
10.7	90.3
78.06	21.94
66.89	33.11
20.87	79.13
90.36	9.64
55.03	44.97
0	100
77.52	22.48
80.17	19.83
26.52	73.48
77.52	22.48
80.17	19.83
26.52	73.48
94.98	5.02
68.58	31.42
9.09	90.91
89.29	10.71

In Table 8.8 source proportions attributed to each of the soil and geology sources are different. For example from routine 1 and using mean values, sediment mixture 1 has mainly 59% limestone and 40% rendzina topsoil. In routine two it is attributed 15% rendzina topsoil and 85% clay topsoil and in routines 3 and 4 80% clay and 20% rendzina are attributed. The results are contradictory for each mixture especially between routines 1 and 2. LINDO

unfortunately cannot learn (gain knowledge) from previous experience and realistic environmental knowledge; the linear relationships between variables are taken for each file as it stands. The ranges of contributions modelled for the mean±1sd are large. For instance, for sediment 1 the range of the limestone input varies between 11 and 73%. Often in the routines where the mean±1sd source values have been used other sources are identified which were not identified when using the mean values. For instance for sediment 1 rendzina subsoil is identified rather than limestone when using mean-1sd source values.

Taking another specific example, mixave, routine 1 gave source proportions of 43% limestone, 22% rendzina subsoil and 35% rendzina topsoil, yet in Figure 8.16 the mixave plots are nearer the clays. In routine 2 the sources were 27% rendzinas and 73% clays giving a more reasonable answer. Even for those mixtures lying in clay areas, for example mixture 2, in routine 1 weight was placed on limestone rather than clay as a contributing source; while in routine 4 for mixture 2, source contributions were more realistically between 90 and 100% clays and 0 and 10% rendzina topsoil. Mixture 3, however, in routine 4 has a large overlap in range of contributions ranging between 0 and 83% clays and 17 and 100% rendzina topsoils.

The results can best be explained with reference to Figure 8.16 which is similar to Figure 8.15 but linear vectors have been drawn from the origin to each of the source mean values. The vector for the limestone source is similar to that of the clay subsoils and topsoils, and the two rendzina sources are more separated. In the case of routine 1, the linear programming identifies the limestone over the clays as a large sediment source. The program will not find a realistic solution for the clays but uses the small values of the limestones mathematically to dilute the effects of the rendzinas. Similarly the program does not discriminate the rendzina topsoil and subsoils well: either one or the other is given a substantial proportional contribution. The range of proportions for each mixture between the mean±1sd is large for the rendzina topsoil source and varying by up to 50%.

In routine two, a similar phenomenon occurs, where solutions are found between the clay topsoil and rendzina topsoil, but clay subsoil and limestone largely have zero contributions. There is more continuity in this routine between the mean and mean±1sd results. Variation is large however with contributions between 1 and 50% for the clay and rendzina topsoils. For most of the mixtures in routine 2 where the mean+1sd is used, proportions are given for clay subsoils and topsoils, caused by better discrimination between these values rather than the means and mean-1sd (see Figure 8.16). Routines 3 and 4 gained similar results, with source proportions being split between the rendzina topsoils and clays. In three cases limestone was recognized as contributing sediment particles pulling the model away from the clay contribution through the collinearity of these sources (Figure 8.16). A contributory cause of additivity problems is that the maximum mixture values of the best discriminatory variable, HIRM300, fall outside the range of the source maximum values. This is caused by HIRM300 being a difference parameter rather than an initial measurement. This is not the case for the ferrimagnetic concentration parameters. Also the mean of the rendzina topsoils and subsoils equals that of the mixture averages for HIRM300 which is the reason why a mean of the rendzina top and subsoils has not been used.

8.9 Discussion

The two main soils in this case study represent the best case for the modelling of magnetic properties of transported materials. None of the sources is sufficiently magnetically strong to mask the other sources, even the diamagnetic limestone. The large overlaps in source contributions when solving for a ±1sd range stem from the environmental variability in the soils of the catchment. This variability must outweigh any errors incurred during the artificial mixing experiments presented in Chapter 4. This modelling work includes the statistical variation within the source units, therefore the results can be taken as a good guide even with the large overlapping ranges in contributions from the different sources.

Error terms used in the modelling of 0.1 and 0.5 units of each variable represent large percentages of the original source measurement values. For example for IRM880 an error of 0.5 allows 12.3% error of the rendzina topsoil and 1000% error on the limestone values. The fact that the program cannot find a solution within smaller multiple error space is a factor of the scale between sources based on ferrimagnetic concentration (rather than good discriminatory factors with less variability). These modelling errors account for measurement error on the sources and mixtures as well as variability of the source samples, however.

The results for linear modelling routine 4, a two-source model could have been found using simultaneous equations for each magnetic measurement and the results averaged (Chapter 3). However the advantage of the linear programming technique is that an error term reflecting the variability in the data set can be included and an overall result obtained for many parameters. The results for each mixture for the two topsoil sources seem to make sense in consideration of the environmental conditions at each site. Site 1 for example is fenced from the rendzina fields and the sub-banks are clayey but sediments will be received from upstream where rendzinas may contribute. So the source proportions are probably reasonable at 80% clay and 20% rendzina (Table 8.8)

For the most part the stream beds are armoured with limestone. This therefore has to be considered as a source but unlike the minerogenic soils, limestone particles may not exist in the <63μm fraction but will probably be dissolved in the stream water. Mixture 2 however was collected from a bed which was predominantly clayey and a value of between 90 and 100% clay is realistic. Further upstream from Danes Bottom at the site of mixture 8, soils are again clay but tile drains deliver sediments from rendzina fields to the north of the valley. So a result here of between 27 and 95% clay and 5 and 73% rendzina is typical of those mixtures where there are clear sources of both soil types. Mixtures 6 and 7 from near the head-waters of the larger stream are similar to this where tile drains from rendzina fields (Plate 8.2h) deliver sediments to a predominantly clayey area. These two mixtures however were collected from aggrading areas of the stream where there was a farm track and road partially blocking the streams course. It could be possible that growth and decomposition of marsh plants, bacteria (Fassbinder et al., 1990) or formation of other ferrimagnetic minerals (greigite for instance, Stanjek et al., 1994) especially in the drier months here could be contributing fine-grained ferrimagnetic minerals to the sediments. Mixtures 3, 4, 5, 6 and 7 have more or less 50:50 results for the two topsoils and overlapping ranges but these reflect the clayey subsoils in the streams and

the input of rendzina top soils either from channel banks or the arable fields. Also it is noted that correction for organic matter was not carried out for these soil sources and sediment mixtures as it was believed that the organic content was very low in the <63μm fraction.

Unfortunately it may rarely be the case using magnetism that the channel bank sources and field sources can be discriminated and modelled much more than as topsoil and subsoils. It is clear here that the results are reasonable, even when considering the sediments as sources of the confluence mixture which fall centrally to the other stream sediments. Care must be taken in the interpretation however for the reasons outlined above and at best the modelling results serve only as a guide. Fortunately at this site contamination was at a minimum with only one affected sample. At sites where more contamination is evident in the form of scrap metal, for instance, the sourcing will be made very difficult depending on the effect and time rust metal lasts in the environment and its transportation mode in a river system. Also atmospheric contributions could not be identified significantly in this catchment. Other workers (Foster et al, 1987b, Hunt, 1986 and Thompson and Oldfield, 1986) have tried to quantify the atmospheric contribution in various environments from urban sites to lake sediments, peats and soils.

8.10 Summary

This case study has shown the drawbacks and limitations of the methodological framework as applied to a catchment system. Throughout it has been seen that even when considering only two sources the ranges of proportions can be very large. Natural variability within the catchment has been assessed and included to some extent in the modelling routines. This represents a major step in the application of modelling techniques to catchments where in the past spatial variability of possible sources has not always been fully considered (Chapter 5). The source contributions calculated have given sensible results in terms of the environmental situation of each sediment mixture.

The methodological framework set out by the experimental and theoretical work in Chapters 4 and 5 has been applied to this case study. The methodological routes followed through this case study have been highlighted on Figure 8.17. Delineation of the area of interest involved an identification of 'effective catchment' and sediment sources were identified spatially through field kappa survey. Variograms have identified the boundaries within the catchment related to geology and soil type and have indicated the level of sampling required. In this case data were not transformed and were not as highly inter-correlated as that of the Holderness case study. Even so the results show that inter-correlation on any scale causes many problems for physical geographers to analyse data quantitatively. Classification techniques allowed the source samples to be grouped and four main sediment sources were identified. Linear modelling was however greatly influenced by collinearity and intercorrelation within the data set. Interpretation of future magnetic sourcing results can only be made with regard to the full range of environmental variability as well as experimental errors. In future application of the methodology to catchment studies great difficulties may be encountered when sources are not as well discriminated as those found at Great Rollright.

Figure 8.17 : Methodological framework and routes taken in Great Rollright study

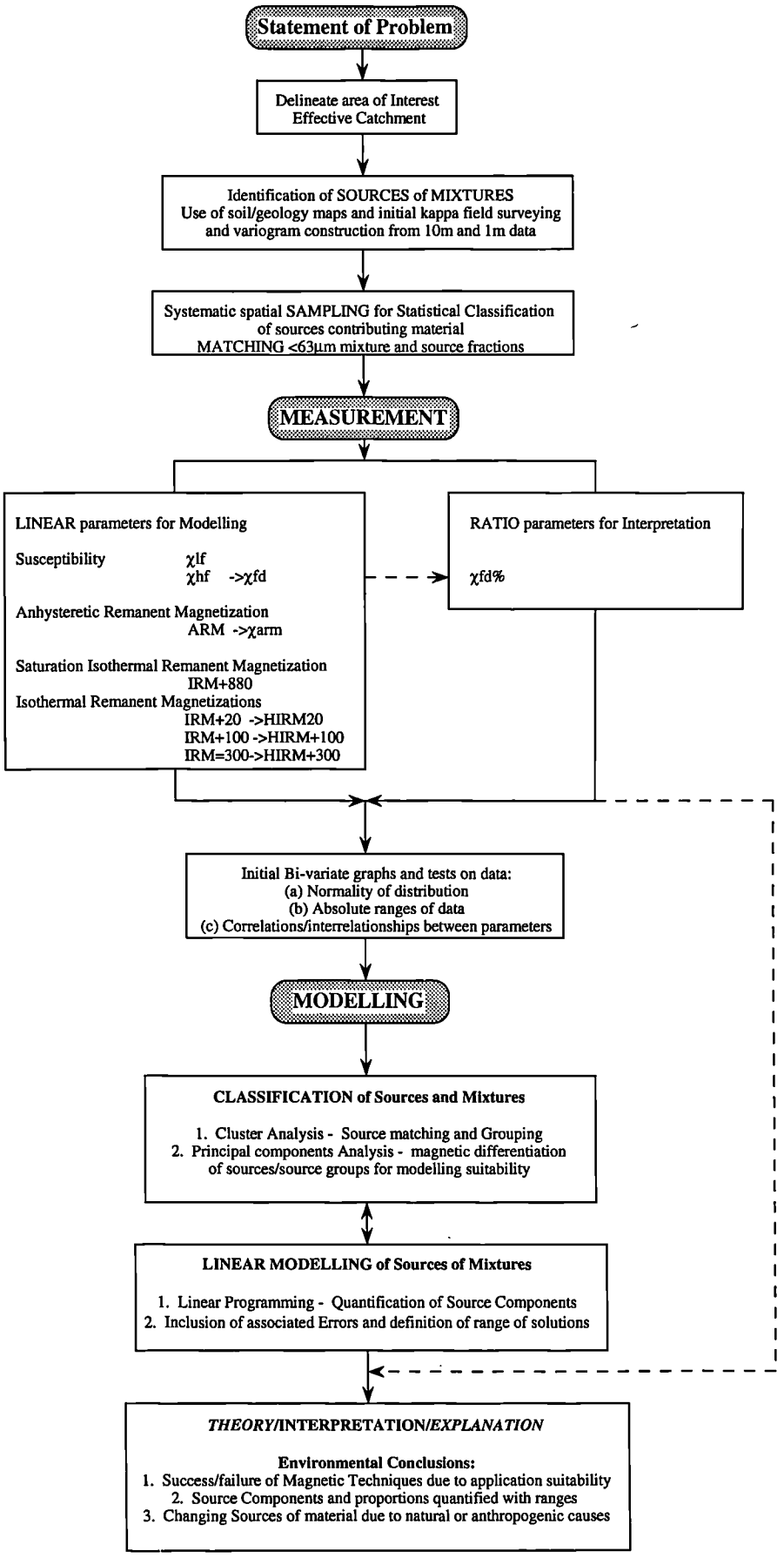

CHAPTER 9

Modelling Minerals in Environmental Materials using Hysteresis Loops

9.1 Introduction and Aims

Less literature is available on the modelling of minerals than on the sources of mixtures. Hysteresis loops can be used to model mixtures of minerals but this is less well evaluated in the literature. An introduction to the use of hysteresis loops is given in Thompson and Oldfield (1986). They illustrate how sediments from Chesapeake Bay were discriminated using hysteresis loops where different shapes of the loops indicate different minerals. Wasilewski (1973) also discusses magnetic hysteresis in natural materials, and presented results for geological samples including basalts, meteor and lunar samples. The materials were discriminated on the basis of their mineral content using coercivity, remanence and magnetization parameters. More recently, Borradaile et al.(1993) have used hysteresis loops and related parameters to discriminate between 116 limestone samples from 92 locations. Pelagic, dolomotized, shallow-subtidal, backreef-lagoonal and reef limestones are found to have different magnetic mineralogies and are either diamagnetic, paramagnetic or ferrimagnetic. For instance pelagic limestones contained MD magnetite grains which had paramagnetic properties. Samples were successfully classified even though they were magnetically very weak, thus highlighting one of the advantages of using accurate magnetic hysteresis data.

Several studies have used hysteresis loops to describe the mineralogies of soils and deposited sediments. Sandgren and Thompson (1990) used hysteresis loops to highlight the mineralogical differences between podzolic subsoils and topsoils developed on sand dunes in Poland. In the study of magnetic properties of Chinese loess, Liu et al (1991) have used hysteresis loops and derived parameters to describe the mineralogy of loess layers. In lake sediment studies Snowball (1993) recently used hysteresis loops to infer mineralogical phases in lake cores in Sweden. Variations in ferrimagnetic and paramagnetic components were described from the curved open sections of the loops at low fields and the constant increase in magnetization at high fields respectively.

No work to date has successfully modelled hysteresis curves of different magnetite grain sizes. The work by Thompson (1986) and Maher and Thompson (1992) represents the most quantitative results of mineral concentrations and different grain size concentrations in materials so far (namely lake sediments and loess/palaeosols respectively). Using synthetic materials Kwun and Burkardt (1986) studied the effects of grain size, hardness and stress on the hysteresis properties of ferromagnetic steels. Grain size was found to have minimal effects on the hysteresis loops of the steels; hardness and stress, however, had a significant influence on the loops. Dunlop et al. (1993) have also studied the effects of particle-size shape and spacing on the hysteresis properties of uniaxial iron particles. Measurements were made parallel and perpendicular to the long axis of the grains and the hysteresis properties were markedly anisotropic (needed for recording media!). Hysteresis loops measured parallel to the long

axis of the grains were rectangular (similar to SD grain characteristics) whilst grains measured at a perpendicular orientation showed little hysteresis. The effects of interaction between grains were studied in magnetite and hematite dilutions by Maurisch et al. (1987). Minerals were crushed mechanically and diluted in volumes of between 0.1-5% (magnetites) and 1-10% (hematites). Unfortunately, no linearity calculations were made on the properties of the dilutions but effects of interaction between grains in the samples significantly affected hysteresis parameters.

In this final case study an attempt is made to model the magnetic minerals found in various environmental materials, mainly soils. Four main groups of minerals can be identified in materials: diamagnetic, paramagnetic, canted-antiferromagnetic and ferrimagnetic minerals. Minerals which belong to these four groups have been discussed in Chapter 2. Primary, secondary (eg. Blakemore, 1975) and atmospheric (eg Hunt et al, 1984) magnetites (and maghemites) contribute to the ferrimagnetic component and hematite, goethite and other clay minerals contribute to the canted-antiferromagnetic component. Transition elements and some clay minerals, salts and some superparamagnetic magnetite grains contribute to the paramagnetic component and finally silica, carbon and organic matter making up the diamagnetic component. Quantification of such components can indicate various sources of minerals in soils including parent materials, soil processes and the atmosphere.

The majority of this work utilizes hysteresis data of known mineral types, but no artificial mixtures are used. Hysteresis data, as outlined in Chapter 2 (and in Paper 3, Appendix 7 in more detail) includes parameters which describe the four magnetic properties listed above. The parameters in use have been shown in Figure 2.2 and are described further in Appendix 1. In this case study these hysteresis parameters have not been intensively used; instead the linearly additive magnetization data measured at 42 fields between ±1000mT were used. Two sets of minerals were used in this study: a set of geological minerals obtained from Birmingham Geology Department and some samples taken from the synthetic database. Figure 9.1 shows diagrammatically the mineral and synthetic source components used for modelling in this chapter and the geological minerals used are shown in Plate 9.1.

The main aims of this chapter are to determine the following magnetic components in soil and sediment samples using the sets of geological and synthetic minerals:

1. The ferrimagnetic component using mineral and synthetic magnetite.
2. The canted-antiferromagnetic component using mineral and synthetic hematite/goethite.
3. The paramagnetic component using mineral lepidocrocite and synthetic manganous carbonate.
4. The diamagnetic component using chalk and synthetic barium sulphate.

Mineral Sources and Soil Sampling

Geological minerals have been included in this study to compare and contrast their properties and modelling results with those of the synthetic minerals. To the author's knowledge such a comparison has not been made before. There are difficulties in choosing mineral sources as there is great variety in the magnetic properties of any one mineral type in the environment and in synthetic minerals. This presents problems of variation in the source

Figure 9.1: Modelling Minerals

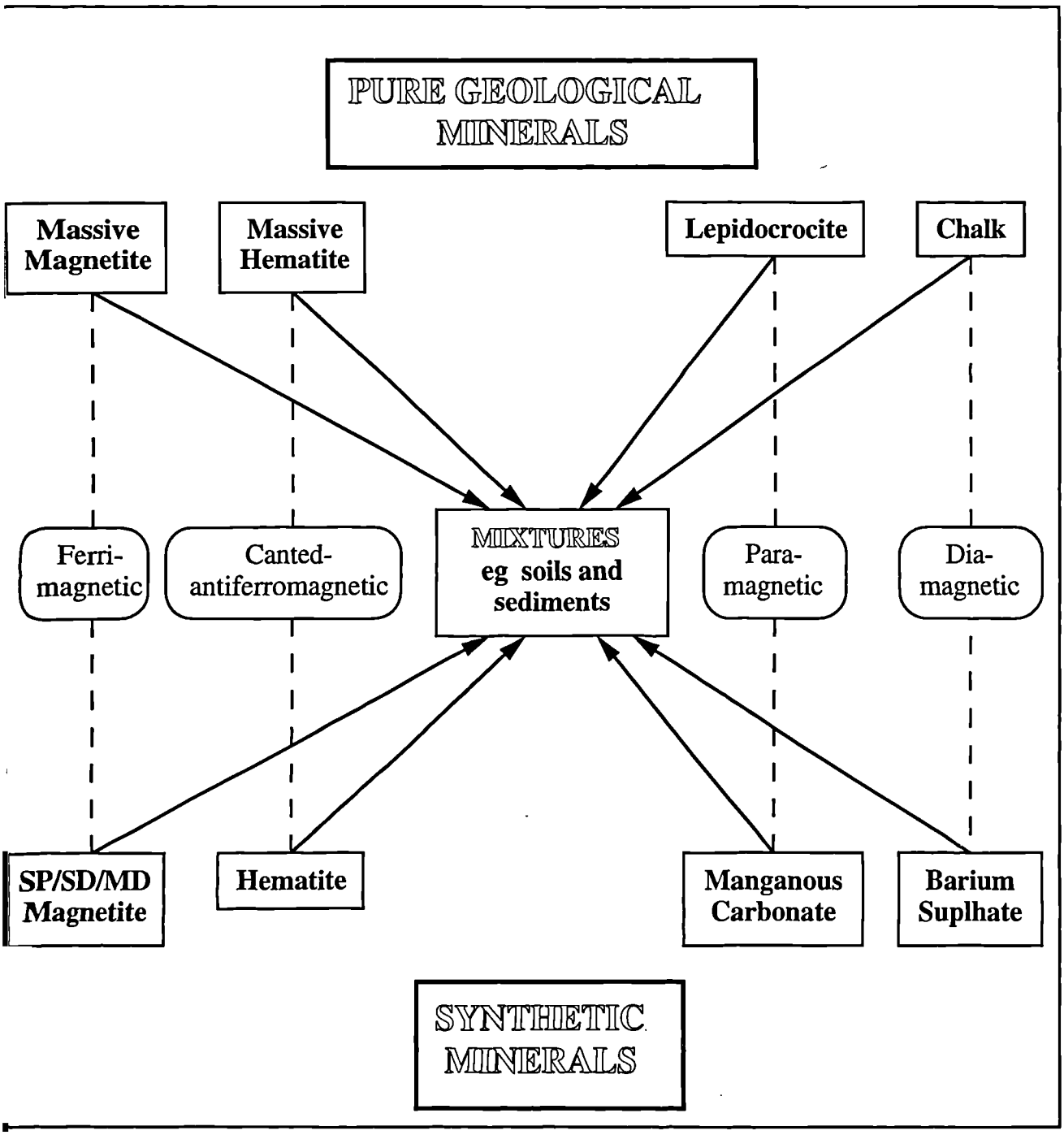

Plate 9.1 a: Massive and crystal magnetite

Plate 9.1 b: Pyrrhotite

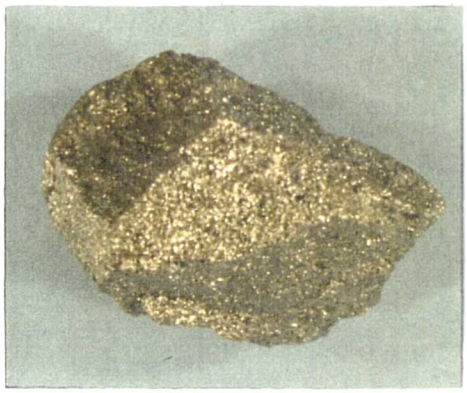

Plate 9.1 c: Crystal maghemite

Plate 9.1 d: Massive hematite

Plate 9.1 e: Lepidocrocite

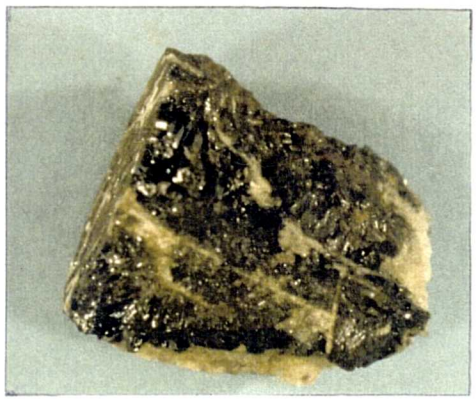

Plate 9.1 f: Goethite

proportion results of the models presented and it has proved difficult to find curves which are satisfactory for mineral modelling. Magnetite curves for SP, SD and MD size grains have been found to be very similar and would be seen as direct multiples in modelling (see Chapter 4, section 4.2.2). Also, when data for sized synthetic magnetites are compared, differences in magnetization and normalized curves are seen. For instance Figure 9.2 shows IRM curves for sized magnetites of Thompson (1986) who produced theoretical curves from some sized magnetite data of Dankers (1978) and Maher's precipitated MT magnetite samples. The equivalent grain sizes do not match in intensity or normalized curve shape. MT samples which are fine grained appear closer to curves between and including the 16 and 256μm curves of Thompson. It was expected that they would plot with the finer grain sizes.

Also in discriminating magnetite grain sizes, Maher and Taylor (1988) proposed χfd% values for MD, SD and SP grains of 0.5, 2 and 10% and Petersen (pers. comm. 1994) presented 12% for SP/SD bacterial magnetite. Such normalized parameters give better discrimination than linearly additive parameters (as shown in Chapter 4). In this chapter synthetic magnetite curves have been amalgamated to produce an average curve of SP, SD and MD MT sample curves measured in this research. This has been done because the curves are not sufficiently numerically different to model individually (collinear and in similar units, see Chapter 4). This is partly controlled by interaction problems where SP and SD grains interact to give MD-like results (see Paper 1, Appendix 7).

Magnetic mineral proportions have been modelled for a number of samples. They include a lake surface sediment (Seeswood Pool) and an organic matter sample taken from under Corsican Pine (Alice Holt Forest, collected by C. White). Modelling results for five contrasting soil profiles are then presented. First a set of three soil profiles taken from Seeswood Pool (See Figure 3.2), including an arable soil, a permanent pasture soil and a woodland soil of the Bromsgrove series. Soils of the Bromsgrove series are well-drained reddish coarse loamy soils with seasonal waterlogging. Secondly, two profiles from Buxton in Yorkshire are studied, a ranker from Earl Sterndale, south-east of Buxton and a peat from near the Cat and Fiddle Public House, west of Buxton (just over the Cheshire border). The ranker is of the Crwbin soil series representing very shallow and well drained loamy over limestone soil. The peat is of the Winter Hill soil series representing acid raw blanket peat which is perennially wet and eroded in places.

9.2 Modelling Minerals

Geological and Synthetic Minerals

The geological minerals used in this study are shown in Plate 9.1 and their hysteresis loops, both mass specific and normalized, are presented in Figures 9.3 and 9.5a respectively. Hysteresis parameter data are presented in Table 9.1 for both sets of minerals and the two initial samples. Figure 9.4 shows the hysteresis curves for the synthetic minerals chosen for this case study. Normalized curves are shown in Figure 9.5b for comparison with those of the geological minerals.

Curves of the geological minerals exhibit the broadest range of any of the hysteresis curves which have been obtained in this research. Magnetite produces a steeply rising curve from the origin which saturates at 400mT. The

Figure 9.2: IRM curves (a) and normalized IRM curves (b) for R Thompson's and B Maher's Magnetites

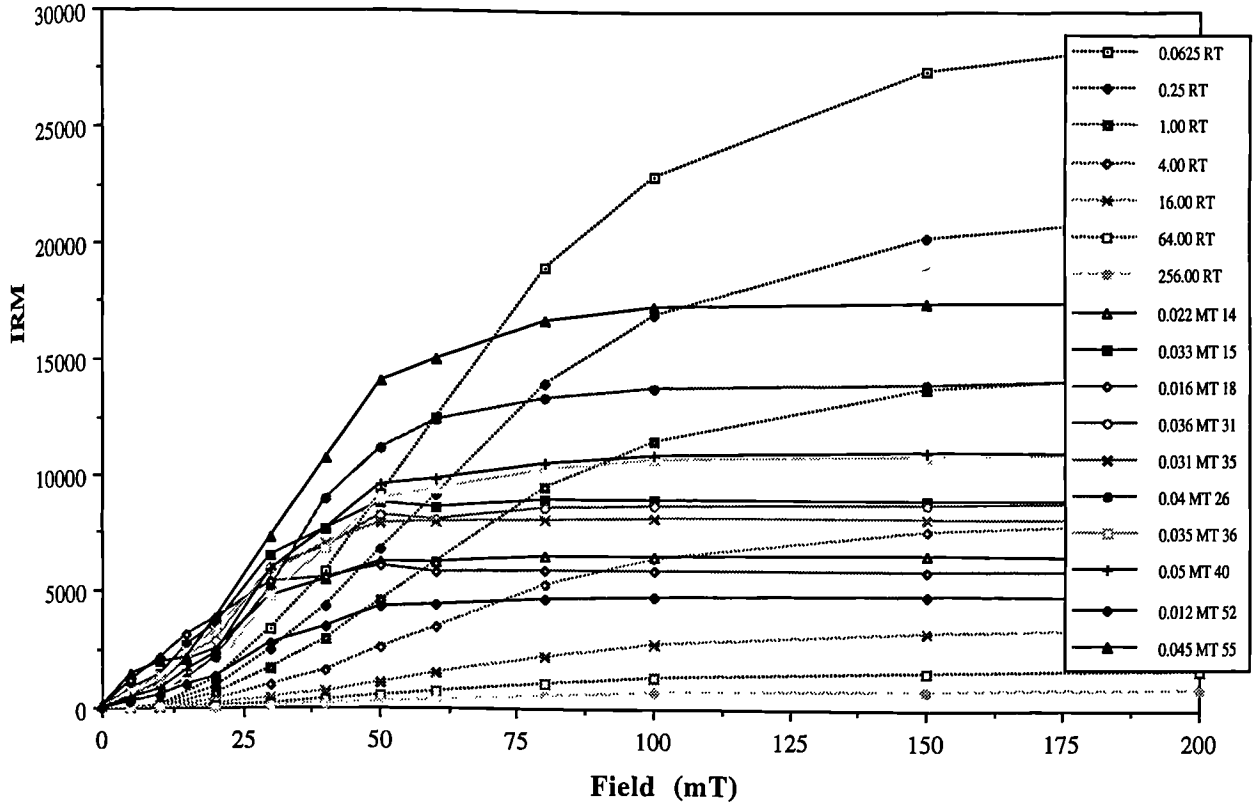

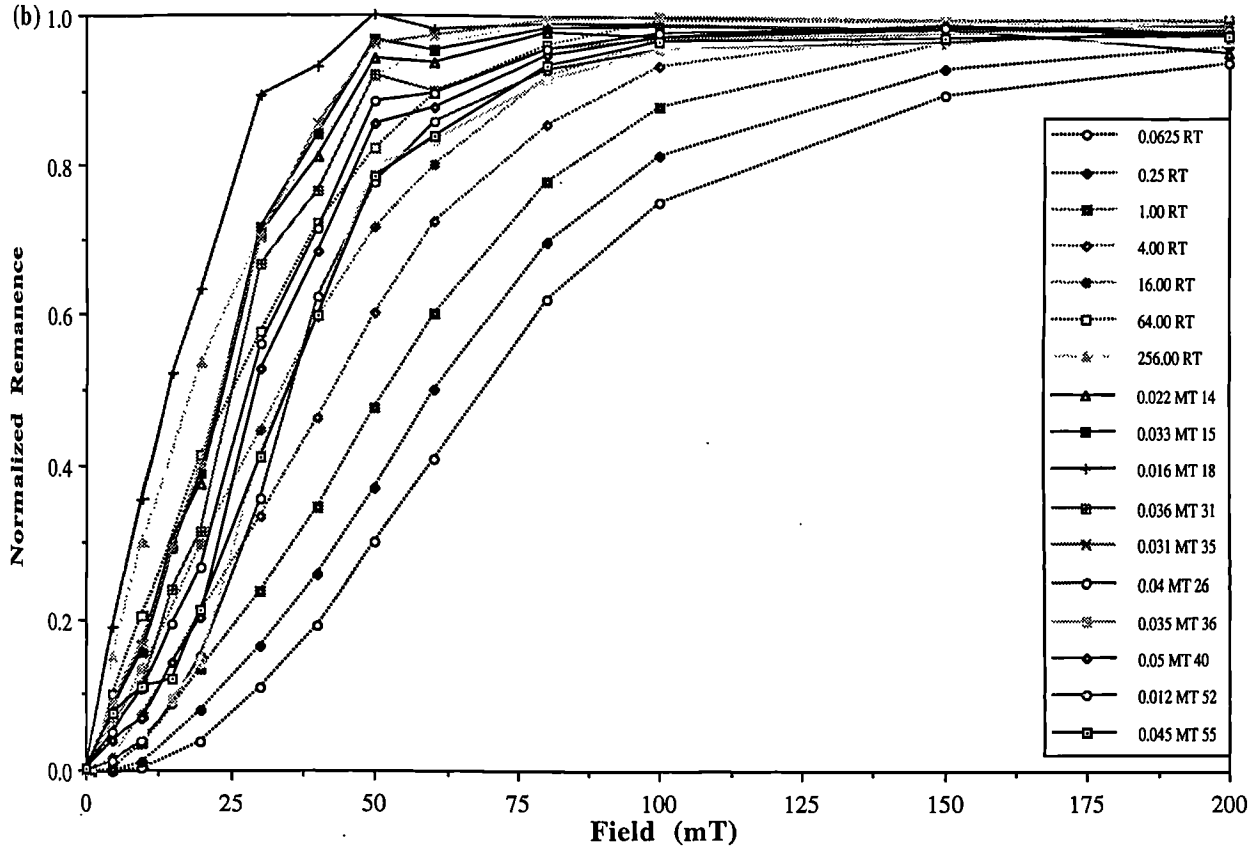

Figure 9.3: Pure Mineral VSM Loops

(a) Massive Magnetite

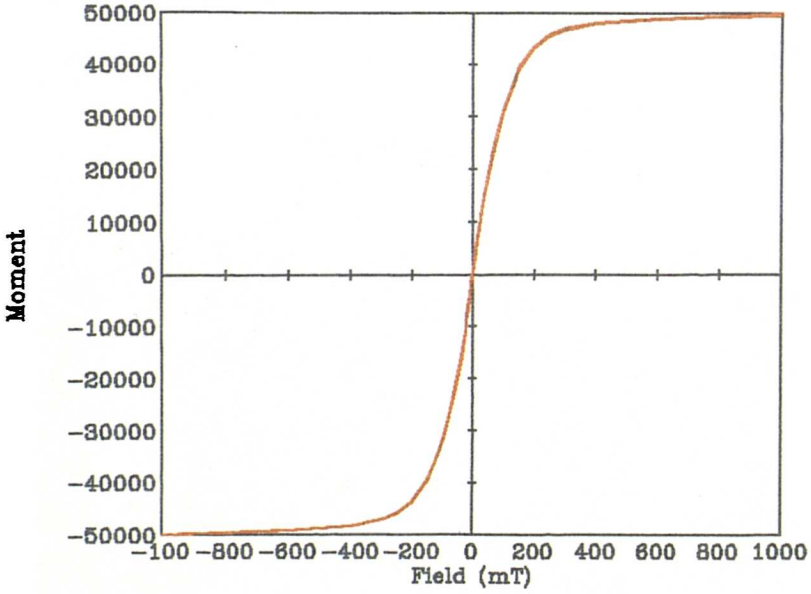

(b) Massive Hematite

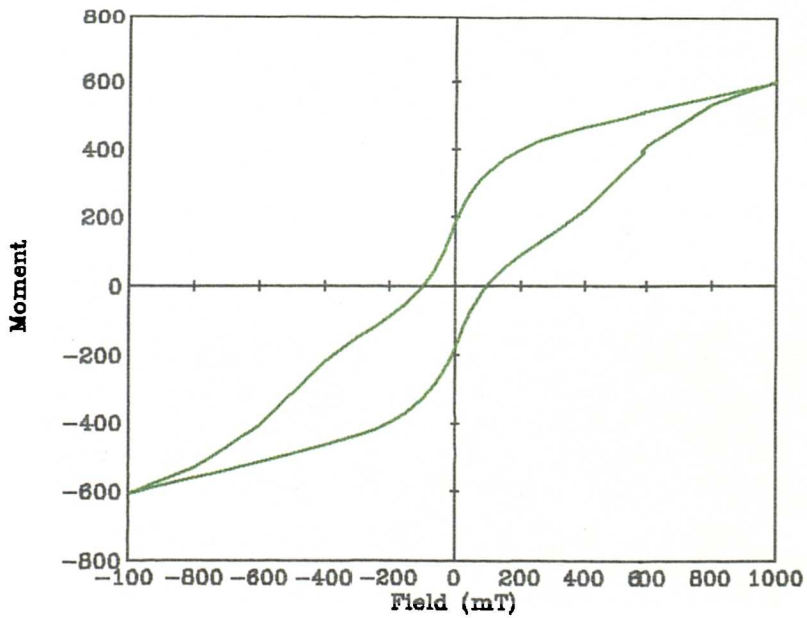

(c) Lepidocrocite

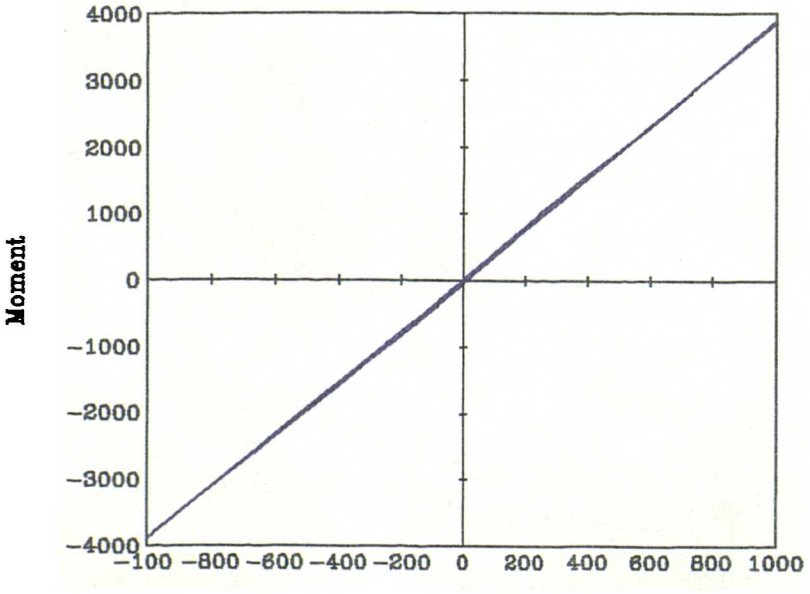

(d) Chalk

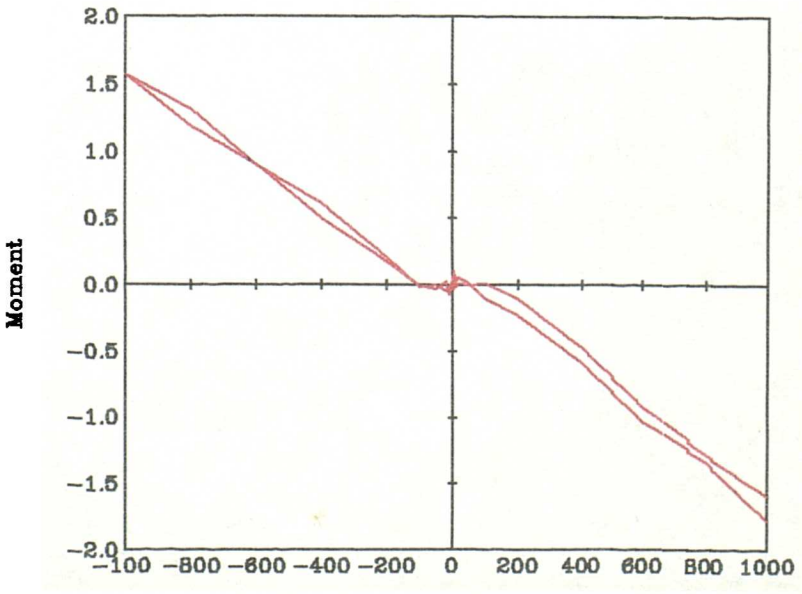

Figure 9.4: Synthetic VSM Loops
(a) SP/SD/MD Magnetite

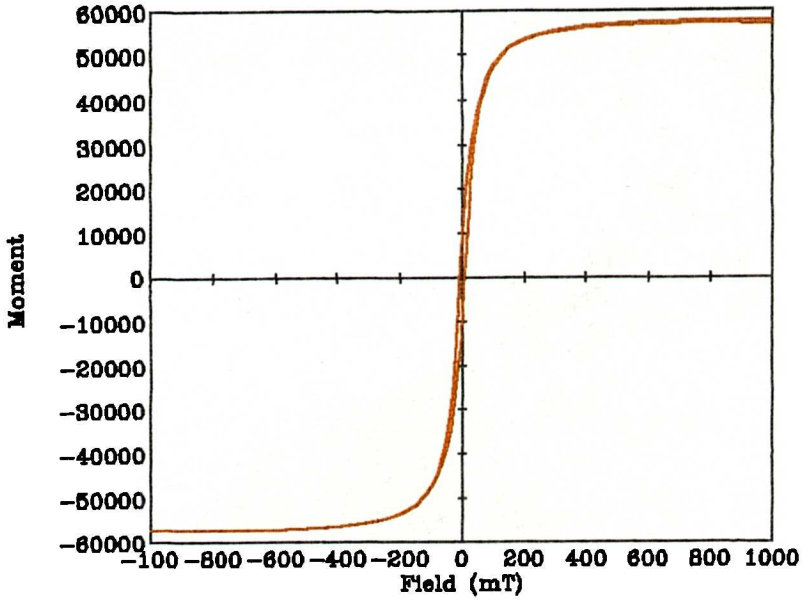

(b) Hematite

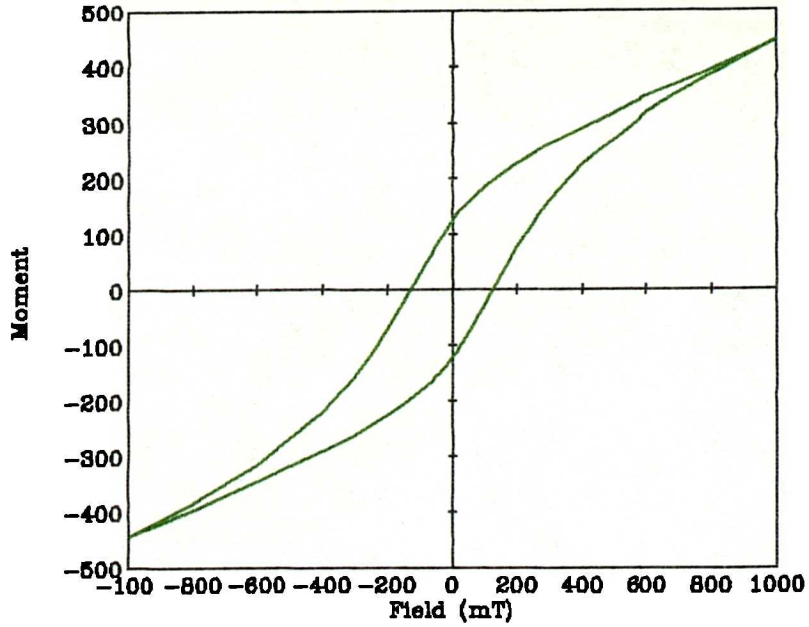

(c) Manganous Carbonate

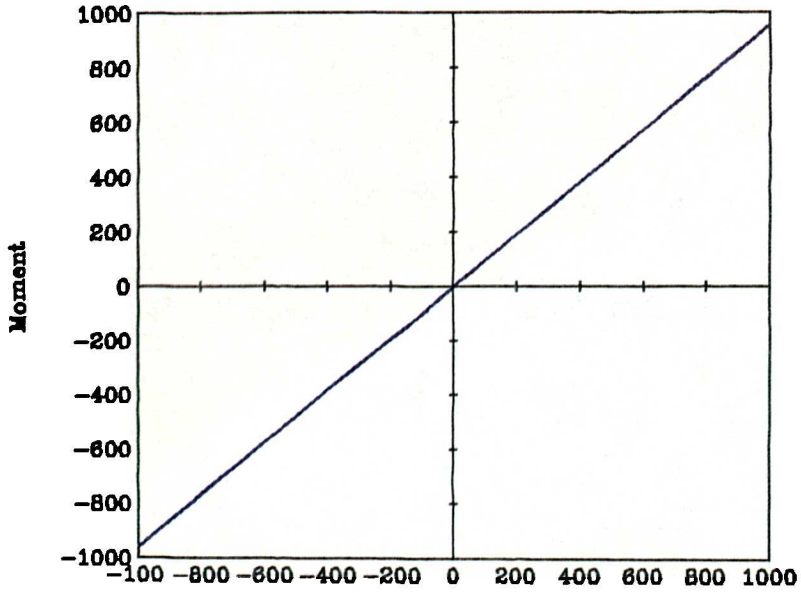

(d) Barium Sulphate

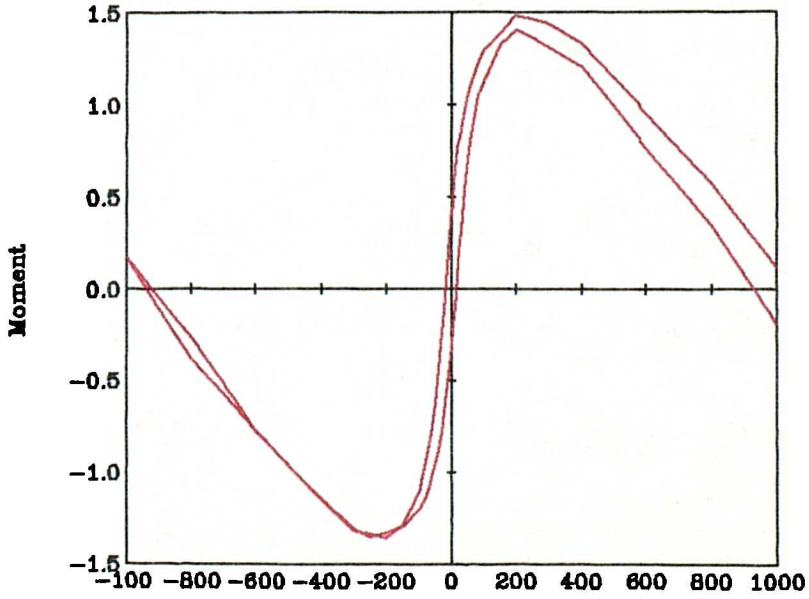

Figure 9.5: Normalized hysteresis loops, (a) Geological Minerals

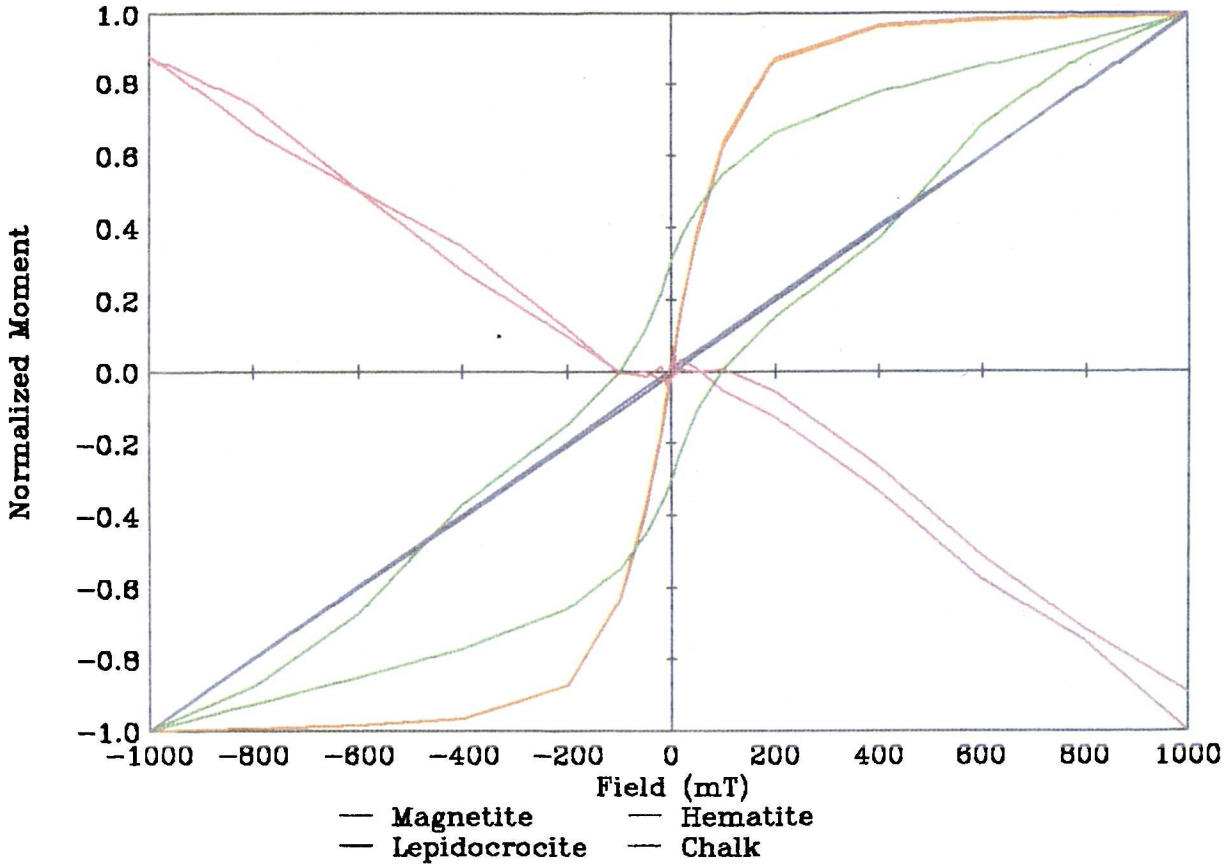

(b) Synthetic Minerals

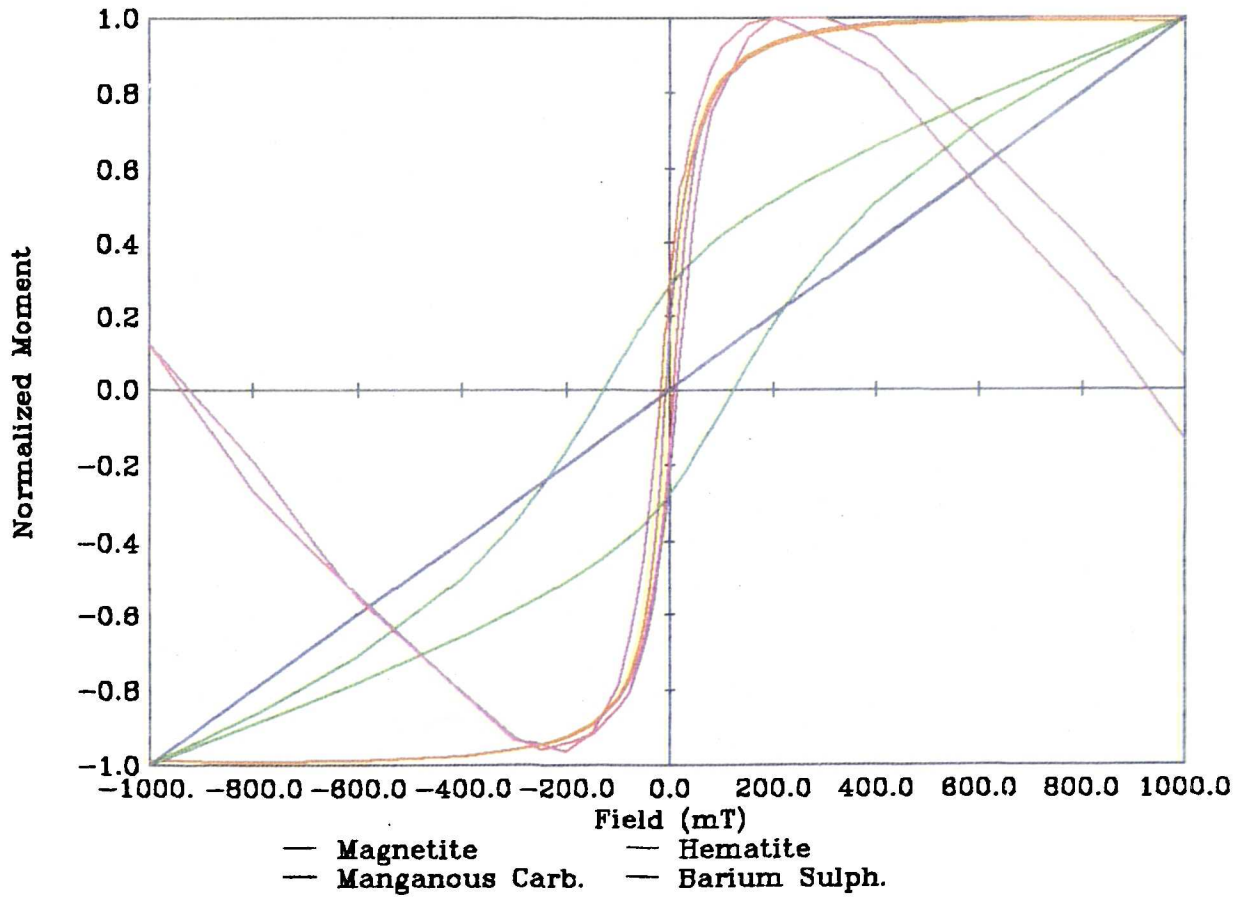

curve is not as steep as that of the synthetic magnetite curve (Figure 9.5) which saturates in less than 200mT. This is also shown by the χlow values of 492 (geological) and 1150 $\mu m^3 kg^{-1}$ (synthetic) respectively. Both magnetite samples have a maximum intensity of 50,000 and 58,000 respectively. The geological magnetite has a small paramagnetic component of 0.13% (0.66 $\mu m^3 kg^{-1}$ calculated from χlow and χhigh) while the synthetic magnetite is 100% ferrimagnetic. In synthetic minerals controlled laboratory precipitation of the SP and SD grains leads to a 100% ferrimagnetic component in the average synthetic curve.

Hematite curves of the geological and synthetic sets are also slightly different (Figures 9.3b and 9.4b). The synthetic curve shows a typical wide loop with high coercivity and saturation at a field greater than 1000mT. The geological hematite exhibited a 'wasp-waisted' shape loop which indicates a small ferrimagnetic component within the mineral structure. The geological hematite also exhibited a higher maximum intensity of 600 $mAm^2 kg^{-1}$ as opposed to 450 $mAm^2 kg^{-1}$ for the synthetic hematite.

Table 9.1: Hysteresis data for geological and synthetic mineral source samples.

VSM SPREADSHEET V1.0 OCTOBER 1993

INPUT Description	INPUT Code	CALC χlow	CALC χhigh (para)	CALC χferri	CALC χpara	CALC χferri	CALC Ms	CALC Mrs	CALC Mrs/Ms	CALC HIRM +100mT	CALC S ratio
			$\mu m^3 kg^{-1}$		%	%	$mAm^2 kg^{-1}$			$mAm^2 kg^{-1}$	
Geological Minerals											
Massive Magnetite	JL-A2	491.97	0.66	491.3	0.13	99.87	44538.4	648.5	0.01	2.54	1.0
Massive Hematite	JL-A4	2.21	0.39	1.82	17.71	82.29	287.62	185.3	0.64	163.55	0.12
Lepidocrocite	JL-A6	0.41	0.49	0.0	100.0	0.0	0.0	3.27	0.0	2.88	0.12
Chalk	LC1C20	-0.16	-0.06	-0.10	N/A	N/A	0.06	-0.20	-3.65	-0.03	0.86
Synthetic Minerals											
Ave Magnetite		921.1	0.0	922.7	0.0	100.0	55697.2	9290.1	0.16	26.43	1.0
Hematite	JD-S4	0.8	0.17	0.63	20.94	79.06	270.58	125.5	0.46	108.5	0.14
MnCO3	GL3K1	1.05	1.0	0.04	95.82	4.18	-9.04	0.35	-0.04	0.09	0.75
BaSO4	GL2K1	-0.02	0.0	-0.02	N/A	N/A	2.31	0.43	0.19	0.05	0.89
SP Magnetite		1149.49	0.0	1152.4	0.0	100.0	54330.5	6482.0	0.12	26.0	0.99
SD Magnetite		768.82	0.0	769.61	0.0	100.0	56608.3	11162.1	0.20	26.7	1.0

Paramagnetic curves exhibit the greatest difference between the two sets of minerals. The concentration element of the two curves (Figures 9.3c and 9.4c) differs by a factor of 4, the geological mineral, lepidocrocite, having the highest concentration. Difficulty was encountered in obtaining a purely synthetic paramagnetic compact material. Paramagnetic materials show no hysteresis as exhibited by the straight curves. Paramagnetic minerals also hold no remanence so Ms and Mrs measurements will be negligible (according to contamination). χlow values for the paramagnetic minerals are also very low namely 0.411 $\mu m^3 kg^{-1}$ for lepidocrocite. Most materials exhibit a paramagnetic component except, as already stated, for the synthetic magnetites.

Chalk exhibited the best diamagnetic curve of the database samples collected (discussed in Chapter 3) while barium sulphate showed the best diamagnetic curve for a synthetic material. However, the barium sulphate (Analr) was contaminated with 0.00002% iron which is shown as a small ferrimagnetic (possibly paramagnetic or ferromagnetic) component (Figure 9.5). Most environmental materials contain a large proportion of diamagnetic material such as silica and organic matter, which for the most part exhibits a negative magnetization. Diamagnetic curves exhibit the weakest magnetizations, the chalk having a maximum intensity of -1.5 mAm^2kg^{-1}.

9.2.1 Initial Examples

Different Minerals

Initially the two 'mixtures' were used to find the differences obtained in the modelling results using the two sets of minerals. The mixtures, as outlined above, are a lake surface sediment and an organic matter sample. The values for the organic matter sample were corrected for 23% loss on ignition giving values for the mineral fraction only. Mass specific and normalized curves for the samples are shown in Figure 9.6. The sediment curve shows a strong paramagnetic component with a small opening in the curve between |200|mT. The organic matter exhibited a larger ferrimagnetic component and this loop also opens between |400|mT. Magnetic extractions were performed on these samples after measurement. For the sediment sample this was carried out using a 200mT hand magnet held against a bottle containing the sediment in water. Plate 9.2a shows a section of the extracted sample which was dispersed in oil onto a slide and examined under a light microscope. Many spherical fly ash particles were seen in the sample (cf McLean, 1991). The organic matter sample was dissolved using hydrogen peroxide and the resulting material dispersed in oil onto a slide. Plate 9.2b again shows fly ash particles attached onto some organic matter. SEM analysis was carried out on the samples and a typical fly ash particle (generally >50μm and MD) is shown in Plate 9.4a. From X-ray diffraction analysis (XRD) the fly ash was found to be 95% iron. The fly ash was found to be similar to those found by Locke and Bertine (1986) and Battarbee *et al.* (1988). Also many bacterial-like chains and aggregates were found in the sediment sample (Plate 9.4b). These were similar to chains found by Farina *et al.* (1990) in sulphur-rich lakes of the southern hemisphere. XRD showed that they were mainly 50% silica and 33% aluminium with 5% iron. In Plate 9.3b an example of fly ash particles extracted from a chimney stack is also shown.

Modelling Minerals

The linear modelling program, LINDO was used (as in chapters 3, 4, 7, and 8) to model the proportions of both sets of mineral sources in the two samples. The linear modelling problem was poorly scaled due to the large magnetization values of the pure magnetite; this is a greater problem with the synthetic sources than with the geological sources. The error terms used in this chapter were set quite large (up to 1000) to counteract the values of the magnetite (in tens of thousands.). The results of this exercise are shown in Table 9.2. The results show that there is little difference between the proportions given to the geological minerals and the synthetic minerals. Using the synthetic minerals in both cases the canted-antiferromagnetic and paramagnetic components are much greater and the diamagnetic component compensates for this. The synthetic minerals and manganous carbonate however are not as likely to be as similar to natural minerals present in the sediment and organic matter as are the geological minerals. In both samples the calculated ferrimagnetic component is zero or extremely small.

Figure 9.6: Lake sed. and org. matter
(a) mass specific hysteresis loops

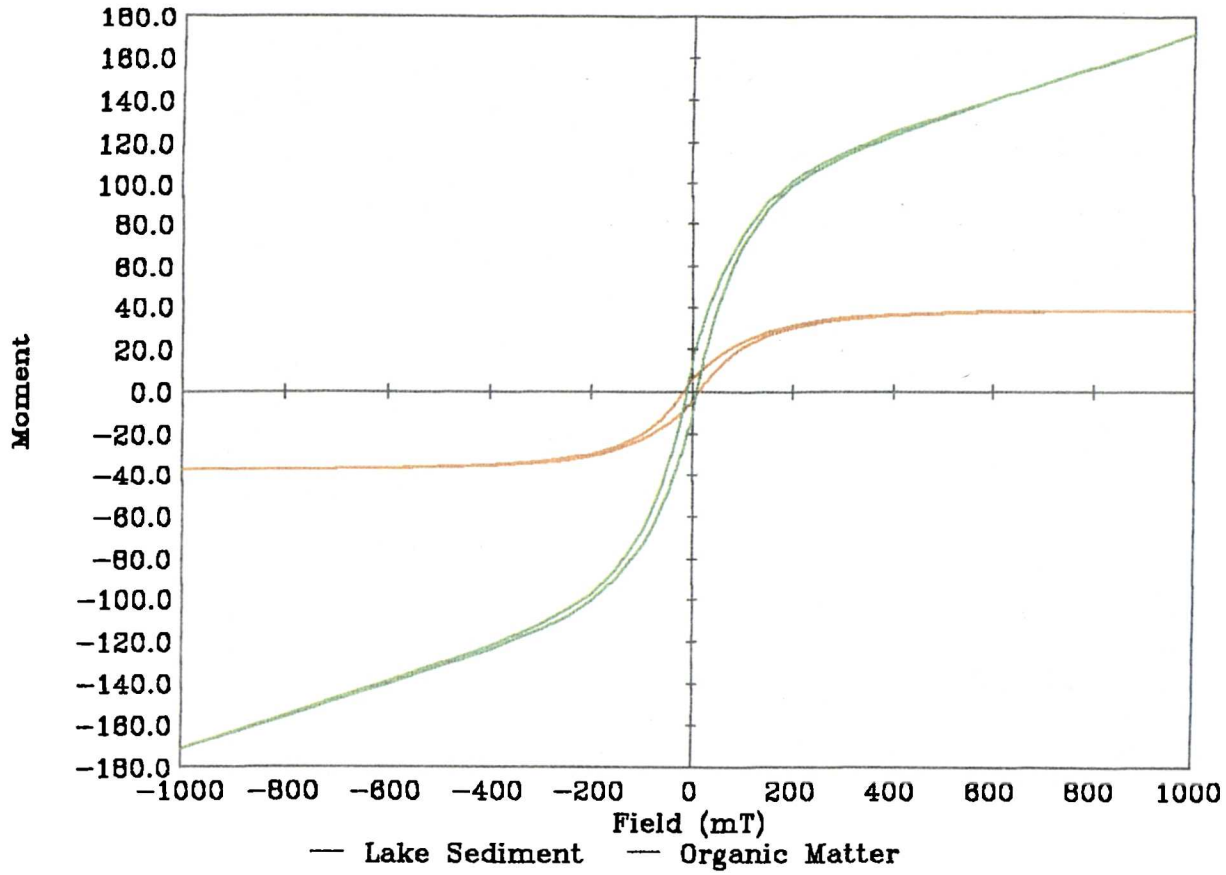

(b) Normalized hystersis loops

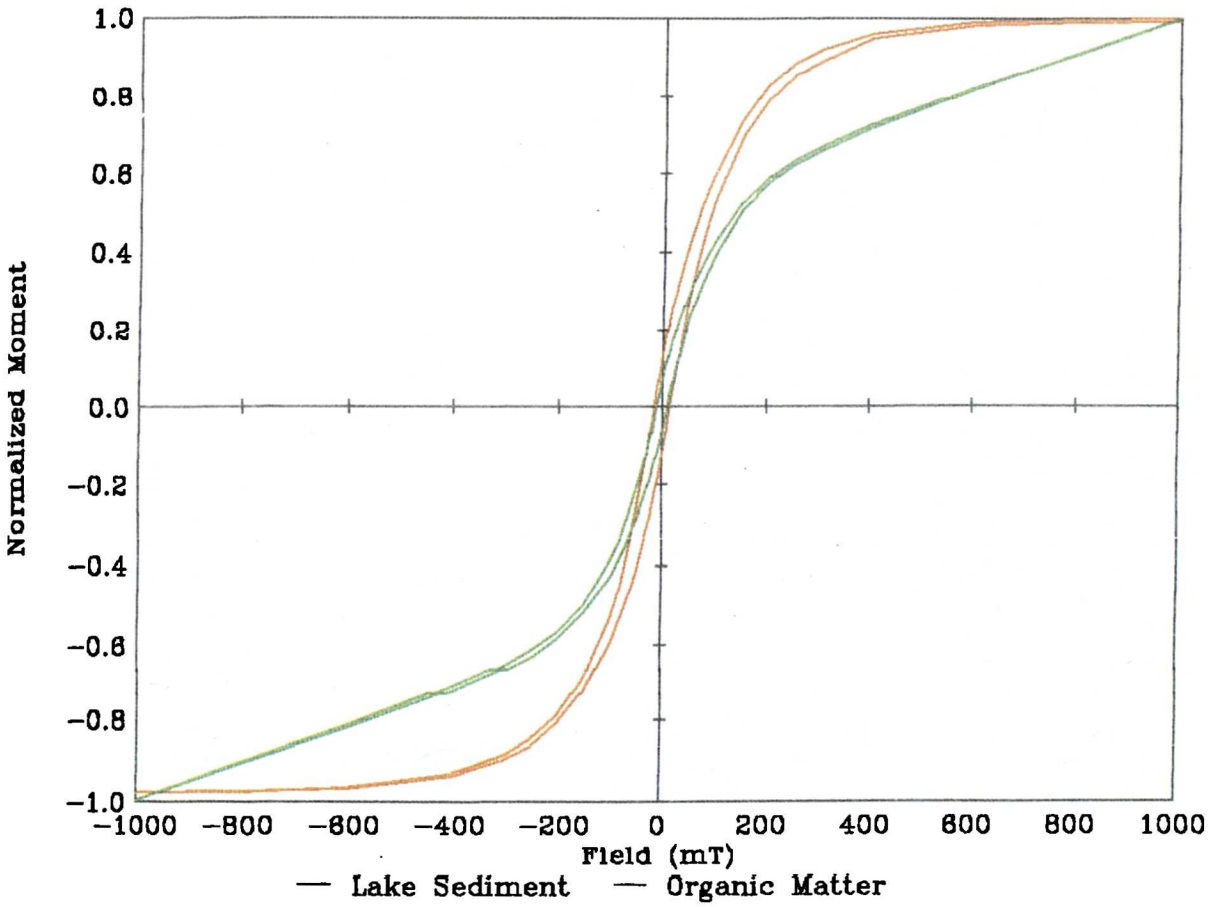

Plate 9.2a: Magnetic extract from Seeswood Pool lake surface sediment (*100)

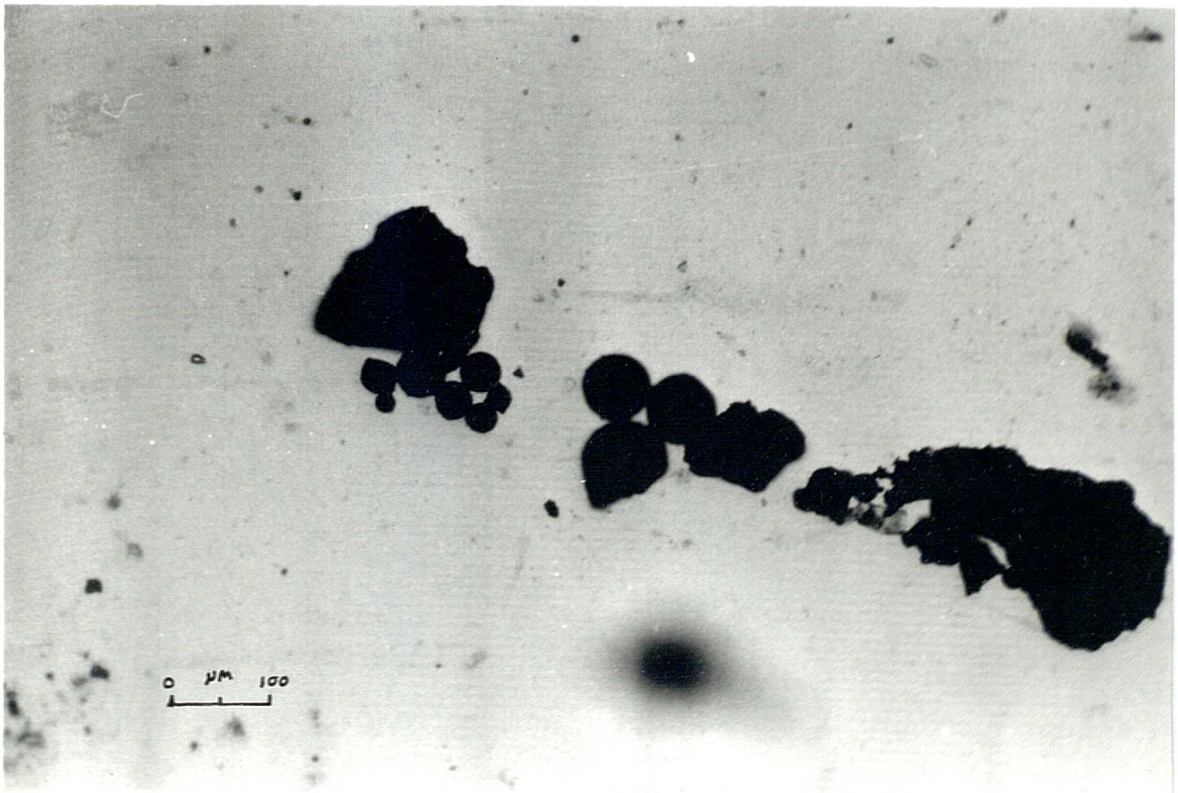

Plate 9.2b: Magnetic extract from Alice Holt Forest organic matter (*100 and inset *400)

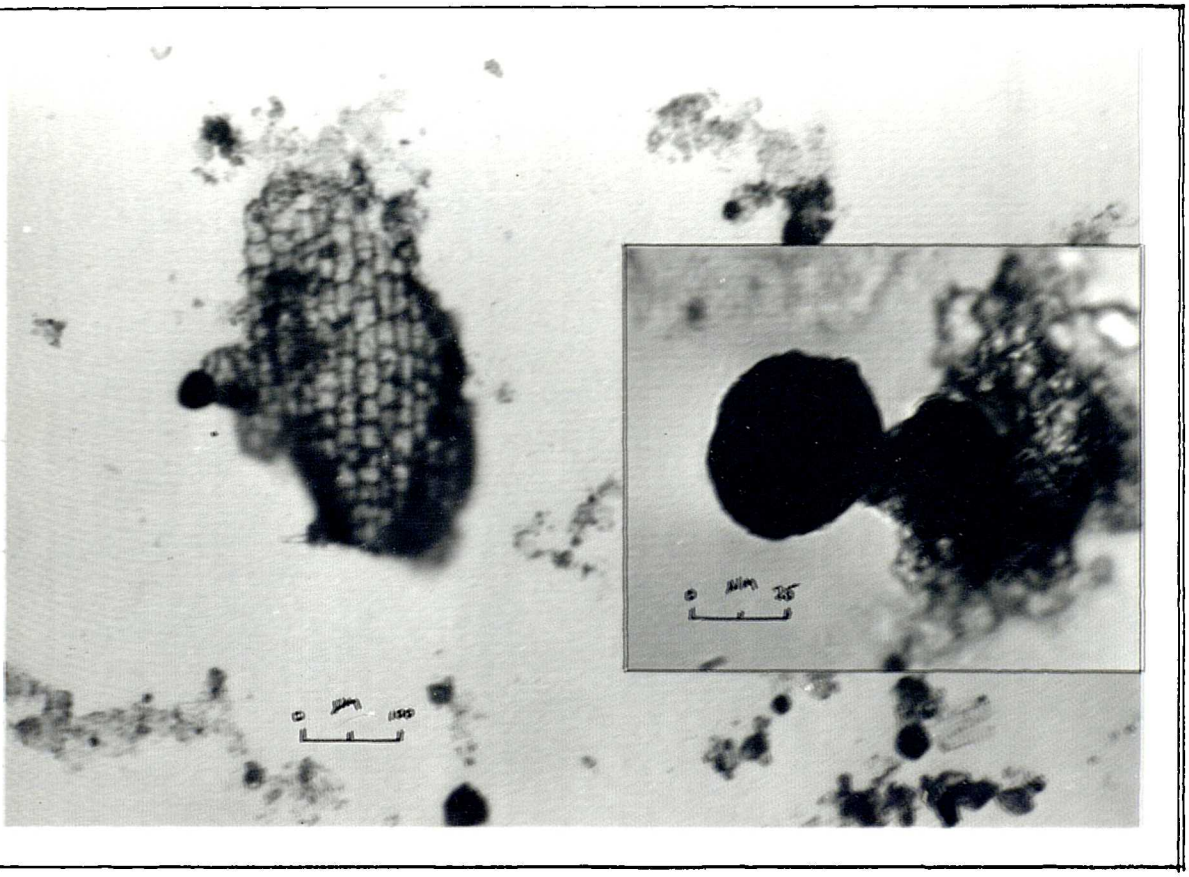

Plate 9.3a: Magnetic extract from Seeswood Pool topsoil (*100)

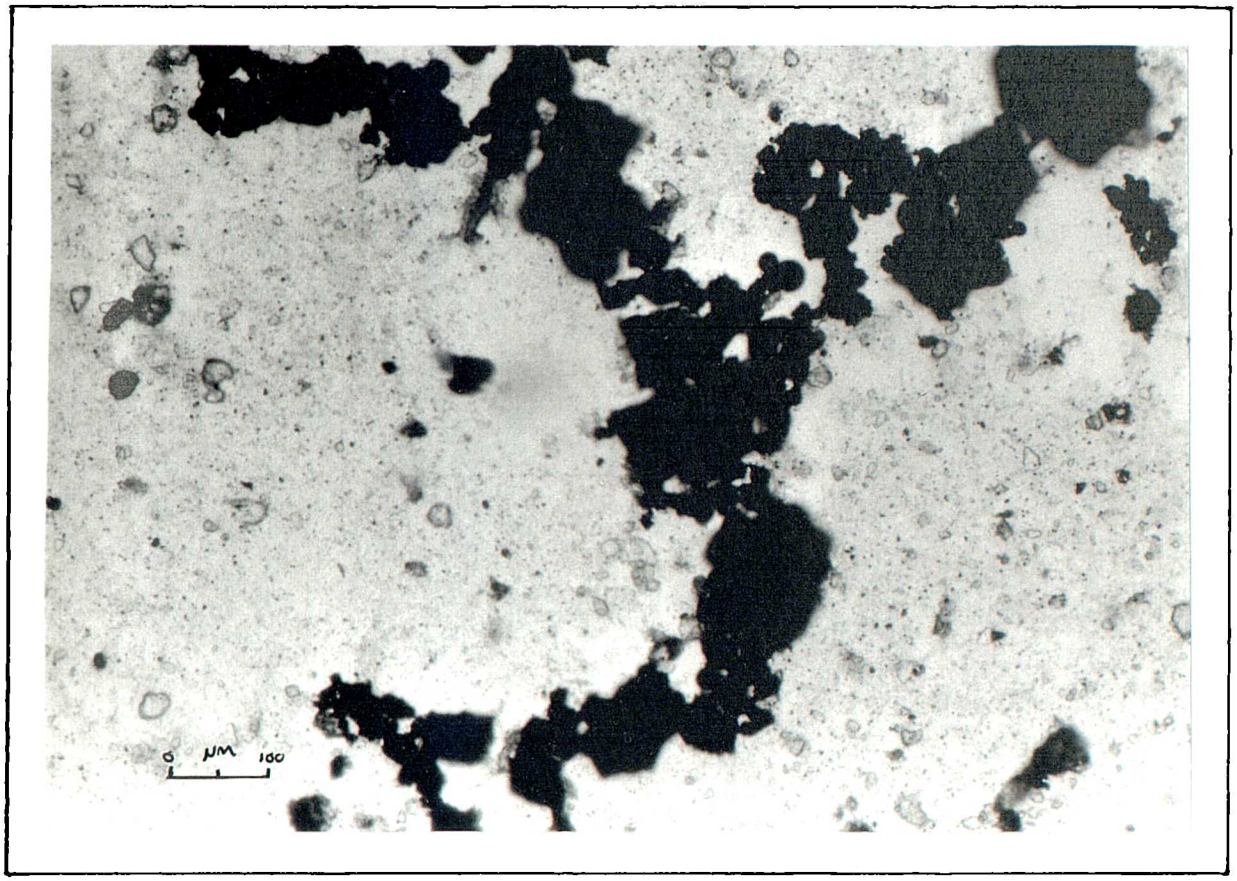

Plate 9.3b: Magnetic extract of Gulson Hospital boiler chimney slag (*100)

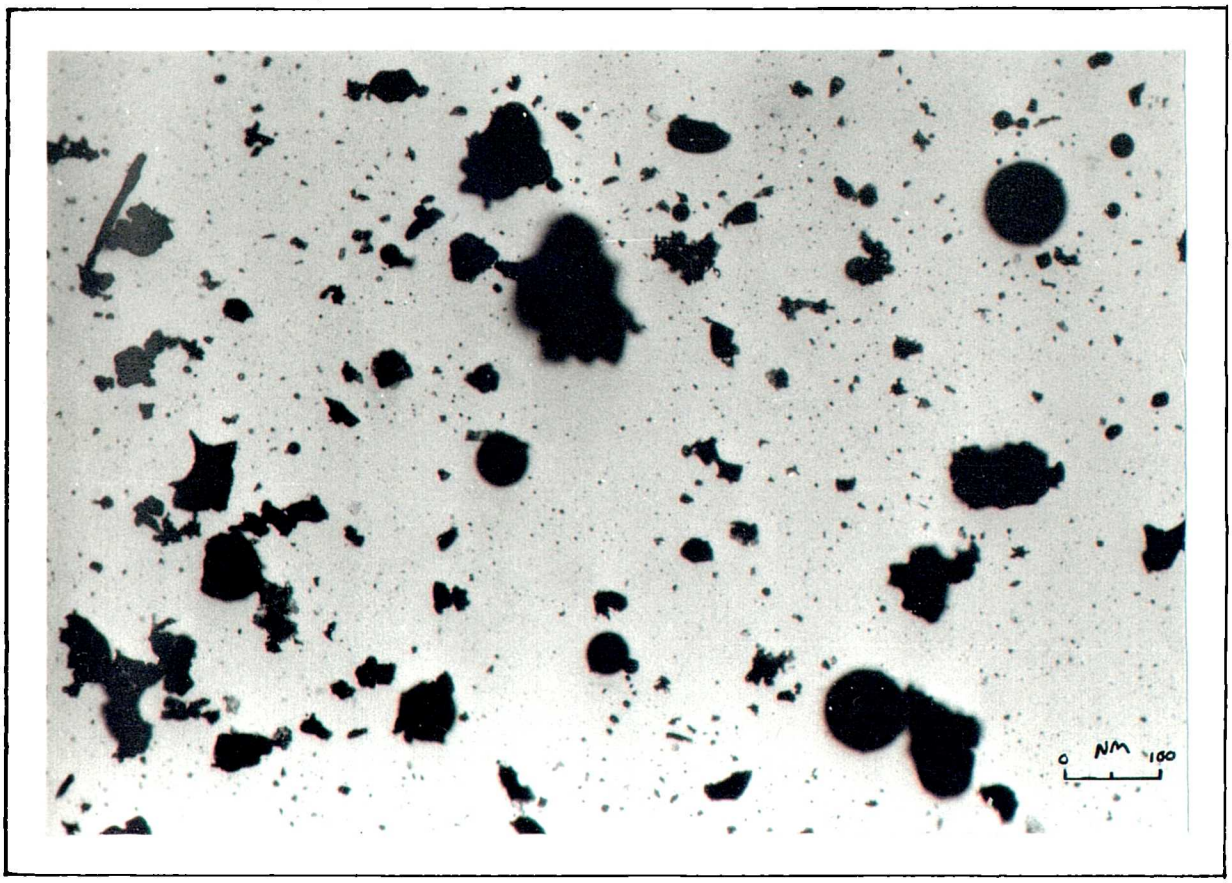

Plate 9.4a: Spherical atmospheric fly ash particle magnetically extracted from Seeswood Pool surface lake sediments

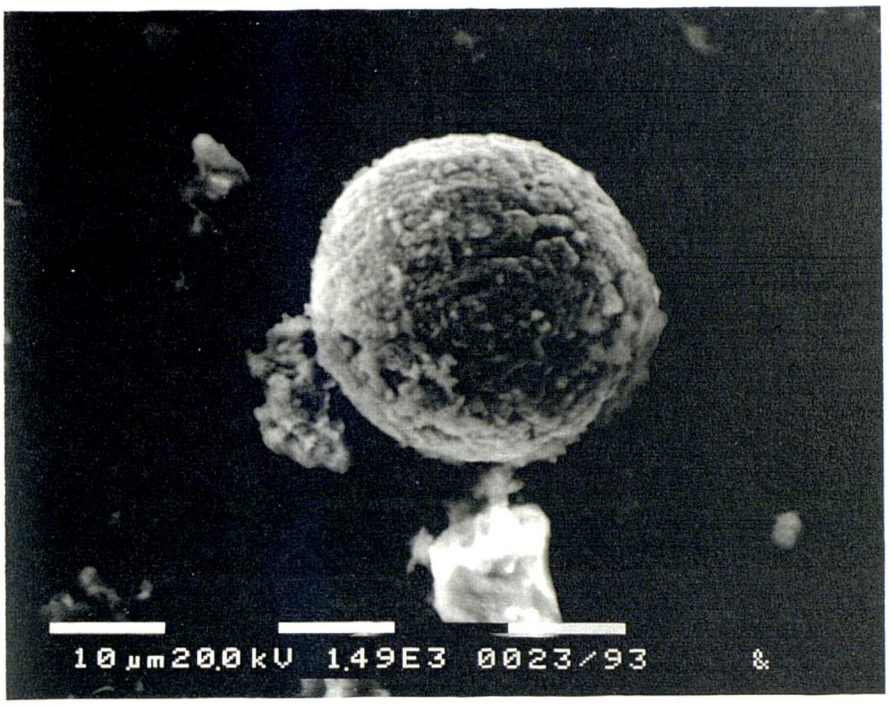

Plate 9.4b: Bacterial aggregate with mucus chain magnetically extracted from Seeswood surface lake sediments (N. Parker, pers. comm.)

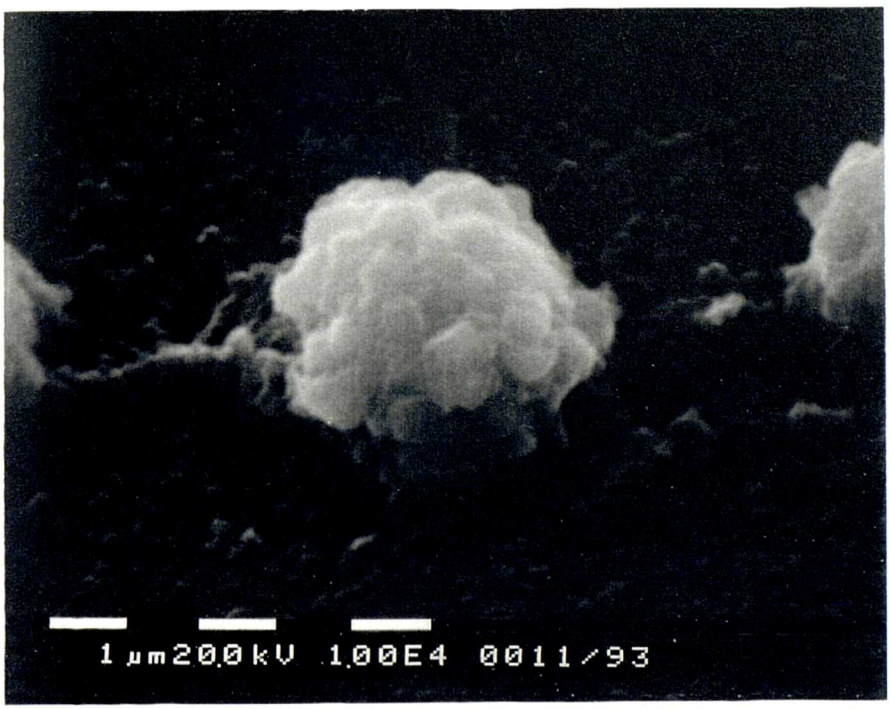

Table 9.2: Linear Modelling results for the sediment and organic materials using both geological and synthetic source sample sets. x1, x2, x3 and x4 are respectively ferrimagnetic, canted-antiferromagnetic, paramagnetic and diamagnetic components.

Sample	**Source and Proportion**			
	x1	**x2**	**x3**	**x4**
Lake Sediment				
Geological Minerals	0	4.27	0.5	95.23
Synthetic Minerals	0	11.85	3.02	85.14
Organic Matter				
Geological Minerals	0	5.25	2.16	92.59
Synthetic Minerals	0	15.12	12.66	72.23

The organic matter sample exhibits a larger paramagnetic component as is shown in Figure 9.6. Both samples have a similar canted-antiferromagnetic component as shown by the similar widths in the two loops. The element of scale in the modelling routine for the magnetite has eliminated this ferrimagnetic component much more than it has the other three components. However it is known that fly ash does contain ferrimagnetic minerals (Locke and Bertine, 1986). Both samples fall within the range of the canted-antiferromagnetic, paramagnetic and diamagnetic components and it seems the proportions have been split between these three components.

Modelling grain sizes

Maher (1988) and work carried out on Maher's samples (largely not presented in this thesis) have shown that there is an overlap in most linearly additive magnetic parameters for SP and MD grain sizes (Chapter 5). This leads to interpretational difficulties without the use of ratio parameters. There are also problems in obtaining or making spherical sized samples with grain distributions within each of the theoretical SP and SD domain size ranges. Maher's samples are cubiod (B. Maher, pers. comm.) which can lead to a 25% variation in the theoretical domain size boundaries (K. O'Grady, pers. comm.). In cuboid grains it is also possible that the domain ranges become smaller as domains can exist in the corners of the cuboid grains (K. O'Grady, pers. comm.). The nature of the grains could also lead to problems in defining their true diameters. However these samples represent the best analogue for the finer ferrimagnetic contents of environmental materials (Paper 1, Appendix 7).

Figure 9.7 shows grain distributions (of approximately 100 grains) for Maher's 10 new MT samples and the theoretical domain boundaries (discussed in Chapter 2) are marked. If the domain boundaries are assumed to be correct it is clear that most of the samples contain grains of SP and SD size and one sample contains all three domain sizes. Only one sample (MT52) contains only SP grains. The distributions are normal on the whole (eg MT35, MT36 and MT40) or negatively skewed (MT18, MT52 and <MT55). This makes finding pure grain size end members impossible.

Also in the sediment and organic matter sample concentration values fall below the magnetite values for different grain size ranges. Because of this only normalized data gives an indication of the grain size of magnetite in any sample. Figure 9.8a shows normalized hysteresis loops for synthetic SP and SD grains and a geological massive magnetite (assumed to contain MD grains). These curves (and χfd% values) can be compared to the normalized

Figure 9.7: Range of Grain Sizes for MT Series

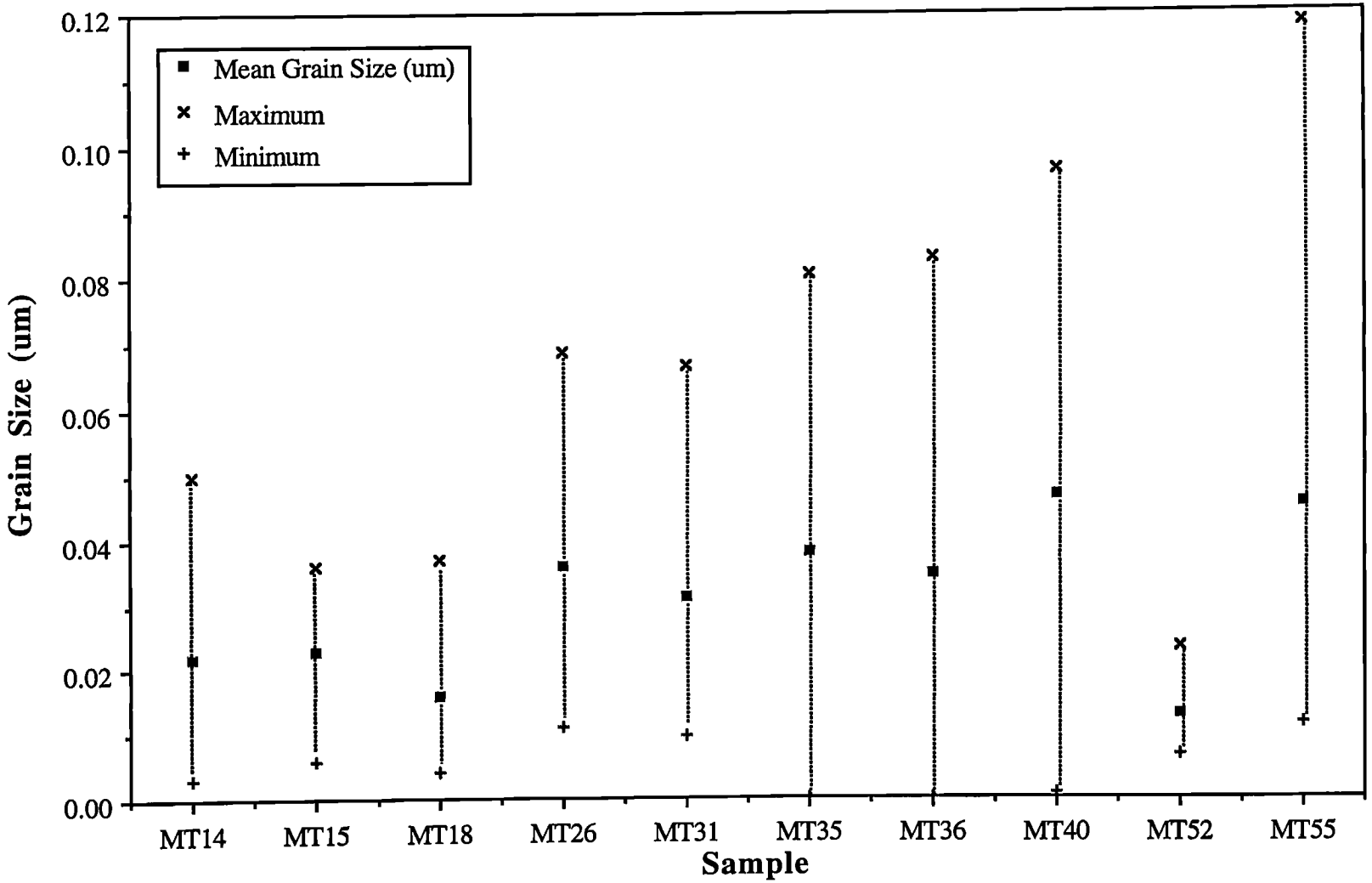

Figure 9.8: Normalized hysteresis loop
(a) different grain size magnetites

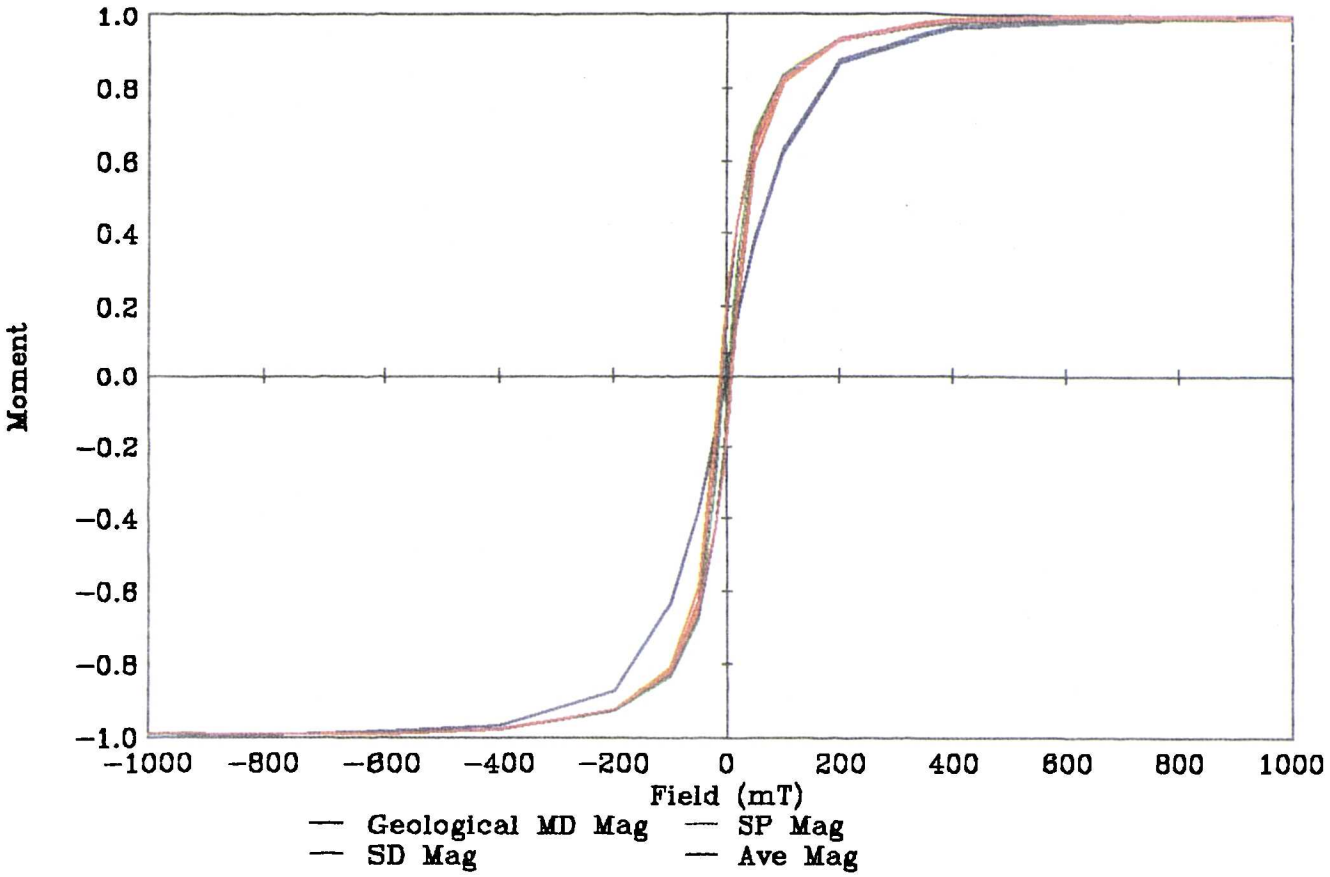

(b) environmental samples containing
atmospheric pollutants

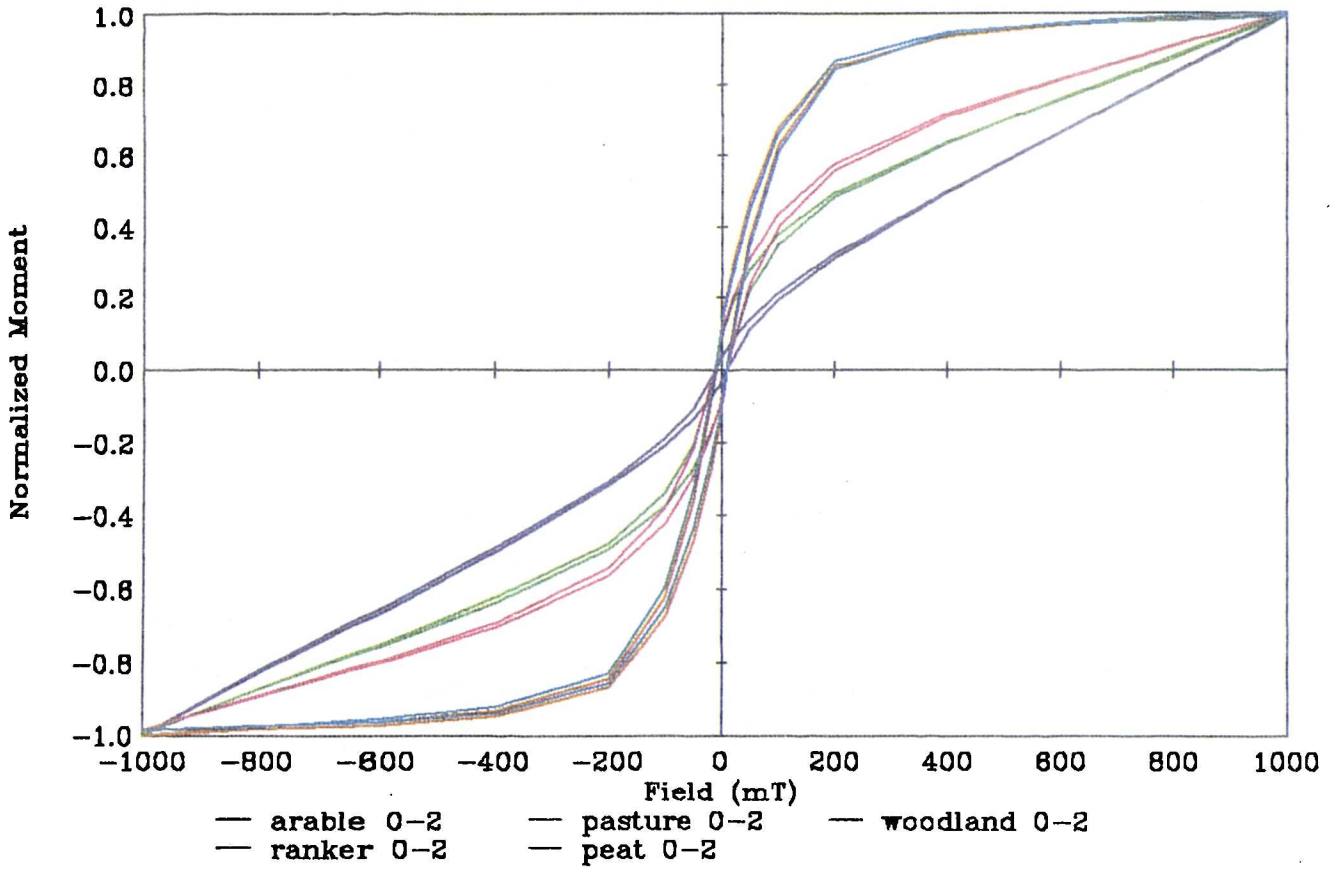

curves of environmental samples. The two samples used for this experiment were a woodland organic matter sample from Seeswood Pool and a contaminated peat (0-2cm) sample from Buxton. Their hysteresis curves are shown in Figure 9.8b. The samples are known to have significant atmospheric components and have low χfd% values of 2.5%. The normalized curves are very similar to the massive magnetite curves rather than the finer-grained synthetic magnetite curves which are much steeper and saturate earlier. Also χfd% values of the SD and SP samples are >5% and the MD magnetite value is <2%.

9.3 Modelling Minerals in Soil Profiles

In this experiment selected horizons of five soil profiles were modelled using the same procedure as in the mineral modelling example above. Four horizons (the organic layer, A and B horizons and parent material) were modelled in each profile representing changes in magnetic properties and mineral composition vertically through the profiles.

All cores were collected using a stainless steel 50cm corer. The samples were air dried, packed in 10ml pots and sub-sampled into 0.4g VSM holders before analysis. χlf, χfd and hysteresis loops of 42 field magnetization measurements were then made on the samples. Susceptibility measurements for the soil profiles are also presented giving an indication of concentrations of magnetic minerals (χlf) and grain size (χfd%) through the profiles. χfd% is especially useful in indicating large atmospheric (coarse-grained) components in organic layers.

9.3.1 Seeswood Soil Profiles

Three soil cores were collected from Seeswood Pool from an area within 10m of one another (see Chapter 3). One 50cm core from each of arable, pasture and woodland land uses was obtained. Brief profile descriptions of the three cores are given in Figure 9.9. The arable profile was homogeneous to a depth of 36cm where in all three profiles the parent material (Keuper Clay and Triassic Sandstone) was seen. Other clear differences occurred between the litter and organic layers in the woodland soil, pasture soil and the top layer of the arable soil. Depths at which VSM samples were taken were 0-2, 16-48, 28-30 and 44-46cm, representing the O, A, B and parent material horizons. When measured, the values were not corrected for loss on ignition in these soils.

The results for χlf can be compared to Dearing et al. (1986) who also made measurements on soil profiles from Seeswood. The results are not similar except for the accumulation of "fly ash" in the woodland soil. Such fly ash has been extracted and photographed for the purposes of this research (Plate 9.3a) and particles are similar to those seen in the sediment at Seeswood Pool (Plate 9.2a)

χlf and χfd% Profiles

χlf and χfd% profiles are shown in Figure 9.10. In the woodland top 10cm of soil there is a concentration of ferrimagnetic magnetic minerals with a χlf of up to 1.4 and low χfd% values of <3. This suggests that the minerals are coarse MD 'magnetite' (ferrimagnetic) grains. The χlf profile for the arable soil is constant throughout and is joined by the woodland and pasture profiles at a depth of 30cm. Much variation occurs in the χfd% profiles

Figure 9.9: Seeswood Pool Soil Profiles, arable (a), pasture (b) and woodland (c)

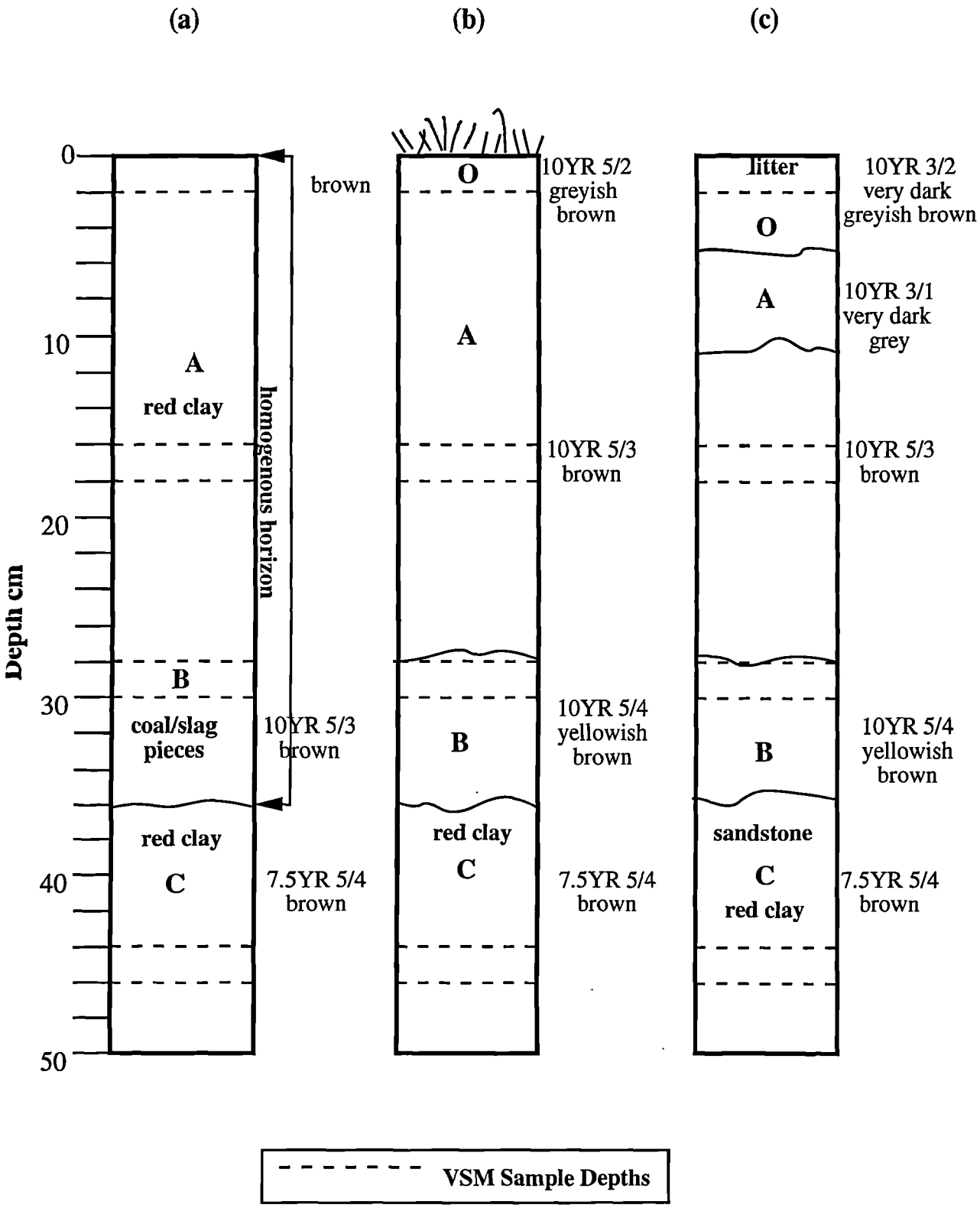

Figure 9.10: Xlf profiles (a) and Xfd% profiles (b) for Seeswood soil cores

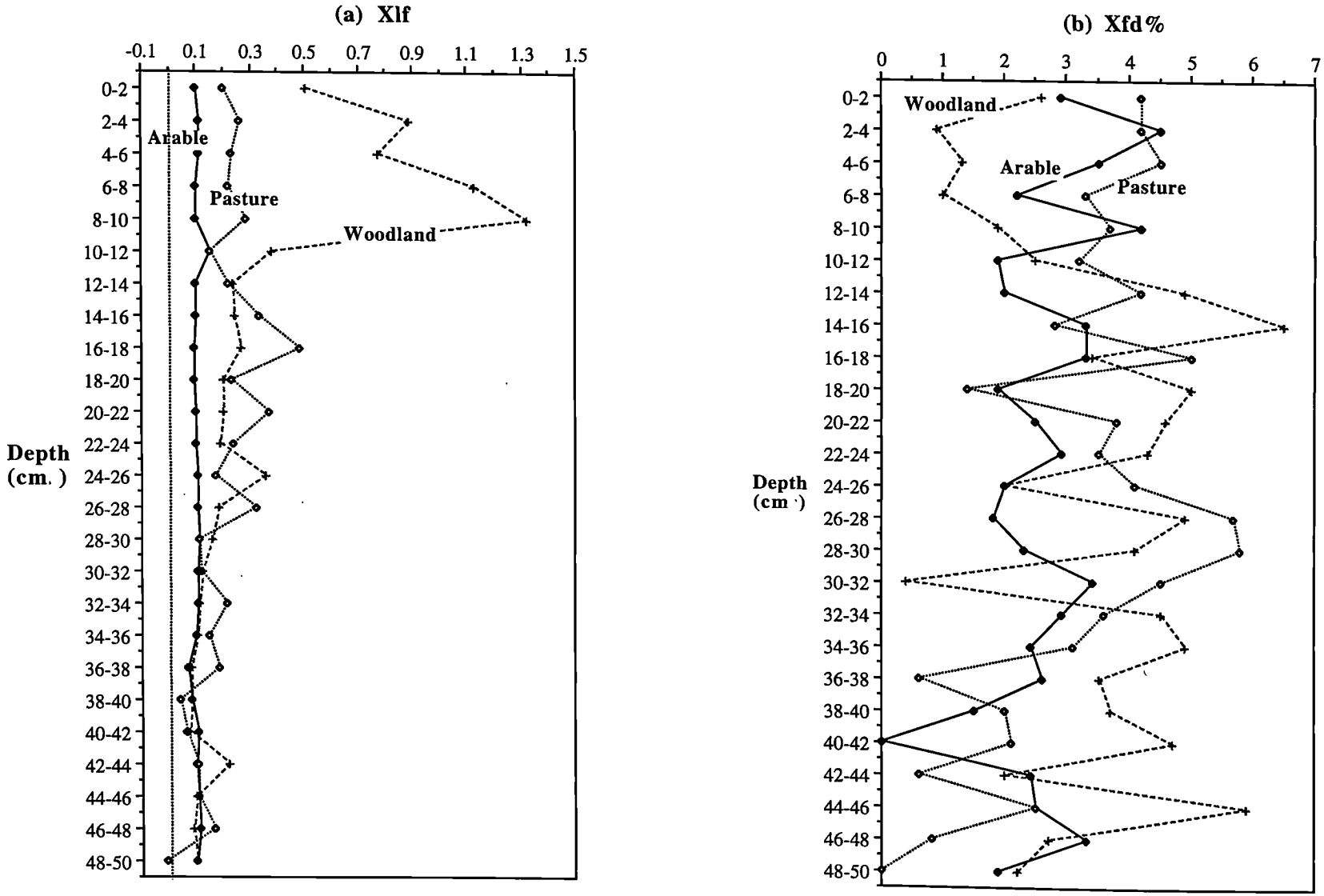

but a clear pattern is seen in the upper layers of the woodland soils. At lower layers the χfd% values are greater in the woodland soils (~4%) than in the arable and pasture soils (~2%), indicating that there may be less destruction through gleying of magnetic minerals in the woodland soils. This is due to the woodland soil being drier and less waterlogged (through vegetation uptake of water) than the two other profiles.

Hysteresis Curves

Mass specific hysteresis curves for the Seeswood soils are presented in Figures 9.11 a-d. Essentially, normalized curves were very similar to these curves as the maximum magnetizations are in similar units. Similar patterns can be seen in the hysteresis loops as that described by the χlf profiles. The woodland soil in the 0-2 layer has by far the greatest magnetization values (Figure 9.11a), next being the pasture soil and then the arable soil. The three curves indicate domination by ferrimagnetic, canted-antiferromagnetic/paramagnetic and paramagnetic minerals respectively. This is also confirmed by the χlow, high and Ms results shown for Seeswood soil cores in Table 9.3.

In the 16-18cm layer (Figure 9.11b) the woodland and pasture soils are extremely similar, indicating canted-antiferromagnetic and paramagnetic minerals and concentrations well above that of the arable soil (approximately 10 mAm^2kg^{-1}). In Figures 9.11c and d the curves are much more similar in magnitude (concentration) and shape (mineral type). At the 28-30cm depth the curves are dominated by canted-antiferromagnetic and paramagnetic minerals. The 44-46cm curves are completely dominated by paramagnetic minerals and exhibit higher χhigh values and lower Ms values in Table 9.3. In Table 9.3 simple percentage ferrimagnetic and paramagnetic components of the total susceptibility have been calculated from the χlow and χhigh results. These give an indication of the minerals contributing to the low field magnetization gradient but are not quantitative in terms of source proportions. They do indicate in this instance, however, the increasing paramagnetic component through the profiles. For instance in the arable soil the paramagnetic component increases from 9% of the total susceptibility in the 0-2cm layer to 50% of the total susceptibility in the 44-46cm layer.

Table 9.3: Hysteresis data for selected horizons of Seeswood arable, pasture and woodland soil profiles.

VSM SPREADSHEET V1.0 OCTOBER 1993

INPUT Description	INPUT Code	CALC χlow	CALC χhigh (para)	CALC χferri	CALC χpara	CALC χferri	CALC Ms	CALC Mrs	CALC Mrs/Ms	CALC HIRM +100mT	CALC S ratio
			$\mu m^3 kg^{-1}$		%	%	$mAm^2 kg^{-1}$			$mAm^2 kg^{-1}$	
Arable											
0-2cm	SP1B1	117.44	10.37	107.07	8.83	91.17	1781.4	355.4	0.2	11.98	0.97
4-6cm	SP1B3	39.99	11.03	28.96	27.57	72.43	2058.7	407.1	0.2	99.56	0.76
8-10cm	SP1B5	44.62	11.79	32.83	26.43	73.57	1548.3	330.9	0.21	102.1	0.69
16-18cm	SP1B9	40.7	11.5	29.2	28.25	71.75	1830.1	356.1	0.19	53.99	0.85
28-30cm	SP1B15	39.79	8.56	31.22	21.53	78.47	1862.3	367.7	0.2	99.0	0.73
44-46cm	SP1B23	47.82	22.6	25.22	47.26	52.74	365.86	258.0	0.71	156.28	0.39

Figure 9.11: Seeswood Pool VSM Loops
(a) 0–2 cm depth

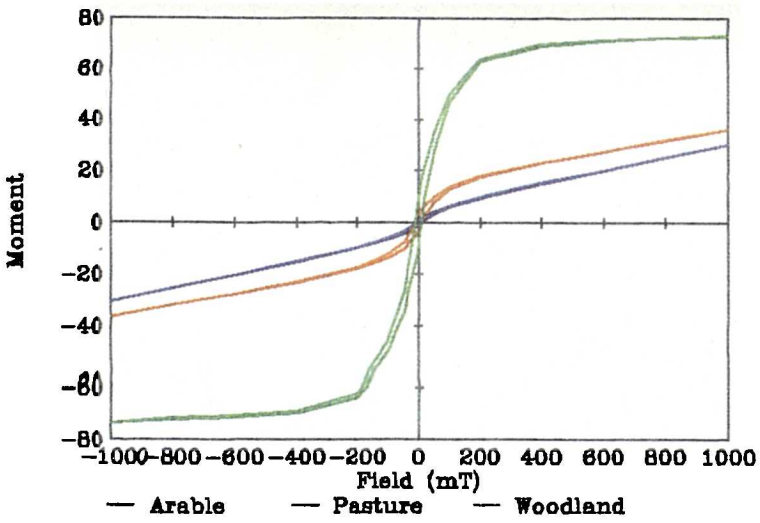

(b) 16–18 cm depth

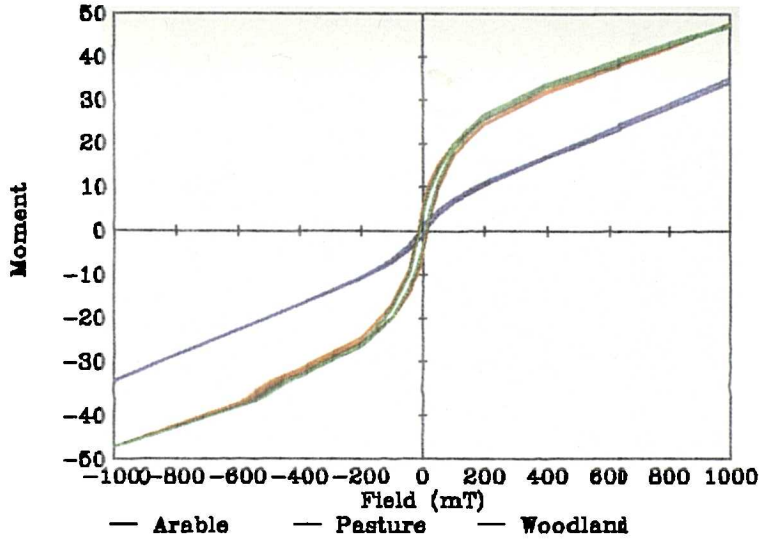

(c) 28–30 cm depth

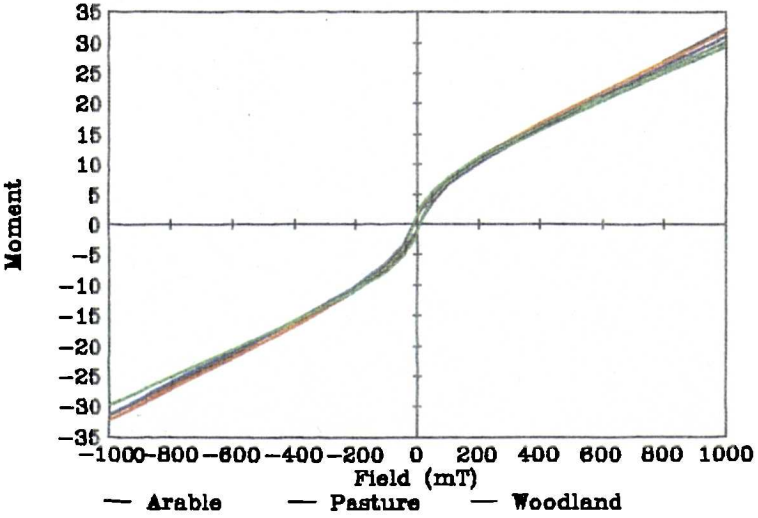

(d) Parent material 44–46 cm depth)

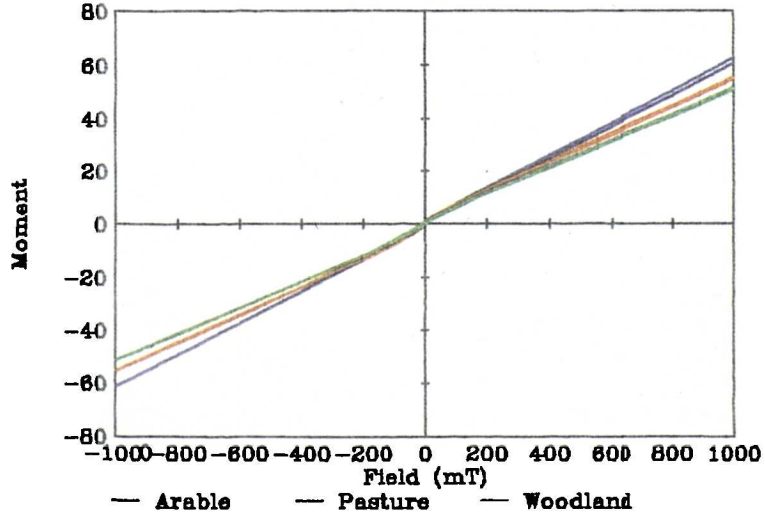

Table 9.3 continued

Description	Code	χlow	χhigh (para)	χferri	χpara	χferri	Ms	Mrs	Mrs/Ms	HIRM +100mT	S ratio
Pasture											
0-2cm	SP2B1	242.75	6.79	235.96	2.8	97.2	4965.0	999.1	0.20	66.71	0.93
4-6cm	SP2B3	86.99	6.99	80.01	8.03	91.97	4012.7	858.9	0.21	205.26	0.76
8-10cm	SP2B5	109.71	9.95	99.76	9.07	90.93	6477.5	1623.3	0.25	616.37	0.62
16-18cm	SP2B9	120.94	9.73	111.2	8.05	91.95	6974.6	1802.8	0.26	480.77	0.73
28-30cm	SP2B15	52.65	8.67	43.98	16.46	83.54	2122.6	444.2	0.21	124.06	0.72
44-46cm	SP2B23	42.01	19.65	22.36	46.77	53.23	1199.1	342.7	0.29	179.1	0.48
Woodland											
0-2cm	SP3B1	262.41	2.48	259.93	0.95	99.05	23107.1	3107.1	0.13	668.6	0.78
4-6cm	SP3B3	364.73	5.31	359.42	1.46	98.54	34372.9	4366.4	0.13	850.7	0.81
8-10cm	SP3B5	516.99	10.54	506.45	2.04	97.96	48352.9	6537.1	0.14	1202.2	0.82
16-18cm	SP3B9	116.37	9.74	106.63	8.37	91.63	8084.9	1264.9	0.16	257.4	0.80
28-30cm	SP3B15	45.28	9.47	35.81	20.92	79.08	2326.9	504.3	0.22	109.19	0.78
44-46cm	SP3B23	39.51	20.33	19.18	51.45	48.55	717.44	250.2	0.35	119.29	0.52

Mineral Modelling

Results from linear modelling for the four horizons in each soil core are presented in Table 9.4. Geological source components have been used to model the soil samples. Diamagnetic proportion results are on average between 90 and 98% while ferrimagnetic components are between zero and 0.0012%. The ferrimagnetic component is, however, detected in the arable horizons and then in all parent material samples to a concentration of between 0.0008 and 0.0012%. The large magnetizations of the woodland organic matter is attributed to the canted-antiferromagnetic component rather than the ferrimagnetic component. In the parent material it should be expected that a much larger paramagnetic component be calculated but this indicates the very small proportions of total mineral content which contribute to the magnetic properties. Also, one problem is that the paramagnetic component of canted-antiferromagnetic materials causes confusion for the linear program.

Table 9.4: Linear Modelling results for arable, pasture and woodland Seeswood soils using geological mineral source set. x1=geological magnetite, x2=geological hematite, x3=lepidocrocite and x4=chalk.

Sample	Source and Proportion			
	x1	x2	x3	x4
0-2 cm..				
Arable	0.0002	0.86	0.71	98.43
Pasture	0	2.88	0.57	96.55
Woodland	0	8.97	0.82	90.21
16-18 cm				
Arable	0.001	0.95	0.8	98.26
Pasture	0	4.62	0.6	94.77
Woodland	0	3.68	0.78	95.53
28-30 cm				
Arable	0.001	0.98	0.73	98.29
Pasture	0	1.0	0.74	98.25
Woodland	0	1.35	0.6	98.04
PM (Keuper Clay)				
Arable	0.0008	0.15	1.62	98.22
Pasture	0.0012	0.35	1.42	98.23
Woodland	0.0012	0.25	1.34	98.41

9.3.2 Buxton Soil Profiles

Two profiles were collected from the area surrounding Buxton, Yorkshire, one a ranker on limestone (SK 081 682) and one a blanket peat (SK 000 719). These profiles were chosen because of their low contributions of primary minerals into the profiles and also, in the case of the peat, few secondary minerals. Both profiles, it was thought, would show similar magnetic properties in upper layers through atmospherically derived minerals; fly ash accumulation in peat has been previously found by Oldfield et al.(1978, 1981) and Williams (1992), for example. Soil profile descriptions are shown in Figure 9.12. The ranker profile shows the shallow nature of the soil on clay and limestone parent material at a depth of 24cm. VSM samples are presented for 0-2, 14-16, 22-24 and parent material layers. The peat was more decomposed from 10cm and a lime contamination layer was present at 8cms. The lime layer could be related to atmospheric fallout of dust from the local lime works. Four peat samples are presented from the profile which represented the most progressive changes in hysteresis loop shape (0-2, 4-6, 14-16 and 22-24cm). When measured the values were not corrected for loss on ignition in these soils.

χlf and χfd% Profiles

Figure 9.13a shows χlf profiles for the two soils and Figure 9.13b shows a χfd% profile for the ranker only (as all kappa measurements of the peat were <10, see Chapter 3). The ranker profile indicates a layer of increased concentration of magnetic minerals at a depth of 14-16cm.. Above this the χlf profile is stable at ~0.4 $\mu m^3 kg^{-1}$. Below the peak the χlf profile reduces to 0.1 $\mu m^3 kg^{-1}$ and then reaches zero in the clay limestone layer below 32cm. The peat profile shows accumulation of magnetic minerals in the top 6cm. and below this a stable profile with diamagnetically affected (negative) measurements. The χlf values of the 0-2cm layers of the peat and the ranker are the same at 0.4 $\mu m^3 kg^{-1}$ indicating that while the magnetic concentration is very low there is similar accumulation of atmospherically derived minerals in both profiles. The χfd% profile for the ranker indicates the accumulation of slightly finer grains in the 14-46cm layer while in the layers above a χfd% of ~4 indicates mainly coarser grains. Below the 14-16cm layer the χfd% drops to zero at 32cms.

Hysteresis Curves

Hysteresis curves for the ranker soil are presented in Figure 9.14a (specific) and b (normalized). Increasingly through the profile there is a change from curved loops (0-2, 14-16cm) to a more paramagnetic loop (22-24cm.) and a diamagnetic curve from the limestone. This is confirmed by the data in Table 9.5 where χlow and Ms values decrease through the profile. Concentration values fall from 125 mAm^2kg^{-1} in the 0-2cm layer to 5 mAm^2kg^{-1} in the limestone. The peat sample curves are shown in Figure 9.15. A large ferrimagnetic concentration dominates the 0-2cm layer (maximum intensity of 70 mAm^2kg^{-1}) and a smaller concentration is seen in the 4-8cm layer (maximum intensity of 12 mAm^2kg^{-1}). The lower layers exhibit diamagnetically dominated curves with tiny ferrimagnetic or other mineral components of <1 mAm^2kg^{-1}. One failure in the VSM spreadsheet occurred when calculating the percentage of χferri and χpara parameters for diamagnetic materials. The failure is the non-recognition of the negative values produced with diamagnetic hysteresis loops. In these cases the parameters are noted as not applicable (N/A: this is shown in Tables 9.4 and 9.5).

Figure 9.12: Buxton Soil Profiles, ranker (a) and peat (b)

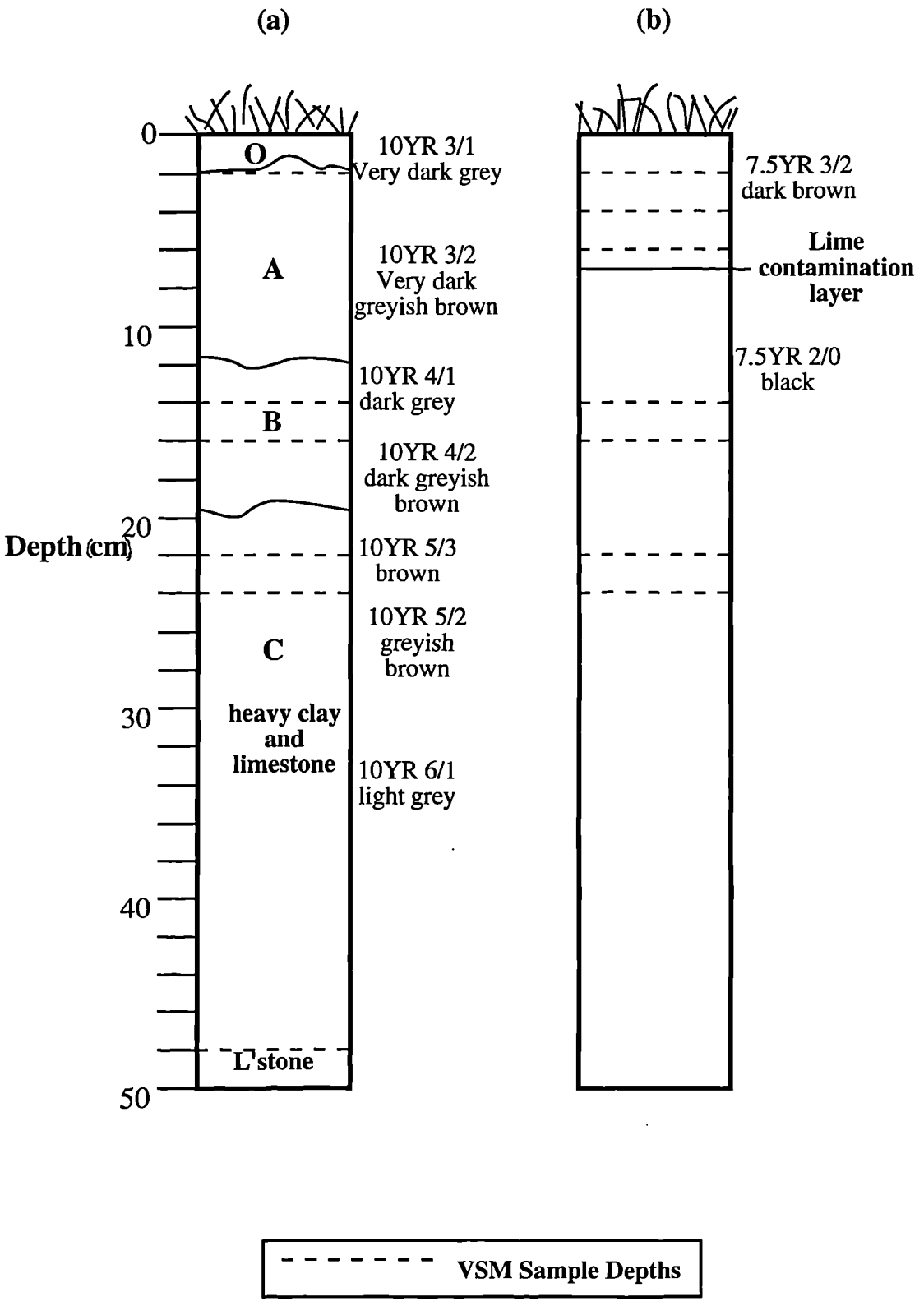

Figure 9.13: Xlf profiles (a) and Xfd% profile (b) for Buxton soil cores

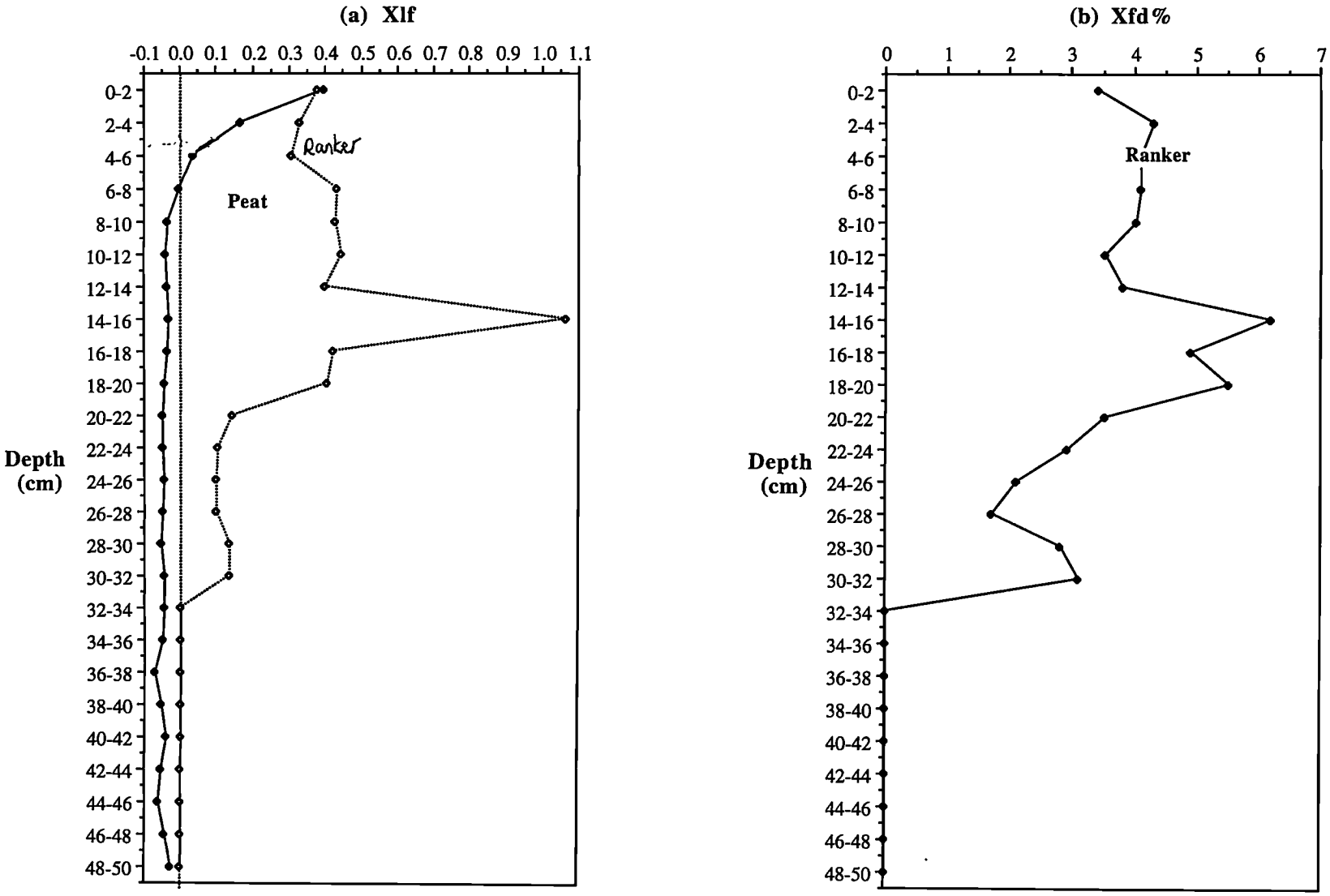

Figure 9.14: Buxton Ranker VSM loops, (a) mass specific

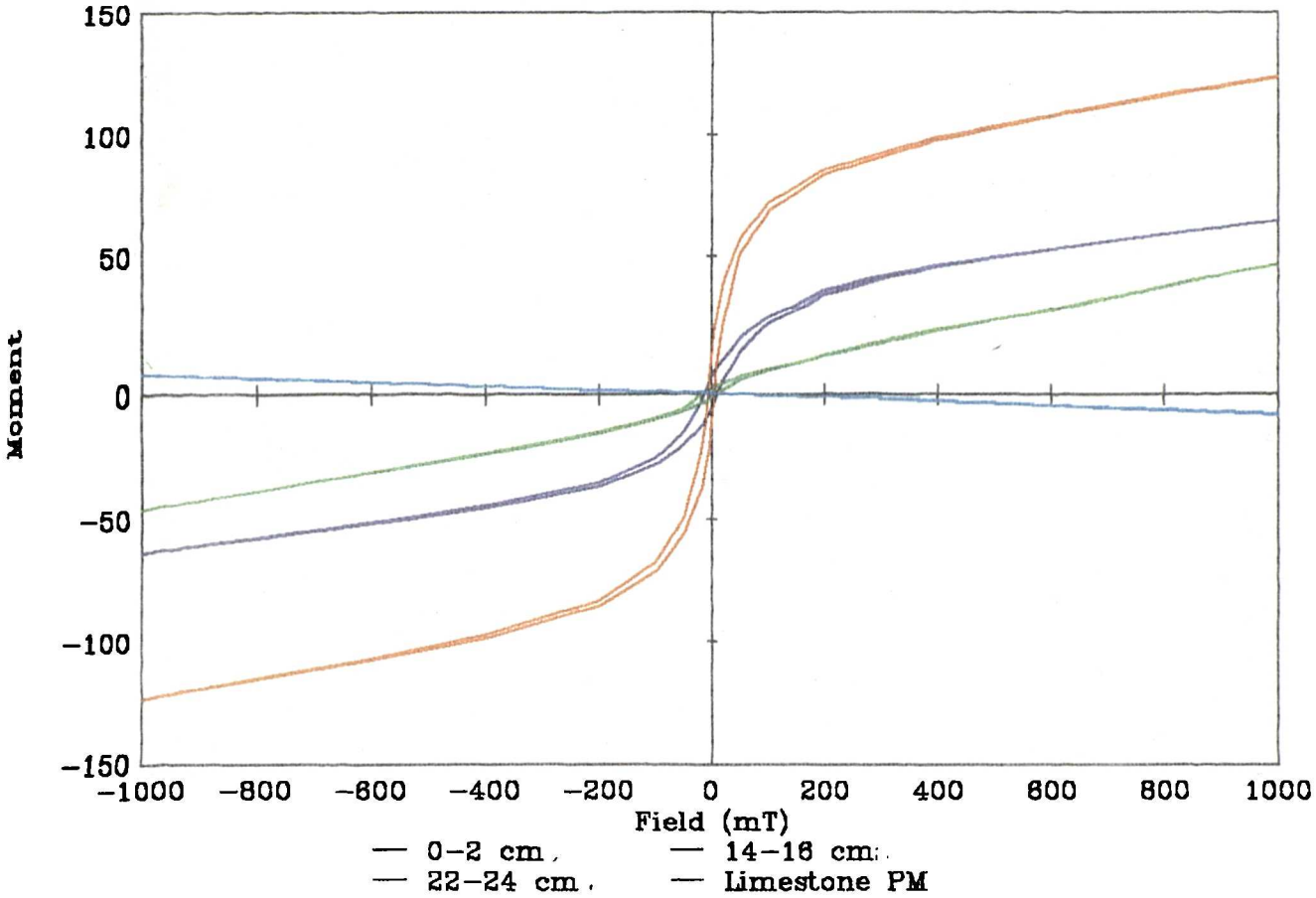

(b) normalized

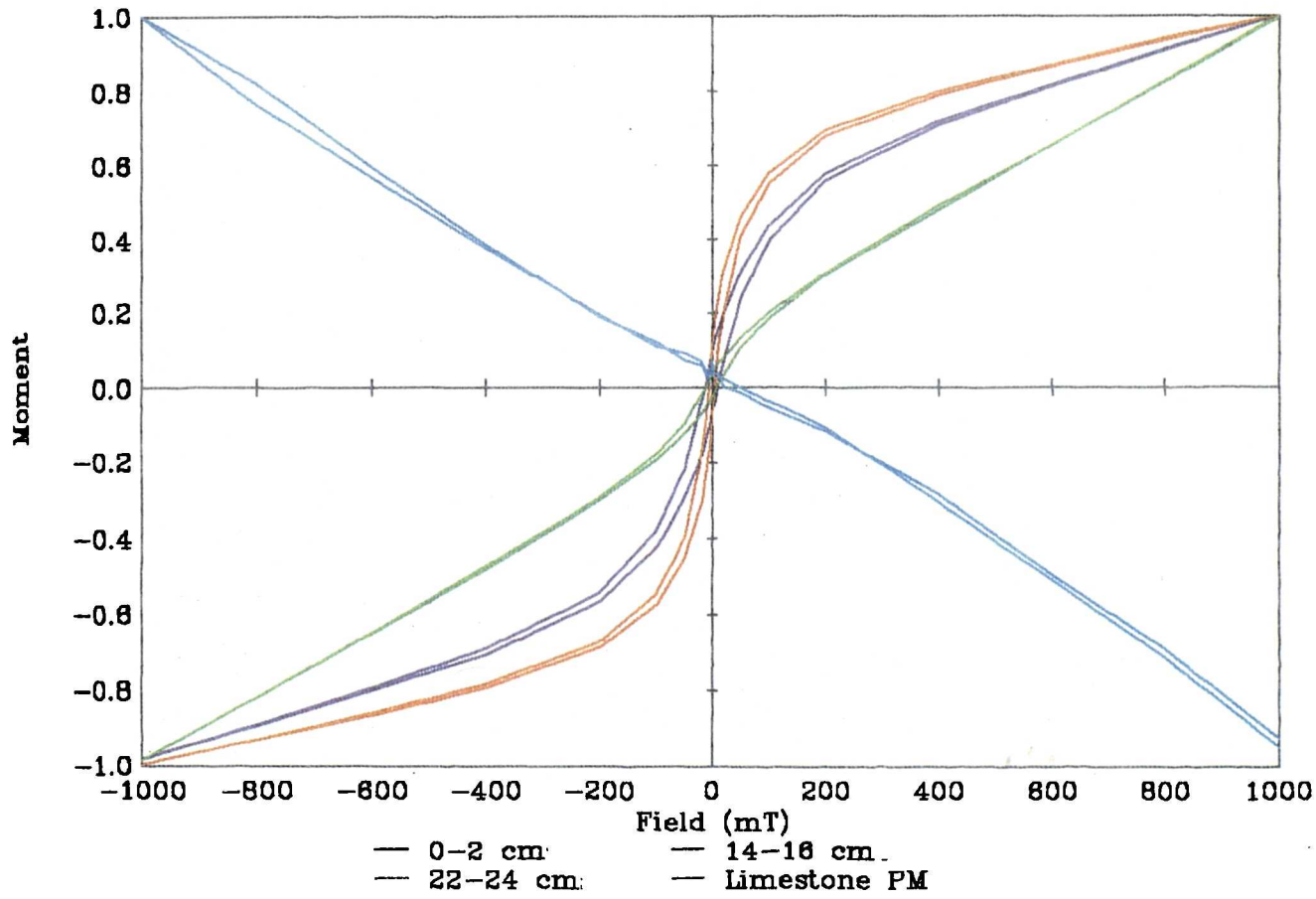

Figure 9.15: Buxton Peat VSM loops, (a) mass specific

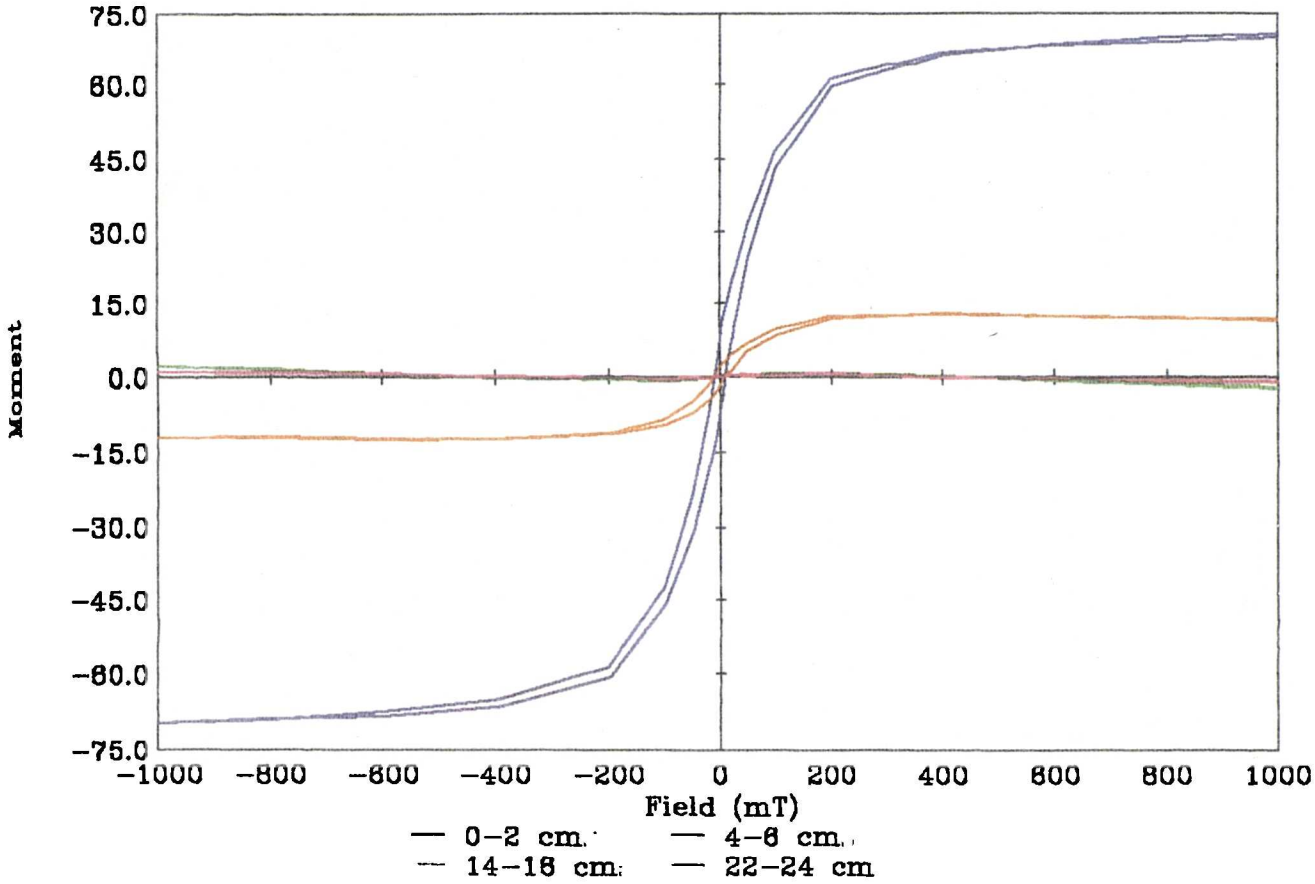

(b) normalized

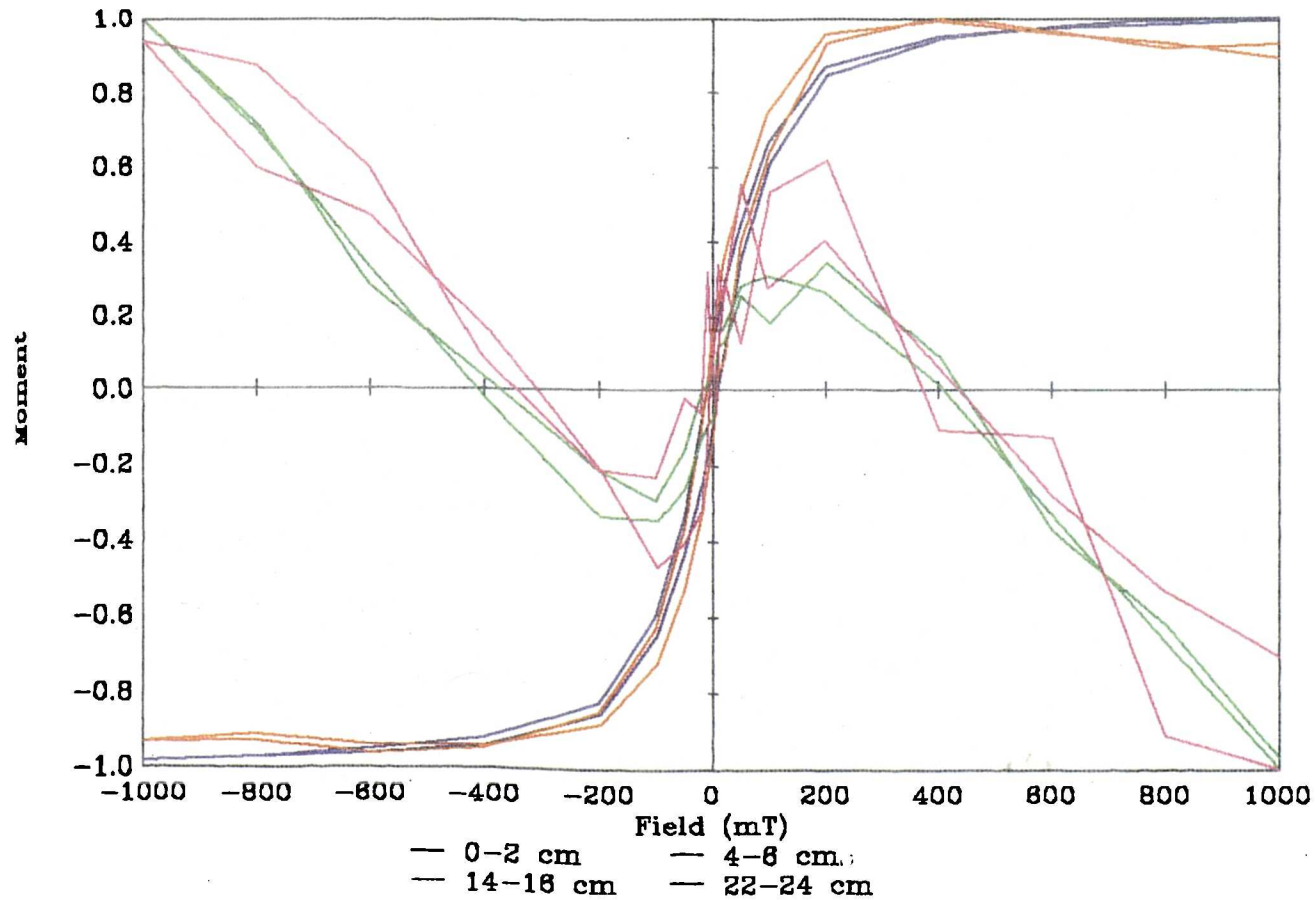

Table 9.5: Hysteresis data for selected horizons of Buxton ranker and peat soil profiles.

VSM SPREADSHEET V1.0 OCTOBER 1993

INPUT Description	INPUT Code	CALC χlow	CALC χhigh (para)	CALC χferri	CALC χpara	CALC χferri	CALC Ms	CALC Mrs	CALC Mrs/Ms	CALC HIRM +100mT	CALC S ratio
			μm^3 kg^{-1}		%	%	mAm^2 kg^{-1}			mAm^2 kg^{-1}	
Ranker											
0-2cm	ES1B1	0.53	0.04	0.50	6.75	93.25	32.59	5.91	0.18	1.15	0.81
14-16cm	ES1B8	1.89	0.05	1.84	2.45	97.55	81.93	12.64	0.15	1.79	0.86
22-24cm	ES1B12	0.12	0.05	0.07	39.94	60.06	7.11	1.69	0.24	0.54	0.68
Limestone	EA1A1	0.01	0.0	0.02	0.0	100.0	0.84	0.57	0.68	0.20	0.64
Peat											
Peat 0-2cm	CF1P1	0.59	0.0	0.59	N/A	N/A	64.77	7.78	0.12	1.43	0.82
Peat 4-6cm	CF1P3	0.02	0.0	0.02	N/A	N/A	13.49	2.0	0.15	0.74	0.63
Peat 14-16cm	CF1P8	-0.07	0.0	-0.08	N/A	N/A	-5.24	0.33	-0.06	0.05	0.83
Peat 22-24cm	CF1P12	-0.06	0.0	-0.06	N/A	N/A	-1.6	0.16	-0.1	-0.07	1.43

Mineral Modelling

Linear modelling results using the geological mineral source components are presented in Table 9.6. Taking the ranker first, the results show that the ferrimagnetic magnetite component is zero throughout except for a value of 0.0003% in the limestone. All layers except the limestone have paramagnetic components of about 1% while the canted-antiferromagnetic component is significantly larger in the 14-16cm layer at 17% (indicated by the width of the hysteresis curve in Figure 9.14). The diamagnetic component in this layer is lower at 82%. The limestone has a realistic diamagnetic component of 99.9997% with a ferrimagnetic component of 0.0003%. This result tends to indicate that generally the results gained using the geological source samples are quite reliable.

Table 9.6: Linear Modelling results for Buxton ranker and peat profiles using geological mineral source set.

Sample	Source and Proportion			
	x1	x2	x3	x4
Ranker				
0-2 cm	0	5.35	0.99	93.66
14-16 cm	0	16.96	0.84	82.2
22-24 cm	0	1.31	1.07	97.62
PM (Limestone)	0.0003	0	0	99.9997
Peat				
0-2 cm	0	8.01	0.89	91.1
4-6 cm	0	1.93	0.095	97.98
14-16 cm	0	0.076	0	99.92
22-24 cm	0.0001	0.1172	0.0034	99.88

The peat samples show large diamagnetic components of 98-99% as expected from their large organic content. In the 0-2cm layer a canted-antiferromagnetic component of 8% and a paramagnetic component of 0.89% is present. It was expected that a ferrimagnetic (magnetite) component would account for the contamination; but this was not the case in the linear modelling results. In the 22-24cm layer a ferrimagnetic component of 0.0001% was detected by

the linear model. This may be representative of all the peat samples but was not seen by the linear modelling in the other layers due to scale problems. In the two lower layers zero and very low percentage paramagnetic components are present; fact the 14-16cm layer appears to show a lower magnetic component overall than the 22-24cm layer. This is also confirmed in Figure 9.15b where the hysteresis curve for the 14-16cm layer shows a reduced magnetic component.

9.4 Discussion

Hysteresis loops give valuable information on the magnetic properties of materials. The choice of minerals which are used as sources in this case study has probably been one of the main limiting factors of the results. The high degree of intercorrelation which exists between magnetization data (always significant to 0.0001% and similar to that shown in Chapter 3 for remanence data) is also a major limitation. Often no ferrimagnetic component was identified in the samples by LINDO but in the case of the organically contaminated samples (Alice Holt, Seeswood Woodland and Buxton peat) the presence of ferrimagnetic fly ash has been confirmed both from the hysteresis loops, microscopically and using XRD. The loss of magnetic minerals in the Seeswood arable and pasture profiles compared to the woodland profile can be attributed to gleying in the soils at this site (Maher, 1986, Dearing et al, 1994). The loss of the magnetic signal in the peat profile can be attributed to the dissolution of the atmospheric magnetite in waterlogged conditions (Williams, 1992). It was of interest to attempt to discriminate both coarse-grained (MD) atmospherically derived magnetic components and fine-grained (SP/SD) pedogenically or bacterially derived magnetic components in environmental materials. This proved to be too difficult, in terms of linear programming, using magnetic measurements. Overall the normalized hysteresis loops and χfd% results are only semi-quantitative.

Simultaneous equations of certain ferrimagnetic mineral-indicating parameters (χferri for example) may give more reliable answers. This is limited in the sense that the result is from one parameter only and not an average result from many parameters. The composition of the soils is given by both the VSM spreadsheet (from susceptibility calculations) and linear modelling of magnetization results. The results are only as reliable as the purity and quality of the source component parameters input into the modelling. Results are directly limited by the large scale values of the ferrimagnetic source components used in the modelling. This adversely affects the results of the modelling and makes the results semi-quantitative at best. Interpretation of the results presented in this chapter requires great care, possibly greater than that taken with sediment source proportion results in Chapters 7 and 8. One advantage of the mineral components used in this chapter, however, are that they are more mineralogically pure than any sediment source components. Sediment sources are more complex as they are essentially non-discrete mixtures of the four mineral source components modelled in this chapter.

9.5 Summary

The methodological framework has again been revised here in accordance with this particular case study and is shown in Figure 9.16. Identification of mineral sources was semi-subjective from a range of natural and synthetic minerals in the sample databases. Measurement was limited to susceptibility and hysteresis loops and calculation of related parameters. Classification of the mineral sources was not successful for reasons explained under classification of the synthetic database in Chapter 3. Modelling of the minerals has been completed and results are affected by the scale of the ferrimagnetic mineral source components and also possibly by the paramagnetic component of the canted-antiferromagnetic minerals. This study has shown that modelling can be accomplished using magnetic mineral sources but that statistical techniques and linear modelling are affected by the scale problem and are ill-conditioned. Also the error terms used in the linear modelling have to be large to compensate for the large magnetite magnetization values. Inclusion of analytical parameters other than magnetic ones would probably have to be included if mineral modelling of soils and sediments is to be more successful.

Figure 9.16: Methodological framework and routes taken in Mineral Modelling study

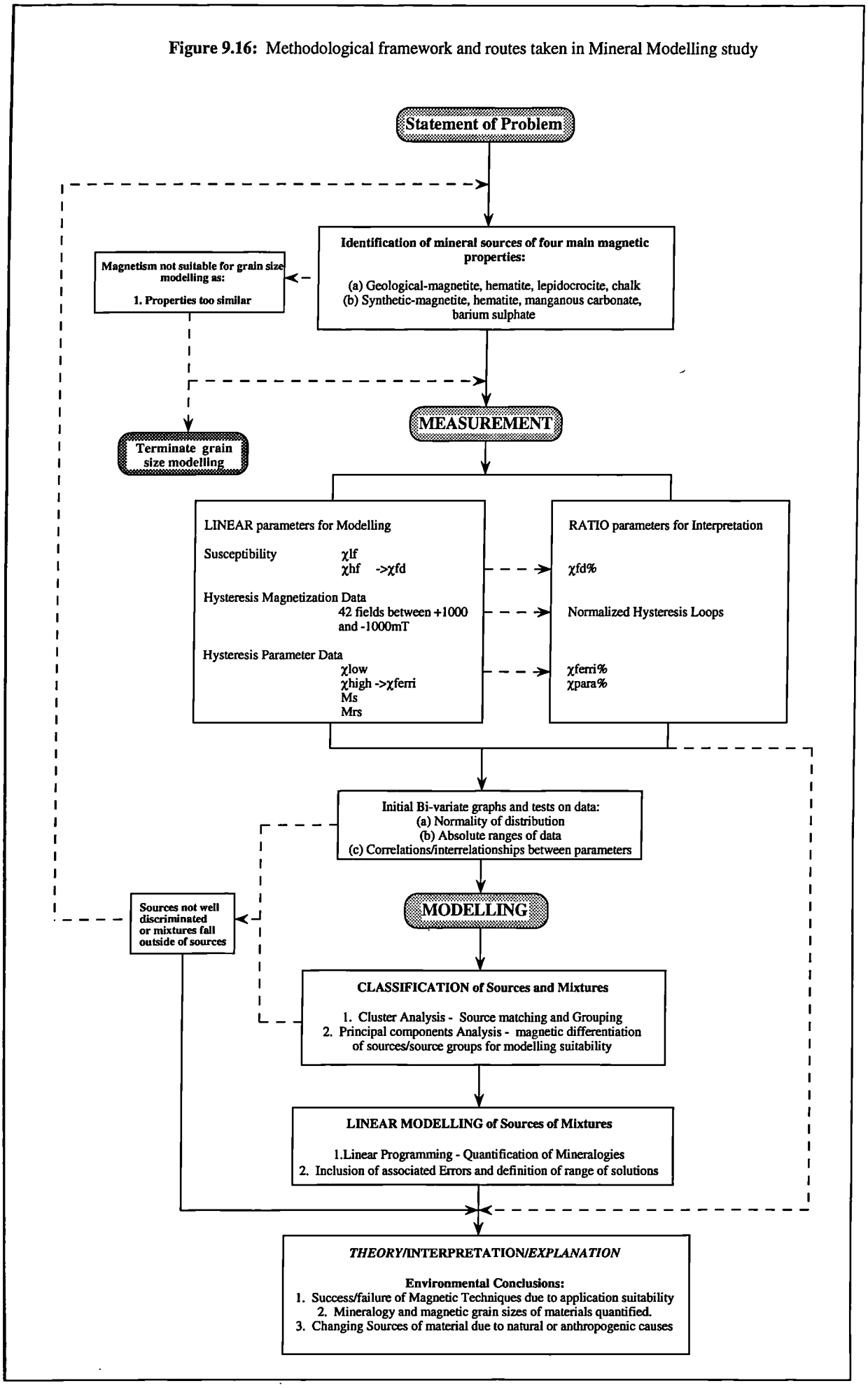

CHAPTER 10
Discussion and Conclusions

The main aims of the research were to evaluate magnetic techniques for modelling the movement of materials and minerals in environmental systems. Overall a *measurement - modelling - interpretation* methodological procedure was to be defined for application of magnetic techniques (Figure 6.1, Chapters 6, 7, 8 and 9). While this research has focused on magnetic techniques it would be valid to transfer this framework to other analytical techniques used in sourcing materials and minerals. The rest of the chapter has been sectioned into the discussion of major findings in each technique used in this research (ie magnetism, source identification, classification and modelling). Sources of error in the methodological procedure are also summarized. The main findings of the three environmental applications of the procedure (Section C) are presented and finally possible improvements to the procedure using further magnetic or other analytical parameters are discussed. Finally the main conclusions of this research are then presented.

10.1 Main Experimental Findings

Magnetism

The limitations imposed on the application of magnetism by the inter-correlation of the magnetic parameters themselves presents the largest single problem in this work. Classification and linear modelling techniques require magnetic parameters to be more independent than many magnetic parameters generally are. Standard concentration parameters (eg χlf and HIRMs) indicate mainly ferrimagnetic mineral and canted-antiferromagnetic mineral groups. Paramagnetic minerals can be identified by moderate susceptibility and zero remanence and diamagnetic minerals by negative susceptibility and zero remanence. With the use of VSM parameters paramagnetic minerals can be identified and quantified more effectively using χhigh. Only normalized and ratio parameters (eg χfd%) give clear indication of magnetic mineral grain sizes.

It has been found that grinding may alter the magnetic properties of materials. This is especially true for materials containing MD grains (Chapter 4 and Appendix 6). Slight changes have also been found in magnetic properties with packing density and dilution (through possible interaction as shown in Paper 1, Appendix 7). Changes may also occur in the mixing of certain materials as seen in Chapter 4 for which no clear answer exists. However, with care, the methodological framework presented in Figure 6.1 can be applied as shown in Section C.

Overall there are limitations in the application of magnetism for quantitative source modelling mainly due to the abundance of ferrimagnetic minerals in the environment. More magnetic parameters which strengthen the weaker magnetic signals (paramagnetic for instance) in the mixture mineral assemblage are required to allow better source discrimination and modelling possibilities.

Source Identification and Variability

There is great need for thorough identification of sources not only through visual observation but also through field survey and statistical discrimination. The preliminary study carried out at Seeswood Pool (Chapter 3) indicated the importance of assessment of sites for magnetic modelling work either by survey or pilot study. Also, the fact that there are different soil units in the catchment does not indicate that there will be successful magnetic differentiation. Verification of actual sediment contribution is of utmost importance as properties of mixtures might fall outside the property range of sources if the identified sources do not contribute material (eg Stober and Thompson, 1979, Yu and Oldfield, 1993). These initial problems led to in-depth testing of the source identification methodology (presented in Chapter 5). The main methodological flaw in many studies can be attributed to unrealistic or subjective sampling strategies which fail to identify or incorporate the true variability of source materials. Identification of such variability may avoid inappropriate application of modelling techniques (especially if that variability causes overlap in the properties of two or more sediment sources). Field surveys and bulking of many samples to incorporate spatial variability are seen to be necessary techniques to incorporate into pilot studies of areas of possible interest.

Chapter 5 presented information on various aspects of variability, from that found in sub-samples of materials to that found in larger spatial areas. Kappa measurements were found to provide information on the concentration and type of minerals. A concentrational classification of types of minerals was applied to field survey results where those values which were below 2 were diamagnetic materials and those over 60 were ferrimagnetic (Figure 5.2). Kappa measurements were used to discriminate between soil and geology types and to indicate areas which might contain magnetically discriminated sources for application of modelling using magnetism. The main advantage of kappa surveys are that they allow fast identification of sites which would be suitable for further magnetic examination and where only tracing of strongly magnetic minerals may be possible.

Experimental variograms of kappa data have been invaluable for verifying boundaries in data from kappa transects, soil and geological boundaries for instance. In many cases the boundaries are not clear cut but a gentle change from one average kappa values to another can be defined (Chapter 8). Variograms have also allowed the spatial dependence of kappa measurements of environmental materials to be assessed. In the case of soil better statistical derivation of sampling grids and numbers of samples has been made.

Multivariate Classification

From initial studies presented in chapter 3 it was clear that parameters used in the classification must be those on which the modelling is to be based. Care must be taken with the distribution of magnetic data (normality) also. Assessment must be made of the interrelationships between parameters especially between those which are calculated from initial measurements (although the relationships between IRM880 and IRM100 with HIRM100 were often not significant). The data used should be unchanged, as initial linear parameters will give as good a result as any linearized data and include only stage one errors (ie initial measurement non-linearity rather than error through fitting techniques).

Significant interrelationships have been found to exist between many magnetic parameters which are used widely in discrimination work. χlf and HIRM+100 seem to provide the best means for classification of most environmental materials where χlf indicates ferrimagnetic minerals and HIRM+100 indicates canted-antiferromagnetic minerals (these parameters often form the PCs in PCA). The intercorrelations between parameters causes ill-conditioning of classification techniques where there are no significant orthogonally related parameters on the basis of which to classify the materials. Cluster analysis has been found to give useful but limited two-dimensional output which is severely affected by positive skew in the data sets. However it is clear that PCA is a good indicator of materials which can be modelled successfully and those which are too magnetically alike or are multiples of one another will fail. It has been found that classification with a few parameters such as χlf, χfd, χarm and HIRM is just as successful as when using all the linear magnetic parameters available.

From classification tests it is clear that without log transformation much information is lost to the mineral concentration scale present within most of the databases. The use of linear non-transformed data also indicates the potential success or failure of linear modelling of the sources as shown in Chapter 3. Log transformation causes the loss of information in datasets with many weak or negative values and PCA techniques fail through this factor. A constant could be added to all parameter values in the dataset to overcome data loss through negative or near zero values; this has not been carried out as yet but must be approached with caution especially when interpreting the data.

Principal components extracted always correspond to ferrimagnetic minerals first and canted-antiferromagnetic minerals second, except in the case of the synthetics database where there are stronger grain size differences between samples. In general it has been found that PCA plots do not contribute further information about the databases than the bi-variate plots. For instance, from the pollution database it is clear that further work in tracing and modelling pollutants using standard magnetic properties would not be successful. Limitations are also shown by the geology database where basic igneous rocks with strong ferrimagnetic signal would mask weaker geologies (Chapter 3).

Overall the classification of magnetic properties is governed by the strong interrelationships seen between the parameters by the statistical routines. At best three PCs can be identified (in a synthetic dataset) representing ferrimagnetic, fine-grained ferrimagnetic and canted-antiferromagnetic minerals. In the environment, however, generally only one or two PCs are identified, ferrimagnetic first and then canted-antiferromagnetic plus paramagnetic plus diamagnetic. The ferrimagnetic component could be removed from the whole exercise however but in 95% of cases (probably nearer 100% in the environment) there are not enough magnetically different minerals left with which to formulate a useful classification. In general, ratio parameters have been found to indicate grain size differences of ferrimagnetic minerals in samples more successfully than linear parameters which are affected by concentrations of minerals.

Modelling

Linear additivity of magnetic parameters was tested and it became clear that many factors affected the success of the linear modelling. First there was wide variation in the environment extending from properties of grain and particle sizes to different soil types. Since great care was taken in the sieving of the bedload and soil experiments such large additivity errors were not expected. In studies of environmental systems where magnetic modelling is engaged a significant difference between identified sources of sediments and secondly a significant difference between the properties of the selected transport fractions of the sources must also exist. The exact particle size ranges of sediments and sources may not be matched exactly as was seen in the River Sowe study. Much depends on the complex processes responsible for the transport of sediments.

Linear magnetic properties have been found to be linear in small concentrations and when using materials less magnetic than the chimney slag. From results of the artificial mixing experiments the magnetic 'distance' needed between materials which can be unmixed successfully was inferred from PCA co-ordination plots. It was found that if the source components occurred in different quadrants of the plot then mixtures of those components will be successful, whereas those of components which occur in the same quadrant are likely to be unsuccessful. The linearity of magnetic properties and specific measuring equipment can be quantified using the linearity errors. The linearity of measurements for each mixture set varies in terms of deviation from unity but in both sets a similar pattern of reduced predicted values compared to actual values exists. Susceptibility measurements had the lowest errors (5-7%, indicating that the Bartington Meter is linear) and remanence measurements made on the Molspin Fluxgate magnetometer were not so linear, with errors generally well over 10%. Linearity of the VSM magnetization data for the mixtures which worked (only 2 of 8) was good with errors of only 6.5% at low positive fields (5mT). Great difficulties were encountered in the mixing of such small samples and this could be the cause of the high failure rate of the VSM mixtures (Chapter 4). Overall results of the 71 artificial mixtures showed that at best only 4 sources of materials could be modelled successfully using magnetism.

There are a number of reasons why linear modelling of magnetic properties may fail. The measurements of artificial mixtures suggested that these include inhomogeneity, equipment linearity and calibration and interaction. Each of these has been tested and no conclusive answer was found (further physical testing of these factors can be found in Paper 1, Appendix 7). Synthetic dilution experiments (not presented in this thesis), where 5 dilutions were made of 15 synthetic minerals, interaction only affected the linearity of χlf measurements in dilutions containing more than 20% of a ferrimagnetic mineral. Such clear results were not gained when testing remanence measurements, however, due to the scale of remanence values overloading the attenuation on the Molspin equipment.

Sources of Error in Modelling

In Table 10.1 a summary of all possible sources of error is given. Many of the errors apply generally to most analytical techniques but those specific to magnetism are given. The table is divided into categories reflecting main sections of the thesis, source identification, classification and modelling for example. The table summarizes the main points made in this Chapter.

Table 10.1: Possible Sources of Error causing poor overall modelling results

General Research Factors	Specific Magnetism Factors
1. General Errors	
(a) Weighing errors	10ml Pots; plus Samples - 6/10g VSM holders; plus samples - 11/0.4g
(b) Equipment accuracy/drift (see Appendix 3)	Corrected on susceptibility meter Molspin calibrated every 10 samples maximum drift 5% (when not warm) VSM drift negligible.
(c) Equipment calibrations batch variation (see Appendix 3)	Suspected demagnetization in Molspin and samples. VSM non zero field on zero remanence measurements. Variation in batch minimal all related samples measured concurrently.
2. Variability of materials	
(a) Within material variation	<15% in environmental materials (<2mm) mostly zero in homogenous chemical materials
(b) Environmental variability	Generally <50% in soil units and <200% in sorted coarse grained materials.
(c) Particle size variability	High and classification is needed on transported grain sizes of potential sources
3. Independence of measurements	
(a) Non-independent ranges	Presence of ferrimagnetic and canted-antiferromagnetic minerals in all databases
(b) Normality of data set	High positive skew in most datasets
(c) Correlation	Highly significant between all parameters except χlf, χfd and HIRM
(d) Collinearity	High collinearity between vectors for sources containing ferrimagnetic minerals
(e) Scale of data set properties	Ferrimagnetic values often hundreds of times that of other minerals
4. Source identification	
(a) Identifying sources	Kappa survey and χlf versus HIRM bi-variate scattergram
(b) Defining sources spatially	Kappa transects and grids and variogram construction at different variability scales
(c) Defining sources statistically	Mean±1sd has been used to define sources

5. Classification and Modelling	
(a) Independent parameters	χlf, χfd and HIRM
(b) Linearity of measurements	χlf = 5-7% and IRMs >10%. VSM (6/8 mixtures) >50%
(c) Ill-conditioning	Caused by much parameter intercorrelation
6. Interpretation	
(a) Measured continuous data	Concentrational parameters (eg χlf and IRM880) for use in source identification, classification and modelling often have double meanings ie concentration/grain size
(b) Derived continuous data	Ratio and normalized parameters (eg χfd%) for use in grain size inference compared to theoretical spherical grain domain sizes
7. Further Work	
(a) More magnetic measurements	Further testing and incorporation of VSM parameters
(b) Other analytical parameters	Colour, particle properties, geochemistry etc

10.2 Main Application Findings

Coastal Systems

At Holderness magnetism was identified as being not suitable to model the sources of the beach mixtures. Successful tracing of the black sand using kappa survey was realised, however, and this would be quicker than using radiometric analysis of the heavy minerals (cf Greenfield, 1989 and Schuilling, 1993). Particular till fractions were matched to the beach sediments according to the dominant particle size of the black sand. Magnetism alone did not identify the source of the black sand; magnetic extraction and microscopy was used to confirm that the tills' small sand fraction contained black sand.

At Holderness kappa surveysidentified the variability of the till and beach units and was also used to trace the movement of black sand on the beaches. The beach kappa transects provided much useful information on the nature of the movement of the black sand on the beaches. Kappa survey would be a more rapid technique than that of radiometric survey presented by Greenfield (1989) and Schuilling (1993) in Denmark. At Lulworth Cove kappa provided invaluable information in a short space of time on the magnetic mineralogy of over twenty geologies and the beach sediments. Also it was found that there was a significant relationship between field and laboratory kappa measurements. The application of field survey then proves to be a useful pre-cursor tool in the suitability of an area for application of further sediment sourcing using magnetic techniques in coastal areas. The identification of black sand at Lulworth which was not as obvious as at Holderness saved time in non-viable application of source

modelling at this site. In the Holderness study linear programming techniques had limited application due to the scale of the ferrimagnetic signal of the black sand but use of kappa survey has much further scope.

Catchment Systems

In contrast to the coastal studies, at Great Rollright delineation of the area of interest involved an identification of 'effective catchment', and sediment sources were identified spatially through field kappa survey. Variograms using kappa data identified the boundaries within the catchment related to geology and soil type and indicated the level of sampling required. The use of kappa surveys allowed identification of the sources and assessment of their variability such that all possible source components could be classified into main source units for quantitative modelling. The use of kappa surveys and associated variograms has allowed definition of soil, geology and land-use boundaries (often there is an overlap) and allowed definition of grid sampling strategies. In other studies where the sources might not be as well discriminated the application of magnetism would be in doubt for quantitative source modelling. Unfortunately it may rarely be the case using magnetism that the channel bank sources and field sources can be discriminated. Quantitative source modelling further than the 'subsoil and topsoil' stage may be difficult in this case. The linear programming results appeared reasonable in the light of the environmental situation of each mixture. Also the confluence mixture which fell centrally to the other stream sediments could be modelled using the upstream sediments as sources.

At Great Rollright linear modelling of the sources was successful. Variability scales were incorporated into the modelling to find the ranges of possible solutions. However error terms used in the modelling of 0.1 and 0.5 units of each variable represent large percentages of the original source measurement values (for example for IRM880 an error of 0.5 represents 12.3% of the IRM880 value of the rendzina topsoil and 1000% error on the limestone values). The fact that the program could not find a solution within smaller multiple error space is a factor of the scale between sources based on ferrimagnetic concentration rather than good discriminatory factors with less variability. These modelling errors accounted for measurement error on the sources and mixtures as well as variability of the source samples. The catchment case study showed the drawbacks and limitations of modelling using magnetic properties as applied to a catchment system. Throughout it has been seen that even when considering only two sources, error can be very large. It is suggested again that if, as in the artificial mixing experiment, one source of each of the four main magnetic parameters was found then modelling of 4 sources would be possible. This would depend on the strength of the ferrimagnetic source however. This study represents a major step in the application of modelling techniques to catchments where in the past spatial variability of possible sources has not been considered. The source contributions calculated have given sensible results in terms of the environmental situation, for example those mixtures from predominantly clay areas were attributed higher clay proportions.

Mineral Modelling

In the third case study hysteresis loops gave information on the magnetic properties of minerals and mixtures. It was found that there are difficulties in finding pure end members to use as sources for environmental mineral mixtures. The choice of minerals that were used as sources in this case study was probably one of the main limiting

factors of modelling minerals. The high degree of intercorrelation which exists between magnetization data is another major limiting factor. The results were not reliable and known ferrimagnetic contents were not recognized in the linear modelling due to the scale of the measurement values.

In the mineral modelling study the linear modelling results were affected by the scale of the ferrimagnetic mineral source components and also possibly by the paramagnetic component of the canted-antiferromagnetic minerals. Great difficulties were encountered in finding pure mineral end members to use in the modelling. The study showed that modelling can be accomplished using magnetic mineral sources but that statistical techniques and linear modelling are affected by the ferrimagnetic scale problem and are ill-conditioned. Error terms used in the linear modelling have to be large to compensate for the large magnetite magnetization values. Overall the modelling of magnetite grain sizes remains qualitative but the modelling of types of minerals has been achieved and can be interpreted with care. Hysteresis loops have proved to be visually useful for cross matching samples (as are IRM curves) as they indicate all four magnetic properties in various sections of the loop (Chapter 9).

10.3 Further Work

Further Application of Magnetic Techniques

There are several further studies which could incorporate magnetic techniques successfully: first, that of tracing of strongly magnetic minerals, and secondly, to identify more effectively the atmospheric component of environmental materials.

In the Holderness and Lulworth studies a means of tracing materials on the beaches was provided by the black sand and further analysis of its associated quartz grain sizes (in terms of density) may prove useful. In Holderness large accumulations of black sands were seen at the foot of Skipsea till cliffs in the summer and sand was not being re-distributed along beaches at this stage. Beaches were 1m thick and layers of the black sands indicating spring and summer storms were clear. In the winter, however, the beaches were much coarser, thinner (5-10cm.) and shingly, but the sand fractions which were present were very black and were re-distributed at every tide into swash lines and areas of lower energy on the beaches. At Lulworth patterns in distribution and concentration of the black sand may indicate the extent of the 'tipped' material. Periodic susceptibility surveys of the beaches may provide useful information on the dynamics of the beaches.

An attempt was made in Chapter 9 to identify and discriminate the atmospheric magnetic component in various soil and sediment samples. So far atmospheric components have been identified by ratios of magnetic parameters (Hunt, 1986, Thompson and Oldfield, 1986) and tracing of the fly ash was done by Scoullos *et al.* (1979) using a correlation between SIRM iron content. Often no ferrimagnetic component was identified in the samples by linear modelling, but in the case of the organically contaminated samples the presence of ferrimagnetic fly ash has been confirmed both from the hysteresis loops and microscopically (see also Paper 4, Appendix 7). The coarse grained fly ash could be indicated from χfd% and normalized hysteresis loops when compared to data for coarse-grained magnetites. This

approach was not quantitative however. Further work might identify a method of separating the ferrimagnetic grain sizes more effectively.

Further Magnetic Parameters

Linear magnetic parameters have been shown to be highly correlated. Further linear magnetic parameters have to be found, or data for other analytical techniques be incorporated with magnetism, if quantitative source modelling using magnetic properties is to be more successful. From Chapter 9 it has been shown that parameters indicating paramagnetic components such as χhigh would be useful to incorporate into classification and modelling techniques. However the linear additivity of VSM measurements is under question (Chapter 4) and until the accuracy of sub-sampling into VSM holders and the linearity of the equipment can be more thoroughly tested such parameters cannot be incorporated. In initial correlation tests of VSM only parameters significant correlation has been found between all parameters except χlow and χferri with HIRM indicating similar problems to the standard parameters.

Incorporating Other Analytical Parameters

If sources are too magnetically alike there is great scope for incorporating other parameters from geochemical or other analysis in linear modelling. This may validate the difference between having to amalgamate two sources into one, or to quantify them individually for example. Other linearly additive parameters which could be included would have to be orthogonally related with magnetic parameters for the best results. Obtaining two or three orthogonally related parameters would result in an improvement in the classification and quantitative modelling of sources of environmental materials. This presents a wider field of further research which needs to:

(a) find parameters which are orthogonally related with magnetic parameters
(b) evaluate the linear additivity of those other parameters

Some analytical parameters such as heavy metal concentrations could be found to be non-correlated in certain situations, lake sediments for instance (S. Charlesworth, pers. comm.). However, correlations have been found between heavy metals and magnetic properties in materials such as atmospheric dusts (Beckwith et al, 1986). But the pollution database results (Chapter 3) indicate that at this stage only tracing of such strongly magnetic materials is possible. Also geochemical parameters measuring concentration of other mineral parameters such as base nutrients and elements might be used. Absorbed ceasium is at present widely applied in sediment sourcing and currently being evaluated for source tracing (Walling and Woodward, 1992). Such radioisotope parameters might not be correlated with magnetic parameters. Some particle size characteristics and description parameters such as those used by Idbeken and Schleyer (1991) could be incorporated. Colour indexing, for instance could be used but would be subject to redox processes however. All techniques have their own level of application suitability however, and have to be evaluated in terms of quantitative modelling for their realistic usefulness.

10.4 *Measurement - Modelling - Interpretation* Procedure

The Procedure

The measurement - modelling - interpretation procedure has been found to be applicable to diverse environmental contexts as shown in Section C. In each case study phases of the procedure can be deleted but none have had to be added. The base set by the theoretical and laboratory work has been sufficient to define a widely applicable procedure. The procedure was presented in Chapter 6 (Figure 6.1) and a discussion of the application of the procedure (Chapters 7, 8 and 9) is given here.

In delineation of the area of interest the Great Rollright study represented the most thorough test. Kappa surveys have been used to identify sources and assess their spatial variability. In the coastal studies kappa surveys have been invaluable in assessing the mineralogical situation and helping to define and classify sources of sediment. It is at this stage in the procedure that an initial assessment of the suitability for modelling application is made. If the situation is that dominant ferrimagnetic minerals exist then tracing may be possible or the study can be terminated. The size of the area in which sources are to be defined presents some problems for the statistical definition of source variability. In larger scale more dynamic environments which are 'open systems' it is difficult to assess the number of samples which are required to statistically represent the sources. In catchment systems this is not as difficult, as a delimitation of contributing area is more straightforward.

The standard measurements which have been found to be most useful are listed in Figure 6.1; IRM curves and hysteresis loops can be added for further indication of the mineralogies of the sources and/or mixtures. Bi-variate scattergrams of χlf and HIRM give the best indication of the possibilities of further application of the procedure. At this stage the normality of the data is also assessed and data can be normalized for classification routine if required. Use of raw data better indicates the realistic possibility of linear modelling however. Correlation between the parameters for a data set also gives clear indication of the most useful parameters to use in discrimination. If the mixture values have been found to fall outside of the range of source values then re-identification of the sources must be carried out.

In the coastal studies and mineral modelling study log-normal distributions were found and log transformation aided multivariate classification but application of linear programming was limited. At Great Rollright, however, the raw data were more normally distributed and classification routines could be undertaken. The application of linear programming was more viable and ranges of source contributions could be identified also.

Cluster analysis and PCA can further identify the groups of samples using more parameters than the bi-variate scattergrams. This takes into account parameters which have weaker contributions to make to the overall classification (χfd and χarm for example). PCA can also identify more clearly those materials which may unmix with more success. In the Holderness study it was clear that linear modelling would be difficult, but in the Great Rollright study classification indicated an increased possibility of modelling of the sources of sediment.

Linear programming has been carried out on subjectively and statistically defined sources of sediment. In the coastal and mineral modelling studies subjective choice of sources to use in modelling was made and this limits the technique. In the coastal study, however, statistical and spatial definition of sources allows more thorough calculation of the range of possible source contributions.

Finally, specific deductive theory/interpretation/explanation procedures can be given for each study undertaken. The main interpretations include reasons for success or failure of the magnetic techniques using this methodology. This success/failure can be defined with respect to initial application suitability rather than inductive reasoning made at the end of an application. For example modelling of Great Rollright sources was more successful than that of Holderness due to the mineralogical situation. But using kappa surveys this potential success or failure can be assessed early on in the procedure application. Either the source or mineral components calculated in the linear modelling can be evaluated against environmental knowledge for the area being studied; this is seen in all the applications made in Section C. Qualitative conclusions can be made for the grain size components in materials from use of normalized data (eg hysteresis loops, Chapter 9). Finally, with sediments representing historical records of source contribution (for instance lake sediments and coastal stratigraphies), changes due to natural or anthropogenic activity can be defined in a more quantitative manner. In contemporary monitoring also, changes in source contribution may also be quantified (from suspended sediments for example) in circumstances where magnetic discrimination is acceptable. Overall however the procedure has been applied successfully to the three main case studies and it is noted that aspects of the procedure may be transferred to techniques other than magnetism.

10.5 Conclusions

Aims

The first aim of this research was to model the movement of environmental materials through environmental systems and therefore be able to identify the sources of mixtures quantitatively. The application of magnetic techniques for this purpose has been tested both in the laboratory (Chapter 4) and in environmental case studies (Chapters 7 and 8). Magnetic properties of soils and geological sediments have been modelled using linear programming and quantitative source proportions have been calculated. Ranges of possible source proportions have been included wherever possible (Chapter 8) and an evaluation of the source proportions answers is also given.

The second aim of the research was to evaluate the prospects for modelling the magnetic mineralogies of natural and synthetic samples in terms of mineral magnetic properties, mineral type and concentration and mineral size. Mineral magnetic properties have been evaluated using four main databases (Chapter 3) and for the most part it has been found that ferrimagnetic minerals dominate most environmental situations (Chapters 3, 4, 7 and 9). Mineral types have been identified in mixtures; this is most effectively done using VSM hysteresis loops where all four main magnetic properties can be individually recognized. Standard parameters indicate mainly two groups of minerals, ferrimagnetic minerals and a combined group of canted-antiferromagnetic/paramagnetic and diamagnetic minerals. In terms of mineral size, great difficulties have been encountered in discriminating grain sizes effectively for linear

modelling. Further linear parameters which may aid this are discussed later in this chapter. At present magnetic mineral grain sizes are best inferred from ratio parameters.

With respect to the first objective, kappa surveys and reconnaissance have been developed to improve the way in which sources are identified and defined in the environment with respect to their spatial variability and likelihood of contribution of sediment. In order to identify the most useful magnetic measurements which can be used in classification and modelling, and so define the limits of the technique, hundreds of correlation and classification tests have shown that the best discriminatory parameters are χlf and HIRM. The third objective was to develop and evaluate the use of magnetic properties in classification techniques for source and mineral identification, discrimination and sample matching from a base of traditional bi-variate discrimination. It was found in testing and comparison of these techniques using the databases that often bi-variate scattergrams give as much information as does PCA. Cluster analysis gives limited two-dimensional information on the data and PCA best defines the distance required between materials in order for successful modelling application. If PCA cannot be carried out (ie only one factor) then the situation is suitable for tracing only.

Linear programming has been used to achieve the fourth objective which was to develop and evaluate the use of magnetic properties in mathematical modelling techniques, for 'unmixing' environmental mixtures of sources and mineralogies and for tracing the movement of materials through environmental systems. The use of magnetic properties has been found to be limited for quantitative source modelling due mainly to intercorrelations between magnetic parameters.

The fifth objective was to identify the most suitable materials which can be modelled according to their magnetic properties. In order to define the application limits of the modelling technique, samples were chosen from the databases for use in artificial mixing experiments (Chapter 4). Chemical reagents were included in the mixtures to provide easily combined diamagnetic and paramagnetic components. The materials chosen were the best found using PCA and set the limits on modelling with materials which are less well discriminated.

Finally, an overall *measurement - modelling - interpretation* methodological procedure was defined from the laboratory and preliminary fieldwork for application to environmental systems of interest (Chapter 6). The procedure has been applied successfully to three case studies and in each case no further methodological work was required (Chapters 7, 8 and 9). In each case separate parts of the methodology were tested, for instance tracing in Chapter 7 and sourcing in Chapter 8. It is proposed that this framework sets the possibilities and limitations of application of magnetism in environmental systems.

Main Experimental Conclusions

1. Major variation of magnetic properties are mappable by kappa which with χlf is the most useful and most linearly additive magnetic parameter.

2. Statistical classification generally gives no more information than a χlf and HIRM+100 bi-variate scatter-plot due to significant correlation and collinearity of linear magnetic parameters.

3. PCA gives an idea of the magnetic distance required between samples if they are to unmix successfully.

4. No more than four sources can be realistically modelled using magnetism and each source has to be contributing at least 5% if strongly magnetic (ferrimagnetic) and 20% if weakly magnetic (diamagnetic, paramagnetic).

5. Variations in the environment can be incorporated in linear modelling but may result in large ranges of possible source contributions.

Main Application Conclusions

1. In bedload and soil fraction modelling, non-linearity has caused failure of simultaneous equations. Linear programming is then the favoured method for 'optimizing' sediment source quantification.

2. In coastal systems application of the methodology resulted in successful tracing of a dominant mineral but unsuccessful quantitative source modelling. Sorted heavy minerals have been found to dominate even a geologically sedimentary area.

3. In catchment studies sediment sources of finer sediments have been quantified where magnetically discriminated sources exist. Incorporations of environmental variability leads to a wide range of possible source contributions. Best results were gained using only two sources.

4. In mineral modelling it has been found that modelling is poorly scaled due to values of the ferrimagnetic component being thousands of times that of all the other components (canted-antiferromagnetic, paramagnetic and diamagnetic). Hysteresis loops are visually useful in determining the presence of certain mineral types and verifying linear programming results using hysteresis data. IRM curves are less useful as the paramagnetic component is not represented.

5. Quantitative grain size mineral modelling has been found to be impossible at this stage as all 'sources' are thousands of times greater than the environmental mixtures. Mathematical dilution of the magnetite data would not be correct. The identification of pedogenic (and bacterial), primary and atmospheric minerals still remains qualitative.

6. Quantification of sediment sources is possible with up to 4 sources but is limited to those studies where magnetic discrimination is at its best. Interpretation of data where only the means of source properties are used required great care. It has been found that by incorporating source spatial variability, large overlapping ranges in source contributions are found.

References

Andrews, J. T. and Jennings, A. E. 1986. Influence of sediment source and type on the magnetic susceptibility of fjord and shelf deposits, Baffin Island and Baffin Bay, N.W.T. *Canadian J. Earth Sci.* **24** (7), 1386-1401.

Appleby, P. G., Dearing, J. A. and Oldfield, F. 1986. Magnetic studies of erosion in a Scottish lake catchment, I Core chronology and correlation. *Limnol. Oceanog.* **30** (6), 1144-1153.

Banerjee, S. K., King, J. and Marvin, J. 1981. A rapid method for magnetic granulometry with applications to environmental studies. *Geophys. Res. Lett.* **8** (4), 333-336.

Battarbee, R. W. (& 15 co-authors). 1988. *Lake acidification in the United Kingdom 1800-1986.* Ensis Publishing, London.

Bazilinski, D. A., Frankel, R. B. and Jannasch, H. W. 1988. Anaerobic magnetite production by a marine, magnetotactic bacterium. *Nature* **334**, 518-519.

Beckett, P. H. T. and Webster, R. 1971. Soil variability: A review. *Soils and Fertilizers* **34**, 1-13.

Beckwith, P. R., Ellis, J. B. and Revitt, D. M. 1986. Heavy metal and magnetic relationships for urban source sediments. *Phys. Earth Planet. Interiors* **42.**

Beckwith, P. R., Ellis, J. B. and Revitt, D. M. 1990. Applications of magnetic measurements to sediment tracing in urban highway environments. *The Science of the Total Environment* **93**, 449-463.

Birks, H. J. B. 1987a. Multivariate Analysis of Stratigraphic Data in Geology: A review. *Chemometrics and Intelligent Laboratoy System* **2**, 109-126.

Birks, H. J. B. 1987b. Multivariate Analysis in Geology and Geochemistry: An Introduction. *Chemometrics and Intelligent Laboratoy System* **2**, 15-28.

Bjorck, S., Dearing, J. A. and Jonsson, A. 1982. Magnetic Susceptibility of Late Weichselian deposits in Southeastern Sweden. *Boreas* **11**, 99-111.

Blakemore, R. P. 1975. Magnetotactic Bacteria. *Science* **190**, 377-379.

Blank, M., Leinen, M. and Prospero, J. M. 1985. Major Asian aeolian inputs indicated by the mineralogy of aerosols and sediments in the western North Pacific. *Nature* **314**, 84-86.

Bloemendal, J., Oldfield, F. and Thompson, R. 1979. Magnetic Measurements used to assess sediment influx at Llyn Goddionduon. *Nature* **280**, 50-53.

Bonnel, M. and Sumner, G. 1992. Autumn and winter daily precipitation areas in Wales, 1982-1983 to 1986-1987. *Int. J. of Climatology* **12**, 77-102.

Borradaile, G. J., Chow, N. and Werner, T., 1993. Magnetic hysteresis of limestones: facies control? *Phys. Earth Planet. Inter.* **76**: 241-252.

Bramley, R. G. V. and White, R. E. 1991. An analysis of variability in the activity of nitrifers in a soil under pasture. I Spatially dependent variability and optimum sampling strategy. *Aust. J. Soil Res.* **29**, 95-108.

Buraymah, J. M. and Webster, R. 1989. Variation in soil properties caused by irrigation and cultivation in the central Gezira of Sudan. *Soil and Tillage Research* **13**, 57-74.

Caitcheon, G. G. 1993. Sediment source tracing using environmental magnetism: A new approach with examples from Australia. *Hydrological Processes* **7** (4), 349-358.

Campbell, G. S. 1985. *Soil Physics with Basic.* Elsevier, Amsterdam, The Netherlands.

Catt, J. A. and Madjett, P. A. 1981. *'The work of W S Bisat FRS on the Yorkshire Coast'.* In J. Neale and J. Flenley (eds), The Quaternary in Britain. Pergamon Press, Oxford.

Chauris, R. 1989. Origine des sables terrigenes des plages: interet de la representation cartographique des pourcentages en differents mineraux Lourdes. L'example de la base de lannion (Bretagne Septentrionde). *Norois* **144**, 391-406.

Chevallier, M. R. and Mathieus, S. 1943. Proprietes magnetiques des poudres D'Hematites (influence des dimensions des grains). *Ann. Phys. Paris* **18**, 258-288.

Coard, M. A. (& 12 co-authors). 1983. Paleolimnological studies of annually-laminated sediments in Loe Pool, Cornwall, UK. *Hydrobiologia* **103**, 185-191.

Cullity, B. D. 1972. *Introduction to magnetic materials.* Addison-Wesley, Reading, Mass..

Curtis, L. F., Courtney, F. M. and Trudgill, S. 1976. *Soils in the British Isles.* Longman, Essex, UK.

Dankers, P. H. M. 1978. Magnetic properties of dispersed natural iron-oxides of known grain size. Unpub. Ph.D. thesis, University of Utrecht.

Dauer, J. P. 1991. A nonstandard curve fitting application in modelling lake depth. *Appl. Math. Modelling* **15**, 329-332.

Dearing, J. A. 1979. The use of magnetic measurements to study particulate flux in lake-watershed ecosystems. Unpublished PhD thesis, University of Liverpool

Dearing, J. A., Elner, J. K. and Happey-Wood, C. M. 1981. Recent sediment flux and erosional processes in a Welsh Upland Lake Catchment based on Magnetic Susceptibility measurements. Quat. *Res.* **16**, 356-372

Dearing, J. A. and Flower, R. 1982. The magnetic susceptibility of sedimenting material trapped in Lough Neagh, N Ireland, and its erosional significance. *Limnol. Oceanog.* **27** (5), 969-975.

Dearing, J. A. 1983. Changing patterns of sediment accumulation in a small lake in Scania, Southern Sweden. *Hydrobiologia* **103**, 59-64.

Dearing, J. A., Maher, B. A. and Oldfield, F. 1985. Geomorphological linkages between soils and sediments: the role of magnetic measurements. In *Geomorphology and Soils*, Eds K. Richards, R. Arnett and S. Ellis. pp245-266. Allen and Unwin, London.

Dearing, J. A., Morton, R. I., Price, T. W. and Foster, I. D. L. 1986. Tracing movements of topsoil by magnetic measurements: Two case studies. *Phys. Earth Planet. Interiors* **42**, 93-104.

Dearing, J. A. 1991. Lake Sediment records of erosional processes. *Hydrobiologia* **214**, 99-106.

Dearing, J. A. 1992. Sediment yield and sources in a Welsh upland lake-catchment during the past 800 years. *Earth Surface Processes and Landforms* **17**, 1-22.

Dossor, J. 1955. 'The coast of Holderness: the problem of erosion'. *Proc. Yorkshire Geolog. Soc.* **30,** 133-145.

Dunlop, D. J. 1971. Magnetic properties of fine-particle Hematite. *Ann. Geophys.* **27** (3), 269-293.

Dunlop, D. J. 1973. Superparamagnetic and single-domain threshold sizes in magnetite. *J. Geophys Res.* **78** (11), 1780-1793.

Dunlop, D. J., Xu, S., Ozdemir, O., AlMawlawi, D. and Moskovits, M. 1993. Magnetic properties of arrays of oriented iron particles as a function of particle size, shape and spacing. *Phys. Earth Planet. Inter.* **76**, 113-121.

Edwards, C. A. 1981. *'The tills of Filey Bay'.* In J. Neale and J. Flenley (eds), The Quaternary in Britain. Pergamon Press, Oxford.

Farina, M., Esquivel, D. M. and Lins de Barros, H. G. 1990. Magnetic iron-sulphur crystals from a magnetotactic microorganism. *Nature* **343**, 256-258.

Fassbinder, J. W., Stanjek, H. and Vali, H. 1990. Occurrence of magnetic bacteria in soil. *Nature* **343**, 161-163.

Flower, R. J., Dearing, J. A. and Nawas, R. 1984. Sediment supply and accumulation in a small Moroccan lake: and historical perspective. *Hydrobiologia* **112,** 81-92.

Foster, I. D. L., Dearing, J. A., Simpson, A. and Carter, A. D. 1985. Lake catchment based studies of erosion and denudation in the Merevale Catchment, Warks, UK. *Earth Surf. Proc. Landf.* **10**, 45-68.

Foster, I. D. L. and Dearing, J. A. 1987a. Quantification of long term trends in atmospheric pollution and agricultural eutrophication: a lake watershed approach. *IAHS Publ. no. 167*, Proc. Vancouver Synmp, 49-63. Wallingford, Oxford.

Foster, I. D. L., Dearing, J. A. and Charlesworth, S. M. 1987b. Paired lake catchment studies: A framework for investigating chemical fluxes in small drainage basins. *Applied Geography* **7**, 115-133.

Foster, I. D. L., Dearing, J. A. and Grew, R. 1988. Lake-catchments: An evaluation of their contribution to studies of sediment yield and delivery processes. Sediment Budgets, *IAHS Publ.***174**, 413-423. Wallingford, Oxford.

Foster, I. D. L., Grew, R. and Dearing, J. A. 1990. Magnitude and frequency of sediment transport in agricultural catchments: A paired lake-catchment study in Midland England. In *Soil Erosion on Agricultural Land.* Eds, J. Boardman, I.D.L. Foster and J. Dearing. Wiley, Chichester.

Foster, I. D. L. (with 7 co-workers). 1991. High energy coastal sedimentary deposits: an evaluation of depositional processes in SW England. *Earth Surface Process and Landform* **16**, 341-356.

Gravenor, C. P. and Wong, T. 1987. Magnetic and pebble fabrics and origin of the Sunnybrook Till, Scarborough, Ontario, Canada. *Canadian J. Earth Sci.* **24** (10), 2038-2046.

Greenfield, M. B., De Meijer, R. J., Put, L. W., Wiersma, J. and Donoghue, J. F. 1989. 'Monitoring beach sand transport by use of Radiogenic heavy minerals'. *Nuclear Geophysics* **3**, 231-244.

Grew, R. 1990. Sediment yield and sources over short and medium timescales in a small agricultural catchment, N Warwickshire, UK. Unpubl PhD Thesis, Coventry Polytechnic.

Haines-Young, R. and Petch, J. 1986. *Physical Geography: Its nature and methods.* Harper and Row, London.

Hakansson, L. and Jannson, M. 1983. *Principles of Lake Sedimentology.* Springer Verlag, Berlin.

Higgit, S. R., Oldfield, F. and Appleby, P. G. 1991. The record of land-use change of soil erosion in the late Holocene sediments of the Petit Lac d'Annecy, Eastern France. *The Holocene* **1** (1), 14-28.

Hilton, J., Davison, W. and Ochsenbein, U. 1985. A mathematical model for analysis of sediment core data: implications for enrichment factor calculation and trace-metal transport mechanism. *Chem. Geol.* **48**, 281-291.

Hilton, J. 1986. A simple model for the interpretation of Magnetic Records in Lacustrine and Ocean Sediments. *Quaternary Research* **27**, 160-166.

Hunt, A., Jones, J. and Oldfield, F. 1984. Magnetic measurements and heavy metals in atmospheric particulates of anthropogenic origin. *Sci. Tot. Env.* **33**, 129-139.

Hunt, A. 1986. The application of mineral magnetic methods to atmospheric aerosol discrimination. *Phys. Earth. Planet. Interiors* **42**, 10-21.

Idbeken, H. and Schleyer, R. 1991. *Source and Sediment: A case study of provenance and mass balance at an active plate margin (Calabria, S Italy)* 1st Ed. Springer Verlag, Berlin.

Jakubovics, J. P. 1987. *Magnetism and magnetic materials.* Inst. of Metals 1987, Bath Press, Bath.

Jiles, D. 1991. *Introduction to magnetism and magnetic materials.* Chapman and Hall, London.

Johnson, H. P. and Hall, J. M. 1978. A detailed rock magnetic opaque mineralogy study of the basalts from the Nazca Plate. *Geophys. J. R. Astr. Soc.* **52**, 45-64

Jones, R. L. and Keen, D. H. 1993. *Pleistocene Environments in the British Isles.* Chapman and Hall, London.

Joreskog, K. G, Klovan, J. E. and Reyment, R. A. 1976. *Geological factor analysis.* Methods in Geomathematics 1. Elsevier, Amsterdam, The Netherlands.

King, J., Banerjee, S. K., Marvin, J. and Ozdemir, O. 1982. A comparison of different magnetic methods for determining the relative grain size of magnetite in natural materials: some results from lake sediments. *Earth and Planetary Science Letters* **59**, 404-419.

Kirkby, M. J., Naden, P. S., Burt, T. P. and Butcher, D. P. 1993. *Computer simulation in Physical Geography.* 2nd edition. Wiley, Chichester.

Kirschvink, J. L. and Gould, J. L. 1981. Biogenic magnetite as a basis for magnetic field detection in animals. *BioSystems* **13**, 181-201.

Kleinman, M. T. 1980. Identifying and estimating the relative importance of sources of airborne particulates. *Sci. Tot. Env.* **14** (1), 62-65.

Kukla, G., Heller, F., Liu, X. M., Xu, T. C., Liu, T. S. and An, Z. A. 1988. Pleistocene climates in China dated by Magnetic susceptibility. *Geology* **16**, 811-814.

Kukla, G. and An, Z. 1989. Loess stratigraphy in Central China. *Palaeogeography, Palaeoclimatology, Palaeoecology* **72**, 203-225.

Kukla, G., An, Z.S., Melice, J.L., Gavin, J. and Xiao, J.L. 1990. Magnetic susceptibility record of Chinese loess. *Transactions of the Royal Society of Edinburgh: Earth Sciences* **81**, 263-288.

Kwun, H. and Burkhardt, G. L. 1987. Effects of grain size, hardness, and skew on the magnetic hysteresis loops of ferromagnetic steels. *J. Appl. Phys.* **61**, 1576-1579.

Laslett, G. M., McBratney, A. B., Pahl, P. J. and Hutchinson, M. F. 1987. Comparison of several spatial prediction methods for soil pH. *J. Soil Sci.* **38**, 325-41.

Le Borgne, E. 1955. Susceptibilite Magnetique Anormale du Sol Superficiel. *Annales de Geophysique* 399-419.

Leeks, G. J., Lewin, J. and Newson, M. D. 1988. Channel change, fluvial geomorphology and river engineering: The case of the Afon Trannon, Mid Wales. *Earth Surf. Proc. Landf.* **13**, 207-223.

Lees, J. A. and Dearing, J. A. 1994. Use of VSM Generated Hysteresis Loops in Environmental Magnetism: Advantages and Comparisons to Other Measuring Equipment. *Environmental Magnetism Laboratory Working Paper No. 1.* Geography Division, Coventry University.

Lehmann, R. 1991a. Uncertainty analysis for a linear programming model for acid rain abatement. *Atmospheric Environment* **25A** (2), 231-240.

Lehmann, R. 1991b. On properties of linear programming models for acid rain abatement. *Atmospheric Environment* 25A (2), 401-410.

Liu, X. M., Xu, T. C. and Liu, D. S 1988. Anisotropy of magnetic susceptibility and origin of the chinese Loess and its significance to the Quaternary research. *Science in China* **B 33** (2), 235-245.

Longworth, G. and Tite, M. S. 1977. Mossbauer and magnetic susceptibility studies of iron oxides in soils from archaeological sites. *Archaeometry* **19** (1), 3-14.

Locke, G. and Bertine, K. K. 1986. Magnetite in sediments as an indicator of coal combustion. *Appl. Geochem.* **1** (3), 345-356.

Maher, B. A. 1986. Characterization of soils by mineral magnetic measurements. *Phys. Earth Planet. Interiors* **42**, 76-92.

Maher, B. A. 1988. Magnetic properties of some synthetic sub-micron magnetites. *Geophys. J.* **94**, 83-96.

Maher, B. A. and Taylor, R. M. 1988. Formation of ultrafine-grained magnetite in soils. *Nature* **336**, 368-371.

Maher, B.A. and Thompson, R. 1992. Paleoclimatic Significance of the mineral magnetic record of the Chinese loess and paleosols. *Quaternary Research* **37**, 155-170.

Mauritsch, H., Becke, M., Kropacek, V., Zelinska, T. and Hejda, P. 1987. Comparison of the hysteresis characterization of synthetic samples with different magnetite and haematite contents. *Phys. Earth Planet. Inter.* **46**, 93-99.

McBratney, A. B. and Webster, R. 1981. Spatial dependence and classification of the soil along a transect in northern Scotland. *Geoderma* **26**, 63-82.

McBratney, A. B. and Webster, R. 1983. How many observations are needed for regional estimation of soil properties. *Soil Science* **135**, 177-183.

McLean, D. 1991. Magnetic spherules in lake sediments. *Hydrobiologia* **214**, 91-97.

Mohan, C. and Gundu Rao, C. 1992. A mathematical approach to the petrogenesis of the Upper Siwalik conglomerates (L. Pleistocene) of the Jammu Region, Northwest India. *J. Geol. Soc. of India* **39**, 223-228.

Mooers, H. D. 1990. Discriminating texturally similar tills in Central Minnesota by graphical and multivariate techniques. *Quat. Res.* **34**, 133-147.

Mullins, C. E. 1977. Magnetic susceptibility of the soil and its significance in soil science - a review. *J. Soil Sci.* **28**, 223-246.

Nezhdanova, I. K. and Suetin, Yu. P. 1987. Investigations of magnetic susceptibility of soils in connection with anthropogenic activity. (English Summary) *Geologiya I Geografiya* **4**, 82-85

Nightingale, A. 1991. Magnetic properties of river sediments. Unpubl. HND Dissertation, Coventry Polytechnic.

Norusis, M. J. 1988. SPSS/PC+ Advanced Statistics V2.0 for the IBM/XT/AT and PS/2. NORUSIS/SPSS INC.

Odeh, I. O. A., Chittlebobough, D. J. and McBratney, A. B. 1991. Elucidation of soil-landform interrelationships by canonical ordination analysis. *Geoderma* **49**, 1-32.

Oldfield, F., Dearing, J. A., Thompson, R., and Gattett-Jones, S. E. 1978a. Some magnetic properties of lake sediments and their possible links with erosion rates. *Pol. Arch. Hydrobiol.* **25** (1&2), 321-331.

Oldfield, F., Thompson, R. and Barber, K. E. 1978b. Changing Atmospheric Fallout of magnetic particles recorded in recent ombrotrophic peat sections. *Science* **199**, 679-680.

Oldfield, F., Rummery, T. A., Thompson, R. and Walling, D. E. 1979. Identification of suspended sediment sources by means of magnetic measurements: Some preliminary results. *Water Resources Res.* **15** (2), 211-218.

Oldfield, F. 1981. Artificial magnetic enhancement of stream bedload: a hydrological application of superparamagnetism. *Phys. Earth Planet. Interiors* **26**, 107-124.

Oldfield, F., Barnosky, C., Leopold, E. B. and Smith, J. P. 1983. Mineral magnetic studies of lake sediments: A brief review. *Hydrobiol.* **103**, 37-44.

Oldfield, F. 1985. Magnetic differentiation of atmospheric dusts. *Nature* **317**, 516-518.

Oldfield, F., Worsley, A. T. and Baron, A. F. 1985. Lake sediments and evidence for agricultural intensification: A case study from the Highlands of Papua New Guinea. In *Prehistoric Intensive Agriculture in the Tropics.* Ed. I. S. Farrington. Allen and Unwin, London.

Oldfield, F. and Clark, R. L. 1990. Lake Sediment-based Studies of Soil Erosion. In *Soil Erosion on Agricultural Land.* Eds, J. Boardman, I.D.L. Foster and J. Dearing. 201-230. Wiley, Chichester.

Oldfield, F. 1991. Environmental Magnetism - A personal perspective. *Quaternary Science Reviews* **10**, 73-85.

Oliver, M. A. and Webster, R. 1986. Combining nested and linear sampling for determining the scale and form of spatial variation of regionalized variables. *Geographical Analysis* **18**, 229-242.

Oliver, M. A. and Webster, R. 1987a. The elucidation of soil pattern in the Wyre Forest of the West Midlands, England I: Multivariate Distribution. *J. Soil Science* **38**, 279-291.

Oliver, M. A. and Webster, R. 1987b. The elucidation of soil pattern in the Wyre Forest of the West Midlands, England II: Spatial Distribution. *J. Soil Science* **38**, 293-307.

Oliver, M. A. 1987. Geostatistics and its application to soil science. *Soil Use and Management* **3**, 8-19.

Oliver, M. A. and Webster, R. 1991. How Geostatistics can help you. *Soil Use and Man.* **7**, 206-217.

O'Reilly, W. 1984. Rock and Mineral Magnetism. Chapman and Hall. London.

Ozdemir, O. and Banerjee, S. K. 1982. A preliminary study of soil samples from west-central Minnesota. *Earth Planet. Sci. Lett.*, **59**: 393-403.

Parry, L. G. 1965. Magnetic properties of dispersed magnetite powders. *Phil. Mag.* **11**, 303-12

Pearce, F. 1993. 'When the tide comes in...'. *New Scientist* **137** (1854), 23-27.

Peart, M. R. and Walling, D. E. 1988. Techniques for establishing suspended sediment sources in two drainage basins in Devon, UK: A comparative assessment. In Sediment Budjets, Proc. of the Porto Alegre Symposium. *IAHS Publication No.* **174**, 269-279. Wallingford, Oxford.

Petersen, N., von Dobeneck, T. and Vali, H. 1986. Fossil bacteria magnetite in deep-sea sediments from the south Atlantic Ocean. *Nature* **320**, 611-615.

Petrovsky, E., Hejda, P, Kropacek, V and Subrt, J. 1993. Experimental determination of magnetic interactions within a system of synthetic haematite particles. *Phys. Earth Planet. Inter.* **76**, 123-130.

Petts, G. and Foster, I. D. L. 1985. Rivers and landscape. Arnold, London.

Pringle, A. W.. 1981. *'Beach development and coastal erosion in Holderness, North Humberside'.* In J. Neale and J. Flenley (eds), The Quaternary in Britain. Pergamon Press, Oxford.

Quarmby, N. A., Townshend, J. R. G., Settle, J. J., White, K. H., Milnes, M., Hindle, T. L. and Silleos, N. 1992. Linear mixture modelling applied to AVHRR data for crop area estimation. *Int. J. Remote Sensing* **13** (3), 415-425.

Robertson, D. 1989. Alternating Field Demagnetization and ARM acquisition using "Molspin" apparatus: Guide for Studients. University of Liverpool.

Robertson, D. 1990. Molspin Magnetometer and Bartington Susceptibility Meter: Dimensions, Units and Calibration. University of Liverpool

Rossman, L. A. 1976. Comment on 'A general linear approach to stream water quality modelling', by Mansur Arbabi and Jack Elzinga. *Water Resources Research* **12**, 823-824.

Rummery, T. A., Bloemendal, J., Dearing, J. A. and Oldfield, F. 1979. The persistence of fire-induced magnetic oxides in soils and lake sediments. *Ann. Geophys.* **35**, 103-107.

Sandgren, P. and Thompson, R. 1990. Mineral magnetic characteristics of podzolic soils developed on sand dunes in the Lake Goosciaz catchment, central Poland. *Phys. Earth Planet. Inter.* **60**: 297-313.

Saucy, D. A., Anderson, J. R. and Buseck, P. R. 1991. Aerosol Particle Characteristics determined by combined cluster and principal component analysis. *J. Geophysical Research* **96**, (D4), 7407-7414.

Settle, J. J. and Drake, D. J. 1993. Linear mixing and the estimation of ground cover proportions. *Int. J. Remote Sensing* **14** (6), 1159-1177.

Schuilling, R. D., De Meijer, R. J., Riezebos, H. J. and Scholten, M. J. 1985. 'Grain size distributions of different minerals in a sediment as a function of their specific density. *Geologie en Mijinbouw* **64**, 199-203.

Schwertmann, U. and Taylor, R. M. 1977. Iron oxides. In *Minerals in soil environments.* J. B Dixon (Ed.), 145-180. Madison: Soil Science Society of America.

Schwertmann, U. 1988. Some properties of Soil and Synthetic Iron Oxides. *Iron in Soils and Clay Minerals.* Ed's J.W. Stucki; pp203-250. D. Reidel, Dordrecht.

Scoullos, M., Oldfield, F. and Thompson, R. 1979. Magnetic monitoring of Marine Particulate Pollution in the Elefsis Gulf, Greece. *Marine Pollution Bulletin* **10**, 287-291.

Shaw, G. and Wheeler, D. 1985. *Statistical Techniques in Geographical Analysis.* Wiley, Chichester.

Singer, M. J. and Fine, P. 1989. Pedogenic factors affecting magnetic susceptibility of Northern Californian soils. *Soil Sci. Soc. Am. J.* **53**, 1119-1127.

Smith, J. P., Fullen, M. A. and Tavner, S. 1990. Some magnetic and geochemical properties of soils developed on Triassic substrates and their use in the characterization of colluvium. In *Soil Erosion on Agricultural Land. Ed's.* J. Boardman, I. D. L. Foster, J. A. Dearing; J. 255-272. Wiley, Chichester.

Snowball, I. 1993. Mineral magnetic properties of Holocene lake sediments and soils from the Karsa valley, Lappland, Sweden, and their relevance to palaeoenvironmental reconstruction. *Terra Nova* **5**, 258-270.

Stacey, F. D. 1963. The physical theory of rock magnetism. *Advances in Physics* **12**, 45-133.

Stanjek, H., Fassbinder, J. W. E., Vali, H., Wagele, H. and Graf, W. 1994. Evidence of biogenic greigite (ferrimagnetic Fe3S4) in Soil. *J. Soil Science. in press.*

Stewart, H. B. and Thompson, J. M 1986. On the border between calm and chaos. *Non-linear dynamics and Chaos.* Wiley, Chichester.

Stober, J. C. and Thompson, F. 1979. An investigation into the source of magnetic minerals in some Finnish lake sediments. *Earth Planet. Sci. Lett.* **45**, 464-474.

Stott, A. P. 1986. Sediment tracing in a reservoir-catchment system using a magnetic mixing model. *Phys. Earth Planet. Interiors* **42**, 105-112.

Taylor, R. M and Schwertmann, U. 1974. Maghemite in soils and its origins I Properties and Observations on soil Maghemites. *Clay Minerals* **10**, 299-310 .

Taylor, R. M., Maher, B. A and Self, P. G. 1987. Magnetite in soils: I the synthesis of single domain and superparamagnetic magnetite. *Clay Minerals* **22**, 411-422.

Thompson, R., Battarbee, R. W., O'Sullivan, P. E. and Oldfield, F. 1975. Magnetic Susceptibility of lake sediments. *Limnol. Oceanogr.* **20** (5), 687-698.

Thompson, R. and Morton, D. J. 1978. Magnetic Susceptibility and particle-size distribution in recent sediments of the Loch Lomond drainage basin, Scotland. *J. Sedimentary Petrology* **49** (3), 801-811.

Thompson, R., Bloemendal, J., Dearing, J. A., Oldfield, F., Rummery, T. A., Stober, J. C. and Turner, G. M. 1980. Environmental Applications of Magnetic Measurements. *Science* **207** (4430), 481-6.

Thompson, R., Bradshaw, R. H. W., and Whitley, J. E. 1986. The distribution of ash in Icelandic lake sediments and the relative importance of mixing and erosional processes. *J. Quat. Sci.* **1**, 3-11.

Thompson, R. 1986. Modelling magnetization data using SIMPLEX. *Phys. Earth Planet. Interiors* **42**, 113-127.

Thompson, R. and Oldfield, F. 1986. *Environmental Magnetism.* Allen and Unwin, London.

Tite, M. S. and Mullins, C. 1971. Enhancement of the magnetic susceptibility of soils on archeological sites. *Archeometry* **13** (2), 209-219.

Tite, M. S. 1972. The influence of geology on the magnetic susceptibility of soils on archeological sites. *Archeometry* **13** (2), 229-236.

Vadyunina, A. F. and Babanin, V. F. 1972. Magnetic susceptibility of some soils in the USSR. *Soviet Soil Science* , 588-599.

Walden, J., Smith, J. P. and Dackombe, R. V. 1987. 'The use of mineral magnetic analyses in the study of glacial diamicts: a pilot study'. *J. Quaternary Science*, **2**, 73-80.

Walden, J., Whittaker, R. J. and Hill, J. 1991. The use of mineral magnetic analyses as a aid in investigating the recent volcanic disturbance history of the Krakatua Islands, Indonesia. *The Holocene*, **1**, 262-268.

Walden, J., Smith, J. P. and Dackombe, R. V. 1992. The use of simultaneous R- and Q-Mode Factor Analysis as a tool for assisting interpretation of Mineral magnetic Data. *Mathematical Geology* **24**, 227-247.

Walling, D. E., Peart, M. R., Oldfield, F. and Thompson, R. 1979. Suspended sediment sources identified by magnetic measurements. *Nature* **281**, 110-113.

Walling, D. E. and Bradley, S. B. 1990. Some applications of caesium 137 measurements in the study of erosion, transport and deposition. Erosion, transport and deposition processes. Proc. of the Jerusalem Workshop, March-April, 1987). *IAHS publication no.* **189**, 179-203. Wallingford, Oxford.

Walling, D. E. and Woodward, J. D., 1992. Use of radiometric fingerprints to derive information on suspended sediment sources. Erosion and sediment transport monitoring programmes in river basins. Proc. of Oslo Symp.

August 1992. *IAHS publication no.* **210**. Wallingford, Oxford.

Wasilewski, P. J. 1973. Magnetic Hysteresis in natural materials. *Earth Planet. Sci. Lett.* **20**, 67-72.

Webster, R. and Burrough, P. A. 1972. Computer based soil mapping of small area from sample data. I Multivariate classification and ordination. *J. Soil Science* **23**, 211-221.

Webster, R. and Oliver, M. A. 1990. *Statistical Methods in Soil and Land Resource Survey*. Oxford University Press.

Webster, R. and Boag, B. 1992. Geostatistical analysis of cyst nematodes in soil. *J. Soil Science* **42**, 583-595.

Webster, R. and Oliver, M. A. 1992. Sample adequately to estimate variograms of soil properties. *J. Soil Science* **43**, 177-192.

Wickramagamage, P. and Fisher, G. C. 1988. The numerical classification of soils: A case study using data from West Sussex, England. *J. Soil Science* **39**, 139-153.

Williams, M. 1992. Evidence for the dissolution of magnetite in Scottish peats. *Quat. Res.* **37**, 171-182.

Williams, R. D. and Cooper, J. R. 1990. Locating soil boundaries using magnetic susceptibility. *Soil Science* **150**, 889-895.

Winston, W. L. 1991. *Operations Research: Applications and Algorithms.* Second Edition. PWS-Kent, USA.

Yu, L. 1989. Environmental applications of mineral magnetic measurements; towards the quantitative approach. Unpub. Ph.D. thesis, University of Liverpool.

Yu, L. and Oldfield, F. 1989. 'A multivariate model for identifying sediment source from magnetic measurements'. *Quat. Res.*, **32**, 168-181.

Yu, L. and Oldfield, F. 1993. Quantitative sediment source ascription using magnetic measurements in a reservoir-catchments system near Nijar, S.E. Spain. *Earth Surf. Proc. Landf.* **18**, 441-454.

Zhou, M. M. and Yi, L. J. 1989. Atmospheric pollution in Beiging, China, as recorded in sediments of the Summer Palace Lake. *Environmental Conservation.* **16** (3), 233-236.

Annex

Environmental Magnetism Bibliography

Compiled by J. A. Lees: 20th November, 1991
Last Updated 12th July, 1994.

AEOLIAN

Blank, M., Leinen, M. and Prospero, J. M. 1985. Major Asian aeolian inputs indicated by the mineralogy of aerosols and sediments in the western North Pacific. *Nature* **314**, 84-86.

Hovan, S. A., Rea, D. K., Pisias, N. G. and Shackleton, N. J. 1989. A direct link between the China loess and marine $d^{18}O$ records: aeolian flux to the north Pacific. *Nature* **340**, 296-298.

Kukla, G. and An, Z. 1989. Loess stratigraphy in Central China. *Palaeogeography, Palaeoclimatology, Palaeoecology* **72**, 203-225.

Kukla, G. et al 1988. Pleistocene climates in China dated by Magnetic susceptibility. *Geology* **16**, 811-814.

Kukla, G., An, Z.S., Melice, J.L., Gavin, J. and Xiao, J.L. 1990. Magnetic susceptibility record of Chinese loess. *Transactions of the Royal Society of Edinburgh: Earth Sciences* **81**, 263-288.

Liu, X.-M., Shaw, J., Liu, T., Heller, F. and Yuan, B. 1991. Magnetic mineralogy of Chinese Loess and its Significance.

Maher, B.A. and Thompson, R. 1991. Mineral Magnetic record of the Chinese loess and paleosols. *Geology* **19**, 3-6.

Maher, B.A. and Thompson, R. 1992. Paleoclimatic Significance of the mineral magnetic record of the Chinese loess and paleosols. *Quaternary Research* **37**, 155-170.

Xiu-Ming, L et al 1988. Anisotropy of magnetic susceptibility and origin of the chinese Loess and its significance to the Quaternary research. *Science in China* **B 33** (2), 235-245.

Zhou, L. P. et al 1990. Partly pedogenic origin of magnetic variations in Chinese loess. *Nature* **346**, 737-9.

ARCHAEOLOGY

Hartwell, B. 1988. A Soil Resistivity Survey at Hauley's Fort. *Emania, Bulletin of the Navan Research Group* **4**, 21-23.

Hedley, I. and Wagner, J.-J. 1990. A Magnetic Investigation of Roman and Pre-Roman pottery. *Archaeometry '90*, Birkhauser Verlag Basel. 275-284

Oldfield, F., Krawiecki, A, Maher, B. A., Taylor, J. J. and Twigger, S. 1985. The role of mineral magnetic measurements in archaeology. *Palaeoenvironmental Investigations: Research,* Fieller, N. R. J., Gilbertwon, D. D. and Ralph, N. G. A. (Eds). 29-43

Wagner, J. -J. and Hedley, I. 1989. Properties magnetiques de ceramiques anciennes. *Methoden zur Erhalung von Kulturgutern*, Schweizer, F. and Villiger, V (Eds). P Haupt, Bern. 215-222

ATMOSPHERIC POLLUTION

Chester, R. et al 1984. The distribution of natural and non-crustal ferrimagnetic minerals in soil sized particulates from the Mediterranean atmosphere. *Water, Air and Soil Pollution* **23**, 25-35.

Clymo, R. S. et al 1990. The record of atmospheric deposition on a rainwater-dependent peatland. *Phil. Trans. R. Soc. Lond.* **B 327**, 331-338.

Hunt, A., Jones, J. and Oldfield, F. 1984. Magnetic measurements and heavy metals in atmospheric particulates of anthropogenic origin. *Sci. Tot. Env.* **33**, 129-139.

Hunt, A. 1986. The application of mineral magnetic methods to atmospheric aerosol discrimination. *Phys. Earth. Planet. Interiors* **42**, 10-21.

Kleinman, M. T. 1980. Identifying and estimating the relative importance of sources of airborne particulates. *Sci. Tot. Env.* **14** (1), 62-65.

Locke, G. and Bertine, K. K. 1986. Magnetite in sediments as an indicator of coal combustion. Appl. *Geochem.* **1** (3), 345-356.

Oldfield, F., Brown, A. and Thompson, R. 1978. The effect of microtopography and vegetation on the catchment of airborne particles measured by remanent magnetism. *Quat. Res.* **12**, 326-332.

Oldfield, F., Thompson, R. and Barber, K. E. 1978. Changing Atmospheric Fallout of magnetic particles recorded in recent ombrotrophic peat sections. *Science* **199**, 679-680.

Oldfield, F. 1985. Magnetic differentiation of atmospheric dusts. Nature 317, 516-518.

Oldfield, F. and Richardson, N. 1990. Lake sediment magnetism and atmospheric deposition. *Phil. Trans. R. Soc. Lond.* **B 327**, 325-330.

Richardson, N. 1986. The mineral magnetic record in recent ombotrophic peat synchronized by fine resolution pollen analysis. *Phys. Earth Planet. Interiors* **42**, 48-56.

Rippey, B. 1990. Sediment chemistry and atmospheric contamination. *Phil. Trans. R. Soc. Lond.* **B 327**, 311-7

Windom, H. L. 1969. Atmospheric dust records in permanent snowfields: Implications to marine sedimentation. *Geol. Soc. Am. Bull.* **80**, 761-782.

Zhou, M. M. and Yi, L. J. 1989. Atmospheric pollution in Beiging, China, as recorded in sediments of the Summer Palace Lake. *Environmental Conservation.* **16** (3), 233-236.

BIOGENIC MAGNETITE

Bazilinski, D. A., Frankel, R. B. and Jannasch, H. W. 1988. Anaerobic magnetite production by a marine, magnetotactic bacterium. *Nature* **334**, 518-519.

Farina, M., Esquivel, D. M. and Lins de Barros, H. G. 1990. Magnetic iron-sulphur crystals from a magnetotactic microorganism. *Nature* **343**, 256-258.

Fassbinder, J. W., Stanjek, H. and Vali, H. 1990. Occurrence of magnetic bacteria in soil. *Nature* **343**, 161-163.

Karlin, R., Lyle, M. and Heath, G. R. 1987. Authigenic magnetite formation in suboxic marine sediments. *Nature* **326**, 490-493.

Kirschvink, J. L. and Gould, J. L. 1981. Biogenic magnetite as a basis for magnetic field detection in animals. *BioSystems* **13**, 181-201.

Lovely, D. R., Stolz, J. F., Nord, G. L. and Phillips, E. J. P. 1987. Anaerobic production of magnetite by a dissimilatory iron-reducing microorganism. *Nature* **330**, 252-254.

Mann, S., Sparks, N. H. C., Frankel, R. B., Bazylinski, D. A. and Jannasch, H. W. 1990. Biomineralization of ferrimagnetic greigite (Fe_3S_4) and iron pyrite (FeS_2) in magnetotactic bacteria. *Nature* **343**, 258-261.

Petersen, N., von Dobeneck, T. and Vali, H. 1986. Fossil bacteria magnetite in deep-sea sediments from the south Atlantic Ocean. *Nature* **320**, 611-615.

Stolz, J. F, Chang, S. R. and Kirschvink, J. L. 1986. Magnetotactic bacteria and single-domain magnetite in hemipelagic sediments. *Nature* **321**, 849-851.

Vali, H. and Kirschvink, J. L. 1989. Magnetofossil dissolution in a palaeomagnetically unstable deep-sea sediment. *Nature* **339**, 203-206.

EXPLORATION

Anon. The quest for Diamagnetic magnetite. Geoscience and Technology Inc.

Barton, R. H., Tomlinson, W. D. and Bartington, G. W. 1988. Use of seabottom magnetic susceptibility measurements in hydrocarbon exploration. Sixth Thematic conference "*Remote Sensing for Exploration Geology*" May 16-19.

Foote, R. S. 1985. Results of horizontal gradient interpretation of low-altitude cesium vapor magnetometer data compared with measurement of rock magnetic susceptibility of... *Unconventional methods in exploration for petroleum and natural gas, Symposium IV. 1-9.*

Hood, P. J., Holroyd, M. T. and McGrath, P. H. 1979. Magnetic methods applied to base metal exploration. In *Geophysics and Geochemistry in the search for metallic ores* **31**, 77-104.

Mares, S. 1984. Geophysical Well Logging. *Introduction of Applied Geophysics.* 474-525

GENERAL APPLICATIONS

Clark, R. 1989. Environmental Magnetism in Australia and Papua New Guinea. *EOS* 28th November. pp 1512.

Oldfield, F. 1983. The role of magnetic studies in palaeohydrology. In *Background to palaeohydrology.* Ed. K. J. Gregory.

Oldfield, F. 1983. Man's impact on the environment: some recent perspectives. Geography 245-256

Oldfield, F. 1991. Environmental Magnetism - A personal perspective. Quaternary Science Reviews 10, 73-81

Thompson, R et al 1980. Environmental Applications of Magnetic Measurements. *Science* **207** (4430), 481-6.

GEOLOGY

Ade-Hall, J. M. et al 1968. A detailed opaque petrological and magnetic investigation of a single Tertiary Lava flow from Skye, Scotland - I Iron-titanium Oxide Petrology.

Aubourg, C., Rochette, P. and Vialon, P. 1990. Directions de transport revelees par la fabrique magnetique des Terres Noires subalpines (Alpes francaises) C. *R. Acad. Sci. Paris, Serie II* **310**, 1341-1346.

Hart, M. and Fuller, M. 1988. Magnetization of a dolomite bed in the Monterey formation: Implications for diagenesis. *Geophys. Res. Lett.* **15** (5), 491-494.

Johnson, H. P. and Hall, J. M. 1978. A detailed rock magnetic opaque mineralogy study of the basalts from the Nazca Plate. *Geophys. J. R. Astr. Soc.* **52**, 45-64

Mayhew, M. A. and LaBreque, J. L. 1987. Crustal geologic studies with Magsat and surface magnetic data. *Reviews of Geophys.* **25** (5), 971-981.

Tucker, D. H. et al 1980. The characteristics and interpretation of regional gravity, magnetic and radiometric surveys in the Pine Creek Geosyncline. *Proc. Int. Symp. on the Pine Creek Geosyncline.*

GLACIAL SEDIMENTS

Gravenor, C. P. and Wong, T. 1987. Magnetic and pebble fabrics and origin of the Sunnybrook Till, Scarborough, Ontario, Canada. *Canadian J. Earth Sci.* **24** (10), 2038-2046.

Walden, J. 1987. The use of mineral magnetic analysis in the study of glacial diamicts: A pilot study. *J. Quat. Sci.* **2**, 73-80.

GREIGITE

Anders, L. Greigite, the thio-spinel of iron; A new mineral. 1964. Skinner, B.J., Erd, R.C. and Grimaldi, F.S. *The American Mineralogist* **49**, 5 and 6, 543-555

Stanjek, H., Fassbinder, J. W. E., Vali, H., Wagele, H. and Graf, W. 1994. Evidence of biogenic greigite (ferrimagnetic Fe3S4) in Soil. *J. Soil Science. in press.*

HEMATITE

Chevallier, M. R. and Mathieus, S. 1943. Proprietes magnetiques des poudres D'Hematites (influence des dimensions des grains). *Ann. Phys. Paris* **18**, 258-288.

Collinson, D. W. 1968. An estimate of the Haematite content of sediments by magnetic analysis. *Earth and Planetary Science Letters* **4**, 4, 417-421.

Dunlop, D. J. 1971. Magnetic properties of fine-particle Hematite. *Ann. Geophys.* **27** (3), 269-293.

Petrovsky, E. et al. 1993. Experimental determination of magnetic interactions within a system of synthetic haematite particles. *Phys. Earth Planet. Inter.* **76**, 123-130.

Townsend Smith, T. 1916. The magnetic properties of Hematite. *Physics Review.* **8**, 721-737.

HYSTERESIS

Borradaile, G. J., Chow, N. and Werner, T., 1993. Magnetic hysteresis of limestones: facies control? Phys. Earth Planet. Inter., **76**: 241-252.

Day, R., Fuller, M. and Schmidt, V. A. 1977. Hysteresis properties of titanomagnetites: Grain size and compositional dependence. *Phys. Earth Planet. Interiors* **13**, 260-267.

Jiles, D. C. and Atherton, D. L. 1986. Theory of ferromagnetic hysteresis. *J. Mag. Mag. Mater.* **61**, 48-60.

Kwun, H. and Burkhardt, G. L. 1987. Effects of grain size, hardness, and stress on the magnetic hysteresis loops of ferromagnetic steels. *J. Appl. Phys.* **61** (4), 1576-1579.

Mauritsch, H., Becke, M., Kropacek, V., Zelinka, T. and Hejda, P. 1987. Comparison of the hysteresis of synthetic samples with different magnetite and haematite contents. *Physics of the Earth and Planetary Interiors* **46**, 93-99.

Novikov, V. F. and Fateev, I. G. 1983. Magnetic hysteresis in simultaneous action of static and dynamic stresses. *Soviet J. N.D.T.* **18**, 489-492.

Senanayake, W. E. and McElhinny, M. W. 1981. Hysteresis and Susceptibility characteristics of magnetite and titanomagnetites: interpretation of results from Basaltic rock. *Phys. Earth Planet. Interiors* **26**, 47-55.

Shah, M. B. and Bose, M. S. C. 1984. Magnetic NDT technique to evaluate fatigue damage. *Phys. Stat. Sol.* **86**, 275-281.

Stoner, E. C. and Wohlfarth, E. P. 1948. A mechanism of magnetic hysteresis in heterogenous alloys. *Phil. Trans. Roy. Soc.* **A 240**, 599-642.

Szpunar, B. and Szpunar, J. A. 1984. Influence of stresses on the hysteresis curve in constructional steel. *IEEE Trans. Mag.* **20** (5), 1882-1884.

Wasilewski, P. J. 1973. Magnetic Hysteresis in natural materials. *Earth Planet. Sci. Lett.* **20**, 67-72.

Willcock, S. N. M. and Tanner, B. K. 1983. Harmonic analysis of B-H loops of constructional steel. *IEEE Trans. Mag.* **19** (5), 2145-2147.

IRON OXIDES

Allen, E. T, Crenshaw, J.L. and Johnston, J. 1912. The mineral sulphides of iron. *American Journal of Science* **33**, 195, 169-217.

Bloomfield, C. 1949. Some observations on gleying. J. Soil Science 1 (2), 205-211.

Bloomfield, C. 1952. The distribution of iron and aluminium oxides in gley soils. J. Soil Science 3 (2), 167-171.

Blume, H. P. 1988. The fate of iron during soil formation in humid-temperate environments. In *Iron in Soils and Clay Minerals.* Ed's J.W. Stucki; D. Reidel, 749-777.

Coey, J. M. D. 1988. Magnetic properties of Iron in soil iron oxides and clay minerals. In *Iron in Soils and Clay Minerals.* Ed's J.W. Stucki; D. Reidel, 397-466.

Dankers, P. H. M. 1978. Magnetic properties of dispersed natural iron-oxides of known grain size. Unpublished PhD Thesis.

Eggleton, R. A. et al. 1988. Introduction to crystal structures of iron containing minerals. In *Iron in Soils and Clay Minerals.* Ed's J.W. Stucki; D. Reidel, 141-164.

Fisher, W. R. 1988. Macrobiological reactions of iron in soils. *In Iron in Soils and Clay Minerals*, ed. J. W. Stucki. D. Reider Publ. Co., 715-748.

Fitzpatrick, R.W. 1988. Iron Compounds as indicators of pedogenic processes: Examples from the Southern Hemisphere. In *Iron in Soils and Clay Minerals.* Ed's J.W. Stucki; D. Reidel, 351-396.

Gangas, N. H. et al 1973. MOSSBAUER studies of small particles of iron oxides in soil. *Clay and Clay Minerals* **21**, 151-160.

Goodman, B. A. 1988. The characterization of iron complexes with soil organic matter. In *Iron in Soils and Clay Minerals.* Ed's J.W. Stucki; D. Reidel, 677-687.

Hilton, J. et al 1986. Iron mineralogy in sediments. A Mossbauer study. *Geochemica et Cosmochimica Acta* **50**, 2147-2151.

Longworth, G. and Tite, M. S. 1977. Mossbauer and magnetic susceptibility studies of iron oxides in soils from archaeological sites. *Archaeometry* **19** (1), 3-14.

Mullins, C. E. and Tite, M.S. 1973. Preisach Diagrams and Magnetic Viscosity Phenomena for Soils and Synthetic Assemblies of Iron Oxide Grains. *Journal of Geomagnetism and Geoelectricity* **25**, 213-229.

Olson, R. V. 1958. Total Iron. 963-973.

Rumble, D. 1976. Oxide minerals in metamorphic rocks. *Mineralogical Soc. of America.*

Schwertmann, V. and Taylor, R. M. 1977. Iron oxides. In *Minerals in soil environments.* Dixon and Weed.

Schwertmann, U. 1988. Some properties of Soil and Synthetic Iron Oxides. *Iron in Soils and Clay Minerals.* Ed's J.W. Stucki; D. Reidel. 203-250.

Schwertmann, U. 1988. Occurrence and Formation of Iron Oxides in various Pedoenvironments. *Iron in Soils and Clay Minerals.* Ed's J.W. Stucki; D. Reidel. 267-308.

LAKE ACIDIFICATION

Fritz, S. C. et al 1989. Paleolimnological evidence for the recent acidification of Llyn Hir, Dyfed, Wales. *J. Paleolimnol.* **2**, 245-262.

Oldfield, F and Clark, R. L. 1990. Environmental History - The Environmental evidence. In *The Silent Countdown Brimblecombe*, Pfister; Springer-Verlag Berlin.

LAKE SEDIMENTS

Anderson, N. J. and Rippey, B. 1988. Diagenesis of magnetic minerals in the recent sediments of a eutrophic lake. *Limnol. Oceanogr.* **33** (6), 1476-1492.

Appleby, P. G., Dearing, J. A. and Oldfield, F. 1986. Magnetic studies of erosion in a Scottish lake catchment, I Core chronology and correlation. *Limnol. Oceanog.* **30** (6), 1144-1153.

Bennett, K. D., Fossitt, J. A., Sharp, M. J. and Switsur, V. R. 1990. Holocene vegetational and environmental history at Loch Lang, South Uist, Western Isles, Scotland. *New Phytologist* **114**, 281-298.

Bloemendal, J., Oldfield, F. and Thompson, R. 1979. Magnetic Measurements used to assess sediment influx at Llyn Goddionduon. *Nature* **280**, 50-53.

Bradshaw, R. and Thompson, R. 1985. The use of magnetic measurements to investigate the mineralogy of Icelandic lake sediments and to study catchment processes. *Boreas* **14**, 203-215.

Caitcheon, G. et al. 1988. The lake Burly Griffin Study: Its implications for Catchment management. Conference on Ag. Eng., Hawksbury Agricultural College NSW, 25-29 September, 1988.

Coey, J.M.D. 1975. Iron in a post-glacial lake sediment core; a Mossbauer effect study. *Geochimica et Cosmochimica Acta.* **39**, 401-415.

Dearing, J. A., Elner, J. K. and Happey-Wood, C. M. 1981. Recent sediment flux and erosional processes in a Welsh Upland Lake Catchment based on Magnetic Susceptibility measurements. *Quat. Res.* **16**, 356-372.

Dearing, J. A., Foster, I. D. L. and Simpson, A.D. 1982. Timescales of denudation: The lake-drainage basin approach. Recent developments in the Explanation and Prediction of Erosion and Sediment Yeild. *IAHS.* Publ. No. **137**, 351-360.

Dearing, J. A. and Flower, R. 1982. The magnetic susceptibility of sedimenting material trapped in Lough Neagh, N Ireland, and its erosional significance. *Limnol. Oceanog.* **27** (5), 969-975.

Dearing, J. A. 1983. Changing patterns of sediment accumulation in a small lake in Scania, Southern Sweden. *Hydrobiologia* **103**, 59-64.

Dearing, J. A. et al 1987. Lake sediments used to quantify the erosional response to land use change in southern sweden. *Oikos* **50**, 60-78.

Dearing,J. A. and Foster,I. D. L. 1986. Lake sediments and palaeohydrological studies. In *Handbook of Holocene Palaeoecology and Palaeohydrology.* Ed. B.E. Burglund; J. Wiley, Chichester. pp67-143.

Dearing, J. A. 1991. Lake Sediment records of erosional processes. *Hydrobiologia* **214**, 99-106.

Dearing, J. A. 1992. Sediment yield and sources in a Welsh upland lake-catchment during the past 800 years. *Earth Surface Processes and Landforms* **17**, 1-22.

Dickson, J. H. et al 1978. Palynology, Palaeomagnetism and radiometric dating of Flandrian marine and freshwater sediments of Loch Lomond. *Nature* **274** (5671), 548-553.

Edwards, K. J. and Rowntree, K. M. 1980. Radiocarbon and palaeoenvironmental evidence for changing rates of erosion at a Flandrian stage site in Scotland. In *Timescales in Geomorphology.* Ed's. R. A. Cullingford, D. A. Davidson, J. Lewin.

Elner, J. K. and Happey-Wood, C. M. 1980. The history of two linked but contrasting lakes in North Wales and chemistry in sediment cores. *J. Ecol.* **68**, 95-121.

Flower, R. J., Dearing, J. A. and Nawas, R. 1984. Sediment supply and accumulation in a small Moroccan lake: and historical perspective. *Hydrobiologia* **112**, 81-92.

Foster, I. D. L. et al. 1985. Lake catchment based studies of erosion and denudation in the Merevale Catchment, Wraks, UK. *Earth Surf. Proc. Landf.* **10**, 45-68.

Foster, I. D. L., Dearing, J. A. and Grew, R. 1988. Lake-catchments: An evaluation of their contribution to studies of sediment yield and delivery processes. Sediment Budgets, *IAHS Publ.***174**, 413-423.

Gaillard, M. J. et al. 1991. A late Holocene record of land use history, soil erosion, lake trophy and lake level fluctuations at Bjanesjosjon, South Sweden.

Higgit, S. R. et al. 1991. The record of land-use change of soil erosion in the late Holocene sediments of the Petit Lac d'Annecy, Eastern France. *The Holocene* **1** (1), 14-28.

Hilton, J. 1985. A conceptual framework for predicting the occurrence of sediment focusing and sediment redistribution in small lakes. *Limnol. Oceanogr.* **30** (6), 1131-1143.

Hilton, J. and Lishman, J. P. 1985. The effects of Redox changes on the magnetic susceptibility of sediments from a seasonally anoxic lake. *Limnol. Oceanogr.* **30** (4), 907-909.

Hilton, J., Davison, W. and Ochsenbein, U. 1985. A mathematical model for analysis of sediment core data: implications for enrichment factor calculations and trace-metal transport mechanisms. *Chem. Geol.* **48**, 281-91.

Hilton, J., Lishman, J. P. and Allen, P. V. 1986. The dominant processes of sediment distribution and focusing in a small, eutrophic, monomictic lake. *Limnol. Oceanogr.* **31** (1), 125-133.

Manjuatha, B. R. and Shankar, R. 1993. Magnetic sedimentological studies of Netruvatic and Gupur River bed sediments, W coast of India. *in press.*

Muller, G. 1969. Diagenetic Changes in Interstitial Waters of Holocene lake Constance Sediments. *Nature* **224**, 258-259.

Oldfield, F. et al 1978. Some magnetic properties of lake sediemnts and their possible links with erosion rates. *Pol. Arch. Hydrobiol.* **25** (1&2), 321-331.

Oldfield, F., Barnosky, C., Leopold, E. B. and Smith, J. P. 1983. Mineral magnetic studies of lake sediments: A brief review. *Hydrobiol.* **103**, 37-44.

Oldfield, F. 1983. The role of magnetic studies in palaeohydrology. In *Background to Palaeohydrology.* Ed. K. J. Gregory; J. Wiley.

Oldfield, F., Worsley, A. T. and Baron, A. F. 1985. Lake sediments and evidence for agricultural intensification: A case study from the Highlands of Papua New Guinea. In *Prehistoric Intensive Agriculture in the Tropics.* Ed. I. S. Farrington.

Oldfield, F. 1988. Magnetic and element analysis of recent lake sediments from the Highland of papua New Guinea. *J. Biogeography* **15**, 529-553.

Oldfield, F. 19 Recent ecological history of small drainage basins in the western and Southern highlands of Papua New Guinea. Research Report, University of Lancaster.

Oldfield, F., Maher, B. A. and Appleby, P. G. 1989. Sediment source variations and lead-210 inventories in recent Potomac Estuary sediment cores. *J. Quat. Sci.* **4** (3), 189-200.

Oldfield, F. 1990. Magnetic measurements of recent sediments from Big Moose Lake, Adirondack Mountains, N.Y., USA. *J Paleolimnol.* **4**, 93-101.

Sandgren, P. and Risberg, J. 1990. Magnetic mineralogy of the sediments in Lake Adran, E. Sweden, and an interpretation of early Holocene water level changes. *Boreas* **19**, 57-68.

Selleck, B. W. 1974. Heavy minerals in the sands of Southern and eastern Lake Ontario. Proc. 17th Conf. Great Lakes Research 1974. *Int. Assoc. Great Lakes Res.* pp697-703.

Snowball, I. and Thompson, R. 1988. The occurrence of Greigite in sediments from Loch Lomond. *J. Quat. Sci.* **3 (2)**, 121-125.

Snowball, I. and Thompson, R. 1990. A mineral magnetic study of Holocene sedimentation in Lough Catherine, Northern Ireland. *Boreas* **19**, 127-146 .

Stober, J. C. and Thompson, F. 1977. Palaeomagnetic secular variation studies of Finnish lake sediment and the carriers of remanence. *Earth Planet. Sci. Lett.* **37**, 139-149.

Stott, A. P. 1987. Medium term effects of afforestation in sediment dynamics in a water supply catchment: A mineral magnetic interpretation of reservoir deposits in the Macclesfield forest, N.W. England. *Earth Surface Process and Landform* **12**, 619-630 .

Thompson, R. et al 1975. Magnetic Susceptibility of lake sediments. *Limnol. Oceanogr.* **20** (5), 687-698.

Thompson, R. and Morton, D. J. 1978. Magnetic Susceptibility and particle-size distribution in recent sediments of the Loch Lomond drainage basin, Scotland. *J. Sedimentary Petrology* **49** (3), 801-811.

Thompson, R., Bradshaw, R. H. W. and Whitley, J. E. 1986. The distribution of ash in Icelandic lake sediments and the relative importance of mixing and erosion processes. *J. Quat. Sci.* **1** (1), 3-11.

Yu, L. et al 1990. Paleoenvironmental implications of magnetic measurements on sediment core from Kunming Basin, Southwest China. *J. of Paleolimnology* **3**, 95-111.

MAGNETITE

Bate, G. 1952. Statistical stability of the Preisach diagram as a provenance indicator. *J. of Sedimentary Petrology* **60** (6), 940-951.

Bazilinski, D. A., Frankel, R. B. and Jannasch, H. W. 1988. Anaerobic magnetite production by a marine, magnetotactic bacterium. *Nature* **334**, 518-519.

Cisowski, S. 1981. Interacting and non interacting single domain behaviour in natural and synthetic samples. *Phys. Earth Planet. Inter.* **26**, 56-62

Dankers, P. 1981. Relationship between median destructive field and remanent coercive forces for dispersed natural magnetite, titanomagnetite and hematite. *Geophys. J. R. astr. Soc.* **64**, 447-461.

Dunlop, D. J. 1973. Superparamagnetic and single-domain threshold sizes in magnetite. *J. Geophys Res.* **78** (11), 1780-1793.

Farina, M., Esquivel, D. M. and Lins de Barros, H. G. P. 1990. Magnetic iron-sulphur crystals from a magnetotactic microorganism. *Nature* **343**, 256-258.

Fassbinder, J. W. E., Stanjek, H. and Vali, H. 1990. Occurrence oF magnetic bacteria in soil. *Nature* **343**, 161-3.

Grigsby, J. D. 1990. Detrital Magnetite as a provenance indicator. *J. of Sedimentary Petrology* **60** (6), 940-951.

Karlin, R., Lyle, M. and Heath, G. R. 1987. Authigenic magnetite formation in suboxic marine sediments. *Nature* **326**, 490-493.

Kirschvink, J. L. and Gould, J. L. 1981. Biogenic magnetite as a basis for magnetic field detection in animals. BioSystems **13**, 181-201.

Kirschvink, J. L. 1982. Paleomagnetic evidence for fossil biogenic magnetite in Western Crete. *Earth and Planetary Science Letters* **59**, 388-392.

Levi, S. and Merril, R. I. 1978. Properties of single-domain, pseudo-single-domain and multidomain magnetite. *J. Geophys. Res.* **83** (B1), 309-323.

Lovely, D. R., Stolz, J. F., Nord, G. L. and Phillips, E. J. P. 1987. Anaerobic production of magnetite by a dissimilatory iron-reducing microorganism. *Nature* **330**, 252-254.

Lowrie, W. and Fuller, M. 1971. On the alternating field demagnetization characteristics of multi domain thermoremanent magnetization in magnetite. *J. Geophys. Res.* **76** (26), 6339-6349.

Maher, B. A. 1988. Magnetic properties of some synthetic sub-micron magnetites. *Geophys. J.* **94**, 83-96.

Mann, S., Sparks, N. H. C., Frankel, R. B., Bazylinski, D. A. and Jannasch, H. 1990. Biomineralization of ferrimagnetic greigite (Fe3S4) and iron pyrite (FeS2) in magnetotactic bacterium. *Nature* **343**, 258-261.

McNeill, D.F. 1990. Biogenic Magnetite from surface Holocene Carbonate Sediments, Great Bahama Bank. *J. of Geophysical Research* **95** (B4), 4363-4371.

Mullins, C. E. and Tite, M. S. 1973. Magnetic viscosity, quadrature susceptibility and frequency dependance of susceptibility in single-domain assemblages of magnetite and maghemite. *J. Geophys. Res.* **78** (5), 804-809.

Parry, L. G. 1965. Magnetic properties of dispersed magnetite powders. *Phil. Mag.* **11**, 303-12

Petersen, N., von Dobeneck, T. and Vali, H. 1987. Fossil bacterial magnetite in deep sea-sediments from the South Atlantic Ocean. Nature 320, 611-615,

Potter, D. K. and Stephenson, A. 1986. The detection of fine particles of magnetite using anhysteretic and rotational remanent magnetizations. *Geophys. J. R. Astr. Soc.* **87**, 569-582.

Setty, K. B. and Raju, D. R. 1988. Magnetite content as a basis to estimate other major heavy mineral content in the sand deposit along the Nizampatnam Coast, Guntur Dist., Andhra Pradesh. *J. Geolog. Soc. India* **31**, 491-4.

Smith, P. P. K. 1978. The identification of single-domain titanomagnetite particles by means of transmission electron microscopy. *Canadian Journal of Earth Science* **16**, 375-379.

Stolz, J. F., Chang, S. R. and Kirschvink, J. L. 1986. Magnetotactic bactera and single-domain magnetite in hemipelagic sediments. *Nature* **321**, 849-851.

Stolz, J. F., Lovley, D. R. and Haggerty, S. E. 1990. Biogenic Magnetite and the magnetization of sediments. *J. Geophys. Res.* **95** (B4), 4355-4361.

Taylor, R. M, Maher, B. A. and Self, P. G. 1987. Magnetite in Soils: I. The synthesis of single-domain and superparamagnetic magnetite. *Clay Minerals* **22**, 411-422.

Vali, H. and Kirschvink, J. L. 1989. Magnetofossil dissolution in a palaeomagnetically unstable deep-sea sediment. *Nature* **339**, 203-206.

MAGNETIZATION

Atherton, D. L. and Jiles, D. C. 1983. Effects of stress on the magnetization of steel. *IEEE Trans. Mag.* **19** (5), 2021-2023.

Langman, R. 1985. The effect of stress on the magnetization of mild steel at moderate field strengths. *IEEE Trans. Mag.* **21** (4), 1314-1320.

MARINE & COASTAL SEDIMENTS

Andrews, J. T. and Jennings, A. E. 1986. Influence of sediment source and type on the magnetic susceptibility of fiord and shelf deposits, Baffin Island and Baffin Bay, N.W.T. *Canadian J. Earth Sci.* **24** (7), 1386-1401.

Bloemendal, J. and deMenocal, P. 1989. Evidence for a change in the periodicity of tropical climate at 2.4 Myr from whole core magnetic susceptibility measurements. *Nature* **342**, 897-900.

Bonnet, P. J. P, Appleby, P. G. and Oldfield, F. 1988. Radionuclides in Coastal and Estuarine Sediments from Wirral and Lancashire. *The Science of the Total Environment* **70**, 215-236.

Cannell, J. E. T. et al. 1990. Contrasting magnetic properties in LEG 107 sediments: Preservation and alteration of titanomagnetite at adjacent sites. Proc. Ocean Drilling Prog. Scientific Results 107, 113-128.

Channell, J. E. T. and Hawthorne, T. 1990. Progressive dissolution of titanomagnetites at ODP Site 653 (Tyrrhenian Sea). *Earth Planet. Sci. Lett.* **96**, 469-480.

Chauris, R. 1989. Origine des sables terrigenes des plages: interet de la representation cartographique des pourcentages en differents mineraux Lourdes. L'example de la base de lannion (Bretagne Septentrionde). Norois **144**, 391-406.

Curry, W. B. and Lohmann, G. P. 1990. Reconstructing past particle fluxes in the Tropical Atlantic Ocean.*Paleoceanography* **5** (4), 487-505.

Foster, I. D. L. et al 1991. High energy coastal sedimentary deposits: an evaluation of depositional processes in SW England. *Earth Surface Process and Landform* **16**, 341-356.

Haggerty, S. E. 1970. *Magnetic Minerals in Pelagic Sediments.* Carnegie Intitution Yearbook, 68 papers from the Geophysical Laboratory, Carnegie Institute 1560, 332-336.

Hilton, J. 1986. A simple model for the interpretation of Magnetic Records in Lacustrine and Ocean Sediments. *Quaternary Research* **27**, 160-166.

Karlin, R. and Levi, S. 1985. Geochemical and sedimentological control of the magnetic properties of hemipelagic sediments. *J.of Geophysical Research* **90** (B12), 10373-92.

Karlin, R. and Levi, S. 1983. Diagenesis of magnetic minerals in Recent haemipelagic sediments. *Nature* **303**, 327-330.

King, J. W. and Channel, J. E. T. 1991. Sedimentary Magnetism, Environmental Magnetism, and Magnetostratigraphy. *Reviews of Geophysics* 358-370.

Kirschvink, J. and Chang, S. R. 1984. Ultrafine-grained magnetite in deep sea sediments: Possible bacterial magnetofossils. *Geology* **12**, 559-562.

Kobayashi, K. and Nomura, M. 1974. Ferromagnetic Minerals in the Sediment Cores Collected from the Pacific Basin. *J. Goephysics* **40**, 501-512.

Lovlie, R., Lowrie, W. and Jacobs, M. 1971. Magnetic Properties and Mineralogy of four deep sea cores. *Earth and Planetary Science Letters* **15**, 157-168.

Lowrie, W. and Heller, F. 1982. Magnetic Properties of Marine Limestones. *Reviews of Geophysics and Space Physics* **20** (2), 171-192.

Poutiers, J. et Noel, M. 1985. Relations entre des proprietes physiques (densite et susceptibilite magnetiques) et la lithologie de sediments du Golfe de Gascogne. *Bull. Soc. Geol. France* **8**, 9-20.

Robinson, S. G. 1986. The late Pleistocene palaeoclimatic record of North Atlantic deep sea sediments revealed by mineral-magnetic measurements. *Phys. Earth Planet. Interiors* **42**, 22-47.

Sachs, S. D. and Ellwood, B. B. 1988. Controls on magnetic grain-size variations in the Argentine Basin, South Atlantic Ocean. *Deep-Sea Res.* **35** (6), 929-942.

Scoullos, M., Oldfield, F. and Thompson, R. 1979. Magnetic monitoring of Marine Particulate Pollution in the Elefsis Gulf, Greece. *Marine Pollution Bulletin* **10**, 287-291.

MISCELLANEOUS

Bussiere, J. F. 1986. On line measurement of the microstructure and mechanical properties of steel. *Mater. Eval.* **44**, 560-567.

Dasgupta, S. 1984. Characterization of magnetic dispersions: rheological, mechanical and magnetic properties. *IEEE Trans. Magn. Magn. Mat.* **20** (1), 7-12.

Evans, M. E. and Wayman, M.L. 1970. An investigation of small magnetic particles by means of electron microscopy. *Earth Planet. Sci. Lett.* **9**, 365-370.

Freishac, F. 1935. Uber die magnetische Nachwirkung. *Ziltschrift Fur Physik* **94**, 277-302.

Jackson, M. W., Gruber, W., Marvin, J. and Banerjee, S.K. 1988. Partial anhystereitc remanence and its anisotropy: Applications and grainsize-dependance. *Geophysical Research Letters* **15** (5), 440-443.

Kolm, H., Oberteuffer, J. and Kelland, D. 1975. A recent advance in the generation of strong magnetic fields opens the way to removing very weakly magnetic particles from mixtures. One novel application of the new process is purifying wastewater. *Scientific American* 47-54

Koster, E. 1984. Recommendation of a simple and universally applicable method for measuring the switching field distribution of magnetic recording media. *IEEE Trans. Magn. Magn. Mat.* **20** (1), 81-83.

Kusnetsov, I. A., Somova, V. M. and Bashkirov, Y. P. 1972. Magnetic, Electrical, and mechanical parameters of 45KhN and 45KhNMFA steels after various heat treatments. *Soviet J. NDT* **8**, 506-511.

Mayo, P. I. at al 1990. Interaction effects in longitudinally orientated and non-orientated barium hexaferrite tapes. *IEEE Trans. Magn.* **26** (5), 1894-1896.

McCary, R. O. 1971. Saturation Magnetic Recording Process. *IEEE Trans. Magn.* **7** (1), 4-16.

Mikeev, M. N. et al 1978. Coercive force measurement methods of inspecting the quality of heat and thermochemical treatments of steel and iron parts. *Soviet J. NDT* **14**, 9-16.

Mikheev, M. N. 1983. Magnetic Structure Analysis. *Magnetic and electromagnetic Methods* **19**, 1-8.

O'Grady, K. 1991. Magnetic pigment dispersions (A tutorial review). *J. Magn. Magn. Mat.* **95**, 341-355.

Ozima, M. and Larson, E. E. 1967. Study on irreversible change of magnetic properties of some ferromagnetic minerals. *J. Geomag. Geoelectr.* **19** (2), 117-127.

Preisach, F. 1935. Uber die magnetische Nachwirkung. *Zeitschrift Fur Physik* **94**, 277-302.

Rodigin, N. M. and Syrochkin, V. P. 1972. Feasability of electromagnetic inspection for the strength and hardness of structural steel under elastic tension. **9**, 453-460.

Scholten, P. C. and Felius, J .A. P. 1990. The magnetical and rheological behavior of aggregating magnetic suspensions. *J. Magn. Magn. Mat.* **85**, 107-113.

Shcherbinina, V. A. et al 1972. Using ferroprobes for testing the rails of electromagnetic wagon/defectoscopes. *Soviet J. N.D.T.* **8**, 641-647.

Spratt, G. W. D., Fearson, M., Bissell, P. R., Chantrell, R. W., Lyberatos, P. and Wohlfarth, E. P. 1988. Interaction fields and the anhysteretic susceptibility of recording media. *IEEE Trans. Mag.* **24**, 1895-1897

Zatsepin, N. N. et al 1982. Possibilities of the nondestructive magnetic inspection of hardness of 32Kh2NVMBR high-strength steel. *Soviet J. N.D.T.* **19**, 158-159.

MODELLING

Banarjee, S. K., King, J. and Marvin, J. 1981. A rapid method for magnetic granulometry with applications to environmental studies. *Geophys. Res. Lett.* **8** (4), 333-336.

Chantrell, R. W. and O'Grady, K. 1992. Remanence Curves of Fine Particle Systems II: Theoretical Studies of Interactions. (Draft)

Dean, B. et al 1990. The mathematical modelling of the acquisition of gyroremanent magnetization in a single domain particle. *J. Appl. Phys.* **67** (9), 4481-4483.

el Hilo, M., Kelly, P. E., O'Grady, K. and Popplewell, J. 1989. Determination of easy axis distribution in recording media. *IEEE Trans. Magn.* **26** (1), 210-212.

Gull, S. F. and Daniell, G. J. 1978. Image reconstruction from incomplete and noisy data. *Nature* **272**, 686-690.

Hilton, J., Davison, W. and Ochsenbein, U. 1985. A mathematical model for analysis of sediment core data: implications for enrichment factor calculation and trace-metal transport mechanism. *Chem. Geol.* **48**, 281-1.

Hilton, J. 1986. Normalized magnetic parameters and their applicability to palaeomagnetism and environmental magnetism. *Geology* **14**, 887-889.

King, J. et al 1982. A comparison of different magnetic methods for determining the relative grain size of magnetite in natural materials: some results from lake sediments. *Earth Planet. Sci. Lett.* **59**, 404-419.

O'Grady, K. 1990. Magnetic characterization of recording media. *IEEE Trans. Magn. Magn. Mat.***26** (5), 1870-5.

O'Grady, K. and Chantrell, R. W. 1992. Remanence curves of Fine Particle Systems I: Experimental Studies. *in press.*

Skilling, J. and Bryan, R. K. 1984. Maximum entropy image reconstruction general algorithm. *Mon. Not. R. Astr. Soc.* **211**, 111-124.

Stott, A. P. 1986. Sediment tracing in a reservoir-catchment system using a magnetic mixing model. *Phys. Earth Planet. Interiors* **42**, 105-112.

Thompson, R. 1986. Modelling magnetization data using SIMPLEX. *Phys. Earth Planet. Interiors* **42**, 113-127.

Tomika, G. J. et al 1990. Magnetic viscosity, susceptibility and fluctuation fields in sintered NdFeB. *IEEE Trans. on Magnetics* **26** (5), 2655-2657.

Yu, L. and Oldfield, F. 1989. A Multivariate Model for identifying Sediment Source from Magnetic measurements. *Quaternary Research* **32**, 168-181.

Yu, L. and Oldfield, F. 1993. Quantitative sediment source ascription using magnetic measurmeents in a reservoir-catchments system near Nijar, S.E. Spain. Earth Surf. Proc. Landf. 18, 441-454.

ORIGINS OF MAGNETIC MINERALS IN SOILS

Babanin, V. F., Karpachevskiy, L.O., Opalenko, A.A. and Shoba, S. A. 1976. Forms of Fe compounds in concretions from various soils. *Soil Chemistry* (translated from: Pochvovedeniye) **5**, 132-138.

Fischer, W. R. and Schwertmann, V. 1975. The formation of hematite from amorphous iron (III) hydroxide. *Clays and Clay Minerals* **23**, 33-37.

Fitzpatrick, R.W. and Le Roux, J. 1975. Pedogenic and solid solution studies on iron-titanium minerals. *Proceedings of the International Clay Conference* 585-599.

Maher, B. A. and Taylor, R. M. 1988. Formation of ultrafine-grained magnetite in soils. *Nature* **336**, 368-371.

McClay, K. R. 1974. Single-domain magnetite in the Jimberlana Norite, W Australia. *Earth Planet. Sci. Lett.* **21**, 367-376.

Schwertmann, U. and Fechter, H. 1984. The influence of aluminium on iron oxides: XI Aluminium-substituted maghemite in soils and its formation. *Soil Science Society of America Journal* **48**, 1462-1463.

Taylor, R. M and Schwertmann, U. 1974. Maghemite in soils and its origins I Properties and Observations on soil Maghemites. *Clay Minerals* **10**, 299-310.

Taylor, R. M and Schwertmann, U. 1974. Maghemite in soils and its origins II Maghemite Synthesis at ambient temperature and pH7. *Clay Minerals* **10**, 299-310.

Taylor, R. M., Maher, B. A and Self, P. G. 1987. Magnetite in soils: I the synthesis of single domain and superparamagnetic magnetite. *Clay Minerals* **22**, 411-422.

PALAEOMAGNETISM

Abrahamsen, N. 1978. Towards a Pleistocene-Holocene Magnetostratigaphy in the Southern Baltic sea. (Draft)

Abrahamsen, N. and Readman, P. W. 1980. Geomagnetic variation recorded in Older (>=23 000 BP) and Younger Voldia Clay (~14 000 BP) at Norre Lingby, Denmark. *Geophys. J. R. Astr. Soc.* **62**, 329-344.

Ade-Hall, J. M. 1963. A correlation between Remanent Magnetism and Petrological and Chemical Properties of Tertiary basalt Lavas from Mull, Scotland.

Aitken, M. J. 1974. Phyics and Archeology. In *Physics and Archeology*. Clarendon Press; Oxford.

Bjorck, S. and Sandgren, P. 1986. A 2000 year geomagnetic record from two Late Weichselian sequences in southeastern Sweden. *Geologiska Foreningens i Stockholm Forhandlingar* **108**, 21-29.

Brown, G. 1953. The occurrence of Lepidocrocite in some British Soils. *Journal of Soil Science* **4** (2), 220-228.

Clark, R. M. and Thompson, R. 1978. An objective method for smoothing palaeomagnetic data.*Geophys. J. R. Astr. Soc.* **52**, 205-213.

Clark, R. M. and Thompson,R. 1984. Statistical comparison of palaeomagneitc directional records from lake sediments. *Geophys. J. R. Astr. Soc.* **76**, 337-368.

Collinson, D. W. 1965. The remanent magnetisation and magnetic properties of Red Sediments. *Geophys. J. R. Astr. Soc.* **10**, 105-126.

Collinson, D. W. 1974. The role of pigment and specularite in the remanent magnetism of Red Sandstone. *Geophys. J. R. Astr. Soc.* **38**, 253-264.

Dickson, J. H. et al 1978. Palynology, Palaeomagnetism and Radiometric Dating of Flandrian marine and freshwater sediments of Loch Lomond. *Nature* **274**, 548-553.

Dunlop, D. J. 1972. Magnetic mineralogy of unheated and heated red sediments by coercivity spectrum analysis. *Geophys. J. R. Astr. Soc.* **27**, 37-55.

Frankel, R. B. 1981. Magnetiostatic Bacteria at the Geomagnetic Equator. *Science* 212, 1269-1270.

Fuller, M. D. 1970. Geophysical aspects of palaeomagnetism. *CRC Critical Reviews in Solid State Sciences* **1**, 137-219.

Henshaw, P. and Merril, R.T. 1979. Characteristics of Drying Remanent Magnetization in Sediments. Earth and Planetary Science letters **43**, 315-320.

Hus, J. J. 1990. The magnetic properties of siderite concretions and the CRM of their oxidation products. *Phys. Earth Planet. Interiors* **63**, 41-57.

Huttunen, P. and Stober, J. 1980. Dating of palaeomagnetic records from Finnish Lake sediment cores using pollen analysis. *Boreas* **9**, 193-202.

Idnrum, M. and Schmidt, P. W. 19 Palaeomagnetic dating of weathered profiles. (Chapter VIII).

Karlin, R. and Levi, S. 1986. Diagenesis of magnetic minerals in recent haemipalagic sediments. *Nature* **303**, 327-330.

Karlin, R. 1990. Magnetite Diagenesis in marine Sediments from the oregon Continental margin. *J. Geophys. Res.* **95** (B4), 4405-4419.

Kent, D. V. 1982. Apparent correlation of palaeomagnetic intensity and climatic records in deep sea sediments. *Nature* **299**, 538-539.

King, J. W., Banergee, S. K., Marvin, J. and Lund, S. 1983. Use of small amplitude palaeomagnetic fluctuations for correlation and dating of continental climatic changes. *Palaeogeogr., Palaeoclimatol., Palaeoecol.* **42**, 167-83

Mackereth, F. J. H. 1971. On the variations in direction of the horizontal component of remanent magnetization in lake sediments. *Earth Planet. Sci. Lett.* **12**, 332-338.

McElhinny, M. W. 1977. Palaeomagnetism and Plate Tectonics. *Palaeomagnetism and Plate Tectonics*. Times University Press.

Morner, N.-A. 1975. Palaeomagnetism and the relation between Bredakra Delta and the Fjaras Stadial and the Gothenburg Magnetic Excursion. *Geologiska Foreningens i Stockholm Forhandlingar* **97**, 298-301.

Morner, N.-A., Lansers, J.P. and Hospers, J. 1971. Late Weichselian Palaeomagnetic Reversal. *Nature Physical Science* **234**, 173-174.

Morner, N.-A. and Lanser, J.P. 1974. Gothenburg Magnetic 'Flip'. *Nature* **251**, 408-409.

Morner, N.-A. 1976. Pleistocene/Holocene Boundary. *Boreas* **5**, 262-269

Morner, N.-A. 1988. Terrestrial Variations with given Energy, Mass and Momentum Budgets; Paleoclimate, Sea-Level, Paleomagnetism, Differential Rotation and Geodynamics. Secular Solar and Geomagnetic Variations in the Last 10,000 Years. F.R. Stephenson and A.W. Wolfendale. Kluwer Academic. 455-478

Noel, M and Tarling, D. H. 1975. The Laschamp geomagnetic 'event'. *Nature* **253**, 705-706.

Noel, M. 1975. The palaeomagnetisn of varved clays from Blekinge southern Sweden. *Geologiska Foreningens i Stockholm Forhandlingar* **97**, 357-367.

Noel, M. 1988. Paleomagnetism of Cave Sediments fron Mynydd Llangattwg. *Cave Sci.* **1** (1), 3-9.

O'Reilly, W. 1976. Magnetic Materials in the crust of the earth. *Rep. Prog. Phys.* **39**, 857-908.

Oldfield, F. and Thompson, R. 1979. Geomagnetic polarity measurements from Pleistocene depostis in Southwest France and their chronological implications. *Geological J.* **14** (2), 117-126.

Sandgren, P. 1986. Late Weichselian secular variation from the Torrberga Basin, S. Sweden.*Phys. Earth Planet. Interiors* **43**, 160-172.

Schmidt, P. W. and Embleton, B. J. 1976. Palaeomagnetic results from sediments of the Perth Basin, W. Australia and their bearing on the timing of regional laterization. *Palaeogeogr., Palaeoclimatol., Palaeoecol.* **19**, 257-273.

Schmidt, P. W., Currey, D. T. and Ollier, C. D. 1976. Sub-basaltic weathering, Damsites, Palaeomagnetism and the age of laterization. *J. Geol. Soc. Australia* **23**, 367-370.

Schmidt, P. W., Taylor, G. and Walker, P. H. 1982. Palaeomagnetic dating and stratigraphy of a Cainozoic Lake near Cooma, NSW. *J. Geolog. Soc. Australia* **29**, 49-53.

Schmidt, P. W., Prasad, V. and Ramam, P. K. 1983. Magnetic ages of some Indian Laterites. *Palaeogeogr., Paleoclimatol., Palaeoecol.* **44**, 185-202.

Schmidt, P. W. and Ollier, C. D. 1988. Palaeomagnetic Dating of Late Cretaceous to Early Tertiary weathering in New England, NSW Australia. *Earth Sci. Rev.* **25**, 363-371.

Thompson, R. 1974. Palaeomagnetism. *Sci. Prog. Oxford* **61**, 349-373.

Thompson, R. 1974. Palaeomagnetic study of Hoxnian lacustrine sediments. *Archeometry* **16**, 233-245.

Thompson, R. and Kelts, K. 1974. Holocene sediments and magnetic stratigraphy from Lakes Zug and Zurich, Switzerland. *Sedimentology* **21**, 577-596.

Thompson, R. 1975. Long period European Geomagnetic Secular Variation Comfirmed. *Geophys. J. R. Astr. Soc.* **43**, 847-859.

Thompson, R. and Berglund, B. 1976. Late Weichselian geomagnetic 'reversal' as a possible example of the reinforcement syndrome. *Nature* **263**, 490-491.

Thompson, R. 1977. Stratigraphic consequences of palaeomagnetic studies of Pleistocene and recent sediments. *J. Geol. Soc. Lond.* **133**, 51-59.

Thompson, R. and Turner, G. M. 1979. British geomagnetic curve 10 000 yrs BP for dating European Sediments. *Geophys. Res. Lett.* **6**, 249-252.

Thompson, R. 1982. A comparison of geomagnetic secular variation as recorded by historical, archaeomagnetic and palaeomagnetic measurements. *Phil. Trans. R. Soc. Lond.* **306**, 103-112.

Thompson, R. and Barraclough, D. R. 1982. Geomagnetic secular variation based of spherical Hharmonic and cross validation analyses of historical and archeomagnetic data. *J Geomag. Geoelectr.* **34**, 245-263.

Thompson, R. and Clark, R. M. 1982. A robust least-squares Gondwanan apparent polar wanderer path and the question of palaeomagnetic assessment of Gondwanan reconstructions. *Earth Planet. Sci. Lett.* **57**, 152-158.

Thompson, R. and Edwards, K. J. 1982. A Holocene palaeomagnetic record and a geomagnetic master curve from Ireland. *Boreas* **11**, 335-349.

Thompson, R. 1983. Global Holocene magnetostratigraphy. *Hydrobiol.* **103**, 45-51.

Thompson, R. 1983. 14C Dating and Magnetostratigraphy. *Radiocarbon* **25**, 229-238.

Thompson, R. Palaeomagnetic Correlation and Dating.

Turner, G. M. and Thompson, R. 1981. Lake sediment record of the geomagnetic secular variation in britain during Holocene times. *Geophys. J. R. Astr. Soc.* **65**, 703-725.

Turner, G. M. and Thompson, R. 1982. Detransformation of the British geomagnetic secular variation record for Holocene Times. *Geophys. J. R. Astr. Soc.* **70**, 789-792.

Wilson, R.L. 1960. Palaeomagnetism in northern Ireland Part I. *The Thermal Demagnetization of Natural Magnetic Moments in Rocks.* 45-58.

Wilson, R.L. 1960. Palaeomagnetism in northern Ireland Part II. *On the Reality of a Reversal of the Earth's magnetic field.* 59-69.

RIVERS

Caitcheon, G. G. 1993. Sediment source tracing using environmental magnetism: A new approach with examples from Australia. *Hydrological Processes* **7** (4), 349-358.

Leeks, G. J., Lewin, J. and Newson, M. D. 1988. Channel change, fluvial geomorphology and river engineering: The case of the Afon Trannon, Mid Wales. *Earth Surf. Proc. Landf.* **13**, 207-223.

Nightingale, A. 1991. Magnetic properties of river sediments. HND Dissertation, Coventry Polytechnic.

Oldfield, F., Rummery, T. A., Thompson, R. and Walling, D. E. 1979. Identification of suspended sediment sources by means of magnetic measurements: Some preliminary results. *Water Resources Res.* **15** (2), 211-218.

Oldfield, F. 1981. Artificial magnetic enhancement of stream bedload: a hydrological application of superparamagnetism. *Phys. Earth Planet. Interiors* **26**, 107-124.

Oldfield, F., Maher, B.A., Donoghue, J. and Pierce, J. 1985. Particle-size related, mineral magnetic source sediment linkages in the Rhode River catchment, Maryland, USA. *J. of the Geological Society of London* **142**, 1035-1046.

Walling, D. E., Peart, M. R., Oldfield, F. and Thompson, R. 1979. Suspended sediment sources identified by magnetic measurements. *Nature* **281**, 110-113.

ROCK MAGNETISM

Ade-Hall, J. M. 1963. A correlation between remanent magnetism and petrological and chemical properties of Tertiary Basalt Lavas From Mull, Scotland.

Akimoto, S. 19 Magnetic Susceptibility of ferromagnetic minerals contained in igneous rocks. **2** (20), 47-56.

Bloemendal, J., Lamb, B. and King, J. 1988. Paleoenvironmental Implications of Rock Magnetic Properties of Late Quaternary Sediment Cores from the Eastern Equatorial Atlantic. *Paleoceanography* **3**, 61-87.

Chernyuk, M. V. 1971. Distribution of the magnetic susceptibility values of intrusive rocks.*IOS Izvestija* 225-9.

Chevallier, P. R. 1951. Proprietes magnetiques de L'oxyde ferrique rhomboedtique (fe2 O3~). *J. Phys. Radium* **12**, 172-188.

Chevallier, R., Mathieu, S. and Vincent, E.A. 1954. Iron-titanium oxide minerals in layered gabbros of the Skaergaard intrusion, E. Greenland. Part II. Magnetic Properties. *Geochemica et Cosmochimica Acta* **6**, 27-34

Cisowski, S. M. 1980. The relationships between the magnetic properties of terrestrial igneous rocks and the composition and internal structure of their component fe-oxide grains. Geophys. *J. R. Astr. Soc.* **60**, 107-122.

Clark. D. A. 1983. Comments on Magnetic Petrophysics. *Bull. Aust. Soc. Explor. Geophys.* **14**,49-62.

Collinson, D.W. 1965. Depositional Remanent Magnetization in Sediments. *Journal of Geophysical Research* **70**, 4663-4668.

Collinson, D.W. 1986. Ferrous and Ferric iron in Red Sediments and Their magnetic Properties. Geophysics Journal Royal Astrological Soceiety **16**, 531-542.

Davis, P. M. and Evans, M. E. 1974. Interacting single-domain properties of magnetite intergrowths. *J. Geophys. Res.* **81** (5), 989-994.

Dekkers, M. J. 1989. Magnetic properties of natural pyrrhotite II High- and low- temperature behaviour of Jrs and TRM as a function of grain size. *Phys. Earth Planet. Interiors* **57**, 266-283.

Doh, S.-J., King, J. W. and Leinen, M. 1988. A rock magnetism study of giant piston core LL44-GPC3 from the central North Pacific and its palaeoceanographic implications. *Paleoceanography* **3** (1), 89-111.

Dunlop, D. J. et al 1973. Indecies of multidomain magnetic behaviour in basic igneous rocks: Alternating field demagnetization, Hysteresis and Oxide Petrology. *J. Geophys. Res.* **78** (8),1387-1393.

Dunlop, D. J. 1981. The rock magnetism of fine particles. *Phys. Earth Planet. Interiors* **26**, 1-26.

Frankel, J. J. 1966. Some mineralogical observations on Australian Lateritic rocks. *Australian J. Science* **29** (4), 115-117.

Haggerty, S. E. 1979. The aeromagnetic mineralogy of igneous rocks. *Canadian J. Earth Sci.* **16**, 1281-1293.

Hamilton., N. 1963. Susceptibility Anisotropy Measurements on some Silurian Siltstones. *Nature* **197**, 170-1.

Henkel, H. 1976. Studies of density and magnetic properties of rocks from N Sweden. *Pure and Applied Geophys.* **11** (4), 235-249.

Irving, E. and Major, A. 1964. Post-Depositional Remanent Magnetization in a Synthetic Sediment. Sedimentology **3**, 135-143.

Janak, F. 1971. Magnetic susceptibility of various rock types and its significance for geophysics and geology. *Geophys. Prospecting* **20**, 375-384.

Janak, F. 1973. A brief outline of the magnetic susceptibility anisotropy of various rock types. *Studia Geoph. et Geod.* **17**, 123-130.

Johnson, H.P., Kinoshita, H. and Merrill, R.T. 1975. Rock Magnetism and Palaeomagnetism of Some North Pacific Deep-Sea Sediments. *Geological Society of America Bulletin* **86**, 412-420,

Kato, Y. On the Magnetic Moment of the Residual Magnetism of the Rock.

Kropacek, V. and Miroslav, K. 1968 Magnetism and ferromagnetism of natural minerals of the spinel group. *Studia Geoph et Geod.* **12**, 385-397.

Kropacek, V. 1971. Distribution of the values of matural remanent magnetization and magnetic susceptibility of some minerals. *Studia Geoph. et Geod.* **15**, 340-352.

Kropacek, V. and Miroslav, K. 1971. Magnetism of natural Phrrhotite, haematite and ilmenite. *Studia Geoph. et Geod.* **15**, 161-172.

Larson, E. et al 1969. Stility of remanent magnetization of igneous rocks. *Geophys. J. R. Astr. Soc.* **17**, 263-92.

McIntyre, J. I. 1980. Geological significance of magnetic patterns related to magnetite in sediments and metasediments - A review. *Bull. Aust. Soc. Explor. Geophys.* **11** (1&2), 19-33.

Molynuex, L., Thompson, R., Oldfield, F. and Lonemore, M.E. 1972. Rapid Measurement of the Remanent Magnetization of Long Cores of Sediment. *Nature* **237**, 42-43.

Nagata, T and Akimoto, S. 19. Magnetic transition points of volcanic rocks. *J. Geomagn. Geoelectr.* **2** (9), 29-33

O'Rielly, W. 1984. Rock and Mineral Magnetism. Blackie.

Soffel, H. C. 1969. The origin of thermoremanent magnetization of two basalts containing homogenous single phase titanomagnetite. *Earth Planet. Sci. Lett.* **7**, 201-208.

Stacey, F. D. 1963. The Physical theory of Rock Magnetism. *Advances in Physics* **12**, 45-133.

Stephenson, A. 1967. The Effect of Heat Treatment on the Magnetic Properties of the Old Red Sandstone. *Geophysics Journal Royal Atronomical Society* **13**, 425-440.

Turner, P. 1975. Depositional magnetization of Carboniferous Limestones from the Craven Basin of Northern England. Sedimentology **22**, 563-581.

Wilson, R.L. 1963. Magnetic Properties and Normal and Reversed Natural Magnetization in the Mull lavas 424-39.

Vincent, E.A. and Phillips, R. 1954. Iron-titanium oxide minerals in layered gabbros of the Skaergaard intrusion, East Greenland. Part I. Chemistry and ore-microscopy. *Geochemica et Cosmochimica Acta* **6**, 1-26.

SOILS

Alekseyev, A. O. et al 1989. Magnetic susceptibility of soils in a catena. *Soviet Soil Science* **21** (1), 78-86.

Babanin, V. F. 1971. Magnetic susceptibility of some groups of soils in the European USSR. *Soviet Soil Science* **4**, 122-124.

Babanin, V. F. 1973. The use of magnetic susceptibility measurements in identifying forms of iron in soils. *Soviet Soil Science* 487-493.

Bagina, O. L. et al. 1990. Magnetoviscous properties of ash soils of Kamchalka and their use for dating. *Soviet Soil Science* **22** (5), 109-118.

Bjorck, S., Dearing, J. A. and Jonsson, A. 1982. Magnetic Susceptibility of Late Weichselian deposits in Southeastern Sweden. *Boreas* **11**, 99-111.

Dearing, J. A., Maher, B. A. and Oldfield, F. 1985. Geomorphological linkages between soils and sediments: the role of magnetic measurements. In *Geomorphology and Soils*, Eds K. Richards, R. Arnett and S. Ellis. Allen and Unwin, 245-266.

Dearing, J. A. et al 1986. Tracing movements of topsoil by magnetic measurements: Two case studies. *Phys. Earth Planet. Interiors* **42**, 93-104.

Dearing, J. A., Alstrom, K., Bergman, A., Regnell, J. and Sandgren, P. 1990. Recent and long-term records of soil erosion from Southern Sweden. In *Soil Erosion on Agricultural Land* Eds J. Boardman, I. D. L. Foster, J. A. Dearing; J. Wiley.

Fine, P. et al 1989. Role of pedogenesis in distribution of magnetic susceptibility in two Californian chronosequences. *Geoderma* **44**, 287-306.

Gaillard, A. J., Dearing, J. A., El-Daoushy, F., Enell, M. and Hakansson, H. 1991. A late Holocene record of land use history, soil erosion, lake trophy and lake level fluctuations at Bjaresjosjon (South Sweden), *J. Paleolimnology* **6**, 51-81.

Harvey, A. M. et al 1981. Dating of post glacial landforms in the central Howgills. *Earth Surface Process and Landforms* **6**, 401-412.

Le Borgne, E. 1955. Susceptibilite Magnetique Anormale du Sol Superficiel. *Annales de Geophysique* 399-419.

Le Borgne, E. 1960a. Influence du Feu sur les Proprietes Magnetiques du Sol et sur Celles du Schiste et du Granite. *Annales de Geophysique* **16** (2), 159-195.

Le Borgne, E. 1960b. Etude Experimentale du Trainage Magnetique dans le Cas d,un Ensemble de Grains Magnetiques tres Fins Disperses dane une Substance non Magnetique. *Annales de Geophysique* 445-494.

Lushkin, A. A., Rumyantseva, T. I. and Kovrigo, V. P. 1968. Magnetic Susceptibility of the principal soil in the Udmurt ASSR. *Scientific Communications* 88-93.

Maher, B. A. 1984. The Origins and Transformations of Magnetic Minerals in soils. Unpubl PhD Thesis, University of Liverpool

Maher, B. A. 1986. Characterization of soils by mineral magnetic measurements. *Phys. Earth Planet. Interiors* **42**, 76-92.

Mullins, C. E. 1977. Magnetic susceptibility of the soil and its significance in soil science - a review. *J. Soil Sci.* **28**, 223-246.

Nezhdanova, I. K. and Suetin, Yu. P. 1987. Investigations of magnetic susceptibility of soils in connection with anthropogenic activity. (English Summary) *Geologiya I Geografiya* **4**, 82-85.

Oades, J. M. and Townsend, W. N. 1963. The detection of ferromagnetic minerals in soils and clays. *Journal of Soil Science* **14** (2), 179-187.

Ozdemir, O. and Barargee, S. K. 1982. A preliminary magnetic study of soil samples from west-central Minnesota. *Earth Planet. Sci. Lett.* **59**, 393-403.

Rummery, T. A., Bloemendal, J., Dearing, J. A. and Oldfield, F. 1979. The persistence of fire-induced magnetic oxides in soils and lake sediments. *Ann. Geophys.* **35**, 103-107.

Sandgren, P. and Thompson, R. 1990. Mineral magnetic characteristics of podzolic soils developed on sand dunes in the Lake Gosciaz catchment, Central Poland. *Phys. Earth Planet. Interiors* **60**, 297-313.

Seminov, A. S. 1988. Measurements of the magnetic susceptibility of soil. (English Summary). *Geologiya I Geografiya* **3**, 35-44.

Singer, M. J. and Fine, P. 1989. Pedogenic factors affecting magnetic susceptibility of Northern Californian soils. *Soil Sci. Soc. Am. J.* **53**, 1119-1127.

Smith, J. P., Fullen, M. A. and Tavner, S. 1990. Some magnetic and geochemical properties of soils developed on Triassic substrates and their use in the characterization of colluvium. In *Soil Erosion on Agricultural Land. Ed's.* J. Boardman, I. D. L. Foster, J. A. Dearing; J. Wiley.

Tite, M. S. and Mullins, C. 1971. Enhancement of the magnetic susceptibility of soils on archeological sites. *Archeometry* **13** (2), 209-219.

Tite, M. S. 1972. The influence of geology on the magnetic susceptibility of soils on archeological sites. *Archeometry* **13** (2), 229-236.

Tite, M. S. and Linnington, R. E. 1975. Effect of climate on the magnetic susceptibility of soils. *Nature* **256**, 565-566.

Vadyunina, A. F. and Babanin, V. F. 1972. Magnetic susceptibility of some soils in the USSR. *Soviet Soil Science* , 588-599.

Vadyunina, A. T., Babanin, V. F. and Koutun, V. A. 1974. Magnetic susceptibility of the separates of some soils. *Soviet Soil Science* , 106-110.

Vadyunina, A. F. and Smirnov, YU. A. 1976. Natural remanent magnetization of some soil. *Soviet Soil Science* **8**, 471-478.

SUSCEPTIBILITY

Collinson, D. W., Molyneux, L. and Stone, D. B. 1963. A total and anisotropic magnetic susceptibility meter Journal of Scientific Instruments **40**, 310-312.

Hamilton, A. C., Magowan, W. and Taylor, D. 19 Use of the Bartington meter to determine the magnetic susceptibility of organic rich sediments from W. Uganda. Dept. Env Sci., New University of Ulster.

Robertson, D. 1990. Molspin Magnetometer and Bartington Susceptibility Meter: Dimensions, Units and Calibration. University of Liverpool

Williams, R. D. and Cooper, J. R. 1990. Locating soil boundaries using magnetic susceptibility. Soil Science 150, 889-895.

VOLCANIC ERUPTIONS

Johnston, M. J. S. and Stacey, F. D. 1969. Transient Magnetic Anomolies accompanying Volcanic Eruptions in New Zealand. *Nature* **224**, 1289-1290.

WATER POLLUTION

Beckwith, P. R., Ellis, J. B. and Revitt, D. M. 1986. Heavy metal and magnetic relationships for urban source sediments. *Phys. Earth Planet. Interiors* **42.**

Beckwith, P. R., Ellis, J. B. and Revitt, D. M. 1990. Applications of magnetic measurements to sediment tracing in urban highway environments. *The Science of the Total Environment* **93**, 449-463.

Brilhante, O., Daly, L. and Trabuc, P. 1989. Application du magnetism a la detection des pollutions causees par les metaux lourds dans l'environment. *C. R. Acad. Sci. Paris. Serie II.***309**, 2005-2012.

APPENDIX 1

Magnetic Measurements and their interpretation: Routine and VSM

Listed in this appendix are the measurements made routinely and used extensively throughout this research (identified by *). Standard parameters are given in part 1 and Vibrating Sample Magnetometer (VSM) parameters in part 2. Parameters derived from calculations of primary measurements are also included (identified by +). In Part three a list is given of the minerals and certain grain sizes of minerals which are indicated by the main linear parameters. Part 3 gives a brief interpretation of the mineral properties and mineral grain sizes which is indicated by each linear parameter. Part 4 gives a definition of linear additivity which applies to the magnetic parameters marked *.

Part 1: Standard Parameters

K and χ^* Magnetic Susceptibility: The ratio of magnetisation induced to intensity of the magnetizing field. This is measured within a small magnetic field (0.1 mT) and is reversible (no remanence is induced). Measurement is on a volume (K) or mass specific (χ) basis. Measurement is roughly proportional to the concentration of ferrimagnetic minerals within a sample. Susceptibility is also sensitive to changes in grain size.

Instrumentation: Single sample susceptibility sensor (Bartington Instruments Ltd).

Units: K (dimensionless); χ ($\mu m^3\ kg^{-1}$)

χfd^+ Frequency Dependent Susceptibility: The variation of susceptibility between two frequencies. Large values of this parameter indicate the presence of ferrimagnetic grains lying at the stable single domain/superparamagnetic boundary (0.02 μm). At higher frequencies of measurement, a proportion of these grains will become blocked in and will no longer contribute to χ as superparamagnetic but as single domain grains. Values of high-frequency (χhf) can be expected to be proportionatly lower than χlf; with weak samples ($\kappa lf < 10$) χfd is prone to instrumental limitations.

$$\chi fd\ (\%) = \frac{\chi lf - \chi hf}{\chi lf} \cdot 100$$

Instrumentation: Dual Frequency (0.46 and 4.6 kHz) susceptibility sensor. (Bartington Instruments Ltd)

Units: Mass Specific ($nm^3\ kg^{-1}$) or as a percentage (%)

ARM* Anhysteretic Remanent magnetization: Anhysteretic remanence is acquired when a sample is subjected to a decreasing alternating field with a weak steady field super-imposed. This parameter is sensitive to the concentration of fine grain sizes (stable single domain; 0.02 - 0.04μm)) of ferrimagnetic minerals in a sample. High values indicate the presence of ferrimagnetic grains close to the Superparamagnetic/Viscous boundary (~0.02-0.04um).

Instrumentation: Anhysteritic magnetizer (maximum a.c. field 100 mT; direct field 0.04 mT)
Fluxgate magnetometer (Molspin Ltd)

Units: $mA\ m^2\ kg^{-1}$

SIRM880mT* Saturation Isothermal Remanent Magnetization: The highest level of magnetic remanence that can be induced in a sample by application of a high field. SIRM is an indicator of the volume concentration of magnetic minerals in a sample, but also responds to grain size variations.

Instumentation: Pulse magnetiszer (maximum field 880 mT) (Molspin Ltd)
Fluxgate magnetometer (Molspin Ltd)

Units: $mA\ m^2\ kg^{-1}$

IRM20mT* 'Soft' Isothermal Remanence Magnetization: Can be used for approximating the concentration of remanence carrying ferrimagnets.

Instrumentation: Pulse magnetizer, Fluxgate magnetometer.

Units: $mA\ m^2\ kg^{-1}$

IRM100mT* 'Hard' Isothermal Remanent magnetization: SIRM - IRM100mT, can be used for approximating the concentration of remanence carrying haematite and goethite in a sample.

Instrumentation: Pulse magnetizer, Fluxgate magnetometer.

Units: $mA\ m^2\ kg^{-1}$

IRM300mT* 'Hard' Isothermal Remanent magnetization: SIRM - IRM300mT, can be used for approximating the concentration of remanence carrying haematite and goethite in a sample also, but is more sensitive than IRM-100mT.

Instrumentation: Pulse magnetizer, Fluxgate magnetometer.

Units: $mA\ m^2\ kg^{-1}$

χARM^{+} Susceptibility of ARM: ARM/DC biasing Field used (0.04mT = 31.84 Am^{-1}). Sensitive for fine grain sizes, values increase steeply with decreasing grain size (Dankers, 1978)
Instrumentation: Pulse magnetizer, Fluxgate magnetometer.
Units: $\mu m^3 kg^{-1}$

$\chi ARM/SIRM^{+}$ Susceptibility of ARM/Saturation Isothermal Remanent Magnetization: This parameter is sensitive to grain size dimentions in magnetite and maghemite. Increases in magnetite grain size are indicated by an increase in the value of the ratio, therefore a value of 0.1 indicates coarse grained primary crystals and 1.0 indicates very fine probably pedogenic secondary crystals (Yu,1989).
Instrumentation: Pulse magnetizer, Fluxgate magnetometer.
Units: kAm^{-1}

ARM/χ^{+} High values indicate finer grain sizes, around stable single domain (SSD), of ferrimagnetic minerals in a sample (Banerjee et al, 1981; King et al, 1982).
Units: $10^2 Am^{-1}$

$SIRM/\chi^{+}$ The ratio of these parameters can be diagnostic of either mineralogy type (e.g., a low - theoretically zero ratio indicates the presence of paramagnetic minerals) or where samples have similar mineral types and concentrations, the dominant magnetic grain size. SIRM/χ is reduced by increased ferrimagnetic versus imperfect antiferromagnetic contribution, by increased grain size from SD upwards, by an increase in SP contribution to χ. comparison to other ratios and quotients makes it possible to identify mass contributory causes of variation in SIRM/χ
Units: $10^2 Am^{-1}$

$SIRM/ARM^{+}$ Also indicates stable single domain grains in a sample. High values (>100) generally indicate multidomain grains, low values (<30) indicate stable single domain dominance (Oldfield and Yu, 1991). The higher the concentration of SSD the lower the value of SIRM/ARM.

$(Bo)cr^{*}$ Demagnetization Parameter: The reverse field strength (mT) required to return a magnetized sample from its SIRM to zero is termed the coercivity of remanence $(B_o)cr$.
Instrumentation: Pulse magnetizer, Fluxgate magnetometer.
Units: mT

'S' ratio^{+} Demagnetization Parameter: The ratio is obtained using IRM100mT (a backfield discriminates between ferrimagnetic and antiferromagnetic mineral types) and SIRM.

$HIRM_n^{*}$ High Field Remanent Magnetization: HIRM is loss of magnetization after saturation expressed on a specific basis (SIRM - IRM100). The total concentration of remanence carrying hematites can be approximated. HIRM300 is generally more sensitive to remanence carying canted-antiferromagnetic minerals also
Instrumentation: Pulse magnetizer, Fluxgate magnetometer.
Units: $mA\ m^2\ kg^{-1}$

$HIRM/\chi lf^{+}$ This ratio indicates the proportion of antiferromagnets to ferrimagnets.
Units: μAm^{-1}

$HIRM/\chi fd^{+}$ This ratio indicates the proportion of antiferromagnets to ferrimagnets of the SD/SP range.
Units: μAm^{-1}

(Adapted from Dankers, 1978; Dearing et al, 1985; Ozdemir and Banerjee, 1982; Yu, 1989; Oldfield and Yu, 1991; Oldfield, 1991)

Part 2: VSM parameters

χlow^{*} Reversible low field susceptibility. Measured either at 1 mT or 5 mT. Like χlf indicates the ferrimagnetic, paramagnetic and canted-antiferromagnetic component of a material minus the diamagnetic component.
Instrumentation: VSM
Units: $\mu m^3 kg^{-1}$

$\chi high^{+}$ Irreversible high field susceptibility. Measured as the gradient of the magnetization slope between 800 and 1000 mT. Indicates the paramagnetic and canted-antiferromagnetic component of a material minus the diamagnetic component. χpara is the mass specific susceptibility of paramagnetic material, χpara% is the percentage paramagnetic susceptibility to the total susceptibility.
Instrumentation: VSM
Units: $\mu m^3 kg^{-1}$

$\chi ferri^{+}$ The mass specific susceptibility component of ferrimagnetic minerals calculated from the difference between χlow and χhigh. Also calculated is the percentage ferrimagnetic component of the total susceptibility (χferri%).
Instrumentation: VSM
Units: $\mu m^3 kg^{-1}$

χpara%$^{+}$ χpara% is the percentage of paramagnetic minerals calculated from χhigh and the total susceptibility.

Ms* The saturation magnetization (at 1000 mT) of the ferrimagnetic component of a material and is calculated by extrapolating the high field magnetisation curve to the y axis (see Figure 1).
Units: mA m^2 kg^{-1}

Mrs* The saturation remanence of a material is the remanence value at zero field following magnetization at 1000 mT, and in theory the same as SIRM.
Instrumentation: VSM
Units: mA m^2 kg^{-1}

Mrs/Ms^{+} Mrs/Ms is the ratio of remanence magnetisation to the saturated magnetisation. In the absence of paramagnetic minerals it gives information about 'magnetite' type and grain sizes.

HIRM100* High Field Remanent Magnetization: HIRM is loss of magnetization after saturation expressed on a specific basis (Mrs - IRM+100). The total concentration of remanence carrying hematites can be approximated.
Instrumentation: VSM
Units: mA m^2 kg^{-1}

'S' ratio^{+} The ratio of IRM+100mT and Mrs and indicates the proportion of soft magnetic minerals such as magnetites to the total remanence carrying mineral content.

Part 3: Linear Parameter Interpretation

Magnetic Parameter	Magnetic Minerals	Grain Sizes (Magnetite)
Standard		
χlf (μ$m^3$$kg^{-1}$)	Ferrimagnetic, Canted-antiferromagnetic Paramagnetic, Diamagnetic	MD, SD, SP
χhf (μ$m^3$$kg^{-1}$)	Ferrimagnetic, Canted-antiferromagnetic Paramagnetic, Diamagnetic	MD, SD (SP=>SD)
χfd (μ$m^3$$kg^{-1}$)	fine-grained ferrimagnetic	SP (SD, MD)
ARM (mAm^2kg^{-1})	fine-grained ferrimagnetic	SP, SD (MD)
IRM20 (mAm^2kg^{-1})	Ferrimagnetic, Canted-antiferromagnetic	MD, SD (zero SP)
IRM100 (mAm^2kg^{-1})	Ferrimagnetic, Canted-antiferromangetic	MD, SD (zero SP)
IRM300 (mAm^2kg^{-1})	Ferrimagnetic, Canted-antiferromangetic	MD, SD (zero SP)
IRM880 (mAm^2kg^{-1})	Ferrimagnetic, Canted-antiferromangetic	MD, SD (zero SP)
HIRM100 (mAm^2kg^{-1})	Canted-antiferromagnetic	MD, SD (zero SP)
VSM		
χlow (μ$m^3$$kg^{-1}$)	Ferrimagnetic, Canted-antiferromagnetic Paramagnetic, Diamagnetic	MD, SD, SP
χhigh (μ$m^3$$kg^{-1}$)	Canted-antiferromagnetic, Paramagnetic, Diamagnetic	MD, SD (SP=>SD)
χferri	fine-grained ferrimagnetic	SP (MD, SD)
Ms (mAm^2kg^{-1})	Ferrimagnetic, Canted-antiferromagnetic	MD, SD, SP
Mrs (mAm^2kg^{-1})	Ferrimagnetic, Canted-antiferromagnetic	MD, SD (zero SP)

Part 4: Linear Additivity: A definition

A definition of linear additivity is given here and relates to all parameters marked with an asterisk (*) in this appendix. In the example shown in Figure A1.1 two sources A and B exist and vectors for two magnetic parameters are drawn on. A line drawn between the measurement values of A and B (*A->B*) gives all possible solutions for mixtures of the sources A and B; given no error at all. Point C is a mixture of A and B but shows some measurement or other error. At this stage simultaneous equations would fail to find a solution as C does not fall on the line *A->B*. However linear programming methods (LINDO for example) would find a solution for Mixture C at the point on *A->B* which is perpendicular with C (marked *). Solutions are therefore found on the line *A->B* at a point which has the shortest distance from C. A defined error range allows such optimization of the overall source and mixture problem. Simultaneous equations can deal with two or three parameters but linear programming can include many parameters and for the example shown in Figure A1.1 the problem would be in multi-dimensional space.

Figure A1.1: Definition of linear additivity
All solutions fall on line A->B

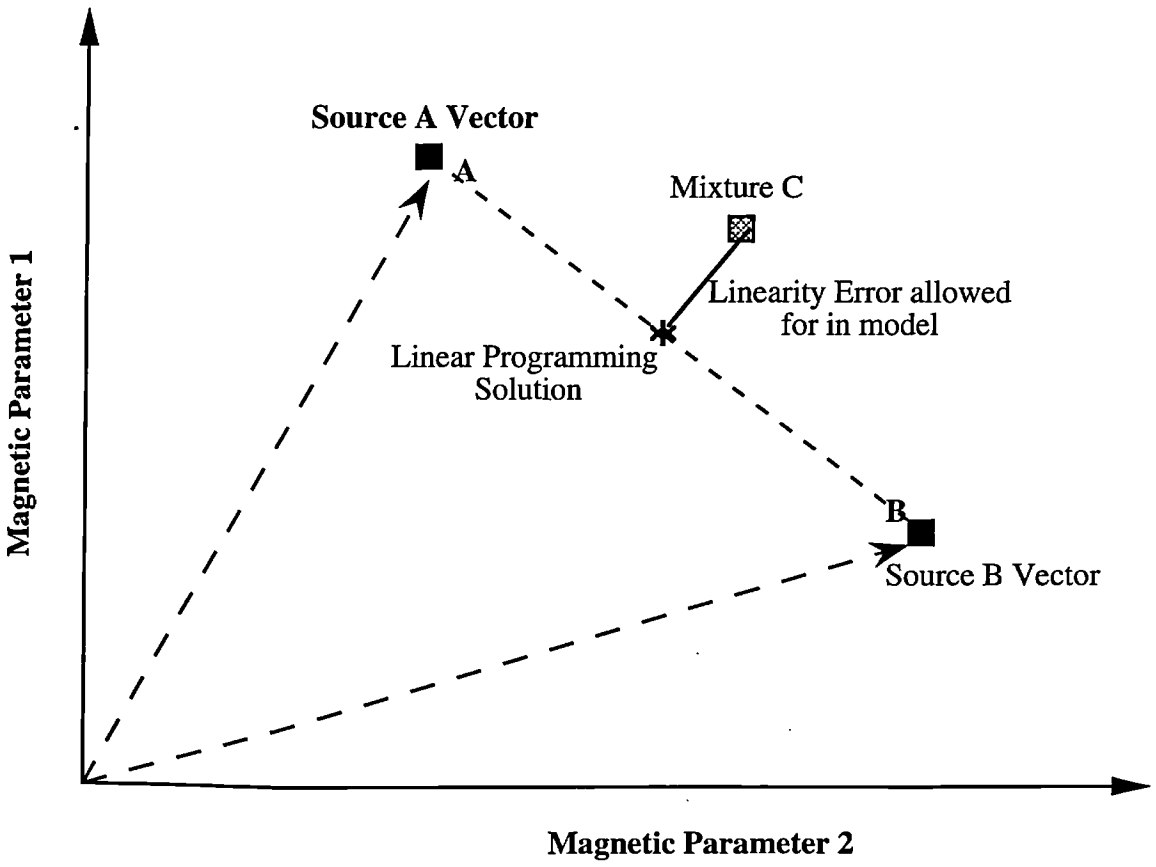

APPENDIX 2

Database Contents and Data Listings

In part 1 of this appendix all samples in each sample database are listed and described. In parts 2 and 3 data from Yu (1991) and Grew (1991), used to test source identification and classification in Chapter 3, are listed.

Part 1: Database Contents

(a) Bedload Database
(b) Chemical database
(c) Coastal database
(d) UK Geological and mineral database
(e) Miscellaneous database
(f) Mixture database
(g) Organic database
(h) Pollution database
(i) Soils database
(j) Synthetics database

(a) Bedload Sample Database

Code	Sample Type	Location	Other Information
FB1Q1-11	Bedload	Finham Brook	Samples 1-5 bulk and 6
FB2Q1-11	Bedload	Finham Brook	to 11 fractions
US1Q1-11	Bedload	Upper Sowe	
LS1Q1-11	Bedload	Lower Sowe 1	
LS2Q1-11	Bedload	Lower Sowe 2	

(b) Chemical Sample Database

Code	Sample Type
GL2K1-5	Barium Sulphate
GL3K1-5	Manganous Carbonate
GL1K1-5-10	Bentonite
SC1K1-3	Sodium Chloride

(c) Coastal Sample Database

Code	Sample Type	Location	Other Information
AB1A1	Diorite	Aldbrough, Holderness	Beach Sample
AB2C1	White Sand	Aldbrough, Holderness	Beach Sample
AB3G1	Grey Till	Aldbrough, Holderness	Cliff Sample
AB4G1	Sandy Till	Aldbrough, Holderness	Cliff Sample
AB5A1	Igneous Rock	Aldbrough, Holderness	Beach Sample
AB6A1	Igneous Rock	Aldbrough, Holderness	Beach Sample
AB7A1	Igneous Rock	Aldbrough, Holderness	Beach Sample
BS1C1	Black Sand	Barmston, Holderness	Beach Sample
BS1C9	Mag Particles	Barmston, Holderness	Beach Sample
BS2C1	Black Sand	Barmston, Holderness	Beach Sample
BS3G1	Grey Till	Barmston, Holderness	Cliff Sample
BS4L1	Lake Sed	Barmston, Holderness	Cliff Sample
BS5B1	Cliff Topsoil	Barmston, Holderness	Cliff Sample
BS6G1	Iron Stain	Barmston, Holderness	Cliff Sample
BS7G1	Upper Cliff Sand	Barmston, Holderness	Cliff Sample
BS8C1	White Sand	Barmston, Holderness	Beach Sample

BS9B1	Cliff Topsoil	Barmston, Holderness	Cliff Sample
BS10B1	Cliff Subsoil	Barmston, Holderness	Cliff Sample
BS11G1	Cliff PM Till	Barmston, Holderness	Cliff Sample
BS12A1	Jurassic Limestone	Barmston, Holderness	Beach Sample
BD1C1	White Sand	Bridlington, Holderness	Beach Sample
BD2C1	White Sand	Bridlington, Holderness	Beach Sample
BD3C1	White Sand	Bridlington, Holderness	Beach Sample
BD4E1	Blown Sand	Bridlington, Holderness	Dune Sample
BD5C1	Sand and Coal	Bridlington, Holderness	Beach Sample
BD6A1	Chalk	Bridlington, Holderness	Cliff Sample
SH1F1	Salt Marsh	Spurn Head, Holderness	Beach Sample
SH2C1	White (E) Sand	Spurn Head, Holderness	Beach Sample
SH3C1	White (E) Sand	Spurn Head, Holderness	Beach Sample
SH4C1	Black (E) Sand	Spurn Head, Holderness	Beach Sample
SH5A1	Coal	Spurn Head, Holderness	Beach Sample
SH6E1	Dune (E) Sand	Spurn Head, Holderness	Beach Sample
SH7C1	Black (E) Sand	Spurn Head, Holderness	Beach Sample
SH8C1	White (S) Sand	Spurn Head, Holderness	Beach Sample
SH9C1	White (S) Sand	Spurn Head, Holderness	Beach Sample
SH10C1	Black (S) Sand	Spurn Head, Holderness	Beach Sample
SH11E1	Dune (S) Sand	Spurn Head, Holderness	Beach Sample
SB1C1	White Sand	Scarborough, Holderness	Beach Sample
SB2G1	Grey Till	Scarborough, Holderness	Cliff Sample
SB3A1	Red Sandstone	Scarborough, Holderness	Cliff Sample
SB3A2	Yellow Sandstone	Scarborough, Holderness	Cliff Sample
SB3A3	Brick	Scarborough, Holderness	Beach Sample
SB3A4	White Sandstone	Scarborough, Holderness	Cliff Sample
SB3A5	Clinker	Scarborough, Holderness	Beach Sample
FB1C1	Black Sand	Filey Bay, Holderness	Beach Sample
FB2G1	Grey Till	Filey Bay, Holderness	Cliff Sample
FB3G1	Sandy Till	Filey Bay, Holderness	Cliff Sample
FH1C1	White Sand	Flambobough Head, Holderness	Beach Sample
FH2C1	White Cave Sand	Flambobough Head, Holderness	Beach Sample
FH3G1	Sandy Till	Flambobough Head, Holderness	Cliff Sample
FH4A1	Chalk	Flambobough Head, Holderness	Beach Sample
CT1C1	White Sand	Cleethorpes, East Anglia	Beach Sample
MT1C1	White Sand	Mablethorpe, East Anglia	Beach Sample
StA1C1	Beach Mixture	Silly Isles, Cornwall	Beach Sample
StA3C1	Sand	Silly Isles, Cornwall	Beach Sample
StA4C1	Sand	Silly Isles, Cornwall	Beach Sample
StA5C1	Sand	Silly Isles, Cornwall	Beach Sample
StA1B1-18	Soil 0-300	Silly Isles, Cornwall	Cliff Samples
LC1A1	Portland	Lulworth Cove, Dorset	Cliff Sample
LC1A2	Purbeck	Lulworth Cove, Dorset	Cliff Sample
LC1A3	Purbeck Sandstone	Lulworth Cove, Dorset	Cliff Sample
LC1A4	Brown/Grey Soil/Clay	Lulworth Cove, Dorset	Cliff Sample
LC1A5	White Sandstone	Lulworth Cove, Dorset	Cliff Sample
LC1A6	Grey Clay	Lulworth Cove, Dorset	Cliff Sample
LC1A7	Blue Clay	Lulworth Cove, Dorset	Cliff Sample
LC1A8	Yellow Sandstone	Lulworth Cove, Dorset	Cliff Sample
LC1A9	Iron Sandstone	Lulworth Cove, Dorset	Cliff Sample
LC1A10	Lignite	Lulworth Cove, Dorset	Cliff Sample
LC1A11	Ironstone	Lulworth Cove, Dorset	Cliff Sample
LC1A12	Red Clay	Lulworth Cove, Dorset	Cliff Sample
LC1A13	Black S'stone	Lulworth Cove, Dorset	Cliff Sample
LC1A14	White Clay	Lulworth Cove, Dorset	Cliff Sample
LC1A15	Sandstone and Iron	Lulworth Cove, Dorset	Cliff Sample
LC1A16	Quartz Conglom	Lulworth Cove, Dorset	Cliff Sample
LC1A17	Orange, Red, Pink Clay	Lulworth Cove, Dorset	Cliff Sample
LC1A18	Greystone	Lulworth Cove, Dorset	Cliff Sample
LC1A19	Greensand	Lulworth Cove, Dorset	Cliff Sample
LC1A20	Chalk	Lulworth Cove, Dorset	Cliff Sample
LC1A21	Hard Chalk	Lulworth Cove, Dorset	Cliff Sample
LC1A22	Low X Sand	Lulworth Cove, Dorset	Beach Sample
LC1A23	High X Sand	Lulworth Cove, Dorset	Beach Sample
LC1A24	Chalky Sand	Lulworth Cove, Dorset	Beach Sample

(d) UK Geological and Mineral Database

1. Existing Rock Database (A. Lovejoy, 1991)

Laboratory Code	Rock Store Code	Rock Type	Group	Location	Geological Age
A4	A4	Granite	Course Acid Igneous	Noirmont, Jersey	Cadomian
A11	A11	Biotite Granite	Course Acid Igneous	Peterhead, Scotland	Caledonian
A24	A24	Microgranite	Fine Acid Igneous	Isle of Aran	Tertiary
BO2	BO2	Rhyolite	Fine Acid Igneous	Cwm Tryffan, Gwynedd	Ordovician
B12	B12	Aegirine-Albite Porphyry	Course Acid Igneous	(Erratic) R. Inver, Sutherland	Caledonian
B5	B5	Felsite Porphyry	Medium Acid Igneous	Inchnadamph, Sutherland	Caledonian
B14	B14	Flow Vesiculated Felsite	Course Acid Igneous	Isle of Aran	Tertiary
BC23	BC23	Pitchstone	Fine Acid Igneous	Corrygills, Isle of Man	Tertiary
AC2	AC2	Quartz-Syenite	Course Intermediate Igneous	Loch Borolan, Sutherland	Caledonian
XY3	XY3	Markfieldite	Intermediate Igneous	East Midlands	Pre-Cambrian
AC3(1)	AC3(1)	Borolonite	Intermediate Igneous	Lock Borolan, sutherland	Caledonian
AC3(2)	AC3(2)	Borolonite	Intermediate Igneous	Borolan Quarry, Sutherland	Caledonian
AE2	AE2	Hornblende Diorite	Course Intermediate Igneous	Green Island, Jersey	Cadomian
BA1	BA1	Andesite	Fine Intermediate Igneous	Exeter Traps, Dunchideock, Devon	Permian
AF1	AF1	Gabbro	Course Basic Igneous	Isle of Skye	Eocene
BE2	BE2	Dolerite	Medium Basic Igneous	Loch Assynt, Sutherland	Inverian
BC2	BC2	Basalt	Fine Basic Igneous	Whin Sill, Northumberland	Carboniferous
AG1	AG1	Cromaltite	Ultra Basic Igneous	Ledmore, Sutherland	Caledonian
AO5	AO5	Pegamite	Ultra Basic Igneous	S. W. Coll, Western Isles	Lewisian
BF8	BF8	Conglomeratic Tuff	Ultra Basic Igneous	Elan Valley, Powys	Ordovician
CO1	CO1	Lewisian Gneiss	Course Metamorphic	Loch Assynt, Sutherland	Scourian
CO3	CO3	Orthogneiss	Course Metamorphic	Beacon Malvern, Worcestershire	Pre-Cambrian
DO1	DO1	Schist	Med Metamorphic	Start Point, Devon	Hercynian
DO3	DO3	Schist	Med Metamorphic	Holyhead, Anglesey	Pre-Cambrian
XY1	XY1	Slate	Fine Metamorphic	Wales	Unknown
DA4	DA4	Dolomitized Limestone	Fine Metamorphic	Assynt, Sutherland	Cambro-Ordovician
GE2	GE2	Mudstone	Fine Sedimentary	North Wales	Lower Palaeozoic
GA2	GA2	Shale	Fine Sedimentary	Wales	Lower Palaeozoic
GB1	GB1	Siltstone	Fine Sedimentary	Shropshire	Silurian
XY2	XY2	Red Sandstone	Medium Sedimentary	West Midlands	Unknown
FC2	FC2	Coarse-Grained Arkose	Medium Sedimentary	Assynt, Sutherland	Torridonian
HA18	HA18	Shelly Limestone	Medium Sedimentary	Unknown	Unknown
FB1	FB1	Eriboll Quartzite	Course Sedimentary	Loch Assynt, Sutherland	Lower Cambrian
E15	E15	Brodick Breccia	Course Sedimentary		

2. *Additions to Existing Database (August, 1992)*

RC A1	A14	Adamellite Granite	Course Acid Igneous	Shap, Westmorland	Caledonian
RC A2	BE3	Dolerite	Medium Basic Igneous	Durness, Sutherland	Caledonian
RC A3	CO13	Marble	Course Metamorphic	Tiree, W. Isles	Caledonian
RC A4	DO5	Schist	Fine Metamorphic	Stack of Glencoul, Sutherland	Moinian
RC A5	DO14	Slate	Fine Metamorphic	Monument, Anglesey	Pre-Cambrian
RC A6	E10	Conglomerate	Fine Conglomerate	Torquay, Devon	New Red Sandstone
RC A7	E12	Conglomerate	Fine Conglomerate	Ironbridge, Shropshire	Old Red Sandstone
RC A8	E18	Quartz Conglomerate	Course Conglomerate	Ellesmere Moraine, Cheshire	Lower Cambrian/Ordovician
RC A9	FA10	Greensand	Medium Sedimentary	Folkestone, Kent	Lower Cretaceous
RC A10	FB6	Quartzite	Med/Fine Metamorphic	Holyhead, Anglesey	Pre-Cambrian
RC A11	FC3	Sandstone	Medium Sedimentary	Ranshaw Rocks, Staffordshire	Namurian
RC A12	FE1	Greywacke	Fine Sedimentary	Jersey Shales, St. Aubins, Jersey	Brioverian
RC A13	GE3	Mudstone	Fine Sedimentary	Loch Awe, Sutherland	L. Cambrian
RC A14	H1	Oolite	Fine Sedimentary	Edgehill, Warwickshire	L. Jurassic
RC A15	H2	Oolite	Fine Sedimentary	Isle of Purbeck, Dorset	Portlandian, U. Jurassic
RC A16	HA4	Limestone	Fine Sedimentary	Dudley, Worcestershire	Silurian
RC A17	HB1	White Chalk	Fine Sedimentary	Kent	Cretaceous
RC A18	HB3	Red Chalk	Fine Sedimentary	Hunstanton, Kent	Cretaceous
RC A19	HO3	Limestone	Fine Sedimentary	Avon Gorge, Somerset	Avonian, L. Carboniferous
RC A20	AG10	Serpentenite	Coarse Ultra-Basic Igneous	Lizard, Cornwall	Hercynian
RC A21	B2	Quartz Porphyry	Fine Acid Igneous	Withiel, Cornwall	Permian
RC A22	BA7	Andesite	Fine Acid Igneous	Grimley Quarry, Leicestershire	Pre-Cambrian
RC A23	CO17	Hornstone	Course Metamorphic	Charnwood Forest, N. Leicestershire	Pre-Cambrian
RC A24	FC5	Millstone Grit	Medium Sedimentary	Derbyshire	Namurian
RC A25	GD1	Pipe Clay	Fine Sedimentary	Bournemouth, Hampshire	Eocene
RC A26	GD5	Red Marl	Fine Sedimentary	Leicestershire	Triassic

3. *Mineral Samples*

Laboratory Code	Mineral Type	Obtained From	Geological Formation
JL-A1	Magnetite (Fe_3O_4 oxides)	Birmingham Geology Dept.	Igneous viens, replacement deposits
JL-A2	Massive Magnetite	Birmingham Geology Dept.	Igneous viens
JL-A3	Crystal Hematite (Fe_2O_3 oxides)	Birmingham Geology Dept.	Igneous viens, hydrothermal replacement deposits
JL-A4	Massive Hematite	Birmingham Geology Dept.	Igneous viens, hydrothermal replacement deposits
JL-A6	Lepidocrocite (FeOOH hydroxides)	Birmingham Geology Dept.	Secondary mineral with Goethite
JL-A8	Goethite (FeOOH hydroxides)	Birmingham Geology Dept.	Oxidation of iron rich deposits
JL-A9	Pyrrhotite (FeS sulphides)	Birmingham Geology Dept.	Magmatic igneous deposits (esp. ultra-basic rocks)

4. Other Samples

Laboratory Code	Rock Type	Group	Location	Geological Age
LC1A1	Portland	Medium Sedimentary	Lulworth Cove	Jurassic
LC1A2	Purbeck	Medium Sedimentary	Lulworth Cove	Jurassic
LC1A3	Purbeck Sandstone	Medium Sedimentary	Lulworth Cove	Jurassic
LC1A4	Brown/Grey Soil/Clay	Fine Sedimentary	Lulworth Cove	Cretaceous
LC1A5	White Sandstone	Medium Sedimentary	Lulworth Cove	Cretaceous
LC1A6	Grey Clay	Fine Sedimentary	Lulworth Cove	Cretaceous
LC1A7	Blue Clay	Fine Sedimentary	Lulworth Cove	Cretaceous
LC1A8	Yellow Sandstone	Medium Sedimentary	Lulworth Cove	Cretaceous
LC1A9	Iron Sandstone	Medium Sedimentary	Lulworth Cove	Cretaceous
LC1A10	Lignite	Medium Sedimentary	Lulworth Cove	Cretaceous
LC1A11	Ironstone	Course Sedimentary	Lulworth Cove	Cretaceous
LC1A12	Red Clay	Fine Sedimentary	Lulworth Cove	Cretaceous
LC1A13	Black Sandstone	Medium Sedimentary	Lulworth Cove	Cretaceous
LC1A14	White Clay	Fine Sedimentary	Lulworth Cove	Cretaceous
LC1A15	Sandstone and Iron	Medium Sedimentary	Lulworth Cove	Cretaceous
LC1A16	Quartz Conglomerate	Course Sedimentary	Lulworth Cove	Cretaceous
LC1A17	Orange, Red and Pink Clay	Fine Sedimentary	Lulworth Cove	Cretaceous
LC1A18	Greystone	Fine Sedimentary	Lulworth Cove	Cretaceous
LC1A19	Upper Greensand	Medium Sedimentary	Lulworth Cove	Cretaceous
LC1A20	Lower Chalk	Fine Sedimentary	Lulworth Cove	Cretaceous
LC1A21	Hard Chalk	Fine Sedimentary	Lulworth Cove	Cretaceous
AB1A1	Diorite	Fine Igneous	Holderness Coastline	-
AB5A1	Igneous Rock	Fine Igneous	Holderness Coastline	-
AB6A1	Igneous Rock	Fine Igneous	Holderness Coastline	-
AB7A1	Igneous Rock	Fine Igneous	Holderness Coastline	-
BS12A1	Limestone	Medium Sedimentary	Holderness Coastline	Jurrasic
BD6A1	Chalk	Fine Sedimentary	Holderness Coastline	Cretaceous
SH5A1	Coal	Medium Sedimentary	Holderness Coastline	Carboniferous
SB3A1	Red Sandstone	Medium Sedimentary	Holderness Coastline	Triassic
SB3A2	Yellow Sandstone	Medium Sedimentary	Holderness Coastline	Triassic
SB3A3	Brick	Man made	Holderness Coastline	-
SB3A4	White Sandstone	Medium Sedimentary	Holderness Coastline	Triassic
SB3A5	Clinker	Man made	Holderness Coastline	-
StA1A19	Granitic Head	Course Igneous/Sedimantary	St. Agnes, Silly Isles	Intrusive volcanic

(e) Miscellaneous Sample Database

Code	Sample Type	Location	Other Information
CS1X1-5	Chimney Slag	Gulson Rd Hospital, Coventry	Packing Expiment
PS1B1-5	Corley Topsoil	Corley, North Warwickshire	
CS1X6-13	Chimney Slag	Gulson Rd Hospital, Coventry	Dilution Experiment
PS1B6-13	Corley Topsoil	Corley, North Warwickshire	
TS1B1-3	Corley Topsoil	Corley, North Warwickshire	Burning Experiment
RS1A1-3	Red Sandstone	Corley Rocks, North Warwickshire	
RC1A1-3	Keuper Clay	Seeswood Pool, North Warwickshire	
SC1K1-3	Sodium Chloride		

(f) Artificial Mixture Sample Database

1. Mixing Experiment 1

Code	Sample Type	Location	Other Information
CM1B1-10	Arable Topsoil	Corley Moor, Warks	
SP1A1-10	Keuper Clay	Seeswood Pool, Warks	
BH1Y1-10	Mine Spoil	Bedworth Heath, Warks	
GH1X1-10	Chimney Slag	Gulson Hospital, Coventry	
GL1K1-10	Bentonite		
DM1A1-10	Coal	Daw Mill	
JL-Z1-20	Mixtures		Mixtures of 2 or more of the above in varying proportions

2. Mixing Experiment 2

SP1A11-15	Keuper Clay	Seeswood Pool	
CM1B11-15	Arable Topsoil	Corley Moor	
BH1Y11-15	Mine Spoil	Bedworth Heath	
FB1Q12-16	Bedload	Finham Brook 2, Coventry	
GL2K1-5	Barium Sulphate		
GL3K1-5	Manganous Carbonate		
JL-Z21-45	Environmental Mixtures		Mixtures of 2 or more of the above environmental materials in varying proportions
JL-Z46-71	Chemical & Environmental Mix.		Mixtures of 2 or more of the above in varying proportions

(g) Organic Sample Database

Code	Sample Type	Location	Other Information
EW1N1-10	Pine Needles	Elkin Wood, Corley, Warks	Taken from 10ft height
EW1Nf1-10	Fallen Needles	Elkin Wood, Corley, Warks	Taken from woodland floor
EW1P1-10	Tree Bark	Elkin Wood, Corley, Warks	Taken at breast height
EW1B1-10	Organic Matter	Elkin Wood, Corley, Warks	0-5cms

(h) Pollution Samples Database

Code	Sample Type	Location (Warwickshire)	Other Information
HP1A1	coal	Coventry Colliery	
HP1M1	brickette	Coventry Homefire Plant	Smokeless fuel
MF1H1	Fablon	Manor Farm, Bennets Rd	Env. Health 13/1/92 - 21/1/92. Reflectance = 96.6
IC1H1	Fablon	Ivy Cottage, Fivefield Rd	Env. Health 13/1/92 - 21/1/92. Reflectance = 94
FR1H1	Fablon	56, Fivefield Rd	Env. Health 13/1/92 - 21/1/92. Reflectance = 95
FR2H1	Fablon	Fivefield Rd	Env. Health 13/1/92 - 21/1/92. Reflectance = 95.4
BR1H1	Fablon	52, Bennets Rd	Env. Health 13/1/92 - 21/1/92. Reflectance = 86
TH1H1	Fablon	The Hollies, Bennets Rd	Env. Health 13/1/92 - 21/1/92. Reflectance = 90
AP1H1-10	Fablon	Unknown	Env. Health
CW1H1	Fine Dust	Cement Works	Env. Health
CW1H2	Course Dust	Cement Works	Env. Health
CW1H3	Leaves	Cement Works	Env. Health
CW1H4	Fine Dust	Cement Works	Env. Health
AP1H1-6	Filters	Council Offices	Env. Health
AP3H1	Filters	Foxford School	Env. Health
AP4H1	Filters	Lythalls Lane	Env. Health
AP5H1	Filters	Radford Comm. Centre	Env. Health
DM1B1	Roadside Soil	Daw Mill Colliery	
DM1H1	Road Dust	Daw Mill Colliery	Collected from Drain Grill
DM1N1	Leaves	Daw Mill Colliery	Hawthorn
DM1N2	Leaves	Daw Mill Colliery	Elderberry
KP1B1	Roadside Soil	Coventry Colliery	
KP1N1	Leaves	Coventry Colliery	Hawthorn
HP1B1	Roadside Soil	Coventry Homefire Plant	
HP1N1	Leaves	Coventry Homefire Plant	Hawthorn
BE1M1	Road Dust	Cement Works	Bayton Ind. Estate.
BE1M2	Cement	Cement Works	Bayton Ind. Estate.
BE2H1	Road Dust	Redland Clay Tiles	Bayton Ind. Estate.
BE2A1	Red Clay	Redland Clay Tiles	Bayton Ind. Estate.
BE2M1	Tile	Redland Clay Tiles	Bayton Ind. Estate.
BE3H1	Deposit	Bayton Ind. Estate	Collected from underside of railway bridge
BE3N1	Leaves	Bayton Ind. Estate	Hawthorn
RR1B1	Roadside Soil	Radford Road	Central Reservation
RR1N1	Leaves	Radford Road	Central Reservation
BR1B1	Roadside Soil	Bennets Road	Motorway Bridge over Corley Services
JL1X1	Exhaust	-	'V' Redg. Volvo 244 DL
JL1X2	Exhaust	-	'Y' Redg. Mini 1000
JL1X3	Exhaust	-	'J' Redg. Simson 50cc Motorcycle
GH1X1	Chimney Slag	Gulson Hospital	from Boiler House
DM1A1	Coal	Daw Mill Colliery	
CV1A1	Fine Dust	Gulson Hospital	Collected using a car vac
CV1A2	Fine Dust	Gulson Hospital	Collected using a car vac
CV1A3	Course Dust	Gulson Hospital	
CV1N1	Leaves	Gulson Hospital	London Plane (70 cut discs)
CV1N2	Leaves	Gulson Hospital	Hawthorn (40)
CV1N3	Leaves	Gulson Hospital	Cherry (50)
CV1N4	Leaves	Gulson Hospital	Laurel (50)
CV1N5	Leaves	Gulson Hospital	Box
CV1N6	Leaves	Gulson Hospital	Catoneaster
CV1N7	Leaves	Gulson Hospital	Budlia
CV1N8	Leaves	Gulson Hospital	Cypress
DM2X1	Ash	Rural	Domestic Coal Fire
DM3X1	Soot	Rural	Domestic Coal Fire

(i) Soil Sample Database

1. Soil Profiles

Code	Soil Type	Location	Depth (cm)	Geology	NGR	Soil Series
CL1B1-8	Brown Earth	Corley, Warks	0-70	Permo Triassic Sandstone	SP 289 852	Bromsgrove
TMT1B1-18		Twelve Mile Tank, New South Wales, Australia	0-118	Sandstone		
CC1B1-16	Humo Ferric Podzol (Buried Soil at 35cms)	Canock Chase, Staffs	0-80	Permo Triassic Conglomerates	SJ 987 183	Goldstone
FD1B1-8	Stagnohumic Gley	Foel Dinas, Dinas Mawddwy, Dyfed	0-70	Paleozoic Slates/Mudstones	SH 851 145	Hafren
HR1B1-6	Argillic Brown Earth	Housedale Rigg, Scarborough	0-61	Jurassic Limestone	SE 87 87	Anglezarke
HR2B1-6	Argillic Brown Earth	Housedale Rigg, Scarborough	0-51	Jurassic Limestone	SE 87 87	Anglezarke
HR3B1-5	Rendzina	Housedale Rigg, Scarborough	0-30	Jurassic Limestone	SE 87 87	Anglezarke
HR4B1-6	Rendzina	Housedale Rigg, Scarborough	0-34	Jurassic Limestone	SE 87 87	Anglezarke
HR5B1-7	Podsolized Brown Earth	Housedale Rigg, Scarborough	0-75	Calcareous Grits	SE 87 87	Anglezarke
HR6B1-8	Iron Pan Podzol	Housedale Rigg, Scarborough	0-62	Calcareous Grits	SE 87 87	Anglezarke
FB1B1-3	Brown Podsol	Foel Benddin, Dinas Mawddwy, Dyfed	0-50	Paleozoic Mudstone/Slate	SH 859 153	Manod
SI1B1-16	Iron Pan Stagnopodzol	St Agnes, Scilly Isles	0-100	Granitic Head	SW 883 071	Hexworthy
AH1B1-3	Stagnogley	Alice Holt Forest, Hampshire	0-50	Jurassic/ Cretaceous Clays	SU 124 258	Denchworth
NYM1B1-11	Podsolized Brown Earth	Housedale Rigg, Scarborough	0-55	Calcareous Grits	SE 87 87	Anglezarke
LG1B1-10	Podzol	Llyn Geiryonydd, N. Wales	0-50	Slates	SH 76 60	
SP1B1-25	Stagnogley	Seeswood Pool, Warks	0-50	Keuper Marl		
SP2B1-24	Stagnogley	Seeswood Pool, Warks	0-50	Keuper Marl		
SP3B1-25	Stagnogley	Seeswood Pool, Warks	0-50	Keuper Marl		
ES1B1-16	Ranker	Earl Standale, Yorkshire	0-32	Limestone		
CF1P1-25	Peat	Cat and Fiddle, Cheshire	0-50	Limestone		
Ccm1B1-15	Stagnogley	Corley Common, Warks	10-15	Keuper Marl		Bromsgrove
Ccm1B16-30	Stagnogley	Corley Common, Warks	25-30	Keuper Marl		Bromsgrove
Ccm1B31-45	Stagnogley	Corley Common, Warks	40-45	Keuper Marl		Bromsgrove

2. Topsoil Samples

Code	Soil Type	Location	Depth (cm)	Geology	NGR	Soil Series
AHCP1B1-75	Stagnogley	Alice Holt Forest, Corsican Pine Plot, Hampshire	0,10,40	Jurassic/ Cretaceous Clays	SU 124 258	Denchworth
AHOK1B1-75	Stagnogley	Alice Holt Forest Oak Plot, Hampshire	0,10,40	Jurassic/ Cretaceous Clays	SU 124 258	Denchworth

Code	Grid Ref	Site	Soil Type	Geology	Map Symbol
TE1B1	423 624	Southam, A423	Calcareous Pelosols	Lower Lias	411b
TE2B1	446 476	Mollington, A423	Brown Earth	Middle Lias	544
TE3B1	448 216	Wooton, A423	Typical Brown Calcareous Earths	Great Oolite	511a
TE4B1	455 187	Wooton, A423	Brown Rendzina	Cornbrash	343a

TE5B1	398 055	Stanton Harcourt, A415	Typical Brown Calcareous Earths	Oxford Clay	511h
TE6B1	482 956	Drayton, A4017	Typical Argillic Brown Earth	Kimmerage Clay	571
TE7B1	444 890	West Hendred, A417	Typical Argillic Brown Earths	Chalk/ Greensand	571i
TE8B1	432 894	West Hendred, A417	Typical Argillic Brown Earths	Upper Greensand	571i
TE9B1	447 876	West Hendred, A417	Grey Rendzinas	Chalk	342c
TE10B1	480 840	West Ilsley, A34	Brown Rendzinas	Chalk	343h
TE11B1	485 846	Chilton, A34	Typical Brown Calcareous Soils	Chalk	571f
TE12B1	482 737	Cheively, A34	Typical Argillic Brown Earths	Oldhaven Beds	571j
TE13B1	485 630	Burghclere, A34	Pelo-argillic Podzols	Bagshot Beds	634
TE14B1	466 258	Steeple Aston, A423	Ferritic Brown Earths	Upper Lias	544a
TE15B1	404 789	Coombe Abbey, A427	Typical Stagnogley Soils	Keuper Clay	711b

Code	Grid ref	Soil	Geology	Land-use	Colour
GR1B1	318 302	Rendzina	Chipping Norton Limestone	Arable	10YR 4/3
GR1B2	adjacent			Wooded/fenced	10YR 3/1
GR1B3	"				10YR 5/2
GR2B1	318 306	Rendzina	Chipping Norton Limestone	Rough Grass	10YR 4/3
GR2B2	adjacent			Open/marches	10YR 3/2
GR2B3	"				10YR 4/3
GR3B1	308 310	Pelo-stag	Clay	Arable	10YR 6/4
GR3B2	adjacent			Wooded/fenced	10YR 3/1
GR3B3	"				10YR 5/2
GR4B1	308 314	Pelo-stag	Clay	Pasture	10YR 4/2
GR4B2	adjacent			Open/fenced/	10YR 3/2
GR4B3	"			bushes	10YR 4/2
GR5B1	322 302	Rendzina	Great Oolite	Arable	10YR 4/2
GR5B2	adjacent			Open/fenced/	10YR 3/2
GR5B3	"			bushes	10YR 5/3
GR6B1	326 302	Rendzina	Great Oolite	Arable	10YR 4/3
GR6B2	adjacent			Open/fenced/	10YR 4/3
GR6B3	"			bushes	7.5YR 4/3
GR7B1	330 302	Rendzina	Great Oolite	Arable	10YR 3/2
GR7B2	adjacent			Open/fenced/	10YR 5/3
GR7B3	"			bushes	10YR 4/2
GR8B1	330 306	Rendzina	Great Oolite	Arable	10YR 4/3
GR8B2	adjacent			Wooded/fenced	10YR 5/3
GR8B3	"				10YR 5/6
GR9B1	330 310	Clay/Rend	Clay/CG	Arable/Pasture	10YR 4/4
GR9B2	adjacent			Open/marches	10YR 4/2
GR9B3	"				2.5YR 4/3
GR10B1	330 314	Pelo-stag	Clay	Pasture	10YR 4/2
GR10B2	adjacent			Open	10YR 3/2
GR10B3	"				10YR 6/3
GR11B1	330 318	Pelo-stag	Clay	Arable	10YR 6/4
GR11B2	adjacent			Open/bushes	10YR 5/2
GR11B3	"				10YR 5/3
GR12B1	330 322	Pelo-stag	Clay	Arable	10YR 4/2
GR12B2	adjacent			Open/bushes	10YR 4/3
1GR12B3	"				10YR 5/4

StA2B1	Podzol, Silly Isles Burned Topsoil
StA2B2	Podzol Silly Isles Burned Topsoil

(j) Synthetic Sample Database

1. MT Series (Chemically Precipitated-Maher pers. comm.)

Code	Mineral	Grain Size (μm)	Mass (g)
BM-S1 (MT14)	Magnetite	0.022	0.0105
BM-S2 (MT15)	Magnetite	0.023	0.0115
BM-S3 (MT18)	Magnetite	0.016	0.0112
BM-S4 (MT26)	Magnetite	0.036	0.0099
BM-S5 (MT31)	Magnetite	0.031	0.0118
BM-S6 (MT35)	Magnetite	0.04	0.0131
BM-S7 (MT36)	Magnetite	0.035	0.0122
BM-S8 (MT40)	Magnetite	0.05	0.013
BM-S9 (MT52)	Magnetite	0.012	0.0128
BM-S10 (MT55)	Magnetite	0.045	0.0127

2. Miscellaneous Samples

Code	Mineral	Grain Size (μm)	Mass (g)	Description
JD-S1	Geothite		Bulk	Dusky Red (10R 3/3) (aFe2o3)
JD-S2	Hematite	0.2	Bulk	Red (10R 4/6)
JD-S3	Hematite		Bulk	Red (10R 4/6) (E3044)
JD-S4	Hematite		Bulk	Red (10R 4/8 (E3044)
JD-S5	Magnetite		5% (Sand)	Dark Grey (2.5Y 4/0)
JD-S6	Magnetite		10% (Sand)	Dark Grey (2.5Y 4/0)
JD-S7	Magnetite		Bulk	Very Dark Grey (2.5Y 3/0)
JD-S8	Magnetite		Bulk	Very Dark Grey (2.5Y 3/0)
JD-S9	Maghemite		Bulk	Strong Brown (7.5YR 5/6) Beyer 8070 Oxide, Batch 72
JD-S10	Maghemite		Bulk	Black (2.5Y 2/0) B Maher, MT 31.
JD-S11	Magnetite	0.45	Bulk	Black (2.5Y 2/0) Bayferrox AC 5113M, Fe3o4
JD-S12	Hematite	0.7	Bulk	Red (10R 4/6) Beferrox 8010, Fe203
JD-S13	Geothite		1% (CaCo3)	Dusky Red (10R 3/3) (aFe2o3)
JD-S4	Hematite	0.2	1% (CaCo3)	Red (10R 4/6)
JD-S15	Hematite		1% (CaCo3)	Red (10R 4/6) (E3044)
JD-S16	Hematite		1% (CaCo3)	Red (10R 4/8 (E3044)
JD-S17	Magnetite		1% (CaCo3)	Dark Grey (2.5Y 4/0)
JD-18	Magnetite		1% (CaCo3)	Dark Grey (2.5Y 4/0)
JD-S19	Magnetite		1% (CaCo3)	Very Dark Grey (2.5Y 3/0)
JD-S20	Magnetite		1% (CaCo3)	Very Dark Grey (2.5Y 3/0)
JD-S21	Maghemite		1% (CaCo3)	Strong Brown (7.5YR 5/6) Beyer 8070 Oxide, Batch 72
JD-S22	Maghemite		0.5% (CaCo3)	Black (2.5Y 2/0) B Maher, MT 31.
JD-S23	Magnetite	0.45	1% (CaCo3)	Black (2.5Y 2/0) Bayferrox AC 5113M, Fe3o4
JD-S24	Hematite	0.7	1% (CaCo3)	Red (10R 4/6) Beferrox 8010, Fe203

3. Magnox Samples (Commercially Manufactured)

JD-S25	Hematite		Bulk	Alpha-311, Red Iron Oxide Fe2o3
JD-S26	Magnetite		Bulk	B-350, Black Iron Oxide
JD-S27	Magnetite		Bulk	B353, Black Iron Oxide
JD-S28	Magnetite		Bulk	TMB-100, Black Iron Oxide
JD-S29	Magnetite		Bulk	TMB-104, Black Iron Oxide
JD-S30	Maghemite		Bulk	HD-494, Dark Brown Cobalt Modified Gamma Iron Oxide
JD-S31	Maghemite		Bulk	HD-485, Dark Brown Gamma Iron Oxide
JD-S32	Maghemite		Bulk	HHO-311, Dark Brown Gamma Iron Oxide
JD-S33	Maghemite		Bulk	HHO-375, Dark Brown Gamma Iron Oxide
JD-S34	Maghemite		Bulk	HHO-385, Dark Brown Gamma Iron Oxide
JD-S35	Maghemite		Bulk	K-300, Dark Brown Gamma Iron Oxide
JD-S36	Maghemite		Bulk	HR-350, Dark Brown Gamma Iron Oxide
JD-S37	Geothite		Bulk	Yellow-350, Yellow Iron Oxide, FeooH
JD-S38	Geothite		Bulk	Yellow-375, Yellow Iron Oxide
JD-S39	Hematite		Bulk	Red Platelet Type U90 (Deanshangar) (Ray Gilson)
JD-S70	Hematite		Bulk	Alpha-485, Red Iron Oxide, Fe2o3

Samples JD-S40 to JD-S54 and JD-S70 are 20% mixtures in CaCo3 of the above Magnox samples. Samples JD-S55 to JD-S69 and JD-S72 are 1% mixtures of the above Magnox samples.

Part 2: Data from Yu (1989)

Sample	χlf	χhf	χfd	ARM	SIRM	ARM/ χ	SIRM/ χ	SIRM/ ARM	S-20mT
101-S1	21.35	20.19	5.41	37.77	1474.56	1.77	69.08	39.04	27.18
101-S2	24.65	23.12	6.20	58.15	1617.26	2.36	65.60	27.81	29.23
101-S3	28.67	26.76	6.65	57.67	1984.10	2.01	69.19	34.41	30.31
101-S4	37.47	34.48	7.97	68.93	2105.44	1.84	56.19	30.54	33.80
101-S5	34.77	32.00	7.97	59.17	1668.88	1.70	48.00	28.20	32.83
101-S6	26.64	24.93	6.41	54.65	1846.21	2.05	69.31	33.78	30.00
101-S7	22.46	21.33	5.05	38.75	1510.25	1.73	67.26	38.97	27.85
101-S8	20.45	19.32	5.51	35.13	1364.84	1.72	66.72	38.85	27.51
101-S9	19.95	18.88	5.37	35.22	1319.99	1.77	66.16	37.47	27.49
101-S10	33.37	31.39	5.93	62.36	2927.47	1.87	87.72	46.94	28.99
101-S11	46.77	42.77	8.55	83.50	2558.54	1.79	54.71	30.64	32.85
101-S12	40.33	37.62	6.72	91.18	2995.81	2.26	74.10	32.85	31.90
101-S13	19.87	18.32	7.81	29.29	1032.58	1.47	51.96	35.25	28.92
101-S14	20.92	19.67	5.97	37.69	1428.63	1.80	68.29	37.90	27.60
101-S15	24.00	22.33	6.95	46.67	1802.44	1.94	75.10	38.62	28.74
101-S16	29.56	27.26	7.77	43.62	1657.43	1.48	56.07	38.00	29.98
101-S17	14.32	13.54	5.42	21.26	1027.14	1.48	71.73	48.30	25.90
101-S18	16.53	15.52	6.08	22.06	1246.91	1.33	75.42	56.52	25.31
109-S0	12.50	11.37	9.01	26.05	1243.33	2.08	99.43	47.72	29.21
109-S1	19.54	18.59	4.87	29.07	1163.08	1.49	59.52	40.01	28.06
109-S2	24.48	23.22	5.16	41.49	1339.92	1.70	54.74	32.29	29.57
109-S3	24.61	23.32	5.26	52.03	1714.73	2.11	69.66	32.96	29.35
109-S4	23.73	22.43	5.46	47.15	1685.58	1.99	71.02	35.75	28.78
109-S5	25.36	23.58	7.03	43.62	1514.21	1.72	59.71	34.72	31.15
109-S6	28.42	26.24	7.68	60.08	2102.20	2.11	73.96	34.99	30.83
109-S7	24.60	22.63	8.01	49.89	1952.77	2.03	79.38	39.14	28.87
109-S8	23.36	21.61	7.48	47.08	1797.42	2.02	76.94	38.18	29.16
109-S9	19.74	18.29	7.36	41.95	1606.82	2.13	81.40	38.30	28.18
109-S10	20.67	18.97	8.24	41.41	1595.16	2.00	77.18	38.52	28.75
109-S11	21.71	19.73	9.14	33.52	1320.34	1.54	60.83	39.39	29.32
109-S12	22.43	20.75	7.51	31.18	1021.41	1.39	45.54	32.76	29.94
109-S13	32.29	29.69	8.06	65.43	2227.10	2.03	68.98	34.04	30.12
109-S14	35.60	32.55	8.57	66.98	2166.78	1.88	60.87	32.35	31.28
109-S15	20.92	19.67	5.98	27.20	1094.33	1.30	52.32	40.24	29.67
109-S16	18.17	17.17	5.51	39.67	1393.19	2.18	76.66	35.12	28.86
109-S17	18.74	17.55	6.37	41.17	1389.92	2.20	74.17	33.76	28.94
109-S18	20.78	19.54	5.95	30.87	1020.65	1.49	49.11	33.06	29.56
109-S19	18.14	16.98	6.37	38.55	1435.89	2.12	79.14	37.24	27.84
109-S20	21.89	20.28	7.35	33.83	923.95	1.55	42.20	27.31	29.68
109-S21	18.08	16.48	8.86	21.79	925.15	1.21	51.17	42.25	26.92
111-S1	28.15	26.04	7.50	41.52	1698.77	1.47	60.34	40.92	30.81
111-S2	20.02	18.94	5.38	35.27	2962.63	1.76	147.98	84.00	30.25
111-S3	13.48	12.89	4.40	22.65	2284.70	1.68	169.51	100.89	30.94
111-S4	25.25	24.09	4.58	29.46	3399.78	1.17	134.66	115.40	29.97
111-S5	15.26	14.67	3.87	24.55	2580.10	1.61	169.12	105.08	32.99
111-S6	25.60	23.62	7.75	46.01	1349.71	1.80	52.72	29.33	31.11
110-S1	2.64	2.53	4.35	6.90	191.01	2.61	72.33	27.68	27.01
110-S2	11.30	11.09	1.84	15.58	608.52	1.38	53.83	39.07	25.29
Nan-P1	16.58	16.45	0.79	0.75	32.12	0.05	1.94	42.87	20.40
Nan-P2	17.98	17.86	0.68	0.38	18.08	0.02	1.01	47.18	17.63
Nan-P3	17.59	17.46	0.72	0.40	22.93	0.02	1.30	57.74	13.55
Nan-P4	10.42	10.30	1.17	0.84	33.90	0.08	3.25	40.30	19.75
Nan-sub1	4.67	4.40	5.83	3.45	154.02	0.74	32.99	44.59	24.31
Nan-sub2	5.23	4.91	6.03	2.73	127.77	0.52	24.41	46.74	20.54
Nan-sub3	5.07	4.80	5.31	2.92	147.07	0.58	29.02	50.35	17.48
Nan-sub4	4.75	4.52	4.80	3.15	152.03	0.66	32.02	48.25	15.99
Tal-P1	1.48	1.37	7.43	0.98	83.37	0.66	56.31	85.07	16.25
Tal-P2	1.97	1.86	5.35	1.11	86.64	0.56	43.98	78.05	16.31
Tal-P3	1.50	1.42	5.26	1.07	80.07	0.71	53.38	74.83	16.82
Tal-P4	1.75	1.65	5.76	1.28	96.55	0.73	55.17	75.43	16.29
Tal-P5	1.39	1.30	6.45	1.38	96.34	0.99	69.31	69.81	16.95
Tal-sub1	6.33	5.76	8.97	5.54	927.11	0.88	146.44	167.21	12.59
Tal-sub2	7.93	7.17	9.64	7.75	737.93	0.98	93.09	95.18	15.92
NPar	15.95	15.54		2.54	154.13	9.66	39.08	62.93	87.38
NSub	6.47	6.38		1.46	174.91	27.02	18.71	34.34	60.03

Sample	χlf	χhf	χfd	ARM	SIRM	ARM/ χ	SIRM/ χ	SIRM/ ARM	S-20mT
TalPar	4.48	4.25		5.20	135.14	30.15	15.86	29.67	54.90
TalSub	12.02	11.34		5.69	1188.97	98.93	10.56	17.67	25.94
Surf1	21.18	19.92		5.95	1784.88	84.26	29.49	53.70	78.48
Surf2	37.65	35.17		6.60	2891.12	76.78	31.87	58.11	84.61
Mix	22.86	21.64		5.32	1347.88	58.96	27.41	55.88	86.65

Sample	S-40	S-100	S-300	IRM-20	IRM-40	IRM-100	IRM-300	HIRM-100	HIRM-300
101-S1	52.25	80.03	93.48	-400.79	-770.46	-1180.09	-1378.42	294.47	96.14
101-S2	55.51	81.31	93.81	-472.73	-897.74	-1314.99	-1517.15	302.27	100.11
101-S3	56.39	82.30	94.18	-601.38	-1118.83	-1632.91	-1868.63	351.19	115.47
101-S4	61.21	84.36	94.92	-711.64	-1288.74	-1776.15	-1998.48	329.29	106.96
101-S5	60.14	83.60	93.94	-547.89	-1003.66	-1395.18	-1567.75	273.70	101.13
101-S6	56.04	81.48	93.92	-553.86	-1034.62	-1504.29	-1733.96	341.92	112.25
101-S7	52.50	79.57	93.35	-420.60	-792.88	-1201.71	-1409.82	308.54	100.43
101-S8	52.18	78.85	92.92	-375.47	-712.17	-1076.18	-1268.21	288.66	96.63
101-S9	52.88	79.37	93.08	-362.87	-698.01	-1047.68	-1228.65	272.31	91.34
101-S10	55.20	83.59	95.88	-848.67	-1615.96	-2447.07	-2806.86	480.40	120.61
101-S11	60.54	84.82	95.64	-840.48	-1548.94	-2170.15	-2446.99	388.39	111.55
101-S12	59.17	84.33	95.37	-955.66	-1772.62	-2526.37	-2857.10	469.44	138.71
101-S13	53.88	79.58	93.70	-298.62	-556.35	-821.73	-967.53	210.85	65.05
101-S14	53.04	79.54	93.79	-394.30	-757.75	-1136.33	-1339.91	292.30	88.72
101-S15	54.78	81.32	94.42	-518.02	-987.38	-1465.74	-1701.86	336.70	100.58
101-S16	56.44	83.16	95.54	-496.90	-935.45	-1378.32	-1583.51	279.11	73.92
101-S17	52.21	77.91	92.68	-266.03	-536.27	-800.24	-951.95	226.90	75.19
101-S18	52.04	81.33	94.43	-315.59	-648.89	-1014.11	-1177.46	232.80	69.45
109-S0	52.27	75.59	93.47	-363.18	-649.89	-939.83	-1162.14	303.50	81.19
109-S1	52.51	78.25	92.92	-326.36	-610.73	-910.11	-1080.73	252.97	82.35
109-S2	55.28	80.34	93.63	-396.21	-740.71	-1076.49	-1254.57	263.43	85.35
109-S3	55.33	80.64	93.59	-503.27	-948.76	-1382.76	-1604.82	331.97	109.91
109-S4	53.82	79.44	93.30	-485.11	-907.18	-1339.02	-1572.65	346.56	112.93
109-S5	55.53	80.00	93.65	-471.68	-840.84	-1211.37	-1418.06	302.84	96.15
109-S6	55.25	80.23	93.28	-648.11	-1161.47	-1686.60	-1960.93	415.60	141.27
109-S7	55.09	78.95	93.69	-563.76	-1075.78	-1541.71	-1829.55	411.06	123.22
109-S8	54.29	78.72	93.66	-524.13	-975.82	-1414.93	-1683.46	382.49	113.96
109-S9	52.44	77.21	93.06	-452.80	-842.62	-1240.63	-1495.31	366.19	111.51
109-S10	53.19	77.68	93.20	-458.61	-848.47	-1239.12	-1486.69	356.04	108.47
109-S11	54.31	78.18	93.11	-387.12	-717.08	-1032.24	-1229.37	288.10	90.97
109-S12	55.62	80.90	93.86	-305.81	-568.11	-826.32	-958.70	195.09	62.71
109-S13	56.29	80.75	94.30	-670.80	-1253.63	-1798.38	-2100.16	428.72	126.94
109-S14	57.66	81.50	94.55	-677.77	-1249.37	-1765.93	-2048.69	400.85	118.09
109-S15	53.73	78.83	92.43	-324.69	-587.98	-862.66	-1011.49	231.67	82.84
109-S16	53.05	77.45	92.35	-402.07	-739.09	-1079.03	-1286.61	314.16	106.58
109-S17	54.39	79.09	93.42	-402.24	-755.98	-1099.29	-1298.46	290.63	91.46
109-S18	54.25	77.31	92.21	-301.70	-553.70	-789.06	-941.14	231.59	79.51
109-S19	52.66	77.25	92.64	-399.75	-756.14	-1109.23	-1330.21	326.66	105.68
109-S20	55.45	79.30	92.61	-274.23	-512.33	-732.69	-855.67	191.26	68.28
109-S21	51.96	77.67	92.36	-249.05	-480.71	-718.56	-854.47	206.59	70.68
111-S1	56.63	82.67	95.07	-523.39	-962.01	-1404.37	-1615.02	294.40	83.75
111-S2	58.96	87.54	96.77	-896.20	-1746.77	-2593.49	-2866.94	369.14	95.69
111-S3	60.35	89.22	97.48	-706.89	-1378.82	-2038.41	-2227.13	246.29	57.57
111-S4	62.07	93.24	100.00	-1018.91	-2110.24	-3169.95	-3399.78	229.83	0.00
111-S5	61.90	90.01	97.81	-851.17	-1597.08	-2322.35	-2523.60	257.75	56.50
111-S6	55.47	78.09	93.00	-419.89	-748.68	-1053.99	-1255.23	295.72	94.48
110-S1	44.87	75.80	91.35	-51.59	-85.71	-144.79	-174.49	46.22	16.52
110-S2	47.00	72.79	89.19	-153.89	-286.00	-442.94	-542.74	165.58	65.78
Nan-P1	40.21	68.04	89.03	-6.55	-12.92	-21.85	-28.60	10.27	3.52
Nan-P2	35.04	64.89	88.06	-3.19	-6.34	-11.73	-15.92	6.35	2.16
Nan-P3	28.67	62.10	88.31	-3.11	-6.57	-14.24	-20.25	8.69	2.68
Nan-P4	34.75	58.64	84.34	-6.70	-11.78	-19.88	-28.59	14.02	5.31
Nan-sub1	42.77	61.90	83.93	-37.44	-65.87	-95.34	-129.27	58.68	24.75
Nan-sub2	38.66	63.70	87.54	-26.24	-49.40	-81.39	-111.85	46.38	15.92
Nan-sub3	33.82	60.19	86.68	-25.71	-49.74	-88.52	-127.48	58.55	19.59
Nan-sub4	32.30	57.45	84.12	-24.31	-49.11	-87.34	-127.89	64.69	24.14
Tal-P1	30.29	52.25	79.00	-13.55	-25.25	-43.56	-65.86	39.81	17.51
Tal-P2	30.83	51.28	79.74	-14.13	-26.71	-44.43	-69.09	42.21	17.55
Tal-P3	31.39	52.72	80.15	-13.47	-25.13	-42.21	-64.18	37.86	15.89
Tal-P4	31.20	52.00	80.47	-15.73	-30.12	-50.21	-77.69	46.34	18.86

Sample	S-40	S-100	S-300	IRM-20	IRM-40	IRM-100	IRM-300	HIRM-100	HIRM-300
Tal-P5	29.57	51.72	80.08	-16.33	-28.49	-49.83	-77.15	46.51	19.19
Tal-sub1	17.37	24.70	47.09	-116.72	-161.04	-229.00	-436.58	698.11	490.53
Tal-sub2	23.67	31.70	52.19	-117.48	-174.67	-233.92	-385.13	504.01	352.80
NPar	96.98	27.35	96.18	134.68	149.48	42.16	148.24	111.98	5.89
NSub	86.13	14.49	85.71	105.00	150.65	25.34	149.92	149.57	25.00
TalPar	81.45	9.93	80.61	74.19	110.07	13.42	108.94	121.72	26.20
TalSub	47.36	6.30	46.69	308.42	563.10	74.91	555.13	1114.07	633.84
Surf1	93.37	17.87	92.58	1400.77	1666.54	318.96	1652.44	1465.92	132.44
Surf2	95.58	19.84	95.14	2446.18	2763.33	573.60	2750.61	2317.52	140.51
Mix	94.34	19.05	94.45	1167.94	1271.59	256.77	1273.07	1091.11	74.81

Part 3: Data from Grew (1991)

Sample	χlf	χfd	χfd (%)	SIRM	IRM -100	S	SIRM/ χlf	HIRM	HIRM/ χlf
TpSx	0.24	10.10	3.90	3.80	-2.36	0.62	14.60	0.71	0.11
SbSx	0.08	3.60	3.10	0.86	-0.13	0.15	9.80	0.51	0.17
Ptx	0.22	11.30	4.00	4.40	-3.04	0.69	16.20	0.68	0.10
Pt0-5x	0.26	11.20	4.10	3.90	-2.65	0.68	15.50	0.66	0.10
Pt5-10x	0.26	10.10	3.90	4.20	-2.94	0.70	13.30	0.62	0.07
Pt10-25x	0.32	13.70	4.10	5.00	-3.35	0.67	14.00	0.78	0.11
Pt45-50x	0.11	3.20	3.50	1.10	-0.21	0.19	9.40	0.53	0.16
Abx	0.28	10.60	4.10	4.50	-2.93	0.65	16.40	0.72	0.10
Ab0-5x	0.21	9.00	4.10	3.10	-1.86	0.60	15.00	0.55	0.13
Ab5-10x	0.25	9.20	4.10	3.10	-1.95	0.63	16.80	0.64	0.11
Ab10-25x	0.20	6.70	4.70	3.20	-1.76	0.55	15.00	0.65	0.14
Ab45-50x	0.08	3.20	4.50	0.75	-0.11	0.14	9.90	0.34	0.15
Wdx	0.25	5.20	3.10	3.60	-1.37	0.38	12.40	0.88	0.13
Wd0-5x	0.44	10.50	2.40	7.10	-3.91	0.55	16.20	1.65	0.13
Wd5-10x	0.21	4.70	3.00	3.00	-1.29	0.43	13.30	0.71	0.16
Wd10-25x	0.15	5.20	4.30	1.30	-0.31	0.24	8.70	0.40	0.10
Wd45-50x	0.14	2.60	2.60	1.00	0.22	-0.22	12.00	0.72	0.23
I9-A1:0-5	0.13	7.80	6.50	1.64	-0.95	0.58	12.62	0.34	0.04
G4-P2:0-5	0.14	5.50	3.90	1.40	-0.74	0.53	10.00	0.66	0.12
F5-W2:0-5	0.38	6.90	1.80	5.87	-3.70	0.63	15.45	1.09	0.16
J9-A1:0-5	0.21	9.30	4.30	2.69	-1.83	0.68	12.81	0.43	0.05
E4-A2:0-5	0.10	0.75	0.78	1.19	-0.21	0.18	11.90	0.49	0.65
J7-A1:0-5	0.37	7.90	2.10	4.89	-3.91	0.80	13.22	0.49	0.06
J10-A1:0-5	0.28	12.80	4.70	3.62	-2.28	0.63	12.93	0.67	0.05
G5-W2:0-5	0.51	15.50	3.00	8.00	-5.44	0.68	15.69	1.28	0.08
J8-A1:0-5	0.17	9.00	5.10	2.60	-1.74	0.67	15.29	0.43	0.05
I8-A1:0-5	0.21	9.40	4.20	3.31	-1.89	0.57	15.76	0.71	0.08
E5-A2:0-5	0.13	4.00	3.10	2.90	-1.48	0.51	22.31	0.71	0.18
F3-W2:0-5	0.36	9.10	2.50	6.09	-3.47	0.57	16.92	1.31	0.14
E2-P2:0-5	0.31	15.40	5.00	3.49	-2.06	0.59	11.26	0.72	0.05
Q5-P1:0-5	0.24	12.00	5.00	3.14	-2.36	0.75	13.08	0.39	0.03
M5-P2:0-5	0.30	14.40	4.90	3.12	-2.37	0.76	10.40	0.37	0.03
N5-P2:0-5	0.22	0.40	0.20	2.37	-1.87	0.79	10.77	0.25	0.63
N4A-P2:0-5	0.23	16.40	7.30	2.00	-1.54	0.77	8.70	0.23	0.01
O5-P2:0-5	0.13	5.40	4.10	1.49	-1.06	0.71	11.46	0.22	0.04
N4-P2:0-5	0.21	10.00	4.90	2.55	-1.43	0.56	12.14	0.56	0.06
M4-P2:0-5	0.27	15.60	5.90	2.77	-2.66	0.96	10.26	0.06	0.00
N4B-P2:0-5	0.17	2.00	1.20	2.72	-1.63	0.60	16.00	0.54	0.27
P5-P2:0-5	0.15	4.40	2.90	1.98	-1.52	0.77	13.20	0.23	0.05
R2-P2:0-5	0.36	26.20	7.30	5.04	-3.53	0.70	14.00	0.76	0.03
R4-P2:0-5	0.23	9.80	4.30	3.76	-2.41	0.64	16.35	0.68	0.07
S4-P2:0-5	0.14	15.40	4.30	6.17	-4.01	0.65	44.07	1.08	0.07
S2-P2:0-5	0.26	6.80	2.60	5.03	-3.37	0.67	19.35	0.83	0.12
P6-A1:0-5	0.33	19.90	6.10	5.37	-3.97	0.74	16.27	0.70	0.04
R3-P2:0-5	0.42	16.10	3.90	7.35	-4.63	0.63	17.50	1.36	0.08
T3-P2:0-5	0.40	12.80	3.20	9.34	-5.60	0.60	23.35	2.00	0.16
S3-P2:0-5	0.40	18.50	4.60	6.18	-4.45	0.72	15.45	0.87	0.05
O4-P2:0-5	0.16	5.40	3.20	2.30	-1.22	0.53	14.38	0.54	0.10
O3-P2:0-5	0.40	11.60	2.80	6.00	-4.20	0.70	15.00	0.90	0.08
I7-Fm1:0-5	0.40	5.90	1.40	7.50	-4.65	0.62	18.75	1.43	0.24
F4-W2:0-5	0.51	0.16	0.30	8.40	-2.60	0.31	16.47	2.90	18.13

Sample	χlf	χfd	χfd (%)	SIRM	IRM -100	S	SIRM/ χlf	HIRM	HIRM/ χlf
I9-A1:45-50	0.09	1.30	1.40	0.78	0.27	-0.34	8.67	0.52	0.40
G4-P2:45-50	0.09	3.70	4.10	0.63	0.23	-0.36	7.00	0.43	0.12
F5-W2:45-50	0.13	3.20	2.30	1.55	0.11	-0.07	11.92	1.05	0.33
J9-A1:45-50	0.05	2.00	4.10	0.54	0.08	-0.15	10.80	0.23	0.12
E4-A2:45-50	0.07	2.70	4.00	0.72	0.36	-0.50	10.29	0.18	0.07
J7-A1:45-50	0.10	1.30	1.30	1.23	-0.82	0.67	12.30	0.20	0.15
J10-A1:45-50	0.11	6.80	6.50	0.84	-0.51	0.61	7.64	0.16	0.02
G5-W2:45-50	0.06	0.40	0.60	0.64	0.09	-0.14	10.67	0.36	0.91
J8-A1:45-50	0.12	3.40	2.70	0.88	-0.25	0.28	7.33	0.34	0.10
I8-A1:45-50	0.09	2.40	2.50	0.71	0.23	-0.32	7.89	0.48	0.20
E5-A2:45-50	0.04	5.40	12.90	0.58	-0.06	0.11	14.50	0.52	0.10
F3-W2:45-50	0.07	2.70	3.60	0.73	0.15	-0.20	10.43	0.44	0.16
E2-P2:45-50	0.07	4.40	6.10	1.02	0.13	-0.13	14.57	0.44	0.10
Q5-P1:45-50	0.08	3.80	4.80	0.72	-0.24	0.34	9.00	0.24	0.06
M5-P2:45-50	0.11	5.50	4.90	0.77	-0.33	0.43	7.00	0.22	0.04
N5-P2:45-50	0.09	2.60	2.60	0.60	-0.14	0.23	6.67	0.23	0.09
N4A-P2:45-50	0.08	3.00	3.80	0.82	-0.35	0.43	10.25	0.23	0.08
O5-P2:45-50	0.12	2.00	1.80	0.93	-0.69	0.74	7.75	0.12	0.06
N4-P2:45-50	0.14	2.60	1.90	1.18	0.31	-0.26	8.43	0.74	0.28
M4-P2:45-50	0.10	1.90	2.10	0.67	-0.20	0.30	6.70	0.23	0.12
N4B-P2:45-50	0.10	2.40	2.40	1.16	-0.50	0.43	11.60	0.66	0.28
P5-P2:45-50	0.08	1.80	2.10	0.93	0.27	-0.29	11.63	0.33	0.18
R2-P2:45-50	0.14	2.00	1.50	0.83	-0.58	0.70	5.93	0.12	0.06
R4-P2:45-50	0.05	1.40	0.70	0.62	-0.06	0.10	12.40	0.56	0.40
S4-P2:45-50	0.13	2.60	3.60	0.78	-0.08	0.10	6.00	0.20	0.08
S2-P2:45-50	0.08	2.70	3.50	0.66	0.53	-0.81	8.25	1.19	0.44
P6-A1:45-50	0.06	3.30	5.50	0.51	-0.10	0.19	8.50	0.40	0.12
R3P2:45-50	0.26	9.70	3.80	4.41	-2.91	0.66	16.96	0.75	0.08
T3-P2:45-50	0.05	0.40	0.90	6.10	-0.67	0.11	122.00	2.70	6.75
S3-P2:45-50	0.05	7.90	16.40	0.38	-0.19	0.50	7.60	0.10	0.01
O4-P2:45-50	0.09	2.10	2.20	0.58	0.07	-0.12	6.44	0.65	0.31
O3-P2:45-50	0.20	1.90	0.90	2.80	-1.76	0.63	14.00	0.52	0.27
I7-Fm1:45-50	0.09	3.30	3.50	0.61	0.19	-0.31	6.78	0.80	0.24
F4-W2:45-50	0.08	3.00	3.00	0.86	0.69	-0.80	10.75	0.46	0.15
StrBedx 0.10	3.60	2.30	2.30	-1.20	0.52	23.50	0.53	0.27	
SusS184-5x				10.00	-6.90	0.69		1.55	
SusS185-6x				22.60	-14.01	0.62		4.29	
SusS186-7x				13.60	-7.75	0.57		2.92	
SusS184-7x				14.20	-8.95	0.63		2.63	
SusS284-5x				5.90	-3.01	0.51		1.45	
SusS285-6x				9.20	-4.51	0.49		2.35	
SusS286-7x				5.70	-2.34	0.41		1.68	
SusS284-7x				6.90	-3.04	0.44		1.93	
Ap86-7 0.00			0.18	-0.00			0.09		
ApEA285-6	0.00			1.49	-0.00			0.75	
Ap1853-1983	9.00				-0.00			0.00	
Top<2.75μm	0.31			3.75	-2.06	0.55	11.90	0.75	
Top2.75-8μm	0.38			6.98	-4.82	0.69	18.00	1.08	
Top8-23μm	0.29			6.28	-4.14	0.66	20.00	1.06	
Top23-63μm	0.11			3.25	-1.95	0.60	24.00	0.64	
Sub<2.75μm	0.17			1.72	0.45	-0.26	10.50	0.91	
Sub2.75-8μm	0.20			2.84	-1.79	0.63	14.50	0.48	
Sub8-23μm	0.15			2.56	-1.64	0.64	16.50	0.43	
Sub23-63μm	0.08			1.44	-0.72	0.50	18.90	0.35	
Top1:<2.75μm	0.41			5.44	-3.59	0.66	13.20	0.93	
Top1:2.75-8μm	0.52			10.00	-7.20	0.72	19.30	1.43	
Top1:8-23μm	0.40			9.51	-6.28	0.66	21.40	1.61	
Top1:23-63μm	0.16			4.81	-2.79	0.58	26.80	0.97	
Top1:63-125μm	0.31			6.42	-4.11	0.64	19.50	1.17	
Top1:>125μm	0.33			8.85	-5.58	0.63	25.30	1.62	
Top2:<2.75μm	0.32			3.88	-2.60	0.67	12.00	0.64	
Top2:2.75-8μm	0.38			7.07	-4.81	0.68	18.70	1.14	
Top2:8-23μm	0.30			6.01	-4.03	0.67	20.50	0.97	
Top2:23-63μm	0.11			3.09	-1.88	0.61	23.80	0.60	
Top2:63-125μm	0.20			3.75	-2.21	0.59	17.90	0.77	
Top2:>125μm	0.14			3.01	-1.78	0.59	18.80	0.62	
Top3:<2.75μm	0.19			2.00	-0.66	0.33	10.40	0.67	

Sample	χlf	χfd	χfd (%)	SIRM	IRM -100	S	SIRM/ χlf	HIRM	HIRM/ χlf
Top3:2.75-8μm	0.24			3.87	-2.55	0.66	15.90	0.66	
Top3:8-23μm	0.18			3.33	-2.16	0.65	18.20	0.59	
Top3:23-63μm	0.07			1.84	-1.12	0.61	21.40	0.35	
Top3:63-125μm	0.10			1.94	-1.07	0.55	16.20	0.44	
Top3:>125μm	0.10			1.55	-0.87	0.56	14.10	0.34	
Sub1:<2.75μm	0.19			1.83	0.53	-0.29	9.70	0.65	
Sub1:2.75-8μm	0.25			3.98	-2.95	0.74	17.10	0.50	
Sub1:8-23μm	0.21			3.64	-2.69	0.74	17.00	0.46	
Sub1:23-63μm	0.08			1.74	-1.06	0.61	21.30	0.34	
Sub1:63-125μm	0.13			2.52	-1.61	0.64	19.40	0.46	
Sub1:>125μm	0.10			2.00	-1.32	0.66	20.00	0.34	
Sub2:<2.75μm	0.15			1.53	0.46	-0.30	10.30	0.99	
Sub2:2.75-8μm	0.20			2.40	-1.46	0.61	12.10	0.46	
Sub2:8-23μm	0.12			1.70	-0.92	0.54	14.50	0.38	
Sub2:23-63μm	0.05			0.87	-0.31	0.36	17.50	0.28	
Sub2:63-125μm	0.07			0.94	-0.23	0.24	13.40	0.35	
Sub2:>125μm	0.05			0.58	-0.01	0.01	11.60	0.29	
Sub3:<2.75μm	0.16			1.81	0.40	-0.22	11.50	1.10	
Sub3:2.75-8μm	0.15			2.15	-1.18	0.55	14.30	0.48	
Sub3:8-23μm	0.13			2.34	-1.47	0.63	12.00	0.46	
Sub3:23-63μm	0.09			1.71	-0.86	0.50	18.90	0.42	
Sub3:63-125μm	0.10			1.43	-0.69	0.48	15.90	0.37	
EA2:0-2 0.13	0.90	0.80	1.86	-1.32	0.71	14.08	0.27	0.30	
EA2:2-4 0.21	1.10	0.50	3.60	-2.59	0.72	17.54	0.50	0.46	
EA2:4-6 0.20	8.70	4.50	3.44	-2.48	0.72	17.66	0.48	0.06	
EA2:6-8 0.25	6.60	2.70	4.23	-3.17	0.75	17.27	0.53	0.08	
EA2:8-10	0.27	4.70	1.80	4.57	-3.48	0.76	17.25	0.54	0.12
EA2:10-12	0.25	1.90	0.70	4.40	-3.29	0.75	17.69	0.56	0.29
EA2:12-14	0.35	7.80	2.20	5.91	-4.57	0.77	16.89	0.67	0.09
EA2:14-16	0.32	2.10	0.60	5.52	-4.28	0.78	17.24	0.62	0.29
EA2:16-18	0.39	8.80	2.30	7.09	-5.59	0.79	18.18	0.75	0.09
EA2:18-20	0.36	9.60	2.60	6.27	-5.02	0.80	17.23	0.63	0.07
EA2:20-22	0.33	3.50	1.10	6.12	-4.77	0.78	18.60	0.68	0.19
EA2:22-24	0.38	16.30	4.30	7.13	-5.57	0.78	18.96	0.78	0.05
EA2:24-26	0.39	5.80	1.50	7.69	-5.91	0.77	19.51	0.89	0.15
EA2:26-28	0.38	10.70	2.80	7.44	-5.90	0.79	19.73	0.77	0.07
EA2:28-30	0.37	7.40	2.00	7.30	-5.98	0.82	19.73	0.66	0.09
EA2:30-32	0.38	9.00	2.40	7.66	-6.03	0.79	20.33	0.82	0.09
EA2:32-34	0.37	15.60	4.30	7.06	-5.62	0.79	19.25	0.74	0.05
EA2:34-36	0.42	11.30	2.70	9.97	-8.33	0.84	23.50	0.82	0.07
EA2:36-38	0.37	7.10	1.90	7.57	-6.06	0.80	20.30	0.76	0.11
EA2:38-40	0.42	7.30	1.70	8.66	-6.86	0.79	20.62	0.90	0.12
EA2:40-42	0.39	9.60	2.40	8.03	-7.90	0.98	20.49	0.07	0.01
EA2:42-44	0.31	5.60	1.80	6.41	-5.07	0.79	20.82	0.67	0.12
EA2:44-46	0.38	14.70	3.90	8.14	-6.33	0.78	21.32	0.91	0.06
EA2:46-48	0.32	9.90	3.10	6.98	-5.28	0.76	22.10	0.85	0.09
EA2:48-50	0.31	7.20	2.30	6.59	-4.86	0.74	21.38	0.86	0.12
EA2:50-52	0.36	12.40	3.50	7.21	-5.44	0.75	20.31	0.89	0.07
EA2:52-54	0.39	13.70	3.50	8.29	-6.26	0.76	21.26	1.01	0.07
EA2:54-56	0.37	22.20	6.10	7.13	-5.46	0.77	19.53	0.84	0.04
EA2:56-58	0.32	12.70	4.00	10.12	-6.36	0.63	31.83	1.88	0.15
EA2:58-60	0.35	16.40	4.70	7.21	-3.47	0.48	20.43	1.87	0.11
EA2:60-62	0.31	12.80	4.10	5.16	-2.94	0.57	16.54	1.11	0.09
EA2:62-64	0.25	18.00	7.10	3.81	-2.18	0.57	15.00	0.82	0.05
EA2:64-66	0.24	12.30	5.10	3.32	-1.87	0.56	13.79	0.73	0.06
EA2:66-68	0.28	16.40	5.80	4.32	-2.39	0.55	15.19	0.96	0.06
EA2:68-70	0.23	2.30	1.00	3.48	-1.10	0.32	15.39	1.19	0.52
EA2:70-72	0.22	8.30	3.90	3.21	-1.55	0.48	14.94	0.83	0.10
EA2:72-74	0.21	13.40	6.30	3.08	-1.36	0.44	14.58	0.86	0.06
EA2:74-76	0.22	11.10	5.10	3.14	-1.33	0.42	14.27	0.91	0.08
EA2:76-78	0.19	9.70	5.20	2.90	-1.32	0.45	15.60	0.79	0.08
EA2:78-80	0.17	3.40	2.10	2.60	-1.17	0.45	15.64	0.71	0.21
EA2:80-82	0.18	10.70	5.80	2.69	-1.13	0.42	14.63	0.78	0.07
EA2:82-84	0.19	12.40	6.40	2.67	-0.99	0.37	13.81	0.84	0.07
EA2:84-86	0.19	6.00	3.10	2.68	-0.93	0.35	14.01	0.87	0.15
EA2:86-88	0.18	1.00	0.50	2.49	-0.75	0.30	13.62	0.87	0.87
EA2:88-90	0.17	6.40	3.90	2.35	-0.52	0.22	14.05	0.91	0.14

Sample	χlf	χfd	χfd (%)	SIRM	IRM -100	S	SIRM/ χlf	HIRM	HIRM/ χlf
EA2:90-92	0.17	8.00	4.60	2.33	-0.43	0.19	13.44	0.95	0.12
EA2:92-94	0.18	11.00	6.30	2.34	-0.42	0.18	13.39	0.96	0.09
EA2:94-96	0.17	8.70	5.20	2.21	-0.44	0.20	13.13	0.88	0.10
EA2:96-98	0.15	5.90	3.90	1.90	-0.26	0.14	12.58	0.82	0.14
EA2:98-100	0.39	13.60	3.50	7.75	-5.98	0.77	19.71	0.89	0.07
EA2:50-52b	0.34	2.70	0.80	6.35	-5.27	0.83	18.67	0.54	0.20
EA2:52-54b	0.36	0.00	0.00	7.37	-5.86	0.80	20.40	0.76	ERR
EA2:54-56b	0.40	2.50	0.60	8.79	-7.02	0.80	21.75	0.89	0.35
EA2:56-58b	0.30	7.80	2.60	6.15	-4.77	0.78	20.70	0.69	0.09
EA2:58-60b	0.33	7.40	2.20	6.89	-5.28	0.77	20.63	0.80	0.11
EA2:60-62b	0.35	10.00	2.90	7.10	-5.43	0.76	20.47	0.84	0.08
EA2:62-64b	0.34	14.10	4.10	6.78	-5.15	0.76	19.72	0.82	0.06
EA2:64-66b	0.33	5.90	1.80	6.95	-4.75	0.68	20.98	1.10	0.19
EA2:66-68b	0.30	0.00	0.00	7.32	-4.44	0.61	24.31	1.44	ERR
EA2:68-70b	0.41	8.80	2.20	10.07	-6.37	0.63	24.80	1.85	0.21
EA2:70-72b	0.30	15.30	5.10	4.92	-2.45	0.50	16.46	1.23	0.08
EA2:72-74b	0.31	17.40	5.70	4.74	-2.56	0.54	15.48	1.09	0.06
EA2:74-76b	0.29	19.80	6.70	4.57	-2.47	0.54	15.59	1.05	0.05
EA2:76-78b	0.30	16.70	5.60	4.34	-2.39	0.55	14.51	0.97	0.06
EA2:78-80b	0.29	14.30	5.00	4.50	-2.60	0.58	15.62	0.95	0.07
EA2:80-82b	0.27	13.40	5.00	4.19	-2.27	0.54	15.44	0.96	0.07
EA2:82-84b	0.25	3.00	1.20	3.88	-1.96	0.50	15.59	0.96	0.32
EA2:84-86b	0.25	21.80	8.80	3.70	-1.74	0.47	14.92	0.98	0.05
EA2:86-88b	0.23	7.60	3.30	3.21	-1.53	0.47	14.03	0.84	0.11
EA2:88-90b	0.23	19.80	8.80	3.21	-1.30	0.41	14.21	0.96	0.05
EA2:90-92b	0.22	8.70	4.00	3.26	-1.56	0.48	14.97	0.85	0.10
EA2:92-94b	0.22	6.90	3.10	3.28	-1.61	0.49	14.82	0.84	0.12
EA2:94-96b	0.21	9.20	4.50	2.89	-1.25	0.43	13.98	0.82	0.09
EA2:96-98b	0.19	22.40	11.60	2.71	-1.03	0.38	14.13	0.84	0.04
EA2:98-100b	0.18	4.30	2.40	2.43	-0.75	0.31	13.44	0.84	0.20
EA2:100-102	0.18	7.80	4.40	2.41	-0.60	0.25	13.72	0.91	0.12
EA2:102-104	0.18	11.80	6.70	2.30	-0.52	0.23	13.14	0.89	0.08
EA2:104-106	0.17	15.20	8.70	2.18	-0.45	0.21	12.52	0.87	0.06
EA2:106-108	0.17	5.20	3.10	0.24	-0.28	1.19	1.41	0.98	0.19
EA2:108-110	0.17	29.80	17.80	2.14	-0.45	0.21	12.81	0.85	0.03
EA2:110-112	0.16	22.00	14.20	2.04	-0.36	0.18	13.14	0.84	0.04
EA2:112-114	0.16	13.20	8.40	1.90	-0.36	0.19	12.11	0.77	0.06
EA2:114-116	0.16	7.80	5.00	1.85	-0.41	0.22	11.80	0.72	0.09
EA2:116-118	0.15	12.60	8.20	1.76	-0.49	0.28	11.40	0.63	0.05
EA2:118-120	0.15	9.70	6.30	1.89	-0.49	0.26	12.35	0.70	0.07
EA2:120-122	0.17	7.60	4.50	2.14	-0.69	0.32	12.66	0.73	0.10
EA2:122-124	0.18	7.80	4.40	2.25	-0.89	0.40	12.68	0.68	0.09
EA2:124-126	0.18	9.60	5.40	2.21	-0.87	0.39	12.57	0.67	0.07
EA2:126-128	0.17	6.00	3.60	2.10	-0.73	0.35	12.63	0.68	0.11
EA2:128-130	0.16	0.90	0.50	2.07	-0.71	0.34	12.80	0.68	0.76
EA2:130-132	0.15	3.30	2.10	1.91	-0.66	0.34	12.40	0.63	0.19
EA2:132-134	0.14	0.70	0.50	1.78	-0.61	0.34	12.43	0.58	0.83
EA2:134-136	0.13	0.80	0.60	1.88	-0.62	0.33	14.34	0.63	0.78
EA2:136-138	0.13	4.00	3.10	1.85	-0.57	0.31	14.43	0.64	0.16
EA2:138-140	0.12	2.10	1.70	1.79	-0.46	0.25	14.94	0.67	0.32
EA2:140-142	0.12	6.60	5.60	1.53	-0.36	0.24	12.99	0.59	0.09
EA2:142-144	0.09	4.40	5.00	0.97	0.00	0.00	10.88	0.49	0.11
EA2:144-146	0.09	2.40	2.60	1.07	0.01	-0.01	11.33	0.54	0.22
EA2:146-148	0.09	5.50	6.10	0.98	-0.01	0.01	10.88	0.48	0.09
EA2:148-150	0.07	13.60	18.50	0.83	0.00	0.00	11.23	0.41	0.03

APPENDIX 3

Magnetic Instrumentation: Its calibration and accuracy

The instrumentation used for each magnetic measurement made in this research (listed in Appendix 1b) has been tested for linearity in measurement and accuracy here. Thompson and Oldfield (1986) give fuller descriptions of the equipment used. The purpose of this section is to research the drift and linear accuracy of the equipment based at Coventry University. It must be noted that sensitive equipment should generally be positioned in temperature controlled rooms to eliminate drift variation by changes in ambient temperature. Circuitry such as AC and DC bridges and Darlington transistor pairs are highly sensitive to temperature changes although effects will lag behind the temperature change when in sealed units. Such conditions are not present in the Coventry laboratory.

3.1 Susceptibility Meter (MS2B)

Susceptibility is defined as the proportionality constant between magnetization (A/m) and the applied magnetic field (A/m, Robertson, 1990). It is expressed here in units of $\mu m^3 kg^{-1}$. The Bartington MS2 (Plate A3.1) meter has a response dependent on both the amount of material present and its susceptibility. This response has the dimensions of volume (m^3).

Drift was measured on the magnetic Susceptibility Meter (Bartington-MS2B) and the Molspin. Figures A3.1a and b exhibit drift in 'air' measurement on the susceptibility meter over a period of 80 minutes. This experiment led to the meter being left to warm up for at least 45 minutes before measurements were made. The high frequency measurement drifted about 10 units and low frequency drifted about 15 units. Drift in the new sensor is more linear than that of the older sensor leading to increased accuracy between before and after air measurements.

3.2 AC Field Magnetometer

The measurement of anhysteretic remanent magnetization (ARM) involves the application of a weak magnetic field superimposed on a stronger alternating field and then measured in the Molspin Fluxgate 'Minispin' magnetometer. The value of ARM (in units of mAm^2kg^{-1}) depends on several factors (Robertson, 1989):

1. The maximum intensity of the alternating field (maximum 100mT)
2. The rate at which the alternating field diminishes (4-32μT per cycle)
3. The size of the biassing field (controlled with current up to 100μT, generally 40μT)
4. The blocking field spectrum (coercivity spectrum) of the sample

An experiment was conducted on this piece of equipment (Plate A3.2) to test the linearity between current and ARM. Two samples were repeatedly given an ARM at increasingly greater currents (biassing fields).

Plate A3.1. Bartington MS2 Susceptibility meters

Plate A3.2. Molspin Instruments AC Field Magnetometer

Plate A3.3. Molspin Instruments Fluxgate 'Minispin' Magnetometer and free standing Vibrating Sample Magnetometer

Figure A3.1: Susceptibility meter intensity decay of air measurement on low frequency (Klf); old sensor (a) and new sensor (b)

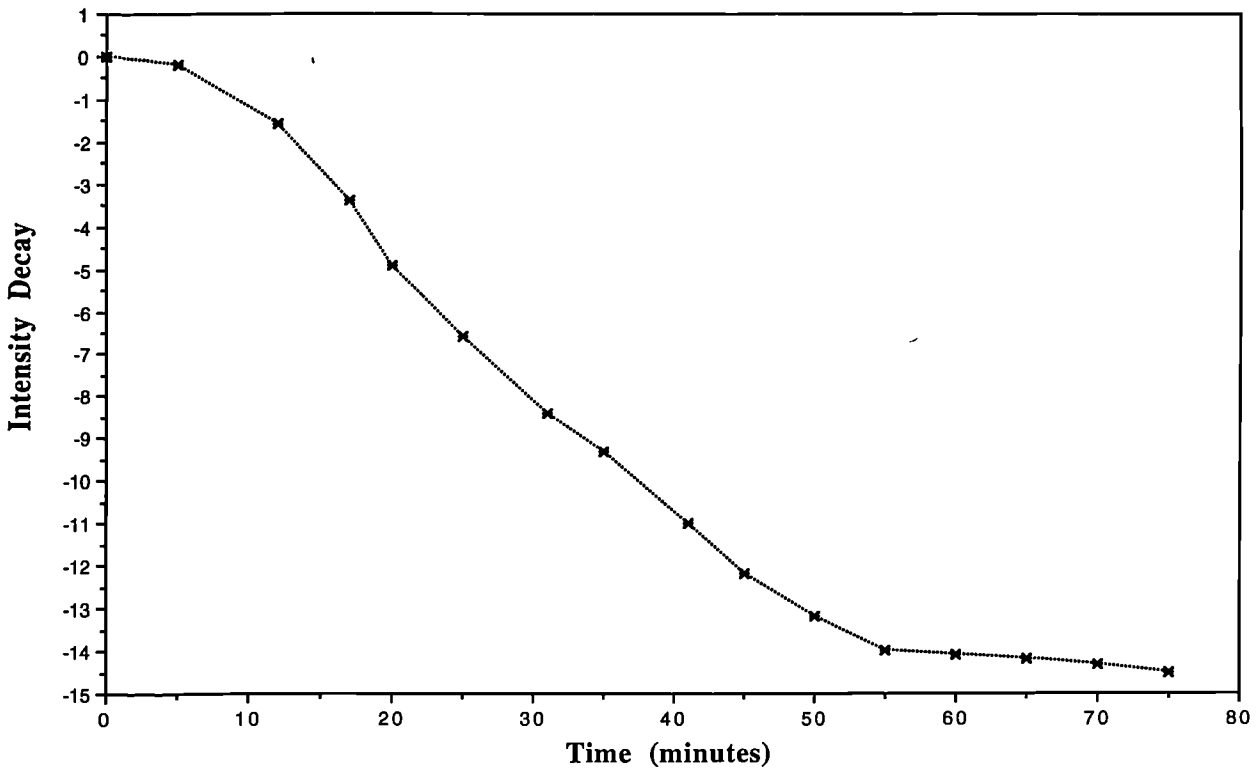

(b)

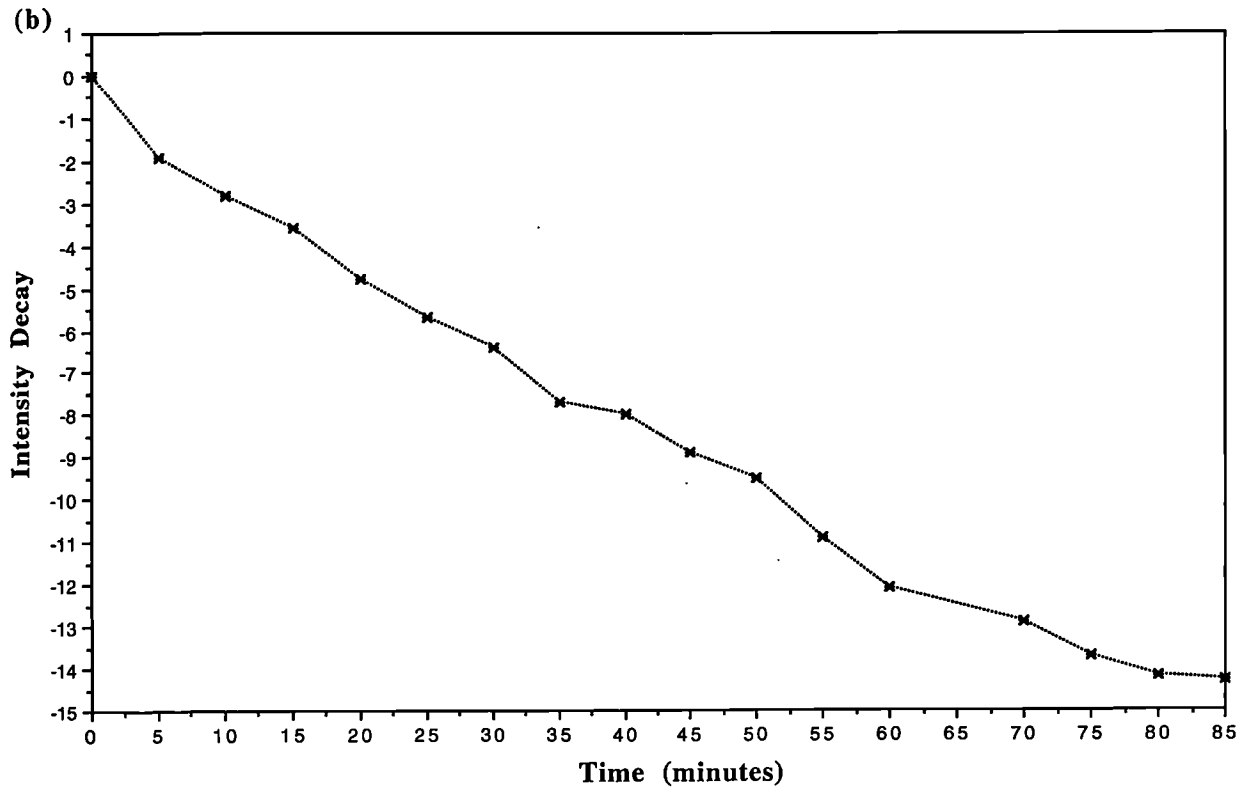

Sample 1: NYM1B1 - North Yorkshire Moors Topsoil Sample

Sample 2: DM3X1 - Chimney Soot collected from a domestic coal fire chimney.

The relationship between current (controlling biassing field) and ARM and also χarm is shown in Figure A3.2. The results are good and fairly linear within an allowed experimental error for the soil sample but a curve is seen in the coal sample after 4.0 amps (set at 3.5 amps for 40μT). There is no clear effect (from interaction for example) in these samples between the fields of 0 and 100μT and ARM measurements are routinely made using 40μT rather than any other or varying field.

3.3 Molspin

A similar experiment was conducted on the two Molspin magnetometers in the laboratory. The new Molspin (Plate A3.3) drifted 6 units (0.65 % error) while the older Molspin drifted 20 units (2.2% error) in 80 minutes. Figures A3.3a and b show the results of these tests. The new Molspin has a much more linear drift than that of the older Molspin. This led to the newer Molspin being used regularly except in periods of mechanical breakdown.

3.4 Calibration of VSM Coventry with Bangor VSM

Cross calibration of the Coventry Vibrating Sample magnetometer (Plate A3.3) (VSM) was required. A VSM at University of Wales, Bangor was used to measure samples which had been already processed in Coventry. Problems have occurred with the Coventry VSM in that while most measurements are very reliable, zero field remanence is not. In many cases at a zero field, a field of approximately 5mT exists which can be up to 7% of the total saturation remanence of a magnetite sample.

Normalized hysteresis loops for two of the MT Series magnetites are shown in Figures A3.4a and b, loops generated at Bangor for the same samples are shown in Figure A3.5a and b. It is clear that the hysteresis loops compare quite well, although Coventry loops are plotted with only 98 points, whereas Bangor curves have 1026 points. Generally the accuracy and sensitivity in measuring environmental samples was better at Coventry. An improved program was requested from the supplier to bring zero field measurements closer to zero. Much better results were then gained to within 0.1mT of zero.

The units of remanence convert from 100mT = 1000 Oe

emu/g = mA m^2 kg^{-1} devided by 10^{-3}

Figure A3.2: Current (biassing field) versus ARM and Xarm

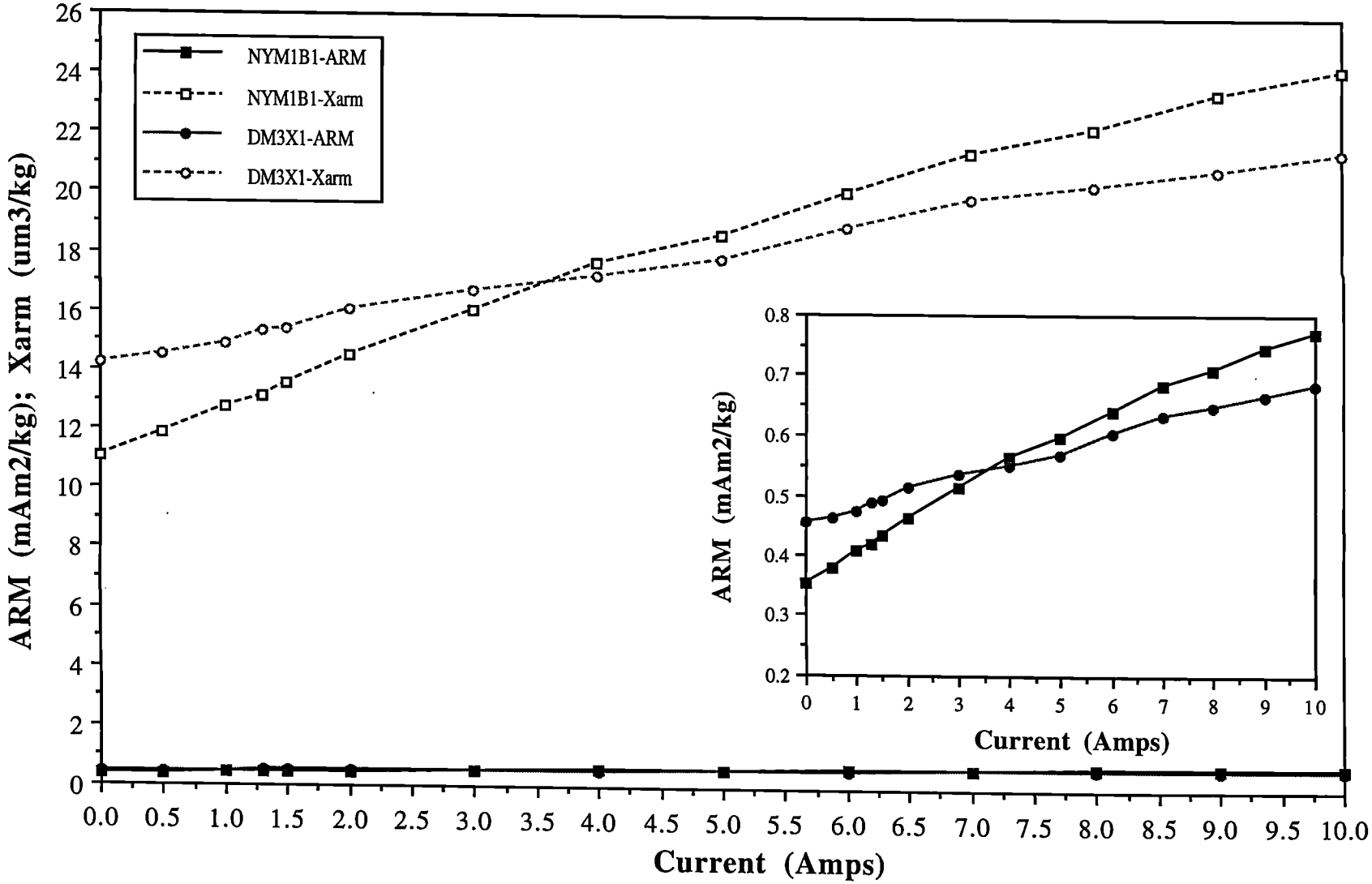

Figure A3.3: Molspin intensity decay curve for calibration sample (Calibration: 928 at 0 minutes); new Molspin (a) and old molspin (b)

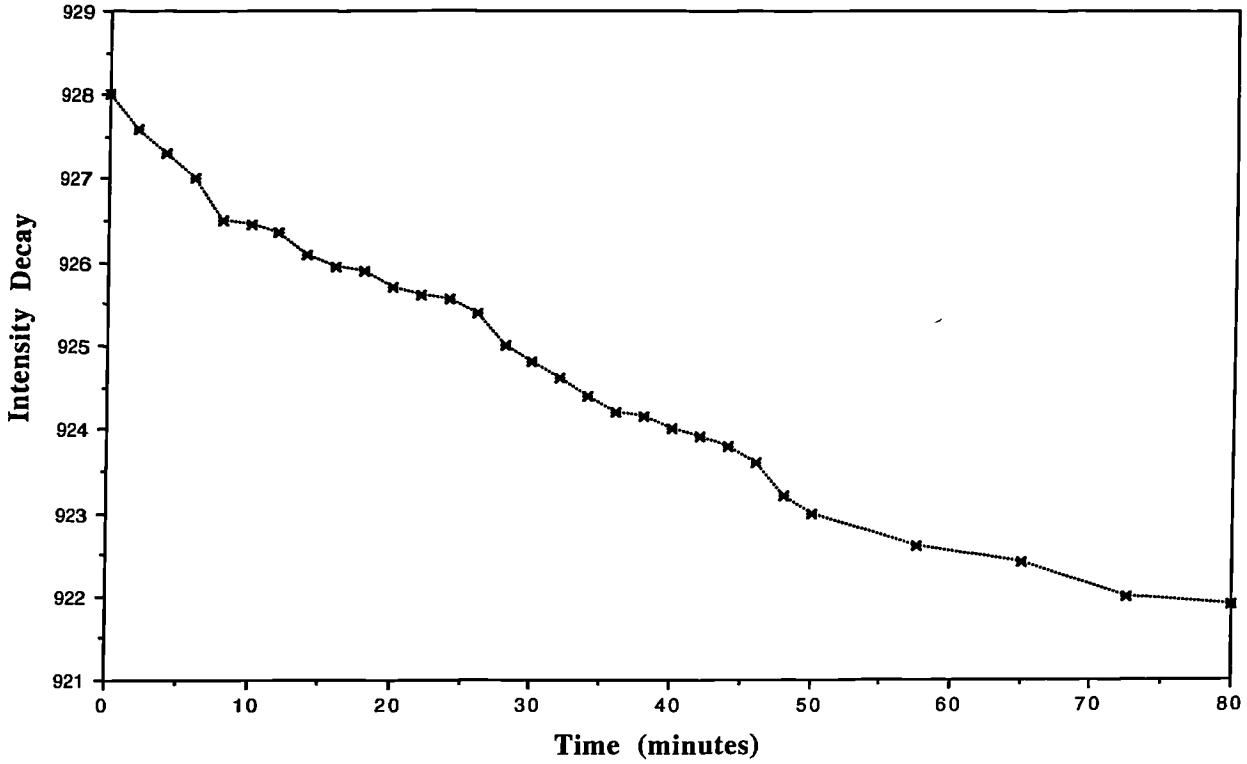

(b)

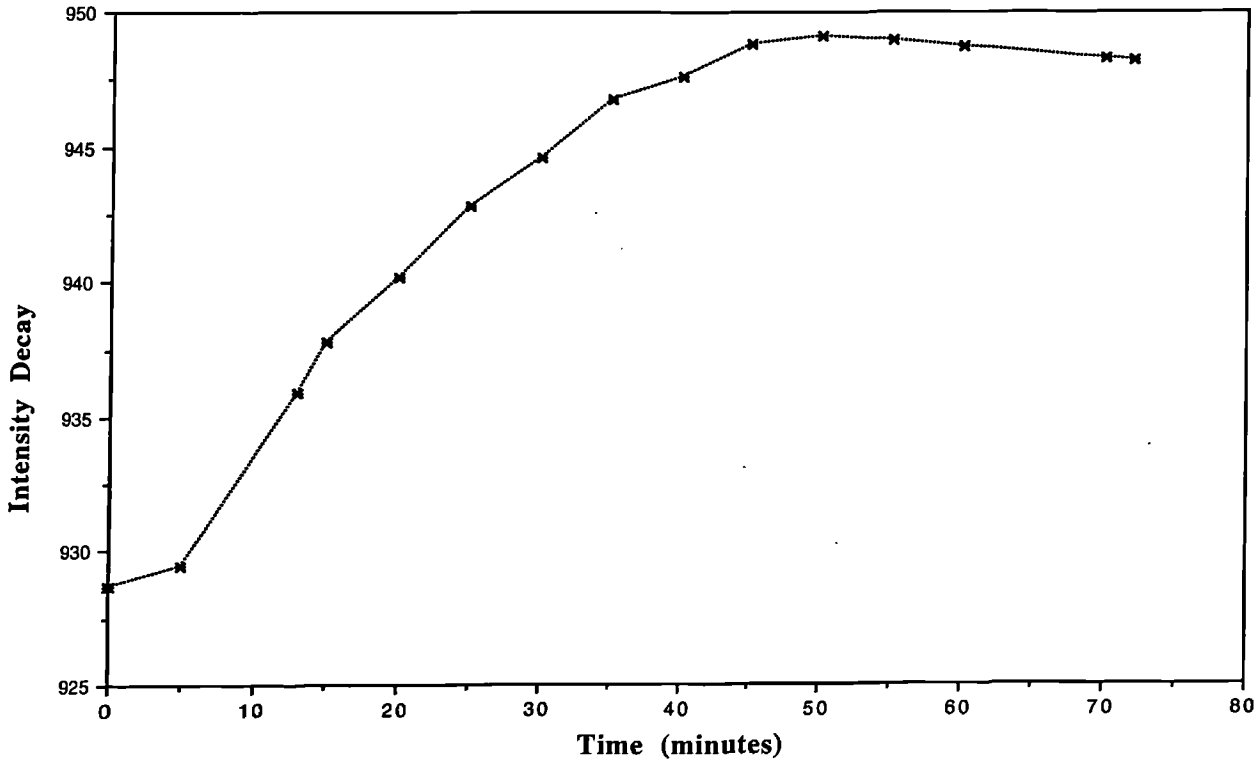

Figure A3.4: Coventry Hysteresis Loops

(a) MT55

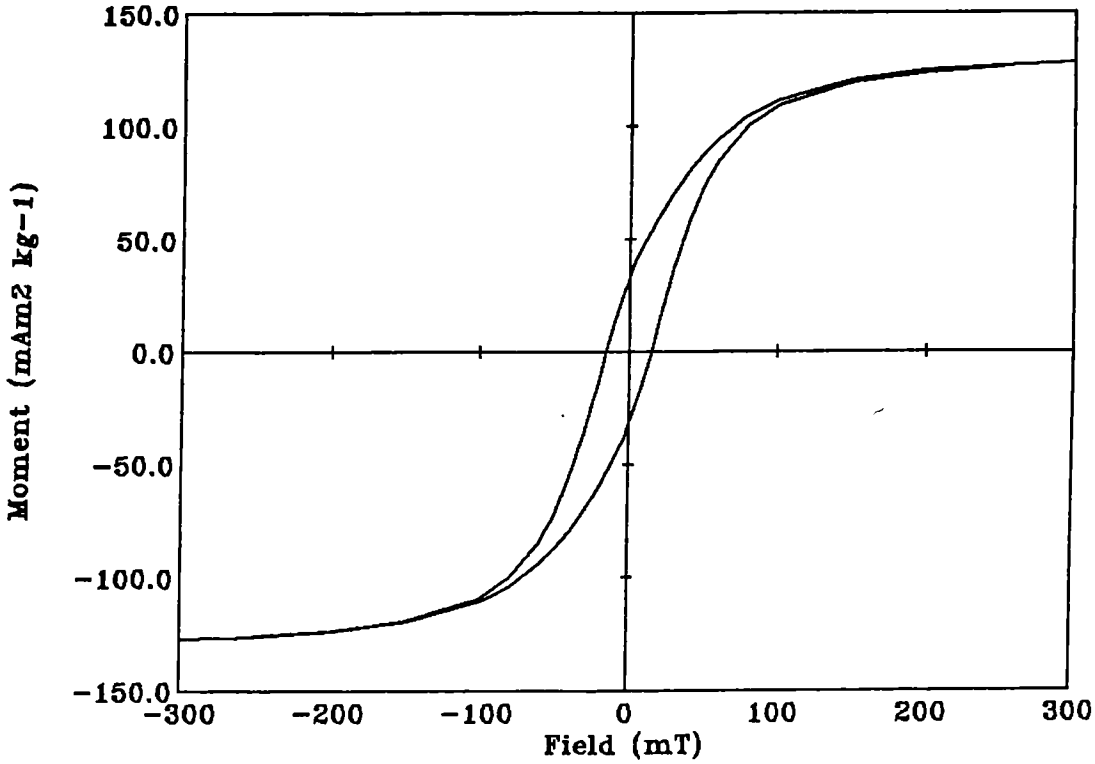

(b) MT14

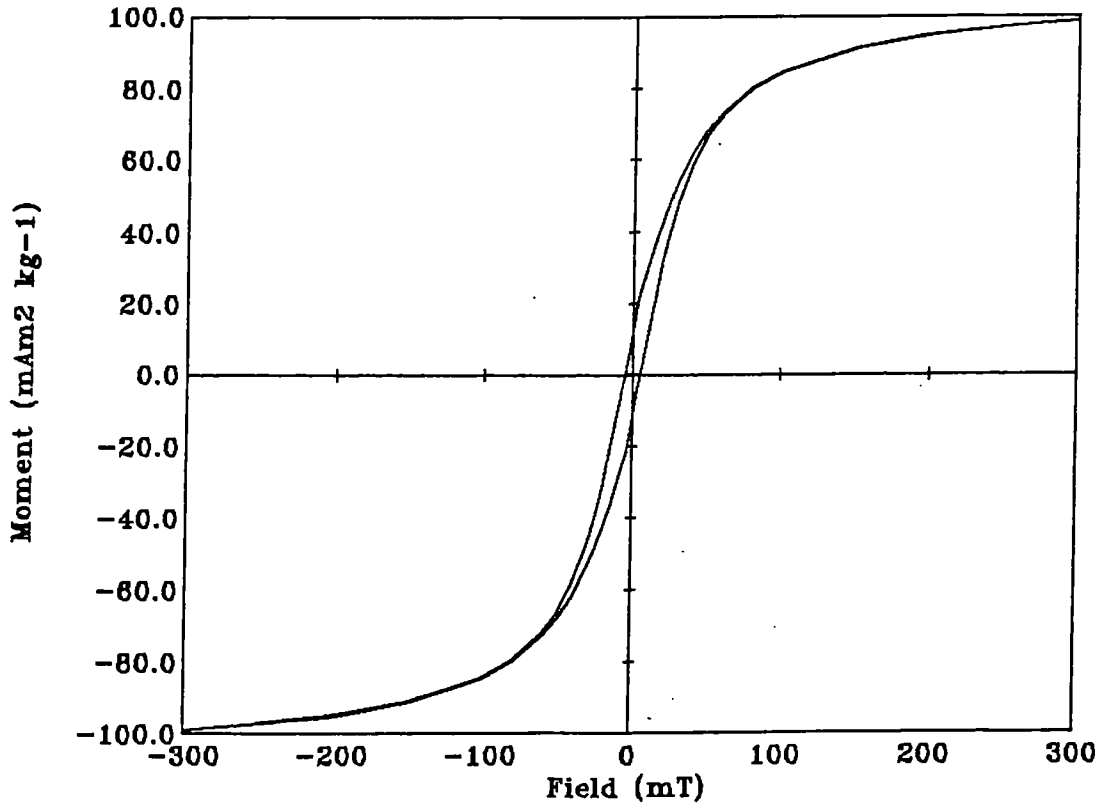

Figure A3.5: Bangor VSM hysteresis curves for MT55 (a) and MT14 (b)

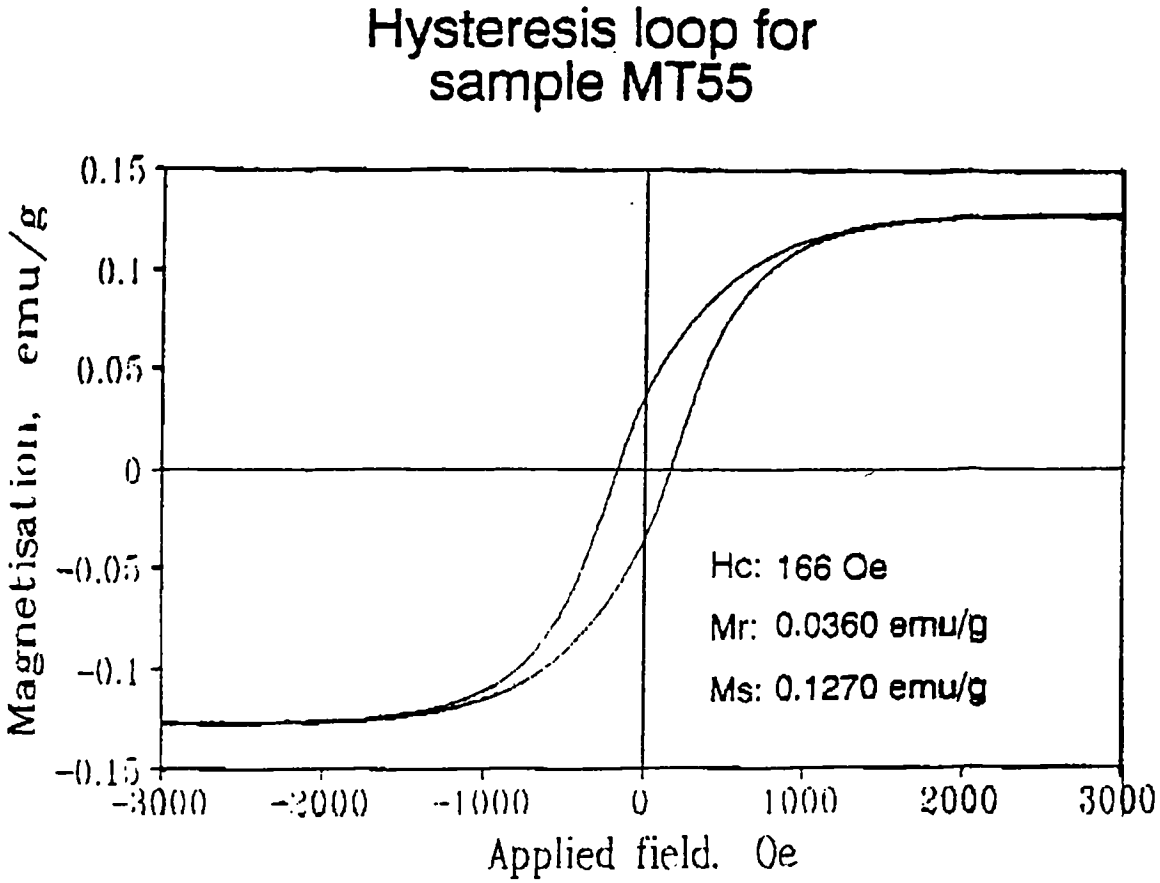

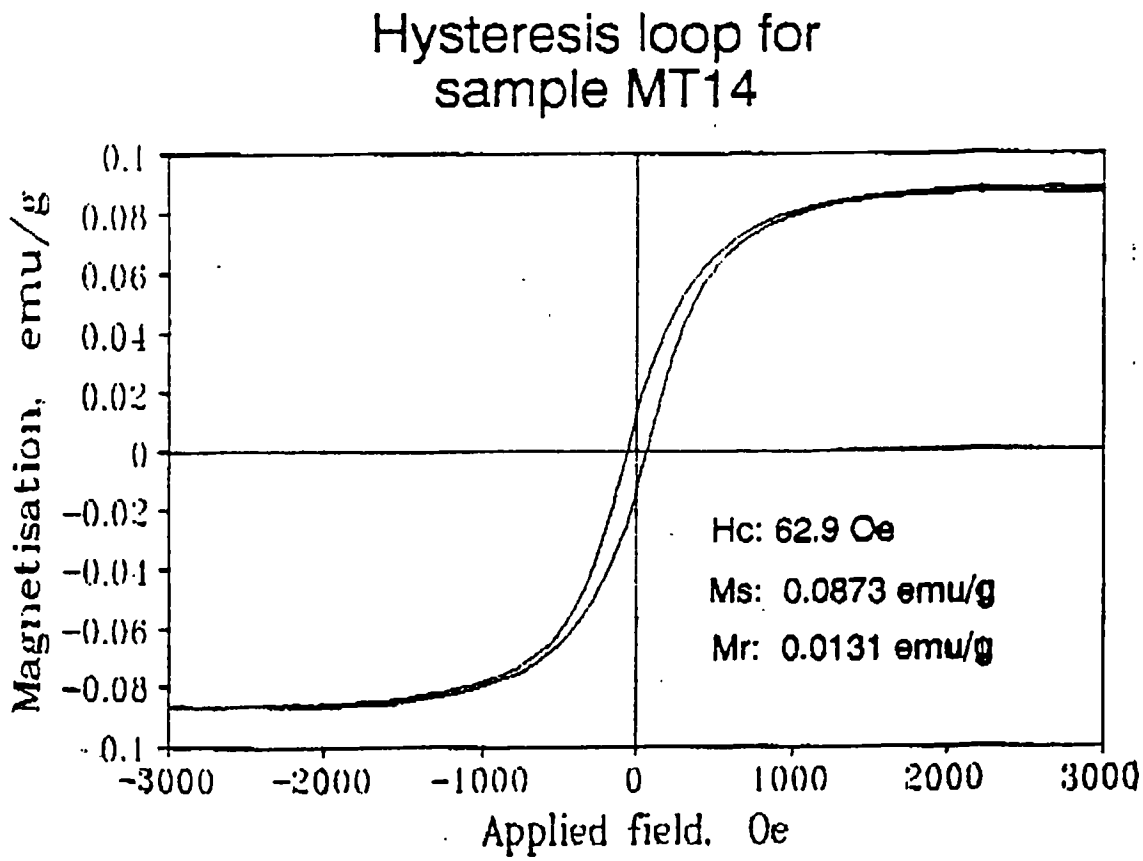

APPENDIX 4

Selected library of IRM Curves and Hysteresis Loops

Selected sample IRM curves generated using the Molspin pulse magnetizers and Molspin Fluxgate 'Minispin' Magnetometer and the VSM and VSM hysteresis loops are given in this appendix. Environmental and synthetic materials selected for their wide ranging magnetic properties from the IRM curve and hysteresis loop databases have been chosen.

IRM curves are shown in part 1 (Figure A4.1a-l). All IRM curves have been normalized for comparison between magnetically strong and weak materials. Examples of ferrimagnetic sample curves are shown in figures a, d, e, h and k and canted-antiferromagnetic sample curves are shown in figures b, c, e and j. Figures c and f show examples of paramagnetic materials. Diamagnetic effects are shown by negative values for example by barium sulphate (figure f and g). Figure l shows the sensitivity of the equipment when the tiny ferrimagnetic component in chalks and limestones can be measured. Paramagnetic components are not shown in remanence curves but can bee seen for the same samples in the following hysteresis loops.

Hysteresis loops are shown in part 2 (Figures A4.2a-l) and a table of other magnetic properties is given in Table A4.1. For further information on VSM hysteresis loops and data refer to Appendix 7 part 3. Figures for Ms give an indication of the scale of magnetic mineral concentration in the samples shown. Ferrimagnetic curves are shown in figures a, d, e and j. Canted-antiferromagnetic curves are shown in figures b (hematite also 'wasp waisted'). Paramagnetic components can be seen in most curves for example Goethite in figure b and true paramagnetic curves can be seen in figures c, d, f, g, h and i and diamagnetic components are shown in figures f (barium sulphate), g, h and i. Most curves show a mixture of minerals and ferrimagnetic, canted-antiferromagnetic and paramagnetic components, figures k and l for example.

Figure A4.1a:
Magnetite and Maghemite

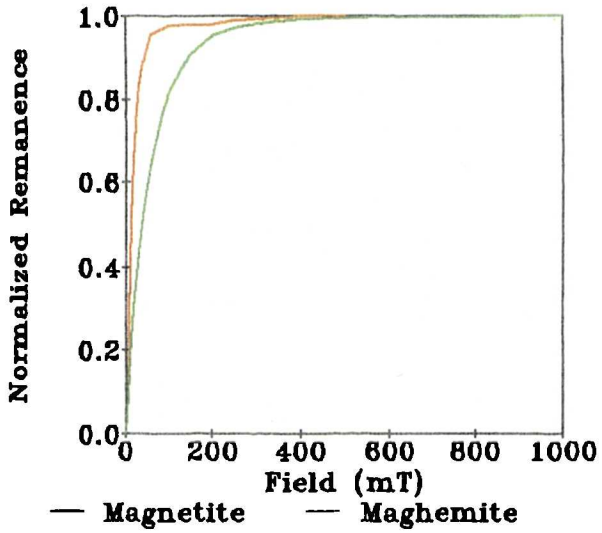

Figure A4.1b:
Hematite and Goethite

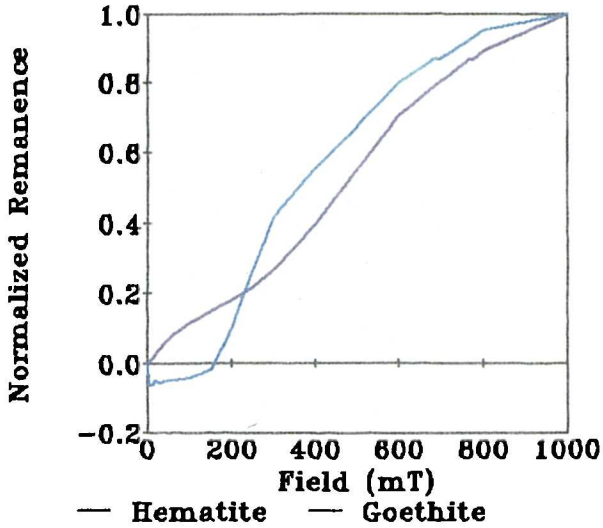

Figure A4.1c:
Lepidocrocite and Pyrrhotite

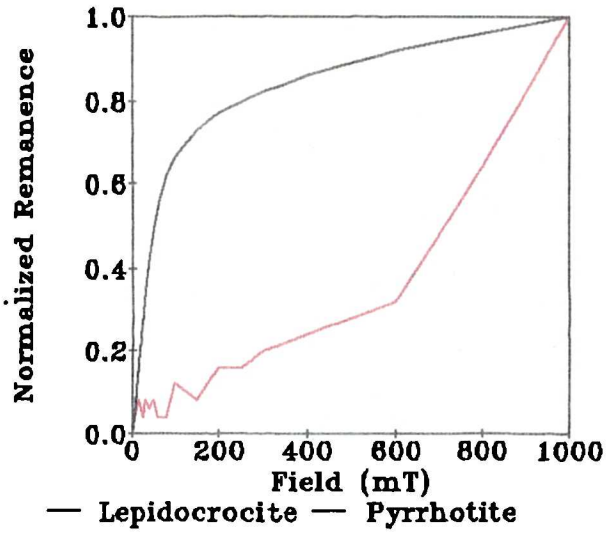

Figure A4.1d:
Arable topsoil and Mine Spoil

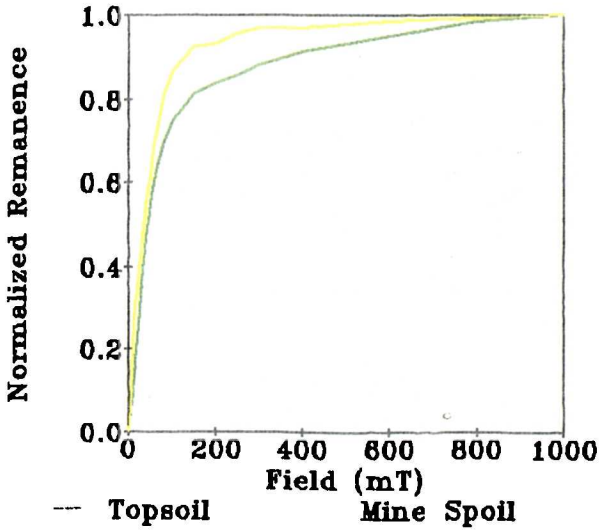

Figure A4.1e:
Keuper Clay and Bedload

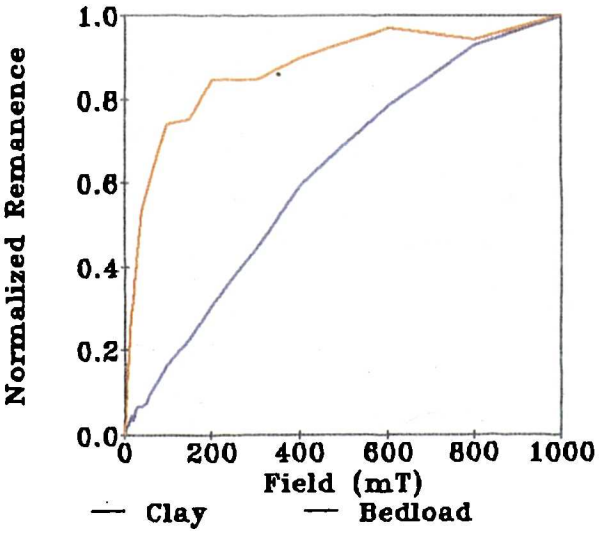

Figure A4.1f:
Barium Sulphate; Manganous Carbonate

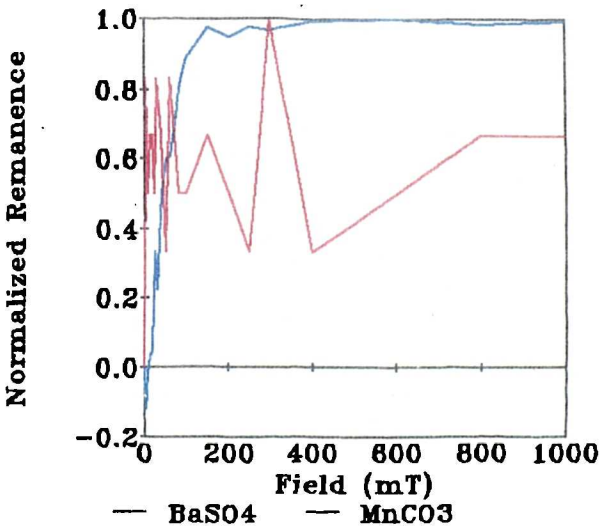

Figure A4.1g:
Peats

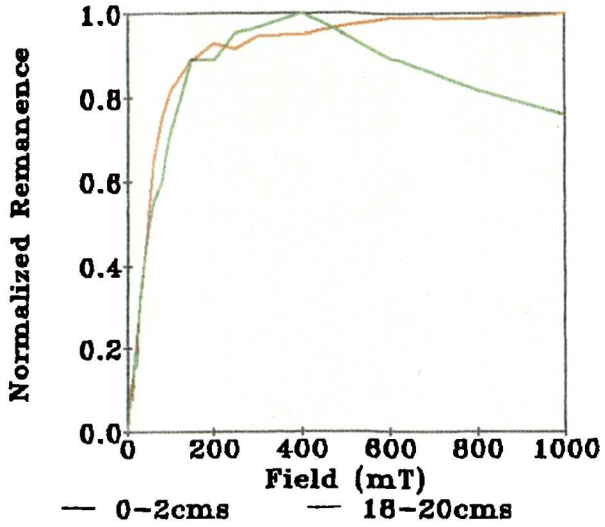

Figure A4.1h:
Brown Earths

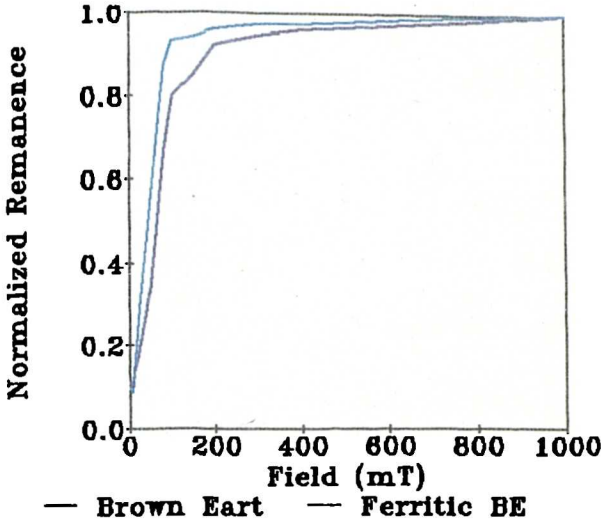

Figure A4.1i:
Rendzina; Stagnogley

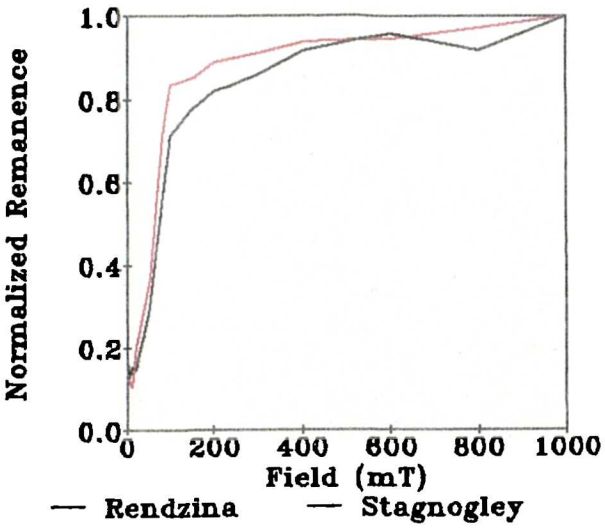

Figure A4.1j:
Skipsea and Withernsea Tills

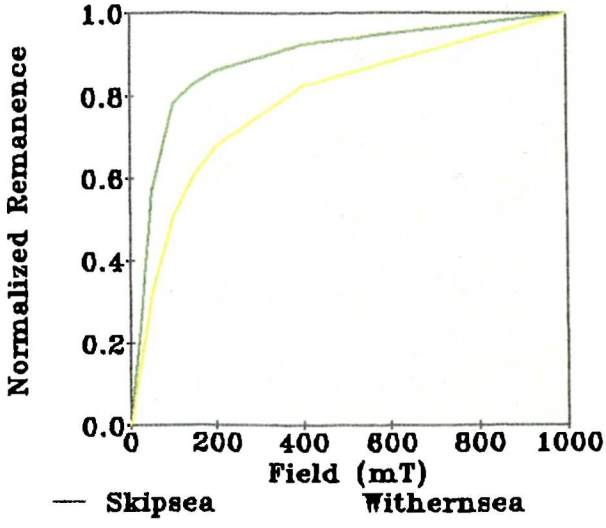

Figure A4.1k:
Diorite and Coal

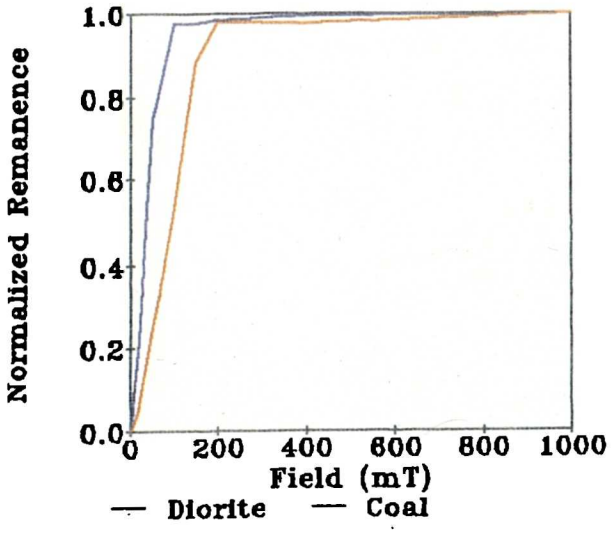

Figure A4.1l:
Limestone and Chalk

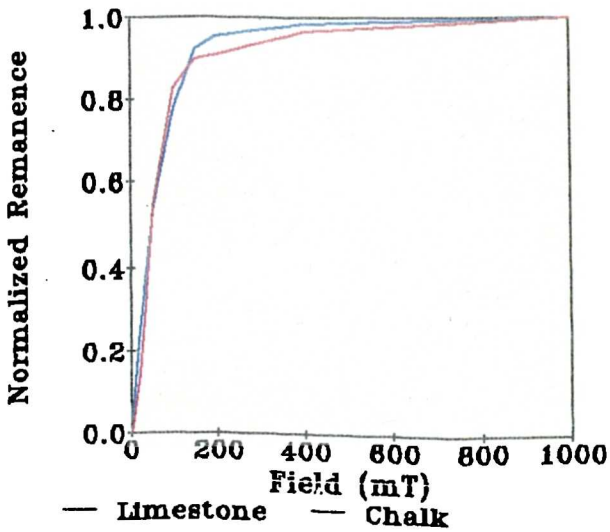

Table A4.1. VSM data for the samples whose hysteresis curves are shown (missing values marked N/A indicate values for diamagnetic materials which are not calculated by the spreadsheet)

VSM SPREADSHEET V1.0 OCTOBER 1993

Values of moment from printout or calculate moment as calcfac*S*attfac

INPUT Description	INPUT Code	CALC χlow	CALC χhigh (para)	CALC χferri	CALC χpara	CALC χferri	CALC Ms	CALC Mrs	CALC Mrs/Ms	CALC HIRM +100mT	CALC S ratio 100/100
		$\mu m^3 kg^{-1}$			%	%	$mAm^2 kg^{-1}$			$mAm^2 kg^{-1}$	
Massive Magnetite	JL-A2	491.97	0.66	491.31	0.13	99.87	44538.4	648.49	0.01	2.54	1.
Crystal Maghemite	JL-A3	31.87	0.50	31.37	1.58	98.42	2972.5	662.19	0.22	124.44	0.81
Massive Hematite	JL-A4	2.21	0.39	1.82	17.71	82.29	287.62	185.33	0.64	163.55	0.12
Lepidocrocite	JL-A6	0.41	0.49	-0.08	100	0	-1.83	3.27	-1.79	2.88	0.12
Goethite	JL-A8	24.72	0.27	24.45	1.10	98.90	110.99	104.03	0.94	-0.26	1.00
Pyrrhotite	JL-A9	13.73	0.41	13.32	3.01	96.99	1480.47	194.89	0.13	65.33	0.66
Keuper Clay	SP1A1	0.11	0.09	0.03	77.28	22.72	4.42	3.32	0.75	2.76	0.17
Top Soil	CM1B1	0.39	0.02	0.37	5.44	94.56	26.94	6.19	0.23	1.55	0.75
Mine Spoil	BH1Y1	0.06	0.00	0.06	6.55	93.45	10.87	1.01	0.09	0.13	0.87
Finham Brook Bedload	FB1Q1	0.16	0.01	0.15	7.35	92.65	10.59	1.99	0.19	0.51	0.74
Barium Sulphate	GL2K1	-0.02	0.00	-0.02	N/A	N/A	2.31	0.43	0.19	0.05	0.89
Manganous Carbonate	GL3K1	1.05	1.00	0.04	95.82	4.18	-9.04	0.35	-0.04	0.09	0.75
Diorite	AB1A1	64.26	0.23	64.03	0.36	99.64	1437.6	-	-	-	-
Withernsea Till	BS3G1	0.52	0.05	0.47	8.80	91.20	16.30	-	-	-	-
Skipsea Till	BS7G1	0.83	0.02	0.81	2.14	97.86	25.19	-	-	-	-
Jurr Limestone	BS12A1	0.05	0.05	-0.01	100	0	-0.56	-	-	-	-
Coal	SH5A1	0.01	0.01	0.00	73.84	26.16	-3.28	-	-	-	-
Quartz Conglomerate	LC1A16	-0.03	0.00	-0.03	N/A	N/A	1.25	0.11	0.09	0.08	0.26
White Sandstone	LC1A5	0.00	0.00	0.01	N/A	N/A	0.43	0.16	0.38	0.02	0.90
Lignite	LC1A10	0.03	0.01	0.01	53.74	46.26	-0.83	0.23	-0.27	0.01	0.97
Chalk	LC1C20	0.07	0.06	0.02	N/A	N/A	-0.06	0.20	-3.65	0.03	0.86
Pyrite Grains	LC1C26	0.05	0.06	-0.01	100	0	1.58	0.15	0.09	0.02	0.88
Iron Grains	LC1C25	329.09	4.43	324.65	1.35	98.65	37486.5	3903.0	0.10	318.75	0.92

Figure 4.2a:
Magnetite and Maghemite

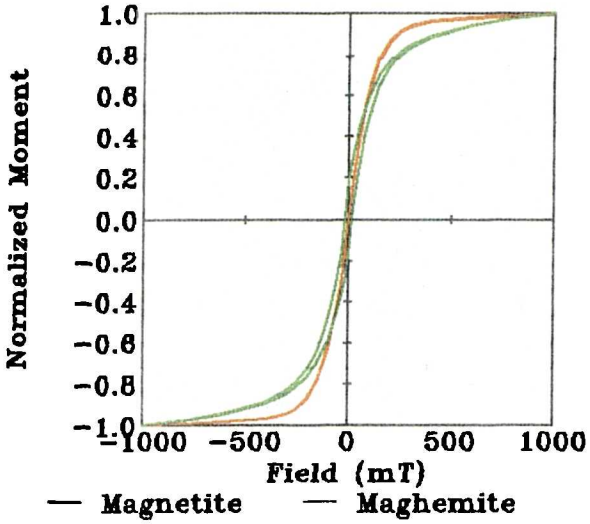

Figure 4.2b:
Hematite and Goethite

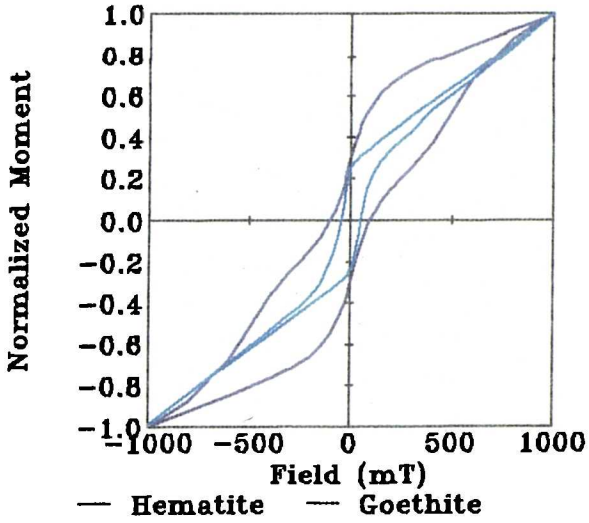

Figure 4.2c:
Lepidocrocite and Pyrrhotite

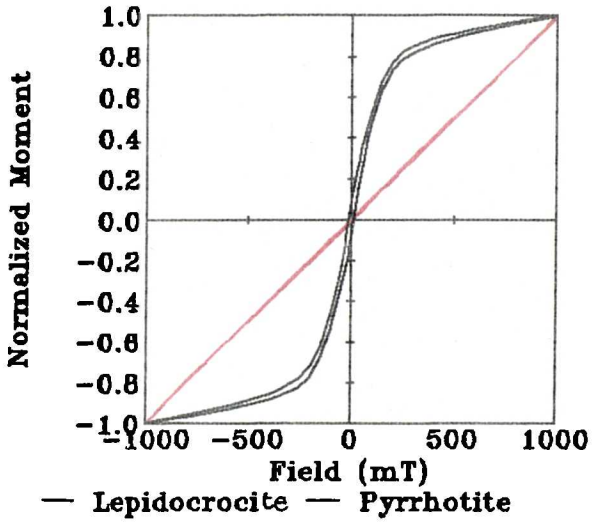

Figure 4.2d:
Iron and Pyrite Grains

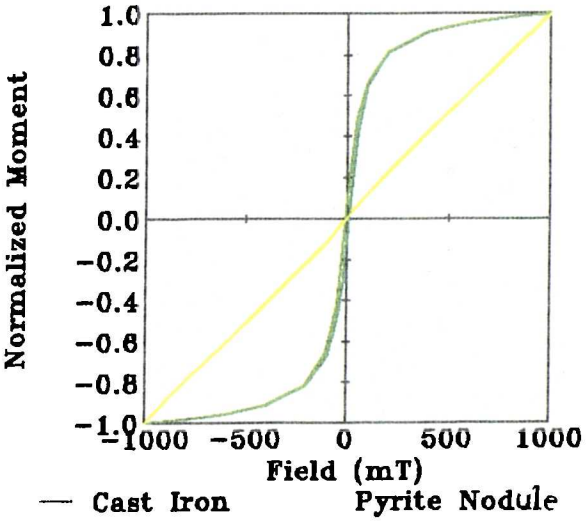

Figure 4.2e:
Lake Sediment and Organic Matter

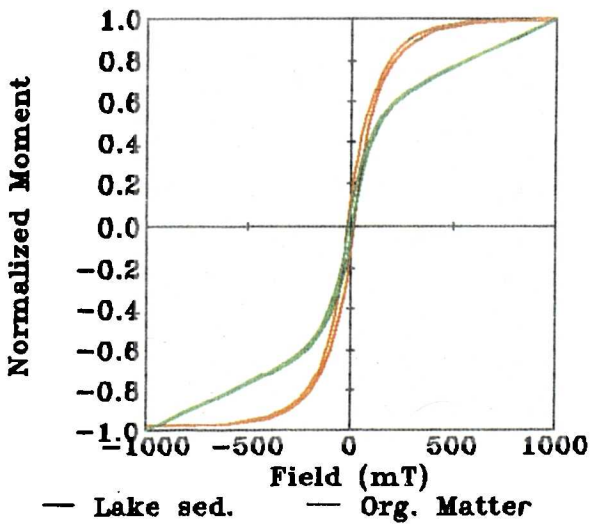

Figure 4.2f:
Barium Sulphate; Manganous Carbonate

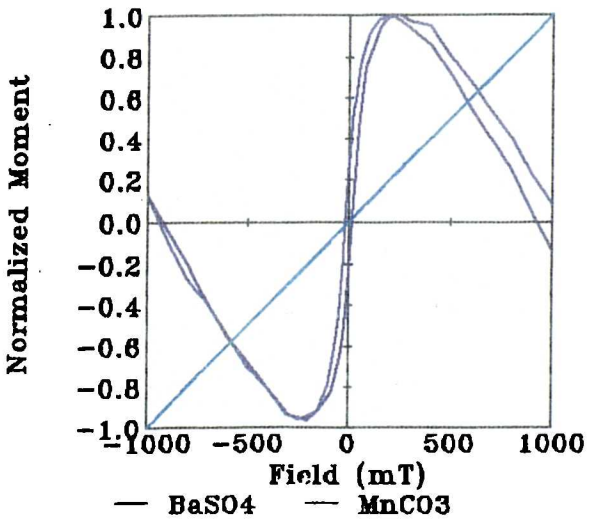

Figure 4.2g:
Peat and Lignite

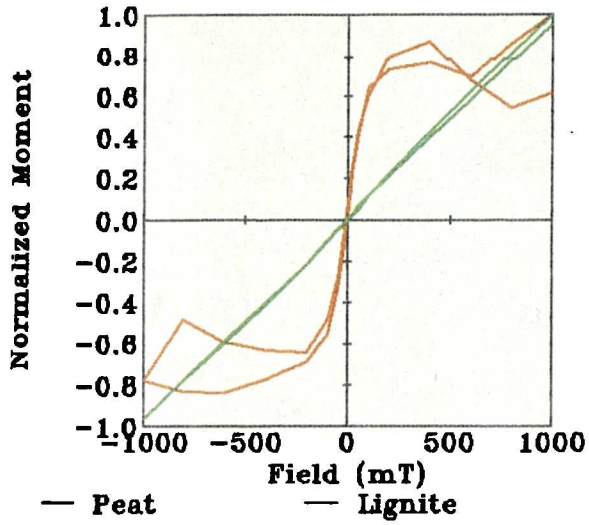

Figure 4.2h:
White Sandstone and Quartz Grit

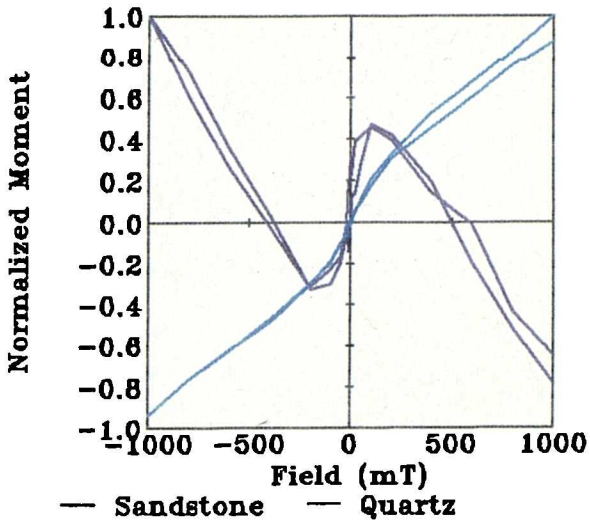

Figure 4.2i:
Limestone and Chalk

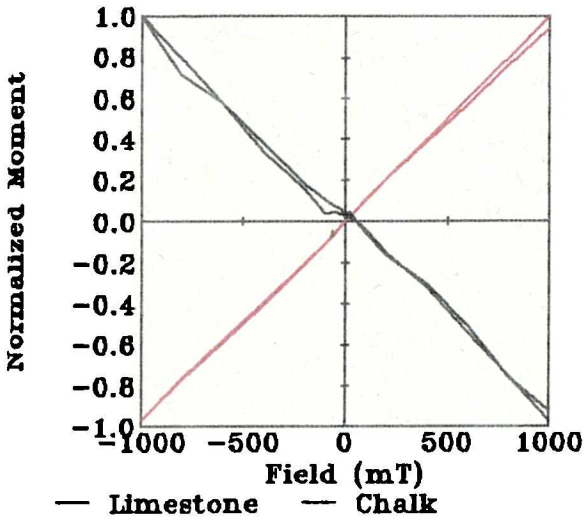

Figure 4.2j:
Coal and Diorite

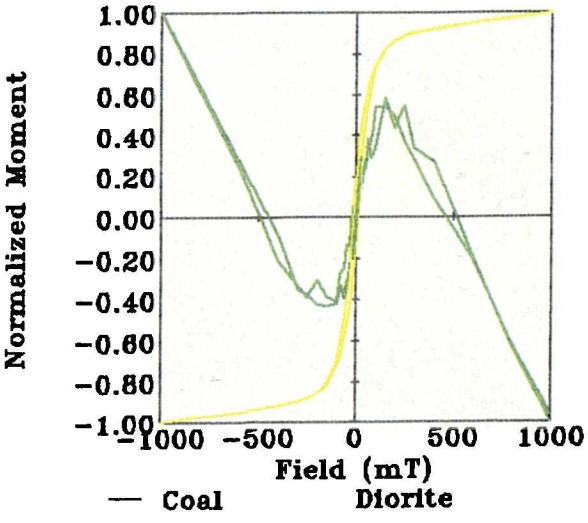

Figure 4.2k:
Skipsea and Withernsea Tills

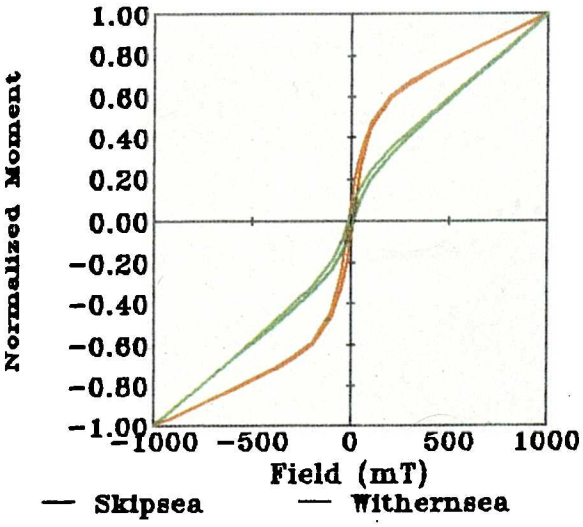

Figure 4.2l:
Rendzina and Stagnogley

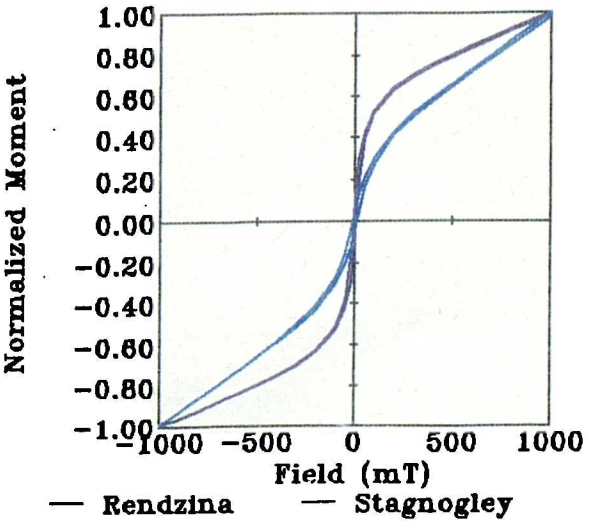

APPENDIX 5

Computer Program Listings

Listed in this appendix are all computer programs written for and adapted for this research. Programs are written in Turbo Basic programming language mainly for data handling and formatting for transfer between programs. The semi-variogram program adapted from Campbell (1985) is also listed. In part three an example is given of the data matrix input file and LINDO files used in this research.

5.1. Data handling programs

(a) MPSGENS - Strips tabs from spreadsheet text files (written by F. P. Lockett).

(b) MPSGEN3 - Formats MPSGENS into .MPS files for Lindo input (version 3) (written by F. P. Lockett).

(c) MPSCOMP - Compares two .MPS (Lindo) files, one input and one output side by side to ensure correct and error free data entry (written by F. P. Lockett).

(d) TABn - Inputs tabs between all data in columns for spreadsheet entry (versions for files with various column numbers

5.2. Other programs

(e) SEMIVARI - Calculates semivariance, auto-covariance, auto-correlation and population statistics for transect or grid data (adapted from Campbell, 1985).

1. Data handling programs

(a) MPSGENS

```
 10 Rem   MPSGENs.BAS  FPL  9-NOV-92
 20 print "MPSGENs Generates .mps data file for Lindo from .sat file"
 22 print "by first removing tab characters to produce a .dat file"
 24 print
 45 input "filename ",f$  :ip$=f$+".sat"  :op$=f$+".dat"
 46 input "number of magnetic parameters",m
 50 Open "I",#98,ip$    :open "o",#99,op$
 60 input #98,ff$       :print #99,op$
 70 for i=1 to 2*m+1
100 line input #98,a$
110 l=len(a$) :b$=" "
130 for k=1 to l
140  r$=right$(left$(a$,k),1)
145  if r$="       " then goto 160   :rem tab right
150  b$=b$+r$        :goto 170
160  b$=b$+" "                :rem space
170 next k
180 print b$   :print #99,b$
190 next i
200 close #98   :close #99
210 print "stop"
220 stop
```

(b) MPSGEN3

```
 10 Rem   MPSGEN3.BAS   FPL   27-OCT-92
 20 Rem   Generates .mps data file for Lindo
 22 Rem   From plain data file containing
 24 Rem   m x n matrix A & m-vectors b and er where n<=6
 26 Rem   A data must be padded out to 6 reals per line
 28 Rem   This version does not specify x>=0 and e>=0
 30 Dim   a(30,30),b(30),er(30)
 45 input "filename ",f$  :ip$=f$+".dat"  :op$=f$+".mps"
 50 Open "I",#98,ip$    :open "o",#99,op$
 60 input #98,ff$
 65 input #98,m,n
 70 for i=1 to m
 72   input #98,a(i,1),a(i,2),a(i,3),a(i,4),a(i,5),a(i,6)
 74 next i
 80 for i=1 to m
 82   input #98,b(i),er(i)
 84 next i
 90 close #98
100 rem
110   Print #99,"NAME    LINDO GENERATED MPS FILE( MIN)"
112   Print #99,"ROWS"
120   Print #99,"  N  1"
130 For i=1 to m
132   Print #99,using "  L ##";i*2
134   Print #99,using "  G ##";i*2+1
140 Next i
150 For i=1 to m
152   Print #99,using "  L ##";m*2+1+i
156 Next i
160 Rem For i=1 to m+n
162 Rem  Print #99,using "  G ##";m*3+1+i
166 Rem Next i
170   Print #99,using "  E ##";m*3+2
210   Print #99,"COLUMNS"
220 E$ ="    E#        ##    #######.####"
222 E2$="    E##       ##    #######.####"
230 For i=1 to m
232   p$=E$
234   If i>9 then p$=E2$
235   Print #99,using p$;i,         1, 1
240   Print #99,using p$;i,i*2       ,-1
245   Print #99,using p$;i,i*2    +1, 1
250   Print #99,using p$;i,m*2  +i+1, 1
255   Rem Print #99,using p$;i,m*3+n+i+1, 1
260 Next i
270 X$ ="    X#        ##     #######.####"
272 X2$="    X##       ##     #######.####"
280 For j=1 to n
282  p$=X$
284  if j>9 then p$=x2$
285  For i=1 to m
290   If a(i,j) = 0 goto 310
300   Print #99,using p$;j,i*2     , a(i,j)
305   Print #99,using p$;j,i*2  +1, a(i,j)
310  Next i
335   Rem Print #99,using p$;j,m*3+j+1, 1
370   Print #99,using p$;j,m*3  +2, 1
```

```
380 Next j
410  Print #99,"RHS"
420 r$="   RHS      ##     #######.####"
430 For e=1 to m
435  Print #99,using r$;e*2   ,b(e)
440  Print #99,using r$;e*2  +1,b(e)
460 Next e
480 For e=1 to m
485  Print #99,using r$;m*2+e+1,er(e)
490 Next e
495  Print #99,using r$;m*3+2  ,1
510  Print #99,"ENDATA"
512  Print    "ENDATA"
```

(c) MPSCOMP

```
10  Rem   MPSCOMP.BAS   FPL   9-NOV-92
20  print "MPSCOMP compares two MPS files, displaying lines side by side"
24  print
45  input "first . mps filename ",f1$  :f1$=f1$+".mps"
46  input "second. mps filename ",f2$  :f2$=f2$+".mps"
48  input "number of magnetic parameters and components ",m,n
50  Open "I",#98,f1$    :open "I",#99,f2$
60  c=0
70  for i=1 to 2*m*n+n+10*m+8
100  line input #98,a$  :line input #99,b$
110  print a$+"   "+b$
120  c=1+c
130  if c<20 then goto 190
140  c=0  :input x
190 next i
200 close #98   :close #99
210 print "stop"
220 stop
```

(d) TABn

```
10  Rem   TAB6.BAS  JAL   20-NOV-92
20  PRINT "TAB inputs a TAB character before every column of data"
30  PRINT
40  INPUT "Filename  ",f$  :ip$=f$+".sat"  :op$=f$+".tbs"
50  INPUT "Number of numeric rows in file  ",n
60  Open "I",#98,ip$   :OPEN "o",#99,op$
62  INPUT #98,ff$      :PRINT #99,op$
65  FOR k=1 TO n
70  INPUT #98,a,b,c,d,e,f
80  PRINT #99,a;"          ";b;"      ";c;"      ";d;"      ";e;"      ";f
90  NEXT k
95  PRINT a;"    ";b;"      ";c;"      ";d;"      ";e;"      ";f;
100 PRINT "STOP"
110  STOP
```

2. Other programs

(e) SEMIVARI

```
10  REM PROGRAM 7.1 PROGRAM FOR COMPUTING CORRELATION,
20  REM COVARIANCE, AND SEMIVARIANCE OF A SET OF DATA
30  REM Version 7.2 JAL 8/12/93
40  INPUT "FILENAME ",f$  :ip$=f$+".SAT"  :op$=f$+".DAT"
50  INPUT "NO OF DATA",N
60  OPEN "i",#98,ip$   :OPEN "o",#99,op$
70  INPUT #98,f$       :PRINT #99,op$
80  S=0:T=0:Q=N/3
90  DIM X(N),C(Q),G(Q),R(Q)
100  LINE INPUT #98,F$
110  FOR I=1 TO N
115     INPUT #98,X(I)
120     S=S+X(I)
125  NEXT I
130  CLOSE #98
135  PRINT #99,Z$
140  XB=S/N
142  FOR I=1 TO N
144    T =T+(X(I)-XB)^2
146  NEXT I
148  V =T/N:SD=V^0.5
150  PRINT #99, "Sum =";S;"Mean =";XB;"Var =";V;"SD =";SD
160  PRINT #99,"Lag";" ";"Autocov";"      ";"Autocor";"      ";"Semivar"
180  FOR K=0 TO Q
190     FOR I=1 TO N-K
200       C(K)=C(K)+(X(I)-XB)*(X(I+K)-XB)
210       G(K)=G(K)+(X(I)-X(I+K))^2
220     NEXT I
230    C(K)=C(K)/(N-K-1)
240    G(K)=.5*G(K)/(N-K-1)
250    R(K)=C(K)/C(0)
260     PRINT #99, USING "########.###";K;C(K);R(K);G(K)
270  NEXT K
280  CLOSE #99
290  PRINT "STOP"
300  STOP
```

5.3 Example LINDO data files

The data in Table A5.1 represents the matrix of source (x) and mixture magnetic data which is created in a spreadsheet. The file is then saves as a test file, translated using MPSGENS and MPSGEN3 into a format readable by LINDO. Once the file is read into LINDO the routine looks like that shown in Table A5.2. The errors in this routine are set quite low at 0.1 and the routine aims to minimize the errors whilst finding a solution for x1, x2, x3 and x4 subject to the constraint x1 + x2 + x3 + x4 = 1.

Table A5.1. Matrix of Source (x) parameter values for Great Rollright Mixture 1 and associated errors. The file is then transferred into LINDO for minimization.

MIX1.dat
(Filename.extention)
10 4
(Number of Parameters, Number of Sources)

Magnetic	**x1**	**x2**	**x3**	**x4**	**x5**	**x6**
Parameter 1	0.006	0.371	0.141	0.647	0	0
Parameter 2	0.006	0.340	0.135	0.595	0	0

Table A5.1 continued

Parameter 3	0.015	3.103	0.030	4.590	0	0
Parameter 4	0.016	2.428	0.934	4.074	0	0
Parameter 5	0.002	0.474	1.116	0.863	0	0
Parameter 6	0.008	2.069	0.720	3.523	0	0
Parameter 7	0.012	2.329	0.831	3.959	0	0
Parameter 8	0.013	1.954	0.285	3.211	0	0
Parameter 9	0.007	0.360	0.825	0.551	0	0
Parameter 10	0.003	0.099	7.839	0.115	0	0

	Mixture	*Error*
Parameter 1	0.2	0.1
Parameter 2	0.19	0.1
Parameter 3	1.37	0.1
Parameter 4	1.69	0.1
Parameter 5	0.25	0.1
Parameter 6	1.36	0.1
Parameter 7	1.61	0.1
Parameter 8	1.44	0.1
Parameter 9	0.33	0.1
Parameter 10	0.09	0.1

Table A5.2. LINDO file of mixture 1 showing minimization of errors (En) which are set at 0.1 for all parameters subject to the constraint x1 + x2 + x3 + x4 = 1.

```
Parameter    x1          x2          x3          x4          Mixture
-E1 + 0.006 x1 + 0.371 x2 + 0.141 x3 + 0.647 x4 <= 0.2
 E1 + 0.006 x1 + 0.371 x2 + 0.141 x3 + 0.647 x4 >= 0.2
-E2 + 0.006 x1 + 0.340 x2 + 0.135 x3 + 0.595 x4 <= 0.19
 E2 + 0.006 x1 + 0.340 x2 + 0.135 x3 + 0.595 x4 >= 0.19
-E3 + 0.015 x1 + 3.103 x2 + 0.030 x3 + 4.590 x4 <= 1.37
 E3 + 0.015 x1 + 3.103 x2 + 0.030 x3 + 4.590 x4 >= 1.37
-E4 + 0.016 x1 + 2.428 x2 + 0.934 x3 + 4.074 x4 <= 1.69
 E4 + 0.016 x1 + 2.428 x2 + 0.934 x3 + 4.074 x4 >= 1.69
-E5 + 0.002 x1 + 0.474 x2 + 1.116 x3 + 0.863 x4 <= 0.25
 E5 + 0.002 x1 + 0.474 x2 + 1.116 x3 + 0.863 x4 >= 0.25
-E6 + 0.008 x1 + 2.069 x2 + 0.720 x3 + 3.523 x4 <= 1.36
 E6 + 0.008 x1 + 2.069 x2 + 0.720 x3 + 3.523 x4 >= 1.36
-E7 + 0.012 x1 + 2.329 x2 + 0.831 x3 + 3.959 x4 <= 1.61
 E7 + 0.012 x1 + 2.329 x2 + 0.831 x3 + 3.959 x4 >= 1.61
-E8 + 0.013 x1 + 1.954 x2 + 0.285 x3 + 3.211 x4 <= 1.44
 E8 + 0.013 x1 + 1.954 x2 + 0.285 x3 + 3.211 x4 >= 1.44
-E9 + 0.007 x1 + 0.360 x2 + 0.825 x3 + 0.551 x4 <= 0.33
 E9 + 0.007 x1 + 0.360 x2 + 0.825 x3 + 0.551 x4 >= 0.33
-E10 + 0.003 x1 + 0.099 x2 + 7.839 x3 + 0.115 x4 <= 0.09
 E10 + 0.003 x1 + 0.099 x2 + 7.839 x3 + 0.115 x4 >= 0.09
Param. Error
 E1 <= 0.1
 E2 <= 0.1
 E3 <= 0.1
 E4 <= 0.1
 E5 <= 0.1
 E6 <= 0.1
 E7 <= 0.1
 E8 <= 0.1
 E9 <= 0.1
 E10 <= 0.1
Constraint
 x1 + x2 + x3 + x4 = 1
```

APPENDIX 6

Dilution and Packing Density Experiments

The factors of dilution of magnetic minerals and packing density were tested in experiments. It was believed that dilution and packing could affect the magnetic properties of a material and cause non-linearity between source and mixture samples for example.

6.1 Effects of Packing density on magnetic properties of materials

It was envisaged that packing density may affect the magnetic properties of materials packed with differential force (Roy Carey pers. comm.). Variations during packing of samples could then mean that slight variations in properties would be present and cause further non-linearity of mixing results. Magnetic particles packed closer together interact, especially in samples of highly magnetic materials such as synthetic minerals (magnetites for example). This could lead to a reduction in measurement values.

Ten samples, five of a topsoil and five of a burnt chimney slag were packed using different forces (using a press) into 10ml pots. The two materials were finely ground and the <63μm fraction was used. Difficulties were encountered in obtaining a wide range of packing densities however. Measurements made were χlf, χhf, ARM, IRM880 and IRM-100. Figure A6.1a-d shows the results for the soil samples and A6.2a-d for the slag samples. Variations of 3g were obtained in the sample masses and small variations are present in the concentration measurements (χlf and IRM880). The largest difference is 2 χlf units between slag samples 3 and 5. Ratio parameters indicating grain size and mineralogical changes (S ratio) are fairly constant. The changes in measurement value are well within the variation expected in the material taken from a number of sub-samples (Chapter 4). Little pattern with packing density of the samples is seen. It was therefore concluded that for environmental samples, even magnetically strong materials, packing density was not contributing to non-linearity over and above factors such as the initial homogeneity of materials.

Figure A6.1: Packing density effects on topsoil, samples weights (a), Xlf (b), IRM880 (c) and S ratio (d)

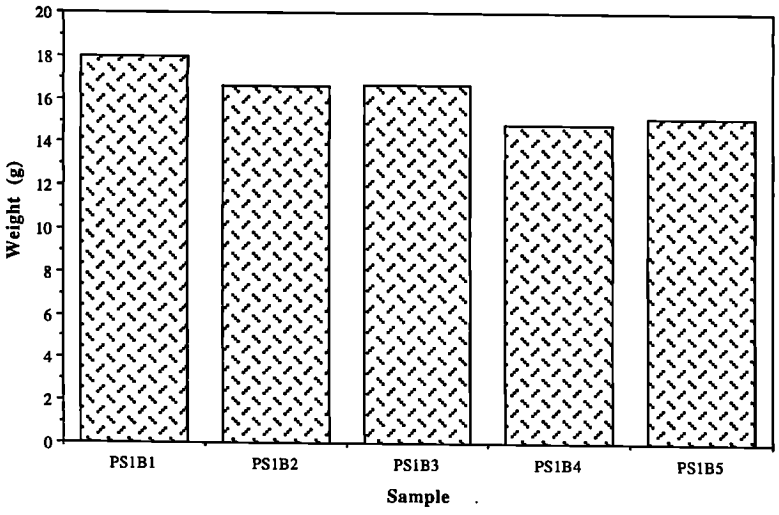

(b)

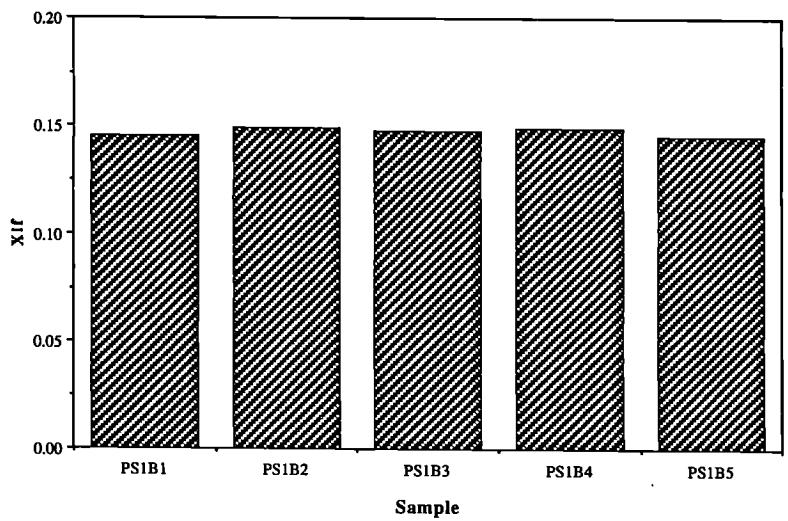

(c)

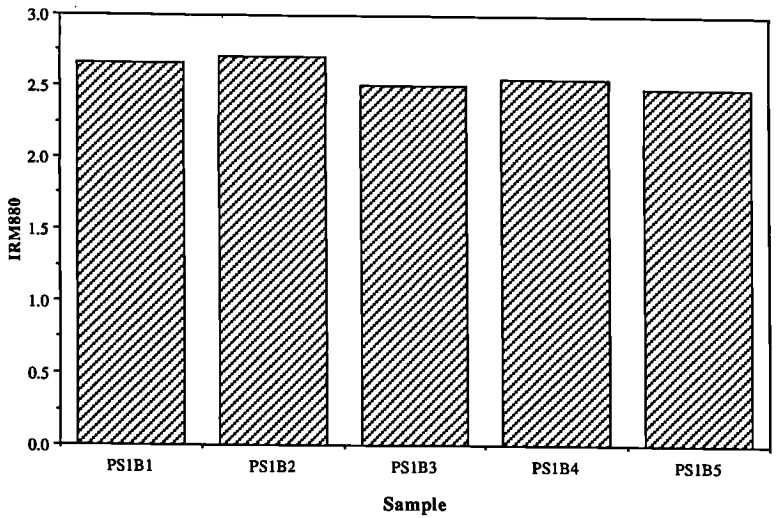

(d)

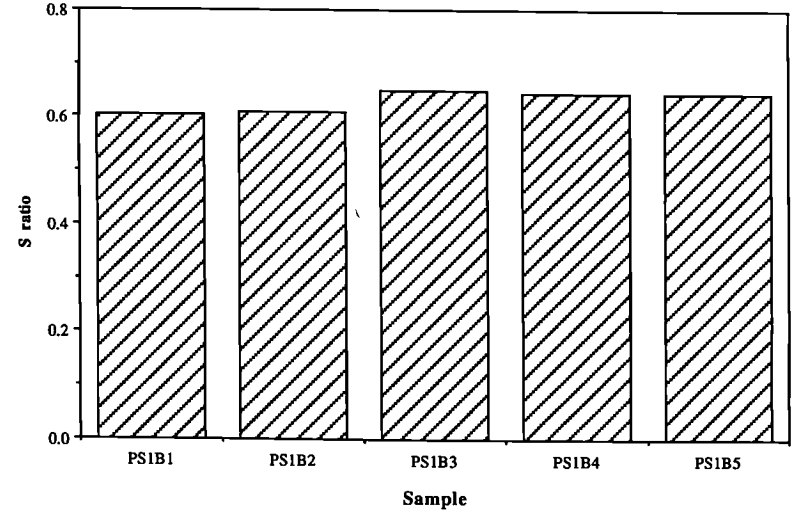

Figure A6.2: Packing density effects on chimney slag, samples weights (a), Xlf (b), IRM880 (c) and S ratio (d)

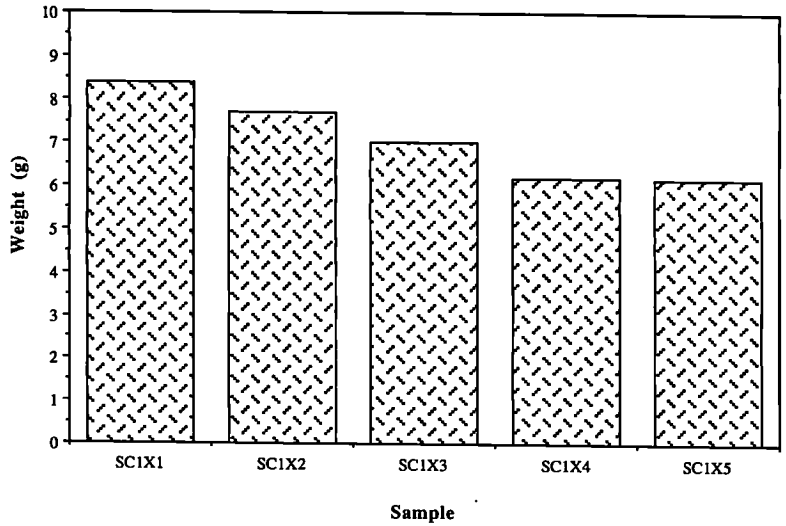

(b)

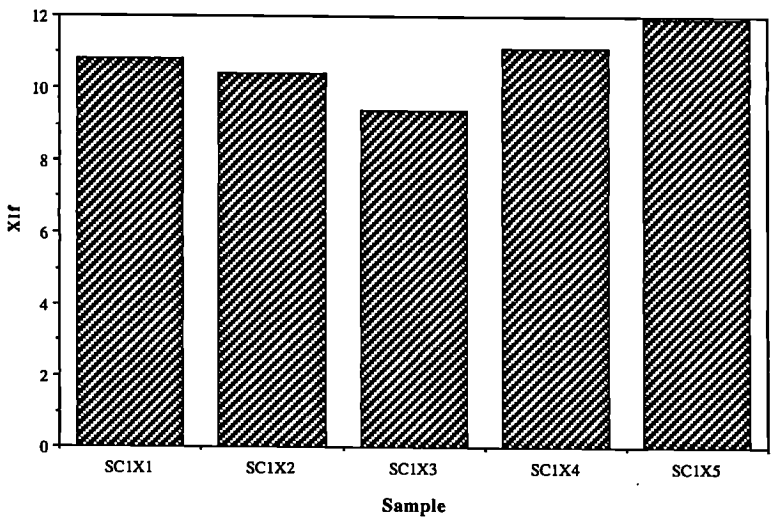

(c)

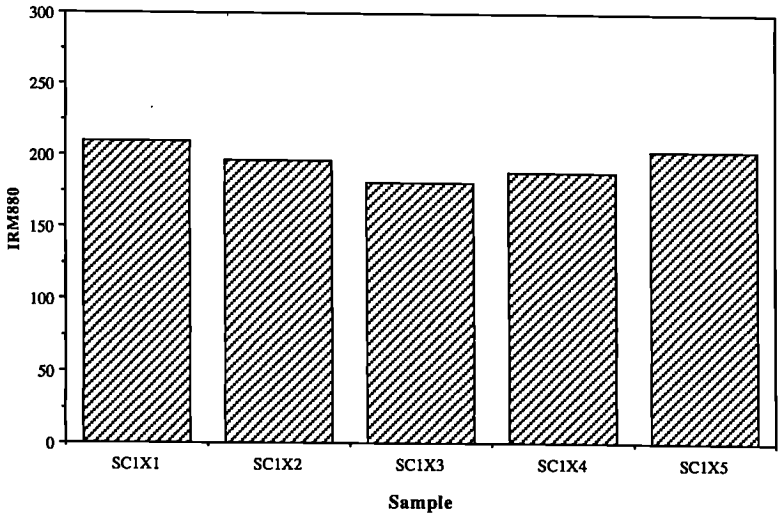

(d)

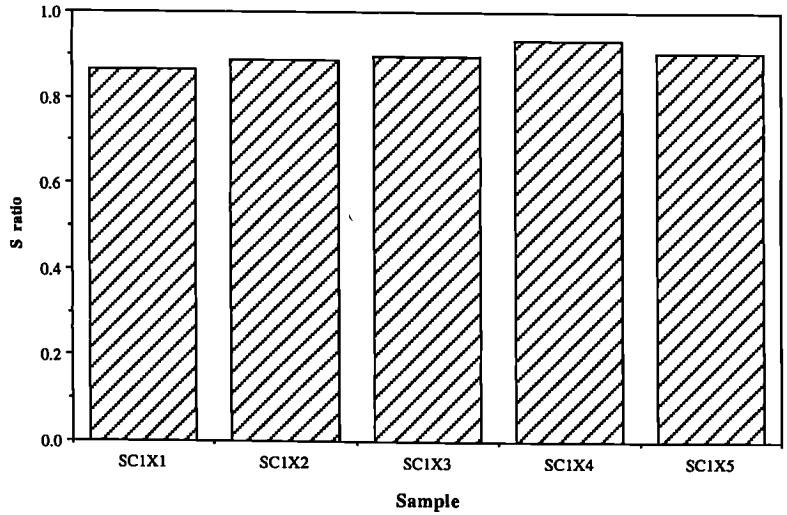

6.2 Effects of dilution on magnetic properties of materials

The same topsoil and slag materials were used in this experiment also. Eight dilutions of each material was made using Analr calcium carbonate (CaCO3). Table A6.1 lists the dilutions made. Weighed proportions of each material was thoroughly mixed to a total weight of 6g and potted into 10ml pots. Measurements made were χlf, χhf, ARM, IRM880 and IRM-100 and 10 sub-samples of the CaCO3 were measured to assess background magnetic properties.

Figures A6.3a-c and A6.4a-c give the results for χlf, IRM880 and S ratio measurements. The CaCO3 measurements for χlf and IRM880 are -0.001 um3 kg-^{1} and 0.037 mAm^{2}kg-^{1} respectively. It must be noted that the soil kappa measurements are subject to some error while the chimney slag kappa measurements were all >10 (see also Chapter 3). In both dilution sets there is a distinct increase in the 0.1% dilutions and a slight increase in 1% dilutions. This phenomenon is interesting for S ratio measurements and may be a factor of the sensitivity of the measurements rather than a true phenomenon. In the case of the chimney slag however, S ratio is constant apart from the 15% dilution which shows a natural variation effect.

Table A6.1. Dilutions made using topsoil and CaCO3 and slag and CaCO3

Sample No	Dilution (%)	Sample Wt (g)	Dilutant Wt (g)
1	100 (bulk)	6	0
2	75	4.5	1.5
3	50	3	3
4	20	1.2	4.8
5	15	0.9	5.1
6	10	0.6	5.4
7	5	0.3	5.7
8	1	0.06	5.94
9	0.1	0.006	5.994

The results may indicate an interaction effect in the materials which is increasingly eliminated towards small dilutions. Measurements made on the soil dilutions however are prone to equipment sensitivity levels at such minute dilutions. The slag however should not reflect this. The results also indicate that if a strongly magnetic sample is mixed in a proportion of greater than 5% with a much weaker material then a non-linearity in the result will occur. This is also shown in the mixing experiments in Chapter 4.

Figure A6.3: Dilution experiment results for topsoil in calcium carbonate, Xlf (a), IRM880 (b) and S ratio (c)

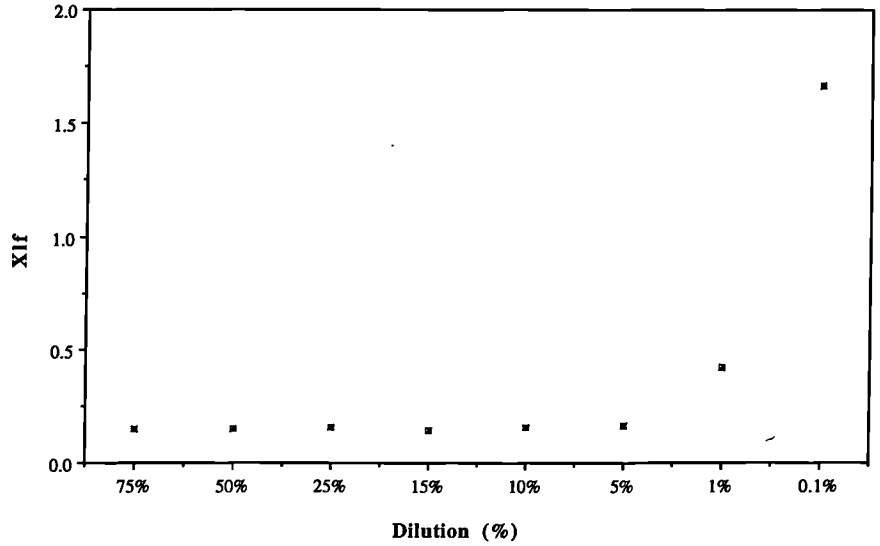

(b)

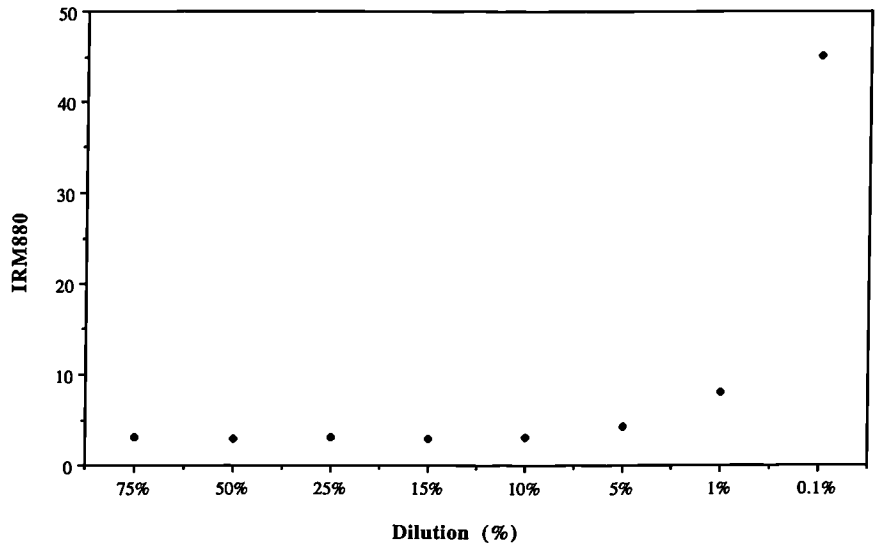

(c)

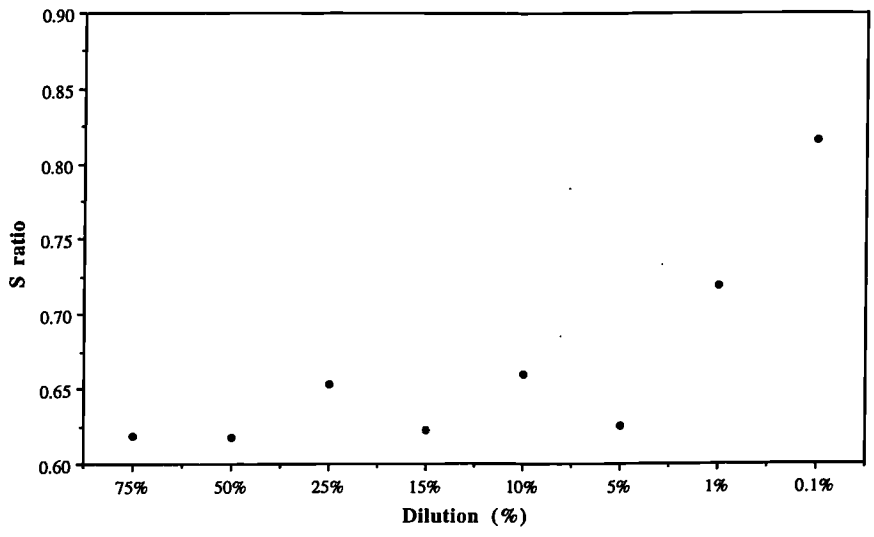

Figure A6.4: Dilution experiment results for chimney slag in calcium carbonate, Xlf (a), IRM880 (b) and S ratio (c)

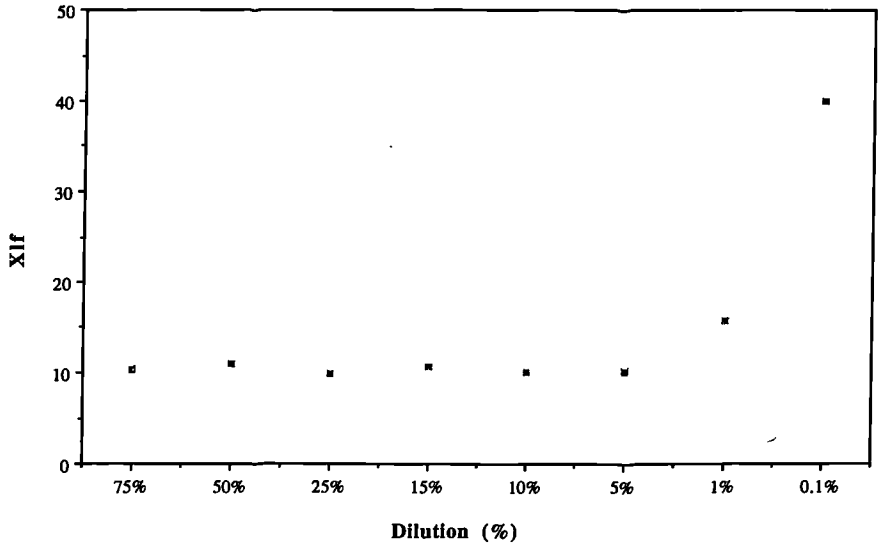

(b)

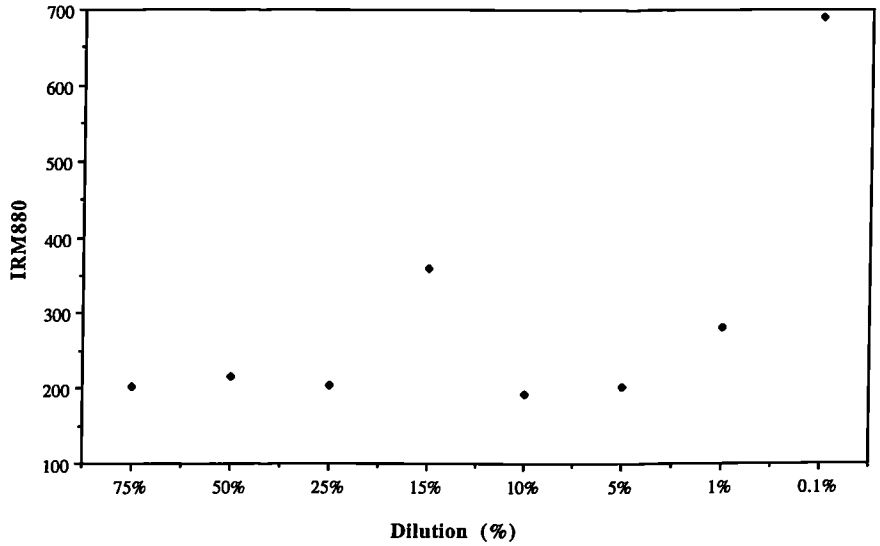

(c)

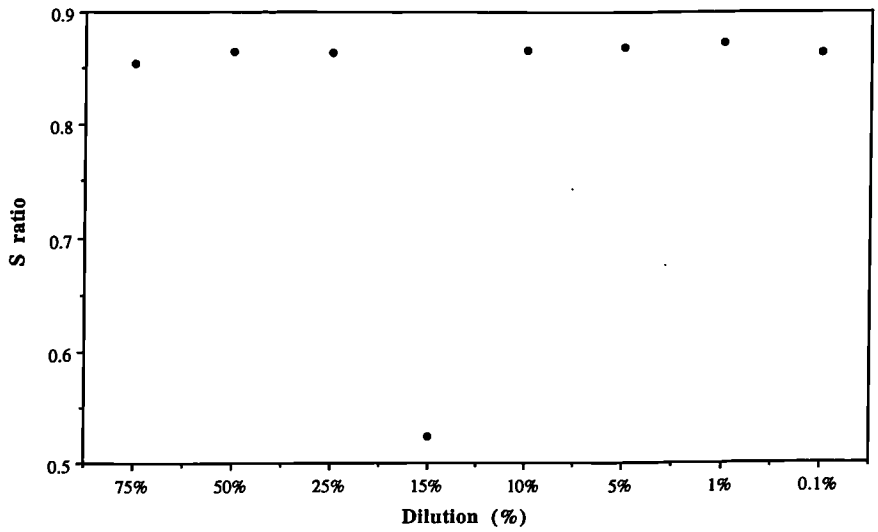

APPENDIX 7

Papers and internal reports

Part 1: Lees, J. A. 1993. Hysteresis Properties of Environmental and Synthetic Materials: Linear Additivity and Interaction Effects. *Manuscript Submitted to Geophysical Journal International.*

Part 2: Lees, J. A. and Pethick, J. S. 1993. Problems associated with Quantitative Magnetic Sources of Sediments of the Holderness Coastline, North Yorkshire, UK. *Manuscript Submitted to Earth Surface Process and Landform.*

Part 3: Lees, J. A. and Dearing, J. A. 1994. Use of VSM Generated Hysteresis Loops in Environmental Magnetism: Advantages and Comparisons to Other Measuring Equipment. *Environmental Magnetism Laboratory Working Paper No. 1.* Geography Division, Coventry University.

Hysteresis properties of mixtures of environmental and synthetic materials: Linear additivity and Interaction effects

Joan A. Lees

June, 1993

ABSTRACT

Mineral magnetic measurements have been used recently to classify and linearly model the sources of sediments through environmental systems. To enable wider application of linear modelling techniques using magnetic properties research has been conducted in the first part using laboratory mixtures of up to 6 source materials including both natural environmental materials and synthetic compounds. It has been found that even with the most magnetically differentiable materials difficulties are encountered with the linear modelling of the sources of the mixtures. The focus of this paper is an investigation into the causes of the failure of linear modelling on laboratory mixtures. These included source homogeneity, calibration and linearity of measuring equipment, magnetic viscosity of materials and the changing physical characteristics of the source materials once mixed together, in terms of interaction effects. In tests of linear-additivity χlf is the most reliable parameter while IRM$_{880}$ suffers from a systemmatic error in the predicted results. Results have shown that in the best controlled conditions where the sources are identified and are artificially mixed together, the results of linear modelling are quite poor and at best 4 sources can be mixed.

Key Words: Environmental Magnetism, linear modelling, laboratory mixtures

1. Introduction

The ability to model quantitatively the movement of materials, river sediments or pollutants for example, through environmental systems is of utmost importance today. Recently in Environmental Magnetism there has been a move from the more qualitative studies to those which begin to quantify the movement of source materials and their proportions in resulting environmental mixtures (Yu and Oldfield, 1989 and 1993). The mineralogy of individual sources is also of great interest, where the individual magnetic minerals and grain sizes can be identified quantitatively (Thompson, 1986). This paper presents investigation of the physical properties of environmental materials and mixtures is required to assess the suitability of modelling magnetic properties. The main assumption made of magnetic measurements are that they are linearly additive and therefore can be used in the linear calculations used in linear modelling and multivariate statistics. Testing the linear additivity is difficult, but a vital prerequisite to the use of magnetic properties in environmental modelling.

Source heterogeneity is a property of individual materials being traced or quantified which is not sufficiently taken into account in the modelling techniques. Potential sources of lake sediment cores and stream sediments used in tracing experiments are often only characterized by tens of samples. If natural variability is such that, for example to lower the standard deviation of a property of a source samples need to be taken every 100m^2 then, much of the tracing and quantification work to date is at best only a very rough guide. In this work natural variability has only

been studied in terms of sub-sample homogeneity not spatial variability in the environment.

In the mixing of environmental materials, little is known of the new physical criteria which arise in the mixture. Interaction effects arising from the mixing of different grain sizes and different minerals are focused upon in this work. Even though dispersion of the magnetic fraction in natural samples could be thought to be good, as the percentage concentration is often less than 1% (in rocks for example, Dunlop, 1981), there is scope for the concentration of iron oxides, with inclusions and coatings and also the clustering of bacterial magnetosomes. Magnetic minerals may be concentrated in areas due to their density also, so dispersion of magnetic minerals in environmental materials may not be as good as some laboratory dispersions. This work represent experiment on the properties of laboratory mixtures of environmental and synthetic materials, however, so limitations on the techniques can be set before environmental applications are made.

2. Methodology and Experimental Procedure

2.1 Setting the hypotheses

The following hypotheses are the possible contributory causes of error in the linear additivity of laboratory mixtures made at Coventry and are the factors investigated here:

(1) Source inhomogeneity: The mean of the sub sample population used in forward calculation does not account for certain mixtures having above or below average magnetic properties. (Even more of a problem in the environment than in laboratory experiment)

(2) Experimental error in the linearity of measuring equipment over higher attenuator scales than x 1, results in higher errors at larger scales.

(3) The presence of viscous grains in certain sources (eg topsoils) cause a rapid loss of IRM in the sources and less loss in the mixtures with lower proportions of the same sources. This is a linear effect but might be affected by inhomogeneity of the sources.

(4) Grain interactions are higher in the sources than in the mixtures which cause a relative reduction in the predicted calculation. This could possibly be caused by a strongly interacting material (eg chimney slag) having many particle-particle interactions which lessen once dispersed in a mixture. Alternatively source samples will contain more particles which may have high internal demagnetizing fields which are then 'diluted' in the mixtures.

2.2 Sample preparation

The material used in the experiments are listed in Table 1. Materials were chosen on the basis that they were as magnetically different as possible. The dominant magnetic properties of the materials are also given, for instance, the arable topsoil is dominated by fine-grained ferrimagnetic minerals while the Keuper (red) clay is dominated by canted-antiferromagnetic minerals with high coercivities. Analr chemical compounds were also included to give paramagnetic and diamagnetic materials. For mixing experiment 1 samples were air dried and sieved using a 2mm sieve, the bulk sample was used in the mixtures. Ten subsamples were packed into plastic 10ml pots. For mixing experiment 2 samples were air dried and finely ground until apparently homogenous (all material was <63μm), five subsamples were prepared. Coefficients of variations could then be calculated for the subsamples to quantify source homogeneity. Source materials were added to a plastic tray in various proportions until approximately 12 grams was reached, each source added being weighed at each stage. The percentage of each source was then calculated and used in the forward calculations. Each mixture was mixed thoroughly and carefully packed into a 10ml pot. Pots were completely filled to minimize varying sample volumes and packing densities.

As mixtures made up into 10ml pots could not be accurately subsampled into 0.5g holders (for measurement on the Vibrating Sample Magnetometer), five new mixtures (Mixtures 72 - 76) were made.

2.3 Measurement and interaction parameters

Magnetic measurement was made on all the samples, sources and mixtures, at the same time. This avoided any calibration changes between the sources and mixtures. Low field and high field susceptibility (χlf, χhf) were measured on a Bartington MS2 system. Anhysteretic remanent magnetization (ARM) was imparted using a Molspin AC field demagnetizer and susceptibility of ARM (χarm) was calculated. Isothermal remanence measurements at fields (mT) of 0, 5, 10, 15, 20, 50, 100, 150, 200, 250, 300, 400, 600, 880mT and a backfield of -100mT were imparted using Molspin pulse magnetizers and all remanence measurements were made using a

Molspin 'Minispin' Fluxgate Magnetometer. $HIRM_{-100}$ was calulated from IRMs 880 and -100 as an indicator of canted-antiferromagnetic minerals (Oldfield, 1991)

In order to test the interaction problem, source materials and some mixtures were further analysed. One axis alternating current (AC) and direct current (DC) demagnetization curves were measured at fields of 0, 5, 10, 15, 20, 40, 80, and 100 mT. Values of coercivity of remanence (Hcr), remanent acquisition coercivity (H'_{cr}) and the median destructive field of IRM ($H_{1/2I}$) were found from these (see Figure 1). A measure of the interaction field (H_{int}) is also made as the difference between H'_{cr} and H_{cr} (Spratt, et al 1988). Wohlfarth's R ratio values were read from the point of intersection of the IRM acquisition curve and the DC demagnetization curve projected onto the y axis and the R value was also read from the AC demagnetization curve (Maher, 1988) for comparison. Source materials a1, a2, a3, a5 and a6 and five new mixtures (nos. 72-76) were made up into 0.5g Vibrating Sample Magnetometer (VSM Molspin Instruments) and hysteresis loops were measured, saturation magnetization (M_S), remanent saturation magnetization (M_{rs}) and coercivity (H_C) were taken from these curves (Figures 3).

In order to test the linearity of magnetic measurements artificial mixing experiments were undertaken. Firstly twenty different source materials, some natural and some synthetic compounds were measured and classified using concentration dependent (linear) magnetic measurements (low and high frequency susceptibility, χ_{lf} and χ_{hf} in μm^3 kg^{-1} and a range of isothermal remanence measurements, ARM, IRM_{880} and IRM_{-100} in $mAm^2\ kg^{-1}$). Cluster analysis and principal components analysis were performed on the data and eight sources were chosen for their different magnetic properties. Ratios of parameters were not included in this analysis as they are not linearly additive and therefore were not suitable for the modelling techniques applied here. Two artificial mixing experiments were carried out, 71 mixtures were made using up to 6 sources of varying magnetic properties and grain sizes (Table 1). For mixing experiment 1, 10 subsamples of each source were measured and the mean used in the calculations, in experiment 2 five subsamples were measured. The actual measurement of the mixtures was compared to that of a forward calculation of the sum of the source measurements multiplied by their proportions in the mixture. The example given is for 'saturation' isothermal remanent magnetization (IRM_{880mT}):

$$\text{Predicted } IRM_{880i} = \sum_{i}^{n} IRM_{880i} * x_i$$

Where IRM_{880i} = Actual measurement of IRM_{880} of source i

x_i = proportion of source i in the mixture

where i = 1, 2, 3, ...n

An error term was calculated from this data as the difference between predicted measurement and actual measurement as a percentage of the predicted measurement.

3. Experimental Results

3.1 Linear Additivity Results

It was found that susceptibility (χ) measurements were within a 5% error and usually lower than 2% (Figure 2a). Remanence measurements however had associated errors of up to 15% (mean of 71 mixtures, Figure 1b). This error was large enough to cause poor prediction of the known source proportions using linear programming techniques (cf. Yu and Oldfield, 1989).

In Figure 2b the predicted measurement values are lower than the actual measurement values and a systematic offset exists. The failure of the linear programming is caused by this offset in remanence measurements and as we need more than susceptibility to characterize materials when using linear programming and classification techniques the phenomenon prompted further investigation. It must however also be noted that some mixtures do fall on the line y=x marked in Figure 2, and that the error shown by other mixtures is actually reasonably constant over all scales.

Figure 2c gives overall results of the success of the 71 artificial mixtures in terms of the number of sources and the percentage error between the predicted and the actual mixture measurement results (as described in section 2). It can be seen that although the best possible source materials were chosen even some mixtures with only two and three sources failed.

3.2 Sample Homogeneity

To compare the variation between the 10 subsamples of each of the sources the coefficient of variation (CV%) was used (see Webster and Oliver, 1990). CV% is calculated as follows:

$$CV\% = \frac{\text{standard deviation } (\sigma)}{\text{mean } (x)} * 100$$

Table 2 gives the results of the coefficient of variation for mass specific (linear) measurements, for the two experiments. The variability is reduced slightly in the ground samples but variables which take the difference of two measurements (χ_{fd} and HIRM-100) have large variation of up to 26% (ground Keuper clay) and 27% (coal). For χ_{lf} and ARM the coefficient of variation is low and only up to 10% and 15 % for coal and bedload samples. However these results show that significant variation in the magnetic fraction of samples exists even in ground laboratory materials and chemical compounds. The three chemical compounds used, Bentonite, Barium sulphate and Manganous Carbonate all have high mass-specific χ_{fd} coefficient of variation values which reflects the error of measurement of χ_{lf} and χ_{hf} in these extremely weak samples (thus χ_{fd} would not be used in linear programming)

The variability range of the subsamples was tested using IRM_{880mT} values for experiment 2 mixtures. The largest and smallest measurement values of the source subsamples were used in two separate recalculations of the predicted measurement values. It was found that this made little change in the outcome and the systematic offset remained. The variability here may explain some of the error but does not explain the offset seen in all the remanence data.

3.3 Calibration of equipment

Calibration of the Molspin Minispin involves use of a thin section of magnetic tape with previously calibrated saturation magnetization of 928 mAm^{-1} which is set into a wooden block of similar dimensions to the 10ml plastic pots used for samples. It is suggested that there may be some error involved in the calibration of 10ml cylindrical pots in this way and that a calibration sample of similar size and shape to the samples is needed. This presents many difficulties however, in the type of material which could be used in these quantities.

In order to test the calibration a cross calibration with a vibrating sample magnetometer (VSM) using IRM_{880} (Molspin) and Mrs (VSM) measurements was made. The VSM is calibrated using a small piece of paramagnetic palladium rod with a saturation magnetization of 31.23 mAm^2 at 1000mT. The VSM samples measured in this paper were given a magnetization of 1000mT in the VSM and their remanence at zero field was recorded. The samples were then inserted into an empty 10ml pot vertically so as to keep the sample in the same measurement orientation; and remanence was re-measured on the Molspin. The results of this exercise are given in Table 3 and shown graphically in Figure 4. The results show that although the Molspin gives lower results (up to 20%) the relative percentage is not different over the range of strengths of materials as shown in Table 3. It is not perceived therefore that the calibration of the Molspin for making remanence measurement is worse over larger attenuation ranges. A reduction in the Molspin measurement could be due to some loss of IRM over the time it took to finish VSM measurements. It must be noted here that a residual field of approximately 0.5 to 1.5mT has been detected on remanence measurements made on paramagnetic materials using the VSM in another experiment. This is caused by the sample remaining between the pole magnets whilst a zero field measurement is made. This differs to the Molspin as the sample is not remote from the source of the initial magnetization. This could have accounted for the higher VSM remanence measurements but upon correction for the residual field (creating 0.07 $mAm^2\ kg^{-1}$ moment) the values of Mrs were not considerably lower for most of the samples.

3.4 Viscosity of Source Samples

The presence of viscous grains in the samples was not believed to be a problem in the samples as generally there was greater error in larger grained samples (single domain Keuper clay) and most of the mixtures containing topsoil as a source worked well. The remanence values of the samples were taken c.20 seconds from imparting a magnetization so time differences were kept to a minimum. The effects of viscosity should act linearly throughout the source and mixture system but may be affected by source homogeneity. The ratio $\chi_{fd}\%$ is often used to implicate the presence of viscous grains in samples (Maher, 1988), however the $\chi_{fd}\%$ results of the sources and mixtures used in this study were very low, the highest being the topsoil sample with a value of 5.8%. The case for viscous effects creating the systematic offset in the remanence data was therefore not valid.

3.5.1 Interaction effects

IRM and both demagnetization curves were plotted to find values for the interaction parameters (these mainly indicate SD interparticle interactions, Cisowski, 1981). For non-interacting grains the curves should be symmetrical, for interacting grains the IRM curve is steeper at higher fields (with higher coercivity) and the demagnetization curve higher at low fields (with lower coercivity) (Cisowski 1981). Investigations into possible complex interaction effects included the use of three coercivity parameters defined by Dankers (1981). First the coercivity of remanence (H_{cr}) and secondly, the median destructive field of IRM ($H_{1/2I}$) have been used in the characterization of the stability of remanence carrying minerals in rocks. Thirdly, coercivity of remanence acquisition (H'_{cr}) indicates the field strength required to magnetize a material to half of its saturation remanent magnetization. Ratios of these parameters indicate the relative amounts of interaction in a material. In materials with no interaction, $H'_{cr} = H_{cr} = H_{1/2I}$, where the grains in the material are homogenously distributed and randomly orientated (Dankers 1981). This relation should hold true for hematites, but for magnetites $H'cr > Hcr > H_{1/2I}$, therefore ratios $H'cr/Hcr$ and $H_{1/2I}/H_{cr}$ in a non-interacting material will equal 1. It is reported that ratios of $H'cr/Hcr$ with values of 1 to 1.5 indicate strong interaction fields (Maher 1988) while $H_{1/2I}/H_{cr}$ may be more indicative of shape anisotropy of grains rather than packing density (Dunlop 1981). However $H'cr/Hcr$ at a value of 1 should indicate no interaction so values greater than 1.5 have been interpreted as having interactions in this study. Dankers found that for dispersed minerals of grain sizes between 5 and 250μm the following relationship exists:

$$H'_{cr} - H_{cr} = H_{cr} - H_{1/2I} \quad \text{or} \quad H'_{cr} + H_{1/2I} = 2H_{cr} \quad (1)$$

Dunlop (1986) and Maher (1988) report a similar relationship for fine grained magnetites and this relationship is found to be a reasonable description of the samples in this paper indicating that in coarser grain sizes (multidomain) larger internal demagnetizing fields may be important whereas in finer grain sizes interparticle interaction will dominate. The ratios H'_{cr}/H_{cr} and $H_{1/2I}/H_{cr}$ are plotted in Figure 5 for the environmental samples, a few MT samples (Maher 1988, hysteresis parameters measured by the author) and Dankers' hematites, magnetites and titanomagnetites using his published coercivity data (Dankers 1981). It can be seen that while $H'cr/Hcr$ is approximately 1 for a few samples (bentonite, Keuper clays), $H_{1/2I}/H_{cr}$ has a different constant value of approximately 0.6, these data are shown in Table 4. The environmental samples which are mixtures of many minerals and grain sizes fall within the bounds of the pure minerals of Dankers (1981), however chimney slag, coal and mixtures containing these do not fall into this region (source proportions of these mixtures are given in Table 1). Interestingly, the MT samples fall further towards Danker's titanomagnetite/hematite samples indicating that the ultrasonic dispersion of these appears to be better than some of the environmental samples, where clusters or concentrations of magnetic minerals may exist.

In this paper R ratios are compared from the DC demagnetization curve and compared to the AC demagnetization curve (used by Maher 1988), the results are presented in Table 4. R values taken from the DC curves are less than those of the AC curves. The AC (one axis) demagnetization seems less effective at reducing remanence at lower fields than the DC demagnetization where the magnetization direction of particles is reversed rather than reduced. Also of interest is the change in R value with the grinding of source samples for mixing experiment 2. There is a reduction in the DC R value in the ground mine spoil of 0.04 and in Keuper clay of 0.06, indicating that MD grains could have possibly been broken into smaller more interacting grains of near single domain (SD) size. A similar pattern is shown by the $\chi_{fd}\%$ results, slight reduction in $\chi_{fd}\%$ is seen in all ground samples compared to the bulk counterparts which seems to display the opposite to the R values results. χ_{arm} shows an increase in the ground samples for all four compared source materials indicating the decrease in grain size with grinding. In the topsoil however there is little change. R values of the chemical compounds are comparable to those of the environmental materials, even though iron concentrations of these homogenous materials is as little as 0.001%. The fact that there is a contamination in these materials allows their remanence measurement. The superparamagnetic (SP) grains of the manganous carbonate (classified as SP in Figure 6) are interacting and could clump to produce SD like effects. The χ_{fd} (%) result for manganous carbonate is very low however and is affected by the dia- and paramagnetic components in this material. The R values of the mixtures fall within the range of the source components which indicates that perhaps this ratio does not tell us enough of the type of interaction between the magnetic particles of a material.

To enable some grain size classification of the sources and mixtures, Hc has been plotted against Hcr (Figure 6) and Mrs/Ms against Hcr/Hc (Figure 7). Values for SD magnetite, MD magnetite and hematite (Thompson and Oldfield, 1986) have been plotted onto Figure 7 for comparison. The mean grain size of the MT samples indicate that they are SP (0.016, 0.022, 0.023μm) and SD (0.036μm). The actual grain size distributions include SP and SD grains (Maher 1988) and here the samples act as MD (0.016, 0.022, 0.023μm) and PSD (0.036μm) grains (cf. Thompson

and Oldfield, 1986). The shape of these grains is important, as they are cuboid (B. Maher, pers. comm.) they have a larger volume than other synthetic acicular grains and appear as larger grains having lower coercivities than expected. Also in cuboid grains there may exist some small domains in the corners of the grains which contribute to the lower coercivities. Dankers (1981) also reports that the coercivity of acicular single domain grains is larger than that of equidimensional grains. There is scope then for internal demagnetization and interparticle interactions in these samples, the environmental samples display similar phenomenon. Mixtures of the manganous carbonate and Keuper clay (Mix 52, 75, 75r) act as MD materials while mixtures of Keuper clay and PSD materials (mine spoil, Mix 72, 73) appear as PSD materials.

3.5.2 χarm and Hint results

ARM is a parameter which is extremely sensitive to interaction effects (Sigiura, 1979). It seems sensible therefore that using the scheme of Spratt et al (1988) χarm is compared to another measure of the interaction field, H_{int}, where:

$$H_{int} = H'_{cr} - H_{cr} \quad 2$$

H_{int} is thought to be representative of many body interactions (interparticle). A linear relationship between χarm and the inverse of H_{int} was found by Spratt et al (1988) where an increase in χarm followed a decrease in the interaction field (brought about by heating) in SD synthetic powders and audio and visual magnetic tapes. Relation 2 can also be directly related to relation 1 and results can be directly compared. Figure 8 shows the results of this paper in comparison to those of Spratt et al (1988). As values of $1/H_{int}$ move toward zero interaction effects are increased. H_{int} results comply reasonably with those of the R values, interaction fields (H_{int}) are similar or greater in bulk samples than in ground samples. This indicates that the type of interaction measured here could be different to that of the R value where internal properties within large particles seem to be indicated; here interparticle interactions are indicated. However it must be noted that the interaction in these samples (from R values) although comparable to those of Spratt et al (1988) the χarm values are less affected. The R values are comparable to those of Maher (1988), but the χarm values here are much higher. The low χarm intensity of the manganous carbonate does compare however, indicating increased interaction mechanisms in this material. There is one exceptional sample in the data set, the bulk Keuper clay indicates much more interaction than its ground counterpart even though R values are very similar for these two source materials, this is generated by a larger than expected Hcr value (Table 4).

4. Discussion

The solving of source proportions in mixtures using magnetic properties, whether laboratory or natural, presents many interesting but complex problems. Results from laboratory mixtures, where the actual outcome can be tested against the predicted outcome, have been extremely difficult to interpret. In the environment where we may never know the true source contributions to mixtures, it is of utmost importance to define or quantify, from laboratory experiment, limitations of linear modelling of sediment or mineral sources. The experimental mixtures have to a certain extent given an indication of the complex problems of quantifying source contributions magnetically and enabled limits to be set on the number and types of materials which can be modelled successfully.

Much work has been done on precipitated (Maher 1988), broken and sieved (Dankers 1981) and natural (Dunlop 1981) magnetite minerals. Little investigation has been done on the mixing of minerals or natural materials (whole assemblages of different minerals and grain sizes and oxidation states) of soil, sediments, dusts and anthropogenic sediment sources such as spoil heaps and atmospheric contributions, which may contribute to sediment mixtures. Mixing of synthetic minerals such as hematite and magnetite has proved difficult as the strength of the ferrimagnetic components, unless diluted to minute amounts, masks the hematite property. The mixing of environmental samples which will contain similar small quantities in an already dispersed state seems sensible, even though the exact mineralogical and grain size properties are known and interaction will occur. The dispersion of pure minerals of discreet grain sizes has proved to be very complex, yet data such as Maher's (1988) MT series is invaluable in the modelling of environmental magnetites and provides one of the best analogues for use with natural materials (as shown here also).

Magnetic properties of materials are affected by many contributory factors including grain size distributions, grain shapes, domain configurations, dispersion, interaction and mineral types. Some of these have been discussed here, interaction in the source samples has been found to be of similar proportions to the mixtures (from R values) but may be of a different type of interaction.

5. Conclusions

(1) Magnetic variability has been proven to exist in magnetic properties even for finely ground materials and chemical compounds. Tests using the entire range of experimental data have shown that the variability is not the cause of the systematic error in the remanence data however.

(2) Calibration of the Molspin has been tested and data is reliable against the VSM. Increasing inaccuracy with increasing attenuator scales on the Molspin is thought not to be the cause of the remanence data errors.

(3) Any loss in remanence caused by the presence of viscous grains or even by non-constant timing whilst magnetizing and measuring remanences would not be greater for the sources than the mixtures. Low χ_{fd} (%) results indicate that there are few viscous grains present in the samples.

(4) Complex grain interactions have been found to exist in the sources and mixtures. The R values of the mixtures fall within those of the sources but it is proposed that H'_{cr}/H_{cr} and $H_{1/2I}/H_{cr}$ ratios indicate some possible differences in the type of interactions between the source materials and the mixtures.

Continued study of the effects of mixing environmental and other materials together is needed before accurate and solid interpretations of modelling results of environmental mixtures can be made. The results show that there are complex properties caused by the mixing of materials and the cause of the systematic error found in the 71 laboratory mixtures. It is suggested that hypothesis 4, the case for complex interaction effects must be considered very seriously. Tests of the other hypotheses have eradicated them as being the major cause of non linearity of magnetic properties when mixing. With the use of various types of measuring equipment it is suggested that calibration and linearity are tested by using artificial mixtures. Once an average error value of the non linearity is known for any single piece of equipment a correction factor can be introduced such that the results presented in Figure 1 are brought more to unity ($y = x$). This correction can also be made for future environmental sediment sourcing studies measured using this equipment.

In the environment sorting of particles (possibly magnetic grain sizes in themselves) could lead to a large difference in internal properties of mixtures to those of the sources which may contain a wider assemblage of grain sizes, densities and concentrations of minerals. Denser particles, magnetites for example, even though small enough for transportation may be preferentially sorted and deposited in high concentrations in areas different to those of the mixture in question. Thus the mixture may have higher concentrations of magnetic materials than the sources of the materials and therefore more potential for interaction effects upon measurement.

Environmental variability is different to that found for samples in this paper, as the same source material would not be as intensively subsampled for a source tracing exercise. The variability of natural samples is therefore potentially much higher, for example, it has been found (by the author) that in a transect of 455m, field measurements of χ_{lf} made every 5m reveal a coefficient of variation of 57% for topsoil and 15% for subsoil. Also small highly magnetic particles in some sources may not be transferred to environmental mixtures in the same quantities, resulting in variation. Such variability either has to be excluded in mixing models and a realistic conclusion drawn as to the effect of variability on the results; or the variability to be taken into account in the modelling.

Acknowledgements

I would like to thank Professor Roy Chantrell and Dr Kevin O'Grady for invaluable research discussion on fine particle physics. I thank Dr John Dearing for his support and discussion of my research. I am also grateful to Dr Barbara Maher for allowing re-measurement of her new MT samples and for discussion on aspects of my work. Dr Pete Lockett provided much help with the mathematics and modelling and Dr John Dearing and Sue Charlesworth read an earlier draft of this paper and I thank them for their useful comments. This work represents part of a research project funded by PCFC and held at Coventry University.

References

Cisowski, S. 1981. Interacting and non-interacting single domain behaviour in natural and synthetic samples. Phys. Earth Planet. Inter., 26:56-62

Dankers, P. 1981. Relationship between median destructive field and remanent coercive forces for dispersed natural magnetite, titanomagnetite and hematite. Geophys. J. R. astr. Soc., 64:447-461

Day, R., Fuller, M. and Schmidt, V.A. 1977. Hysteresis properties of titanomagnetites: grain size and compositional dependence. Phys. Earth Planet. Inter., 13:260-267

Dearing, J.A., Lees, J.A. and White, C. 1993. Mineral magnetic properties of gleyed soils under different forest stands. Draft in prep.

Dunlop, D.J. 1981. Rock magnetism of fine particles. Phys. Earth Planet. Inter., 26:1-26

Maher, B.A. 1988. Magnetic properties of some synthetic sub-micron magnetites. Geophysical J., 94:83-96

Oldfield, F. 1991. Environmental Magnetism - A personal perspective. Quaternary Science Reviews 10, 73-85.

Spratt, G.W.D., Fearson, M., Bissell, P.R., Chantrell, R.W., Lyberatos, P. and Wohlfarth, E.P. 1988. Interaction fields and the anhysteretic susceptibility of recording media. IEEE Trans. Mag., 24:1895-1897

Thompson, R. 1986. Modelling magnetization data using SIMPLEX. Phys. Earth Planet. Inter. 42:113-127

Thompson, R. and Oldfield, F. 1986. Environmental Magnetism. Allen and Unwin.

Wasilewski, P.J. 1973. Magnetic hysteresis in natural materials. Earth Planet. Sci. Lett., 20:67-72

Yu, L. and Oldfield, F. 1989. A multivariate model for identifying sediment source from magnetic measurements. Quat. Res., 32:168-181

List of Tables

1. Source materials used in the artificial mixing experiments and their magnetic properties and source components of mixtures analsyed in this paper
2. Coefficient of variation on subsamples measured for artificial mixing experiments 1 and 2 (10 and 5 subsamples respectively)
3. Calibration data for the Molspin and VSM. Error is expressed as the difference between the VSM and the Molspin as a percentage of the VSM value
4. Hysteresis data for environmental and chemical reagent sources and mixtures and data for MT samples (Hcr and H'cr from Maher 1988)

List of Figures

1. Part IRM acquisition, AC and DC demagnetization curves (ground mine spoil) defining the coercivity parameters and R value used
2. Predicted versus Actual Measurements for (a) low frequency susceptibility and (b) saturation isothermal remanent magnetization (880mT). (c) shows the success rates for the mixing experiments in terms of the number of sources and the percentage difference error between predicted and actual mixture measurement.
3. Hysteresis loop for Keuper clay defining hysteresis parameters used
4. VSM IRM_{1000mT} remanence measurement versus Molspin IRM_{1000mT} remanence measurement for calibration test
5. H'cr/Hcr versus $H1_{/2}I$/Hcr indicating the amount of interaction by deviation of both from 1. Where H'cr/Hcr > 1 and $H1_{/2}I$/Hcr <1 interactions are present.
6. Hc versus Hcr for some of the source materials, mineral data from Thompson and Oldfield (1986) is added (after Wasilewski 1973)
7. Mrs/Ms versus Hcr/Hc for some of the source samples, mineral data from Thompson and Oldfield (1986) is added (after Day et al 1977)
8. Xarm versus inverse of Hint for environmental and chemical samples, results of Spratt et al (1988) are drawn on for comparison.

Table 1

Mixing Experiment 1

Component	*Dominant Magnetic Property*
a1 Arable Topsoil, Corley (Bromsgrove Series)	Ferrimagnetic
a2 Keuper Clay (Seeswood Pool, N Warks)	Canted Antiferromagnetic
a3 Mine Spoil (Soil and Coal Spoil)	Ferrimagnetic
a4 Chimney Slag (Gulson Hosp Boiler)	Ferrimagnetic
a5 Coal (Daw Mill Colliery)	Canted Antiferromagnetic
a6 Commercial Bentonite	Antiferromagnetic

Mixture 5	38% a1, 25% a3, 18% a4, 8% a5, 11% a6
Mixture 6	7% a1, 7% a2, 33% a3, 17% a5, 36% a6
Mixture 15	44% a1, 29% a2, 15% a5, 12% a6
Mixture 19	51% a2, 30% a4, 19% a5
Mixture 20	28% a1, 10% a2, 24% a3, 10% a4, 4% a5, 24% a6

Mixing Experiment 2

Component	*Dominant Magnetic Property*
a1 Arable Topsoil (Bromsgrove Series)	Ferrimagnetic
a2 Keuper Clay (Seeswood Pool, N Warks)	Canted Antiferromagnetic
a3 Mine Spoil (Newdigate Colliery)	Ferrimagnetic
a4 Bedload (Finham Brook, Coventry)	Ferrimagnetic
a5 Barium Sulphate	Diamagnetic
a6 Manganous Carbonate	Paramagnetic

Mix 21	56% a1, 44% a2
Mix 23	42% a2, 58% a3
Mix 28	26% a1, 74% a3
Mix 40	15% a1, 43% a2, 42% a4
Mix 52	63% a2, 37% a6
Mix 69	37% a3, 39% a4, 13% a5, 11% a6
Mix 72	26% a1, 74% a3
Mix 73	71% a2, 29% a3
Mix 74	35% a1, 65% a2
Mix 75	82% a1, 18% a6
Mix 76	38% a2, 62% a5
Mix 74rep.	57% a1, 43% a2
Mix 75rep.	42% a1, 58% a6

Table 3

Sample	VSM Mrs (mAm^2/kg)	Molspin Mrs (mAm^2/kg)	% Difference ((VSM-Mol)/VSM*100)
Chimney Slag	317.1	253.0	20.2
Daw Mill Coal	27.6	23.4	15.0
Keuper Clay	3.1	2.9	7.3
Topsoil	7.5	6.5	13.2
Mine Spoil	12.8	11.4	11.3
Baruim Sulphate	0.4	0.4	16.9
Manganous Carbonate	0.5	0.002	95.5
Mix 72	11.4	9.9	12.6
Mix 73	6.4	5.6	11.3
Mix 74r	4.9	4.2	15.9
Mix 75r	2.1	1.8	16.6
Mix 76	1.9	1.9	3.6

Table 2

Mixing Experiment 1

Variable	Keuper Clay	Arable Topsoil	Mine Spoil	Chimney Slag	Coal	Bentonite
χlf ($\mu m^3/kg$)	0	3.5	5.8	4.9	5.4	0
χhf ($\mu m^3/kg$)	0	3.6	5.8	4.9	5.4	0
χfd (nm^3/kg)	20.3	4.9	21.0	15.7	13.9	133
ARM (mAm^2/kg)	0	0	14.3	10.3	10.0	0
χarm ($\mu m^2/kg$)	7.1	5.0	9.7	9.8	9.7	20
IRM880mT (mAm^2/kg)	6.5	8.8	8.6	2.3	8.8	5.9
IRM-100mT (mAm^2/kg)	7.1	9.3	10.3	2.9	10.3	9.1
HIRM (mAm^2/kg)	6.5	10.1	9.4	11.8	27.3	0

Mixing Experiment 2

Variable	Ground Keuper Clay	Ground Arable Topsoil	Ground Mine Spoil	Ground Chimney Slag	Ground Bedload	Barium Sulphate	Manganous Carbonate
χlf ($\mu m^3/kg$)	0	0	1.0	7.9	7.7	0	0
χhf ($\mu m^3/kg$)	0	3.5	1.0	7.8	7.7	0	0
χfd (nm^3/kg)	26.4	5.2	14.1	12.8	19.8	37.0	13.3
ARM (mAm^2/kg)	0	0	0	5.4	0	0	0
χarm ($\mu m^2/kg$)	0	1.1	0.8	5.4	3.1	0	0
IRM880mT (mAm^2/kg)	0.8	2.7	1.2	5.2	7.2	6.1	0
IRM-100mT (mAm^2/kg)	1.1	3.6	1.2	4.4	13.0	0	0
HIRM (mAm^2/kg)	0.9	1.9	1.9	25.2	6	50	0

Table 4

Sample	χlf	χfd	χarm	IRM880	R Ratios		Hcr	H'cr	H1/2I	H'cr	H1/2I	1
	(μm^3/kg)	(%)	(nm^3/kg)	(mAm^2/kg)	AC Demag	DC Demag	(mT)	(mT)	(mT)	Hcr	Hcr	Hi
Chimney Slag	12.450	0.665	32.398	218.655	0.165	0.156	13.0	33.0	3.0	2.538	0.231	0.05
Ground Chimney Slag	10.832	0.535	34.433	209.166	0.29	0.20	23.0	43.0	12.4	1.87	0.539	0.05
Mine Spoil	0.966	0.679	1.785	9.529	0.3	0.22	30.0	53.0	15.2	1.767	0.507	0.044
Ground Mine Spoil	1.020	0.526	2.560	12.088	0.28	0.18	30.0	53.0	15.0	1.767	0.5	0.044
Keuper Clay	0.084	3.390	0.138	2.032	0.46	0.4	420.0	350.0	283.0	0.833	0.674	0.014
Ground Keuper Clay	0.087	1.415	0.184	2.476	0.34	0.34	353.0	337.0	208.0	0.955	0.589	0.062
Topsoil	0.291	5.807	2.527	4.846	0.325	0.25	33.0	50.0	17.78	1.515	0.539	0.059
Ground topsoil	0.309	5.247	2.889	4.988	0.315	0.25	30.0	43.0	14.76	1.433	0.492	0.077
Bedload	0.135	1.595	0.670	2.244	0.39	0.32	30.0	63.0	14.56	2.1	0.485	0.03
Coal	3.160	0.400	2.520	22.255	0.245	0.146	13.0	33.0	8.0	2.538	0.615	0.05
Bentonite	0.071	0.719	0.051	0.157	0.39	0.3	33.0	40.0	22.44	1.212	0.68	0.143
Barium Sulphate	0.010	2.703	0.058	0.345	0.285	0.21	33.0	53.0	19.0	1.606	0.576	0.05
Manganous Carbonate	1.099	0.226	0.002	0.003	0.31	0.24	33.0	60.0	19.0	1.818	0.576	0.037
Mixture 5	3.046	0.531	7.357	56.681	0.27	0.20	23.0	37.0	14.3	1.609	0.622	0.071
Mixture 6	0.793	0.496	1.179	8.144	0.26	0.20	30.0	53.0	15.34	1.767	0.511	0.044
Mixture 15	0.515	0.987	1.146	5.912	0.27	0.21	33.0	67.00	16.2	2.030	0.491	0.029
Mixture 19	3.982	0.910	10.248	75.73	0.255	0.14	17.0	40.0	10.0	2.353	0.588	0.044
Mixture 20	1.640	0.813	4.246	31.47	0.275	0.22	27.0	40.0	13.69	1.481	0.507	0.077
Mixture 21	0.205	5.536	1.792	3.919	0.325	0.28	47.0	73.0	22.5	1.553	0.479	0.038
Mixture 28	0.847	1.245	2.930	11.082	0.27	0.22	30.0	53.0	14.04	1.767	0.468	0.044
Mixture 40	0.121	4.235	0.778	2.574	0.325	0.21	67.0	150.0	21.3	2.239	0.318	0.012
Mixture 69	0.551	0.403	1.387	5.962	0.285	0.2	27.0	53.0	16.875	1.963	0.625	0.038

Table 4 cont

	Mrs (Am^2/kg)	Ms (Am^2/kg)	Hcr (mT)	Hc (mT)	H'crH1/2I (mT)	(mT)	Mrs / Mr	Hcr / Hc	H'cr / Hcr	H1/2I / Hcr
Ground Keuper clay	0.003	0.007	335.0	31.0			0.434	10.806		
Ground Topsoil	0.009	0.05	27.0	9.5			0.179	2.842		
Ground Minespoil	0.013	0.146	36.0	7.0			0.088	5.143		
Barium Sulphate	0.000	0.001	46.0	15.5			0.264	2.968		
Mixture 72	0.011	0.125	39.0	7.0			0.088	5.571		
Mixture 73	0.006	0.055	54.0	10.0			0.111	5.4		
Mixture 74	0.004	0.014	75.0	14.0			0.270	5.357		
Mixture 76	0.002	0.004	221.0	25.0			0.496	8.84		
Manganous Carbonate	0.000	0.0	33.0	0.001			0.0			
Mixture 75	0.002	0.002	54.0	1.5			0.912	36.0		
Mixture 74r	0.004	0.014	75.0	10.5			0.299	7.143		
Mixture 75r	0.002	0.002	54.0	2.0			0.982	27.0		
Ground Keuper clay	0.003	0.005	353.0	30.5			0.577	11.574		
Ground Topsoil	0.005	0.022	30.0	11.0			0.242	2.727		
Ground Minespoil	0.015	0.195	30.0	6.0			0.078	5.0		
Bedload	0.002	0.010	30.0	9.5			0.19	3.158		
Barium Sulphate	0.000	0.001	33.0	16.0			0.302	2.062		
Manganous Carbonate	0.000	0.000	33.0	0.0			0.0			
Mixture 23	0.010	0.092		6.5			0.108			
Mixture 52	0.001	0.0		1.5			0.0			
Chimney Slag	0.314	0.49	13.0	8.0			0.641	1.625		
Daw Mill Coal	0.026	0.118	13.0	4.5			0.223	2.889		
MT14 (0.022µm)	0.054	0.543	19.0	4.5	22.5	11.5	0.1	4.222	1.184	0.605
MT15 (0.023µm)	0.053	0.605	19.0	5.0	22.5	11.5	0.088	3.8	1.184	0.605
MT18 (0.016µm)	0.046	0.536	13.5	3.0	14.0	8.5	0.087	4.5	1.037	0.63
MT26 (0.036µm)	0.094	0.639	20.0	8.0	25.0	15.5	0.146	2.0	1.25	0.775
MT31 (0.031µm)	0.079	0.540		7.5		11.5	0.147			
MT35 (0.04µm)	0.113	0.650		11.5		11.5	0.174			
MT36 (0.035µm)	0.071	0.461		10.0		8.5	0.153			
MT40 (0.05µm)	0.070	0.542		8.0		15.5	0.13			
MT52 (0.012µm)	0.039	0.520		3.5			0.075			
MT55 (0.045µm)	0.148	0.649		14.0			0.227			

Figure 1

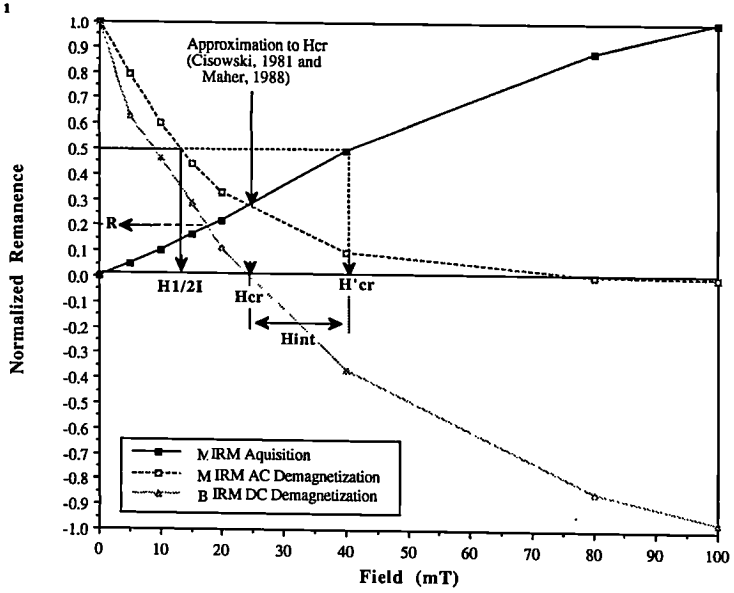

Figure 1a

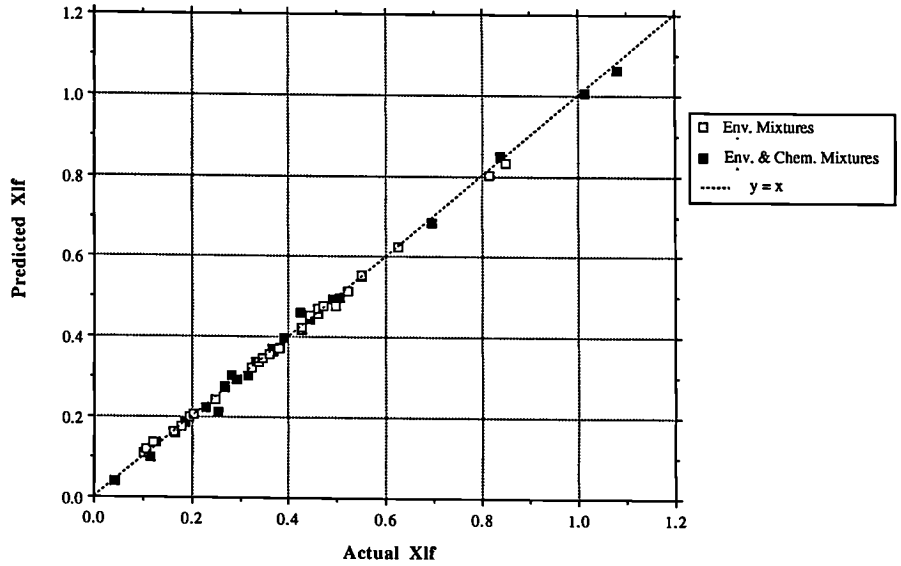

Figure 1b

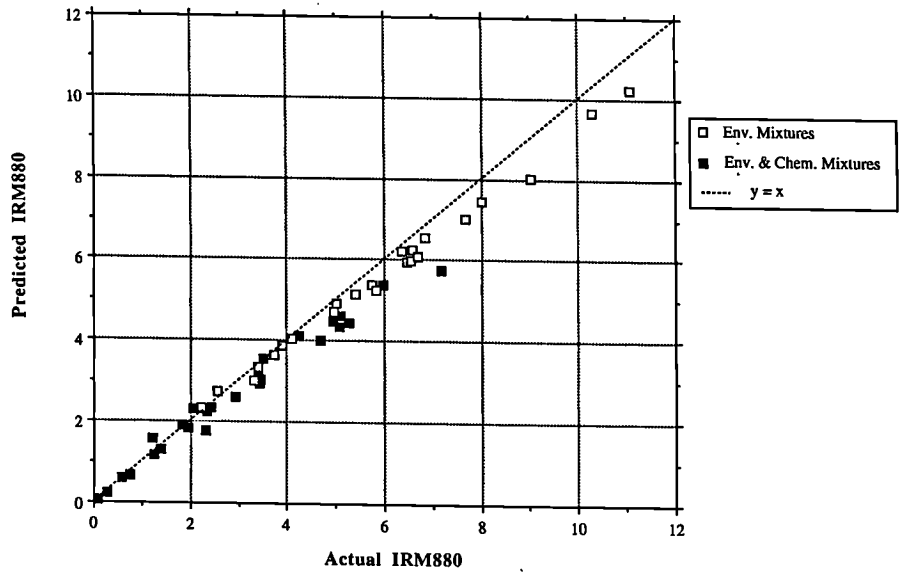

Figure 1c

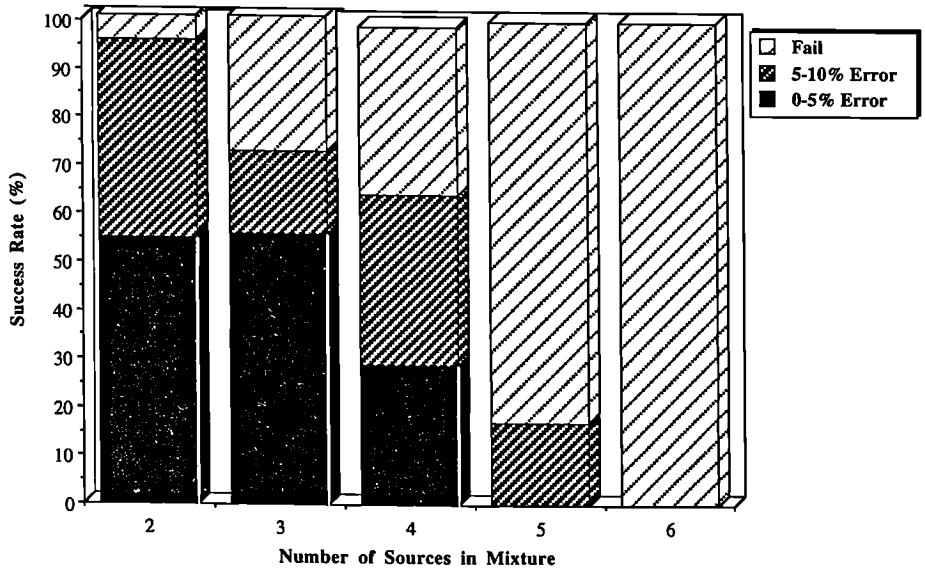

Figure 3

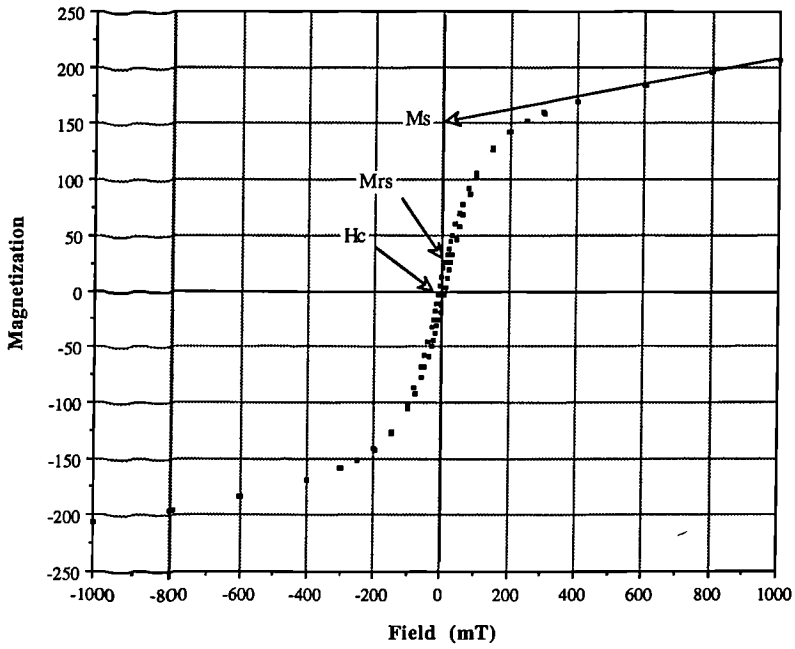

Figure 4

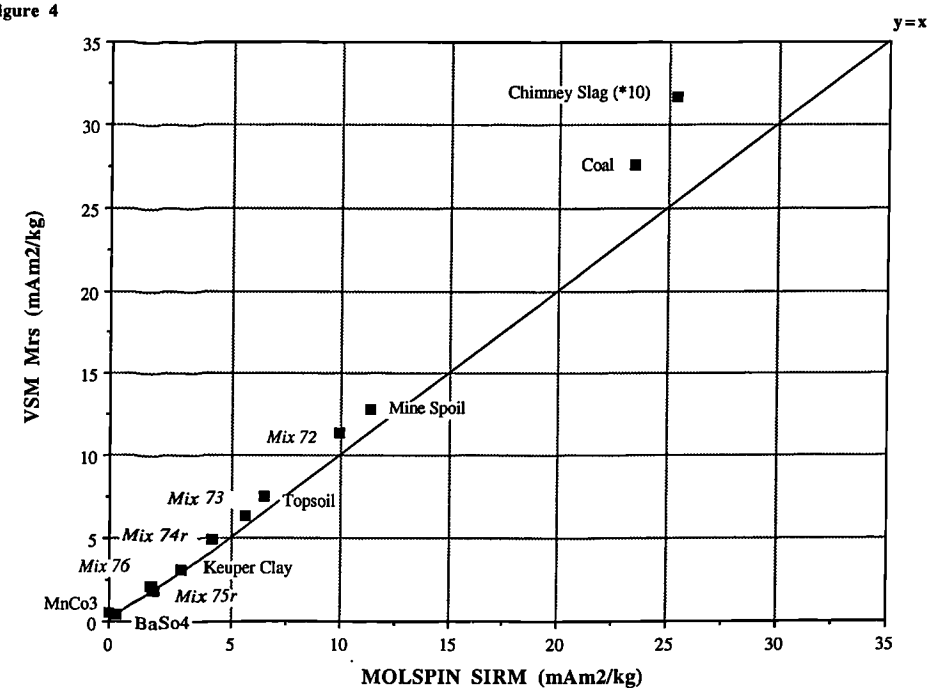

Figure 5

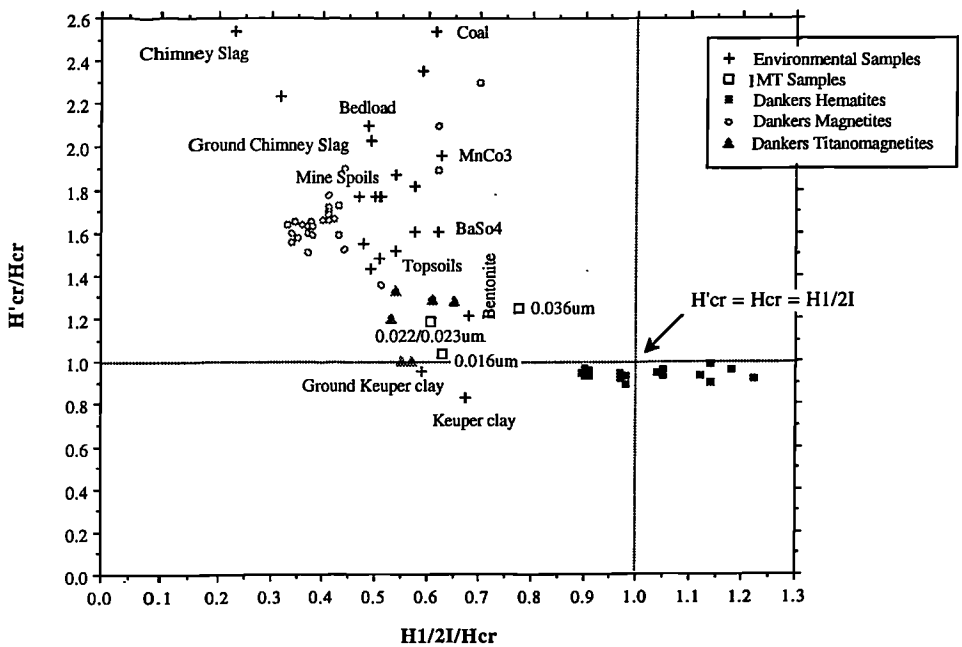

Figure 7

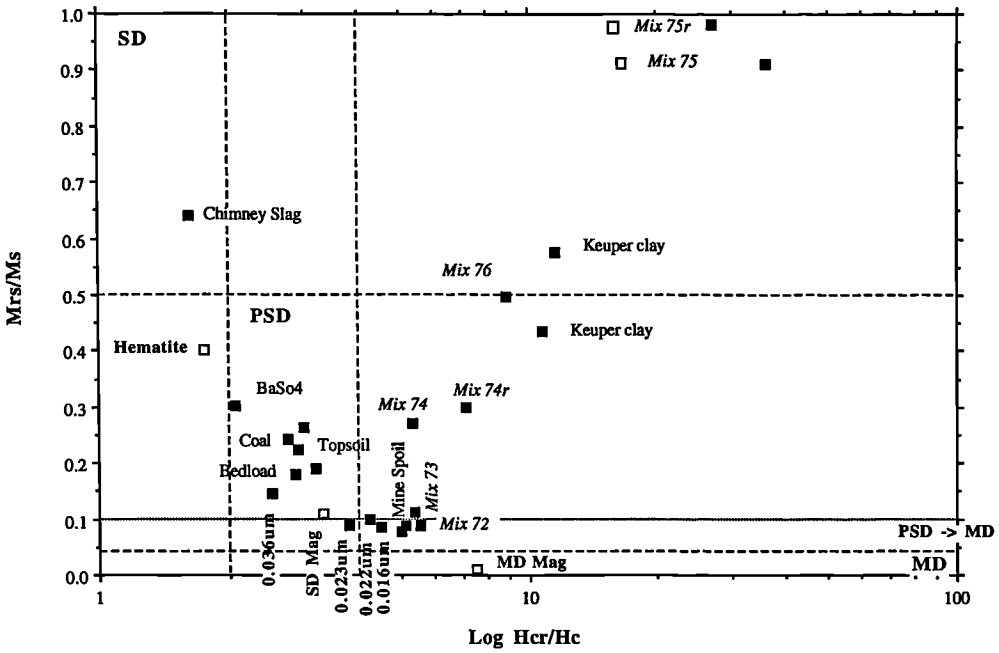

Figure 6

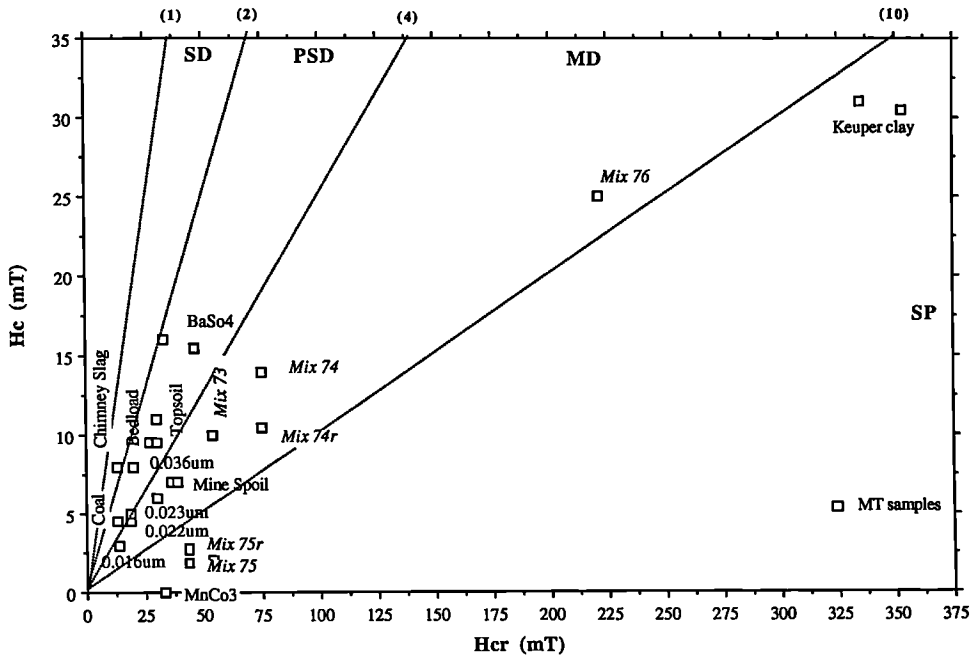

Figure 8

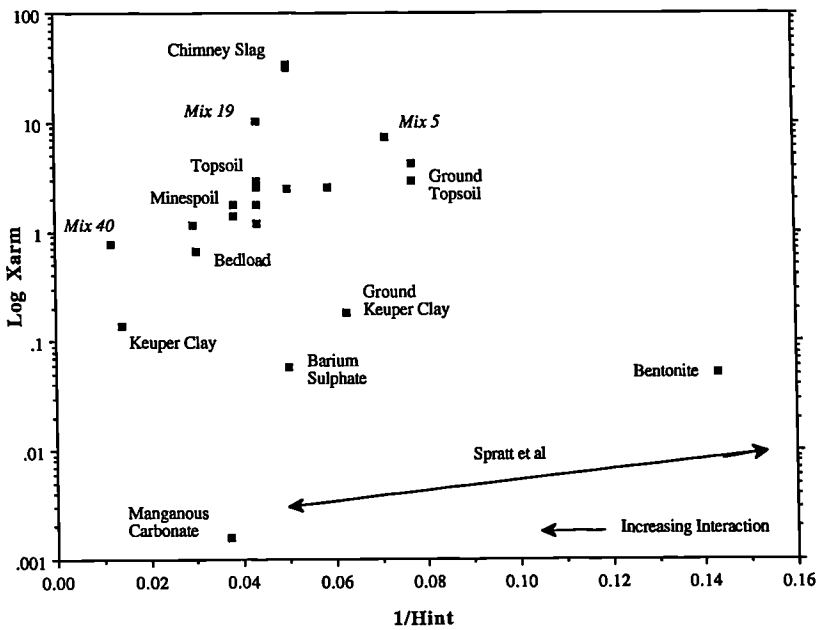

SHORT COMMUNICATION

PROBLEMS ASSOCIATED WITH QUANTITATIVE MAGNETIC SOURCING OF SEDIMENTS OF THE HOLDERNESS COASTLINE, NORTH YORKSHIRE, UK.

J. A. LEES[1] and J. S. PETHICK[2]
November, 1993

1. *Centre for Environmental Research and Consultancy, Geography Division, School of Natural and Environmental Sciences, Coventry University, Priory Street, Coventry, CV1 5FB*

2. *Director of the Institute of Estuarine and Coastal Studies, University of Hull, Hull, HU6 7RX*

ABSTRACT

There are many problems associated with beach tracing and sand provenance in coastal studies over short and long timescales. Here an attempt has been made to trace the source sediments of the beaches along the Holderness coastline between Scarborough and Mablethorpe using magnetic techniques. The methodology employed involves classification and modelling of sediment sources and mixtures using their magnetic properties. Focus is given to a strong ferrimagnetic black sand (heavy mineral) which dominated the magnetic signal of the beach mixtures. Quantifying and tracing this mineral will indicate wave energy and sediment movement processes along this coastline. The paper presents results so far.

KEY WORDS Coastal sediment sourcing, Beach tracing, Mixtures, Magnetic field survey, Coastal erosion.

INTRODUCTION

The beaches and cliffs of the Holderness coastline (Figure 1) are eroding rapidly at an average rate of 2 metres per year. This Figure is a conservative estimate in some local areas where erosion may have increased with the building of local sea defences. This problem is compounded by the naturally unstable till cliffs of the area. Along most of the Holderness coastline the low water mark is moving inland at a rate of 1m per year due to rising sea levels (Pearce, 1993) and isostatic readjustment of the land after the last glaciation.

Along the coastline of Holderness it is estimated that 480 square kilometres of land have fallen into the sea along with 36 villages since Roman times (Pearce, 1993). This stretch of coastline is the North Sea's largest single source of sediment; some of the coarser sediment moves south to Spurn Head (a natural spit) while finer sediments move off-shore and may eventually reach the Essex saltmarshes or the coastlines of Denmark, the Netherlands and Germany (Dosser, 1955; Pethick in Pearce, 1993). There are four specific questions which are proposed in this study, first, can the beach be sourced magnetically; second, what is the source of the black sand and can it be quantified; third, where do the till materials go and finally can magnetic techniques be used successfully to infer coastal processes and the redistribution of coastal sediments.

The main objective of this study was to source the beach sediments along a section of the eastern coastline of Britain and to identify the number of lithological units which contribute sediment. The aims of the study are as follows:

1. To use magnetic properties to identify and quantify the sources of the beach sediment.
2. To find the source of and quantify a specific sediment on the beach and to trace that sediment using magnetism.
3. To evaluate the use of magnetism in the classification and modelling of coastal sediments.

Magnetic techniques have been used in modelling and sediment sourcing by a number of workers (Thompson, 1986, Yu and Oldfield, 1989) and have been evaluated for use in classification and linear modelling by the author (Lees, 1993). Also glacial tills have been magnetically differentiated by Walden et al (1987). Little has been done in the area of coastal sediment sourcing using magnetism. However heavy minerals on beaches have been traced using radiometric survey (Greenfield, 1989; Schuilling, 1985).

AREA OF STUDY

The chosen area, the coastline between Scarborough and Mablethorpe (Figure 1), includes coastal features such as Spurn Head (shingle spit) a chalk headland (Flamborough Head) and salt marshes in and south of the Humber Estuary (Spurn Head and Saltfleet). The solid geology of the area is given on Figure 1, the only site at which the

chalk is clearly visible on the coast is at Flamborough head where the chalk is uplifted and resistant. Between Flamborough north to Filey and south to Spurn the beaches are backed by glacial tills with complex stratigraphies. South of Spurn at Cleethorpes and Mablethorpe the till cliffs were not evident and the beaches of the area were wide and receive mainly Humber estuary sediments.

The glacial tills of the area are of the Wolstonian and late Devensian ages. A Wolstonian basement till is thought to exist below the Devensian tills (Jones and Keen, 1993) but this was not observed at sampling locations. The tills which were sampled in the field are, first, a dark brown drab till termed Skipsea till which lies at the base of the cliffs. This was only exposed from Mappleton northwards. Secondly, between Hornsea and Spurn a red/purple till outcrops (Withernsea Till), the limit of which is marked on Figure 1. The Withernsea till overlays the Skipsea till and in between them in places there are lacustrine varved sediments with clear laminations and sand and gravel layers. At Barmston (outside the Withernsea till limit) there is a complex stratigraphy where a sand layer/till of approximately 7m in depth overlies the Skipsea Till and is clearly bedded which suggests a fluvio-glacial origin. Above this was a clearly defined soil profile with dark topsoil (50cm) and weathered subsoil (1m). A till similar to the Withernsea till has been identified in Filey Bay (Edwards, 1981), but it was difficult to distinguish between the Filey tills and Withernsea tills in the field. The till cliffs range in height from 1m to 30m along the coastline, at the sites studied the cliffs were about 15m in height lowering to 1m at the landward end of Spurn. The tills carry many erratics and these were considered as potential sources for the beach. Many erratics were local chalks and limestones with negligable magnetic mineral input, some igneous and sedimentary rocks.

The beaches were found to consist of mainly quartz sands and the black sand which was identified microscopically as basalt crystals. The black sand was concentrated in lines parallel to and near to the cliffline and in summer clear banding of the black sand could be seen in the beach profile. In winter, black sand was concentrated at the surface of the beach and no depth banding was apparent as shingle underlay about 5 cm of sand. Shingle contained different rocks from the tills with many flint and limestone pebbles.

METHODOLOGY AND TECHNIQUES

Preliminary study

Sources of the beaches were defined primarily from solid and drift geology maps and secondly from observations in the field. Sources of all contemporary materials on the beaches of Holderness were included, this does not account for the original sources of the glacial till and erratics or the direction of circulation and deposition of North Seas sediments. Only landward sources of sediment were included and the glacial tills were considered the main source of material to the beach. Seaward sources proved too difficult to sample. Many other beach materials such as wreckage from sea defences, housing collapse and industrial waste seemed to be very localised and were not included. The only material which was well distributed on beaches other than the sand and shingle was washed coal, this could have come from mine waste tips locally or further north or from the tills (it was seen in Skipsea Till), this was included in the study.

Field survey

Initial fieldwork included a survey using a hand held magnetic susceptibility meter and D loop sensor (Bartington Instruments Ltd) which measures Kappa (volume susceptibility). The variability of the tills and the beach sands was found using 50 measurements (Table 2). Beach Kappa transects were carried out at Barmston, Mappleton and Tunstall in order to trace the black sands over the beach profiles. Transects were surveyed every 5m using an Abney level and field kappa was measured every 1m along the transect, resultant profiles are shown in Figure 5.

Sampling and sample preparation

Spot samples of tills, black sands near the cliffs and white sands towards the sea were taken. Other samples included erratics from the tills and other geological specimens were collected from the beach. Some data were available from a magnetic database of British geologies also.

In total, fifty three samples were collected, air dried, sieved at 2mm and packed into 10ml pots ready for magnetic measurement. Remaining samples were sieved into 6 particle size ranges (Figure 2) and where enough material existed fractions were packed again for magnetic measurement. Magnetic black sand particles were extracted using a 200mT hand magnet and dispersed in magnetically weak calcium carbonate so that magnetic properties of the black sand could be obtained.

Magnetic measurement

A range of magnetic measurements were made on bulk and fractioned samples including low and high frequency susceptibility (χ_{lf} and χ_{hf} in $\mu m^3\ kg^{-1}$, at frequencies 0.47 and 4.7kHz, measured on a Bartington MS2

instrument), anhysteretic remanent magnetisation (ARM in $mAm^2\ kg^{-1}$ measured on a Molspin Fluxgate magnetometer). Isothermal remanent magnetisations were measured at various fields between zero and 880 milli Tesla (IRMs in $mAm^2\ kg^{-1}$, measured on a Molspin Fluxgate magnetometer) so that IRM curves (growth of remanence with field) could be plotted. Ten hysteresis curves were also measured on a Vibrating Sample Magnetometer (VSM, Molspin Ltd) for clear graphical representation of magnetic properties of sources and mixtures.

Susceptibility is a measure of the total ferrimagnetic component of a sample and the difference between two frequencies of susceptibility measurement ($\chi_{fd}\%$) indicate ferrimagnetic grains which are smaller than approximately 0.03μm. High $\chi_{fd}\%$ values indicate ferrimagnetic grains formed in soils rather than primary minerals from rocks. Remanence measurements indicate all remanence carrying minerals in a sample; ARM indicates finer grain sizes as does $\chi_{fd}\%$ but includes canted-antiferromagnetic minerals. IRM curves and IRM_{880mT} indicate acquisition of remanence and the largest acquisition value obtainable in this laboratory. The rate of acquisition indicates different minerals types. Hysteresis loops were used to graphically show the contribution of paramagnetic minerals in the samples as paramagnetic minerals do not hold a remanence and are therefore not indicated by remanence measurements. Saturation magnetisation (Ms) at 1000mT was used from the hysteresis loops to model the black sand. This measurement, of the total magnetic component of a sample, is not affected by interaction; however the small VSM samples are prone to inhomogeneity through sub-sampling especially in coarser materials. Fuller description of measurements may be found in Thompson and Oldfield (1986).

RESULTS

Discrimination of Sediment Sources

Particle size analysis indicated that in general white sands (taken 50m from the cliffs) were between 125μm and 1mm with 50 to 80% lying between 250 and 500μm. Black sand mixtures collected from the foot of the cliffs ranged from 63μm to 2μm, the dominant black sand fraction was 125 to 250μm and was associated with coarser quartz sands with 55% being between 500μm and 1mm. This reflects grain size and density relationships similar to those found by Schuiling (1983), where heavy minerals are deposited with coarser grains of lighter minerals. The tills particle size distributions ranged between <63μm and >2mm, with 80% between <63μm and 250μm. Cliff topsoils had a more normally distributed particle size distribution (Figure 2).

The colour of the particle size samples did not infer the source of the black sand. The source of the black sand was found to be upper cliff sands, sandy lenses and in the Skipsea Tills between Barmston and Bridlington. This was inferred from the susceptibility results, the black sand was not easily spotted in particle size distributions but upon magnetic extraction of cliff sand, black sand was found and compared magnetically, using $\chi_{fd}\%$ values of particle size samples, and microscopically to the beach black sand.

The magnetic measurements were highly interrelated and classification schemes such as principal components analysis were not applicable. The inter-correlation was caused by the dominance in the mixtures of the strong ferrimagnetic black sand. There was no other material with a sufficiently different magnetic property to counteract this effect. It was found that classification of the sources could be achieved successfully using only χ_{lf} and $\chi_{fd}\%$ indicating concentrations of ferrimagnetic minerals and their grain size respectively (Figure 3). The beach mixtures do not have $\chi_{fd}\%$ values over 1% indicating the coarser grain sizes present, whilst in the till, topsoil and saltmarsh samples much finer ferrimagnetic grains are present and $\chi_{fd}\%$ results are greater than 2. These results are highly related to the actual particle size results and reflect the energy of the environments in which each material was created and deposited. The finer magnetic minerals contributing to the $\chi_{fd}\%$ of the topsoils and tills are not found in the beach. Any analysis of new samples could then be restricted to these two indices for this particular environment and mineralogical situation.

Hysteresis loops indicated that the two tills and sandy lenses contribute both ferrimagnetic and paramagnetic minerals to the beach, but in the beach only coarser ferrimagnetic minerals remain. Hysteresis loops (normalised to Ms) for the 125-250μm sand fractions of the Withernsea, Skipsea till, cliff sand and a black sand beach mixture from Barmston are shown in Figure 4. It can be inferred that the ferrimagnetic minerals from mainly the upper cliff sand and Skipsea Tills contribute to the beach but are more concentrated in the beach than in the original source.

Quantification of black sand

The χ_{lf} and Ms values for the black sand dispersions were used to calculate the amount of black sand in the Barmston cliff sands. χ_{lf} has been found to be the most reliably linear magnetic measurement in laboratory tests (Lees, 1993) and from preliminary experiment Ms is more reliably linear than remanence measurements but prone to

sub sampling variability as shown by the calculation for the Skipsea till.

Upper cliff sand, bulk sample:

χlf ($\mu m^3 kg^{-1}$): 0.0556% black sand in till matrix

Ms ($mAm^2 kg^{-1}$): 0.05999% black sand in till matrix

Skipsea Till bulk sample:

χlf ($\mu m^3 kg^{-1}$): 0.0665% black sand in till matrix

Ms ($mAm^2 kg^{-1}$): 0.0388% black sand in till matrix

Modelling of the beach was impossible in terms of the general bulk of sand as the black sand dominated the magnetic properties; in linear modelling of the beach sand mixtures the solutions were 100% sandy cliff materials and 0% of all other source including erratics. However from the above calculations estimates of the contributions of black sand from the sandy cliffs to the beach can be made; taking a 1m section of cliff and beach where the sandy material comprises 7m of the cliff and the beach is 50m long and erosion rates are 2m yr (depth of beach not accounted for):

Upper cliff sand, bulk sample:

χlf ($\mu m^3 kg^{-1}$): covering of black sand on 50 * 1m surface of beach = 0.156cm

Ms ($mAm^2 kg^{-1}$): covering of black sand on 50 * 1m surface of beach = 0.168cm

Skipsea Till bulk sample:

χlf ($\mu m^3 kg^{-1}$): covering of black sand on 50 * 1m surface of beach = 0.186cm

Ms ($mAm^2 kg^{-1}$): covering of black sand on 50 * 1m surface of beach = 0.109 cm

However the black sands are generally concentrated in the first 10m of the beach, near the cliffs or in swash lines so re-calculating the above for 10m of beach gives 0.778cm, 0.84cm, 0.93cm and 0.54cm respectively. The lighter fractions could also be calculated as inputs from the cliff to the beach from the sandy cliffs at specific points along the cliffs by using the other 99.94% of the sand. Sand fractions from the other tills would have to be included also.

The great advantage of the magnetic property of the black sand is that it can be traced and mapped in the field very quickly as shown in Figure 7. The laboratory susceptibility measurements were calibrated with the field susceptibility measurements by counting and measuring black sand grains of different grain sizes held in 2 * 6cm sellotape strips. The results of this experiment are given in Table 3. There was a good linear relationship between the kappa of the sellotape strips and the number of grains and the following were calculated:

kappa of 1 grain of black sand = 0.0222
kappa 1g of black sand = 4033.33
where 1g = 181,682 grains

The field sensor measures approximately 75% of the total susceptibility as measured by the laboratory susceptibility meter (Bartington Instruments Ltd) in 6cm depth of material. If a kappa measurement on the beach was 75, the total susceptibility would be approximately 100. The number and weight of grains being measured can be estimated using the above calculations, this assumes that all the magnetic minerals on the beach are black sand grains:

kappa of 100 $\simeq$ 4505 grains of black sand
$\simeq$ 0.025 g of black sand

This gives an indication of the quantity of black sand in a homogenous area of beach being measured ($270cm^2$ by 6cm depth). Field susceptibility transects, shown in Figure 5, indicate concentrations of the black sand found in swash lines, at the turn of the tide and in low velocity steeper areas of the beach. At Mappleton black sand was deposited in the lee of granite groynes built parallel to the cliffline. The Mappleton transects also indicate changes to the beach profiles between and beyond the groynes since they were constructed in 1989. The major change being that the waves are reflected and broken by the granite groynes and do not proceed up the beach to the cliff foot, the difference is 9m. The transects indicate how the magnetic surveys can be used to map the distribution of the black sand and thus coastal processes on the beach.

DISCUSSION

There four specific questions raised in the introduction can be fully answered here. The beach can be sourced magnetically but only in terms of the ferrimagnetic black sand fractions in the till which limits the application of magnetism here. The tills are magnetically weaker and less variable than the beach sands and the different tills can be discriminated. Erratics and till sands are the major contributing sources of the beaches between Scarborough and Spurn. Estuarine sands may contribute to beaches south of the Humber Estuary. The black sand could be used to trace the movement of its associated larger grains of the lighter fractions of the beach, probably down to Spurn head. The black sand is delimited to the north by the outcrop of Oolite near Scarborough, where the tills end. Beach zones are variable because of sorting and zones of different minerals, particle sizes and particle densities are created. It is clear from both particle size distributions and magnetic measurement that the fines from the tills are removed and enter North Sea circulation and are deposited elsewhere. The southward movement of the black sand is interrupted by the Humber River as it was not found in Mablethorpe and Cleethorpes sands, here the sand flow must move out into the sea.

The input and amount of black sand can been fully quantified at specific points along the coastline at the moment. Further, more intensive magnetic surveys could reveal the spatial extent and movement of the black sand possibly more easily than that done using radiometric surveys elsewhere. Calculations of the energy required to move the black sand might indicate possible modelling avenues of the movement of sands in this area using the black sand as a tracer, as in this preliminary study. Past energy requirements, preserved in raised coastal stratigraphies, could be indicated also by the presence of heavy minerals like the black sand when magnetically analysed (David Smith pers. comm.). Certainly in the present environment spatial concentrations of the black sand indicates the day to day and season to season processes as shown by the transects.

CONCLUSIONS

The magnetic properties of sediments of the Holderness coastline have been evaluated for use in sourcing and modelling the beaches. One ferrimagnetic mineral in cliff sand deposits above the Skipsea tills and North of the Withernsea till limit dominated the magnetic properties of the beaches between Filey and Spurn. The Black sand is found in Filey bays in the small coves of Flamborough Head and from Bridlington to Spurn and could be used as a tracer for the coarser materials moving along the beaches towards Spurn Head.

The contribution of the black sand from the tills and its concentration on the beaches has been quantified for the Barmston site. Further modelling could include estimates of the spatial distribution of the black sands along the entire coastline concerned. Even with the fast rates of erosion the tills actually contribute little to the beaches in the area, much fine material is lost.

The main limitation of using magnetism here is that measurements are highly inter-correlated due to the magnetic property of the black sand. Mixture measurements were greater by orders of magnitude than the source measurements. However magnetic tracing in the field could provide valuable information quickly through regular monitoring of the processes occurring and the wave energies along this coastline.

ACKNOWLEDGEMENTS

Acknowledgments are due to Dr John Dearing for making useful comments on an earlier draft and for guidance with this work. Dr David Keen provided useful discussions on the geological aspects of this work, Dr Ian Foster and Professor Smith provided invaluable discussions and encouragement and Dr Ian Foster made corrections and useful comments on the paper. Sue Charlesworth made productive comments on an earlier draft. Rebecca Dann provided practical help in the field. This work was funded by a PCFC grant held at Coventry University and contributes towards the senior authors thesis.

REFERENCES

Bisat, W. S. 1939. 'The relationship of the 'Basement clays' of Dimlington, Bridlington and Filey Bays'. *The Naturalist*, May 1st, 133-125.

Catt, J. A. and Madjett, P. A. 1981. *'The work of W S Bisat FRS on the Yorkshire Coast'.* In J. Neale and J. Flenley (eds), The Quaternary in Britain. Pergamon Press, Oxford.

Dossor, J. 1951. 'The coast of Holderness: the problem of erosion'. *Proc. Yorkshire Geological Society* **30,** 133-145.

Edwards, C. A. 1981. *'The tills of Filey Bay'.* In J. Neale and J. Flenley (eds), The Quaternary in Britain. Pergamon Press, Oxford.

Greenfield, M. B. et al. 1989. 'Monitoring beach sand transport by use of Radiogenic heavy minerals'. *Nuclear Geophysics* **3**, 231-244.

Jones, R. L. and Keen, D. H. 1993. *Pleistocene Environments in the British Isles.* Chapman and Hall.

Lees, J. A. 1993. 'Hysteresis properties of mixtures of environmental and synthetic materials: Linear additivity and Interaction effects'. Draft Manuscript.

Lees, J. A. and Dearing, J. A. 1994. Use of VSM Generated Hysteresis Loops in Environmental Magnetism: Advantages and Comparisons to Other Measuring Equipment. *Environmental Magnetism Laboratory Working Paper No. 1.* Geography Division, Coventry University.

MacGarvin, M. 1990. *Greenpeace the seas of Europe: The North Sea.* Collins and Brown, London.

Pearce, F. 1993. 'When the tide comes in...'. *New Scientist* **137** (1854), 23-27.

Pringle, A. W.. 1981. *'Beach development and coastal erosion in Holderness, North Humberside'.* In J. Neale and J. Flenley (eds), The Quaternary in Britain. Pergamon Press, Oxford.

Schuilling, R. D. et al 1985. 'Grain size distributions of different minerals in a sediment as a function of their specific density. *Geologie en Mijinbouw* **64**, 199-203.

Steers, J. A. 1969. *'The coastline of England and Wales'.* Cambridge University Press. 2nd Edition, chapter 10, p 406-419.

Thompson, R. 1986. 'Modelling magnetization data using SIMPLEX'. *Phys. Earth Planet. Inter.* **42**, 113-127

Thompson, R. and Oldfield, F. 1986. *Environmental Magnetism.* Allen and Unwin.

Walden, J., Smith, J. P. and Dackombe, R. V. 1987. 'The use of mineral magnetic analyses in the study of glacial diamicts: a pilot study'. *J. Quaternary Science*, **2**, 73-80.

Yu, L. and Oldfield, F. 1989. 'A multivariate model for identifying sediment source from magnetic measurements'. *Quat. Res.*, **32**, 168-181.

LIST OF FIGURES

Figure 1. Location of study area and sampling sites. The limit of Withernsea till is marked on (Catt, 1987a in Jones and Keen)

Figure 2. Particle size distributions for samples from Barmston

Figure 3. Low frequency susceptibility (χ_{lf} μm^3 kg^{-1}) and frequency dependent susceptibility (χ_{fd}%) classification for the bulk samples. The samples are dominated by different concentrations (χ_{lf}) or grains sizes (χ_{fd}%) of ferrimagnetic minerals and a classification is marked.

Figure 4. Hysteresis loops of 125-250μm fractions of the Skipsea, Withernsea tills and black sand indicating the dominance of paramagnetic minerals in the tills and ferrimagnetic minerals in the black sand

Figure 5. Beach and kappa transects for three sites along the Holderness coastline, indicating the distribution of black sand down the beach related to beach profile and coastal processes.

Table I. Erratics reported in the tills (Catt and Madgett, 1981) and those measured (*).

Skipsea Till	Withernsea Till
chalk*, pink chalk, liassic shales*	chalk*, greywackes*
Carboniferous limestone*	Carboniferous limestone*
limestone*, Magnesian limestone*	Magnesian limestone*
Bunter Sandstone*, yellow sandstone*	Triassic shales, Liassic shales*
Scottish granites*, granites*	Cheviot porphyrites, igneous pebbles*
Norwegian larvikite*, Diorite*	
grey flints*, black flints*	
green greywackes*, rhomb porphyry	
Cheviot porphyrites, quartz porphyry*	

Table II. Variability results for the kappa surveys of the tills and beach sediments and for granite boulders used to build the groynes at Mappleton (Coefficient of variation (%) is sd/mean * 100).

Site/sample	Mean	standard deviation	coefficient of variation (%)	number in sample
Barmston				
beach transect	87.95	64.58	73.44	70
Skipsea till	36.88	4.86	13.19	50
sandy till	46	7.75	16.86	50
Mappleton				
beach transect 1	267.25	188.81	70.65	35
beach transect 2	217.42	157.79	72.58	35
cross beach survey	452.9	119.57	26.4	50
Withernsea Till	20.52	1.88	9.16	50
Granite groynes	536.78	527.41	98.25	50
Tunstall				
beach transect	187.54	90.18	48.09	70
Withernsea till	20.58	2.72	13.22	50

Table III. Calibration between numbers of black sand grains of different sizes and kappa measurements.

Grain Size	No of grains	Calculated actual wt (g)	Kappa	Kappa per grain
75-90	3876	0.0213	71	0.0183
90-125	2156	0.0119	39	0.0181
125-180	2312	0.0127	42	0.0182
180-250	2015	0.0111	51	0.0253
250-300	1837	0.0101	47	0.0256
300-500	539	0.0030	15	0.0278
Mean	2123	0.0117	44	0.0222
Sample	**Calculated no of grains**	**Actual wt (g)**	**Kappa**	**Kappa per grain**
Mixture	817	0.0045	18.15	0.0222

Figure 1: Area of Study showing solid geology and sampling sites

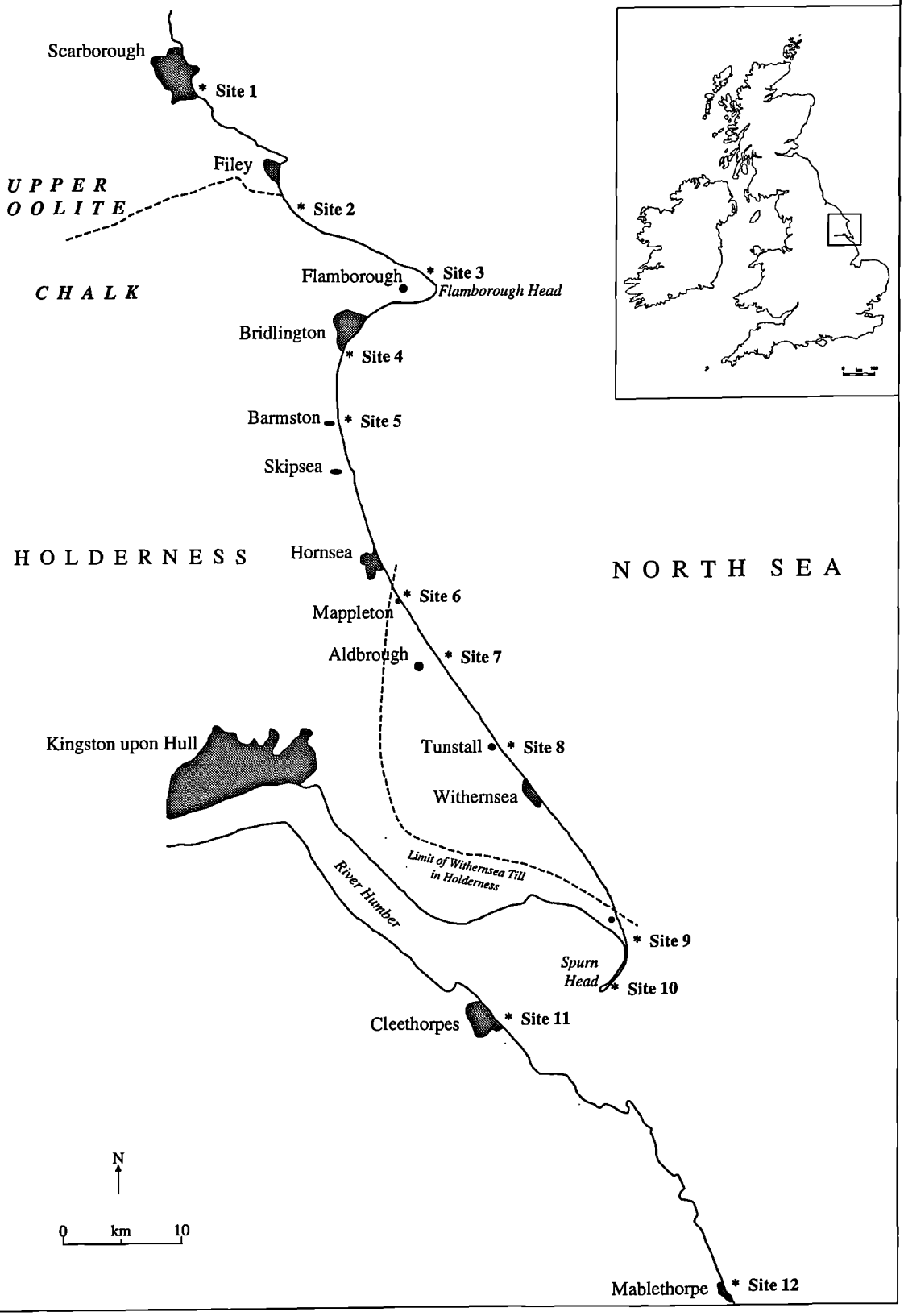

Figure 2

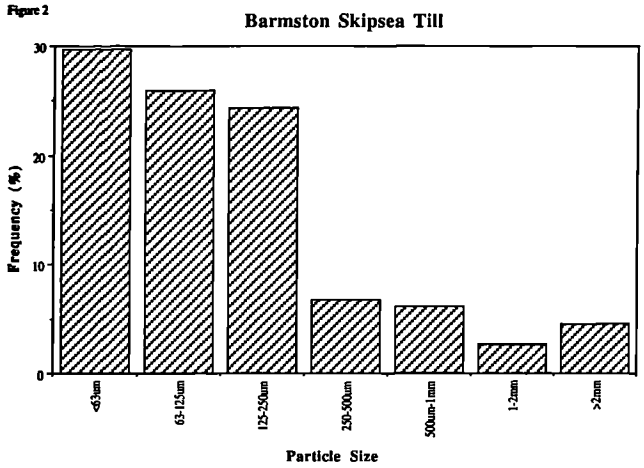
Barmston Skipsea Till
Frequency (%)
0
10
20
30
<63um
63-125um
125-250um
250-500um
500um-1mm
1-2mm
>2mm
Particle Size

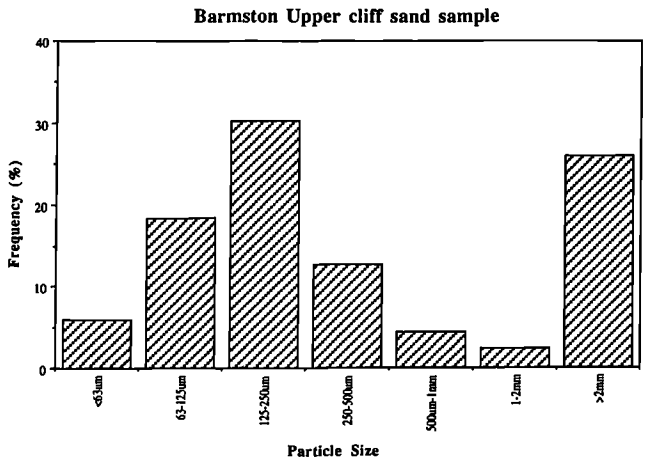
Barmston Upper cliff sand sample
Frequency (%)
0
10
20
30
40
<63um
63-125um
125-250um
250-500um
500um-1mm
1-2mm
>2mm
Particle Size

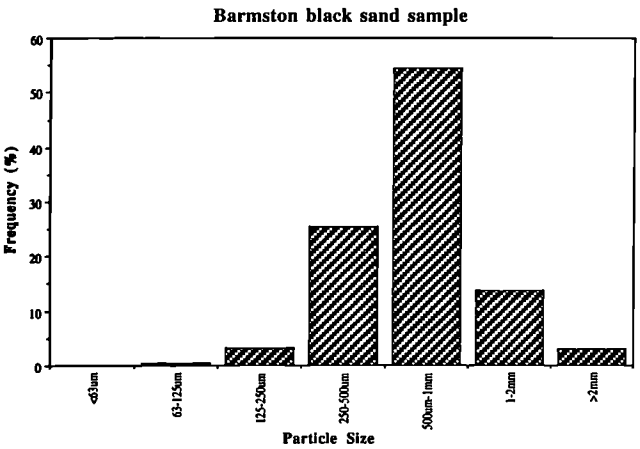
Barmston black sand sample
Frequency (%)
0
10
20
30
40
50
60
<63um
63-125um
125-250um
250-500um
500um-1mm
1-2mm
>2mm
Particle Size

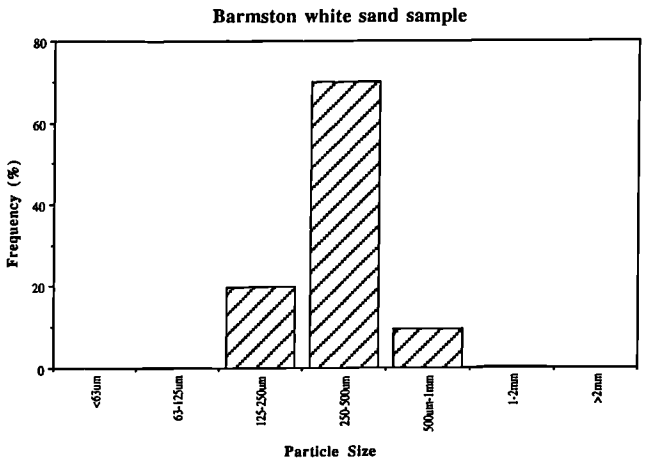
Barmston white sand sample
Frequency (%)
0
20
40
60
80
<63um
63-125um
125-250um
250-500um
500um-1mm
1-2mm
>2mm
Particle Size

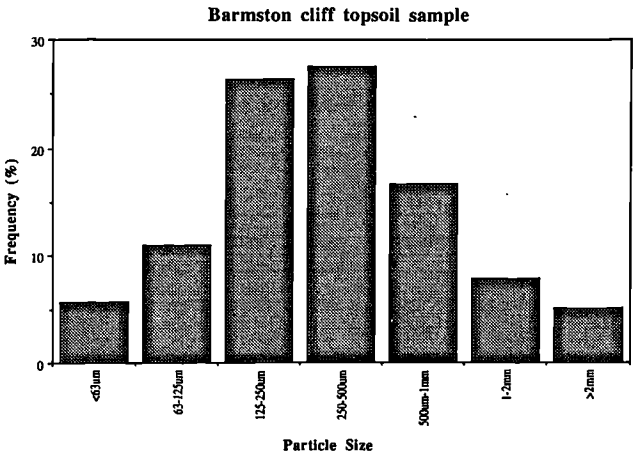
Barmston cliff topsoil sample
Frequency (%)
0
10
20
30
<63um
63-125um
125-250um
250-500um
500um-1mm
1-2mm
>2mm
Particle Size

Figure 3

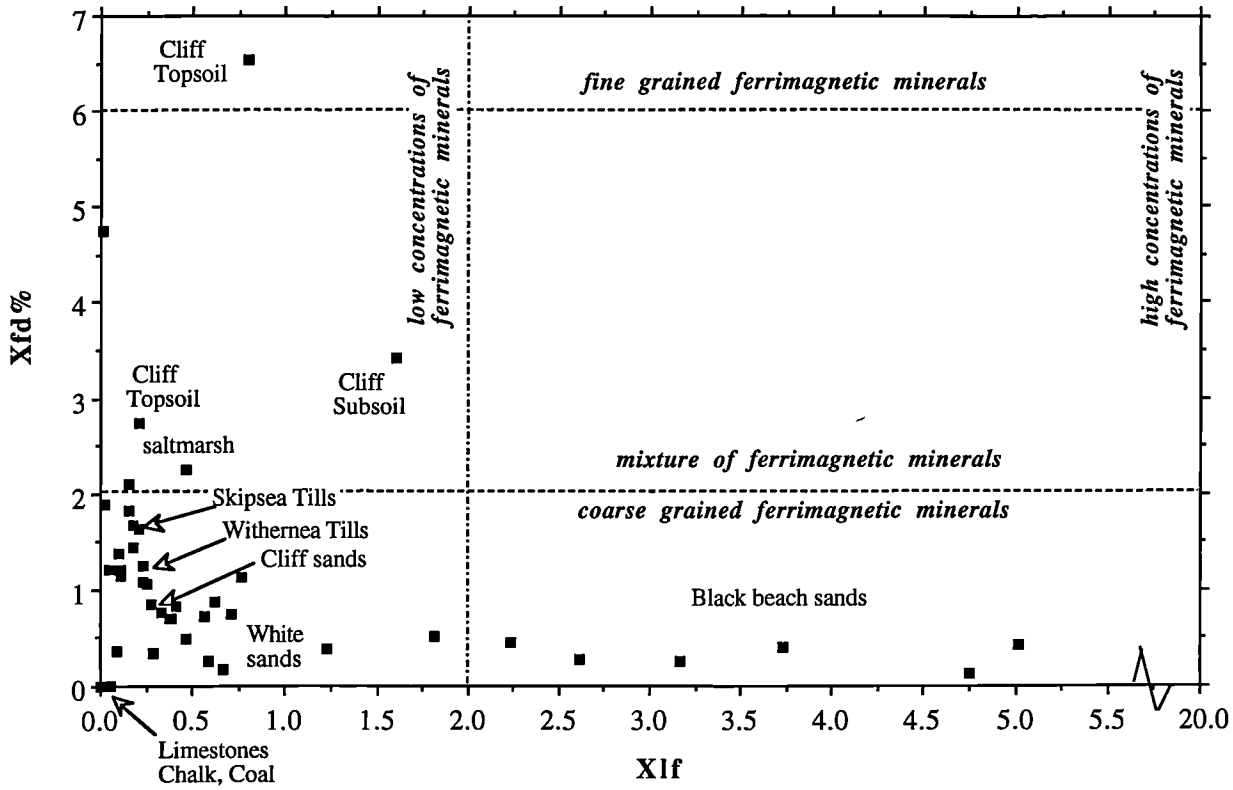

Figure 4:

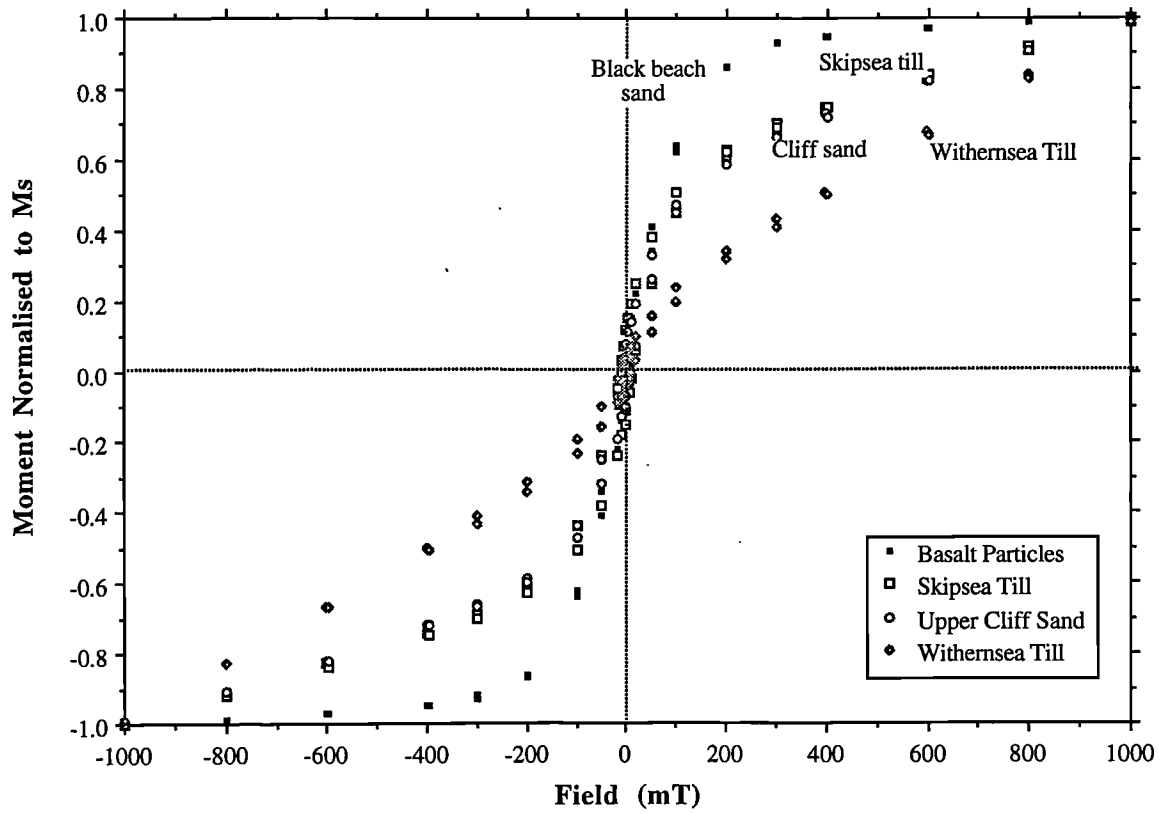

Figure 5

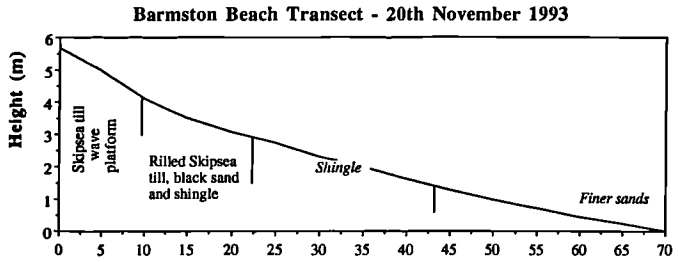
Barmston Beach Transect - 20th November 1993
Height (m)
Skipsea till wave platform
Rilled Skipsea till, black sand and shingle
Shingle
Finer sands

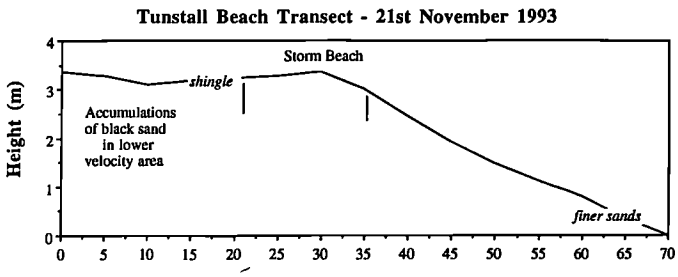
Tunstall Beach Transect - 21st November 1993
Height (m)
Storm Beach
shingle
Accumulations of black sand in lower velocity area
finer sands

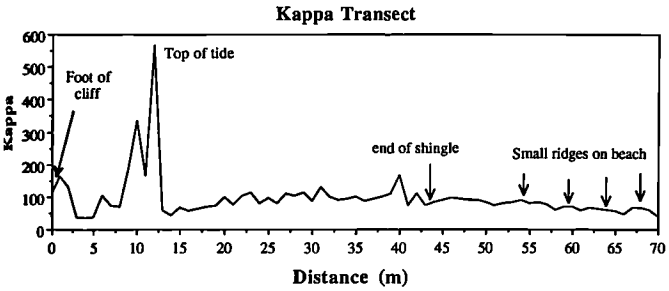
Kappa Transect
Kappa
Foot of cliff
Top of tide
end of shingle
Small ridges on beach
Distance (m)

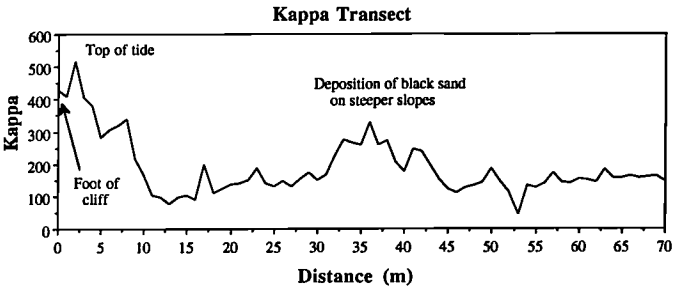
Kappa Transect
Kappa
Top of tide
Deposition of black sand on steeper slopes
Foot of cliff
Distance (m)

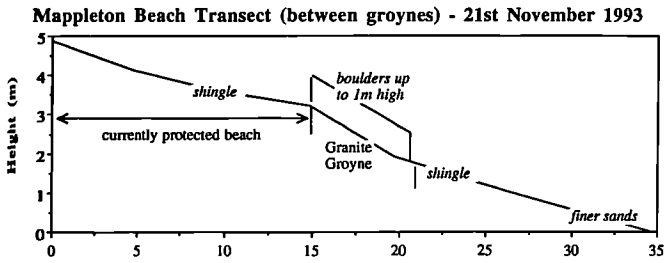
Mappleton Beach Transect (between groynes) - 21st November 1993
Height (m)
shingle
boulders up to 1m high
currently protected beach
Granite Groyne
shingle
finer sands

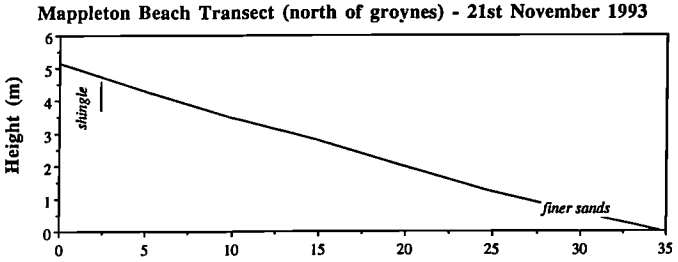
Mappleton Beach Transect (north of groynes) - 21st November 1993
Height (m)
shingle
finer sands

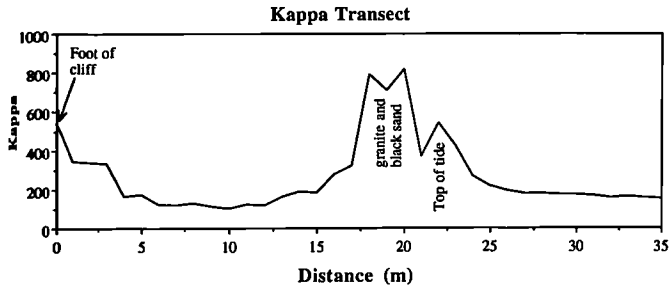
Kappa Transect
Kappa
Foot of cliff
granite and black sand
Top of tide
Distance (m)

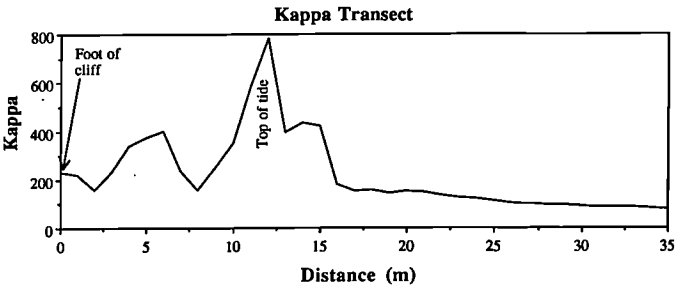
Kappa Transect
Kappa
Foot of cliff
Top of tide
Distance (m)

Use of VSM generated hysteresis loops in Environmental Magnetism: Advantages and comparison to other measuring equipment.

J. A. Lees and J. A. Dearing

Centre for Environmental Research and Consultancy, Geography Division, School of Natural and Environmental Science, Coventry University, Priory Street, Coventry, CV1 5FB.

28th February, 1994

ABSTRACT

Vibrating Sample Magnetometers (VSM) are increasingly used in the field of Environmental Magnetism for characterizing materials and modelling their magnetic properties. This paper presents the range of uses of the VSM for initial sample characterization, matching and modelling of sources and environmental mixtures. The advantages and disadvantages of the VSM are described and calibration experiments with other equipment have been undertaken.

Key Words: Environmental Magnetism, hysteresis loops, Nuvo Vibrating Sample Magnetometer (VSM), environmental modelling, technical calibration.

INTRODUCTION

Over the past few years, the use of vibrating sample magnetometers has been widening in the field of environmental magnetism. The ability to produce continuous measurements of both in-field and remanent magnetization through magnetic fields (generally between 1 Tesla and -1 Tesla) presents many advantages over the standard procedure of measuring low field susceptibility and a few parameters of remanence magnetization on different equipment. The hysteresis loops give clear graphical representations of the magnetic properties of materials from which is often more easily interpretable at a glance than sets of numbers for standard measurements. The loops are measured on a single piece of equipment which optimizes sample preparation, measurement and data handling time, and eliminates calibration comparisons between different measuring equipment. This is also an advantage in environmental modelling studies where greater accuracy in measurement means less error in solving for the source proportions of sediments. Thompson and Oldfield (1986) stated that the 'hysteresis diagram and parameters provide the most comprehensive magnetic characterization of natural materials without extravagant specialisation or excessive cost'.

This paper reviews the use of the Molpsin 'Nuvo' vibrating sample magnetometer (VSM) in providing hysteresis data for use in studies of environmental magnetism. Direct comparisons are made between measurements made on the 'Nuvo' VSM and the Molspin pulse magnetizer/fluxgate spinner magnetometer system and the Bartington MS2 susceptibility system.

HYSTERESIS DATA AND THEIR MEASUREMENT

Parameters which have been used consistently in environmental magnetism are initial low-field susceptibility and isothermal remanence measurements, and derived ratios which are used to discriminate between different materials. Table 1 gives a comprehensive summary of the most widely used parameters. With the use of the VSM many more parameters are available from the magnetization curve and the full hysteresis loop, including susceptibility at any field (eg. χ_{low}, χ_{high}), Ms (saturation magnetization) and Hc (coercive force). Figure 1 shows the range of data which can be produced in a matter of half an hour for a sample of semi-pure massive hematite. The hysteresis parameters in Table 1 are defined on the diagram.

An introduction to the use of hysteresis loops is given in Thompson and Oldfield (1986). They illustrate how sediments from Chesapeake Bay were discriminated according to hysteresis loops. Wasilewski (1973) also discusses magnetic hysteresis in natural materials, and presents results for geological samples including basalts, synthetic minerals and lunar samples. The materials were discriminated on the basis of their mineral content using coercivity parameters. More recently, Borradaile et al (1993) have used hysteresis loops and related parameters to discriminate between 116 limestone samples from 92 locations. Pelagic, dolomotized, shallow-subtidal, backreef-lagoonal and reef limestones are found to have different magnetic mineralogies and are either diamagnetic, paramagnetic or ferrimagnetic. Samples were successfully classified even though they were magnetically very weak, thus highlighting one of the advantages of highly accurate magnetic hysteresis data. Also Sandgren and Thompson (1990) used hysteresis loops to highlight the mineralogical differences between podzolic subsoils and topsoils

developed on sand dunes in Poland. In the study of magnetic properties of Chinese loess, Liu et al (1991) have used hysteresis loops and derived parameters to discribe the mineralogy of loess layers.

ADVANTAGES OF THE 'NUVO' VSM

1. Full IRM, magnetization curves and hysteresis loops can be measured on the same sample for 20 fields in half an hour. Traditional magnetization and measurement of IRM curves take several hours.

2. Once set in the VSM, the sample is not removed for measurement whereas the traditional method of obtaining susceptibility and remanence measurements involves different sample configurations so increasing the chance of error and inaccuracy.

3. Repeatability of the fields is extremely good. In a typical IRM curve of 20 field measurements and 20 zero field measurements, zero field was reached 100% (with VZ facility set at 0.1) and the specified magnetization fields were reached with an average field error of 0.75mT (1.713% error). By comparison, the repeatability of remanence measurements using a pulse magnetometer was lower due to small errors in setting the field using an analogue dial. Overall this means that measurement of weak samples on the VSM, such as peats and chemical compounds, will be much more accurate and reliable.

4. Higher accuracy of measurement will improve the prospects for linear modelling of the sources of environmental mixtures. Laboratory tests have shown that linearity errors of artificial mixtures are as low as 2% at higher field measurements. However care has to be taken as the source samples have to be mixed together to formulate only 0.4 grams of mixture sample; inhomogeneity and weighing errors become greater than in the traditional 10 ml pots used in standard equipment listed in Table 1.

USING THE VSM IN ENVIRONMENTAL MAGNETISM

Characterisation of samples

The VSMs mainstream use is in the magnetic description of environmental samples. The manufacturer provides a calibration sample of paramagnetic ferrous sulphate, or similar. We prefer to use a small piece of palladium rod set into a standard plastic sample holder. The moment of the rod is calculated from its mass and known mass-specific moment, and is highly stable. The Coventry calibration sample is 31.23 mA m^{-1} at 1000 mT. Selected data from the initial magnetization and IRM curves of samples are fed into a specially designed Microsoft WORKS VSM spreadsheet at Coventry which then calculates several further magnetic parameters. The VSM hysteresis loops, magnetization and remanence curves show immediately the types of minerals and their approximate contribution to the magnetic properties of a material. The examples presented here are taken from a database of 200 analysed materials. Figure 2 shows a range of loops which were obtained for 'pure' geological minerals and the spreadsheet output from the mineral data shown in Figure 2 is given in Table 2.

Modelling

Sources of Laboratory and Environmental Mixtures

The data of the VSM has been evaluated for use in the modelling of sources of environmental mixtures. Linear modelling routines are used in order to quantify the sources of mixtures of sediments using magnetic parameters. Only linearly additive data can be used, such as susceptibility, remanence and magnetization data. Linearity tests have been done using data of artificial laboratory mixtures where the exact proportions of sources are known. These tests have shown that at high fields (eg 800 mT) an error of 2% is typical. On low field measurements (eg 5 mT) however errors of 50 to 100% are typical; here slight variations in field settings have a greater effect on the linearity of the data.

Two examples are presented here, first an artificial laboratory mixture and second a real mixture of suspended sediments. Figure 3a shows a mixture made from 99.975% manganous carbonate (MnCO3) and 0.025% basalt crystals of approximately 125 mm. Table 3 presents some source predictions obtained using the hysteresis data of the two sources in linear programming (advanced from simultaneous equations by the incorporation of an error term). An error term is given where the difference between predicted result and actual measured result is calculated as a percentage of the predicted result.

Hysteresis loops for two suspended sediment sources (a and b) and one suspended sediment mixture (c) are presented in Figure 3b. No tests of the actual source proportions can be done here but an accuracy similar or even better to the

laboratory results can be expected if it is assumed that the mixing in environmental situations is superior to laboratory mixing where the sources are thoroughly mixed. However drawbacks in environmental situations include the variability and the movement of specific grain sizes.

Modelling Mineralogies of Materials

Modelling the proportions of magnetic minerals in materials can also be undertaken but problems of source data are great. The major problem is whether to use data for synthetic minerals of known grain sizes or just to use geological mineral data such as that in Figure 2 where purity of the minerals comes into question. Failing any in-depth analysis of the mineralogical content the VSM spreadsheet has been used to calculate percentage proportions of the ferrimagnetic and paramagnetic susceptibility using low (χ_{low} μm^3kg^{-1}) and high field (χ_{high} μm^3kg^{-1}) susceptibility. Changes in the size of these parameters are shown clearly in the progression from topsoil to parent material in the hysteresis loops shown in Figure 4.

Measurement of Weakly and Strongly Magnetic Samples

In the environment, materials which are of use in studies of sediment movement or pollution are often either found in low proportions, such as suspended sediments, or are magnetically weak, such as peats, leaves and suspended sediments. There is a facility on the VSM to correct weak samples for the diamagnetic background signal of the sample holder. Samples with a maximum magnetization as low as 2.3 mAm^2kg^{-1} and maximum remanence as low as 0.428 mAm^2kg^{-1} (Barium Sulphate) have been measured and successfully used in mixing experiments in the laboratory. Values for peat samples have been as low as 1.12 mAm^2kg^{-1} (maximum magnetization) and 0.299 mAm^2kg^{-1} (maximum remanence). In a study of suspended stream sediments from weakly magnetic sedimentary deposits, repeatable measurements were made on folded millipore filter papers holding c. 0.02 g of sediment, equivalent to a sediment concentration in the river of c. 80 mg l^{-1}

Very strong samples have been measured on the VSM in small proportions where they must be dispersed in a non-magnetic matrix such as calcium carbonate. The highest value of Ms to date is 67792.35 mAm^2kg^{-1} for a fine grained dispersed synthetic magnetite. A value of 42010.3 mAm^2kg^{-1} for a natural basalt crystal was also measured. In both cases, the ferrimagnetic material represented approximately 1% of the total mass of the VSM sample within a non magnetic matrix (99%). Strong samples are likely to show a demagnetisation effect, whereby an internal field created by highly magnetic particles counteracts and reduces the effective field around the sample. This will have the effect of reducing the magnetisation values from their maximum at any field. Whilst this problem cannot be totally overcome it can be lessened by changing the sample geometry (Cullity, 1972, O'Grady pers. Comm.). For the Nuvo VSM, demagnetisation factors will be reduced in samples which are disc shaped. This can be done by reducing the height of the standard 'cylindrical' holder to c.1 mm. Also where highly magnetic minerals are to be measured, dispersion is essential to at least 1% of the total sample weight (c. 0.4 g)

CALIBRATION OF THE VSM WITH THE BARTINGTON MS2 SUSCEPTIBILITY SYSTEM

Comparison of low field susceptibility (χ_{low}) and low frequency susceptibility (χ_{lf})

It should be noted initially that the VSM measures low and high field susceptibility (χ_{low}, χ_{high}) and the Bartington MS2 measures low field susceptibility at low and high frequencies (χ_{lf}, χ_{hf}). Although not directly comparable these measurements indicate the volume of ferrimagnetic minerals in a material. χ_{lf} is measured at 0.1 mT at a frequency of 4.6 mHz and has proved to be the most reliably linear measurement in laboratory tests, with an average linearity error (from 70 artificial mixtures) of 2%. This validates the usefulness of the cross calibrations. Measurement of χ_{low} on the VSM has been measured at 1 mT and 5 mT, the 5 mT value being more reliable in terms of field repeatability; thus 5 mT values are discussed in this paper.

A more comprehensive cross-calibration was undertaken using 93 materials, including pure minerals, synthetic minerals, peats, soils, rocks and chemical reagents. Data for χ_{low} at 5 mT (μm^3kg^{-1}) from the VSM was compared to χ_{lf} (μm^3kg^{-1}) from the MS2. Figure 5a shows the relationship between the two measurements. The two sets of values are related by the equation $y = 1.3169x + 5.9194$ with a correlation coefficient of 0.975 significant to 0.001.

Deviation from a $y = x$ (ie 1:1) relationship is expected, for two main reasons. First, the relationship between field and susceptibility in non-paramagnetic materials is not always linear even at fields under 10 mT (Nagata, 1940). However it must also be noted that the VSM measures at 5 mT and the MS2 at 0.1 mT. Second, the two

measurements use different sample sizes which gives rise to errors caused by material inhomogeneity.

CALIBRATION OF THE VSM WITH THE MOLSPIN PULSE MAGNETIZER/FLUXGATE SPINNER MAGNETOMETER SYSTEM

Comparison of VSM Mrs and Molspin IRM at 1000 mT

In this experiment the problem of sample homogeneity is not present as the same samples are measured each time. A group of samples shown in Table 4 were potted into VSM (0.4 g) holders and magnetized in the VSM at 1000 mT; Mrs was then measured on the VSM. The samples were then fitted vertically into a 10 ml sample pot adaptor and IRM_{1000mT} was measured on the Molspin. This avoided any problems of sample inhomogeneity, but did introduce the problem of using a small sample size (0.4 g cf. 10 g) in the Molspin which has yet to be addressed. The difference in time span between measurement on the VSM and Molspin is not considered important here as the samples chosen were not viscous. The results are presented both in Table 4 and in Figure 5b. A linear relationship exists between the two sets of values and they are correlated to 0.998, significant to 0.001. It was noted that paramagnetic material had non-zero remanence values on the VSM. It has been calculated that an average moment of 0.07 mAm^2kg^{-1} exists when the field is shown as zero. This moment value is the equivalent to between 0.125 and 1.5 mT. The reasons for this are not clear, but may be due to errors in the field detection setup. In any case, the value defines the accuracy of the VSM measurements at zero field. If all remanace data are corrected for this 'background value', the VSM values are still higher than those of the Molspin, but paramagnetic results are much improved.

CONCLUSIONS

1. The Molspin 'Nuvo' VSM provides a satisfactory means for obtaining magnetization and remanent data on environmental samples in fields between 1000 and -1000 mT. Sample characterization can be performed quickly and efficiently and may be used in modelling the sources of mixtures as shown.

2. Limitations to obtaining accurate and repeatable results are set by sample size and the magnetic moment of sample. As a guide, measurements should be undertaken on full sample holders, equivalent to c.0.4 g. It may be possible to reduce the mass to 0.02-0.04 g if the material is dispersed throughout the holder's volume. A diamagnetic correction should be used when the saturation magnetisation of a sample in less than 3 mAm^2 by using an average measurement of sample holders. It will be difficult to measure 0.4 g of material satisfactorily with saturation magnetisation values lower than 1 mAm^2kg^{-1}. The mean 'remanent' magnetisation values of a number of paramagnetic materials at zero field should be measured and used to correct all magnetisation data.

3. Susceptibility measurements at 5 mT compare reasonably well with data from the Bartington Instruments MS2 system. A better relationship exists for remanent magnetisation data at 1000 mT between the Molspin pulse magnetiser/spinner magnetometer and Molspin VSM. However, the errors are probably too large to allow data from the VSM and alternative equipment to be mixed but they give a very useful guide.

ACKNOWLEDGEMENTS

We would like to thank Lindsay Molyneux for his advice, Kevin O'Grady for advice and for providing a calibration sample, Roy Thompson for information and discussions on VSMs, Ian Foster and Angela Gurnell for permission to use data from their samples, and Birmingham Geology Department for providing mineral specimens. The equipment was originally financed by a DTI grant and upgraded using research funds provided by Coventry University

REFERENCES

Borradaile, G. J., Chow, N. and Werner, T., 1993. Magnetic hysteresis of limestones: facies control? Phys. Earth Planet. Inter., **76**: 241-252.

Cullity, B. D. 1972. Introduction to magnetic materials. Addison-Wesley, Reading, Mass.

Dankers, P. H. M. 1977. Magnetic properties of dispersed natural iron-oxidws of known grain size. Unpub. Ph.D. thesis , University of Utrecht.

Dearing, J. A., Maher, B. A. and Oldfield, F. 1985. Geomorphological linkages between soils and sediments: the role of magnetic measurements. in Richards, K.,Arnett, R. R. and Ellis, S. (Eds) Geomorphology and Soils, George Allen and Unwin.

Liu, X., Shaw, J., Liu, T., Heller, F. and Yuan, B. 1991. Magnetic mineralogy of Chinese Loess and its significance. (in press).

Nagata, T. 1940. Some Physical properties of the lavas of volcanoes Asama and Mihara II: Magnetic susceptibility. Bull. Earthquake Res. Inst., **18**: 102-135.

Oldfield, F. and Yu, L, 1993. Quantitative sediment source ascription using magnetic measurements in areservoir-catchment system near Nijar,S.E. Spain. Earth Surf. Proc. Landf., **18**: 441-454.

Oldfield, F. 1991. Environmental Magnetism- a personal perspective. Quaternary Science Reviews, **10**: 73-85.

Ozdemir, O. and Banerjee, S. K. 1982. A preliminary study of soil samples from west-central Minnesota. Earth Planet. Sci. Lett., **59**: 393-403.

Sandgren, P. and Thompson, R. 1990. Mineral magnetic characteristsics of podzolic soils developed on sand dunes in the Lake Goosciaz catchemnt, central Poland. Phys. Earth Planet. Inter., **60**: 297-313.

Senanayake, W. E. and McElhinny, M. W., 1981. Hysteresis and susceptibility characteristics of magnetite and titanomagnetite: interpretation of results from basaltic rocks.Phys. Earth Planet. Inter., **26**: 47-55.

Thompson, R. and Oldfield, F. 1986. Environmental Magnetism, George Allen and Unwin, London.

Wasilewski, P. J., 1973. Magnetic hysteresis in natural materials. Earth Planet. Sci. Lett., **20**: 67-72.

Yu, L. 1989. Environmental applications of mineral magnetic measurements; towards the quantitative approach. Unpub. Ph.D. thesis, University of Liverpool.

Yu, L. and Oldfield, F. 1989. A multivariate model for identifying sediment source from magnetic measurements. Quaternary Research, **32**: 168-181.

LIST OF FIGURES

Figure 1. IRM curve, magnetization curve and hysteresis loop for a sample of semi-pure massive hematite. Parameters used in this study are marked.

Figure 2. Hysteresis loops obtained for four geological mineral samples. (a) Magnetite, (b) Impure Hematite, (c) Lepidocrocite, (d) Geothite. The impure hematite gives a 'wasp waisted' loop indicating a ferrimagnetic component.

Figure 3. (a) Hysteresis loops for $MnCO_3$ and basalt crystals and for a mixture of the two (b) Hysteresis loops for two suspended sediments and their mixture.

Figure 4. Hysteresis loops for (a) a topsoil (0-2cms), (b) A horizon (16-18cms), (c) horizon (28-30cms) of a stagnogley soil and (d) the parent material Keuper clay.

Figure 5. (a) χ_{low} (VSM) versus χ_{lf} (MS2) for 93 synthetic and environmental samples. (b) Mrs (VSM) versus IRM (Molspin). In both cases the linear relationship is calculated and shown.

LIST OF TABLES

Table 1. (a) Hysteresis parameters measured on Molspin magnetometer and Bartington MS2 systems (all measured on 10ml samples). (b) Hysteresis parameters measured on Nuvo VSM (all measured on 0.4g samples).

Table 2. Microsoft WORKS VSM Spreadsheet output for the minerals shown in Figure 2.

Table 3. (a) Linear modelling results of the $MnCo^3$ and basalt crystal mixture and error terms of the comparison between actual measured result and predicted result. (b) Linear modelling results of the suspended sediment sources and mixture.

Table 4. Mrs (VSM) and IRM (Molspin) both measured at 1000mT. An error term is calculated as the difference between the two expressed as a percentage of the predicted result.

Table 1. (a) Standard Hysteresis parameters and the equipment used to measure them (all measured on 10ml samples). (b) V Hysteresis parameters (all measured on 0.4g samples).

(a)

K and χ Magnetic Susceptibility: The ratio of magnetisation induced to intensity of the magnetizing field. This is measured within a small magnetic field (0.1 mT) and is reversible (no remanence is induced). Measurement is on a volume (K) or mass specific (χ) basis. Measurement is roughly proportional to the concentration of ferrimagnetic minerals within a sample. Susceptibility is also sensitive to changes in grain size.

Instrumentation: Single sample susceptibility sensor (Bartington Instruments Ltd).
Units: K (dimensionless); χ ($\mu m^3\ kg^{-1}$)

χfd Frequency Dependent Susceptibility: The variation of susceptibility between two frequencies. Large values of this parameter indicate the presence of ferrimagnetic grains lying at the stable single domain/superparamagnetic boundary (0.02 μm). At higher frequencies of measurement, a proportion of these grains will become blocked in and will no longer contribute to χ as superparamagnetic but as single domain grains. Values of high-frequency (χ_{hf}) can be expected to be proportionatly lower than χ_{lf}; with weak samples (K_{lf}< 10) χfd is prone to large instrumental errors.

$$\chi fd\ (\%) = \frac{\chi_{lf} - \chi_{hf}}{\chi_{lf}} \cdot 100$$

Instrumentation: Dual Frequency (0.46 and 4.6 kHz) susceptibility sensor. (Bartington Instruments Ltd)
Units: Mass Specific ($nm^3\ kg^{-1}$) or as a percentage (%)

IRM Saturation Isothermal Remanent Magnetization: The highest level of magnetic remanence that can be induced in a sample by application of a high field. IRM_{880} is an indicator of the volume concentration of magnetic minerals in sample, but also responds to mineral type and grain size variations.

Instumentation: Pulse magnetiszer (maximum field 880 mT) (Molspin Ltd)
Fluxgate magnetometer (Molspin Ltd)
Units: $mAm^2\ kg^{-1}$

IRM_{20mT} 'Soft' Isothermal Remanence Magnetization: IRM_{20mT} can be used for approximating the concentration of remanence carrying ferrimagnets.

Instrumentation: Pulse magnetizer, Fluxgate magnetometer.
Units: $mA\ m^2\ kg^{-1}$

IRM_{-100mT} 'Hard' Isothermal Remanent magnetization: IRM_{880} - IRM_{100mT}, can be used for approximating the concentratio remanence carrying canted antiferromagnetic haematite of goethite in a sample.

Instrumentation: Pulse magnetizer, Fluxgate magnetometer.
Units: $mA\ m^2\ kg^{-1}$

IRM_{-300mT} 'Hard' Isothermal Remanent magnetization: IRM_{880} - IRM_{300mT}, can be used for approximating the concentratio remanence carrying canted antiferromagnetic haematite of goethite in a sample also, but is more sensitive than IRM-100mT.

Instrumentation: Pulse magnetizer, Fluxgate magnetometer.
Units: $mA\ m^2\ kg^{-1}$

IRM_{880}/χ The ratio of these parameters can be diagnostic of either mineralogy type (e.g., a low - theoretically zero ratio indicates the presence of paramagnetic minerals) or where samples have similar mineral types and concentrations, dominant magnetic grain size. Reduced by increased ferrimagnetic versus canted antiferromagnetic contribution, by increased grain size from SD upwards, by an increase in SP contribution to χ. comparison to other ratios and quotients makes it possible to identify mass contributory causes of variation in IRM_{880}/χ

Units: $kA\ m^{-1}$

$(B_o)_{cr}$ Demagnetization Parameter: The reverse field strength (mT) required to return a magnetized sample from its IRM_{88} zero is termed the coercivity of remanence $(B_o)_{cr}$.

Instrumentation: Pulse magnetizer, Fluxgate magnetometer.
Units: mT

'S' ratio Demagnetization Parameter: The ratio is obtained using IRM 100mT (a backfield discriminates between ferrimagnetic and antiferromagnetic mineral types) and IRM_{880}.

HIRM High Field Remanent Magnetization: HIRM is loss of magnetization after saturation expressed on a specific basis (IRM_{880} minus IRM-100). The total concentration of remanence carrying canted antiferromagnetic hematites car approximated.

Instrumentation: Pulse magnetizer, Fluxgate magnetometer.
Units: $mA\ m^2\ kg^{-1}$

HIRM/χ_{lf} This ratio indicates the proportion of antiferromagnets to ferrimagnets.

Units: kAm^{-1}

HIRM/χfd This ratio indicates the proportion of antiferromagnets to ferrimagnets of the SD/SP range.

Units: kAm^{-1}

(Dankers, 1977; Dearing et al, 1985; Ozdemir and Banerjee, 1982; Yu, 1989; Oldfield, 1991; Oldfield and Yu, 1993)

(b)

χlow Reversible low field susceptibility. Measured either at 1 mT or 5 mT. Like χ_{lf} indicates the ferrimagnetic, paramagnetic and canted-antiferromagnetic component of a material minus the diamagnetic component.
Instrumentation: VSM
Units: $\mu m^3 kg^{-1}$

χhigh Irreversible low field susceptibility. Measured as the gradient of the magnetization slope between 800 and 1000 mT Indicates the paramagnetic and canted-antiferromagnetic component of a material minus the diamagnetic component.

χpara is the mass specific susceptibility of paramagnetic material, χpara% is the percentage paramagnetic susceptibility to the total susceptibility.
Instrumentation: VSM
Units: $\mu m^3 kg^{-1}$

χferri The mass specific susceptibility component of ferrimagnetic minerals calculated from the difference between χlow χ_{high}. Also calculated is the percentage ferrimagnetic component of the total susceptibility (χ_{ferri}%).
Instrumentation: VSM
Units: $\mu m^3 kg^{-1}$

Ms The saturation magnetization (at 1000 mT) of the ferrimagnetic component of a material and is calculated by extrapolating the high field magnetisation curve to the y axis (see Figure 1).
Units: $mA\ m^2 kg^{-1}$

Mrs The saturation remanence of a material is the remanence value at zero field following magnetization at 1000 mT, in theory the same as IRM_{880}.
Instrumentation: VSM
Units: $mA\ m^2 kg^{-1}$

Mrs/Ms Mrs/Ms is the ratio of remanence magnetisation to the saturated magnetisation. In the absence of paramagnetic minerals it gives information about 'magnetite' type and grain sizes.

$HIRM_{+100mT}$ High Field Remanent Magnetization: HIRM is loss of magnetization after saturation expressed on a specific basis (Mrs - IRM_{+100}). The total concentration of remanence carrying hematites can be approximated.
Instrumentation: VSM
Units: $mA\ m^2 kg^{-1}$

'S' ratio The ratio of IRM_{+100mT} and Mrs and indicates the proportion of soft magnetic minerals such as magnetites to the total remanence carrying mineral content.

Table 2. Microsoft WORKS VSM Spreadsheet output for the minerals shown in Figure 2.

VSM SPREADSHEET V1.1 - OCTOBER 1993 - JAD&JAL

Values of moment from printout or calculate moment as calfac*S*attfac

Description	INPUT Code	INPUT holder mass g	INPUT sample holder g	INPUT +sample g	INPUT exact Residual at 0mT	INPUT exact field at 5mT	INPUT enter moment values from VSM forward mag and irms for fields in mT mag 5 mT	rem 0 mT	mag 100 mT	rem 0 mT	mag 800 mT	rem 0 mT	mag 1000mT	rem 0 mT
Magnetite	JL-A2	6.916	7.368	0.451	0.07	5.4	954.6	32.1	12899.1	291.6	20298.8	295.5	20346.2	292.8
Hematite	JL-A4	6.894	7.399	0.506	0.07	5.4	4.867	0.403	82.925	11.005	271.498	84.103	303.025	93.682
Lepidocrocite	JL-A6	6.896	7.133	0.237	0.07	5.5	0.496	0.031	9.486	0.093	73.346	0.496	91.791	0.775
Geothite	JL-A8	6.914	7.270	0.356	0.07	5.5	38.595	37.603	47.306	37.138	101.401	37.138	116.870	37.045

Continued:

	CALC χ_{low} μAm^2kg^{-1}	CALC χ_{high} (para) μAm^2kg^{-1}	CALC χ_{ferri} μAm^2kg^{-1}	CALC χ_{para} percent	CALC χ_{ferri} percent	CALC Ms mAm^2kg^{-1}	CALC Mrs mAm^2kg^{-1}	CALC $Mrs/_{Ms}$	CALC HIRM +100mT mAm^2kg^{-1}	CALC S ratio $100/_{1000}$
Magnetite	491.972	0.659	491.313	0.134	99.866	44538.4	648.494	0.015	2.540	0.996
Hematite	2.208	0.391	1.817	17.706	82.294	287.616	185.325	0.644	163.555	0.117
Lepidocrocite	0.411	0.487	-0.076	118.618	-18.618	-1.832	3.271	-1.786	2.879	0.120
Geothite	24.717	0.272	24.446	1.099	98.901	110.994	104.030	0.937	-0.261	1.003

Table 3. (a) Linear modelling results of the $MnCo^3$ and basalt crystal mixture and error terms of the comparison between actual measured result and predicted result. (b) Linear modelling results of the suspended sediment sources and mixture.

Parameter	Manganous Carbonate (99.75%)	Basalt Crystals (0.25%)	Predicted Measurement	Actual Meas.	% Error
χ_{low} (μAm^2kg^{-1})	1.048	527.6	2.397	2.364	-1.38
χ_{ferri} (μAm^2kg^{-1})	0.044	526.5	1.3	1.36	4.422
Ms (mAm^2kg^{-1})	9.036	42010.3	120.53	114.04	-5.69
Mag 200mT(mAm^2kg^{-1})	191.86	36982.8	299.05	286.0	-4.56
Mag 600mT(mAm^2kg^{-1})	572.15	41120.7	661.57	675.91	2.12

Table 4. Mrs (VSM) and IRM_{880} (Molspin) both measured at 1000mT. An error term is calculated as the difference between the two expressed as a percentage of the predicted result.

Sample Code	VSM Mrs (mAm2/kg)	MOl. Mrs (mAm2/kg)	VSM-MOL MOL (%)	VSM-MOL (mAm2/kg)	Remanence (mT)	Moment (mT)
SP1A12	3.118	2.891	7.28	0.227	45	2
CM1B12	7.504	6.512	13.22	0.992	2	1
BH1Y12	12.841	11.396	11.253	1.445	5	1
GL2K2	0.42	0.349	16.905	0.071	7	5
GL3K2	0.4934	0.022	95.54	0.471	>1000	4
GH1X1	317.091	252.975	20.22	64.116	>1000	33
DM1A1	27.56	23.414	15.04	4.146	>1000	14
MIX 72	11.35	9.922	12.581	1.428	10	1
MIX 73	6.346	5.629	11.298	0.717	12	1.5
MIX 74R	4.938	4.157	15.816	0.781	15	3
MIX 75R	2.123	1.77	16.63	0.353	5	1
MIX 76	1.923	1.855	3.536	0.068	27	0.125

Figure 1 (a)

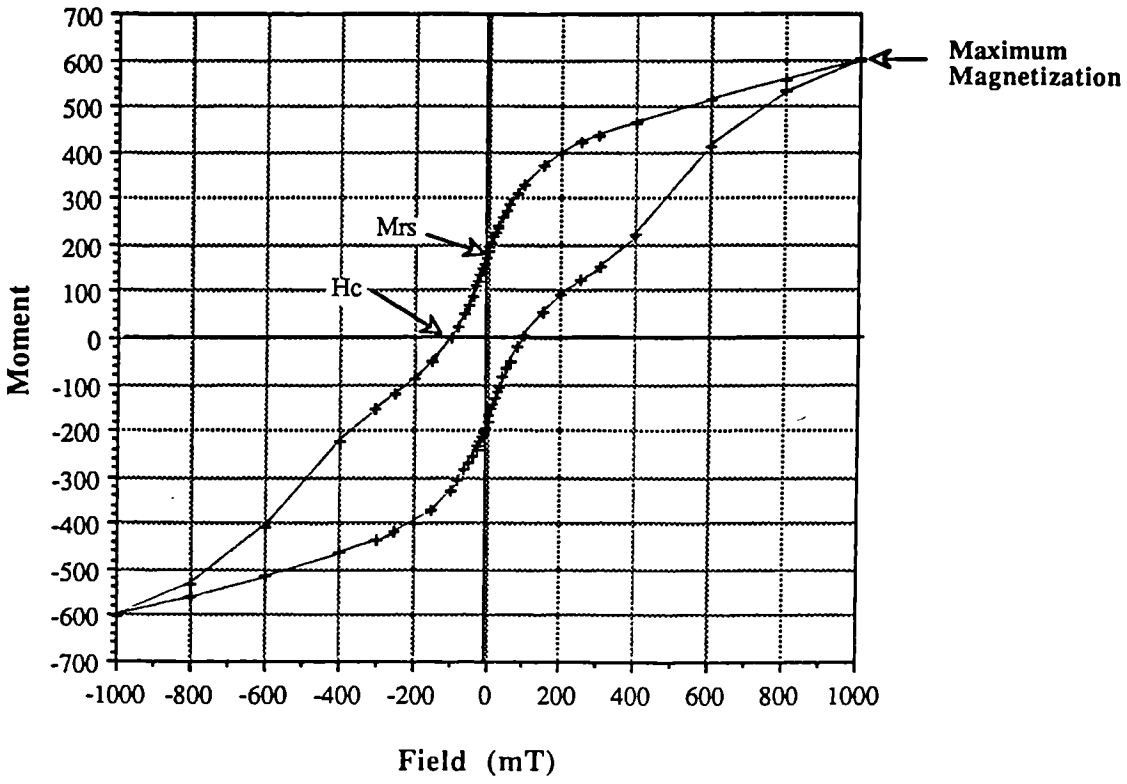
Massive Hematite
Maximum Magnetization
Mrs
Hc
Moment
700
600
500
400
300
200
100
0
-100
-200
-300
-400
-500
-600
-700
-1000 -800 -600 -400 -200 0 200 400 600 800 1000
Field (mT)

(b)

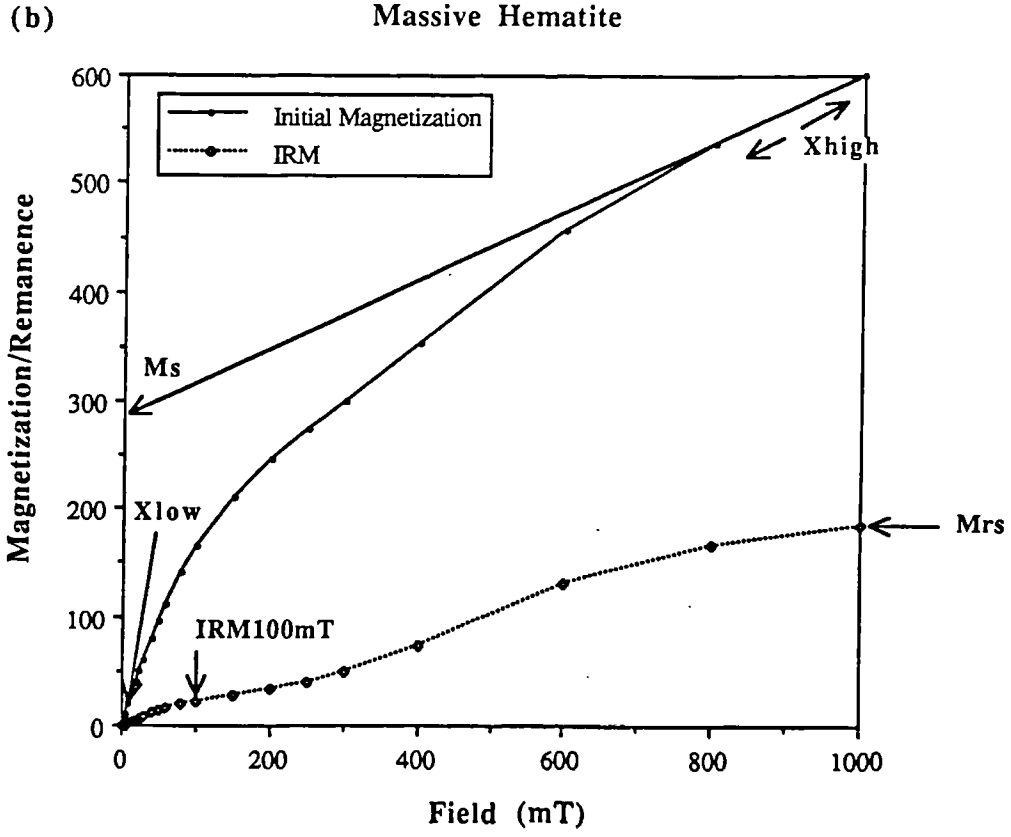
Massive Hematite
Initial Magnetization
IRM
Xhigh
Ms
Xlow
IRM100mT
Mrs
Magnetization/Remanence
600
500
400
300
200
100
0
0 200 400 600 800 1000
Field (mT)

Figure 2 (a) Massive Magnetite

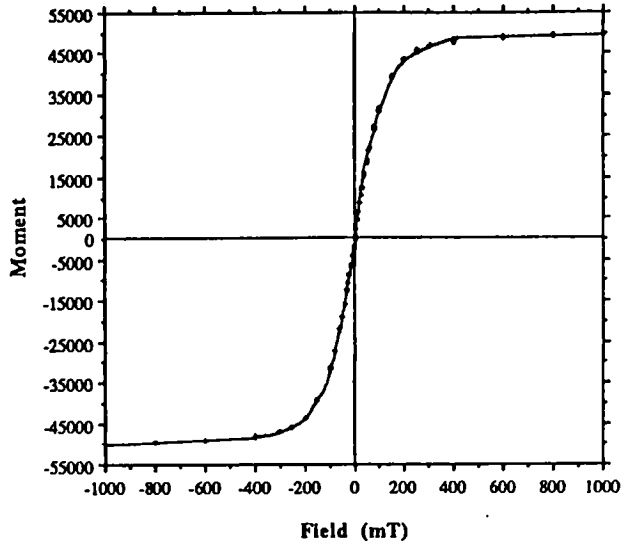

(b) Massive Hematite

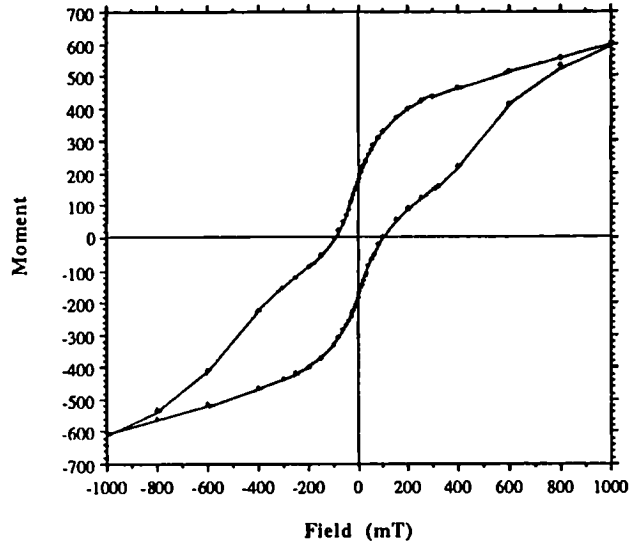

(c) Lepidocrocite

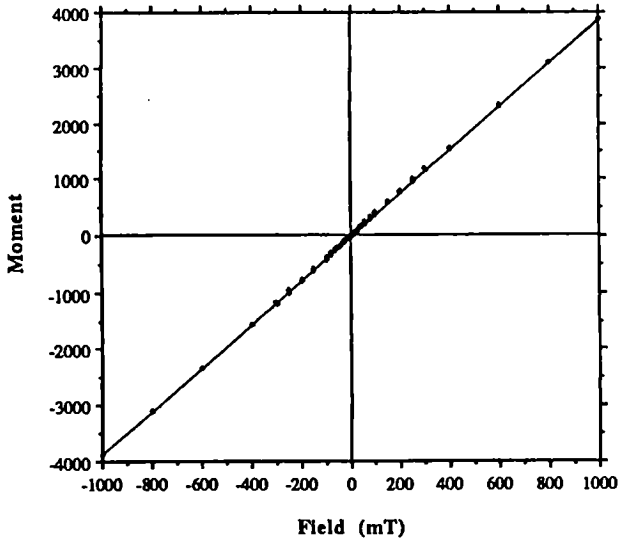

(d) Goethite

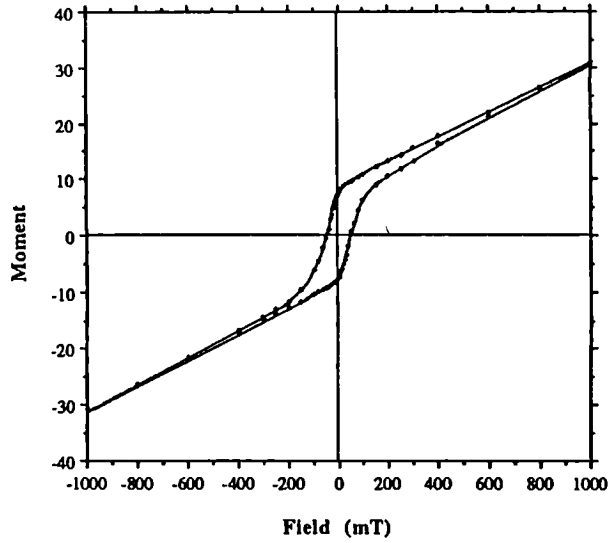

Figure 3 (a)

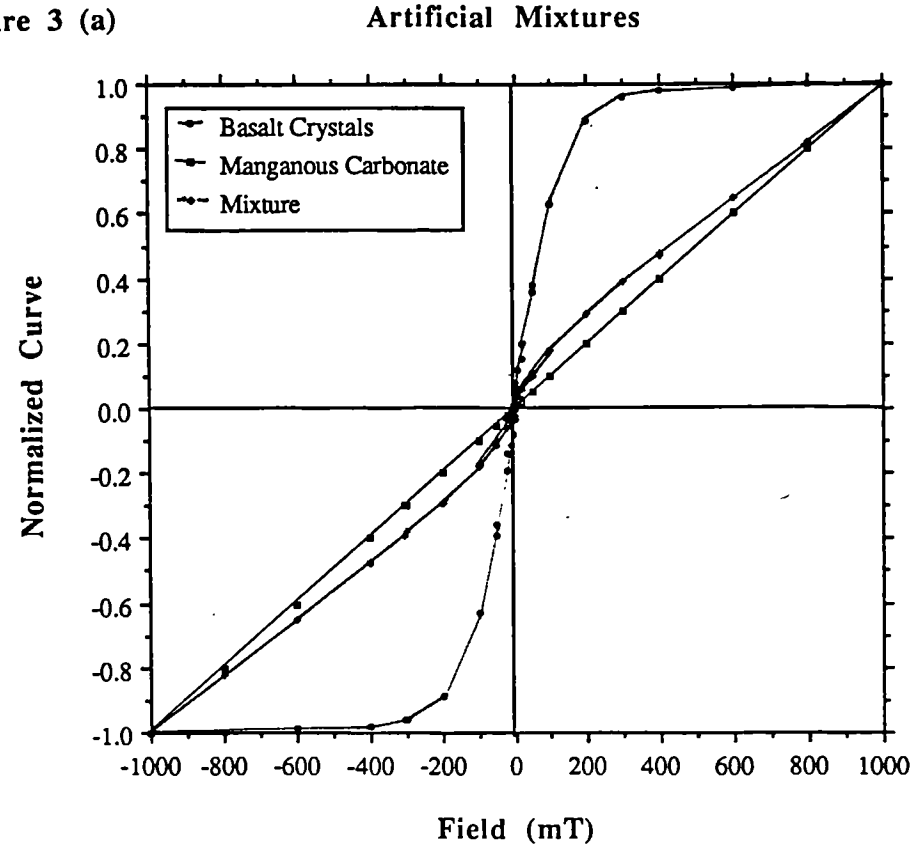
Artificial Mixtures
Basalt Crystals
Manganous Carbonate
Mixture
Normalized Curve
1.0
0.8
0.6
0.4
0.2
0.0
-0.2
-0.4
-0.6
-0.8
-1.0
-1000 -800 -600 -400 -200 0 200 400 600 800 1000
Field (mT)

(b)

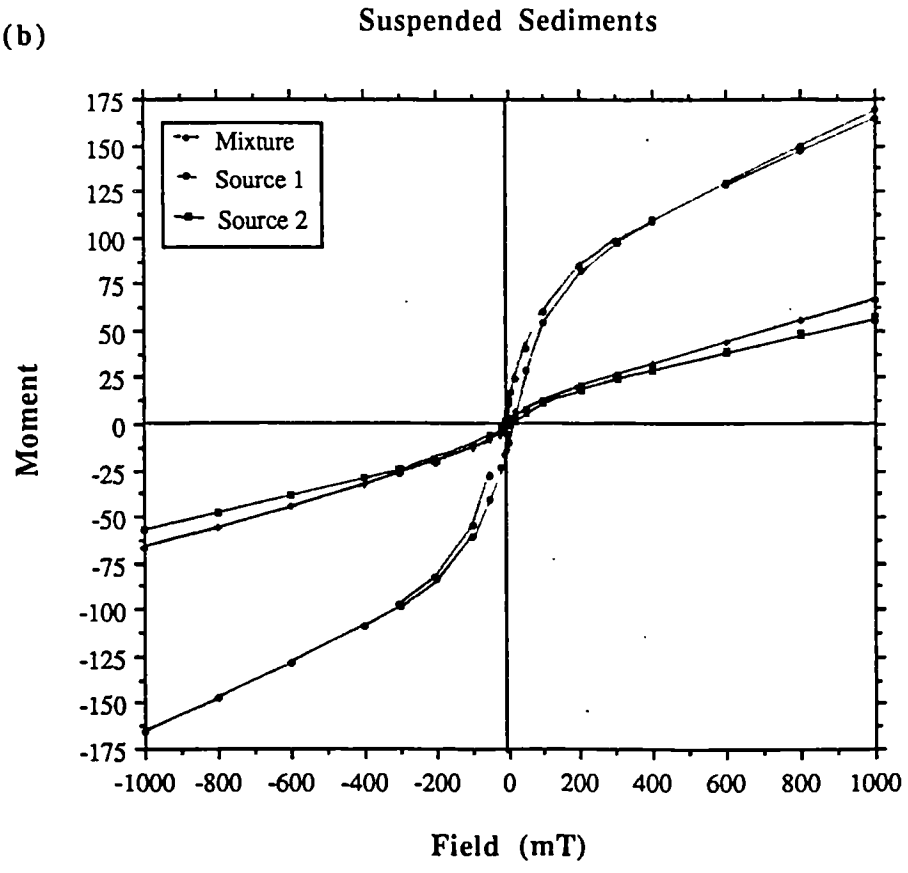
Suspended Sediments
Mixture
Source 1
Source 2
Moment
175
150
125
100
75
50
25
0
-25
-50
-75
-100
-125
-150
-175
-1000 -800 -600 -400 -200 0 200 400 600 800 1000
Field (mT)

Figure 4 (a)

Topsoil 0-2cms

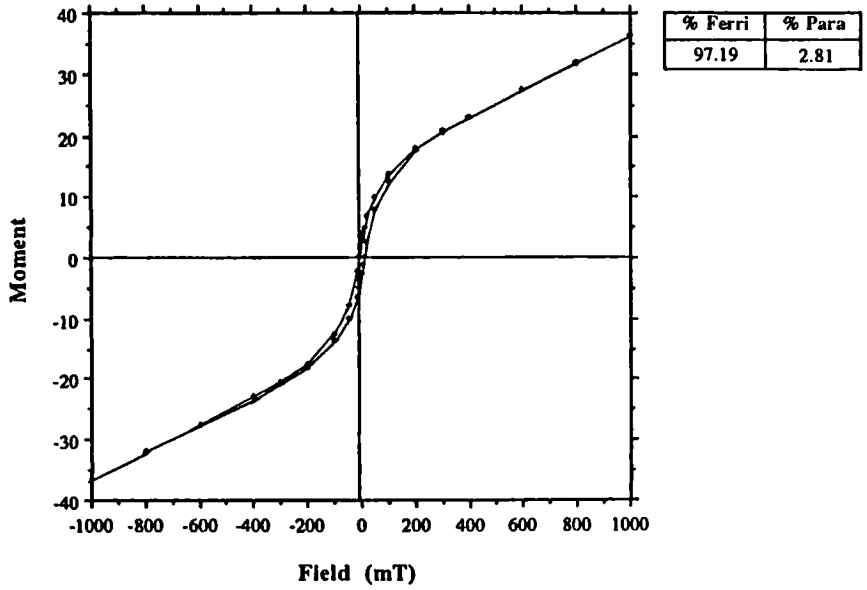

% Ferri	% Para
97.19	2.81

(b)

A Horizon 16-18cms

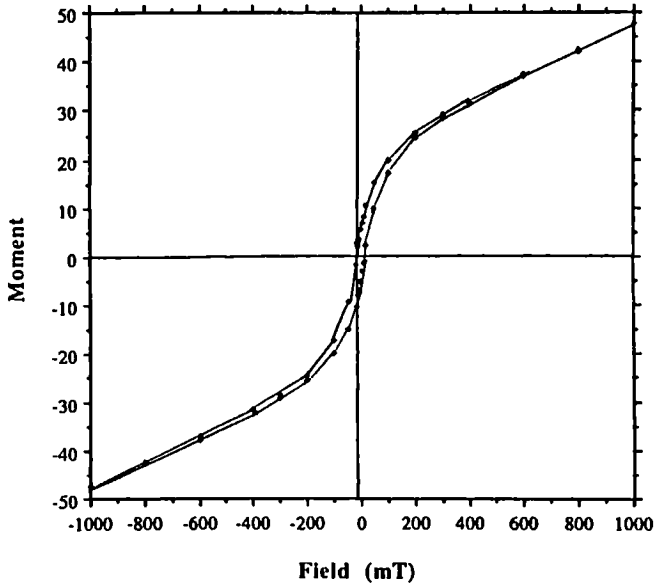

% Ferri	% Para
91.38	8.62

(c)

B Horizon 28-30cms

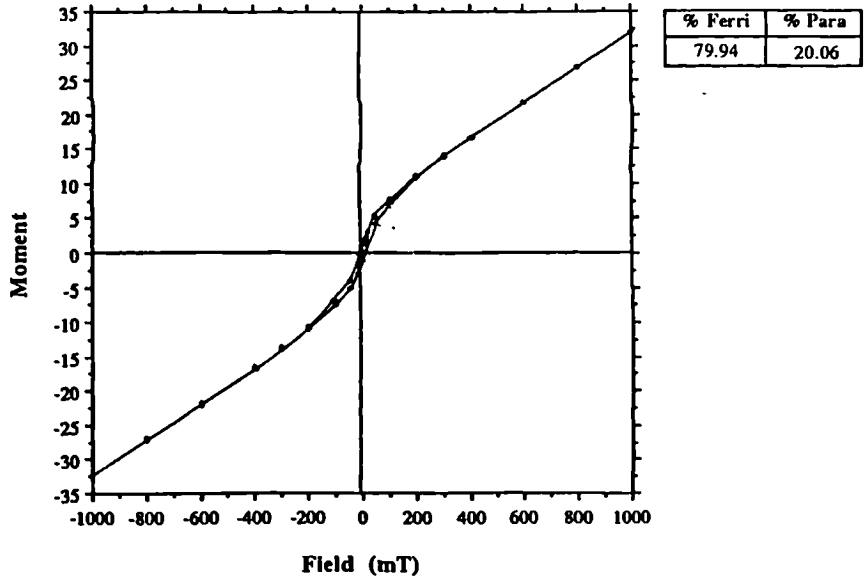

% Ferri	% Para
79.94	20.06

(d)

Parent Material

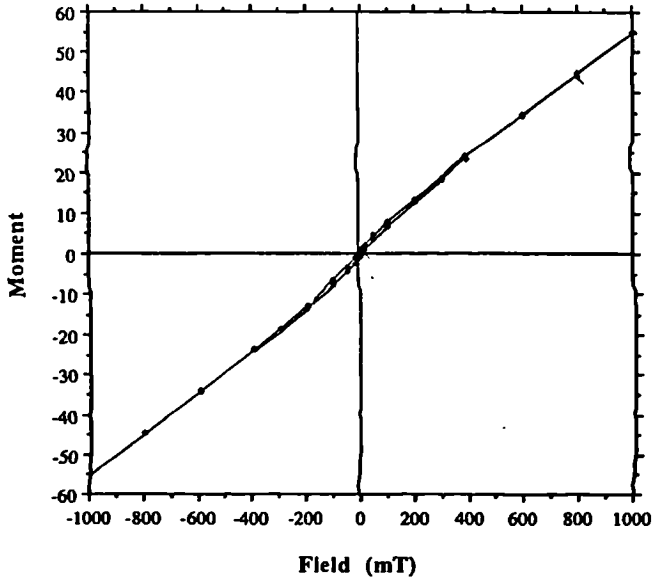

% Ferri	% Para
37.06	62.94

Figure 5 (a)

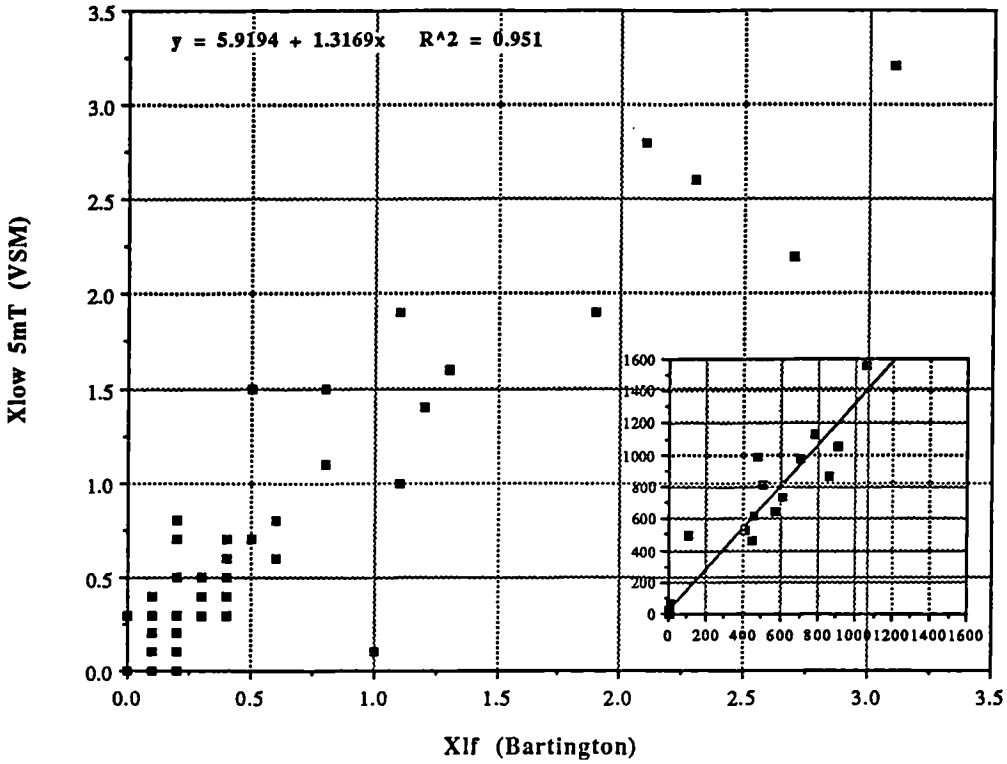
y = 5.9194 + 1.3169x R^2 = 0.951
Xlow 5mT (VSM)
Xlf (Bartington)
0.0
0.5
1.0
1.5
2.0
2.5
3.0
3.5
0
200
400
600
800
1000
1200
1400
1600

(b)

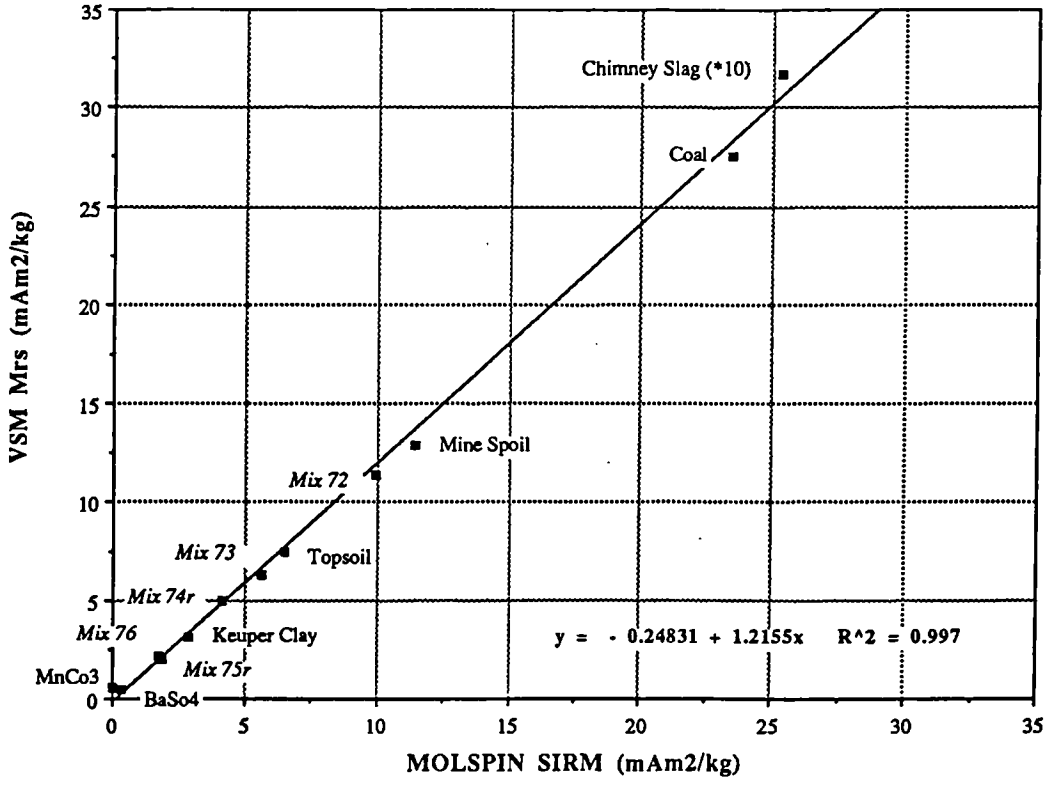
VSM Mrs (mAm2/kg)
MOLSPIN SIRM (mAm2/kg)
Chimney Slag (*10)
Coal
Mine Spoil
Mix 72
Mix 73
Topsoil
Mix 74r
Mix 76
Keuper Clay
Mix 75r
MnCo3
BaSo4
y = - 0.24831 + 1.2155x R^2 = 0.997
0
5
10
15
20
25
30
35